British Journal of Pharmacology

February 1995

Volume 114 Number 3 pages 563–732

British Journal of Pharmacology (1995) 114, 563–569

Potentiation by endothelin-1 of cholinergic nerve-mediated contractions in mouse trachea via activation of ET_B receptors

[1]Peter J. Henry & Roy G. Goldie

Department of Pharmacology, University of Western Australia, Nedlands, 6009, Australia

1 We have previously shown that endothelin-1-induced contraction of mouse isolated tracheal smooth muscle was mediated via both ET_A and ET_B receptors. In the current study, we have investigated endothelin-1-induced potentiation of cholinergic nerve-mediated contractions in mouse isolated trachea and have characterized pharmacologically the endothelin receptors mediating this response.

2 Electrical field stimulation (EFS; 70 V, 0.5 ms duration, 10 s train, 0.1–60 Hz) of mouse isolated trachea caused frequency-dependent, monophasic contractions (magnitude of contraction of 60 Hz was $56 \pm 4\%C_{max}$ ($n = 6$), where C_{max} is the contractile response to 10 μM carbachol). EFS-induced contractions were abolished by either 0.1 μM atropine or 3 μM tetradotoxin, but were not affected by 1 μM hexamethonium, indicating that they were induced by stimulation of postganglionic cholinergic nerves. In contrast, contractions induced by exogenously applied acetylcholine were inhibited by atropine, but not by either tetrodotoxin or hexamethonium.

3 The ET_B receptor-selective agonist, sarafotoxin S6c, caused marked concentration-dependent potentiation of EFS-induced contractions in mouse isolated tracheal segments. At 0.1 nM, sarafotoxin S6c exerted no direct contractile effect, but significantly increased a standard EFS-induced contraction of $20\%C_{max}$ by $8 \pm 2\%C_{max}$ (i.e. 1.4 fold, $n = 5$, $P < 0.05$). At higher concentrations, 10 nM sarafotoxin S6c induced a large, transient contraction (peak response of $74 \pm 2\%C_{max}$ at 10 min; $3 \pm 2\%C_{max}$ at 45 min) and enhanced the standard EFS-induced contraction by $30 \pm 4\%C_{max}$ (i.e. 2.5 fold, $n = 5$, $P < 0.01$). In contrast, 10 nM sarafotoxin S6c did not enhance contractile responses to exogenously applied acetylcholine ($n = 6$).

4 Endothelin-1 also modulated EFS-induced contractions. At 0.1 nM, endothelin-1 exerted no direct contractile effect, but significantly increased the standard EFS-induced contraction of $20\%C_{max}$ by $7 \pm 2\%C_{max}$ (i.e. 1.35 fold, $n = 5$, $P < 0.05$). At 1 nM, endothelin-1 induced a small, sustained contraction ($16 \pm 3\%C_{max}$) and increased the standard EFS-induced contraction by $19 \pm 2\%C_{max}$ (i.e. 1.95 fold, $n = 5$, $P < 0.01$). Finally, 10 nM endothelin-1 induced a large, sustained contraction ($98 \pm 8\%C_{max}$), but the EFS-induced contraction was significantly reduced from $20\%C_{max}$ to $6 \pm 4\%C_{max}$ ($n = 6$, $P < 0.05$). In contrast, in the presence of 3 μM BQ-123 (ET_A receptor-selective antagonist), 10 nM endothelin-1 induced a transient contraction mediated via ET_B receptors (peak response of $59 \pm 10\%C_{max}$ at 10 min; $8 \pm 2\%C_{max}$ at 45 min). Under these conditions, the standard EFS-induced contraction was increased by $26 \pm 1\%C_{max}$ (i.e. 2.3 fold, $n = 6$, $P < 0.01$).

5 The potentiation of EFS-induced contractions produced by 1 nM endothelin-1 was not mediated by ET_A receptors, since 3 μM BQ-123 did not diminish this effect ($n = 6$). Furthermore, 1 nM endothelin-1 did not potentiate EFS-induced contractions in preparations in which the function of the ET_B receptor-effector system had been attenuated by desensitization ($n = 6$).

6 In summary, endothelin-1 potentiates cholinergic nerve-mediated contractions in mouse isolated trachea, apparently by activating prejunctional ET_B receptors. This neuronal pathway offers an additional mechanism through which endothelin-1 may elevate bronchomotor tone.

Keywords: Endothelin-1; sarafotoxin S6c; endothelin receptors; electrical field stimulation; parasympathetic nerves; cholinergic nerves; airway smooth muscle

Introduction

There is accumulating evidence that the elevated levels of endothelin-1 detected in the airways during asthma may contribute to the bronchial obstruction associated with this airways disease (Springall *et al.*, 1991; Hay *et al.*, 1993a). For example, it is well established that many of the changes in the airway wall that lead to bronchial obstruction, including bronchoconstriction, mucous gland hypersecretion and airway wall thickening (oedema and airway smooth muscle proliferation) can be induced by endothelin-1 in various experimental systems (Advenier *et al.*, 1990; Henry *et al.*, 1990; Shimura *et al.*, 1992; Mullol *et al.*, 1993; Pons *et al.*, 1991; Ercan *et al.*, 1993; Noveral *et al.*, 1992; Tomlinson *et al.*, 1994). To date, most attention has focussed on the marked bronchoconstrictor actions of endothelin-1.

The precise mechanisms through which endothelin-1 causes bronchoconstriction is unclear, although a variable combination of direct and indirect actions may be involved. With respect to the direct actions of endothelin-1, airway smooth muscle contains high densities of endothelin receptors (Goldie *et al.*, 1994), that are linked to the influx of extracellular calcium and the release of intracellular calcium (via stimulation of the phosphoinositide pathway); processes known to be intimately associated with airway smooth muscle contraction. Whereas the direct actions of endothelin-1 on airway smooth muscle are well established, there is conflicting evidence as to whether endothelin-1-induced contraction also occurs through an *indirect* mechanism involving the release of secondary mediators. For example, there is general agreement that the *in vivo* bronchoconstrictor actions of endothelin-1 are inhibitable by the cyclo-oxygenase inhibitor, indomethacin, and may be mediated by thromboxane A_2 (Payne & Whittle, 1988; Macquin-Mavier *et al.*, 1989; Lagente *et al.*, 1989). However, in contrast, recent studies by Hay and coworkers have demonstrated that although

[1] Author for correspondence.

endothelin-1 evokes the release of an array of prostanoids from guinea-pig and human airways, they do not appear to have any significant effect on the contractile response (Hay *et al.*, 1993b,c).

An additional potential mechanism through which endothelin-1 might cause bronchoconstriction is neuromodulation. In a recent study of rabbit bronchial segments, McKay and coworkers (1993) reported that the purported neural form of endothelin, endothelin-3 augmented the contractile responses induced by electrical field stimulation of postganglionic cholinergic nerves, via a prejunctional mechanism. Furthermore, endothelin receptors have been demonstrated on the cell bodies, processes and varicosities of cholinergic and adrenergic intramural neurones present in primary cultures of guinea-pig tracheal smooth muscle. Moreover, stimulation of these neuronal endothelin receptors produced a tetrodotoxin-sensitive elevation of calcium and contraction of adjacent smooth muscle cells (Takimoto *et al.*, 1993). The aim of the current study was to characterize pharmacologically the endothelin receptor subtype(s) through which endothelin-1 exerts its enhancing effects on cholinergic nerve-mediated contractions in the airways.

Methods

Mouse isolated tracheal tissue

Male CBA/CaH mice between 8 and 10 weeks of age were obtained from the Animal Resources Centre (Perth, Australia). Mice were anaesthetized with halothane (Fluothane, ICI) and killed by cervical dislocation. The trachea and surrounding tissue was gently dissected free and placed in a Petri dish containing oxygenated Krebs-bicarbonate solution (KBS). The trachea was then dissected free of adhering tissue and cut transversely to yield two tracheal segments of 2–3 mm in length, which were suspended under 0.5 g tension in organ baths containing 3 ml KBS at 37°C, bubbled with 5% CO_2 in O_2. Care was taken to ensure that the tracheal smooth muscle band was always located between the supports to maximize tension recordings. Changes in tracheal smooth muscle tension were recorded isometrically via FT03 force-displacement transducers (Grass Instruments) linked to a Grass Polygraph (Model 7D). Each tracheal segment was equilibrated for 45 min, with changes in KBS every 15 min during this period. The viability of each preparation was then assessed by the cumulative addition of 0.2 μM (submaximally-effective concentration) and 10 μM carbachol (maximally-effective concentration; Henry *et al.*, 1990; 1991). Upon reaching a contraction plateau with 10 μM carbachol ($100\%C_{max}$), preparations were repeatedly washed and rested for a further 20 min. A non-cumulative frequency-response curve was then constructed for each preparation (70 V, 0.5 ms, 10 s train; 0.3, 1, 3, 10 and 30 Hz at 2 min intervals). Electrical field stimulation (EFS) was delivered by a Grass S44 stimulator connected to a stimulus isolation unit (SIU5, Grass Instruments) and a timing devise. Stimuli were applied across the tracheal ring preparations by means of two parallel platinum electrodes. The composition of KBS was (in mM): NaCl 117, KCl 5.36, $NaHCO_3$ 25, KH_2PO_4 1.03, $MgSO_4.7H_2O$ 0.57, $CaCl_2$ 2.5 and glucose 11.1. The cyclo-oxygenase inhibitor, indomethacin (2.5 μM) was present in the KBS during all studies.

Experimental protocols

In each protocol, the contractile responses of four tracheal rings (from two mice) were examined concurrently. One segment was used as a time-control and the remaining three as test preparations.

Nature of EFS-induced responses

To evaluate the role of cholinergic nerves in the contractile responses to EFS (non-cumulative frequency-response curve, 0.1–60 Hz), we investigated the effects of the muscarinic cholinoceptor antagonist, atropine (0.1 μM), the neurotoxin, tetrodotoxin (3 μM) and the ganglion blocker, hexamethonium (1 μM). The influence of these agents on contractile responses to cumulatively applied acetylcholine (10 nM–0.3 mM at 0.5 log concentration increments) was also tested. Each of the three test preparations was exposed to a different antagonist.

Endothelin receptor-mediated modulation of EFS responses

A major aim of the current study was to evaluate the influence of ET_A and ET_B receptor stimulation by sarafotoxin S6c (ET_B receptor-selective agonist) and endothelin-1 (nonselective ET_A/ET_B receptor agonist) on EFS-induced contractions. From the EFS frequency-response curve, an EFS frequency that produced $20\%C_{max}$ was estimated and applied to the preparations at 3 min intervals. After three consecutive, equivalent EFS-induced contractions had been obtained (standard EFS-induced contractions), each of the three test preparations was exposed to a different concentration (0.1 nM, 1 nM or 10 nM) of sarafotoxin S6c or endothelin-1, and the selected frequency of EFS applied every 3 min for a further 45 min. The control preparation was exposed to EFS, but not to an endothelin receptor agonist. A similar protocol was used to investigate the role of ET_A receptors in endothelin-1-mediated modulation of EFS-induced contractions. In these studies, 3 μM BQ-123 (ET_A receptor-selective antagonist) was applied at least 20 min prior to the addition of 1 nM endothelin-1. In addition, in some experiments, preparations were exposed for 40 min to a high concentration (100 nM) of sarafotoxin S6c to desensitize the ET_B receptor-effector system. After this desensitization period, preparations were repeatedly washed for 30 min and the influence of 1 nM sarafotoxin S6c or 1 nM endothelin-1 on EFS-induced contractions determined as described above.

Data analysis

Contractile responses to EFS, acetylcholine and peptides have been expressed as a percentage of the response obtained to a maximally-effective concentration of carbachol (10 μM, $100\%C_{max}$) at the beginning of the experiment. In control (C) and test (T) preparations, the mean of the three initial standard EFS-induced contractions was estimated (C_0, T_0) and subtracted from the subsequent EFS-induced contractions (C_t, T_t) produced at three min intervals over the 45 min period. Thus, at each of these time-points, changes in the magnitude of EFS-induced contractions induced as a function of time and by an endothelin receptor agonist in a test preparation ($\Delta T = T_t - T_0$) and by time alone in a control preparation ($\Delta C = C_t - C_0$) were estimated. Time-related changes in EFS responses were subtracted ($\Delta T_{cor} = \Delta T - \Delta C$) to isolate agonist-induced changes at each time-point. Agonist-induced changes were expressed as mean $\Delta T_{cor} \pm$ s.e.mean of n different preparations. The time-related changes in EFS-induced contractile responses (ΔC) were small and consistent; an increase of $2.9 \pm 0.4\%C_{max}$ was observed at 20 min and of $5.6 \pm 0.7\%C_{max}$ at 45 min ($n = 22$ control preparations).

Drugs

Endothelin-1 and sarafotoxin S6c were purchased from Auspep (Melbourne, Australia) and stored as 50 μM solutions in 0.1 M acetic acid at −70°C. Other drugs used included carbamylcholine chloride, acetylcholine chloride, indo-

methacin, tetrodotoxin, hexamethonium chloride (Sigma Chemical Co, St Louis), atropine sulphate monohydrate (Fluka AG), and BQ-123 (cyclo[D-Trp-D-Asp-L-Pro-D-Val-L-Leu], generous gift from Dr D.W.P. Hay, SmithKline Beecham Pharmaceuticals, King of Prussia). All dilutions were made in saline, stored on ice and protected from light.

Results

EFS-induced contractions in mouse isolated tracheal preparations

EFS (70 V, 0.5 ms duration, 0.3–30 Hz, 10 s train every 2 min) induced frequency-dependent contractions in mouse isolated tracheal segments (Figure 1a). Representative examples of the monophasic contractions induced by EFS are shown in Figures 2a and 4a. EFS-induced contractions were prevented by prior incubation with either the neurotoxin, tetrodotoxin (3 μM) or the muscarinic cholinoceptor antagonist, atropine (0.1 μM), but were not inhibited in the presence of the ganglion blocker, hexamethonium (1 μM) (Figure 1a). These data indicate that the EFS-induced contractions resulted from the activation of postganglionic cholinergic nerves. As expected, contractions induced by exogenously added acetylcholine were inhibited by atropine, but not by tetrodotoxin or hexamethonium (Figure 1b).

Potentiation of EFS-induced contractions by the ET_B receptor-selective agonist sarafotoxin S6c

In mouse isolated tracheal segments, the ET_B receptor-selective agonist, sarafotoxin S6c (10 nM) induced large, transient contractions that peaked within 10 min (74 ± 2%C_{max}, $n = 5$) but which waned towards baseline levels of tone over a 45 min period (3 ± 2%C_{max}, $n = 6$) (Figure 2a). In the presence of 10 nM sarafotoxin S6c, contractile responses to EFS were augmented at all stimulation frequencies tested (0.1–60 Hz) (Figure 2a,b). Thus, the EFS frequency required to produce a contraction of 40%C_{max} in the presence of 10 nM sarafotoxin S6c (0.37 Hz; 95% confidence limits, 0.16–0.85, $n = 6$) was 13.8 fold lower than that in paired control preparations (5.1 Hz; 0.9–28, $n = 6$, $P < 0.01$). Although 10 nM sarafotoxin S6c potentiated contractile responses to EFS, it had no significant effect on responses to exogenously added acetylcholine (Figure 2c). As shown in Figure 3, the extent to which the contractile responses to EFS was enhanced depended upon the concentration of sarafotoxin S6c. Interestingly, at a concentration of 0.1 nM, sarafotoxin S6c induced no direct contractile response but produced a significant potentiation of the EFS-induced contraction (8 ± 2%C_{max}, $n = 5$, $P < 0.05$). The potentiations observed in the presence of 1 and 10 nM sarafotoxin S6c were

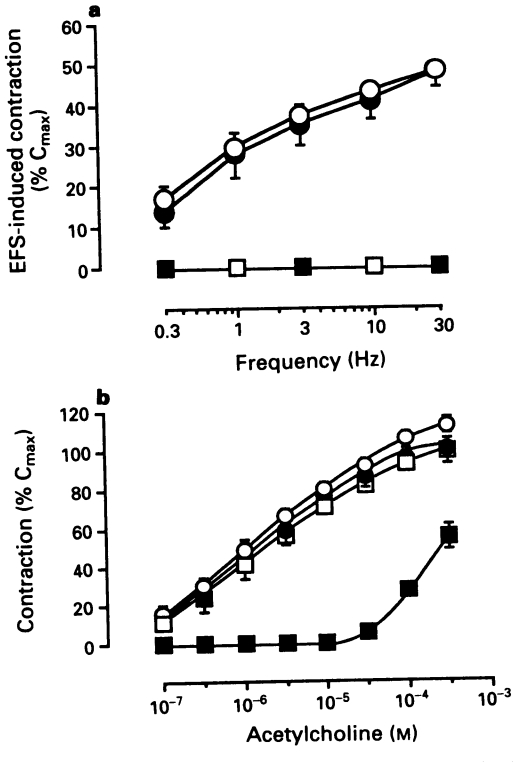

Figure 1 Effect of 0.1 μM atropine (■), 3 μM tetrodotoxin (□) and 1 μM hexamethonium (●) on (a) the EFS frequency-response relationship and (b) acetylcholine concentration-response curves in mouse isolated tracheal segments (control, ○). Shown are the mean ± s.e.mean responses from 3 preparations. Responses in this and subsequent figures are shown as a percentage of the response to a maximally effective concentration of carbachol (10 μM, 100%C_{max}).

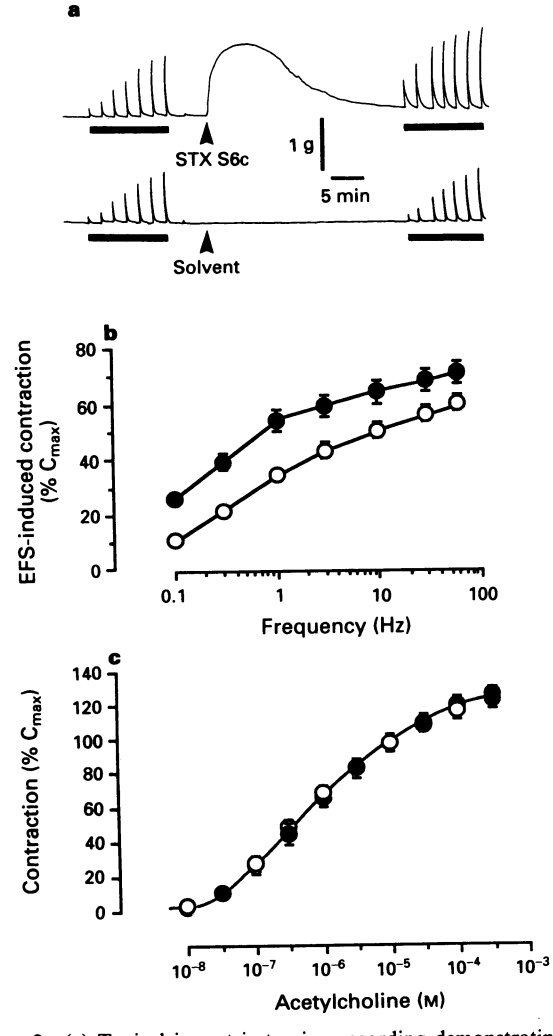

Figure 2 (a) Typical isometric tension recording demonstrating the enhanced EFS-induced contractions of mouse isolated tracheal segments produced in the presence of sarafotoxin S6c (STX S6c). The solid bars represent non-cumulative EFS frequency-response curves (0.1, 0.3, 1, 3, 10, 30 and 60 Hz for 10 s at 2 min intervals) determined in the presence (upper trace) and absence (lower trace, time-control) of 10 nM sarafotoxin S6c. (b) Mean EFS frequency-response curves obtained in the absence (○) and presence (●) of 10 nM sarafotoxin S6c, using the protocol depicted in (a). Shown are the mean ± s.e.mean responses from 6 experiments. (c) Mean cumulative concentration-response curves to acetylcholine obtained in the absence (○) and presence (●) of 10 nM sarafotoxin S6c. Shown are the mean ± s.e.mean responses from 6 experiments.

$23 \pm 2\%C_{max}$ and $30 \pm 4\%C_{max}$ respectively ($n = 5$; $P < 0.01$) i.e. equivalent to a 2.15 and 2.5 fold increase in the standard EFS-induced contraction, respectively.

All contractile responses obtained in the current study have been standardized by expressing them as a percentage of the response obtained to 10 μM carbachol at the beginning of the experiment ($100\%C_{max}$). In additional experiments, we demonstrated that it was unlikely this initial exposure to carbachol (an exogenous cholinoceptor agonist) had any significant effect on subsequent contractile responses to EFS (mediated by the endogenous cholinoceptor agonist acetylcholine). For example, both the EFS frequency-response relationship and the magnitude of the sarafotoxin S6c-induced potentiation of EFS-mediated contractions were found to be independent of whether preparations had been initially exposed to 40 mM KCl (a depolarizing spasmogen) or to 10 μM carbachol ($n = 4$, data not shown).

Modulation of EFS-induced contractions by endothelin-1

In mouse isolated tracheal segments, 10 nM endothelin-1 induced large contractions that peaked at about 10 min ($97 \pm 6\%C_{max}$, $n = 6$) and were sustained for at least 45 min ($98 \pm 8\%C_{max}$, $n = 6$) (Figure 4a, middle trace). In the presence of 10 nM endothelin-1, the upper limit of smooth muscle contraction in these preparations was approached and subsequent EFS-induced contractions were suppressed (Figure 4a,b). However, in the presence of the ET_A receptor-selective antagonist BQ-123 (3 μM), the contractions induced by 10 nM endothelin-1 (Figure 4a, upper trace) closely resembled the transient contractions induced by sarafotoxin S6c (Figure 4a, lower trace). These data are consistent with previous observations that endothelin-1-induced contractions in mouse isolated tracheal preparations were mediated via both ET_A and ET_B receptors (Henry & Goldie, 1994). Under these conditions, endothelin-1 enhanced EFS-induced contractions by $26 \pm 1\%C_{max}$ (i.e. 2.3 fold, $n = 6$) towards the levels of potentiation produced by 10 nM sarafotoxin S6c ($30 \pm 4\%C_{max}$, $n = 5$) (compare Figures 3 and 4). In the presence of lower concentrations of endothelin-1, which induced little (1 nM endothelin-1; $16 \pm 3\%C_{max}$ at 45 min, $n = 5$) or no (0.1 nM endothelin-1, $n = 6$) direct smooth muscle contractile response, EFS-induced contractions were again markedly enhanced (Figure 4b).

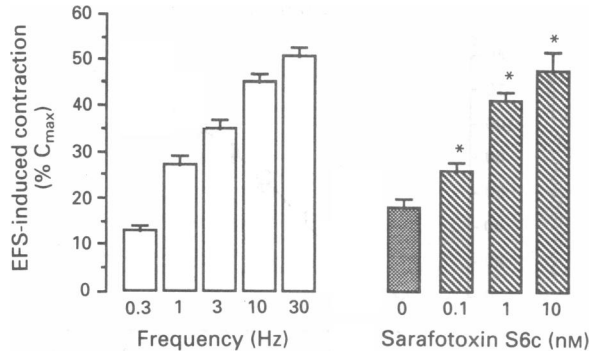

Figure 3 Effect of the ET_B receptor-selective agonist, sarafotoxin S6c on EFS-induced contractions in mouse isolated tracheal segments. From the EFS frequency-response relationship determined in each preparation (open columns), a stimulus frequency was selected that induced a $20\%C_{max}$ contraction (0.5–0.7 Hz, stippled column). The potentiating effect of sarafotoxin S6c on EFS-induced contractions at this stimulus frequency were concentration-dependent (hatched columns). The EFS-induced contractions presented were determined 45 min after the addition of 0.1, 1 or 10 nM sarafotoxin S6c when the residual levels of sarafotoxin S6c-induced contraction were respectively, $0 \pm 0\%C_{max}$ (from a peak of $0 \pm 0\%C_{max}$), $14 \pm 4\%C_{max}$ (peak, 21 ± 5) and $3 \pm 2\%C_{max}$ (peak, 74 ± 2). At each concentration of sarafotoxin S6c, the mean ± s.e.mean responses from 5 animals are presented. $*P < 0.05$, compared to control (stippled column).

Relative contributions of ET_A and ET_B receptor-effector systems in augmenting EFS-induced contractions

Data presented in Figures 3 and 4 showing marked potentiation of EFS-induced contractions by sarafotoxin S6c and by endothelin-1 in the presence of BQ-123, indicate an important role for ET_B receptors in mediating this effect. Additional experiments were performed to establish the extent to which the ET_A receptor-effector system contributed to endothelin-1-induced potentiation of EFS-induced contractions. Firstly, we investigated the influence of 3 μM BQ-123 on the magnitude of the endothelin-1-induced potentiation of

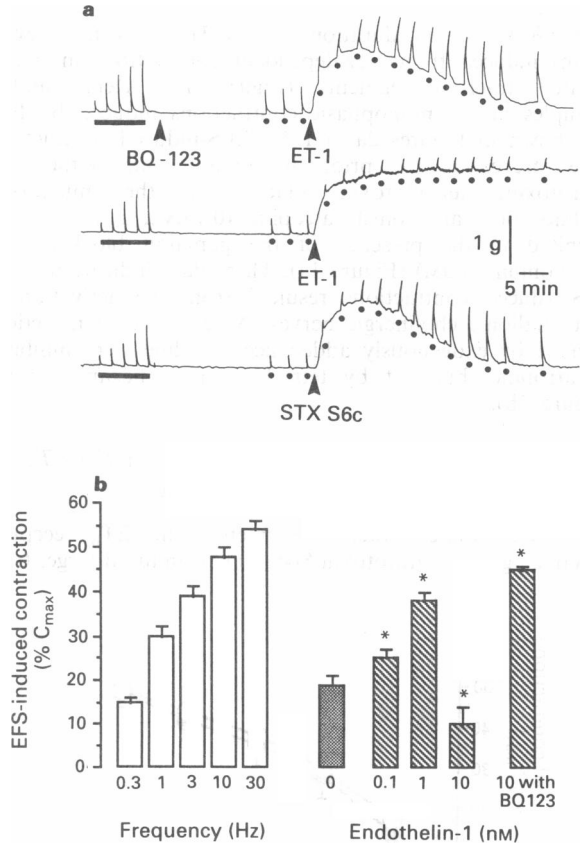

Figure 4 (a) Typical isometric tension recordings demonstrating the effects of 10 nM endothelin-1 (ET-1) on EFS-induced contractions in the presence (upper trace) and absence (middle trace) of 3 μM BQ-123. The solid bars represent non-cumulative EFS frequency-response curves (0.3, 1, 3, 10 and 30 Hz for 10 s at 2 min intervals) and the dots (•) represent the application of a 0.7 Hz stimulus frequency (3 min intervals). In the presence of 10 nM endothelin-1 alone, a large, sustained contraction was induced and EFS-induced contractions were attenuated. However, in the presence of BQ-123, endothelin-1-induced contractions resembled the transient contractions induced by 10 nM sarafotoxin S6c (STX S6c, lower trace) and EFS-induced contractions were augmented. The mean results are shown in (b). (b) Effect of endothelin-1 on EFS-induced contractions in mouse isolated tracheal segments. From the EFS frequency-response relationship determined in each preparation (open columns), a stimulus frequency was selected that induced a $20\%C_{max}$ contraction (0.5–0.7 Hz stippled column). At low concentrations of endothelin-1 (0.1 or 1 nM), EFS-induced concentrations at this stimulus frequency were potentiated (hatched columns). However, unless 3 μM BQ-123 was also present, EFS-induced contractions were suppressed in the presence of 10 nM endothelin-1. The EFS-induced contractions presented were determined 45 min after the addition of 0.1, 1 or 10 nM endothelin-1 when the residual levels of endothelin-1-induced contraction were respectively, $0 \pm 0\%C_{max}$ (from a peak of $0 \pm 0\%C_{max}$), $16 \pm 3\%C_{max}$ (peak, 19 ± 2) and $98 \pm 8\%C_{max}$ (peak, 97 ± 6). In the presence of BQ-123, the residual level of endothelin-1-induced contraction was $8 \pm 2\%C_{max}$, from a peak response of $59 \pm 10\%C_{max}$. At each concentration of endothelin-1, the mean ± s.e.mean responses from 6 animals are presented. $*P < 0.05$, compared to control (stippled column).

EFS-induced contractions. As shown in Figure 5a, BQ-123 produced no significant inhibition of the effects induced by 1 nM endothelin-1. Secondly, studies were performed to determine whether an ET_A receptor-mediated effect could be unmasked following attenuation of the ET_B receptor-effector system by desensitization. Exposure of mouse isolated tracheal segments to a high concentration of sarafotoxin S6c (100 nM) for 40 min prevented the subsequent augmentation of EFS-induced contractions usually produced by 1 nM sarafotoxin S6c (Figure 5b). Under conditions of ET_B receptor desensitization, 1 nM endothelin-1 was also without any significant enhancing effect on EFS-induced contractions (Figure 5b). Together, these studies indicate that ET_A receptor stimulation played no significant role in the potentiation of EFS-induced contractions produced by endothelin-1.

Discussion

In the current study, evidence is provided that endothelin-1 enhances the contractions induced by parasympathetic nerve stimulation via an action on prejunctional ET_B receptors. These studies are in accord with recent reports that endothelin-1 and related peptides modulate cholinergic neurotransmission within the airways (McKay *et al.*, 1993; Takimoto *et al.*, 1993) and are suggestive that neurotransmission may be a relevant mechanism through which endothelin-1 produces bronchoconstriction in diseases of the airways such as asthma.

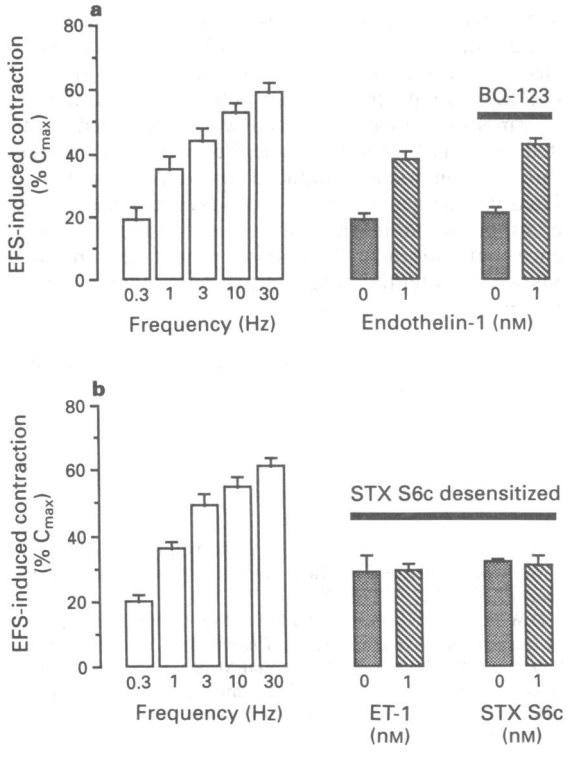

Figure 5 (a) Influence of 1 nM endothelin-1 on EFS-induced contractions in the presence and absence of the ET_A receptor-selective antagonist BQ-123 in mouse isolated tracheal segments. The EFS-induced contractions presented (0.5 Hz; hatched columns) were determined 21 min after the addition of 1 nM endothelin-1 when the residual levels of endothelin-1-induced contraction were $16 \pm 4\%C_{max}$ in the presence of BQ-123, and $16 \pm 3\%C_{max}$ in its absence. (b) Influence of ET_B receptor-desensitization on EFS-induced contractions in the presence and absence of 1 nM endothelin-1 (ET-1) or sarafotoxin S6c (STX S6c). The EFS-induced contractions presented (0.7 Hz, hatched columns) were determined 21 min after the addition of either 1 nM endothelin-1 or 1 nM sarafotoxin S6c. At this time the levels of contraction induced by endothelin-1 and sarafotoxin S6c were $22 \pm 5\%C_{max}$ and $0 \pm 0\%C_{max}$, respectively. In both (a) and (b), the mean ± s.e.mean responses from 6 experiments is presented.

In mouse isolated tracheal preparations, EFS caused monophasic contractions that were abolished by either tetrodotoxin or atropine, but were not inhibited by hexamethonium. Thus, EFS-induced contractions in mouse trachea occurred in response to the release of acetylcholine from postganglionic parasympathetic nerves. These observations are in line with those of others who have recently investigated EFS-induced contractions in mouse trachea (van Oosterhout *et al.*, 1991; Larsen *et al.*, 1992).

A major finding of this study was the concentration-dependent potentiation of contractile responses to EFS produced by the ET_B receptor-selective agonist, sarafotoxin S6c. This effect was seen even at low concentrations of sarafotoxin S6c which exerted little or no direct contractile effect. Potentiation of contractile responses to EFS was observed at all frequencies of stimulation tested, although relatively greater enhancement was observed at the lower stimulus frequencies. This pattern is consistent with that previously seen with tachykinins, thromboxane A_2-mimetics and 5-hydroxytryptamine in several airway preparations including mouse trachea (Tanaka & Grunstein, 1986; Hall *et al.*, 1989; van Oosterhout *et al.*, 1991; Yanawaki *et al.*, 1992) and may represent an important mechanism of bronchoconstriction, since autonomic nerves generally discharge at relatively low frequencies (Widdicombe, 1966; Yanawaki *et al.*, 1992).

Although sarafotoxin S6c markedly potentiated contractions induced by EFS, contractions induced by exogenously added acetylcholine were unaltered. This suggests that sarafotoxin S6c-induced augmentation was not due to postjunctional events such as increased muscarinic receptor binding or attenuated degradation of endogenous acetylcholine. Rather, sarafotoxin S6c probably stimulated prejunctional ET_B receptors on cholinergic postganglionic nerves to facilitate EFS-induced acetylcholine release. These findings are entirely consistent with the recent report by McKay and coworkers (1993) that the ET_B receptor-preferring peptide, endothelin-3, has a prejunctional, neuromodulatory effect on cholinergic parasympathetic nerves in rabbit airways. Confirmation of this postulated mechanism awaits the identification of prejunctional ET_B receptors on cholinergic nerves and the development of more sensitive techniques to assess acetylcholine release from murine airways.

Sarafotoxin S6c and other activators of ET_B receptors, including endothelin-1 are potent spasmogens of airway smooth muscle in many animal species including man (Advenier *et al.*, 1990; Hay *et al.*, 1993c). Thus, these agents potentially have a dual bronchoconstrictor action such that they directly contract airway smooth muscle and can augment neurally-mediated contraction of airway smooth muscle. In this respect, of particular interest was the finding that while the direct contractile effect mediated by ET_B receptor stimulation was transient in nature, its augmentary effect on EFS-induced contractions was relatively resistant to tachyphylaxis. The underlying reasons for these differences are currently unknown. However, the phenomenon of sustained neurally-mediated effects in the face of diminished direct smooth muscle effects has also been observed with tachykinin receptors activated by substance P in canine airways (Tanaka & Grunstein, 1986).

Contractions induced by EFS were also modulated by the nonselective ET_A/ET_B receptor agonist, endothelin-1. At low concentrations of endothelin-1, which induced little or no direct spasmogenic action, EFS-induced contractions were enhanced. On the other hand, at higher concentrations of endothelin-1 which induced large sustained contractions in mouse tracheal smooth muscle preparations, contractions induced by EFS were suppressed as the upper limit of the contractile response in these preparations was approached. However, in the presence of the ET_A receptor-selective antagonist, BQ-123, high concentrations of endothelin-1 induced contractile responses which were similar to the transient contractions induced by sarafotoxin S6c and also

markedly enhanced contractions induced by EFS. Thus, like sarafotoxin S6c, endothelin-1 can enhance EFS-induced contractions by stimulating ET_B receptors.

We investigated the possibility that ET_A receptor activation may also have contributed to the potentiation of EFS-induced contractions produced by endothelin-1. Two indirect approaches were used to investigate the influence of ET_A receptors on endothelin-1-induced potentiation of contractile responses to EFS. Firstly, we investigated whether the potentiation of EFS-mediated contractions produced by endothelin-1 was attenuated in the presence of BQ-123. Secondly, we investigated whether endothelin-1 was able to potentiate EFS-induced contractions, via activation of ET_A receptors, in preparations in which the ET_B receptors had been desensitized by prolonged exposure to high concentrations of sarafotoxin S6c. In neither case was any evidence obtained in support of a role for ET_A receptors in endothelin-1-induced potentiation of EFS-mediated contractions in mouse trachea. These findings are consistent with those of a preliminary report that endothelin-1-induced release of radioactivity from [^{3}H]-choline-labelled guinea-pig airways was not blocked by BQ-123 (Nomura *et al.*, 1994). Thus, although endothelin-1-induced contraction of airway smooth muscle in murine trachea is mediated via the activation of both ET_A and ET_B receptor subtypes (Henry & Goldie, 1994), it appears that the neuromodulatory effects of endothelin-1 were mediated predominantly via the activation of ET_B receptors. Although not available for use in the current study, the recent development of ET_B receptor-selective antagonists such as BQ-788 (Ishikawa *et al.*, 1994) and RES-701-1 (Tanaka *et al.*, 1994) promise to be powerful tools in the further characterization of these neuromodulatory ET_B receptors.

A significant component of endothelin-1-induced bronchoconstriction is attenuated by inhibitors of cyclo-oxygenase and thromboxane A_2 synthase (Payne & Whittle, 1988; Macquin-Mavier *et al.*, 1989; Nambu *et al.*, 1990), indicating that the generation of secondary mediators, such as thromboxane A_2, play an important role in mediating this *in vivo* bronchoconstrictor response. Furthermore, endothelin-1 elevates the levels of numerous prostanoids including thromboxane B_2 (an inactive metabolite of thromboxane A_2), although there are conflicting views as to whether these released prostanoids play a major role in endothelin-1-induced contraction of human or guinea-pig isolated airways preparations (Filep *et al.*, 1990; Hay, 1990; Hay *et al.*, 1993a,b). Nevertheless, the endothelin-1-evoked release of prostanoids might contribute to the overall pulmonary response to endothelin-1, since thromboxane A_2 and stable thromboxane analogues such as U-46619 have been shown to facilitate cholinergic neurotransmission in airways (Chung *et al.*, 1985; Serio & Daniel, 1988). It is unlikely that prostanoids contributed to the endothelin-1-induced potentiation of EFS-mediated contractions observed in the current study because all experiments were performed in the presence of the cyclo-oxygenase inhibitor indomethacin. On the other hand, we cannot unequivocally rule out the possibility that endothelin-1 generated non-prostanoid secondary mediators (e.g. histamine, leukotrienes) or that these mediators may have contributed to the neuromodulatory effects of endothelin-1. However, it is unlikely that this latter mechanism was of major significance in the current study. Firstly, endothelin-1 appears to be a poor generator of histamine and leukotrienes in airways (Hay *et al.*, 1993b). Secondly, the leukotrienes exert little or no direct facilitory effects on cholinergic neurotransmission in airways (Inoue & Ito, 1985; Serio & Daniel, 1988; Jacques *et al.*, 1991). Finally, although the release of secondary mediators within the airways appears predominantly to be an ET_A receptor-mediated process (Hay *et al.*, 1993b,c), the ET_A receptor antagonist, BQ-123 had no significant inhibitory effect on endothelin-1-mediated potentiation of EFS-induced contractions in the current study.

In summary, evidence is provided that endothelin-1 stimulates prejunctional ET_B receptors and thereby potentiates parasympathetic nerve-mediated contractions. This raises the possibility that the elevated levels of endothelin-1, which reportedly exist in the airway wall during disease states including asthma (Springall *et al.*, 1991), may contribute to elevated bronchomotor tone through several mechanisms. Firstly, the potent spasmogenic actions of endothelin-1 on airway smooth muscle have been well established in human isolated bronchial smooth muscle. Secondly, a component of the bronchoconstriction induced by endothelin-1 may be mediated via the generation of secondary mediators. Furthermore, as proposed in the current study, there is emerging evidence that endothelin-1 possesses potent neuromodulatory actions which potentiate the contractile responses induced by cholinergic nerve stimulation.

This work is supported by grants from the National Health and Medical Research Council of Australia.

References

ADVENIER, C., SARRIA, B., NALINE, E., PUYBASSET, L. & LAGENTE, V. (1990). Contractile activity of the three endothelins (ET-1, ET-2 and ET-3) on the human isolated bronchus. *Br. J. Pharmacol.*, **100**, 168–172.

CHUNG, K.F., EVANS, T.W., GRAF, P.D. & NADEL, J.A. (1985). Modulation of cholinergic neurotransmission in canine airways by thromboxane mimetic U46619. *Eur. J. Pharmacol.*, **117**, 373–375.

ERCAN, Z.S., KILINC, M., YAZAR, O., KURKUSUZ, P. & TURKER, A.K. (1993). Endothelin-1-induced oedema in the rat and guinea-pig isolated perfused lungs. *Arch. Int. Pharmacodyn. Ther.*, **323**, 74–84.

FILEP, J.G., BATTISTINI, B. & SIROIS, P. (1990). Endothelin induces thromboxane release and contraction of isolated guinea-pig airways. *Life Sci.*, **47**, 1845–1850.

GOLDIE, R.G., HENRY, P.J., SELF, G.J., KNOTT, P.G., LUTTMANN, M. & HAY, D.W.P. (1994). Endothelin receptor subtype distribution, density and function in human isolated asthmatic and non-diseased bronchus. *Am. Rev. Respir. Crit. Care Med.*, **149**, A472.

HALL, A.K., BARNES, P.J., MELDRUM, L.A. & MACLAGAN, J. (1989). Facilitation by tachykinins of neurotransmission in guinea-pig pulmonary parasympathetic nerves. *Br. J. Pharmacol.*, **97**, 274–280.

HAY, D.W.P. (1990). Mechanism of endothelin-induced contraction of isolated guinea-pig trachea: comparison with rat aorta. *Br. J. Pharmacol.*, **100**, 383–392.

HAY, D.W.P., HENRY, P.J. & GOLDIE, R.G. (1993a). Endothelin and the respiratory system. *Trends Pharmacol. Sci.*, **14**, 29–32.

HAY, D.W.P., HUBBARD, W.C. & UNDEM, B.J. (1993b). Relative contributions of direct and indirect mechanisms mediating endothelin-induced contraction of guinea-pig trachea. *Br. J. Pharmacol.*, **110**, 955–962.

HAY, D.W.P., LUTTMANN, M., HUBBARD, W.C. & UNDEM, B.J. (1993c). Endothelin receptor subtypes in human and guinea-pig pulmonary tissues. *Br. J. Pharmacol.*, **110**, 1175–1183.

HENRY, P.J. & GOLDIE, R.G. (1994). ET_B but not ET_A receptor-mediated contractions to endothelin-1 attenuated by respiratory tract viral infection in mouse airways. *Br. J. Pharmacol.*, **112**, 1188–1194.

HENRY, P.J., RIGBY, P.J., MACKENZIE, J.S. & GOLDIE, R.G. (1991). Effect of respiratory tract viral infection on murine airway β-adrenoceptor function, distribution and density. *Br. J. Pharmacol.*, **104**, 914–921.

HENRY, P.J., RIGBY, P.J., SELF, G.J., PREUSS, J.M. & GOLDIE, R.G. (1990). Relationship between endothelin-1 binding site densities and constrictor activities in human and animal airway smooth muscle. *Br. J. Pharmacol.*, **100**, 786–792.

INOUE, T. & ITO, Y. (1985). Pre- and post-junctional actions of prostaglandin I_2, carbocyclin, thromboxane A_2 and leukotriene C_4 in dog tracheal tissue. *Br. J. Pharmacol.*, **84,** 289–298.

ISHIKAWA, K., IHARA, M., NOGUCHI, K., MASE, T., MINO, N., SAEKI, T., FUKURODA, T., FUKAMI, T., OZAKARI, S., NAGASE, T., NISHIKIBE, M. & YANO, M. (1994). Biochemical and pharmacological profile of a potent and selective endothelin B-receptor antagonist, BQ-788. *Proc. Natl. Acad. Sci. U.S.A.*, **91,** 4892–4896.

JACQUES, C.A.J., SPUR, B.W., JOHNSON, M. & LEE, T.H. (1991). The mechanism of LTE_4-induced hyperresponsiveness in guinea-pig tracheal and human bronchial smooth muscle, *in vitro*. *Br. J. Pharmacol.*, **104,** 859–866.

LAGENTE, V., CHABRIER, O.E., MENCIA-HEURTA, J.-M. & BRAQUET, P. (1989). Pharmacological modulation of the bronchopulmonary action of the vasoactive peptide, endothelin, administered by aerosol in the guinea-pig. *Biochem. Biophys. Res. Commun.*, **158,** 625–632.

LARSEN, G.L., RENZ, H., LOADER, J.E., BRADLEY, K.L. & GELFAND, E.W. (1992). Airway response to electrical field stimulation in sensitized inbred mice; passive transfer of increased responsiveness with peribronchial lymph nodes. *J. Clin. Invest.*, **89,** 747–752.

MACQUIN-MAVIER, I., LEVAME, M., ISTIN, M. & HARF, A. (1989). Mechanisms of endothelin-mediated bronchoconstriction in the guinea-pig. *J. Pharmacol. Exp. Ther.*, **250,** 740–745.

MCKAY, K.O., ARMOUR, C.L. & BLACK, J.L. (1993). Endothelin-3 increases transmission in the rabbit pulmonary parasymphathetic nervous system. *J. Cardiovasc. Pharmacol.*, **22** (Suppl 8), S181–S184.

MULLOL, J., CHOWDHURY, B.A., WHITE, M.V., OHKUBO, K., RIEVES, R.D., BARANIUK, J., HAUSFELD, J.N., SHELHAMER, J.H. & KALINER, M.M. (1993). Endothelin in human nasal mucosa. *Am. J. Respir. Cell Mol. Biol.*, **8,** 393–402.

NAMBU, F., YUBE, N., OMAWARI, N., SAWADA, M., OKEGAWA, T., KAWASAKI, A. & IKEDA, S. (1990). Inhibition of endothelin-induced bronchoconstriction by OKY-046, a selective thromboxane A_2 synthase inhibitor, in guinea-pigs. *Adv. Prostaglandin Thromb. Leukot. Res.*, **21,** 453–456.

NOMURA, A., UCHIDA, Y., SAKAMOTO, T., ISHII, Y., BASSETT, D.J.P., HASEGAWA, S. & HIRATA, F. (1994). Cholinergic nerves are involved in endothelin-1-induced bronchoconstriction. *Am. Rev. Respir. Crit. Care Med.*, **149,** A473.

NOVERAL, J.P., ROSENBERG, S.M., ANBAR, R.A., PAWLOWSKI, N.A. & GRUNSTEIN, M.M. (1992). Role of endothelin-1 in regulating proliferation of cultured rabbit airway smooth muscle cells. *Am. J. Physiol.*, **263,** L317–L324.

PAYNE, A.N. & WHITTLE, B.J.R. (1988). Potent cyclo-oxygenase-mediated bronchoconstrictor effects of endothelin in the guinea-pig *in vivo*. *Eur. J. Pharmacol.*, **158,** 303–304.

PONS, F., TOUVAY, C., LAGENTE, V., MENCIA-HUERTA, J.M. & BRAQUET, P. (1991). Comparison of the effects of intra-arterial and aerosol administration of endothelin-1 (ET-1) in the guinea-pig lung. *Br. J. Pharmacol.*, **102,** 791–796.

SERIO, R. & DANIEL, E.E. (1988). Thromboxane effects on canine trachealis neuromuscular function. *J. Appl. Physiol.*, **64,** 179–188.

SHIMURA, S., ISHIHARA, H., SATOH, M., MASUDA, T., SASAKI, H. & TAKISHIMA, T. (1992). Endothelin regulation of mucous glycoprotein secretion from feline tracheal submucosal glands. *Am. J. Physiol.*, **262,** L208–L213.

SPRINGALL, D.R., HOWARTH, P.H., COUNIHAN, H., DJUKANOVIC, R., HOLGATE, S.T. & POLAK, J.M. (1991). Endothelin immunoreactivity of airway epithelium in asthmatic patients. *Lancet*, **337,** 697–701.

TAKIMOTO, M., INUI, T., OKADA, T. & URADE, Y. (1993). Contraction of smooth muscle by activation of endothelin receptors on autonomic neurons. *FEBS Lett.*, **324,** 77–82.

TANAKA, D.T. & GRUNSTEIN, M.M. (1986). Effect of substance P on neurally mediated contraction of rabbit airway smooth muscle. *J. Appl. Physiol.*, **60,** 458–463.

TANAKA, T., TSUKUDA, E., NOZAWA, M., NONAKA, H., OHNO, T., KASE, H., YAMADA, K. & MATSUDA, Y. (1994). RES-701-1, a novel, potent, endothelin type B receptor-selective antagonist of microbial origin. *Mol. Pharmacol.*, **45,** 724–730.

TOMLINSON, P.R., WILSON, J.W. & STEWART, A.G. (1994). Inhibition by salbutamol of the proliferation of human airway smooth muscle cells grown in culture. *Br. J. Pharmacol.*, **111,** 641–647.

VAN OOSTERHOUT, A.J.M., HOFMAN, G., WOUTERSEN-VAN NIJNANTEN, F.M.A. & NIJKAMP, F.P. (1991). 5-HT_1-like receptors mediate potentiation of cholinergic nerve-mediated contraction of isolated mouse trachea. *Eur. J. Pharmacol.*, **209,** 237–244.

WIDDICOMBE, J.G. (1966). Action potentials in parasympathetic and sympathetic efferent fibres to the trachea and lungs of dogs and cats. *J. Physiol.*, **186,** 56–88.

YANAWAKI, I., TAMAOKI, J., YAMAUCHI, F. & KONNO, K. (1992). Angiotensin II potentiates neurally mediated contraction of rabbit airway smooth muscle. *Resp. Physiol.*, **89,** 239–247.

(Received June 23, 1994
Revised October 11, 1994
Accepted October 14, 1994)

British Journal of Pharmacology (1995) 114, 570-577

An investigation into the mechanism of capsaicin-induced oedema in rabbit skin

P. Newbold & [1]S.D. Brain

Pharmacology Group and Vascular Biology Research Centre, Biomedical Sciences Division, King's College, Manresa Rd., London SW3 6LX

1 Oedema formation induced by intradermal capsaicin has been studied in rabbit skin. The effect of the anti-inflammatory steroid dexamethasone and also of a range of known inhibitors of oedema formation have been investigated in order to elucidate mechanisms involved in capsaicin-induced oedema formation.

2 Oedema formation, in response to intradermally-injected test agents, was measured by the local extravascular accumulation of intravenously injected ^{125}I-labelled albumin. In separate experiments skin blood flow was assessed by the clearance of intradermally-injected ^{133}xenon.

3 Oedema formation induced by intradermal histamine (3 nmol) and bradykinin (1 nmol), when in the presence of vasodilator doses of calcitonin gene-related peptide (CGRP) (3 pmol) or prostaglandin E_1, (PGE_1) (10 pmol), was significantly inhibited ($P<0.01$) in rabbits pretreated with intravenous dexamethasone (3 mg kg^{-1}, -4 h). In contrast dexamethasone had no effect on capsaicin (3 μmol)-induced oedema formation or, on capsaicin (30–100 nmol)-induced blood flow.

4 Oedema formation observed in response to intradermal capsaicin (3 μmol) was significantly inhibited ($P<0.01$) when the selective capsaicin antagonist, ruthenium red (3 nmol) was co-injected. This suggests that the mechanism of capsaicin-induced oedema involves activation of sensory nerves. However, oedema was not inhibited when capsaicin was co-injected with the neurokinin NK_1 receptor antagonist, RP67580 (10 nmol), the NK_2 antagonist SR48960 (10 nmol) or the CGRP antagonist $CGRP_{8-37}$ (300 pmol).

5 Oedema formation induced by capsaicin was not inhibited when co-injected with the histamine H_1 receptor antagonist, mepyramine (3 nmol), the PAF antagonist, WEB 2086 (100 nmol), the bradykinin B_2 receptor antagonist, Hoe140 (1 nmol), or the cyclo-oxygenase inhibitor, indomethacin (10 nmol), suggesting that these mediators do not play a major role in the capsaicin-induced response.

6 Histological analysis of capsaicin-treated skin sites revealed undamaged, intact microvessels and lack of haemorrhage. Further, co-injection of capsaicin with the hydrogen peroxide remover, catalase (2,200 u), had no effect on oedema formation. This suggests that capsaicin does not induce oedema formation secondary to free radical-induced damage.

7 These results indicate that capsaicin-induced oedema in rabbit skin involves activation of sensory nerves. However, the oedema is not inhibited by pretreatment with the anti-inflammatory steroid, dexamethasone. Further the mechanisms which lead to the oedema formation observed after intradermal capsaicin remain unknown.

Keywords: Capsaicin; dexamethasone; oedema; rabbit skin; microvascular permeability; neurogenic inflammation

Introduction

Capsaicin is a well utilized pharmacological tool which is used to activate selectively sensory nerves. Work in many models has shown that capsaicin can activate sensory nerves to induce release of neuropeptides, in particular calcitonin gene-related peptide (CGRP) and substance P (SP) (Lundberg *et al.* 1985; Martling *et al.* 1988; Hua & Yaksh, 1992). It is generally accepted that, in the microcirculation, SP increases microvascular permeability leading to oedema formation whilst CGRP is an extremely potent vasodilator. There is evidence in animal skin that intradermal (i.d.) vasodilators, as a consequence of increasing local blood flow, potentiate oedema formation induced by i.d. mediators of increased microvascular permeability (see Williams & Morley, 1973). This is clearly observed in rat skin where SP and CGRP act together synergistically to potentiate inflammatory oedema formation (Brain & Williams, 1985).

It has previously been shown in rabbit skin that low doses of i.d. capsaicin can induce an increased local skin blood flow whereas high doses of i.d. capsaicin induce local oedema formation (Buckley *et al.* 1990). Similarly in man, it has been shown that topical capsaicin can induce an increase in local skin blood flow (Roberts *et al.* 1992) but higher doses of capsaicin given i.d. induce an oedema response which accompanies the erythema response (Wallengren & Hakanson, 1992). The increase in blood flow induced by low doses of i.d. capsaicin in rabbit skin has now been attributed to the release of CGRP, as the CGRP antagonist $CGRP_{8-37}$ inhibits capsaicin-induced blood flow (Hughes & Brain, 1991; Hughes *et al.*, 1992). The mechanisms responsible for the oedema response in rabbit skin, induced by higher doses of capsaicin have not been previously investigated.

Dexamethasone is an anti-inflammatory glucocorticosteroid with the ability to inhibit oedema induced by a wide range of mediators of increased microvascular permeability. These include platelet activating factor (PAF), bradykinin (BK) and histamine (Ahluwalia *et al.*, 1992; Yarwood *et al.* 1993). It has been proposed that the anti-inflammatory activity of dexamethasone is due to the induction of *de novo* synthesis of the proteins vasocortin and lipocortin-1 (Sautebin *et al.*, 1992 for review). The anti-inflammatory steroids have also been shown to inhibit cytokine production in cellular inflammatory processes and to inhibit the upregulation of adhesion molecules on endothelial cells (Barnes & Adcock,

[1] Author for correspondence.

1993). Recently, sensory nerve endings have been suggested as a possible site of action of anti-inflammatory steroids (Ahluwalia & Flower, 1993a) and Tafler and co-workers (1993) have demonstrated that topical steroid treatment inhibits the flare response to topical capsaicin in human skin.

The aim of this study was to investigate the effect of the anti-inflammatory steroid, dexamethasone on capsaicin-induced oedema and to elucidate the mechanism of action of capsaicin-induced oedema formation in rabbit skin. Some of these data has been previously reported to the British Pharmacological Society (Newbold & Brain, 1994).

Methods

Measurement of skin oedema

Oedema formation was measured by the local accumulation of ^{125}I-labelled human serum albumin ([^{125}I]-HSA) into extravascular tissue from the systemic circulation. (Brain & Williams, 1985). Male New Zealand white rabbits (2.5–3 kg) were anaesthetized with sodium pentobarbitone (Sagatal 30 mg kg^{-1} i.v.). The dorsal skin was shaved with clippers and [^{125}I]-HSA (185 kBq) together with 1 ml 2.5% Evan's blue dye, were injected i.v. via the marginal ear vein. Test agents (0.1 ml i.d.) were injected according to a randomized, balanced site pattern with six replicates for each test agent and with up to 12 different agents in each experiment. After an accumulation period of 30 min a 5 ml blood sample was collected into heparin (10 u ml^{-1}) by cardiac puncture. The blood was centrifuged at 8000 *g* for 5 min and plasma (two 1 ml plasma samples) prepared. The rabbits were killed by anaesthetic overdose and the skin was then removed. Skin sites were punched out (16 mm diameter) and counted together with the plasma samples in a γ-counter (LKB 1282 commpugamma CF). Oedema was expressed as plasma protein extravasation in μl by dividing counts in each skin site by counts in 1 μl of plasma. Results are shown as μl plasma (mean ± s.e.mean) for Figures 1, 2 and 3 whilst results are shown as % of control (mean ± s.e.mean) for Figures 4 and 5. For data expressed as % of control, the results were calculated by comparing oedema responses obtained in the presence of antagonist/inhibitor with control oedema responses induced by the inflammatory mediator(s) injected in the same rabbit. In Table 1 the response to saline (vehicle) was subtracted from all oedema responses and the results were calculated as % inhibition of control response (mean ± s.e.mean).

Measurement of skin blood flow

Blood flow changes were measured in rabbit skin by a ^{133}xenon (^{133}Xe) clearance technique (Williams, 1976; 1979; Hughes & Brain, 1994). Male rabbits (2.5–3 kg) were anaesthetized with sodium pentobarbitone (Sagatal 30 mg kg^{-1}, i.v.) and the dorsal skin shaved.

Test agents were made up in saline in 1 ml volumes containing 0.74 MBq ^{133}Xe and kept at 4°C. Agents were rapidly injected i.d. in 0.1 ml volumes according to a previously determined randomized balanced site pattern with six replicates per test agent and up to nine agents tested per rabbit. After a clearance period of 15 min the rabbits were killed by anaesthetic overdose. The skin was removed and skin sites, together with test agent samples, were counted for radioactivity. Changes in blood flow were expressed as percentage change in ^{133}Xe clearance in test sites compared to clearance in control saline-treated sites (as detailed in Hughes *et al.*, 1994).

Effect of dexamethasone on oedema and blood flow

Test rabbits were pre-injected with dexamethasone at 3 mg kg^{-1} i.v., 4 h prior to i.d. injection of test agents. Control animals were pretreated with saline vehicle by a similar route and pretreatment time. This pretreatment time and dose have previously been shown to inhibit significantly oedema induced by mediators that include PAF (0.1–1 nmol) and BK (10–100 pmol) when injected in the presence of vasodilators in rabbit skin (Yarwood *et al.*, 1993). Oedema induced by capsaicin, as well as by histamine and BK in the presence of a vasodilator, was investigated in test and control rabbits. Blood flow changes induced by capsaicin were investigated in a separate study in test and control rabbits.

In further experiments the effect of dexamethasone on the time course of capsaicin-induced oedema was investigated to establish whether the steroid could modulate the capsaicin response at specific time points over the 30 min measurement period. Capsaicin (3 μmol) or BK (1 nmol) were injected i.d., in 0.1 ml volumes, at 0, 5, 10 and 15 min prior to the i.v. injection of [^{125}I]-HSA such that oedema formation was measured at differing periods (0–30 min, 5–35 min, 10–40 min and 15–45 min) after i.d. injection of capsaicin or BK. Thirty minutes after i.v. [^{125}I]-HSA, the rabbits were killed by anaesthetic overdose and samples evaluated.

The effect of ruthenium red on capsaicin-induced oedema formation was evaluated at doses determined in a previous study (Buckley *et al.*, 1990).

Contribution of vasodilators to capsaicin-induced oedema

The effect of a vasodilator component in capsaicin-induced oedema in rabbit skin was investigated with a range of agents as follows. The CGRP antagonist, $CGRP_{8-37}$, was used at doses of 0.3 and 1 nmol/site. $CGRP_{8-37}$ at a dose of 0.3 nmol/site has been previously shown to inhibit the increase in blood flow induced by capsaicin (100 nmol/site) in rabbit skin (Hughes & Brain, 1991; Hughes *et al.*, 1992). The cyclooxygenase inhibitor, indomethacin, which inhibits the conversion of arachidonic acid (AA) to vasodilator prostaglandins was used at a dose of 10 nmol/site which has been previously shown to abolish the potentiation of oedema induced by BK (0.1 nmol) when given together with AA (3 nmol) in rabbit skin (Hellewell *et al.*, 1992). The nitric oxide synthase inhibitor N^G-nitro-L-arginine methyl ester (L-NAME, 30 nmol) was used at a dose which has been previously shown to inhibit capsaicin-induced blood flow in rabbit skin (Hughes & Brain, 1994).

Effect of inhibitors of mediators of increased microvascular permeability

The effect of a number of antagonists of mediators of increased microvascular permeability were tested against capsaicin-induced oedema in the skin of control rabbits by co-injection with capsaicin (3 μmol). Where possible, the effectiveness of the antagonist was demonstrated by inhibition of oedema induced by the agonist in the presence of a vasodilator dose of CGRP (see Brain & Williams, 1985). The dose of antagonist was chosen as follows: The histamine H_1 receptor antagonist, mepyramine (3 nmol/site), and the PAF antagonist WEB2086 (100 nmol/site) were used at doses previously shown to inhibit effectively oedema induced by histamine (10 nmol/site) or PAF (1 nmol/site) respectively, in the presence of a vasodilator in rabbit skin (Hellewell *et al.*, 1992). The bradykinin B_2 receptor antagonist, Hoe 140, was used at a dose of 1 nmol/site, after preliminary experiments had indicated this to be an appropriate dose to inhibit oedema induced by bradykinin in rabbit skin. The effect of a tachykinin NK_1 antagonist and a tachykinin NK_2 antagonist was also investigated. Neurokinins do not induce oedema formation after intradermal injection in rabbit skin (Brain & Williams, 1985), thus the effectiveness of the antagonists could not be tested in this model. However, the NK_1 antagonist, RP67850, was used at a dose of 10 nmol/site, a dose previously shown to inhibit significantly oedema induced by substance P (30 pmol/site) in the presence of a

vasodilator in guinea-pig skin (Wilsoncroft *et al.*, 1994) and rat skin (unpublished data). The NK_2 receptor antagonist, SR48968, was used at a dose of 10 nmol/site since doses of 6.5 nmol and 65 nmol injected intrathecally have been shown to inhibit neurokinin-induced nociception in the rat (Picard *et al.*, 1993).

The ability of other agents to modulate capsaicin-induced oedema formation was tested as follows. The peptidase trypsin degraded and abolished vasodilator activity of CGRP in rat skin (Brain & Williams, 1988). Trypsin (100 ng) was therefore used in this study to determine if a trypsin-sensitive (i.e. peptide) component was involved in the capsaicin-induced oedema. The involvement of free radicals was investigated by using the free radical remover catalase (2200 u/site) at a dose greater than that shown to be effective in inhibiting albumin transport across endothelial cells *in vitro* (Berman & Martin, 1993).

Histology

Skin sites (16 mm diameter) were fixed in 10% formalin saline for 48 h. They were processed in a Shandon automatic histokinette tissue processor and cast into wax blocks. Tissue sections were cut at 5 μm on a microtome and mounted on glass slides and dried. They were stained by the haematoxylin and eosin method. Sections were rinsed twice with histoclear and then with 70% alcohol in distilled water. They were stained with Ehrlich's haematoxylin for 20 min and washed briefly with water. Sections were differentiated in 1% hydrochloric acid in 70% alcohol and washed well with running tap water. Sections were then counterstained with 5% aqueous eosin and rinsed with distilled water. The slides were dehydrated with 70% alcohol rinsed with histoclear and mounted in diphenyl xylene mountant (DPX). Sections were then examined under a microscope at × 40 magnification

Materials

All drugs were made up in isotonic sterile saline except where specified. Bradykinin, catalase (bovine liver), dexamethasone diphosphate, histamine diphosphate, mepyramine (pyrilamine maleate), N^G-nitro-L-arginine methyl ester (L-NAME) and trypsin were all purchased from Sigma Chemical Co., U.K. Arachidonic acid (sodium salt), indomethacin, platelet activating factor and PGE_1 were also purchased from Sigma but were initially dissolved in ethanol and further diluted with saline prior to injection. Ruthenium red, also purchased from Sigma, was initially dissolved in distilled water and further diluted with saline. Capsaicin (pelargonic acid vanillyl amide, purchased from Fluka Chemical Ltd., U.K.) was initially dissolved in ethanol: Tween 80: saline in the ratio 3:1:6 and further diluted in saline for injection. $CGRP_{8-37}$, D-NAME and human endothelin-1 were purchased from Bachem, U.K. Human α-CGRP was a gift from Dr U. Ney, Celltech, U.K. RP67580 (7,7-diphenyl-2[1-imino-2(2-methoxyphenyl)-ethyl] per hydroisoindol-4-one(3aR,7aR)) was a gift from Dr Garret at Rhône Poulenc Rorer, France. SR48968 ((S)-N-methyl-N[4-(4-acetylamino-4-phenyl piper idino)-2-(3,4-dichlorophenyl) butyl] benzamide) was a gift from Dr X. Edmonds-Alt at Sanofi, France. WEB 2086 (3-(4-(2-chlorophenyl)-9-methyl-6H-thieno-(3,2-f) (1,2,4)-triazola-(4,3-a) (1,4)-diazepine-2-yl)-1-(4-morpholinyl)-1-propanone) was a gift from Boehringer Ingleheim, Germany. Hoe 140 D-Arg-[Hyp^3, Thi^5, D-Tic^7, Oic^8] bradykinin was purchased from Peninsula, U.K. Sagatal (sodium pentobarbitone) was purchased from Rhône Poulenc Rorer, U.K. [^{125}I]-HSA was purchased from Amersham International, U.K. ^{133}Xe was purchased from Megidex, Belgium. Histoclear was purchased from National Diagnostic, U.K. Eoson and DPX (xylene) were purchased from BDH, U.K.

Statistics

Statistical analysis was carried out by two way analysis of variance (ANOVA) and Bonferroni's modified *t*-test used for comparison of multiple site treatment. Where data are expressed as percentages, analysis for significance was carried out on the raw data.

Results

Effect of dexamethasone on rabbit skin oedema

Capsaicin acted in a dose-related manner to induce oedema when injected i.d. in rabbit skin, with results (μl plasma extravasation, mean ± s.e.mean, $n = 4$) as follows: saline i.d. 8.0 ± 1.3 μl, capsaicin 300 nmol 9.9 ± 1.8 μl, 1 μmol 21.1 ± 3.3 μl, 3 μmol 49.2 ± 8.1 μl. In further experiments the effect

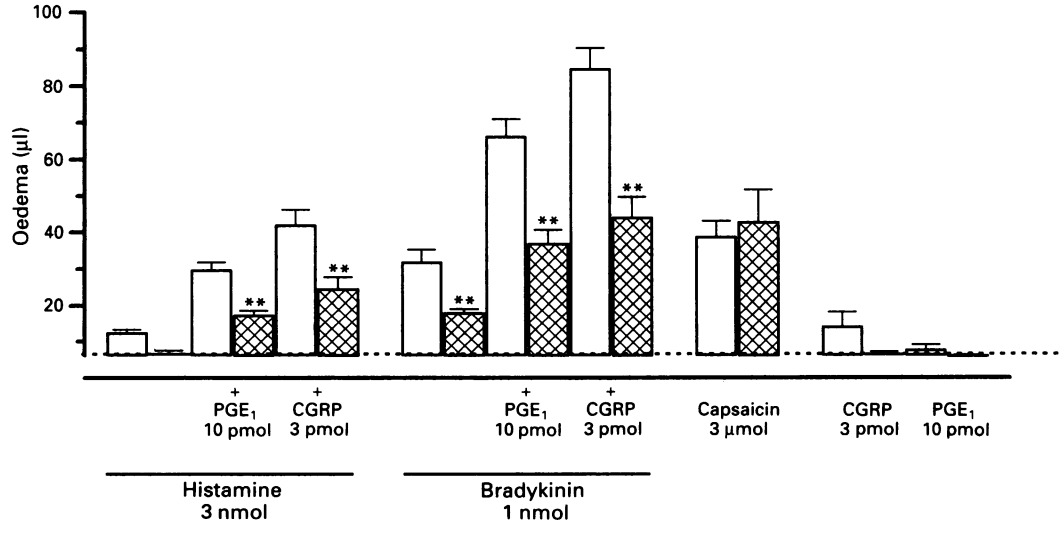

Figure 1 Effect of i.v. dexamethasone on capsaicin, histamine and bradykinin-induced oedema. Test agents were injected alone or together with vasodilator doses of prostaglandin E_1 (PGE_1) or calcitonin gene-related peptide (CGRP) in 0.1 ml volumes i.d. Open columns represent oedema responses (μl) in animals pretreated with saline and cross-hatched columns represent animals pretreated with dexamethasone 3 mg kg^{-1}, i.v. 4 h prior to injection of test agents. The dotted horizontal line represents a basal effect measured at i.d. saline treated sites. Data are means ± s.e. mean ($n = 6$). $^{**}P < 0.01$ compared to response in control saline-treated rabbits.

of dexamethasone on capsaicin 3 μmol/site was investigated. Oedema was induced in the skin of control rabbits with histamine (3 nmol), bradykinin (BK 1 nmol) and capsaicin (3 μmol) as shown in Figure 1. Oedema induced by histamine and BK was potentiated by co-injection with PGE_1 (10 pmol) or CGRP (3 pmol). Oedema induced by histamine when injected together with each vasodilator and induced by BK alone, or when given together with each vasodilator was significantly ($P<0.01$) inhibited in dexamethasone pretreated animals. Oedema induced by capsaicin was similar in dexamethasone-treated rabbits when compared with control rabbits. It can be seen in Figure 2 that in control animals, ongoing oedema formation could be measured at 5, 10 and even 15 min after the injection of capsaicin. Oedema could no longer be measured 10 min after i.d. BK (1 nmol). This suggests that oedema induced by capsaicin in rabbit skin is a long-lasting event when compared with that of BK. Dexamethasone pretreatment had no modulatory effect on the capsaicin-induced oedema time course at any of the time points where oedema was measured after capsaicin injection. However, dexamethasone significantly inhibited BK oedema ($P<0.01$).

Effect of dexamethasone on skin blood flow

Low doses of capsaicin (30–100 nmol, i.d.) dose-dependently increased local skin blood, in the absence of oedema formation, as previously shown (Hughes & Brain, 1991). Dexamethasone pretreatment had no modulatory effect on blood flow induced by capsaicin when compared to responses in control rabbits. Results expressed as % increase in ^{133}Xe clearance compared with saline-injected sites are as follows in control rabbits, capsaicin 30 nmol 33.9 ± 5.1% increase, 100 nmol 49.6 ± 10.8% increase and in dexamethasone-treated rabbits, capsaicin 30 nmol 39.7 ± 4.2% increase, 100 nmol 49.6 ± 9.4% increase (mean ± s.e.mean, $n = 6$ for all data). Further, dexamethasone was without effect on the increased blood flow induced by PGE_1 and CGRP, and clearance of ^{133}Xe was similar in both groups of rabbits indicating that dexamethasone pretreatment did not affect basal blood flow (results not shown).

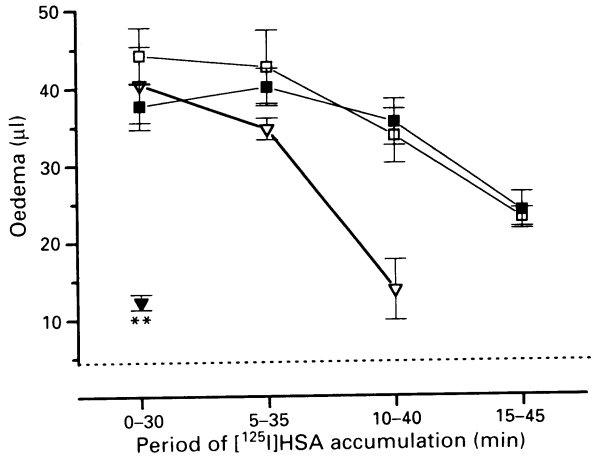

Figure 2 Effect of dexamethasone on the time course of capsaicin-induced oedema. Capsaicin was injected at 0, 5, 10 and 15 min and bradykinin (BK) at 0, 5 and 10 min prior to the systemic injection of ^{125}I-labelled human serum albumin [^{125}I]-HSA such that oedema formation was measured (μl) for 30 min from those time points after i.d. capsaicin and BK: (□) oedema induced by capsaicin (3 μmol) in saline-treated rabbits; (■) oedema induced by capsaicin in dexamethasone (3 mg kg^{-1} i.v., −4 h)-treated rabbits; (▽) oedema to BK (nmol) in saline-treated rabbits; (▼) oedema to BK in dexamethasone-treated rabbits. The dotted line represents the response at saline-injected sites. Data are means ± s.e. mean, $n = 6–7$ for each time point. $^{**}P<0.01$ compared to response in control rabbits.

Effect of ruthenium red on capsaicin-induced oedema

The selective capsaicin antagonist, ruthenium red (RR), was used to investigate whether the capsaicin-induced oedema could be selectively inhibited. RR was co-injected i.d. with the capsaicin. RR at 3 nmol and 10 nmol per site significantly ($P<0.01$) inhibited the capsaicin-induced oedema in a dose-dependent manner. These doses of RR had no effect on BK-induced oedema (Figure 3).

Contribution of vasodilators

The CGRP antagonist $CGRP_{8-37}$ at 300 pmol, significantly inhibited oedema induced by BK given together with CGRP ($P<0.01$). $CGRP_{8-37}$ at 300 pmol and 1 nmol had no inhibitory effect on capsaicin-induced oedema. The cyclo-oxygenase inhibitor, indomethacin at 10 nmol, which significantly ($P<0.01$) inhibited oedema induced by BK given together with arachidonic acid (AA), also had no effect against capsaicin-induced oedema as shown in Figure 4. Combination of $CGRP_{8-37}$ and indomethacin did not further inhibit capsaicin or BK induced oedema formation (results not shown).

Figure 5 shows that co-injection of a vasodilator dose of PGE_1 at 10 pmol significantly potentiated BK-induced oedema ($P<0.01$) but had no modulatory effect on capsaicin-induced oedema. This suggests that there is a maximal vasodilator component present in the capsaicin-injected site which cannot be potentiated further. Co-injection of the vasoconstrictor endothelin-1 (ET-1) significantly inhibited

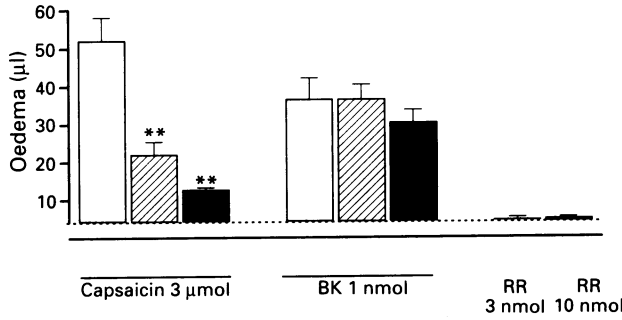

Figure 3 Effect of ruthenium red (RR) on capsaicin- and bradykinin (BK)-induced oedema. RR (3 and 10 nmol) was co-injected with either capsaicin (3 μmol) or BK (1 nmol). The open columns represent control oedema (μl) to either capsaicin or BK; hatched columns represent oedema to capsaicin or BK plus RR (3 nmol) and stippled columns represent oedema to capsaicin or BK plus RR (10 nmol). The dotted horizontal line represents a basal effect measured at i.d. saline-treated sites. Data are means ± s.e.mean ($n = 6$). $^{**}P<0.01$ compared with response in the absence of RR.

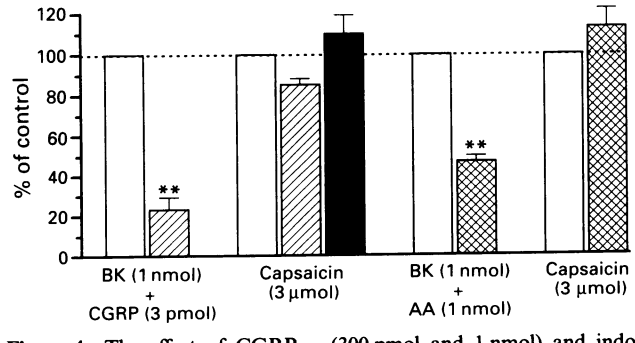

Figure 4 The effect of $CGRP_{8-37}$ (300 pmol and 1 nmol) and indomethacin (10 nmol) on capsaicin-induced oedema. Responses are expressed as a percentage of the control response. Open columns represent responses to control treatment, hatched columns represent co-treatment with $CGRP_{8-37}$ 300 pmol, and solid columns represent co-treatment with $CGRP_{8-37}$ 1 nmol and cross hatched columns represent co-treatment with indomethacin (10 nmol). Responses are means ± s.e.mean, $n = 4–8$. $^{**}P<0.01$ compared to control response.

both BK- and capsaicin-induced oedema which supports the hypothesis that a vasodilator component is present in capsaicin-induced oedema formation. Neither the nitric oxide synthase inhibitor, L-NAME nor its inactive enantiomer D-NAME had any inhibitory effect on capsaicin-induced oedema as shown in Figure 5, suggesting that nitric oxide does not play a major modulatory role.

Effect of inhibitors of increased microvascular permeability

Table 1 shows results of experiments where a number of different inhibitors of increased microvascular permeability were given as co-injections with capsaicin. In other models of inflammation, capsaicin has been shown to release tachykinins such as SP and neurokinin A (NKA) to induce oedema. Hence both the NK_1 receptor antagonist, RP67580 and the NK_2 receptor antagonist, SR48968 were given together with capsaicin. Neither antagonist showed any ability to inhibit the capsaicin response; however, no positive control could be determined since SP itself, even when given together with CGRP, had little oedema inducing capacity in rabbit skin (Brain & Williams, 1985).

Other inhibitors of increased microvascular permeability also had no effect on capsaicin-induced oedema. The histamine H_1 receptor antagonist, mepyramine, (3 nmol) which significantly inhibited histamine (3 nmol) + CGRP (3 pmol)-induced oedema ($P<0.01$); the PAF antagonist WEB 2086, (100 nmol) which significantly inhibited PAF (1 nmol) + CGRP (3 pmol)-induced oedema ($P<0.01$) and the BK B_2 receptor antagonist, Hoe 140, (1 nmol), which significantly inhibited BK (0.1 nmol) + CGRP (3 pmol)-induced oedema ($P<0.01$), all failed to inhibit capsaicin oedema. Further the peptidase, trypsin (100 ng) was co-injected with capsaicin at a dose which significantly inhibited BK (1 nmol) + CGRP (3 pmol)-induced oedema ($P<0.01$); again no inhibitory effect on capsaicin-induced oedema formation was observed. This is evidence that the mediator of increased microvascular permeability may not be peptide in nature.

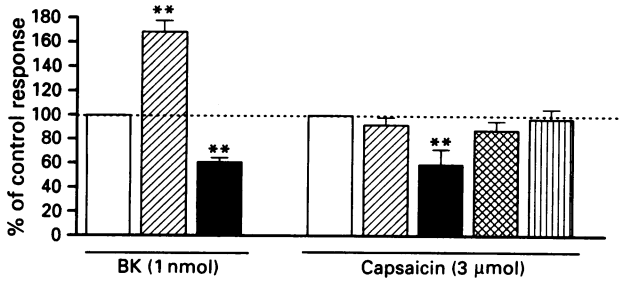

Figure 5 Effect of prostaglandin E_1 (PGE_1, 10 pmol), endothelin-1 (ET-1, 1 pmol), N^G-nitro-L arginine methyl ester (L-NAME, 30 nmol) and D-NAME (30 nmol) on bradykinin (BK)- and capsaicin-induced oedema in rabbit skin. Responses are expressed as a percentage of the control response. Open columns represent responses to control treatment; hatched columns represent co-treatment with vasodilator PGE_1, and stippled columns represent co-treatment with vasoconstrictor ET-1. Cross hatched columns represent co-treatment with L-NAME and vertical bars D-NAME. Responses are means ± s.e. mean, $n = 4-8$. $^{**}P<0.01$ compared to control response.

Effects of catalase and histology

Capsaicin, at the doses injected i.d. may have a neurotoxic effect, possibly leading to the release of free radicals from damaged nerves. The free radical remover catalase (2200 u) was co-injected with capsaicin (3 μmol). Capsaicin induced mean oedema formation of 35.2 ± 8.2 μl ($n = 3$) and capsaicin co-injected with catalase resulted in mean oedema formation of 35.1 ± 5.5 μl ($n = 3$). Thus catalase had no inhibitory effect on capsaicin-induced oedema at the dose given. Histology carried out (Figure 6) indicated that there was no breakdown of microvessel walls induced by the capsaicin as haemorrhage was not observed and the oedema induced was quite distinct since there was no evidence of damage to the aterioles and venules and no evidence of red blood cell leakage into the surrounding tissue. There is evidence of oedema formation in response to capsaicin (Figure 6b) and to BK (Figure 6c) when compared to saline-treated sites (Figure 6a) as indicated by gaps in the extravascular tissue.

Discussion

These results suggest that capsaicin induces oedema in rabbit skin by uncharacterized mechanisms and show that the oedema is insensitive to pretreatment with the anti-inflammatory steroid, dexamethasone given i.v. The lack of inhibition by antagonists of a range of mediators of increased microvascular permeability is indicative that these mediators do not play a major role in mediating capsaicin-induced

Table 1 Effect of co-injected inhibitors of increased microvascular permeability on capsaicin-induced oedema in rabbit skin

		% inhibition of control	
(a) Neuropeptide antagonists	*Capsaicin* (3 μmol)	*Positive control*	n
NK_1			
RP67850 (10 nmol)	−0.5 ± 7.0	ND	5
NK_2			
SR48968 (10 nmol)	−13.0 ± 5.9	ND	4
(b) Other antagonists			
Histamine H_1	Capsaicin (3 μmol)	Histamine (3 nmol) + CGRP (3 pmol)	
Mepyramine (3 nmol)	4.2 ± 8.8	92.1 ± 2.7**	3
PAF		PAF (1 nmol) + CGRP (3 pmol)	
WEB 2086 (100 nmol)	−13.1 ± 19.9	71.1 ± 5.2**	3
Bradykinin B_2		BK (0.1 nmol) + CGRP (3 pmol)	
Hoe140 (1 nmol)	−16.7 ± 11.7	68.6 ± 3.3**	4
(c) Miscellaneous			
Peptidase		BK (1 nmol) + CGRP (3 pmol)	
Trypsin (100 ng)	2.9 ± 5.2	58.0 ± 4.3**	4

Results are expressed as mean ± s.e.mean percentage inhibition of control response which was either capsaicin (3 μmol) or the respective positive control. $^{**}P<0.01$. ND = not determined. The response to saline was subtracted from all oedema responses and results then calculated as percentage inhibition of control. Antagonist were co-injected together i.d. with test agent in 0.1 ml volumes. Mean oedema responses were: capsaicin, 46.8 ± 2.8 μl ($n = 21$); histamine (3 nmol) + calcitonin gene-related peptide (CGRP, 3 pmol), 76.8 ± 28.2 μl; PAF (1 nmol) + CGRP (3 pmol) 40.4 ± 12.2 μl; bradykinin (BK, 0.1 nmol) + CGRP (3 pmol), 63.9 ± 10.4 μl; BK (1 nmol) + CGRP (3 pmol), 52.2 ± 14.7 μl.

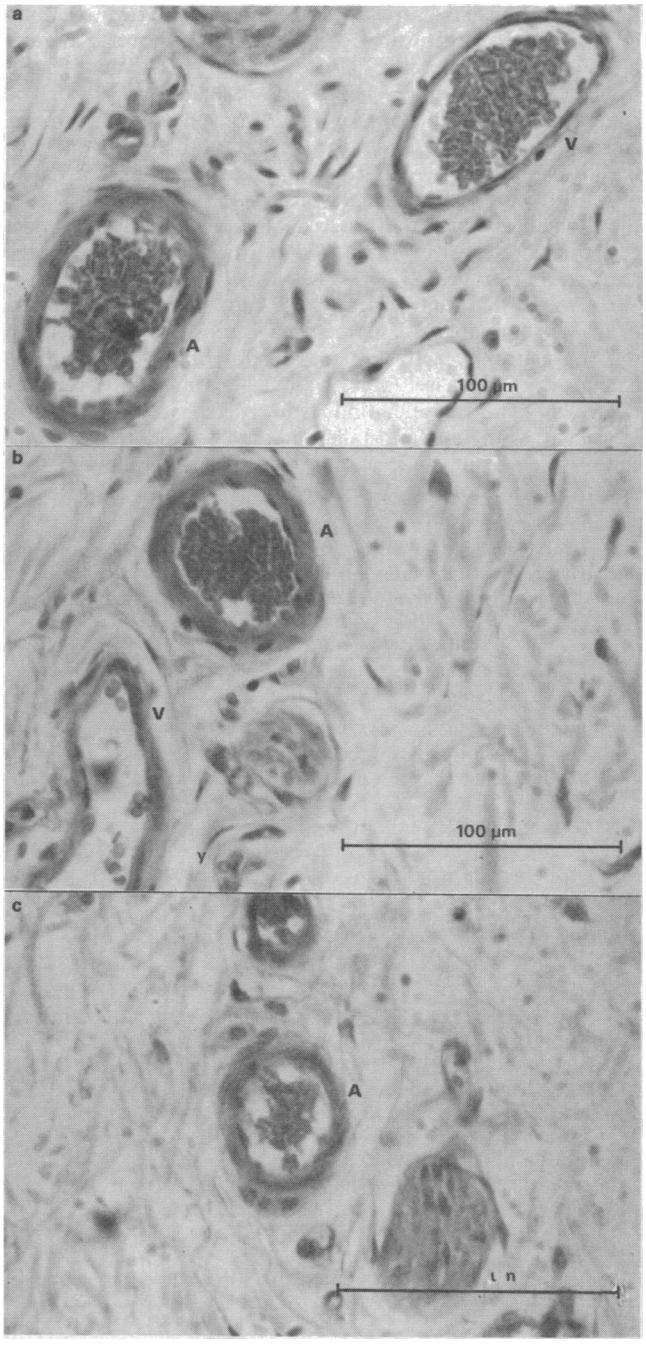

Figure 6 Histological analysis of (a) saline, (b) bradykinin, (1 nmol) and (c) capsaicin (3 µmol) induced oedema in rabbit skin sites by haematoxylin and eosin staining at × 40 magnification. Where indicated an arteriole (A) and/or a venule (V) are shown on the photomicrographs. A scale of 100 µm is shown on each photomicrograph.

oedema. The resistance of the capsaicin-induced oedema to dexamethasone is of interest as, it has been previously shown that pretreatment with anti-inflammatory steroids inhibits the actions of a wide range of mediators of increased microvascular permeability (Ahluwalia *et al.*, 1992; Yarwood *et al.*, 1993). Similarly, pretreatment with dexamethasone significantly inhibited oedema formation to the direct acting mediators of increased microvascular permeability, BK and histamine in this study. The mechanism by which dexamethasone inhibits oedema induced by these direct acting mediators of increased microvascular permeability is probably dependent on *de novo* synthesis of a protein which act directly at the endothelial cell to inhibit plasma leakage since local pretreatment with actinomycin reverses the effect of steroid pretreatment (Bjork *et al.*, 1985; Peers & Flower, 1991). This protein may not be lipocortin-1 since lipocortin-1 has been shown to be ineffective against direct acting mediators of increased microvascular permeability in the rat paw (Cirino *et al.*, 1989).

Tafler and co-workers (1993) showed that topical steroid treatment could inhibit the flare response induced by topical capsaicin in the skin of humans, although this inhibition, whilst significant, was relatively small. In the rat, Ahluwalia & Flower (1993b) demonstrated that topical steroid pretreatment of skin sites using betamethasone, did not inhibit i.d. capsaicin-induced blood flow. In agreement, we have shown that systemic dexamethasone treatment has no effect on capsaicin-induced blood flow in rabbit skin. Conversely though, Ahluwalia & Flower (1993a) showed that topical steroid treatment inhibited the putative sensory neurone component of heat-induced vasodilatation in rat skin. It may be therefore that the sensory nerve involvement in heat-induced vasodilatation is via distinct mechanisms from those involved in capsaicin-induced blood flow and oedema formation and hence one mechanism may be steroid-sensitive and the other not.

The oedema induced by capsaicin in this study was sensitive to co-injection with ruthenium red (RR). RR is a selective inhibitor of capsaicin-induced responses (Buckley *et al.*, 1990; Franco-Cereceda *et al.*, 1991) which was confirmed in our study by the lack of effect on BK-induced oedema. RR is suggested to act at the sensory nerve membrane to inhibit calcium influx induced by capsaicin upon opening of the non-selective cation channel by coupling of capsaicin with a binding site (receptor) found on sensory nerve endings (Takaki *et al.*, 1991). It is proposed that RR inhibits this calcium influx by interfering with sialic acid residues required for the transmembrane transport of calcium (Takaki *et al.*, 1992). The selective inhibitory activity of RR in this model would suggest that the oedema response involves activation of sensory nerve endings by capsaicin and certainly the finding that the increased blood flow induced by lower doses of capsaicin (30–100 nmol) is blocked by $CGRP_{8-37}$ (Hughes *et al.*, 1992) is in agreement with such a suggestion. It is possible that capsaicin can induce oedema formation in rabbit skin by a direct action on the endothelial cell lining of blood vessels, although little evidence of capsaicin binding sites in the periphery exists except for platelets (Hogaboam & Wallace, 1991).

$CGRP_{8-37}$, at doses of 300 pmol and 1 nmol did not inhibit oedema formation when co-injected with capsaicin (3 µmol). This could be because there is a large release of CGRP from capsaicin-activated sensory nerves which it is not possible to block with the doses of $CGRP_{8-37}$ that can be given i.d., or alternatively that CGRP release is not an important factor in capsaicin-induced oedema in rabbit skin. The cyclo-oxygenase inhibitor, indomethacin, also had no effect on capsaicin-induced oedema. Indeed, if prostanoid generation was involved in capsaicin-induced oedema in rabbit skin, some inhibition of capsaicin-induced oedema would be expected in dexamethasone pretreated animals since induced lipocortin-1 would inhibit phospholipase A_2 thus inhibiting eicosanoid production (Blackwell *et al.*, 1980). In addition, the nitric oxide synthase inhibitor, L-NAME, did not modify capsaicin-induced oedema. However, the oedema induced by capsaicin was not further potentiated by the vasodilator, PGE_1 and was inhibited by the vasoconstrictor, ET-1. These latter findings are suggestive that the capsaicin-induced oedema contains a vasodilator component.

In other systems, capsaicin induces microvascular leakage by release of tachykinins from sensory nerves (Murai *et al.*, 1993; Moussaoui *et al.*, 1993). Tachykinins are co-stored with CGRP in sensory nerves and thus can be co-released (Lundberg *et al.*, 1985). Oedema induced by endogenously released or exogenously injected substance P can be inhibited by NK_1 antagonists in the rat (Garret *et al.*, 1991; Murai *et al.*, 1993; Moussaoui *et al.*, 1993) and guinea-pig (Wilsoncroft *et al.*, 1994). Capsaicin-induced oedema in this study was not affect-

ed by co-treatment with either an NK_1 or NK_2 antagonist. This would suggest the mediator of increased microvascular permeability is not a tachykinin. This is further supported by the finding that SP, even when co-administered with CGRP, has little oedema inducing ability in rabbit skin (Brain & Williams, 1985). Our results also suggest that histamine, PAF and BK are probably not involved to a major extent in capsaicin-induced oedema since selective receptor antagonists to these mediators of increased microvascular permeability, when co-injected with capsaicin had no inhibitory effect on oedema formation. Interestingly, trypsin had no inhibitory effect on capsaicin-induced oedema. This would suggest that the mediator of increased microvascular permeability may not be peptide in nature as trypsin does inhibit peptide-mediated responses as shown in this and previous studies (Brain & Williams, 1988).

Capsaicin, given at high doses, is reported to have neurotoxic effects caused by calcium and sodium ion overload of the nerve ending, inducing release of neuropeptides and destruction of the sensory nerve ending (Marsh *et al.*, 1987). Free radicals generated by cell damage, may act on the endothelial cell lining of blood vessels to induce leakage. In particular, hydrogen peroxide has been implicated as important in endothelial barrier dysfunction and leakage (Berman & Martin, 1993). The hydrogen peroxide remover, catalase, had no effect on capsaicin-induced oedema at the dose tested, suggesting that either hydrogen peroxide may not be generated or it is not important in inducing plasma protein leakage induced by capsaicin. Furthermore the histological findings would suggest that oedema induced by i.d. capsaicin is not a result of damage to microvascular blood vessels in the dermal layers of the skin since blood vessels were intact and there were no evidence of erythrocyte leakage into the surrounding tissue.

In conclusion, high doses of i.d. capsaicin induce oedema in the skin of rabbits. This oedema is sensitive to ruthenium red suggesting an activation of sensory nerves although the mediator of increased microvascular permeability remains unknown. The capsaicin-induced oedema is insensitive to treatment with the anti-inflammatory steroid, dexamethasone, which is in contrast to other forms of inflammatory oedema formation.

P.N. is the recipient of a SERC studentship. We would like to thank Sue Barker, Physiology Group, King's College for the histology carried out in this study. We also thank Fisons for support.

References

AHLUWALIA, A. & FLOWER, R.J. (1993a). Investigations into the mechanism of vasoconstrictor action of the topical steroid betamethasone-17-valerate in the rat. *Br. J. Pharmacol.*, **108,** 544–548.

AHLUWALIA, A. & FLOWER, R.J. (1993b). Effect of chronic capsaicin and guanethidine treatment on skin blood flow of the rat. *Agents Actions*, **38,** C16–C18.

AHLUWALIA, A., PEERS, S.H. & FLOWER, R.J. (1992). Steroid inhibition of oedema formation in the rat skin. *Br. J. Pharmacol.*, **106,** 628–631.

BARNES, P.J. & ADCOCK, I. (1993). Anti-inflammatory actions of steroids: molecular mechanisms. *Trends Pharmacol. Sci.*, **14,** 436–441.

BERMAN, R.S. & MARTIN, W. (1993). Arterial endothelial barrier dysfunction: actions of homocysteine and the hypoxanthine-xanthine oxidase free radical generating system. *Br. J. Pharmacol.*, **108,** 920–926.

BJORK, J., GOLDSCHMIDT, T., SMEDEGARD, G. & ARFORS, K.-E. (1985). Methylprednisolone acts at the endothelial cell level reducing inflammatory responses. *Acta Physiol. Scand.*, **123,** 221–223.

BLACKWELL, G.J., CARNUCCIO, R., DI ROSA, M., FLOWER, R.J., PARENTE, L. & PERSICO, P. (1980). Macrocortin: a polypeptide causing the anti-phospholipase effect of glucocorticoids. *Nature*, **287,** 147–149.

BRAIN, S.D. & WILLIAMS, T.J. (1985). Inflammatory oedema induced by synergism between calcitonin gene-related peptide (CGRP) and mediators of increased vascular permeability. *Br. J. Pharmacol.*, **86,** 855–860.

BRAIN, S.D. & WILLIAMS, T.J. (1988). Substance P regulates the vasodilator activity of calcitonin gene-related peptide. *Nature*, **335,** 73–75.

BUCKLEY, T.L., BRAIN, S.D. & WILLIAMS, T.J. (1990). Ruthenium red selectively inhibits oedema formation and increased blood flow induced by capsaicin in rabbit skin. *Br. J. Pharmacol.*, **99,** 7–8.

CIRINO, G., PEERS, S.H., FLOWER, R.J., BROWNING, J.L. & PEPINSKY, R.B. (1989). Human recombinant lipocortin 1 has acute local anti-inflammatory properties in the rat paw edema test. *Proc. Natl. Acad. Sci. U.S.A.*, **86,** 3428–3432.

FRANCO-CERECEDA, A., LOU, Y.-P. & LUNDBERG, J.M. (1991). Ruthenium red inhibits CGRP release by capsaicin and resiniferatoxin but not ouabain, bradykinin or nicotine in guinea-pig heart: correlation with effects on cardiac contractility. *Br. J. Pharmacol.*, **104,** 305–310.

GARRET, C., CARRUETTE, A., FARDIN, V., MOUSSAOUI, S., PEYRONEL, J.-F., BLANCHARD, J.-C. & LADURON, P.M. (1991). Pharmacological properties of a potent selective nonpeptide substance P antagonist. *Proc. Nat. Acad. Sci. U.S.A.*, **88,** 10208–10212.

HELLEWELL, P.G., JOSE, P.J. & WILLIAMS, T.J. (1992). Inflammatory mechanisms in the passive cutaneous anaphylactic reaction in the rabbit: evidence that novel mediators are involved. *Br. J. Pharmacol.*, **107,** 1163–1172.

HOGABOAM, C.M. & WALLACE, J.L. (1991). Inhibition of platelet aggregation by capsaicin. An effect unrelated to actions on sensory afferent neurons. *Eur. J. Pharmacol.*, **202,** 129–131.

HUA, X.-Y. & YAKSH, T.L. (1992). Release of calcitonin gene-related peptide and tachykinins from the rat trachea. *Peptides*, **13,** 113–120.

HUGHES, S.R. & BRAIN, S.D. (1991). A calcitonin gene-related peptide (CGRP) antagonist (CGRP8-37) inhibits microvascular responses induced by CGRP and capsaicin in skin. *Br. J. Pharmacol.*, **104,** 738–742.

HUGHES, S.R. & BRAIN, S.D. (1994). Nitric oxide dependent release of vasodilator quantities of calcitonin gene-related peptide from capsaicin-sensitive nerves in rabbit skin. *Br. J. Pharmacol.*, **111,** 425–430.

HUGHES, S., BRAIN, S., WILLIAMS, G. & WILLIAMS, T. (1994). The assessment of blood flow changes at multiple sites in rabbit skin using a ^{133}Xenon clearance technique. *J. Pharmacol. Toxicol. Methods*, (in press).

HUGHES, S.R., BUCKLEY, T.L. & BRAIN, S.D. (1992). Olvanil: more potent than capsaicin at stimulating the efferent function of sensory nerves. *Eur. J. Pharmacol.*, **219,** 481–484.

LUNDBERG, J.M., FRANCO-CERECEDA, A., HUA, X.Y., HOKFELT, T. & FISCHER, J.A. (1985). Co-existence of substance P and cacitonin gene-related peptide-like immunoreactivities in sensory nerves in relation to cardiovascular and bronchoconstrictor effects of capsaicin. *Eur. J. Pharmacol.*, **108,** 315–319.

MARSH, S.J., STANSFELD, C.E., BROWN, D.A., DAVEY, R. & MCCARTHY, D. (1987). The mechanism of action of capsaicin on sensory C-type neurons and their axons in vitro. *Neuroscience*, **23,** 275–289.

MARTLING, C.-R., SARIA, A., FISCHER, J.A., HOKFELT, T. & LUNDBERG, J.M. (1988). Calcitonin gene-related peptide and the lung: neuronal coexistence with substance P, release by capsaicin and vasodilatory effect. *Regul. Pept.*, **20,** 125–139.

MOUSSAOUI, S.M., MONTIER, F., CARRUETTE, A., BLANCHARD, J.C., LADURON, P.M. & GARRET, C. (1993). A non-peptide NK_1-receptor antagonist, RP 67580, inhibits neurogenic inflammation postsynaptically. *Br. J. Pharmacol.*, **109,** 259–264.

MURAI, M., MAEDA, Y., HAGIWARA, D., MIYAKE, H., IKARI, N., MATSUO, M. & FUJII, T. (1993). Effects of an NK_1 receptor antagonist, FK888, on constriction and receptor antagonist plasma extravasation induced in guinea pig airways by neurokinins and capsaicin. *Eur. J. Pharmacol.*, **236,** 7–13.

NEWBOLD, P. & BRAIN, S.D. (1994). The lack of inhibition of capsaicin-induced oedema by dexamethasone. *Br. J. Pharmacol.*, **112,** 127P.

PEERS, S.H. & FLOWER, R.J. (1991). Site of anti-inflammatory action of dexamethasone in rabbit skin. *Eur. J. Pharmacol.*, **196,** 37–41.

PICARD, P., BOUCHER, S., REGOLI, D., GITTER, B.D., HOWBERT, J.J. & COUTURE, R. (1993). Use of non-peptide tachykinin receptor antagonists to substantiate the involvement of NK_1 and NK_2 receptors in a spinal nociceptive reflex in the rat. *Eur. J. Pharmacol.*, **232,** 255–261.

ROBERTS, R.G.D., WESTERMAN, R.A., WIDDOP, R.E., KOTZMANN, R.R. & PAYNE, R. (1992). Effects of capsaicin on cutaneous responses in humans. *Agents Actions*, **37,** 53–59.

SAUTEBIN, L., CARNUCCIO, R., IALENTI, A. & DI ROSSA, M. (1992). Lipocortin and vasocortin: Two species of anti-inflammatory proteins mimicking the effects of glucocorticoids. *Pharmacol. Res. Commun.*, **25,** 1–12.

TAFLER, R., HERBERT, M.K., SCHMIDT, R.F. & WEIS, K.H. (1993). Small reduction of capsaicin-induced neurogenic inflammation in human forearm skin by the glucocorticoid prednicarbate. *Agents Actions*, **38,** C31–C34.

TAKAKI, M., KIKUTA, A. & NAKAYAMA, S. (1991). Ruthenium red antagonism of the effects of capsaicin mediated by extrinsic sensory nerves on the myenteric plexus neurons of the isolated guinea-pig ileum. *Brain Res.*, **551,** 87–93.

TAKAKI, M., NAKAYAMA, S. & SUGA, H. (1992). Possible mechanism of ruthenium red antagonism of capsaicin-induced action in the isolated guinea-pig ileum. *Eur. J. Pharmacol.*, **211,** 125–127.

WALLENGREN, J. & HAKANSON, R. (1992). Effects of capsaicin, bradykinin and prostaglandin E_2 in the human skin. *Br. J. Dermatol.*, **126,** 111–117.

WILLIAMS, T.J. (1976). Simultaneous measurement of local plasma exudation and plasma changes induced by intradermal injection of vasoactive substance, using ^{131}I albumin and ^{133}Xe. *J. Physiol.*, **254,** 4–5P.

WILLIAMS, T.J. (1979). Prostaglandin E_2, prostacyclin I_2 and the vascular changes of inflammation. *Br. J. Pharmacol.*, **65,** 517–524.

WILLIAMS, T.J. & MORLEY, J. (1973). Prostaglandins as potentiators of increased vascular permeability in inflammation. *Nature*, **246,** 215–217.

WILSONCROFT, P., EUZGER, H. & BRAIN, S.D. (1994). Effect of a neurokinin 1 (NK_1) receptor antagonist on oedema formation induced by tachykinins, carrageenin and an allergic response in guinea-pig skin. *Neuropeptides*, **26,** 405–411.

YARWOOD, H., NOURSHARGH, S., BRAIN, S.D. & WILLIAMS, T.J. (1993). Effect of dexamethasone on neutrophil accumulation and oedema formation in rabbit skin: an investigation of site of action. *Br. J. Pharmacol.*, **108,** 959–966.

(Received June 27, 1994
Revised August 24, 1994
Accepted September 22, 1994)

British Journal of Pharmacology (1995) 114, 578–583

Inhibition of carrageenin-induced rat paw oedema by crotapotin, a polypeptide complexed with phospholipase A_2

[1]Elen C.T. Landucci, Edson Antunes, Jose L. Donato, Renato Faro, Stephen Hyslop, *Sérgio Marangoni, *Benedito Oliveira, †Giuseppe Cirino & Gilberto de Nucci

Departments of *Biochemistry and Pharmacology, UNICAMP, PO Box 6111, 13081-970, Campinas (SP), Brazil and †Department of Experimental Pharmacology, Faculty of Pharmacy, Naples, Italy

1 The effect of purified crotapotin, a non-toxic non-enzymatic chaperon protein normally complexed to a phospholipase A_2 (PLA_2) in South America rattlesnake venom, was studied in the acute inflammatory response induced by carrageenin (1 mg/paw), compound 48/80 (3 μg/paw) and 5-hydroxytryptamine (5-HT) (3 μg/paw) in the rat hind-paw. The effects of crotapotin on platelet aggregation, mast cell degranulation and eicosanoid release from guinea-pig isolated lung were also investigated.

2 Subplantar co-injection of crotapotin (1 and 10 μg/paw) with carrageenin or injection of crotapotin (10 μg/paw) into the contralateral paw significantly inhibited the carrageenin-induced oedema. This inhibition was also observed when crotapotin (10–30 μg/paw) was administered either intraperitoneally or orally. Subplantar injection of heated crotapotin (15 min at 60°C) failed to inhibit carrageenin-induced oedema. Subplantar injection of crotapotin (10 μg/paw) also significantly inhibited the rat paw oedema induced by compound 48/80, but it did not affect 5-HT-induced oedema.

3 In adrenalectomized animals, subplantar injection of crotapotin markedly inhibited the oedema induced by carrageenin. The inhibitory effect of crotapotin was also observed in rats depleted of histamine and 5-HT stores.

4 Crotapotin (30 μg/paw) had no effect on either the histamine release induced by compound 48/80 *in vitro* or on the platelet aggregation induced by both arachidonic acid (1 mM) and platelet activating factor (1 μM) in human platelet-rich plasma. The platelet aggregation and thromboxane B_2 (TXB_2) release induced by thrombin (100 mu ml^{-1}) in washed human platelets were also not affected by crotapotin. In addition, crotapotin (10 μg/paw) did not affect the release of 6-oxo-prostaglandin $F_{1\alpha}$ and TXB_2 induced by ovalbumin in sensitized guinea-pig isolated lungs.

5 Our results indicate that the anti-inflammatory activity of crotapotin is not due to endogenous corticosteroid release or inhibition of cyclo-oxygenase activity. It is possible that crotapotin may interact with extracellular PLA_2 generated during the inflammatory process thereby reducing its hydrolytic activity.

Keywords: Crotapotin; crotoxin; phospholipase A_2; acute inflammation; carrageenin oedema; histamine release; platelet aggregation

Introduction

Crotoxin, the main neurotoxic component of the venom of the South American rattlesnake *Crotalus durissus terrificus*, is a protein complex composed of a phospholipase A_2 (PLA_2) and a polypeptide named crotapotin (Slotta & Fraenkel-Conrat, 1938). The PLA_2 blocks neuromuscular transmission (Brazil, 1966) and is responsible for the neurotoxic and myotoxic activities observed *in vivo* (Gopalakrishnakone *et al.*, 1984). Crotapotin consists of three polypeptides linked by disulphide bridges and is thought to act as a chaperon protein for PLA_2 (Bon *et al.*, 1979). Although crotapotin has been reported to be enzymatically and pharmacologically inactive (Haberman & Breithaupt, 1978; Bon *et al.*, 1979; Verheij *et al.*, 1980; Gopalakrishnakone *et al.*, 1984), it does enhance the toxicity of PLA_2 (Bon, 1982).

PLA_2 is responsible for arachidonic acid mobilization from cell membranes and is believed to play a key role in the inflammatory process (Flower & Blackwell, 1976; Vadas & Pruzanski, 1986; Pruzanski *et al.*, 1993). Extracellular group II PLA_2 levels are elevated in glycogen-induced ascitic fluid in rabbits (Franson *et al.*, 1978) and in the serum of rabbits with experimental endotoxaemia (Vadas & Hay, 1983), of patients with septic shock and rheumathoid arthritis (Pruzanski *et al.*, 1985; Green *et al.*, 1991) and of healthy human volunteers following lipopolysaccharide (LPS) administration (Pruzanski *et al.*, 1992). Since crotapotin binds to PLA_2 *in vitro* (Rubsamen *et al.*, 1971), we have investigated the influence of the former protein on acute inflammatory responses where PLA_2 activation is clearly involved such as in carrageenin-induced rat hind paw oedema (Di Rosa *et al.*, 1971). The actions of crotapotin on mast cell degranulation, platelet aggregation and eicosanoid release (thromboxane A_2 and prostacyclin) from guinea-pig isolated lungs have also been investigated.

[1] Author for correspondence.

Methods

Rat paw oedema

Male Wistar rats (150–200 g) were used. Hind paw oedema was induced by a single subplantar injection of carrageenin (1 mg/paw), 5-hydroxytryptamine (5-HT) (3 μg/paw), compound 48/80 (3 μg/paw) or crotoxin complex (1–10 μg/paw) in the left paw of rats under light ether anaesthesia in a final volume of 0.1 ml. All drugs were dissolved in sterile saline (0.9%). Paw volume was measured immediately before the injection of the irritant and at selected time intervals thereafter with a hydroplethysmometer (model 7150, Ugo Basile, Italy). Crotapotin (1–10 μg/paw) was dissolved in saline (0.9%) and injected into the paw immediately before the irritant. In another set of experiments, crotapotin (10–30 μg kg^{-1}) was given either intraperitoneally or orally 30 min before the local administration of the irritant. Results were expressed as the increase in paw volume (ml) calculated by

subtracting the basal (pre-injection) volume. In some cases, the area under the time-course curve (AUC) was calculated using a trapezoidal rule and the results expressed as ml min^{-1}.

Adrenalectomy procedure

Male Wistar rats (150–200 g) anaesthetized with ether were used. The dorsal part of the animals was shaved and a small incision of 1 cm performed. The adrenal glands were removed and the rats used one week after surgery. During the entire post-surgical period, the rats were allowed to drink only saline. The induction of the oedema induced by carrageenin injection was performed as described above. Sham-operated rats received water instead of saline after surgery.

Depletion of histamine and 5-HT stores

Rats were depleted of their stores of histamine and 5-HT by repeated injections of compound 48/80 (Spector & Willoughby, 1959; Di Rosa *et al.*, 1971). Briefly, a 0.1% (w/v) solution of compound 48/80 in saline was given i.p. morning and evening for eight doses, starting with an evening dose. The dose employed was 0.6 mg kg^{-1} for the first six injections and 1.2 mg kg^{-1} for the last two doses. Crotapotin and carrageenin were given 5–6 h after the last injection of compound 48/80. Histamine and 5-HT depletion was considered efficient since this treatment abolished the oedema induced by compound 48/80 (data not shown; $n = 10$).

Isolation and incubation of peritoneal mast cells

Male Wistar rats (200–300 g) were exsanguinated under ether anaesthesia and 10 ml of Krebs-Ringer phosphate solution (KRP, pH 7.4) were injected into the peritoneal cavity. The abdomen was carefully massaged, the fluid withdrawn and spun at 300 *g* for 5 min at 4°C. The resulting cell pellet (of which mast cells comprised 10%) was gently resuspended in a small volume of KRP. The viability of the mast cells (as assessed by 0.1% (w/v) trypan blue dye exclusion) was approximately 90%. Aliquots of the mast cell suspension (0.5 ml) were warmed to 37°C for 10 min. Compound 48/80 was added to the suspension (final volume of 1.0 ml) and the incubation carried out for a further 20 min. When required, crotapotin was incubated (10 min) with the mast cell suspension before adding compound 48/80. The reaction was stopped by placing the test tubes in ice-cold water. The cells were then centrifuged (300 *g*, 10 min) and the supernatant removed for histamine determination. Krebs-Ringer solution (1.0 ml) was added to the cell pellet which was then boiled at 100°C for 10 min to release residual histamine. Histamine concentrations were determined with a double antibody radioimmunoassay (Biomerica). Histamine release was expressed as a percentage of the total cellular content of the amine. All values (means ± s.e.mean) were corrected for the spontaneous histamine release occurring in the absence of stimulus. The composition of the KRP solution was (mM): NaCl 154, KCl 6.2, $NaHCO_3$ 11.9, NaH_2PO_4 0.3, $MgSO_4$ 1.5, glucose 5.6 and $CaCl_2$ 2.8.

Preparation of platelet-rich plasma and washed platelets: measurement of platelet aggregation and thromboxane B_2 (TXB_2) release

Blood from healthy volunteers who had not taken drugs for at least 15 days was collected by venepuncture into a plastic flask containing 3.8% sodium citrate. Platelet-rich plasma (PRP) was prepared by centrifugation at 200 *g* for 12 min at room temperature. Platelet-poor plasma (PPP) was obtained by centrifuging the remaining blood at 900 *g* for 8 min at room temperature. In some experiments, PRP was centrifuged (900 *g*, 8 min) in the presence of the prostacyclin analogue, iloprost (0.8 nM). The supernatant was removed and the platelet pellet was resuspended in 15 ml of calcium-free oxygenated (95% O_2/5% CO_2) Krebs buffer. Iloprost (0.8 nM) was added again and the platelets were centrifuged (900 *g*, 8 min) at room temperature. The supernatant was aspirated and the pellet resuspended in calcium-free Krebs solution (Radomski & Moncada, 1983). The platelet count was determined automatically (Coulter Counter model T 890, Hileah, Fla., U.S.A.) and adjusted to 1×10^8 cells ml^{-1}.

Calcium chloride (1 mM) was added to the final platelet suspension. A suspension of either PRP or washed platelets (500 μl) was incubated at 37°C for 1 min in a Payton dual-channel aggregometer (Born & Cross, 1963) with continuous stirring at 900 r.p.m. and then stimulated with arachidonic acid (1 mM), platelet-activating factor (PAF; 1 μM) and thrombin (200 mu ml^{-1}). Changes in optical density (OD) were recorded for 5 min after stimulation. For the measurement of TXB_2 release, washed platelet samples were exposed to thrombin (200 mu ml^{-1}) followed by centrifugation for 3 min at full speed in a Beckman microfuge and the supernatant removed and stored at −20°C until assayed. When required, platelets were pre-incubated with either indomethacin (10 μM) or crotapotin (100–500 μg ml^{-1}) before aggregation. The procedure for the determination of TXB_2 levels by radioimmunoassay and the specificity of the antiserum employed have been described elsewhere (Salmon, 1978). The composition of the Krebs solution was (mM): NaCl 137, KCl 2.7, $NaHCO_3$ 11.9, NaH_2PO_4 0.3, $MgSO_4$ 0.8, glucose 5.6 and $CaCl_2$ 1.0.

Guinea-pig isolated lungs

Male guinea-pigs (250–350 g) were actively sensitized by intraperitoneal injection of 50 mg of ovalbumin together with a further 50 mg given subcutaneously (each in 1 ml of 0.9% saline; Payne & De Nucci, 1987). Two weeks later, the animals were anaesthetized with pentobarbitone sodium (Sagatal, 60 mg kg^{-1}, i.p). Following mid-thoracotomy, the pulmonary artery was cannulated and perfused for 5 min with 25 ml of heparinized (10 u ml^{-1}) Krebs solution. The trachea was cannulated and the lungs were removed and suspended in a heated chamber. The lungs were perfused via the pulmonary artery with warmed (37°C) and oxygenated (95% O_2/5% CO_2) Krebs solution at 5 ml min^{-1} and left to stabilize for 20 min (Bakhle *et al.*, 1985). Crotapotin (10 μg ml^{-1}) was infused through the lungs for 30 min at 0.1 ml min^{-1}. Control lungs were infused (0.1 ml min^{-1}) with saline instead of crotapotin. Lung effluent was collected before challenge with ovalbumin and in 4 min fractions after challenge. 6-Oxo-prostaglandin $F_{1\alpha}$ and TXB_2 in the lung effluent were determined by specific radioimmunoassay (RIA) after suitable dilution in RIA buffer without prior extraction or purification.

Materials

λ Carrageenin, compound 48/80, arachidonic acid, 5-hydroxytryptamine, L-α-phosphatidylcholine β-acetyl-γ-O-alkyl (platelet-activating factor), ovalbumin and indomethacin were obtained from Sigma Chemical Co (U.S.A.). Iloprost was obtained from Schering (Germany). [^{3}H]-histamine radioimmunoassay kits was purchased from Biomerica (U.S.A.). 5,6,8,9,11,12,14,15 [^{3}H]-TXB_2 (specific activity 140 Ci $mmol^{-1}$) and 6-oxo-5,6,8,9,11,14,15(n)-[^{3}H]-$PGF_{1\alpha}$, (specific activity 150 Ci $mmol^{-1}$) were obtained from Amersham International (U.K.), respectively. The 6-oxo-$PGF_{1\alpha}$ and TXB_2 antisera were provided by Dr J. Salmon (Wellcome Research Laboratories, Beckenham, UK). All the salts were obtained from Merck (Darmstadt, Germany). *Crotalus durissus terrificus* venom was obtained from the Instituto Butantan (São Paulo, Brazil). Crotoxin and crotapotin were isolated and purified as previously described (Landucci *et al.*, 1994). Heated crotapotin was obtained by heating the protein for 15 min at 60°C.

Statistical analysis

Results are expressed as mean ± s.e.mean for n experiments. In some experiments of rat paw oedema, the area under the time course curve (AUC) was determined by using the trapezoidal rule. Statistical comparison was undertaken by means of Student's unpaired t test (two-tailed) or by analysis of variance (ANOVA) and application of the Bonferroni corrected P value for multiple comparisons. Values of $P<0.05$ were considered as significant.

Results

Effect of crotapotin and crotoxin on carrageenin-induced rat paw oedema

The subplantar injection of carrageenin (1 mg/paw) induced a paw oedema of slow onset (0.21 ± 0.03 ml by the 1st h) and prolonged duration (0.52 ± 0.05 ml by the 3rd h, $n=20$). In contrast, crotoxin (10 μg/paw) induced a paw oedema of rapid onset (0.53 ± 0.03 ml at 0.5 h) and short duration (0.11 ± 0.02 ml at 2 h, $n=15$). The co-injection of crotoxin with carrageenin in the rat paw caused a greater oedema (Figure 1). In contrast to crotoxin, crotapotin (3–100 μg/paw) did not cause oedema formation (data not shown; $n=15$). However, co-injection of crotapotin (1–10 μg/paw; $n=20$) produced a dose-dependent reduction of the carrageenin-induced oedema (Figure 2). Inhibition was also observed when crotapotin (10 μg/paw) was administered in the contralateral paw ($n=10$; Figure 2). In addition, intraperitoneal administration of crotapotin significantly inhibited carrageenin-induced oedema (2.0 ± 0.3, 0.96 ± 0.24 and 0.76 ± 0.25 ml min^{-1}, AUC for control, crotapotin 10 and 30 μg kg^{-1}, respectively, $n=10$, $P<0.05$). Oral administration of crotapotin also inhibited carrageenin-induced oedema (1.60 ± 0.26, 0.70 ± 0.06 and 0.46 ± 0.10 ml min^{-1}, AUC for control, crotapotin 10 and 30 μg kg^{-1}, respectively, $n=10$, $P<0.05$). Subplantar injection of heated crotapotin (10 μg/paw) did not affect carrageenin-induced oedema (2.80 ± 0.30 and 2.70 ± 0.20 ml min^{-1}, AUC for carrageenin-induced oedema in the absence and in the presence of heated crotapotin, respectively, $n=5$).

The carrageenin-induced oedema in adrenalectomized rats was significantly larger when compared to that observed in sham-operated animals. The subplantar injection of crotapotin (10 μg/paw) in adrenalectomized animals also caused a significant inhibition of carrageenin-induced oedema ($n=10$; Figure 3). In rats depleted of histamine and 5-HT by chronic intraperitoneal injection of compound 48/80, the oedema induced by carrageenin was significantly reduced at 1–3 h after injection. In these animals, the co-injection of crotapotin (10 μg/paw) abolished carrageenin-induced oedema ($n=15$; Figure 4).

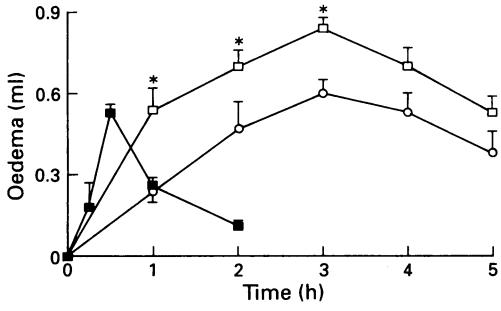

Figure 1 Effect of subplantar injection of crotoxin on carrageenin (1 mg/paw)-induced oedema. Crotoxin (10 μg/paw) was injected alone (■) or co-injected with carrageenin (□) in the rat paw. Control animals received carrageenin with saline (○) instead of crotoxin. The oedema is expressed as the increase in paw volume (ml) above its basal value. Each point represents the mean with s.e.mean from 15 rats. *$P<0.05$ compared to control animals receiving carrageenin with saline.

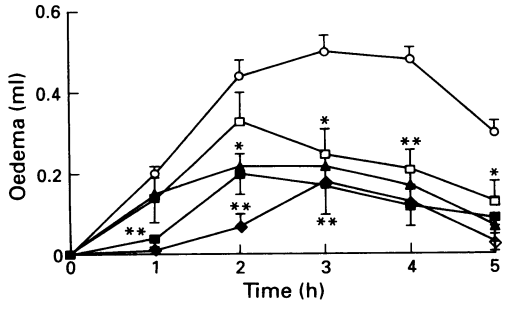

Figure 2 Subplantar injection of crotapotin either together with carrageenin or in the contralateral paw inhibits carrageenin (1 mg/paw)-induced rat paw oedema. Crotapotin was co-injected with carrageenin at doses of 1 (□), 3 (■) and 10 (◆) μg/paw. Crotapotin (10 μg/paw) was also injected in the contralateral paw (▲). Control animals (○) received carrageenin with saline instead of crotapotin. The oedema is expressed as the increase in paw volume (ml) above its basal value. Each point represents the mean with s.e.mean from 10–20 rats. *$P<0.05$, **$P<0.01$ as compared with control rats.

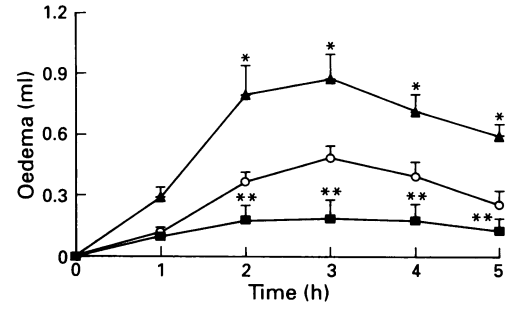

Figure 3 Crotapotin inhibits carrageenin (1 mg/paw)-induced paw oedema in adrenalectomized rats. The animals were adrenalectomized as stated in the Methods. Adrenalectomized rats (▲) showed greater oedema formation than sham-operated animals (○). Subplantar injection of crotapotin (10 μg/paw) in adrenalectomized rats (■) significantly inhibited carrageenin-induced oedema. The oedema is expressed as the increase in paw volume (ml) above its basal value. Each point represents the mean with s.e.mean from 10 rats. *$P<0.05$ compared with sham-operated rats. **$P<0.01$ compared with adrenalectomized rats.

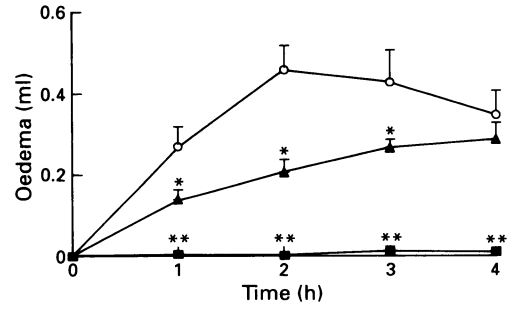

Figure 4 Crotapotin inhibits carrageenin (1 mg/paw)-induced rat paw oedema in rats chronically depleted of histamine and 5-HT. The depletion of these autacoids was performed as stated in the Methods. The oedema induced by carrageenin in the depleted animals (▲) was significantly reduced when compared to control animals (○). Subplantar injection of crotapotin (10 μg/paw) in the depleted rats (■) virtually abolished the oedema. The oedema is expressed as the increase in paw volume (ml) above its basal value. Each point represents the mean with s.e.mean from 15 rats. *$P<0.05$ compared with control rats. **$P<0.01$ compared with depleted animals.

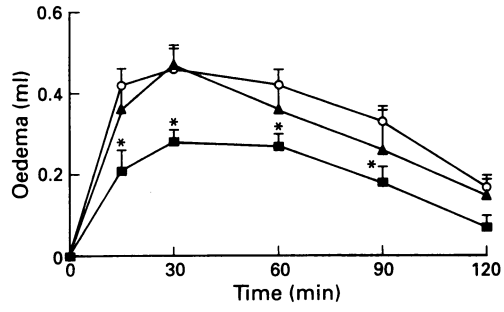

Figure 5 Crotapotin inhibits compound 48/80 (3 μg/paw)-induced paw oedema. Crotapotin was co-injected with compound 48/80 at doses of 3 (▲) and 10 (■) μg/paw. Control animals (○) were injected with compound 48/80 and saline. The oedema is expressed as the increase in paw volume (ml) above its basal value. Each point represents the mean with s.e.mean from 20 rats. $*P<0.05$ compared with control rats.

Effect of crotapotin on compound 48/80 and 5-HT-induced oedema

Subplantar injection of either compound 48/80 (3 μg/paw) or 5-HT (3 μg/paw) induced paw oedema that reached a maximum at 30 min and ended after 2 h. Subplantar injection of crotapotin (3 and 10 μg/paw) inhibited compound 48/80-induced oedema only at the higher dose ($n = 20$; Figure 5). In contrast, crotapotin (10 μg/paw) had no effect on 5-HT-induced oedema (3.90 ± 0.30 ml min $^{-1}$ and 3.20 ± 0.20 ml min^{-1}, AUC in the absence and in the presence of crotapotin, respectively, $n = 5$).

Effect of crotapotin on rat mast cell degranulation in vitro

Crotoxin (30 μg ml^{-1}) induced histamine release ($44.6 \pm 3.0\%$, $n = 5$) from rat peritoneal mast cells. In contrast, crotapotin (100 μg ml^{-1}) did not induce histamine release *per se* ($10.0 \pm 2.0\%$) nor did it affect the compound 48/80 (1.0 μg ml^{-1})-induced histamine release ($68.7 \pm 3.5\%$ and $68.1 \pm 3.0\%$, histamine release in the absence and in the presence of crotapotin, respectively, $n = 3$).

Effect of crotapotin on human platelet aggregation and on TXB_2 release

Crotapotin (50–100 μg ml^{-1}) did not affect the platelet aggregation induced by either PAF (1 μM, $n = 4$) or arachidonic acid (1 mM, $n = 4$) in PRP nor did it influence the platelet aggregation induced by thrombin (200 mu ml^{-1}) in washed platelets ($n = 4$; not shown). Crotapotin (100 and 500 μg ml^{-1}) did not induce TXB_2 release from washed platelets nor did it affect the TXB_2 release induced by thrombin (Table 1).

Effect of crotapotin on 6-oxo-$PGF_{1\alpha}$ and TXB_2 release from sensitized guinea-pig isolated lungs

Infusion of crotapotin (10 μg ml^{-1}) affected neither 6-oxo-$PGF_{1\alpha}$ (14.0 ± 2 and 14.1 ± 2 ng ml^{-1} for control and crotapotin-treated lungs, respectively, $n = 5$) nor TXB_2 (177.2 ± 37.8 and 176 ± 34.9 ng ml^{-1} for control and crotapotin-treated lungs, respectively, $n = 5$) release induced by ovalbumin (100 μg ml^{-1}) in the sensitized guinea-pig lungs.

Table 1 Lack of effect of crotapotin on the release of thromboxane B_2 induced by thrombin in human washed platelets

Treatment	*Thromboxane B_2* (ng ml^{-1})
Basal	4.5 ± 0.3 ($n = 5$)
Thrombin (100 mu ml^{-1})	158.6 ± 18.4 ($n = 5$)*
Crotapotin (500 μg ml^{-1})	3.8 ± 0.2 ($n = 3$)
Crotapotin + Thrombin	177 ± 24.2 ($n = 5$)

$*P<0.01$ when compared to basal values. n represents the number of experiments

Discussion

Our results show that crotapotin (but not the crotoxin complex) significantly inhibited carrageenin-induced rat paw oedema during the early and late phases of the response.

The most frequently encountered mechanism of action amongst anti-inflammatory drugs is the inhibition of prostaglandin synthesis (Vane, 1971; Smith & Willis, 1971). Indeed, carrageenin-induced oedema is mainly characterized by the pivotal role of prostaglandin release (Di Rosa *et al.*, 1971). However, the findings that crotapotin did not inhibit the release of either prostacyclin from guinea-pig lungs or TXB_2 from platelets as well as the aggregation induced by arachidonic acid indicate that this protein has no inhibitory activity on cyclo-oxygenase itself. Since inflamed tissues are known to express inducible cyclo-oxygenase (COX II; Lee *et al.*, 1992; Masferrer *et al.*, 1992), it is possible that crotapotin may interfere with the induction of this enzyme.

Adrenal corticosteroids are well known anti-inflammatory substances. Their anti-inflammatory effects are in part attributed to the synthesis of lipocortins, a family of glucocorticoid-induced proteins with anti-phospholipase activity (Flower, 1988). Lipocortins inhibit carrageenin-induced rat paw oedema presumably by preventing arachidonic acid mobilization from membrane phospholipids (Parente *et al.*, 1984; Flower *et al.*, 1986; Cirino *et al.*, 1989). Our results showing that crotapotin inhibited carrageenin-induced oedema in adrenalectomized rats to the same extent as in sham-operated rats, clearly indicate that the anti-oedematogenic effect of crotapotin is independent of the release of endogenous corticosteroids.

Mast cell degranulation followed by the release of both histamine and 5-HT is the first event in carrageenin-induced oedema (Di Rosa *et al.*, 1971). The finding that the oedema induced by 5-HT was not affected by crotapotin ruled out the possibility that this protein was acting as a 5-HT antagonist. The partial inhibition by crotapotin of compound 48/80-induced oedema suggests that the prevention of mast cell degranulation is a factor which may contribute to its anti-oedematogenic effect in the early stage of the inflammatory process. However, the marked inhibition caused by crotapotin on carrageenin-induced oedema cannot be explained solely by this action since other drugs which also prevent mast cell degranulation are less effective in this type of oedema (Di Rosa *et al.*, 1971). The finding that crotapotin had no effect on the *in vitro* histamine release induced by compound 48/80 may reflect the different mast cell population studied (i.e. paw vs peritoneal mast cells). In other species such as the mouse, bone marrow-derived mast cells have a different granule density, histamine content and histamine releasing capacity compared to peritoneal mast cells (Chiu & Burrall, 1990).

Crotapotin does not bind to membranes but may prevent non-specific binding of the PLA_2 component to them (Bon *et al.*, 1979). This raises the possibility that crotapotin could interact with extracellular PLA_2 generated during the inflammatory process thereby reducing the hydrolytic activity of the latter. Indeed, this type of interaction with other group II PLA_2 has already been shown by Choumet *et al.* (1993). These workers demonstrated the existence of a complex between crotapotin and the single chain PLA_2, agkistrodotoxin and that the formation of this complex enhanced the biological activity of the PLA_2. It is interesting to note that crotapotin is derived by post-translational maturation from a

precursor, proCA, homologous with secreted PLA_2 (Bouchier *et al.*, 1991). Thus, it is not unreasonable to suggest that crotapotin may in someway be able to interact with the secreted group II PLA_2 to reduce its hydrolytic activity. Alternatively, crotapotin may influence PLA_2 activity by interfering with on/off binding rates to membrane surfaces (Berg *et al.*, 1991; Jain *et al.*, 1991).

Crotapotin was effective when given orally. Since it is unlikely that a protein such as crotapotin could resist gastric proteolysis and be absorbed, it is probable that in this circumstance smaller peptide(s) is (are) responsible for the anti-oedematogenic activity observed. For instance, antiflammins are nonapeptides derived from regions of high similarity in uteroglobin and lipocortins and do retain their anti-inflammatory activity (Cirino & Flower, 1987; Cabré *et al.*, 1992). It is interesting to note that the crude venom of *Crotalus durissus terrificus* induces analgesia in mice when given orally (Giorgi *et al.*, 1993). The identification of small crotapotin-derived peptides which retain the anti-inflammatory activity of the parent protein and the delineation of their mechanism of action may widen the perspectives for the development of a new class of anti-inflammatory agents. Actually, *Crotalus durissus terrificus* venom was used clinically in the past for treatment of several diseases, including cancer, epilepsy and leprosy (Jenkins & Pendleton, 1914; Brazil, 1934).

References

BAKHLE, Y.S., MONCADA, S., DE NUCCI, G. & SALMON, J.A. (1985). Differential release of eicosanoids by bradykinin, arachidonic acid and calcium ionophore A23187 in guinea-pig isolated lungs. *Br. J. Pharmacol.*, **86**, 55–62.

BERG, O.G., YU, B.Z., ROGERS, J. & JAIN, M.K. (1991). Interfacial catalysis by phospholipase A_2: Determination of the interfacial kinetic rate constants. *Biochemistry*, **30**, 7283–7297.

BON, C. (1982). Synergism of the two subunits of crotoxin. *Toxicon*, **2**, 105–109.

BON, C., CHANGEUX, J., JENG, T. & FRAENKEL-CONRAT, H. (1979). Postsynaptic effects of crotoxin and of its isolated subunits. *Eur. J. Biochem.*, **99**, 471–481.

BORN, G.V.R. & CROSS, M.J. (1963). The aggregation of blood platelets. *J. Physiol.*, **168**, 178–195.

BOUCHIER, C., BOULAIN, J., BON, C. & MENEZ, A. (1991). Analysis of cDNAs encoding the two subunits of crotoxin, a phospholipase A_2 neurotoxin from rattlesnake venom: the acidic non enzymatic subunit derives from a phospholipase A_2-like precursor. *Biochem. Biophys. Acta*, **1088**, 401–408.

BRAZIL, O.V. (1966). Pharmacology of crystalline crotoxin. II. Neuromuscular blocking action. *Mem. Inst. Butantan*, **33**, 981–992.

BRAZIL, V. (1934). Do emprego da peçonha em terapêutica. *Biol. Med. São Paulo*, **1**, 7–21.

CABRÉ, F., MORENO, J.J., CARABAZA, A., ORTEGA, E., MAULEÓN, D. & CARGANICO, G. (1992). Antiflammins: Anti-inflammatory activity and effect on human phospholipase A_2. *Biochem. Pharmacol.*, **44**, 519–525.

CHIU, H.F. & BURRALL, B.A. (1990). Effects of interleukin 3 on the differentiation and histamine content of cultured marrow mast cells. *Agents Actions*, **31**, 197–203.

CHOUMET, V., SALIOU, B., FIDELER, L., CHEN, Y., GUBENSEK, F., BON, C. & DELOT, E. (1993). Snake venom phospholipase A_2 neurotoxins. Potentiation of a single chain neurotoxin by the chaperon subunit of a two component neurotoxin. *Eur. J. Biochem.*, **211**, 57–62.

CIRINO, G. & FLOWER, R.J. (1987). The inhibitory effect of lipocortin on eicosanoid synthesis is dependent upon Ca^{2+} ions. *Br. J. Pharmacol.*, **92**, 521P.

CIRINO, G., PEERS, S.H., FLOWER, R.J. & PEPINSKY, R.B. (1989). Human recombinant lipocortin 1 has acute local anti-inflammatory properties in the rat paw oedema test. *Proc. Natl. Acad. Sci. U.S.A.*, **86**, 3428–3432.

DI ROSA, M., GIROUD, J.P. & WILLOUGHBY, D.A. (1971). Studies of the mediators of the acute inflammatory response induced in rats in different sites by carrageenin and turpentine. *J. Pathol.*, **104**, 15–29.

FLOWER, R.J. (1988). Lipocortin and the mechanism of action of glucocorticoids. *Br. J. Pharmacol.*, **94**, 987–1015.

FLOWER, R.J. & BLACKWELL, G.J. (1976). The importance of phospholipase A_2 in prostaglandin biosynthesis. *Biochem. Pharmacol.*, **25**, 285–291.

FLOWER, R.J., PARENTE, L., PERSICO, P. & SALMON, J.A. (1986). A comparison of the acute inflammatory response in adrenalectomized and sham-operated rats. *Br. J. Pharmacol.*, **87**, 57–62.

FRANSON, R., DOBROW, R., WEISS, J., ELSBACH, P. & WEGLICKI, W. (1978). Isolation and characterization of a phospholipase A_2 from an inflammatory exudate. *J. Lipid Res.*, **19**, 18–23.

GIORGI, R., BERNARDI, M.M. & CURY, Y. (1993). Hypoalgic effect of the *Crotalus durissus terrificus* (C.d.t.) venom. *Toxicon*, **31**, 133.

GOPALAKRISHNAKONE, P., DEMPSTER, D.W., HAGWOOD, B.J. & ELDER, H.Y. (1984). Cellular and mitochondrial changes induced in the structure of murine skeletal muscle by crotoxin, a neurotoxic phospholipase A_2 complex. *Toxicon*, **22**, 85–98.

GREEN, J.A., SMITH, G.M., BUCHTA, R., LEE, R., HO, K.Y., RAJKOVIC, I.A. & SCOTT, K.F. (1991). Circulating phospholipase A_2 activity associated with sepsis and septic shock is indistinguishable from that associated with rheumatoid arthritis. *Inflammation*, **15**, 355–367.

HABERMANN, E. & BREITHAUPT, H. (1978). The crotoxin complex -an example of biochemical and pharmacological protein complementation. *Toxicon*, **16**, 19–30.

JAIN, M.K., YU, B.Z., ROGERS, J., RANADIVE, G.N. & BERG, O.G. (1991). Interfacial catalysis by phospholipase A_2 dissociation constants for calcium, substrate, products and competitive inhibitors. *Biochemistry*, **30**, 7306–7317.

JENKINS, C.L. & PENDLETON, A.S. (1914). Crotalin in epilepsy. *J. Am. Med. Ass.*, **63**, 1749–1750.

LANDUCCI, E.C.T., CONDINO-NETO, A., ANTUNES, E., PEREZ, A.C., HYSLOP, S., CORRADO, A.P., NOVELLO, J.C., MARANGONI, S., OLIVEIRA, B. & DE NUCCI, G. (1994). Crotoxin induces aggregation of human washed platelets. *Toxicon*, **32**, 217–226.

LEE, S.H., SOYOOLA, E., CHANMUGAM, P., HART, S., SUN, W., ZHONG, H., LIOU, S., SIMMONS, D. & HWANG, D. (1992). Selective expression of mitogen-inducible cyclooxygenase in macrophages stimulated with lipopolysaccharide. *J. Biol. Chem.*, **267**, 25934–25938.

MASFERRER, J.L., SEIBERT, K., ZWEIFEL, B. & NEEDLEMAN, P. (1992). Endogenous glucocorticoids regulate an inducible cyclooxygenase enzyme. *Proc. Natl. Acad. Sci. U.S.A.*, **89**, 3917–3921.

PARENTE, L., DI ROSA, M., FLOWER, R.J., GHIARA, P., MELI, R., PERSICO, P., SALMON, J.A. & WOOD, J.N. (1984). Relationship between the anti-phospholipase and anti-inflammatory effects of glucocorticoid-induced proteins. *Eur. J. Pharmacol.*, **99**, 233–239.

PAYNE, A.N. & DE NUCCI, G. (1987). Anaphylaxis in guinea pigs induced by ovalbumin aerosol in vivo and in vitro methods. *J. Pharmacol. Methods*, **17**, 83–90.

PRUZANSKI, W., VADAS, P. & BROWNING, J.L. (1993). Secretory non-pancreatic group II phospholipase A_2; role in physiologic and inflammatory processes. *J. Lipid. Med.*, **8**, 161–167.

PRUZANSKI, W., VADAS, P., STEFANSKI, E. & UROWITZ, M.B. (1985). Phospholipase A_2 activity in sera and synovial fluids in rheumatoid arthritis and osteoarthritis: its possible role as a proinflammatory enzyme. *J. Rheumatol.*, **12**, 211–220.

PRUZANSKI, W., WILMORE, D.W., SUFFREDINI, A., MARTICH, G.D., HOFFMAN, G.D., BROWNING, J.L., STEFANSKI, E., STERNBY, B. & VADAS, P. (1992). Hyperphospholipasemia A_2 in human volunteers challenged with intravenous endotoxin. *Inflammation*, **16**, 561–570.

RADOMSKI, M.W. & MONCADA, S. (1983). An improved method for washing human platelets with prostacyclin. *Thromb. Res.*, **30**, 383–389.

RUBSAMEN, K., BREITHAUPT, H. & HABERMANN, E. (1971). Biochemistry and pharmacology of the crotoxin complex. I. Subfractionation and recombination of the crotoxin complex. *Naunyn-Schmied. Arch. Pharmacol.*, **270**, 274–288.

SALMON, J.A. (1978). A radioimmunoassay for 6-keto-prostaglandin $F_{1\alpha}$. *Prostaglandins*, **15**, 383–397.

SLOTTA, K.H. & FRAENKEL-CONRAT, H.L. (1938). Schlangengifte, III: Mitteilung Reiningung und krystallization des klapperschangengiftes. *Ber. Dtch. Chem. Ges.*, **71**, 1076–1081.

SMITH, J.B. & WILLIS, A.L. (1971). Aspirin selectively inhibits prostaglandin production in human platelets. *Nature (New Biol.)*, **231**, 235–237.

SPECTOR, W.G. & WILLOUGHBY, D.A. (1959). The demonstration of the role of mediators in turpentine pleurisy in rats by experimental suppression of the inflammatory changes. *J. Pathol. Bact.*, **77**, 1–17.

VADAS, P. & HAY, J.B. (1983). Involvement of circulating phospholipase A_2 in the pathogenesis of the hemodynamic changes in endotoxin shock in rabbits. *Can. J. Physiol. Pharmacol.*, **61**, 561–566.

VADAS, P. & PRUZANSKI, W. (1986). Biology of disease: role of secretory phospholipase A_2 in the pathobiology of disease. *Lab. Investigation*, **55**, 391–404.

VANE, J.R. (1971). Inhibition of prostaglandin synthesis as a mechanism of action for aspirin-like drugs. *Nature (New Biol.)*, **231**, 232–235.

VERHEIJ, H.M., BOFFA, M.C., ROTHEN, C., BRYCKAERT, M., VERGER, R. & DE HAAS, G.H. (1980). Correlation of enzymatic activity and anticoagulant properties of phospholipase A_2. *Eur. J. Biochem.*, **112**, 25–32.

(Received June 26, 1994
Revised September 16, 1994
Accepted September 26, 1994)

British Journal of Pharmacology (1995) 114, 584-591

Regional haemodynamic effects of human and rat adrenomedullin in conscious rats

[1]S.M. Gardiner, P.A. Kemp, J.E. March & T. Bennett

Department of Physiology & Pharmacology, University of Nottingham Medical School, Queen's Medical Centre, Nottingham NG7 2UH

1 Male, Long Evans rats were chronically instrumented with pulsed Doppler flow probes and intravascular catheters to permit assessment of the regional haemodynamic responses to human and rat adrenomedullin, to compare the responses to human adrenomedullin to those of human α-CGRP in the absence and presence of the $CGRP_1$-receptor antagonist, human α-CGRP [8-37], and to determine the involvement of nitric oxide (NO)-mediated mechanisms in the responses to human adrenomedullin, relative to human α-CGRP.

2 Human and rat adrenomedullin (0.3, 1, and 3 nmol kg^{-1}, i.v.) caused dose-dependent hypotension and tachycardia, accompanied by increases in renal, mesenteric and hindquarters flows and vascular conductances. At the lowest dose only, the hypotensive and mesenteric vasodilator effects of rat adrenomedullin were significantly greater than those of human adrenomedullin.

3 Human α-CGRP at a dose of 1 nmol kg^{-1} caused hypotension, tachycardia and increases in hindquarters flow and vascular conductance, but reductions in renal and mesenteric flows, and only transient vasodilatations in these vascular beds. These effects were substantially inhibited by human α-CGRP [8-37] (100 nmol kg^{-1} min^{-1}), but those of human adrenomedullin (1 nmol kg^{-1}) were not; indeed, the mesenteric haemodynamic effects of the latter peptide were enhanced by the $CGRP_1$-receptor antagonist.

4 In the presence of the NO synthase inhibitor, N^G-nitro-L-arginine methyl ester (L-NAME, 183 nmol kg^{-1} min^{-1}), there was only a slight, but significant, inhibition of the hindquarters hyperaemic vasodilator effect of human adrenomedullin, but not that of human α-CGRP.

5 These results indicate that the marked regional vasodilator effects of human (and rat) adrenomedullin are largely independent of NO and, *in vivo*, do not involve $CGRP_1$-receptors.

Keywords: Adrenomedullin (human); rat adrenomedullin; haemodynamics; α-calcitonin gene-related peptide (α-CGRP) (human); α-CGRP [8-37] (human)

Introduction

Recently, a novel peptide, designated adrenomedullin, consisting of 52 amino acids, was isolated from human phaeochromocytoma by Kitamura *et al.* (1993). Although the levels of adrenomedullin were highest in phaeochromocytoma, the peptide was also present in normal adrenal medulla and other human tissues (Kitamura *et al.*, 1993). Subsequently, Sakata *et al.* (1993) detected adrenomedullin in various tissues from normal rats, and showed the peptide was distinct from human adrenomedullin in having 50 amino acid residues, 6 of which differed from the corresponding ones in the human peptide.

The presence of adrenomedullin in normal tissues and plasma (Ichiki *et al.*, 1994), and its synthesis and release by endothelial cells *in vitro* (Sugo *et al.*, 1994), raises the possibility that the peptide has a physiological role in cardiovascular control. This proposition is consistent with the finding that human adrenomedullin exerts a potent hypotensive effect in anaesthetized rats (Kitamura *et al.*, 1993); subsequently, this action was shown to be due to marked vasodilatation, since adrenomedullin increased cardiac index and stroke index (Ishiyama *et al.*, 1993). Interestingly, the hypotensive effect of human adrenomedullin was not accompanied by tachycardia, although Ishiyama *et al.* (1993) acknowledged this may have been due to inhibition of baroreceptor reflex function by the barbiturate anaesthetic they used. It is notable that Sakata *et al.* (1993) found rat adrenomedullin was more potent than human adrenomedullin, both in terms of eliciting hypotension in anaesthetised rats, and in stimulating cyclic AMP levels in platelets.

Recently, Kitamura *et al.* (1994) found plasma levels of adrenomedullin were elevated in patients with hypertension, and suggested the peptide might exert a beneficial arteriolar vasodilator effect in this condition. However, there are no data on the regional haemodynamic changes underlying the hypotensive effects of human or rat adrenomedullin in the absence of anaesthesia. Therefore, the first objective of this work was to determine the dose-relatedness of the regional haemodynamic actions of rat and human adrenomedullin in conscious rats.

Although human, and rat, adrenomedullin show only slight homology with human α-calcitonin gene-related peptide (α-CGRP) (Kitamura *et al.*, 1993), it has been reported that, in the isolated mesenteric vascular bed of the rat, human adrenomedullin caused vasodilatation which was blocked by the $CGRP_1$-receptor antagonist, human α-CGRP [8-37] (Nuki *et al.*, 1993). Since endogenous CGRP is localized to perivascular nerve fibres in the mesenteric vascular bed (Kawasaki *et al.*, 1988; Han *et al.*, 1990), the findings of Nuki *et al.* (1993) could be explained either by human adrenomedullin interacting with $CGRP_1$- receptors, and/or by adrenomedullin releasing endogenous CGRP. However, although exogenous CGRP is a potent vasodilator of the isolated mesenteric vascular bed of the rat (Marshall *et al.*, 1986), systemic administration of human or rat CGRP causes mesenteric vasoconstriction, probably as a reflex response to the systemic hypotension (Gardiner *et al.*, 1988; 1989a,b). Therefore, our second objective was to compare regional haemodynamic responses to human adrenomedullin and human α-CGRP in conscious rats, and to determine the influence of human α-CGRP [8-37] upon them.

There is some evidence that components of the regional

[1] Author for correspondence.

haemodynamic response to infusion of human α-CGRP involve nitric oxide (NO)-mediated mechanisms (Gardiner *et al.*, 1991), but the possible involvement of NO in the haemodynamic effects of human adrenomedullin has not been examined. Therefore, our third objective was to assess the influence of the NO synthase inhibitor, N^G-nitro-L-arginine methyl ester (L-NAME), on responses to human adrenomedullin. However, since L-NAME causes substantial cardiovascular changes (Gardiner *et al.*, 1990a) which could influence responses to human adrenomedullin, independent of an action involving inhibition of NO synthase, we also assessed the effects of human adrenomedullin in the presence of a co-infusion of angiotensin II and vasopressin that, within experimental constraints, simulated the pressor and regional haemodynamic effects of L-NAME. Some of the results have been presented to the British Pharmacological Society (Gardiner *et al.*, 1994).

Methods

Male, Long Evans rats (350–450 g), bred in the Animal Unit in Nottingham, were used for all experiments. Under sodium methohexitone anaesthesia (Brietal, Lilly; 40–60 mg kg^{-1}, i.p., supplemented as required) pulsed Doppler flow probes and intravascular catheters were implanted to monitor renal, mesenteric and hindquarters flow, to measure blood pressure, and to administer substances into the right jugular vein, as described in detail previously (Gardiner *et al.*, 1993). Doppler probes were implanted at least 7 days before intravascular catheters, and the latter were implanted no less than 24 h before experiments were begun in conscious, unrestrained animals. The following protocols were run:

Dose-responses to human or rat adrenomedullin

Separate groups ($n = 8$ in each) of rats were given 3 increasing i.v. doses (0.3, 1.0, 3.0 nmol kg^{-1}) of human or rat adrenomedullin (Groups 1 and 2, respectively), with doses separated by at least 2 h.

Effect of human α-CGRP [8-37] on responses to human α-CGRP or human adrenomedullin

Rats ($n = 8$; Group 3) were randomised to receive human adrenomedullin (1 nmol kg^{-1}) or human α-CGRP (1 nmol kg^{-1}) followed 2 h later by the other peptide. Two hours thereafter, an infusion of human α-CGRP [8-37] (100 nmol kg^{-1} min^{-1}; Gardiner *et al.*, 1990b) was begun and 15 min later, human adrenomedullin or human α-CGRP was again administered (whichever was the peptide given first earlier). After a further 2 h, the infusion of human α-CGRP [8-37] was begun again, and, 15 min later, human adrenomedullin or human α-CGRP was again administered (whichever peptide was given second earlier).

In a separate group of rats ($n = 8$; Group 4) the protocol above was followed, with the exception that an infusion of isotonic saline (154 mmol l^{-1} NaCl) was given instead of human α-CGRP [8-37]. This allowed us to assess the reproducibility of responses to human adrenomedullin and human α-CGRP in the absence of the $CGRP_1$-receptor antagonist.

Effect of L-NAME or vasopressin plus angiotensin II on responses to human α-CGRP or human adrenomedullin

Animals were randomized to receive human adrenomedullin (1 nmol kg^{-1}) or human α-CGRP (1 nmol kg^{-1}) followed 2 h later by the other peptide. A further 2 h later, in one group ($n = 8$; Group 5) of animals, an infusion of L-NAME (183 nmol kg^{-1} min^{-1}; Gardiner & Bennett, 1992) was begun, and 90 min later human adrenomedullin or human α-CGRP was administered (whichever peptide was given first earlier). The infusion of L-NAME was continued and 2 h later, human adrenomedullin or human α-CGRP was again administered (whichever peptide was given second earlier).

In a separate group of rats ($n = 9$; Group 6) the protocol above was followed with the exception that, instead of L-NAME, a co-infusion of vasopressin (3 pmol kg^{-1} min^{-1}) and angiotensin II (33 pmol kg^{-1} min^{-1}) was given, to simulate, as far as possible, the pressor and regional haemodynamic effects of L-NAME. Pilot experiments showed that the co-infusion was more effective in this respect than either peptide alone.

Data analysis

Continuous recordings were made of phasic and mean arterial blood pressure and instantaneous heart rate, together with phasic and mean renal, mesenteric and hindquarters Doppler shift signals. Percentage changes in mean Doppler shift signals were taken as indices of flow changes, and changes in vascular conductance were calculated by dividing mean arterial blood pressure into mean Doppler shift and expressing the change as a %. Within-group analysis was by Friedman's test applied to changes relative to baseline or to integrated responses (areas under or over curves); between group comparisons were made by the Mann-Whitney U test or the Kruskal-Wallis test, as appropriate. A value for $P < 0.05$ was taken as significant.

Drugs and peptides

Human and rat adrenomedullin were obtained from the Peptide Institute through their UK agents (Scientific Research Associates). Human α-CGRP, angiotensin II and arginine vasopressin were obtained from Bachem (UK), and human α-CGRP [8-37] was a gift from Dr R. Foulkes (Celltech Ltd.). L-NAME hydrochloride was obtained from Sigma. All peptides were dissolved in sterile saline (154 mmol l^{-1} NaCl) containing 1% bovine serum albumin (Sigma); L-NAME was dissolved in sterile saline. Bolus injections were given in 100 μl; infusions were at 400 μl h^{-1}. Administration of saline alone in these volumes has no consistent effects.

Results

Resting values for cardiovascular variables in the 6 groups of rats studied are shown in Table 1. There were some slight differences in hindquarters Doppler shift values only.

Dose-responses to human or rat adrenomedullin

Human adrenomedullin caused hypotension and tachycardia, the magnitudes and durations of which were dose-dependent (Figure 1, Table 2). There were significant increases in renal, mesenteric and hindquarters flow with all 3 doses of human adrenomedullin, and these were associated with vasodilatations (Figure 1) which were dose-dependent when expressed as the integrated response (Table 2).

Rat adrenomedullin also caused dose-dependent hypotension, tachycardia and dilatation in the renal, mesenteric and hindquarters vascular beds (Table 2). However, only at the lowest dose did rat adrenomedullin have a greater hypotensive effect than human adrenomedullin; this difference was accompanied by a greater mesenteric vasodilatation only (Table 2).

Effect of human α-CGRP [8-37] on responses to human α-CGRP or human adrenomedullin

Bolus injections of human α-CGRP caused hypotension and tachycardia, together with reductions in renal and mesenteric flow and an increase in hindquarters flow; there were only

transient increases in renal and mesenteric vascular conductance, but a marked hindquarters vasodilatation (Figure 2). Repeated injection of human α-CGRP in the presence of saline evoked responses similar to those above, with the exception that the hindquarters vasodilator response was enhanced (Figure 2). In contrast, in the presence of human α-CGRP [8-37], the hypotensive and tachycardic effects of human α-CGRP were substantially inhibited, as were the reductions in renal and mesenteric flow; indeed, under these circumstances, human α-CGRP evoked a transient increase in renal flow (Figure 2). However, the initial rise in renal vascular conductance was significantly attenuated, and the subsequent renal and mesenteric vasoconstrictions were abolished in the presence of human α-CGRP [8-37], as were the increases in hindquarters flow and vascular conductance (Figure 2).

In the absence of human α-CGRP [8-37], the haemodynamic responses to human adrenomedullin were very reproducible (Figure 3). Interestingly, in the presence of human α-CGRP [8-37], the increases in mesenteric flow and vascular conductance evoked by human adrenomedullin were significantly enhanced; no effect of the latter peptide was inhibited by the $CGRP_1$-receptor antagonist.

Effect of L-NAME or vasopressin plus angiotensin II on responses to human α-CGRP or human adrenomedullin

Prior to infusion of L-NAME or vasopressin plus angiotensin II, responses to bolus injection of human α-CGRP were as described above (Figure 4).

The pressor effects of L-NAME and vasopressin plus angiotensin II were well-matched (Figure 4). However, infusion of vasopressin plus angiotensin II caused significantly greater bradycardia and reductions in renal and mesenteric flow and mesenteric vascular conductance than did L-NAME (Figure 4). In the presence of L-NAME, the integrated tachycardic and renal hyperaemic effects of human α-CGRP were significantly less than in the presence of

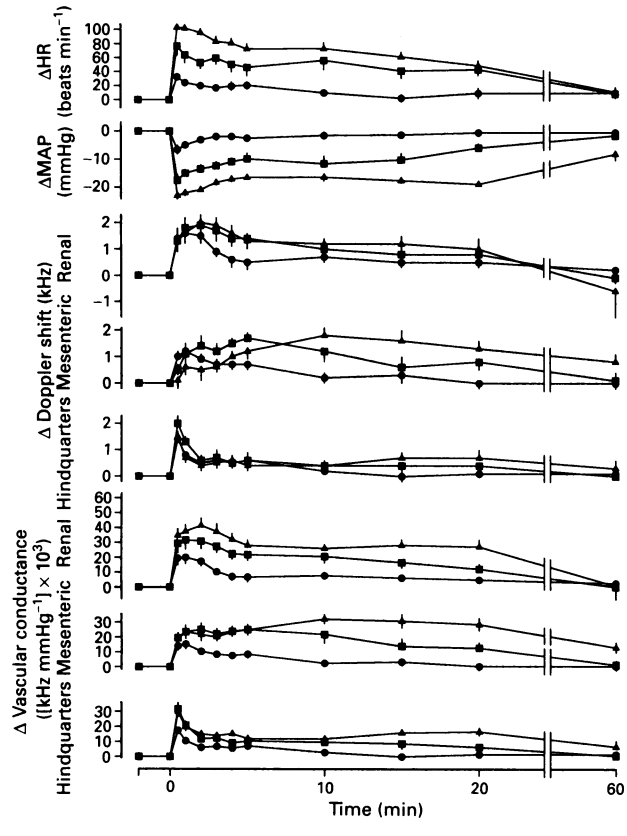

Figure 1 Cardiovascular changes following i.v. bolus injection of human adrenomedullin (●, 0.3 nmol kg^{-1}; ■, 1 nmol kg^{-1}; ▲, 3 nmol kg^{-1}), in the same conscious Long Evans rats ($n = 8$; Group 1). Values are mean ± s.e.mean; for clarity statistics for the integrated responses are shown in Table 2. HR = heart rate; MAP = mean arterial blood pressure.

Table 1 Resting cardiovascular variables in the 6 groups of conscious, Long Evans rats studied (see Methods)

	Group 1	*Group 2*	*Group 3*	*Group 4*	*Group 5*	*Group 6*
Heart rate (beats min^{-1})	338 ± 7	334 ± 6	316 ± 4	319 ± 7	312 ± 4	325 ± 1
Mean blood pressure (mmHg)	105 ± 2	103 ± 2	101 ± 2	103 ± 2	105 ± 1	104 ± 2
Renal Doppler shift (kHz)	7.1 ± 1.2	7.2 ± 0.4	6.8 ± 0.4	6.3 ± 0.5	6.5 ± 0.1	7.0 ± 0.5
Mesenteric Doppler shift (kHz)	6.8 ± 0.5	7.5 ± 0.7	6.1 ± 0.4	7.6 ± 0.7	7.5 ± 1.0	6.8 ± 0.7
Hindquarters Doppler shift (kHz)	4.5 ± 0.3	4.2 ± 0.2	3.6 ± 0.3	3.9 ± 0.5	3.1 ± 0.3[1,2]	3.5 ± 0.2[1]
Renal vascular conductance ([kHz $mmHg^{-1}$]10^3)	67 ± 11	70 ± 4	68 ± 5	62 ± 6	62 ± 2	68 ± 5
Mesenteric vascular conductance ([kHz $mmHg^{-1}$]10^3)	65 ± 5	73 ± 7	60 ± 3	75 ± 9	75 ± 9	66 ± 7
Hindquarters vascular conductance ([kHz $mmHg^{-1}$]10^3)	43 ± 3	41 ± 3	36 ± 3	38 ± 4	29 ± 3	34 ± 2

Values are mean ± s.e.mean.
Superscript numbers $P < 0.05$ versus corresponding groups (Kruskal-Wallis).

Table 2 Integrated (area under or over curve 0–60 min) cardiovascular changes during infusion of human or rat adrenomedullin in 2 separate groups of conscious, Long Evans rats

	Adrenomedullin 0.3 nmol kg^{-1}		*Adrenomedullin* 1.0 nmol kg^{-1}		*Adrenomedullin* 3.0 nmol kg^{-1}	
	Human a	*Rat* b	*Human* c	*Rat* d	*Human* e	*Rat* f
Heart rate (% min)	245 ± 98	378 ± 104	619 ± 82[a]	880 ± 162[b]	758 ± 108[a]	1567 ± 157[b,d]
Mean blood pressure (% min)	−101 ± 35	−284 ± 39[a]	−332 ± 68[a]	−461 ± 97[b]	−790 ± 60[a,c]	−801 ± 67[b,d]
Renal conductance (% min)	675 ± 240	788 ± 152	904 ± 182[a]	1378 ± 252[b]	1814 ± 324[a,c]	2136 ± 245[b,d]
Mesenteric conductance (% min)	362 ± 120	868 ± 143[a]	1175 ± 274[a]	1775 ± 224[b]	1990 ± 308[a,c]	2359 ± 226[b,d]
Hindquarters conductance (% min)	463 ± 111	835 ± 224	1119 ± 281[a]	1343 ± 272	2003 ± 356[a,c]	2034 ± 415[b]

Values are mean ± s.e.mean.
Superscript letters $P < 0.05$ versus corresponding column (Wilcoxon or Mann-Whitney U test, as appropriate).

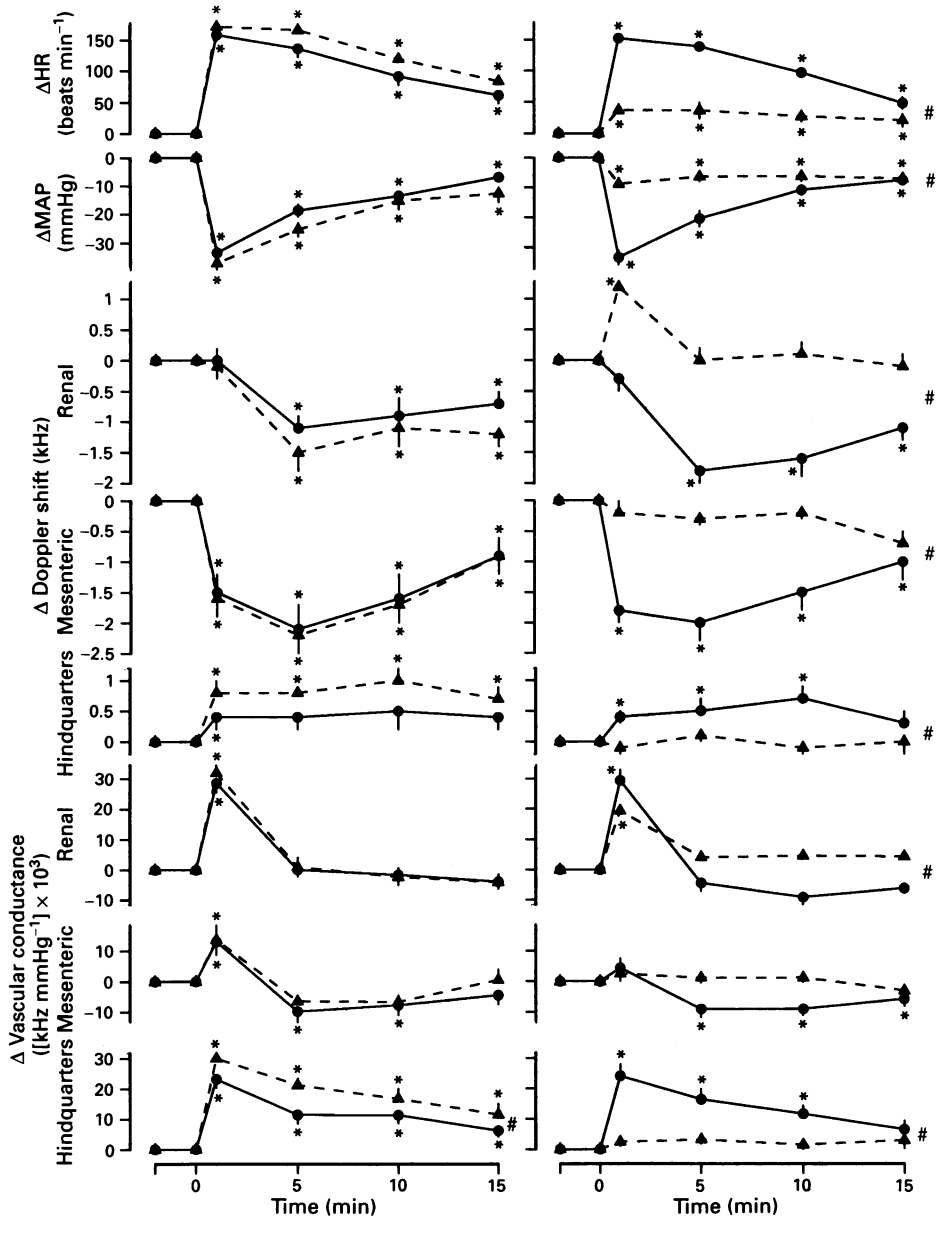

Figure 2 Cardiovascular changes following i.v. bolus injection of human α-calcitonin gene-related peptide (αCGRP) (1 nmol kg^{-1}). Left-hand panels, responses in the absence (●) and during infusion of saline (▲) in the same conscious, Long Evans rats ($n = 8$; Group 3). Right-hand panels, responses in the absence (●) and during infusion of human α-CGRP [8-37] (▲, 100 nmol kg^{-1} min^{-1}) in the same conscious, Long Evans rats ($n = 8$; Group 4). Values are mean ± s.e.mean; $^{*}P < 0.05$ versus baseline (Friedman's test), $^{\#}P < 0.05$ for the difference between the integrated responses in the absence and presence of saline (left-hand panels) or human α-CGRP [8-37] (right-hand panels) (Wilcoxon's test).

vasopressin and angiotensin II; however, the renal, mesenteric and hindquarters vasodilator actions of human α-CGRP were not significantly different in the two conditions (Figure 4).

Prior to infusion of L-NAME or vasopressin plus angiotensin II, responses to human adrenomedullin were as described above (Figure 5).

As in the experiment above, the pressor effects of L-NAME and vasopressin plus angiotensin II were the same, although the bradycardia and reductions in mesenteric and hindquarters flows and vascular conductances in the presence of vasopressin plus angiotensin II were greater than those in the presence of L-NAME (Figure 5).

The integrated tachycardic and hindquarters hyperaemic vasodilator responses to human adrenomedullin were slightly, but significantly, less in the presence of L-NAME than in the presence of vasopressin plus angiotensin II (Figure 5).

Discussion

The present work in conscious rats shows that human adrenomedullin has clear, dose-dependent hypotensive and tachycardic effects. While the changes in mean arterial blood pressure are consistent with previous reports (Kitamura *et al.*, 1993; Ishiyama *et al.*, 1993; Hao *et al.*, 1994), the marked increases in heart rate contrast with the absence of tachycardic responses to human adrenomedullin in anaesthetized rats (Ishiyama *et al.*, 1993) and cats (Hao *et al.*, 1994). This difference is consistent with the heart rate effects of adrenomedullin in our conscious rats being reflex responses to the hypotension, and the absence of tachycardia in the experiments of Ishiyama *et al.* (1993) and Hao *et al.* (1994) being due to inhibition of cardiac baroreflexes by anaesthesia, rather than adrenomedullin having a unique profile of action (Hao *et al.*, 1994).

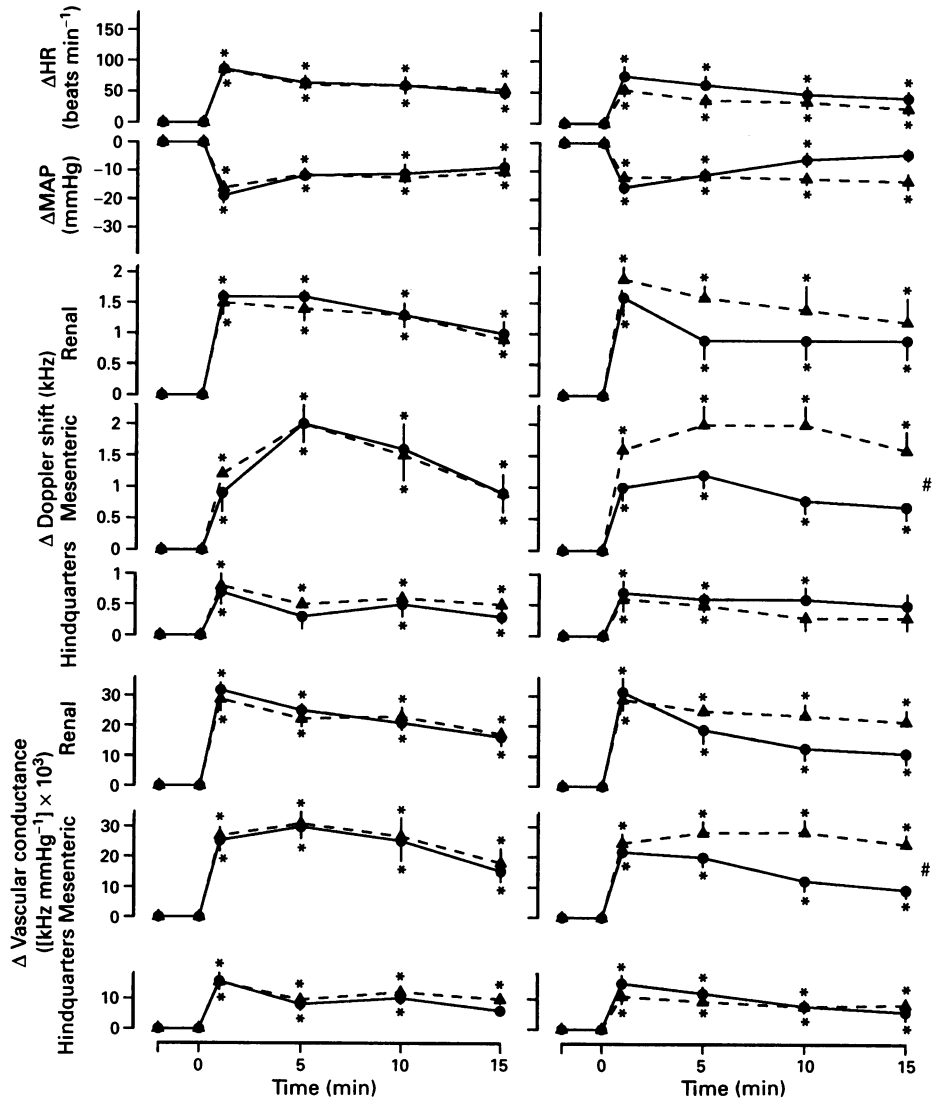

Figure 3 Cardiovascular changes following i.v. bolus injection of human adrenomedullin (1 nmol kg^{-1}). Left-hand panels, responses in the absence (●) and during infusion of saline (▲) in the same conscious, Long Evans rats ($n = 8$; Group 3). Right-hand panels, responses in the absence (●) and during infusion of human α-calcitonin gene-related peptide (α-CGRP) [8-37] (▲, 100 nmol kg^{-1} min^{-1}) in the same conscious, Long Evans rats ($n = 8$; Group 4). Values are mean ± s.e.mean; $^*P < 0.05$ versus baseline (Friedman's test), $^*P < 0.05$ for the difference between the corresponding integrated responses in the absence and presence of human α-CGRP [8-37] (Wilcoxon's test).

It has been reported that rat adrenomedullin has a more potent hypotensive action than human adrenomedullin (Sakata *et al.*, 1993; Lin *et al.*, 1994) in anaesthetized rats. However, such a difference was only apparent at the lowest dose (0.1 nmol kg^{-1}) used in the present study in conscious rats, and that difference was accompanied only by a greater mesenteric vasodilatation.

Although there is some evidence that $CGRP_1$-receptors may be involved in the mesenteric vasodilator effects of human adrenomedullin *in vitro* (Nuki *et al.*, 1993), we could find no evidence for their involvement *in vivo*. Using equimolar doses (1 nmol kg^{-1}) of human α-CGRP and human adrenomedullin, the hypotensive and tachycardic actions of the former were about twice those of the latter. Human α-CGRP caused reductions in renal and mesenteric flows, and only transient increases in renal and mesenteric vascular conductances. In contrast, human adrenomedullin caused marked and persistent increases in renal and mesenteric flows and vascular conductances. Interestingly, however, both human α-CGRP and human adrenomedullin caused increases in hindquarters flows and vascular conductances. Elsewhere, (Gardiner *et al.*, 1988; 1989a) we have suggested that the relative lack of renal and mesenteric vasodilator responses to human α-CGRP was due to activation of counter-regulatory vasoconstrictor mechanisms, such as the renin-angiotensin system (Kurtz *et al.*, 1988). However, since the hypotensive effect of the highest dose of human adrenomedullin (3 nmol kg^{-1}) was similar to that of human α-CGRP at 1 nmol kg^{-1}, it appears that any activation of endogenous vasoconstrictor mechanisms was not able to mask the vasodilator actions of human adrenomedullin. These differences, alone, argue against the latter peptide interacting, directly or indirectly, with $CGRP_1$-receptors, a proposal which is supported by the finding that human α-CGRP [8-37] caused clear inhibition of the haemodynamic effects of human α-CGRP, but not those of human adrenomedullin. It is notable that the inhibition of the hypotensive action of human α-CGRP by human α-CGRP [8-37] was accompanied by clear suppression of its renal and mesenteric vasoconstrictor effects, consistent with these being secondary to the usual hypotension (see above).

Rather than inhibiting the haemodynamic effects of human

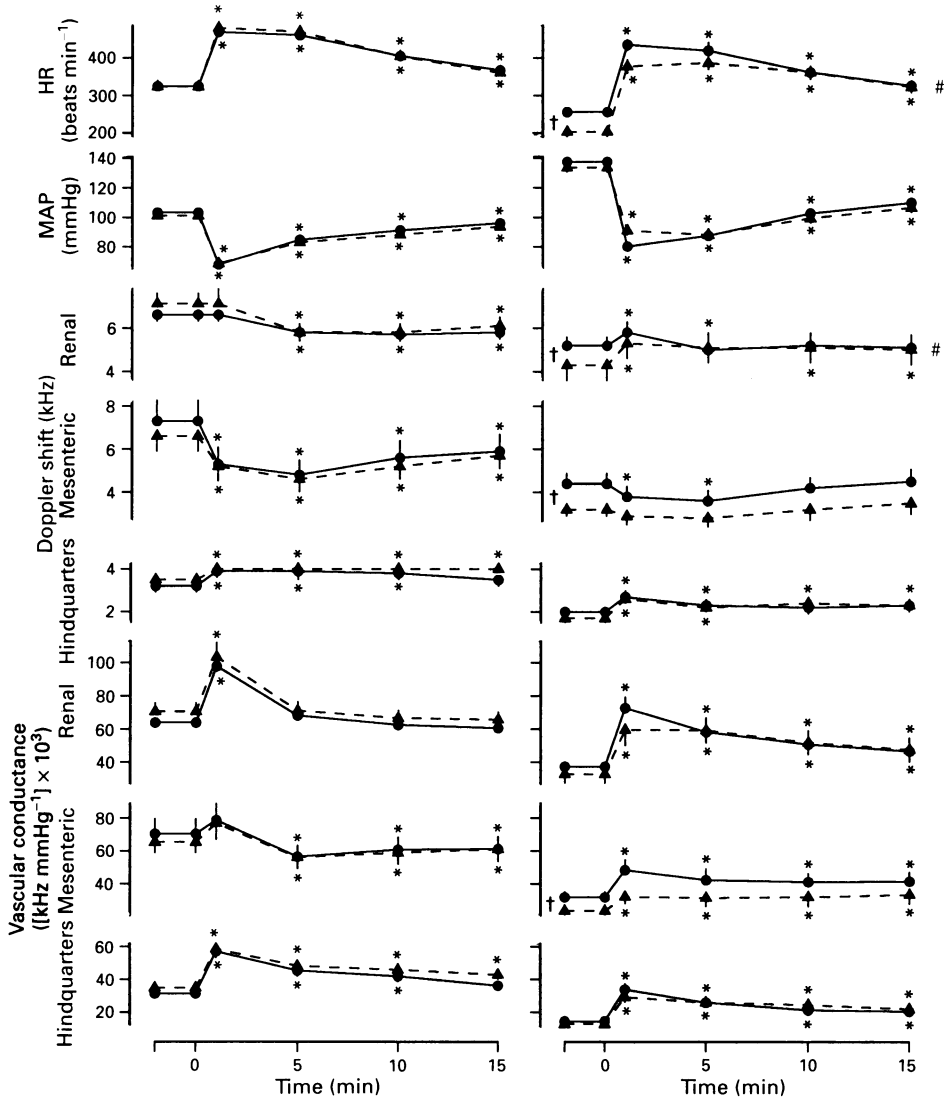

Figure 4 Cardiovascular changes following i.v. bolus injection of human α-calcitonin gene-related peptide (α-CGRP) (1 nmol kg^{-1}) before (left-hand panels, ●) and during infusion of N^G-nitro-L-arginine methyl ester (L-NAME) (right-hand panels, ●) in the same conscious, Long Evans rats ($n = 8$; Group 5), or before (left-hand panels, ▲) and during infusion of vasopressin plus angiotensin II (right-hand panels, ▲) in a separate group of animals ($n = 8$; Group 6). Values are mean ± s.e.mean; $^*P < 0.05$ versus baseline (Friedman's test); †$P < 0.05$ for difference between resting values (Mann-Whitney U test); $^\#P < 0.05$ for difference between integrated responses (Mann-Whitney U test) in the presence of L-NAME or vasopressin plus angiotensin II.

adrenomedullin, the $CGRP_1$-receptor antagonist enhanced its mesenteric haemodynamic action, and tended to do the same in the renal vascular bed. One possibility is that antagonism of the action of endogenous CGRP by human α-CGRP [8-37] sensitizes the mesenteric (and renal) vascular beds to human adrenomedullin. Although speculative, this suggestion is consistent with the finding that human adrenomedullin stimulates cyclic AMP formation in rat vascular smooth muscle cells, and this action is not inhibited by human α-CGRP [8-37] (Ishizaka *et al.*, 1994).

A difference between human α-CGRP and human adrenomedullin was also apparent when the possibility of the involvement of NO was investigated by comparing responses to each peptide in the presence of L-NAME or vasopressin plus angiotensin II to simulate, as far as possible, the haemodynamic effects of the former. Thus, the hindquarters hyperaemic vasodilator effect of human adrenomedullin was only slightly, but significantly, less in the presence of L-NAME than in the presence of vasopressin plus angiotensin II, indicating a small contribution from NO to this response. Such a difference was not apparent for human α-CGRP, although a slow infusion, rather than bolus injection, of the latter peptide appears to activate NO-mediated hindquarters vasodilatation (Gardiner *et al.*, 1991). While it is clear that any involvement of NO in the responses to human adrenomedullin was very marginal, this is an important observation, since it would be reasonable to assume otherwise, considering the marked and widespread vasodilator profile of human adrenomedullin.

Overall, then, human and rat adrenomedullin are potent vasodilator peptides that, unlike human α-CGRP, cause marked increases in renal and mesenteric flows and vascular conductances, as well as hindquarters hyperaemic vasodilatation. While all the haemodynamic effects of human α-CGRP are inhibited by human α-CGRP [8-37], none of the effects of human adrenomedullin are, at least in conscious rats. Contrary to the findings of Nuki *et al.* (1993) these results indicate that the actions of adrenomedullin do not involve $CGRP_1$-receptors, consistent with the recent findings of Ishizaka *et al.* (1994).

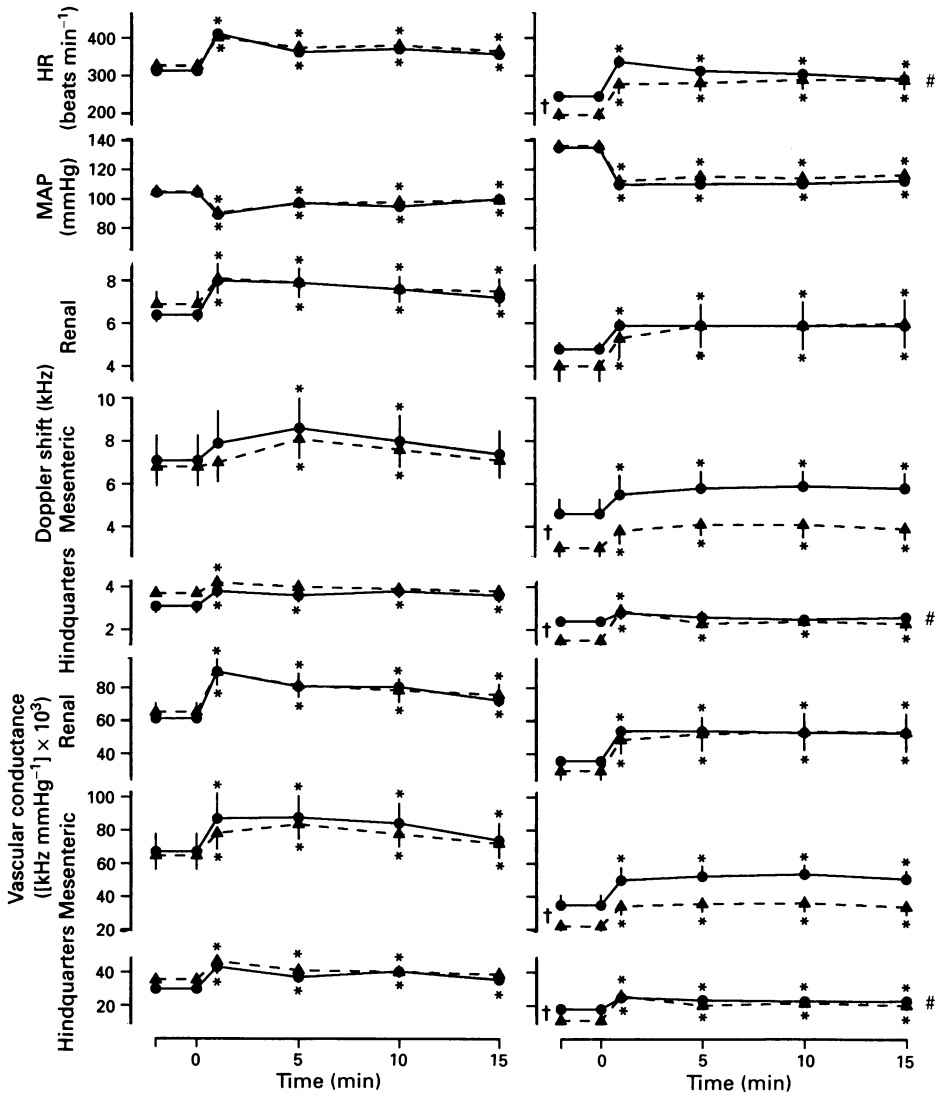

Figure 5 Cardiovascular changes following i.v. bolus injection of human adrenomedullin (1 nmol kg^{-1}) before (left-hand panels, ●) and during infusion of N^G-nitro-L-arginine methyl ester (L-NAME) (right-hand panels, ●) in the same conscious, Long Evans rats ($n = 8$; Group 5), or before (left-hand panels, ▲) and during infusion of vasopressin plus angiotensin II (right-hand panels, ▲) in a separate group of animals ($n = 8$; Group 6). Values are mean ± s.e.mean; $^*P < 0.05$ versus baseline (Friedman's test); $\dagger P < 0.05$ for difference between resting values (Mann-Whitney U test); $^\#P < 0.05$ for difference between corresponding integrated responses (Mann-Whitney U test) in the presence of L-NAME or vasopressin plus angiotensin II.

References

GARDINER, S.M. & BENNETT, T. (1992). Involvement of nitric oxide in the regional haemodynamic effects of perindoprilat and captopril in hypovolaemic Brattleboro rats. *Br. J. Pharmacol.*, **107**, 1181–1191.

GARDINER, S.M., COMPTON, A.M. & BENNETT, T. (1988). Regional haemodynamic effects of depressor neuropeptides in conscious, unrestrained, Long Evans and Brattleboro rats. *Br. J. Pharmacol.*, **95**, 197–208.

GARDINER, S.M., COMPTON, A.M. & BENNETT, T. (1989a). Regional hemodynamic effects of calcitonin gene-related peptide. *Am. J. Physiol.*, **256**, R332–R338.

GARDINER, S.M., COMPTON, A.M. & BENNETT, T. (1989b). Regional haemodynamic effects of human α- and β-calcitonin gene-related peptide in conscious Wistar rats. *Br. J. Pharmacol.*, **98**, 1225–1232.

GARDINER, S.M., COMPTON, A.M., KEMP, P.A. & BENNETT, T. (1990a). Regional and cardiac haemodynamic effects of N^G-nitro-L-arginine methyl ester in conscious, Long Evans rats. *Br. J. Pharmacol.*, **101**, 625–631.

GARDINER, S.M., COMPTON, A.M., KEMP, P.A., BENNETT, T., BOSE, C., FOULKES, R. & HUGHES, B. (1990b). Antagonistic effect of human α-CGRP [8-37] on the *in vivo* regional haemodynamic actions of human α-CGRP. *Biochem. Biophys. Res. Commun.*, **171**, 938–943.

GARDINER, S.M., COMPTON, A.M., KEMP, P.A., BENNETT, T., FOULKES, R. & HUGHES, B. (1991). Haemodynamic effects of human α-calcitonin gene-related peptide following administration of endothelin-1 or N^G-nitro-L-arginine methyl ester in conscious rats. *Br. J. Pharmacol.*, **103**, 1256–1262.

GARDINER, S.M., KEMP, P.A. & BENNETT, T. (1994). Regional haemodynamic effects of adrenomedullin in conscious rats. *Br. J. Pharmacol.*, **112**, Suppl. 562P.

GARDINER, S.M., KEMP, P.A., BENNETT, T., PALMER, R.M.J. & MONCADA, S. (1993). Regional and cardiac haemodynamic effects of N^G, N^G, dimethyl-L-arginine and their reversibility by vasodilators in conscious rats. *Br. J. Pharmacol.*, **110**, 1457–1464.

HAN, S.-P., NAES, L. & WESTFALL, T.C. (1990). Calcitonin gene-related peptide is the endogenous mediator of nonadrenergic-noncholinergic vasodilation in rat mesentery. *J. Pharmacol. Exp. Ther.*, **255,** 423–428.

HAO, Q., CHANG, J.-K., GHARAVI, H., FORTENBERRY, Y., HYMAN, A. & LIPPTON, H. (1994). An adrenomedullin (ADM) fragment retains the systemic vasodilator activity of human ADM. *Life Sci.*, **54,** 265–270.

ICHIKI, Y., KITAMURA, K., KANGAWA, K., KAWAMOTO, M., MATSUO, H. & ETO, T. (1994). Distribution and characterization of immunoreactive adrenomedullin in human tissue and plasma. *FEBS Lett.*, **338,** 6–10.

ISHIYAMA, Y., KITAMURA, K., ICHIKI, Y., NAKAMURA, S., KIDA, O., KANGAWA, K. & ETO, T. (1993). Hemodynamic effects of a novel hypotensive peptide, human adrenomedullin, in rats. *Eur. J. Pharmacol.*, **241,** 271–273.

ISHIZAKA, Y., ISHIZAKA, Y., TANAKA, M., KITAMURA, K., KANGAWA, K., MINAMINO, N., MATSUO, H. & ETO, T. (1994). Adrenomedullin stimulates cyclic AMP formation in rat vascular smooth muscle cells. *Biochem. Biophys. Res. Commun.*, **200,** 642–646.

KAWASAKI, H., TAKASAKI, K., SAITO, A. & GOTO, K. (1988). Calcitonin gene-related peptide acts as a novel vasodilator neurotransmitter in mesenteric resistance vessels of the rat. *Nature*, **335,** 164–167.

KITAMUA, K., ICHIKI, Y., TANAKA, M., KAWAMOTO, M., EMURA, J., SAKAKIBARA, S., KANGAWA, K., MATSUO, H. & ETO, T. (1994). Immunoreactive adrenomedullin in human plasma. *FEBS Lett.*, **341,** 288–290.

KITAMURA, K., KANGAWA, K., KAWAMOTO, M., ICHIKI, Y., NAKAMURA, S., MATSUO, H. & ETO, T. (1993). Adrenomedullin: a novel hypotensive peptide isolated from human pheochromocytoma. *Biochem. Biophys. Res. Commun.*, **192,** 553–560.

KURTZ, A., MUFF, R., BORN, W., LUNDBERG, J.M., MILLBERG, B.-I., GNÄDINGER, M.P., UEHLINGER, D.E., WEIDMANN, P., HÖKFELT, T. & FISCHER, J.A. (1988). Calcitonin gene-related peptide is a stimulator of renin secretion. *J. Clin. Invest.*, **82,** 538–543.

LIN, B., GAO, Y., CHANG, J.-K., HEATON, J., HYMAN, A. & LIPPTON, H. (1994). An adrenomedullin fragment retains the systemic vasodepressor activity of rat adrenomedullin. *Eur. J. Pharmacol.*, **260,** 1–4.

MARSHALL, I., AL-KAZWINI, S.J., HOLMAN, J.J. & CRAIG, R.K. (1986). Human and rat α-CGRP but not calcitonin cause mesenteric vasodilatation in rats. *Eur. J. Pharmacol.*, **123,** 217–222.

NUKI, C., KAWASAKI, H., KITAMURA, K., TAKENAGA, M., KANGAWA. K., ETO, T. & WADA, A. (1993). Vasodilator effect of adrenomedullin and calcitonin gene-related peptide receptors in rat mesenteric vascular beds. *Biochem. Biophys. Res. Commun.*, **196,** 245–251.

SAKATA, J., SHIMOKUBO, T., KITAMURA, K., NAKAMURA, S., KANGAWA, K., MATSUO, H. & ETO, I. (1993). Molecular cloning and biological activities of rat adrenomedullin, a hypotensive peptide. *Biochem. Biophys. Res. Commun.*, **195,** 921–927.

SUGO, S., MINAMINO, N., KANGAWA, K., MIYAMOTO, K., KITAMURA, K., SAKATA, J., ETO. T. & MATSUO, H. (1994). Endothelial cells actively synthesize and secrete adrenomedullin. *Biochem. Biophys. Res. Commun.*, **201,** 1160–1166.

(Received June 30, 1994
Revised September 6, 1994
Accepted October 5, 1994)

British Journal of Pharmacology (1995) 114, 592-597

Interaction of human adrenomedullin $_{13-52}$ with calcitonin gene-related peptide receptors in the microvasculature of the rat and hamster

[1]Judith M. Hall, Lynn Siney, *Howard Lippton, *Albert Hyman, †Jaw Kang-Chang & Susan D. Brain

Pharmacology Group, Biomedical Sciences Division, King's College London, Manresa Road, London, SW3 6LX, U.K; *Department of Surgery, Tulane Medical School, 1430 Tulane Avenue, New Orléans, LA 70112, U.S.A and †Pheonix Pharmaceuticals, 2462 Wyandotte Street, Moutainview, CA 94043, U.S.A.

1 Adrenomedullin (ADM), a recently discovered circulating hypotensive peptide, shares limited sequence homology with the sensory nerve-derived vasodilator, calcitonin gene-related peptide (CGRP). This study compared the vasodilator effect of sequence 13-52 of human adrenomedullin (ADM_{13-52}) with that of human α CGRP (CGRP), in the microvasculature of the hamster cheek pouch and rat skin *in vivo*.

2 Single arterioles (20–40 μm diameter) in the hamster cheek pouch were visualised by intravital microscopy and video recording, and measured by image analysis. Both ADM_{13-52} (1 pmol–0.4 nmol) and CGRP (0.1 pmol–1 nmol) evoked dose-related increases in the diameter of preconstricted arterioles ($n = 6$). ADM_{13-52} (ED_{50} 14 pmol) was 20 fold less active than CGRP (ED_{50} 0.71 pmol). The kinetics of onset and decline of vasodilator responses to both peptides were similar, with vasodilator responses to both peptides reaching a maximum at *ca.* 2 min, and reversing after 10–15 min ($n = 5-7$). The submaximal increase in blood flow evoked by ADM_{13-52} was significantly inhibited ($P<0.05$; $n = 6$) by the $CGRP_1$ receptor antagonist, $CGRP_{8-37}$, at a dose (300 nmol kg^{-1}, i.v.) that we have previously shown to inhibit significantly equivalent vasodilator responses to CGRP in this preparation.

3 In experiments measuring changes in local blood flow in rat skin by a ^{133}xenon clearance technique, intradermal injection of both ADM_{13-52} (3–300 pmol) and CGRP (0.1–30 pmol) evoked dose-related increases in local blood flow. ADM_{13-52} (ED_{50} 27 pmol) was 17 fold less potent than CGRP (ED_{50} 1.6 pmol) ($n = 6$). The submaximal increase in blood flow evoked by both peptides was significantly inhibited ($P<0.02$; $n = 5$) by $CGRP_{8-37}$ (100 nmol kg^{-1}, i.v.).

4 We conclude that ADM_{13-52} is a potent vasodilator in the microvasculature of the hamster and rat *in vivo*. It mediates its vasodilator effect by arteriolar dilatation and this effect is due, at least in part, to the stimulation of $CGRP_1$ receptors.

Keywords: Adrenomedullin; microvasculature; calcitonin gene-related peptide; $CGRP_{8-37}$; hamster cheek pouch; skin (rat); blood flow; vasodilatation; sensory neuropeptide

Introduction

Adrenomedullin (ADM) is a 52 amino acid peptide originally isolated from human phaeochromocytoma tissue (Kitamura *et al.*, 1993a). Human and rat ADM mRNA have subsequently been shown to be expressed in various peripheral tissues of rat and man, including the kidney, lung and adrenal medulla (Kitamura *et al.*, 1993b; Sakata *et al.*, 1993; Ichiki *et al.*, 1994). In man, ADM had been shown to be present at considerable concentrations in the blood (e.g. 3 fmol ml^{-1}, Kitamura *et al.*, 1994a), and in several species has been shown to have potent actions in the vasculature both *in vivo* and *in vitro*. For example, in the anaesthetized rat (Ischiyama *et al.*, 1993) and cat (Hao *et al.*, 1994), intravenous injection of ADM causes a potent and long-lasting hypotensive response, and when infused into the intralobar artery of the cat, evokes vasodilatation in the pulmonary circulation (DeWitt *et al.*, 1994; Lippton *et al.*, 1994). *In vitro*, low doses of ADM evoke vasodilatation in the isolated perfused mesentery of the rat (Nuki *et al.*, 1993). Recently, the 13–52 sequence of human ADM (ADM_{13-52}) has been shown to exhibit the full vasodilator properties of the present peptide, ADM_{1-52}, *in vivo* and *in vitro* (Perret *et al.*, 1993; Hao *et al.*, 1994; Lippton *et al.*, 1994), suggesting that biological activity largely resides in this C-terminal fragment.

ADM and ADM_{13-52} show some limited sequence homology with the sensory nerve-derived vasodilator calcitonin gene-related peptide (CGRP), sharing a six residue ring structure formed by an intramolecular disulphide linkage and a slight homology in the C-terminal amide sequence (Kitamura *et al.*, 1994b, Figure 1). It has recently been suggested that the vasodilator effect of ADM is due to its interaction with CGRP receptors, since vasodilator responses in the rat isolated perfused mesentery evoked by ADM *in vitro* were inhibited by the $CGRP_1$ receptor antagonist $CGRP_{8-37}$ (Nuki *et al.*, 1993). Further, in cultured vascular smooth muscle cells, CGRP displaced binding from specific sites labelled with [^{125}I]-ADM (Eguchi *et al.*, 1994), suggesting an interaction of CGRP and ADM with common receptor sites.

In the present study, we have compared the activity of ADM_{13-52} with human α CGRP (CGRP) in microvascular assays *in vivo*. In the hamster cheek pouch, we investigated the vasodilator effect of the two peptides on single arterioles viewed by intravital microscopy (see Hall & Brain, 1994), and in rat skin, we determined the effect of the two peptides on blood flow using a ^{133}xenon-clearance technique (see Lawrence & Brain, 1992). In both types of experiment, we used the $CGRP_1$ receptor antagonist, human α $CGRP_{8-37}$ (Dennis *et al.*, 1990) to investigate whether the effects of ADM_{13-52} were mediated via stimulation of $CGRP_1$ receptors.

[1] Author for correspondence.

Sequence homology of some peptides compared to α human calcitonin gene-related peptide (α-CGRPh)

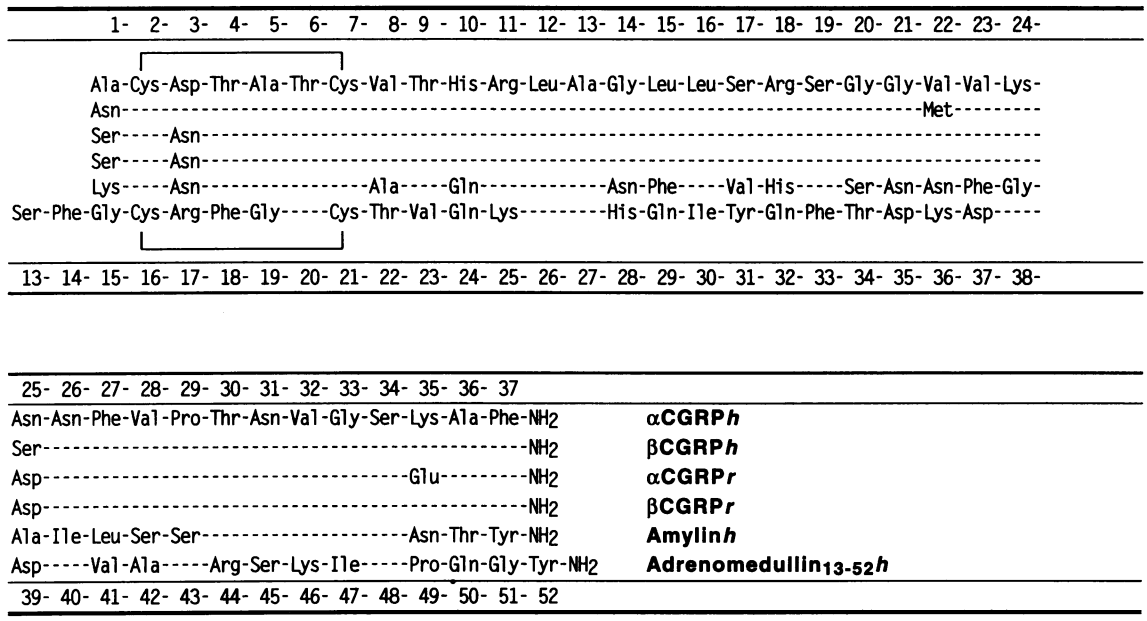

Figure 1 Comparison of amino acid sequences of calcitonin gene-related peptides, amylin, and adrenomedullin$_{13-52}$. Non-identical homologous residues, and the internal disulphide links, are indicated.

Preliminary accounts of this work have been presented to the 14th National Scientific Meeting of the Bayliss and Starling Society (Southampton, England) (Siney *et al.*, 1994a), and a Satellite Symposium of the XIIth IUPHAR Congress, The Second International Symposium of Calcitonin Gene-Related Peptide (Montréal, Canada) (Siney *et al.*, 1994b).

Methods

Hamster cheek pouch

Male golden (Syrian) hamsters (85–106 g) were anaesthetized with sodium pentobarbitone (Sagatal 50 mg kg^{-1}; i.v.) and anaesthesia maintained with 15 mg kg^{-1} pentobarbitone as required. A single layer of vascular membrane was prepared as described by Duling (1973) with some modifications (Hall & Brain, 1994). Briefly, the hamster was placed on a specially designed stage with a central depressed well, the right cheek pouch was carefully everted and placed in the well and pinned to a silicon-rubber ring encircling the window. A single vascular layer was dissected out keeping an intact blood supply, and all connective tissue was removed. In some experiments, the left jugular vein was cannulated (Portex 18 gauge) for intravenous administration of CGRP$_{8-37}$. The tissue was superfused with Krebs-bicarbonate solution (composition mM: NaCl 120, KCl 4.7, $MgCl_2$ 0.12, $CaCl_2$ 0.18, KH_2PO_4 0.4, $NaHCO_3$ 23, glucose 10) at a rate of 4 ml min^{-1} and the Krebs solution, warmed to 35°C, was gassed with 5% CO_2 in air maintained at pH 7.4. An area of microvasculature was selected which allowed an arteriole and adjacent venule (each between 20 and 40 μm in diameter) to be viewed concomitantly. The microvessels were observed with a Leitz Dialux microscope having a 27 × salt-water dipping objective with 10 × eye pieces. Diameters of microvessels were measured with a computerised imaging system (Kompira Limited, Strathclyde, U.K.). In all experiments, arterioles were pre-constricted (by *ca.* 50%) with human endothelin-1 (usually 30–300 pM) superfused 20 min before, and throughout, the experiment. CGRP and ADM$_{13-52}$, dissolved in Krebs solution, were applied topically in 10 μl (or 20 μl for 0.4 nmol ADM$_{13-52}$ in view of the maximum concentration of the stock solution) using a Finn pipette. The CGRP receptor antagonist, CGRP$_{8-37}$ (300 nmol kg^{-1}), dissolved in 0.5 ml saline: bovine serum albumin (BSA;0.1%), was applied i.v. over 1 min, followed by i.v. 0.75 ml saline; BSA over 2 min, 5 min before administration of ADM$_{13-52}$. Following application of test agent, vessel diameter was measure at 15 s, 30 s, 45 s, 1 min, and every minute thereafter, until the dilator response had fully reversed and predilator vessel diameter was recovered.

In experiments comparing the vasodilator activities of CGRP (0.1 pmol–1 nmol) and ADM$_{13-52}$ (1 pmol–0.4 nmol), dose-response curves were obtained by applying single doses of the peptide every 15 min. In half the experiments, the dose-response curve to CGRP was obtained first followed by ADM$_{13-52}$, in the other half, *vice versa*. In all experiments, control responses to the peptide solvent (10 or 20 μl Krebs solution) were measured. In another series of experiments, the CGRP receptor antagonist, CGRP$_{8-37}$, was tested against submaximal vasodilator responses to ADM$_{13-52}$. The response to a submaximal dose of ADM$_{13-52}$ (0.1 nmol) was obtained and this was repeated 30 min later following i.v. administration of CGRP$_{8-37}$ (300 nmol kg^{-1}; i.v.). Reversal of the antagonist effect was determined by obtaining responses to ADM$_{13-52}$ 30 and 60 min after antagonist administration.

Rat skin

The effect of ADM$_{13-52}$ and CGRP on local blood flow was evaluated by local clearance of ^{133}xenon (^{133}Xe) in the dorsal skin of male Wistar rats (200–230 g) following intradermal (i.d.) injection of multiple test agents, as previously described (Williams, 1976; Lawrence & Brain, 1992). Briefly, the rats

were anaesthetized with sodium pentobarbitone (50 mg kg^{-1}) and the dorsal skin was shaved. Each test solution was made up in modified Tyrode solution (composition mM: NaCl 137, KCl 2.7, $MgCl_2$ 1.1, $NaHCO_3$ 11.9, NaH_2PO_4 0.4, glucose 5.6), and equal quantities of ^{133}Xe were mixed with 1 ml samples of each. A 100 µl sample of each test agent was rapidly injected i.d., in duplicate, in random order according to a balanced site pattern. On completion of injections, a 100 µl aliquot of each solution was rapidly injected into vials containing paraffin oil, and immediately capped: the total radioactivity present in 100 µl of each sample could then be counted. After a clearance period of 15 min, the rat was killed, the dorsal skin removed, and the sites punched out. Radioactivity was measured using an automated gamma-counter.

In experiments to compare the vasodilator activities of CGRP and ADM_{13-52}, dose-response curves were determined by the i.d. injection of five dose-levels of the two peptide agonists, at different randomized sites in each rat. In all experiments, control vehicle responses were measured. In a separate series of experiments, the CGRP receptor antagonist, $CGRP_{8-37}$, was tested against the vasodilator responses to ADM_{13-52} and CGRP. Some rats were treated with $CGRP_{8-37}$ (100 nmol kg^{-1}, i.v.) 10 min before i.d. injections, and responses compared to those in control rats also injected 10 min before with vehicle (0.9% saline). Dose-response curves for ADM_{13-52} and CGRP were then determined as before. In all cases, changes in local blood flow were expressed as percentage change in local clearance of ^{133}Xe at test sites, as compared to control sites injected with Tyrode solution (see Lawrence & Brain, 1992). A decrease in clearance indicates a decrease in local blood flow due to vasoconstriction of microvessels.

Source of drugs

Drugs were obtained as follows: pentobarbitone sodium (Sagatal; Rhône Mérieux Ltd, Essex, U.K.) endothelin-1, human αCGRP and human $\alpha CGRP_{8-37}$ (Bachem, Essex, U.K.). ADM_{13-52} was dissolved in saline, all other peptides were dissolved in distilled water and stored at −20°C, peptide dilutions were made up in Krebs or Tyrode solution, as appropriate. All salts were of analytical grade and were obtained from B.D.H, U.K. ADM_{13-52} was synthesized by Dr Jaw Kang-Chang, Pheonix Pharmaceuticals, California, U.S.A.

Expression of results and statistical analysis

Arteriolar vasodilatation in the hamster cheek pouch was calculated as % maximal increase in diameter (compared to pre-constricted diameter). Changes in local blood flow in rat skin were expressed as % change in local clearance of ^{133}Xe at test sites, compared with control sites injected with Tyrode solution. Data from individual experiments were combined, and results are expressed as mean ± s.e.mean of experiments carried out in at least 5 animals for each study. Estimates of ED_{50} with 95% confidence limits, calculated as geometric means were made from individual log concentration-response curves, and are defined as the dose producing 50% of the maximal recorded increase in arteriolar diameter in the hamster cheek pouch, or 50% of maximum response in blood flow in rat skin. The maximum responses evoked by ADM_{13-52} and CGRP were similar in both assays at the highest doses tested. For the hamster cheek pouch experiments, tests for significant differences between log ED_{50}s were made using Student's paired or unpaired t tests, as appropriate. With the rat skin assay, differences between means were assessed by Bonferroni's modified t test, which uses the standard error estimate for analysis of variance, to allow comparison of multiple sites.

Results

Hamster cheek pouch

ADM_{13-52} (1 pmol–0.4 nmol) and CGRP (0.1 pmol-1 nmol) potently evoked arteriolar vasodilatation but had no consistent dilator effect on venules. The time-course of the vasodilatation evoked by both peptides was similar. Figure 2 shows the time-course of vasodilatation of equi-effective doses of ADM_{13-52} (0.1 nmol) and CGRP (10 pmol). The maximal vasodilatation was evoked 2 min after peptide application, and reversed 10–15 min after application. ADM_{13-52} was *ca.* 20 fold less potent than CGRP in evoking arteriolar vasodilatation (Figure 3a), ED_{50} estimates were 14 pmol (1.8–111) and 0.71 pmol (0.2–2.9), respectively. It was not possible to determine the maximal dilator response to ADM_{13-52} in view of the limited concentration of the stock solution; however, the maximal increase in vessel diameter recorded at the highest dose tested was similar for ADM_{13-52} and CGRP (140 ± 25% and 136 ± 28%, respectively). The CGRP receptor antagonist, $CGRP_{8-37}$ (300 nmol kg^{-1}; i.v.), in its own right produced a small constriction in arteriolar tone, which was maximal (at 10.5 ± 1.8) 1.75 min after i.v. injection, but which had essentially reversed after 5 min. $CGRP_{8-37}$ significantly inhibited ($P<0.05$) submaximal vasodilator responses to ADM_{13-52}. The antagonism was partially reversible 30 and 60 min after antagonist administration (Figure 2c). We have previously shown that the same dose of $CGRP_{8-37}$ significantly inhibits submaximal vasodilator responses to CGRP in this preparation (for comparison, a 178% increase in vasodilatation was reduced to 59% by $CGRP_{8-37}$; unpublished observations).

Rat skin

ADM_{15-52} caused a dose-related increase in blood from in the rat cutaneous microvasculature (Figure 4a). However, ADM_{13-52} was shown to be *ca.* 17 fold less potent than CGRP as compared in the same rats, yielding ED_{50} estimates of 27 (22–32) pmol and 1.6 (0.9–2.9) pmol, respectively (Figure 3a). In this system, there was no significant difference in the maximal increase in blood flow induced by the two peptides; 55 ± 6% and 46 ± 4%, for ADM_{13-52} and CGRP, respectively. The antagonist $CGRP_{8-37}$ (100 nmol kg^{-1}) significantly ($P< 0.05$) inhibited ADM_{13-52}-induced increases in blood flow (30–100 pmol/site). Vehicle alone had no significant effect on ADM_{13-52}-induced vasodilatation (Figure 4b). Further, $CGRP_{8-37}$ alone (100 nmol kg^{-1} i.v.), had no significant effect on the clearance at saline-injected sites.

Discussion

This study demonstrates that ADM_{13-52} is a potent vasodilator in the microvasculature of the rat and hamster. It mediates its vasodilator effect by arteriolar dilatation, and the vasodilatation is due, at least in part, to the stimulation of $CGRP_1$ receptors.

Interaction of ADM_{13-52} with CGRP receptors

When applied topically in the hamster cheek pouch, or intradermally in rat skin, microvasculature; both ADM_{13-52} and CGRP, in a dose-related manner, potently evoked arteriolar dilatation, or increased local blood flow, respectively. In both microvasculature preparations, ADM_{13-52} was *ca.* 20 fold less active than CGRP. These results are consistent with results of a recent *in vitro* studying using the full sequence ADM_{1-52} which was found to be *ca.* 10 fold less active than CGRP in the rat isolated perfused mesentery (pD_2 estimates were 8.3 and 9.2 respectively; Nuki *et al.*, 1993).

In the hamster cheek pouch, the time-course of the arteriolar dilatation was similar for ADM_{13-52} and CGRP, with

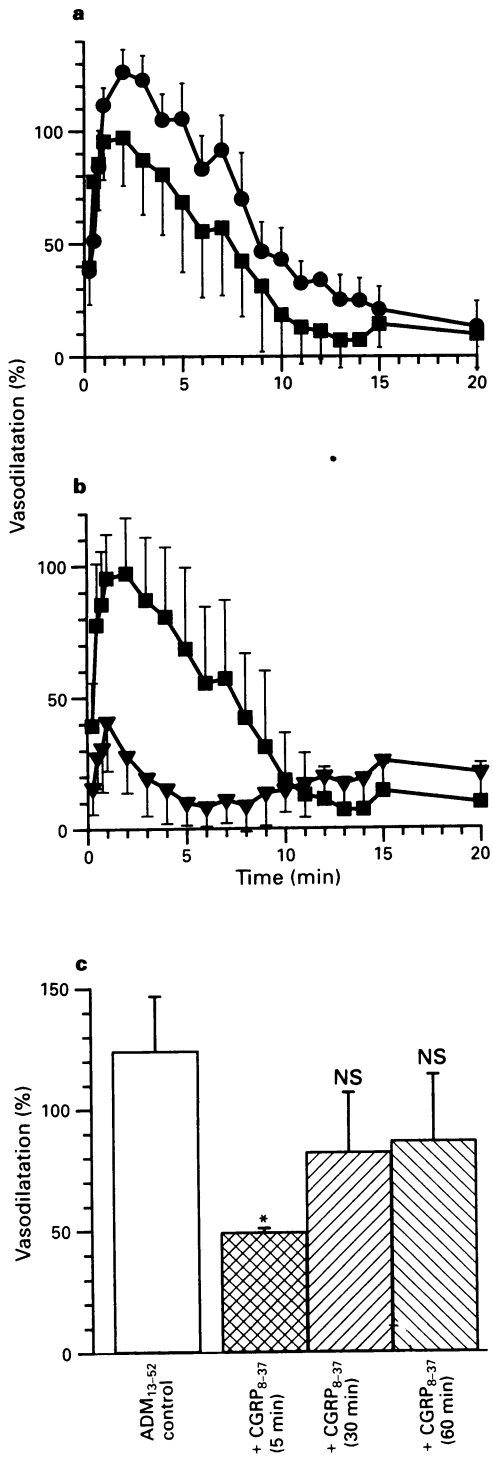

Figure 2 (a) Shows a comparison of time-courses of arteriolar vasodilatation evoked by human adrenomedullin $_{13-52}$ (ADM_{13-53}) (■) and human α calcitonin gene-related peptide (CGRP) (●) in the hamster cheek pouch. Vasodilatation evoked by ADM_{13-52} (0.1 nmol) and CGRP (10 pmol), is expressed as % increase in diameter of arterioles preconstricted (by *ca.* 50%) by human endothelin-1. Vessel diameter was measured 15, 30, 45, 60 s and then every minute up to 20 min after topical application of peptide (in 10 μl Krebs solution). (b) Shows inhibition of submaximal vasodilator responses evoked by ADM_{13-52} (0.1 nmol), Control (■), or after administration of the $CGRP_1$ receptor antagonist $CGRP_{8-37}$ (▼) (300 nmol kg^{-1}, i.v.). (c) Shows inhibition of the maximal vasodilator response evoked by ADM_{13-52} by $CGRP_{8-37}$. Control vasodilatation is shown by the open column, and dilatation recorded 5, 30 and 60 min following intravenous administration of $CGRP_{8-37}$ respectively. Responses are shown as the mean ± s.e.mean in 5–7 hamsters. Vehicle control (10 μl Krebs) produced an 18.6 ± 10.5% increase in arteriole diameter. $^*P<0.05$. NS not significant.

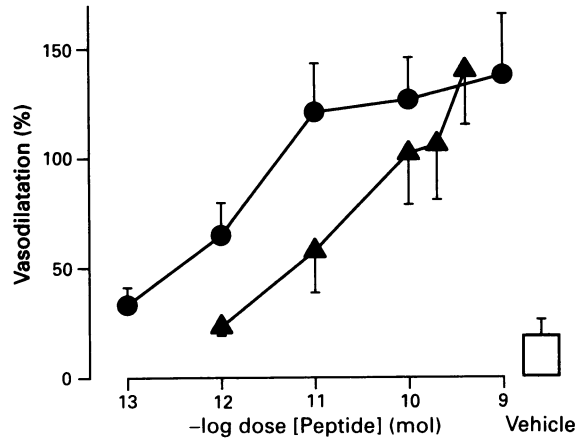

Figure 3 Dose-related vasodilatation in the hamster cheek pouch evoked by human adrenomedullin$_{13-52}$ (ADM_{13-52}) (▲) or human α calcitonin gene-related peptide (CGRP) (●) measured following topical application of peptide (in 10 or 20 μl Krebs solution). Vasodilatation is expressed as maximal % increase in diameter of arterioles preconstricted (by *ca.* 50%) by human endothelin-1, and mean responses, ± s.e.mean, are shown for experiments carried out in 6 hamsters. Estimates of ED_{50} were 14 pmol (1.8–111) and 0.72 (0.2–2.9) pmol, respectively.

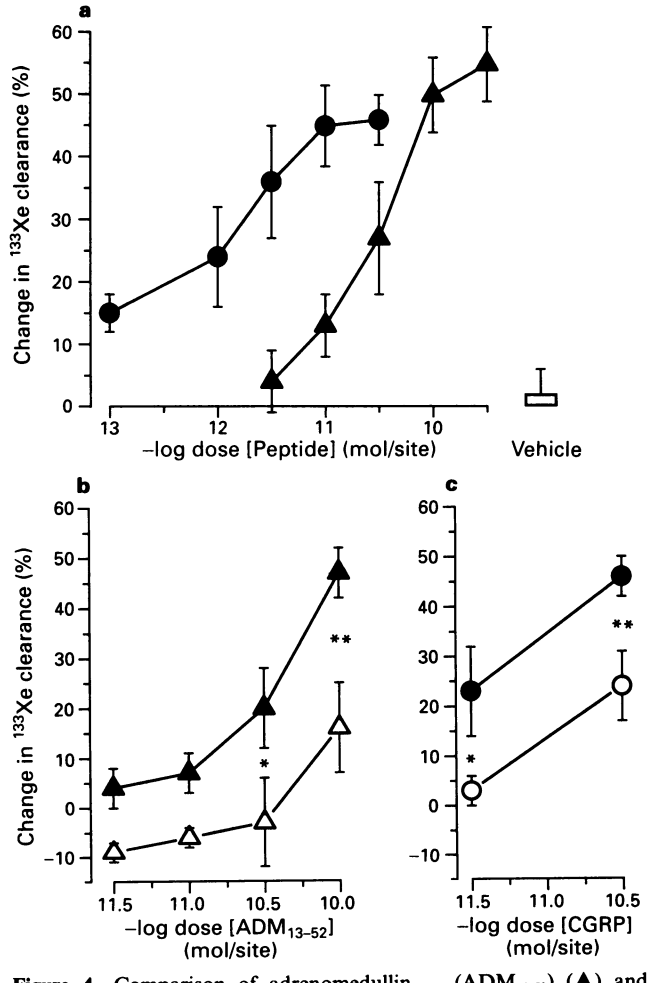

Figure 4 Comparison of adrenomedullin$_{13-52}$ (ADM_{13-52}) (▲) and human α calcitonin gene-related peptide (CGRP) (●) on local blood flow in rat dorsal skin (a). The effect of the antagonist $CGRP_{8-37}$ (100 nmol kg^{-1}, i.v.) against (b) ADM_{13-52}-induced changes in blood flow (test △; vehicle-treated animals/control ▲), and (c) against CGRP (test ○, and control ●). Effects are expressed as percentage change in ^{133}Xe clearance, as indicator of local blood flow, at test sites compared to Tyrode solution injected sites (mean ± s.e.mean; $n = 5$ rats). Dashed line represents blood flow at control Tyrode injected sites. $^*P<0.05$; $^{**}P<0.01$ antagonist *cf.* vehicle control.

dilatation reaching a maximum at 2 min and reversing after 10–15 min. The rate of onset and decline of responses to the two peptides is relatively slow when compared to certain other vasodilators such as substance P (see Hall & Brain, 1993; 1994). CGRP is well known to produce long-lasting microvascular vasodilatation, characterized by a pronounced and well maintained erythema in human skin (Brain *et al.*, 1985), maintained increases in blood flow in rabbit skin (Brain *et al.*, 1985), and prolonged decreases in perfusion pressure in isolated preparations such as the rat mesentery (Claing *et al.*, 1992) and rat kidney (Chin *et al.*, 1994). The similarity in time-course of vasodilator responses to CGRP and ADM_{13-52} suggests a similar mechanism of vasodilatation.

In the microvasculature of both the rat skin and the hamster cheek pouch, the $CGRP_1$ receptor antagonist, $CGRP_{8-37}$, significantly inhibited the vascular effects of both ADM_{13-52} and CGRP. These results with the CGRP receptor antagonist $CGRP_{8-37}$ are consistent with an interaction of ADM_{13-52} with $CGRP_1$ receptors. The doses of $CGRP_{8-37}$ we used to show inhibition of vasodilatation, 100 nmol kg^{-1} and 300 nmol kg^{-1} in the rat skin and hamster cheek pouch, respectively, are comparable with those used previously to exhibit a selective inhibition of CGRP-induced vasodilator responses (Escott & Brain, 1993). $CGRP_{8-37}$ did not inhibit submaximal vasodilator responses to substance P ($n = 5$; unpublished data) in the hamster cheek pouch, again indicating selective block of CGRP receptors. Inhibition of the vasodilator effects of full sequence ADM_{1-52} by $CGRP_{8-37}$ has recently been reported *in vitro* (Nuki *et al.*, 1993; Eguchi *et al.*, 1993); however, our study is the first demonstration of inhibition of ADM_{13-52}-evoked vasodilator responses in the microvasculature *in vivo* by $CGRP_{8-37}$. Further evidence also suggests that ADM, or an ADM-related peptide, can interact with the same receptor sites as CGRP. Thus, in vascular smooth muscle cells in culture, CGRP displaced specific binding sites labelled with ^{125}I-ADM_{1-52} (Eguchi *et al.*, 1994), and in several cell types it has been shown that both ADM and CGRP stimulate the generation of cyclic AMP (Kitamura *et al.*, 1993a; Eguchi *et al.*, 1994).

In terms of structure-activity relationships, it is interesting that peptides with such limited sequence-homology can interact, and stimulate, the same receptors. Indeed, this 'cross-talk' is not limited to CGRP, ADM and its fragments. For example, the 37 amino acid hormone amylin, which exhibits *ca.* 50% sequence homology with CGRP, has also been shown to evoke various biological effects including vasodilatation in the rat isolated perfused kidney (Chin *et al.*, 1994), and inhibition of nerve or spasmogen-evoked contractions of non-vascular smooth muscle (e.g. Giuliani *et al.*, 1992), via an interaction with $CGRP_1$ receptors. The main structural similarity between CGRP, ADM and amylin is the presence of six-residue ring structure formed by an intramolecular disulphide linkage, and a C-terminal amide structure (see Figure 1). It has been previously shown that the N-terminal sequence of CGRP is important for agonist activity of CGRP, in as much as opening or modification of the disulphide bond leads to a considerable loss in vasodilator activity (Tippins *et al.*, 1986; Maggi *et al.*, 1990; Zaidi *et al.*, 1990). This suggests that the disulphide bond may well also be of importance for agonist activity of amylin and adrenomedullin at CGRP receptors. Further, the ability of the N-terminally deleted CGRP fragment, $CGRP_{8-37}$, to act as a receptor antagonist suggests that the C-terminal sequences of amylin and adrenomedullin are important in determining affinity, rather than intrinsic efficacy at the CGRP receptor. This is interesting since Figure 1 shows that the structural homology in the C-terminus sequences of the various naturally-occurring homologues of CGRP is very limited.

In conclusion, we have demonstrated for the first time that ADM_{13-52} is a potent arteriolar vasodilator in the microvasculature, and that its effects in both rat skin and the hamster cheek pouch vasculature are mediated, at least in part, via an interaction with $CGRP_1$ receptors. Currently, it is not established whether the whole of the ADM_{13-52} sequence is required for full biological activity, nor whether ADM_{1-52}, ADM_{13-52}, or another fragment, is the biologically active species secreted *in vivo*. The role of ADM in physiology or pathophysiology remains to be determined, though it is tempting to speculate that, in view of the interaction of ADM and ADM_{13-52} with CGRP receptors, that ADM or an ADM fragment, may have a role as a circulating activator of CGRP receptors and modulator of vascular tone.

We thank the Wellcome Trust and the British Heart Foundation for support. We are grateful to Dr I.K.M. Morton for analysis and preparation of the figures, and Dr U. Ney, Celltech Berkshire, for a gift of CGRP.

References

BRAIN, S.D., WILLIAMS, T.J., TIPPINS, J.R., MORRIS, H.R. & MACINTYRE, I. (1985). Calcitonin gene-related peptide is a potent vasodilator. *Nature*, **313**, 54–56.

CHIN, S.Y., HALL, J.M., BRAIN, S.D. & MORTON, I.K.M. (1994). Vasodilator responses to calcitonin gene-related peptide (CGRP) and amylin in the rat isolated perfused kidney are mediated via $CGRP_1$ receptors. *J. Pharmacol. Exp. Ther.*, **269**, 989–992.

CLAING, A., TÉLÉMAQUE, CADIEUX, A., FOURNIER, A., REGOLI, D. & D'ORLÉANS-JUSTE, P. (1992). Nonadrenergic and noncholinergic arterial dilatation and venoconstriction are mediated by calcitonin gene-related $peptide_1$ and neurokinin-1 receptors, respectively, in the mesenteric vasculature of the rat after perivascular nerve stimulation. *J. Pharmacol. Exp. Ther.*, **263**, 1226–1232.

DENNIS, T., FOURNIER, A., CADIEUX, A., POMERLEAU, F., JOLICOEUR, F.B., ST.PIERRE, S. & QUIRION, R. (1990). $hCGRP_{8-37}$, a calcitonin gene-related peptide receptor heterogeneity in brain and periphery. *J. Pharmacol. Exp. Ther.*, **245**, 123–128.

DEWITT, B.J., CHENG, D.Y., CAMINITI, G.N., NOSSAMAN, B.D., COY, D.H., MURPHY, W.A. & KADOWITZ, P.J. (1994). Comparison of responses to adrenomedullin and calcitonin gene-related peptide in the pulmonary vascular bed of the cat. *Eur. J. Pharmacol.*, **257**, 303–306.

DULING, B.R. (1973). The preparation and use of the hamster cheek pouch for studies of the microcirculation. *Microvasc. Res.*, **5**, 423–429,

EGUCHI, S., HIRATA, Y., KANO, H., SATO, K., WATANABE, Y., WATANABE, T.X., NAKAJIMA, K., SAKAKIBARA, S. & MARUMO, F. (1994). Specific receptors for adrenomedullin in cultured rat vascular smooth muscle cells. *FEBS Lett.*, **340**, 226–230.

ESCOTT, K.J. & BRAIN, S.D. (1993). Effect of a calcitonin gene-related peptide antagonist ($CGRP_{8-37}$) on skin vasodilatation and oedema induced by stimulation of the rat saphenous nerve. *Br. J. Pharmacol.*, **110**, 772–776.

GIULIANI, S., WIMILAWANSKI, S.J. & MAGGI, C.A. (1992). Involvement of multiple receptors in the biological effects of calcitonin gene-related peptide and amylin in rat and guinea-pig preparations. *Br. J. Pharmacol.*, **107**, 510–514.

HALL, J.M. & BRAIN, S.D. (1993). Quantification of the vasodilator effects of CGRP, amylin and $[Cys(ACM)^{2,7}]$-hCGRP on the microvasculature of the hamster cheek pouch *in vivo*. *Neuropeptides*, **24**, 207.

HALL, J.M. & BRAIN, S.D. (1994). Inhibition of NK_1 tachykinin receptor mediated, nitric oxide dependent vasodilatation by SR140333 in the hamster cheek pouch microvasculature *in vivo*. *Br. J. Pharmacol.*, **113**, 522–526.

HAO, Q., CHANG, J-K., GHARAVI, H., FORTENBERRY, Y., HYMAN, A. & LIPPTON, H. (1994). An adrenomedullin (ADM) fragment retains the systemic vasodilator activity of human ADM. *Life Sci.*, **54**, PL265–PL270.

ICHIKI, Y., KITAMURA, K., KANGAWA, K., KAWAMOTO, M., MATSUO, H. & ETO, T. (1994). Distribution and characterization of immunoreactive adrenomedullin in human tissue and plasma. *FEBS Lett.*, **338,** 6–10.

ISCHIYAMA, Y., KITAMURA, K., ICHIKI, Y., NAKAMURA, S., KIDA, O., KANGAWA, K. & ETO, T. (1993). Hemodynamic effects of a novel hypotensive peptide, human adrenomedullin, in rats. *Eur. J. Pharmacol.*, **241,** 271–273.

KITAMURA, K., KANGAWA, K., KAWAMOTO, M., ICHIKI, Y., NAKAMURA, S., MATSUO, H. & ETO, T. (1993a). Adrenomedullin: a novel hypotensive peptide isolated from human pheochromocytoma. *Biochem. Biophys. Res. Commun.*, **192,** 553–560.

KITAMURA, K., SAKATA, J., KANGAWA, K., KOJIMA, M., MATSUO, H. & ETO, T. (1993b). Cloning and characterization of cDNA encloding a precursor for human adrenomedullin. *Biochem. Biophys. Res. Commun.*, **194,** 720–725.

KITAMURA, K., ICHIKI, Y., TANAKA, M., KAWAMOTO, M., EMURA, J., SAKAKIBARA, S., KANGAWA, K., MATSUO, H. & ETO, T. (1994a). Immunoreactive adrenomedullin in human plasma. *FEBS Lett.*, **341,** 288–290.

KITAMURA, K., KANGAWA, K., KOJIMA, M., ICHIKI, Y., MATSUO, H. & ETO, T. (1994b). Complete amino acid sequence of porcine adrenomedullin and cloning of cDNA encoding its precursor. *FEBS Lett.*, **338,** 306–310.

LAWRENCE, E.J. & BRAIN, S.D. (1992). Responses to endothelins in the rat cutaneous microvasculture: A modulatory role of locally produced nitric oxide. *Br. J. Pharmacol.*, **106,** 733–738.

LIPPTON, H., CHANG, J-K., HAO, Q., SUMMER, W. & HYMAN, A.L. (1994). Adrenomedullin dilates the pulmonary vascular bed *in vivo*. *J. Appl. Physiol.*, **76,** 2154–2156.

MAGGI, C.A., ROVERO, P., GIULIANI, S., EVANGELISTA, S., REGOLI, D. & MELI, A. (1990). Biological activity of N-terminal fragments of calcitonin gene-related peptide. *Eur. J. Pharmarcol.*, **179,** 217–219.

NUKI, C., KAWASAKI, H., KITAMURA, K., TAKENAGA, M., KANGAWA, K., ETO, T. & WADA, A. (1993). Vasodilator effect of adrenomedullin and calcitonin gene-related peptide receptors in rat mesenteric vascular beds. *Biochem. Biophys. Res. Commun.*, **196,** 245–251.

PERRET, M., BROUSSARD, H., LEGROS, T., BURNS, A., CHANG, J-K, SUMMER, W., HYMAN, A. & LIPPTON, H. (1993). The effect of adrenomedullin on the isolated heart. *Phamacol. Lett.*, **53,** PL377-PL379.

SAKATA, J., SHIMOKUBO, T., KITAMURA, K., NAKAMURA, S., KANGAWA, K., MATSUO, H. & ETO, T. (1993). Molecular cloning and biological activities of rat adrenomedullin, a hypotensive peptide. *Biochem. Biophys. Res. Commun.*, **195,** 921–927.

SINEY, L., HALL, J.M. & BRAIN, S.D. (1994a). Comparison of the vasodilator peptides adrenomedullin and calcitonin gene-related peptide in the rat cutaneous microvasculature. *Regul. Pept.*, **51,** 292.

SINEY, L., HALL, J.M. & BRAIN, S.D. (1994b). Vasodilator effects of adrenomedullin in the rat cutaneous microvasculature. *Can. J. Physiol. Pharmacol.*, **72,** 51.

TIPPINS, J.R., DI MARZO, V.M., PANICO, M., MORRIS, H.R. & MACINTYRE, I. (1986). Investigation of the structure-activity relationship in human calcitonin gene-related peptide (CGRP). *Biochem. Biophys. Res. Commun.*, **134,** 1306–1311.

WILLIAMS, T.J. (1976). Simultaneous measurement of local plasma exudation and blood flow changes induced by intradermal injection of vasoactive substances using [^{131}I] albumin and [^{133}Xe]. *J. Physiol.*, **254,** 4–5P.

ZAIDI, M., BRAIN, S.D., TIPPINS, J.R., DI MARZO, MOONGA, B.S., CHAMBERS, T.J., MORRIS, H.R. & MACINTYRE, I. (1990). Structure-activity relationships of human gene-related peptide. *Biochem. J.*, **269,** 775–780.

(Received July 15, 1994
Revised September 20, 1994
Accepted October 6, 1994)

British Journal of Pharmacology (1995) 114, 598-601

On the inhibition of prostanoid formation by SK&F 96365, a blocker of receptor-operated calcium entry

Dedicated to Professor Ronald Kurz on the occasion of his 60th birthday

[1]Hans J. Leis, Doris Zach, Evelyn Huber, Laszlo Ziermann, Helmut Gleispach & W. Windischhofer

Dept. of Biochemical Analysis, Univ. Childrens Hospital, Auenbruggerplatz 30, A-8036 Graz, Austria

1 The proposed blocker of receptor-operated calcium channels, SK&F 96365 was shown to inhibit formation of prostaglandin E_2 in two osteoblast-like cell lines, MC3T3-E1 and UMR-106 in a dose-dependent manner at an IC_{50} of 3-4 μM. Inhibition was observed with various stimuli (arachidonic acid, bradykinin and calcium ionophore A23187).

2 This effect was also observed in human platelets, where SK&F 96365 dose-dependently blocked thromboxane biosynthesis and formation of 12-hydroxy-heptadecatrienoic acid after stimulation with arachidonic acid (IC_{50} = 4 μM).

3 The compound had no effect on 12-hydroxy-eicosatetraenoic acid production by human platelets. Additionally, linoleic acid oxidation by soybean 15-lipoxidase was not impaired by SK&F 96365. The results thus provide evidence for cyclo-oxygenase inhibition by SK&F 96365 at concentrations used to block receptor-operated calcium influx.

Keywords: Cyclo-oxygenase; SK&F 96365; prostaglandins; HETE; thromboxane

Introduction

Stimulus-evoked influx of extracellular calcium can be regarded as a fundamental process in cell signalling and response. Ca^{2+} entry via voltage-gated calcium channels is well documented due to the availability of high-affinity ligands (Campbell *et al.*, 1988; Tsien *et al.*, 1988). Studies on the mechanism and function of receptor-mediated calcium entry (RMCE) in non-excitable cells have proved difficult without suitable ligands (Medolesi & Pozzan, 1987; Hallam & Rink, 1989). Recently, it has been proposed that the imidazole compound, SK&F 96365 (1-{β-[3-(4-methoxyphenyl)propoxy]-4-methoxyphenylethyl}-1*H*-imidazole hydrochloride) is an inhibitor of RMCE (Merritt *et al.*, 1990). Numerous studies have been conducted with this ligand for blockade of RMCE, thereby relating a wide range of cellular responses to this inhibitory action. Thus, SK&F 96365 was shown to inhibit muscarinic receptor-mediated tyrosine phosphorylation of phospholipase C-γ (PLC-γ) (Gusovsky *et al.*, 1993) and isolated sarcoplasmatic reticulum Ca^{2+}-ATPase (Mason *et al.*, 1993). The drug also inhibited prostaglandin formation and RMCE in the osteoblast-like cell line, MC3T3-E1 (Leis *et al.*, 1994). In human endothelial cells, diminished prostacyclin production after stimulation with platelet activating factor (PAF) and SK&F 96365-treatment was attributed to the blockade of RMCE (Weber *et al.*, 1993) as well as inhibition of tumour cell growth in human astrocytoma (U373 MG) and neuroblastoma (SK-N-MC) cells (Lee *et al.*, 1993). Besides having an effect on RMCE, SK&F 96365 has also been shown to inhibit cytochrome P-450 mediated reactions (Sheets *et al.*, 1986; Alonso *et al.*, 1991) and reversibly activates non-selective cation channels in human endothelial cells (Schwarz *et al.*, 1994). Thus, the compound may exert multiple effects on fundamental biochemical mechanisms, and caution should be exercised when cellular responses are attributed to its RMCE-blocking activity. This is also suggested by studies on the T-cell leukaemia cell line Jurkat, where the drug blocked calcium influx and imposed a total cell cycle arrest in GM/2, which was reported to be dependent on drug concentration, but not on extracellular calcium (Nordstrom *et al.*, 1992).

Human platelets have been shown to possess receptor-operated calcium channels (ROCC) (Zschauer *et al.*, 1988), and the inhibitory action of SK&F 96365 on ADP- and thrombin-induced platelet activation has been correlated to the blockade of RMCE (Merritt *et al.*, 1990). Therefore the aim of the present study was to investigate, whether SK&F 96365-evoked cellular responses are solely due to its effects on cell calcium homeostasis, or if it also affects other fundamental metabolic events of the cell. Since the compound has been shown to inhibit cytochrome P-450, a similar action on other haeme-proteins like cyclo-oxygenase appears to be very likely.

Methods

Cell culture

MC3T3-E1 cells were cultured routinely in DMEM containing 5% FCS, gentamycin-sulphate (83.4 mg l^{-1}), and L-glutamine (0.584 g l^{-1}) in a humidified atmosphere of 5% CO_2 in 80 cm^2 flasks and transferred to 4 cm^2 12-well culture dishes before experiments. At confluency medium (1 ml) was removed and the cell monolayer incubated in 1 ml of Ca^{2+}-free HEPES-buffered Hanks balanced salt solution (HBSS). After preincubation with the indicated concentrations of SK&F 96365 for 5 min, Ca^{2+} was added to a final concentration of 1 mM. After 10 min, incubations with the appropriate stimuli or vehicle were carried out for 30 min. For prostaglandin measurement, the incubation buffer was removed and processed as described below.

Human platelets were prepared from human plasma as described by Mustard *et al.* (1989) and resuspended in HEPES buffer as described above; 500 µl (10^8 cells) of the suspension was used. Incubation was stopped by addition of 500 µl ice-cold ethanol and thromboxane (TX) B_2, 12-hydroxy-heptadecatrienoic acid (12-HHT) and 12-hydroxy-eicosaetraenoic acid (12-HETE) determined as described below.

[1] Author for correspondence.

Prostaglandin determination

Prostaglandin E_2 (PGE_2) thromboxane B_2 (TXB_2), 12-HHT and 12-HETE were measured by gas chromatography-negative ion chemical ionization mass spectrometry (GC-NICI-MS) (Leis *et al.*, 1987a, b; Mayer *et al.*, 1986; Malle *et al.*, 1987). Briefly, PGE_2 and TXB_2 were converted to their PFB ester-TMS-ether-O-methyloxime derivative. Quantitation was carried out by use of tetradeuterated PGE_2 and ^{18}O-TXB_2 as internal standard. 12-HHT and 12-HETE were quantified as their PFB ester TMS-ether derivatives after catalytical hydrogenation using [$^{18}O_2$]-5-HETE as internal standard. A Fisons Trio quadrupole mass spectrometer coupled to a Carlo Erba GC 8000 was used. GC was performed on a 15 m DB5 fused silica capillary column (Fisons Instruments). The temperature of the splitless Grob injector was kept at 290°C, initial column temperature was 160°C for 1 min, followed by an increase of 40°/min to 310°C. NICI was carried out in the single ion recording mode with methane as a moderating gas.

Activity of soybean 15-lipoxidase was assessed photometrically with linoleic acid as a substrate following the protocol of the manufacturers.

Materials

Bradykinin (BK), arachidonic acid (AA), EGTA, calcium ionophore A23187, soybean lipoxidase, PGE_2 and HEPES buffer were from Sigma Chemical Co. (Munich, Germany). DMEM and foetal calf serum (FCS) were obtained from sera-lab (Vienna, Austria). L-Glutamine was from serva (Vienna, Austria). Trypsin-EDTA was purchased from Böhringer (Mannheim, Germany). Pentafluorobenzyl bromide (PFBBr), *bis*-(N,O-trimethylsilyl)trifluoroacetamide (BSTFA), silylation grade pyridine, acetonitrile, and O-methoxyamine hydrochloride (MOX) were from Pierce Chemical Co. (Rockford, IL, U.S.A.). Culture dishes were from Falcon via Szabo (Vienna, Austria). MC3T3-E1 cells were kindly supplied by Prof. M. Kumegawa, Sakado, Japan. UMR-106 cells were from the American Type Culture Collection, Rockville, Maryland, U.S.A. Deuterated PGE_2 was obtained through MSD Isotopes via IC Chemikalien GmbH (München, Germany). All other chemicals and reagents were from Merck, Darmstadt, Germany. SK&F 96365 was purchased from Biomol, Hamburg, Germany. [^{18}O]-TXB_2 and [^{18}]-5-HETE were prepared as described (Leis *et al.*, 1986).

Results

SK&F 96365 inhibited formation of PGE_2 in arachidonate-stimulated MC3T3-E1 (Figure 1) and UMR-106 cells (Figure 2) in a dose-dependent manner. This inhibitory effect was influenced by the concentration of arachidonic acid used to stimulate cells. IC_{50} values of 3–4 μM SK&F 96365 were obtained in both cell systems. At a drug concentration of 50 μM, PGE_2 production was reduced by more than 95% with up to 10 μM arachidonic acid supplemented. SK&F 96365 at 50 μM also completely inhibited formation of PGE_2 in both cell lines after stimulation with the calcium ionophore A23187 (5 μM) and in MC3T3-E1 cells after treatment with bradykinin (1 μM) (results not shown).

In arachidonate-challenged human platelets, SK&F 96365 blocked synthesis of TXB_2 (Figure 3). This effect was dose dependent with an IC_{50} of 4 μM. The arachidonic acid concentration used was 10 μM. No effect of the compound on TXB_2 formation was seen in the absence of arachidonic acid. Additionally, the cyclo-oxygenase-derived metabolite 12-HHT was also blocked dose-dependently by the drug, following nearly identical kinetics as for TXB_2 (Figure 4). Levels of 12-HETE determined in the same samples, however, were not altered by SK&F 96365 at concentrations up to 50 μM (Figure 4).

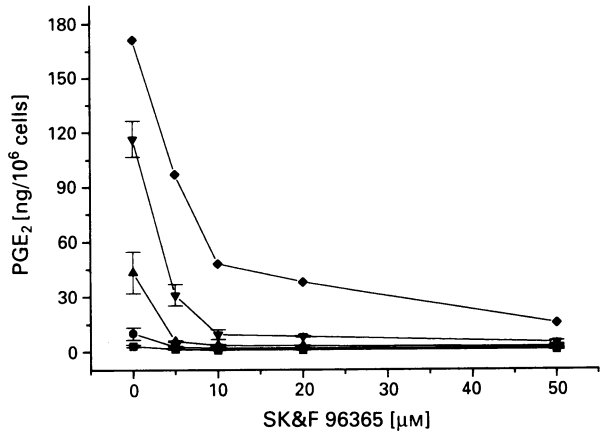

Figure 1 Inhibition of arachidonic acid-induced formation of prostaglandin E_2 (PGE_2) by SK&F 96365 in the clonal murine osteoblast-like cell line, MC3T3-E1. Cells were cultured as described in experimental procedures and preincubated for 5 min with SK&F 96365 in Ca^{2+}-free HEPES buffered HBSS. After addition of Ca^{2+} to a final concentration of 1 mM, preincubation was continued for another 10 min, and incubations with different concentrations of arachidonic acid, 2 μM (■), 4 μM (●), 6 μM (▲), 10 μM (▼) and 20 μM (◆), were subsequently carried out for 30 min. Points represent means ± s.e.mean of 6 determinations.

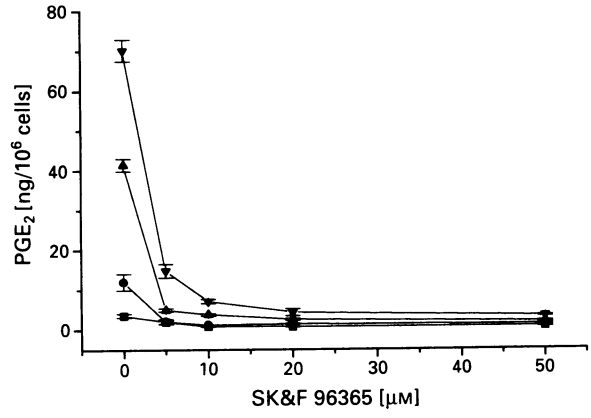

Figure 2 Inhibition of arachidonic acid-induced formation of prostaglandin E_2 (PGE_2) by SK&F 96365 in the rat osteosarcoma cell line, UMR-106. Cells were cultured as described in experimental procedures and preincubated for 5 min with SK&F 96365 in Ca^{2+}-free HEPES buffered HBSS. After addition of Ca^{2+} to a final concentration of 1 mM, preincubation was continued for another 10 min, and incubations with different concentrations of arachidonic acid, 2 μM (■), 4 μM (●), 6 μM (▲) and 10 μM (▼), were subsequently carried out for 30 min. Points represent means ± s.e.mean of 6 determinations.

Hydroperoxide formation from linoleic acid by soybean 15-lipoxidase, as measured by u.v. absorption at 238 nm, was not impaired by concentrations of the drug up to 100 μM (results not shown).

Discussion

With the advent of SK&F 96365, much progress has been made in the elucidation of functional mechanisms of RMCE. However, a variety of additional effects have been demonstrated for the drug, thus caution should be exercised, when biochemical cellular responses are attributed to the ubiquitous event of calcium influx. Our results clearly demonstrate an inhibitory effect of SK&F 96365 on cyclo-oxygenase activity in different cell systems: osteoblast-like cells cloned from 'normal' mouse calvaria, MC3T3-E1 (Kodama *et al.*,

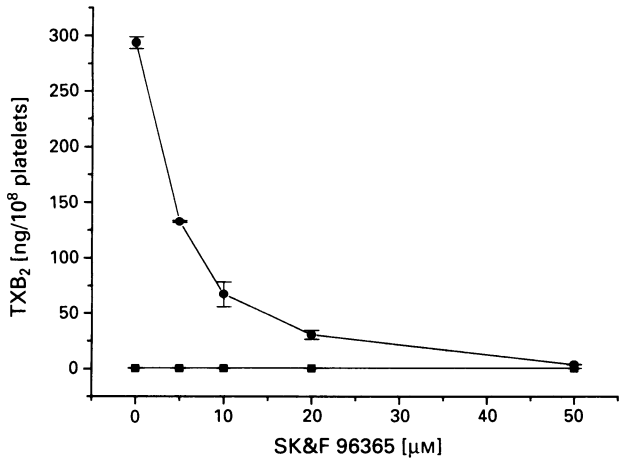

Figure 3 Inhibition of arachidonic acid-induced formation of thromboxane B_2 (TXB_2) by SK&F 96365 in washed human platelets. Cell suspensions were obtained as described in experimental procedures and preincubated for 15 min with SK&F 96365 HEPES buffered HBSS, containing 1 mM Ca^{2+}. Incubations with arachidonic acid (10 μM, ●) or vehicle (■) were subsequently carried out for 30 min. Points represent means ± s.e.mean of 6 determinations.

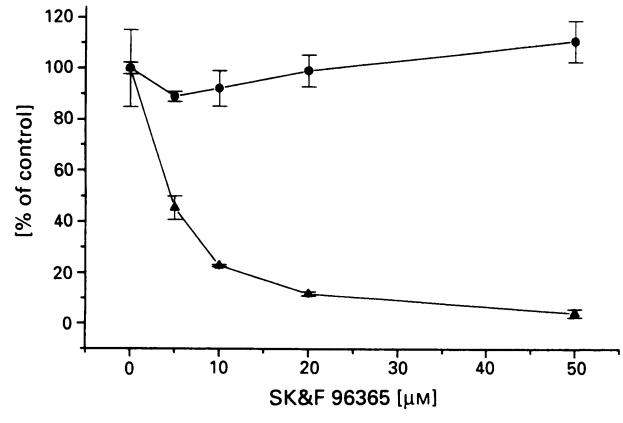

Figure 4 Effect of SK&F 96365 on arachidonic acid-induced formation of 12-hydroxy-eicosaetetraenoic acid (12-HETE, ●) and 12-hydroxy-heptadecatrienoic acid (12-HHT, ▲) in washed human platelets. Cell suspensions were obtained as described in experimental procedures and preincubated for 15 min with SK&F 96365 HEPES buffered HBSS, containing 1 mM Ca^{2+}. Incubations with arachidonic acid (10 μM) were subsequently carried out for 30 min. Points represent means ± s.e.mean of 6 determinations.

1981), osteoblast-like rat osteosarcoma cells (UMR-106), and human platelets. Effects on phospholipases as a primary cause for inhibition (e.g. due to blockade of calcium entry) can be ruled out under these experimental conditions, since exogenous arachidonic acid would be metabolized in any case. Additionally, stimulation of arachidonate metabolism by the calcium ionophore A23187 should bypass any effects on phospholipases related to blockage of RMCE. Since no such stimulation occurs in MC3T3-E1 and UMR-106 cells, the inhibitory effect can be related to the cyclo-oxygenase enzyme. This is supported by the fact that the activity of human platelet 12-lipoxygenase was not at all modulated by the drug, whereas formation of 12-HHT was. From these data it is evident, that SK&F 96365 is a selective blocker of cyclo-oxygenase up to 50 μM. At this concentration RMCE is totally blocked by the compound. Lipoxygenases are obviously not affected, which is confirmed by the lack of any blocking-activity on soybean 15-lipoxidase. Since the inhibitory effect is also dependent on the concentration of arachidonic acid used to stimulate cells, a reversible mode of action is suggested.

Looking at certain cellular responses in the light of the cyclo-oxygenase-blocking activity of the drug, some conclusions from previous studies might require re-interpretation. Thus, a marked inhibitory effect of SK&F 96365 on agonist-stimulated prostacyclin synthesis after pretreatment with platelet activating factor (PAF) in human endothelial cells led to the conclusion, that PAF exerts its effect via sensitizing ROCCs (Weber *et al.*, 1993). Although this might also contribute to the observed effects, diminished prostacyclin production was probably mainly due to cyclo-oxygenase inhibition by SK&F 96365.

Inhibition of tumour cell growth in human U373 MG (astrocytoma) and SK-N-MC (neuroblastoma) cells (Lee *et al.*, 1993) as well as cell cycle arrest in a T-cell leukaemia cell line (Nordstrom *et al.*, 1992) has also been related to inhibition of RMCE by SK&F 96365. In the latter case, the authors suggested a dual mode of action of the drug, since the effect was not influenced by the concentration of extracellular Ca^{2+}. It is well documented that prostaglandins exhibit profound modulatory activity on cell proliferative mechanisms. In mice, *in vivo* enhancement of experimental bone metastasis by recombinant human interleukin-1α is prevented by indomethacin (Arguello *et al.*, 1992) and cyclo-oxygenase inhibitors have been evaluated for their potential role in cancer chemoprevention, due to the stimulatory action of prostaglandins on growth of certain tumour cell lines (Earnest *et al.*, 1992). Furthermore, inhibition of PGE_2 synthesis by dexamethasone reduced proliferation of osteoblasts (Hughes-Fulford *et al.*, 1992) and the mitogenic response of BALB/c 3T3 fibroblasts to epidermal growth factor is abolished by indomethacin (Nolan *et al.*, 1988). It is thus likely, that effects of SK&F 96365 on cell proliferation are not or at least not solely due to diminished RMCE, but may be attributed to impaired prostaglandin synthesis by cyclo-oxygenase inhibition.

The same mechanism can be applied to the inhibitory action of the drug on platelet activation. Reduced formation of the potent proaggregatory TXB_2 certainly prevents platelet aggregation. On the other hand, blockade of RMCE also should have effects on TXB_2 levels due to lack of phospholipase A_2 activation. Again, this implies care in interpreting the experimental results. Nevertheless, the nature of SK&F 96365 as a multiple effector ligand provides the possibility of measuring cumulative effects and in combination with specific cyclo-oxygenase inhibitors, of dissociating the two mechanisms.

In summary, we conclude that the proposed inhibitor of RMCE, SK&F 96365, also blocks cyclo-oxygenase at concentrations even lower than those for blockade of RMCE (50 μM), and that some of the proposed cellular responses may be attributed to this inhibitory action and concomitant reduction of prostanoid formation.

This work was supported by grants from the Fond zur Förderung der wissenschaftlichen Forschung, Austria, project numbers P-9337 and P-10542.

References

ALONSO, M.T., ALVAREZ, J., MONTERO, M., SANCHEZ, A. & GARCIA-SANCHO, J. (1991). Agonist-induced Ca^{2+} influx into human platelets is secondary to the emptying of intracellular Ca^{2+} stores. *Biochem J.*, **280**, 783–789.

ARGUELLO, F., BAGGS, R.B., GRAVES, B.T., HARWELL, S.E., COHEN, H.J. & FRANTZ, C.N. (1992). Effect of IL-1 on experimental bone/bone marrow metastases. *Int. J. Cancer*, **52**, 802–807.

CAMPBELL, K.P., LEUNG, A.T. & SHARP, A.H. (1988). The biochemistry and molecular biology of the dihydropyridine-sensitive calcium channels. *Trends Neurosci.*, **11**, 425–430.

EARNEST, D.L., HIXSON, L.J. & ALBERTS, D.S. (1992). Piroxicam and other cyclooxygenase inhibitors: potential for cancer chemoprevention. *J. Cell. Biochem.-suppl.*, **161**, 156–166.

GUSOVSKY, F., LUEDERS, J.E., KOHN, E.C. & FELDER, C.C. (1993). Muscarinic Receptor-mediated Tyrosine Phosphorylation of Phospholipase C-gamma. *J. Biol. Chem.*, **268**, 7768–7772.

HALLAM, T.J. & RINK, T.J. (1989). Receptor-mediated Ca^{2+} entry: diversity of function and mechanism. *Trends Pharmacol. Sci.*, **10**, 8–10.

HUGHES-FULFORD, M., APPEL, R., KUMEGAWA, M. & SCHMIDT, J. (1992). Effect of dexamethasone on proliferating osteoblasts: inhibition of prostaglandin E_2 synthesis. DNA synthesis, and alterations in actin cytoskeleton. *Exp. Cell. Res.*, **203**, 150–156.

KODAMA, H., AMAGAI, Y., SUDO, S., KASAI, S. & YAMAMOTO, S. (1981). Establishment of a clonal osteogenic cell line from newborn mouse calvaria. *Jpn. J. Oral. Biol.*, **23**, 899–901.

LEE, Y.S., SAYEED, M.M. & WURSTER, R.D. (1993). Inhibition of human brain tumor cell growth by a receptor-operated Ca^{2+} channel blocker. *Cancer Lett.*, **72**, 77–81.

LEIS, H.J., HOHENESTER, E., GLEISPACH, H., MALLE, E. & MAYER, B. (1987a). Measurement of prostaglandins, thromboxanes and hydroxy fatty acids by stable isotope dilution gas chromatography/mass spectrometry. *Biomed. Environ. Mass Spectrom.*, **14**, 617–621.

LEIS, H.J., MALLE, E., MAYER, B., KOSTNER, G.M., ESTERBAUER, H. & GLEISPACH, H. (1987b). Quantitative measurement of 5-, 12-, and 15-hydroxyeicosatetraenoic acid by stable isotope dilution gas chromatography-negative ion chemical ionization mass spectrometry. *Anal. Biochem.*, **162**, 337–344.

LEIS, H.J., MALLE, E., MOSER, R., NIMPF, J., KOSTNER, G.M., ESTERBAUER, H. & GLEISPACH, H. (1986). Preparation of ^{18}O-labelled standards of hydroxy-eicosatetraenoic acids and thromboxanes for quantitative measurement by gas chromatography/mass spectrometry. *Biomed. Environ. Mass. Spectrom.*, **13**, 483–488.

LEIS, H.J., ZACH, D., HUBER, E., ZIERMANN, L., GLEISPACH, H. & WINDISCHHOFER, W. (1994). Extracellular Ca^{2+} sensing by the osteoblast-like cell line. MC3T3-El. *Cell Calcium*, **15**, 447–456.

MALLE, E., NIMPF, J., LEIS, H.J., WURM, H., GLEISPACH, H. & KOSTNER, G.M. (1987). Cyclooxygenase and lipoxygenase metabolites during platelet aggregation: quantitative measurement by negative ion chemical ionization – gas chromatography/mass spectrometry. *Prost. Leukotr. Med.*, **27**, 53–70.

MASON, M.J., MAYER, B. & MYMEL, L.J. (1993). Inhibition of Ca^{2+} transport pathways in thymic lymphocytes by econazole, miconazole, and SK&F 96365. *Am. J. Physiol.*, **264**, C654-C662.

MAYER, B., MOSER, R., LEIS, H.J. & GLEISPACH, H. (1986). Rapid separation of arachidonic acid metabolites by silicic acid chromatography for subsequent quantitative analysis by gas chromatography-mass spectrometry. *J. Chromatogr.*, **378**, 430–436.

MEDOLESI, J. & POZZAN, T. (1987). Pathways of Ca^{2+} influx at the plasma membrane: voltage-, receptor-, and second messenger operated channels. *Exp. Cell Res.*, **171**, 271–283.

MERRITT, J.E., ARMSTRONG, W.P., BENHAM, C.D., HALLAM, T.J., JACOB, R.J., JAXA-CHAMIEC, A., LEIGH, B.K., MCCARTHY, S.A., MOORES, K.E. & RINK, T.J. (1990). SK&F, 96365, a novel inhibitor of receptor-mediated calcium entry. *Biochem. J.*, **271**, 515–522.

MUSTARD, J.F., KINLOUGH-RATHBONE, R.L. & PACKHAM, M.A. (1989). Isolation of human platelets from plasma by centrifugation and washing. In *Methods in Enzymology*, Vol. 169, ed. J. Hawinger, pp. 3–11. New York: Academic press.

NOLAN, R.D., DANILOWICZ, R.M. & ELING, T.E. (1988). Role of arachidonic acid metabolism in the mitogenic response of BALB/c 3T3 fibroblasts to epidermal growth factor. *Mol. Pharmacol.*, **33**, 650–656.

NORDSTROM, T., NEVANLINNA, H.A. & ANDERSON, L.C. (1992). Mitosis-arresting effect of the calcium channel inhibitor SK&F 96365 on human leukemia cells. *Exp. Cell. Res.*, **202**, 487–494.

SCHWARZ, G., DROOGMANS, G. & NILIUS, B. (1994). Multiple effects of SK&F 96365 on ionic currents and intracellular calcium in human endothelial cells. *Cell Calcium*, **15**, 45–54.

SHEETS, J.J., MASON, J.I., WISE, C.A. & EASTABROOK, R.W. (1986). Inhibition of rat liver microsomal cytochrome P-450 steroid hydroxylase reactions by imidazole antimycotic agents. *Biochem. Pharmacol.*, **35**, 487–491.

TSIEN, R.W., LIPSCOMBE, D., MADISON, D.V., BLEY, K.R. & FOX, A.P. (1988). Multiple types of neuronal calcium channels and their selective modulation. *Trends Neurosci.*, **11**, 431–438.

WEBER, C., KRUSE, H.J., SELLMAYER, A., ERL, W. & WEBER, P.C. (1993). Platelet activating factor enhances receptor-operated Ca^{++}-influx and subsequent prostacyclin synthesis in human endothelial cells. *Biochem. Biophys. Res. Commun.*, **195**, 874–880.

ZSCHAUER, A., VAN BREEMEN, C., BÜHLER, F.R. & NELSON, M.T. (1988). Calcium channels in thrombin-activated human platelet membrane. *Nature*, **334**, 703–705.

(Received August 11, 1994
Revised October 3, 1994
Accepted October 7, 1994)

British Journal of Pharmacology (1995) 114, 602-611

Inhibition of muscarinic receptor-induced inositol phospholipid hydrolysis by caffeine, β-adrenoceptors and protein kinase C in intestinal smooth muscle

[1]S.A. Prestwich & T.B. Bolton

Department of Pharmacology and Clinical Pharmacology, St George's Hospital Medical School, Cranmer Terrace, London SW17 0RE

1 The effects of caffeine, isoprenaline, dibutyryl cyclic AMP, isobutylmethylxanthine (IBMX), 12-*O*-tetradecanoylphorbol-13-acetate (TPA) or 1-oleoyl-2-acetylglycerol (OAG), (protein kinase C (PKC) activators), 2-methoxy verapamil (D600), thapsigargin and ryanodine on muscarinic acetylcholine receptor (AChR)-stimulated inositol phospholipid hydrolysis were studied in smooth muscle fragments from the longitudinal layer of the small intestine of the guinea-pig.

2 Incubation of the fragments with the muscarinic agonist, carbachol (CCh) (100 μM) resulted in rapid increases in the levels of all the inositol phosphate isomers with maximal increases in the [^{3}H]-inositol (1,4,5) trisphosphate ([^{3}H]-Ins(1,4,5)P_3) isomer occurring 10 s following incubation.

3 The β-adrenoceptor agonist, isoprenaline (10 μM) and dibutyryl cyclic AMP (10 μM), a membrane permeant analogue of cyclic AMP both reduced the CCh stimulation, but not the basal levels of [^{3}H]-inositol phosphates. This inhibition by dibutyryl cyclic AMP was enhanced in the presence of the phosphodiesterase inhibitor, IBMX. CCh inhibited the isoprenaline-induced increases in the levels of cyclic AMP and this was via a pertussi toxin (PTX)-sensitive G-protein mechanism.

4 TPA (1 μM) and OAG (100 μM) a 1,2-diacylglycerol (DAG) analogue both reduced the CCh-induced increases in [^{3}H]-inositol phosphates levels but neither affected basal values nor the basal levels of cyclic AMP.

5 D600 (10 μM), which blocks voltage-dependent Ca^{2+} channels, also reduced the CCh-stimulated levels of [^{3}H]-inositol phosphates suggesting that some of the agonist-induced increases are due to a potentiating effect of Ca^{2+} entering the cell.

6 Caffeine (0.5-30 mM) significantly inhibited both the basal and CCh-induced increases in all the [^{3}H]-inositol phosphate isomers. Its inhibitory action was not due to increases in cyclic AMP since caffeine had no effect on the levels of cyclic AMP at concentrations up to 30 mM.

7 Incubation with thapsigargin (1 μM) and ryanodine (10 μM) had no effect on either basal or CCh-induced inositol phospholipid hydrolysis or cyclic AMP levels.

8 The results indicate a reciprocal inhibition by β-adrenoceptors and muscarinic AChRs of their effects on cyclic AMP and inositol phosphate levels respectively. Ca^{2+} entering the cell (but not the action of ryanodine or thapsigargin) potentiates while caffeine inhibits muscarinic AChR-induced rises in inositol phosphate levels. Diacylglycerols may exert a negative feedback inhibition on inositol phosphate production.

Keywords: Smooth muscle; inositol phosphates; caffeine; isoprenaline; protein kinase C; 2-methoxy verapamil (D600); cyclic AMP; pertussis toxin.

Introduction

Activation of muscarinic acetylcholine receptors (AChRs) on the longitudinal smooth muscle layer from the small intestine of the guinea-pig increases the activity of phospholipase C (PLC) via a G-protein causing inositol(1,4,5)trisphosphate (Ins(1,4,5)P_3) levels to increase (Best & Bolton, 1986; Prestwich & Bolton, 1994). The Ins(1,4,5)P_3 binds to its receptor on the sarcoplasmic reticulum (Ehrlich & Watras, 1988) which serves as a Ca^{2+} release channel and Ca^{2+} is released from stores down its concentration gradient into the cell; this contributes to the initial transient phase of contraction. Also, Ca^{2+}-induced Ca^{2+} release may be activated via ryanodine receptors on the sarcoplasmic reticulum membrane. Muscarinic AChR activation also causes receptor operated channels in the plasma membrane to open, allowing the influx of cations (mainly Na^+) (Bolton, 1979) and this activation is potentiated by Ca^{2+} released from the sarcoplasmic reticulum stores (Pacaud & Bolton, 1991). The resulting change in membrane potential triggers the opening of voltage-dependent Ca^{2+} channels resulting in Ca^{2+} influx and this contributes to the sustained phase of contraction.

Most smooth muscle relaxation is thought to occur by lowering the $[Ca^{2+}]_i$ and by dephosphorylation of myosin light chain (Gerthoffer & Murphy, 1983). Low levels of $[Ca^{2+}]_i$ are achieved following contraction by several mechanisms, reuptake of Ca^{2+} into the sarcoplasmic reticulum via Ca^{2+} ATPase, increased extrusion by the plasma membrane Ca^{2+} ATPase, Na^+-Ca^{2+} exchange, and by the closure of voltage-operated calcium channels which occurs when the membrane potential is restored or when the membrane hyperpolarizes. An increase in $[Ca]_i$ results in activation of Ca^{2+}-dependent K^+ channels which open causing the membrane to hyperpolarize and this helps to restore the membrane potential towards the resting level. Hyperpolarization caused by increases in K^+ channel activity decreases the opening of the voltage-dependent Ca^{2+} channels that control Ca^{2+} influx and contributes to relaxation. Some of these mechanisms may also contribute to the switching off of inositol phospholipid hydrolysis and thus contribute to relaxation (Quast, 1993).

Hydrolysis of inositol phospholipids produces a bifurcating pathway and 1,2-diacylglycerol (DAG) is produced at the same time as the inositol phosphates (Rana & Hokin, 1990).

[1] Author for correspondence.

The DAG (in conjunction with phosphatidylserine in the membrane) activates Ca^{2+}-dependent protein kinase Cs (PKCs) leading to phosphorylation of proteins (Nishizuka, 1992). PKC may be involved in the tonic component of the contractile response (Rasmussen *et al.* 1988). At the same time PKC may serve as a negative feedback regulator of inositol phospholipid hydrolysis thereby switching off not only the increases in inositol phosphates but also increases in DAG.

Application of caffeine to smooth muscle strips results in a transient contraction by releasing Ca^{2+} from intracellular stores (Matsumoto *et al.*, 1990). The mechanism is independent of Ins(1,4,5)P_3 release, since the effect of caffeine is not inhibited by heparin which prevents the binding of Ins(1,4,5)P_3 to its receptor (Komori & Bolton, 1991). In addition to these contractile effects, caffeine has potent relaxing ability on precontracted smooth muscles (Karaki *et al.*, 1987); it inhibits voltage-dependent Ca^{2+} channels (Hughes *et al.*, 1990); it causes hyperpolarization of the membrane (Van der Bent & Bény, 1991) and inhibits phosphodiesterase activity resulting in increases in the levels of adenosine 3':5'-cyclic monophosphate (cyclic AMP) (Butcher & Sutherland, 1962). Inhibition of Ins(1,4,5)P_3 levels have also been observed (Toescu *et al.*, 1992).

Ryanodine and thapsigargin also cause Ca^{2+} release from sarcoplasmic reticulum stores but by different mechanisms to caffeine. Ryanodine causes Ca^{2+} store depletion by maintaining the Ca^{2+} release channel in a partially open state (Fleischer *et al.*, 1985) and thapsigargin prevents the reuptake of Ca^{2+} into the sarcoplasmic reticulum by inhibiting the Ca^{2+}-ATPase pump of the sarcoplasmic reticulum (not the plasma membrane pump) in smooth muscle (Shima & Blaustein, 1992).

β-Adrenoceptors have been identified on longitudinal smooth muscle cells from the small intestine (Broadley & Grassby, 1985) and are of the β_3-adrenoceptor type (Van der Vliet *et al.*, 1990). Isoprenaline, a β-adrenoceptor agonist has been shown to cause relaxation in smooth muscle as a result of increased protein kinase A activity through increases in cyclic AMP levels (Bülbring & Tomita, 1987) due to activation of adenylyl cyclase via Gs (Iyengar & Birnbaumer, 1981). Activation of β-adrenoceptors has also been shown to result in hyperpolarization of the membrane (Sadoshima *et al.*, 1988), inhibition of Ca^{2+} influx into cells (Abe & Karaki, 1988) and activation of specific kinases (βARKs) (Richardson *et al.*, 1993).

The aim of this study was to determine the effects of drugs that might modify the muscarinic AChR-activated inositol phospholipid pathway. To do this [^{3}H]-inositol-labelled smooth muscle fragments were incubated in the presence of substances which can activate PKC, increase cyclic AMP levels, decrease $[Ca^{2+}]_i$ levels or alter the membrane potential, prior to muscarinic AChR activation. Since several of the substances used have not been shown to elevate cyclic AMP in smooth muscle from guinea-pig small intestine, changes in the levels of cyclic AMP were also determined to see if observed effects could be attributed to increases in adenylyl cyclase activity.

Methods

Preparation and assay of [^{3}H]-inositol-labelled fragments

Guinea-pigs were killed by dislocation of the neck and exsanguinated and longitudinal muscle of the small intestine removed. Contaminating circular muscle was removed and fragments (350 × 350 μm) were prepared by tissue chopping as previously described (Prestwich & Bolton, 1994). The assay for the determination of the levels of [^{3}H]-inositol phosphates was the same as described by Prestwich & Bolton (1991, 1994). Briefly, chopped fragments were incubated in Krebs Ringer buffer of the following composition (final, mM): NaCl 120, KCl 5.9, $NaHCO_3$ 15.4, NaH_2PO_4 1.2, glucose 11.5, $MgCl_2$ 1.2, $CaCl_2$ 2.5 (pH was 7.25 when equilibrated) containing [^{3}H]-inositol and kept in a humidified atmosphere containing 95% O_2/5% CO_2 at 30°C for 20 h. When treated with toxin the fragments were incubated with pertussis toxin (PTX) 6 μg ml^{-1} for 20 h at 30°C. Functional responses of contraction of the fragments to CCh could still be observed after this long incubation period.

For the assay, the tissue (about 1 mg ml^{-1}) was incubated with or without the drug at 37°C. At the end of the incubation, 500 μl 20% trichloroacetic acid and 50 μl 50 mM EDTA were added to stop the assay. The trichloroacetic acid was extracted from the supernatant with water-saturated diethyl ether (4 × 5 ml); the residual ether was removed and the pH of the samples adjusted to 7.0 with 1 M NaOH (5 μl). Protein determination was done on the pellet using the method of Lowry *et al.* (1951). The elution profiles of the labelled inositol phosphate samples were assayed by anion-exchange high performance liquid chromatography (h.p.l.c.) within 7 days using a method modified from Irvine *et al.* (1985) and Batty *et al.* (1985) and described in Prestwich & Bolton (1991). The identity of the various [^{3}H]-inositol phosphate isomers was determined by comparing their elution profiles from the h.p.l.c. with those of labelled standards (see Prestwich & Bolton, 1991). From these standards the following inositol phosphate isomers were identified: [^{3}H]-inositol monophosphates ([^{3}H]-inositol (1) phosphate and [^{3}H]-inositol (4) phosphate) (InsP_1); [^{3}H]-inositol (1,4) bisphosphate (Ins(1,4)P_2); [^{3}H]-inositol (1,3,4) trisphosphate (Ins(1,3,4)P_3); [^{3}H]-inositol (1,4,5) trisphosphate, (Ins(1,4,5)P_3) and [^{3}H]-inositol tetrakisphosphates (InsP_4). From the elution profiles obtained by other workers, the other [^{3}H]-inositol bisphosphate which is labelled sInsP_2 in the figures, is likely to be [^{3}H]-inositol (3,4) bisphosphate. After samples had been expressed as d.p.m. mg^{-1} protein, the agonist stimulated responses were compared with control values and the results expressed as % change compared to control. The effects the various agents had on basal and CCh-stimulated [^{3}H]-inositol phosphate formation were usually determined after a 10 min incubation at 37°C with the agent unless otherwise stated. Under these conditions CCh (100 μM) was added 10 s before the end of the 10 min incubation period.

Cyclic AMP determination

Smooth muscle fragments were prepared and incubated as previously described (Prestwich & Bolton, 1991) when measuring [^{3}H]-inositol phophates. Initial experiments to determine agonist responses (data not shown) were carried out in the absence of the phosphodiesterase inhibitor, isobutylmethylxanthine (IBMX) but no changes in the basal cyclic AMP levels could be seen with isoprenaline. Therefore for the cyclic AMP measurements the fragments were incubated in KRB containing 1 mM IBMX. After incubation with or without drug (for 10 min) with and without CCh, (100 μM) 10 s before the end, the reaction was stopped with 10% (final) trichloroacetic acid. The trichloroacetic acid was removed by diethyl ether extraction, the samples neutralized, lyophilized and reconstituted in water. The cyclic AMP formed was determined by competition binding assay with a radiolabelled kit from Amersham International Ltd. The results are expressed as either pmol mg^{-1} protein or % change compared to control.

Materials

1-Oleoyl-2-acetylglycerol (OAG), ryanodine, thapsigargin, 12-*O*-tetradecanoylphorbol-13-acetate (TPA) and pertussis toxin (PTX) were obtained from Calbiochem. [^{3}H]-inositol and the [^{3}H]-cyclic AMP assay kit were obtained from Amersham International Ltd. [^{3}H]-inositol contained a PT6 tablet which

absorbed any radiolysis products, which meant no purification of the label was necessary before use. All the other chemicals and drugs were obtained from either Sigma Chemical Co. Ltd or BDH.

Data analysis

The average protein concentration in mg/tube was 1.1 ± 0.02 ($n = 20$). The data are expressed as the mean ± s.e. mean % change over control of at least three paired experiments performed on different occasions. Intra-assay variance was very small and highly significantly less ($P<0.001$) than the variance between guinea-pigs. Tests of pair differences from zero were therefore applied. The statistical significance was assessed by use of a Student's t test. P values that were less than 0.05 were considered to be significant. Calculations were performed using the computer programme INSTAT (GraphPAD software, U.S.A.).

Results

It was found previously, using the experimental protocol adopted here, that the maximum increase in the [^{3}H]-Ins(1,4,5)P_3 isomer during muscarinic AChR activation with a concentration of 100 μM CCh occurs at 10 s following application and thereafter the level returns towards the basal value (Prestwich & Bolton, 1994). Also, Konno & Takayanagi (1989) showed that 100 μM CCh was the concentration required to obtain a maximal release of Ca^{2+} from the sarcoplasmic reticulum for the guinea-pig ileum at 37°C. Therefore drugs were usually applied for the 10 min prior to application of 100 μM CCh for 10 s to determine the effects on CCh-induced increases in [^{3}H]-inositol phosphates.

Caffeine

Incubation of the smooth muscle fragments with 20 or 30 mM caffeine for 5 or 10 min caused a time-dependent decrease in the basal levels of all [^{3}H]-inositol phosphates (Figure 1). However, 1 min after application of caffeine a very small increase in the basal levels of all of the [^{3}H]-inositol phosphates except [^{3}H]-InsP_1 and [^{3}H]-sInsP_2 occurred when compared to control. A 10 min incubation in either 20 or 30 mM caffeine significantly reduced basal levels of all the [^{3}H]-inositol phosphates (Figure 1). Concentrations of caffeine of 3 mM or more have been shown to release Ca^{2+} from intracellular stores; however, when smooth muscle fragments were incubated with different concentrations of caffeine from 0.5 mM to 20 mM for 10 min, although a small increase in levels of some [^{3}H]-inositol phosphates was seen at the lower concentrations of caffeine (0.5–1 mM), at higher concentrations (10 and 20 mM) there was a concentration-dependent decrease in basal levels of [^{3}H]-inositol phosphates (Figure 2). These effects of caffeine were not altered in the presence of 0.5 μM atropine, a concentration which inhibited more than 95% of the CCh-stimulated increases in the levels of the [^{3}H]-inositol phosphates in these fragments.

The presence of increasing concentrations of caffeine from 0.5 mM to 20 mM, prior to addition of the CCh, significantly inhibited in a concentration-dependent manner the CCh-induced increases (10 s, 100 μM) in the levels of [^{3}H]-inositol phosphates (Figure 3). A 10 min incubation in the presence of 0.5 mM caffeine inhibited the CCh-induced production of [^{3}H]-Ins(1,4,5)P_3 by 34% and a 10 min incubation with 20 mM caffeine the CCh-induced production of all the [^{3}H]-inositol phosphates by ≥95% (Figure 3).

Ryanodine (10 μM, 10 min) or thapsigargin (1 μM, 10 min) at concentrations shown to deplete Ca^{2+} stores in smooth muscle (Hisayama *et al.* 1990; Low *et al.* 1991) had no effect

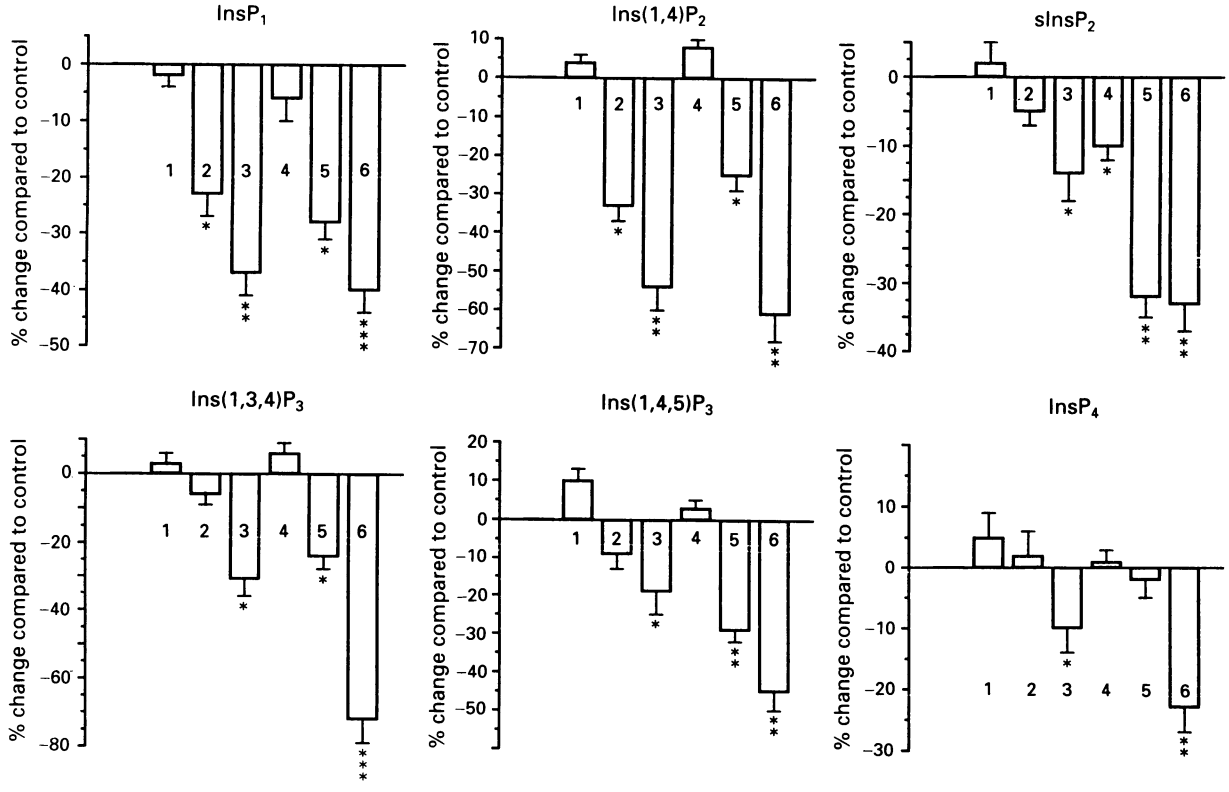

Figure 1 The effect of incubation in caffeine for different times on basal levels of [^{3}H]-inositol phosphates. [^{3}H]-inositol-labelled smooth muscle fragments were incubated with 20 mM caffeine for 1 min **(1)**, 5 min **(2)** or 10 min **(3)** or incubated with 30 mM caffeine for 1 min **(4)**, 5 min **(5)** or 10 min **(6)**. Results represent the mean ± s.e. mean of three experiments performed on separate occasions and are expressed as the % change in [^{3}H]-inositol phosphates compared to control where the control is in the absence of caffeine. $*P<0.05$, $**P<0.01$, $***P<0.001$.

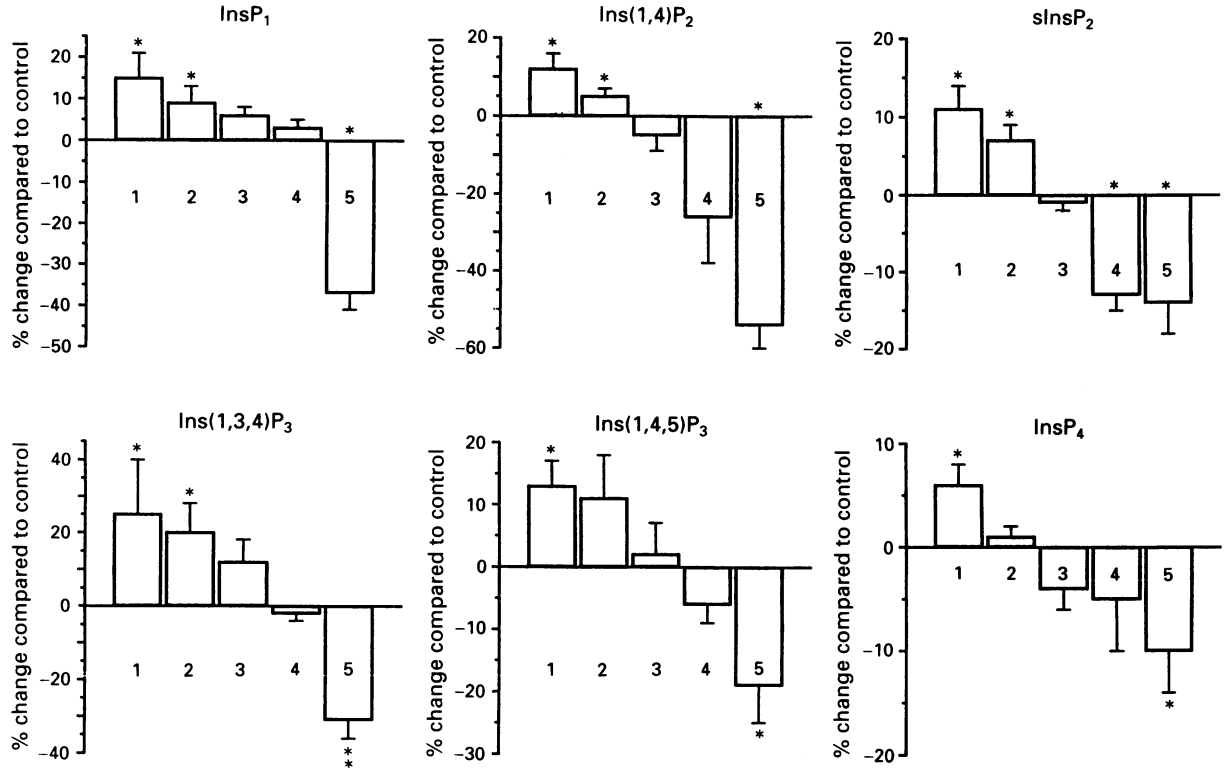

Figure 2 The effect of caffeine at various concentrations on basal levels of [^{3}H]-inositol phosphates. [^{3}H]-inositol-labelled smooth muscle fragments were incubated with 0.5 mM **(1)**, 1 mM **(2)**, 3 mM **(3)**, 10 mM **(4)**, and 20 mM **(5)** caffeine for 10 min. Results represent the mean ± s.e. mean of three experiments performed on separate occasions and are expressed as the % change in [^{3}H]-inositol phosphates compared to control where the control is in the absence of caffeine.

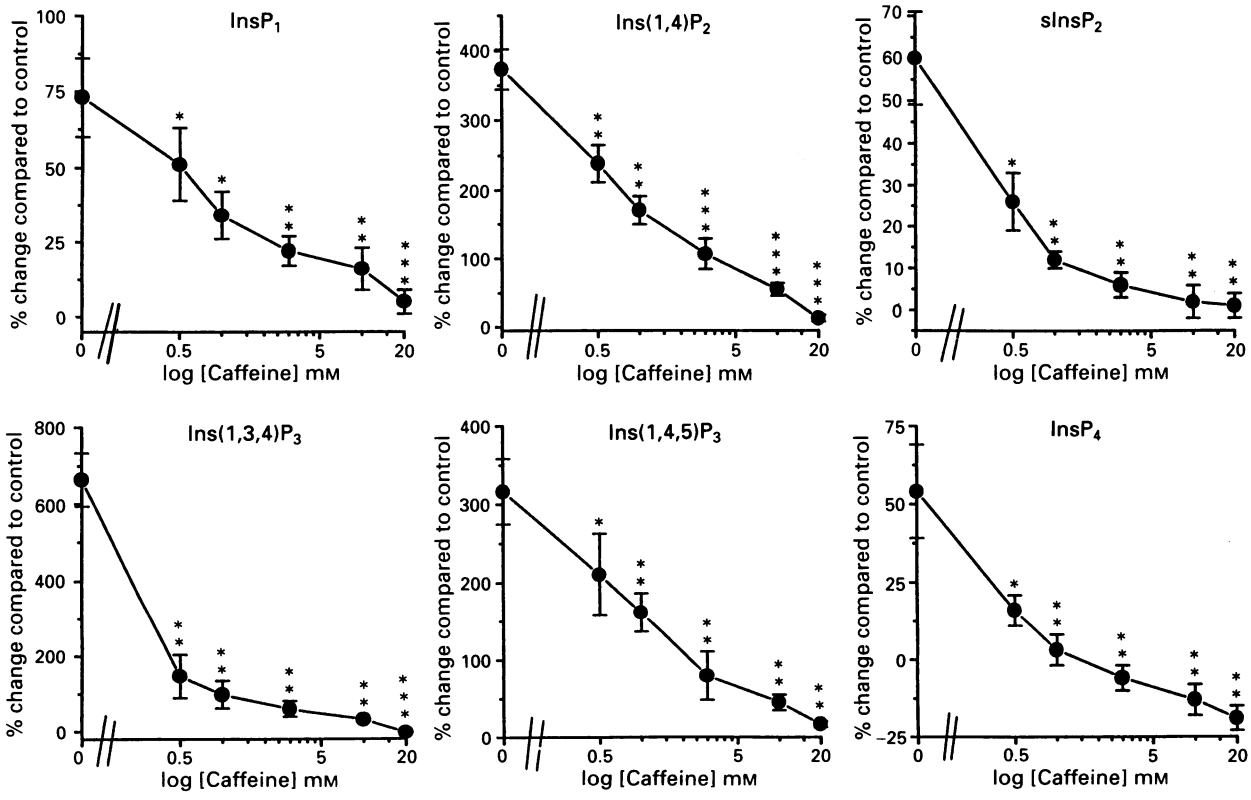

Figure 3 The effect of caffeine on the carbachol (CCh)-induced increases in [^{3}H]-inositol phosphates. [^{3}H]-inositol-labelled smooth muscle fragments were incubated in the presence of different concentrations of caffeine for 10 min. CCh (100 μM) was added for 10 s before the end and the reaction stopped. Results represent the mean ± s.e. mean of three experiments performed on separate occasions and are expressed as the % change in [^{3}H]-inositol phosphate compared to control and except when caffeine was absent, the values were calculated from the formula $((Y-X)/X) \times 100\%$ where X is the d.p.m. in the presence of caffeine alone and Y is the d.p.m. in the presence of caffeine and CCh. When caffeine was absent Y and X are the d.p.m. in the presence and absence of CCh respectively.

on either the basal (6.3 ± 2.6% change compared to control) or CCh-induced increase in the levels of [^{3}H]-inositol phosphates.

β-Adrenoceptor activation

Incubation with the β-adrenoceptor agonist, isoprenaline (10 μM, 10 min) had no significant effect on the basal levels of [^{3}H]-inositol phosphates (5.3 ± 3.4% decrease compared to control). However, incubation with isoprenaline prior to application of CCh (100 μM) for 10 s resulted in a significant decrease in the CCh-induced increases in the levels of all the [^{3}H]-inositol phosphates compared to CCh alone (Figure 4). Since isoprenaline increases the levels of cyclic AMP in smooth muscle and other tissues (Iyengar & Birnbaumer, 1981) fragments were incubated with a cyclic AMP analogue, dibutyryl cyclic AMP (10 μM, 10 min) under the same conditions as for isoprenaline and this also reduced the CCh-stimulation of [^{3}H]-inositol phosphates by almost the same amount (Figure 4). IBMX (1 mM) alone caused a small inhibition of the CCh effects on labelled inositol phosphates (Figure 4). When smooth muscle fragments were incubated in the presence of dibutyryl cyclic AMP (10 μM) plus IBMX (1 mM) the response of most isomers to CCh was almost completely inhibited (Figure 4).

Protein kinase C

To determine whether increased PKC activity, which may occur following muscarinic AChR activation and inositol phospholipid hydrolysis, could affect the CCh-induced increases in the levels of the [^{3}H]-inositol phosphates, fragments were incubated with the phorbol ester, TPA. Incubation of smooth muscle fragments for 10 min with TPA (1 μM) had no effect on basal release of [^{3}H]-inositol phosphates (data not shown) but significantly inhibited the time-dependent increases in the levels of [^{3}H]-inositol phosphates seen in the presence of CCh (100 μM) (Figure 5) (at least $P<0.05$ at all time points). A 10 min incubation with TPA prior to application of CCh for 10 s, also significantly inhibited increases in the levels of all the [^{3}H]-inositol phosphates produced by 0.1–100 μM CCh (Figure 6). When smooth muscle fragments were incubated for 2 h with TPA (1 μM) prior to addition of CCh, the inhibition of CCh-induced increases in levels of [^{3}H]-inositol phosphates was greater (Table 1). Incubation with the DAG analogue, OAG (100 μM), for either 10 min or 2 h resulted in similar inhibitions of CCh-induced increases in the levels of [^{3}H]-inositol phosphates as seen with TPA (Table 1).

2-Methoxyverapamil (D600)

Incubation of the smooth muscle fragments with the voltage-dependent Ca^{2+} channel antagonist D600 (10 μM) for 10 min prior to addition of CCh (100 μM) significantly reduced the early (2 s to 120 s) CCh-stimulated increases in the levels of all the [^{3}H]-inositol phosphates (Figure 7). The peak CCh-induced response of [^{3}H]-Ins(1,4,5)P_3 was significantly inhibited by 41% at 10 s ($P<0.05$) and by 62% at 2 min ($P<0.05$).

Cyclic AMP measurements

IBMX (1 mM, 10 min) increased the basal levels of cyclic AMP from 2.01 ± 0.26 pmol mg^{-1} protein to 36 ± 2.7 pmol mg^{-1} protein ($n = 5$). Changes in basal cyclic AMP levels

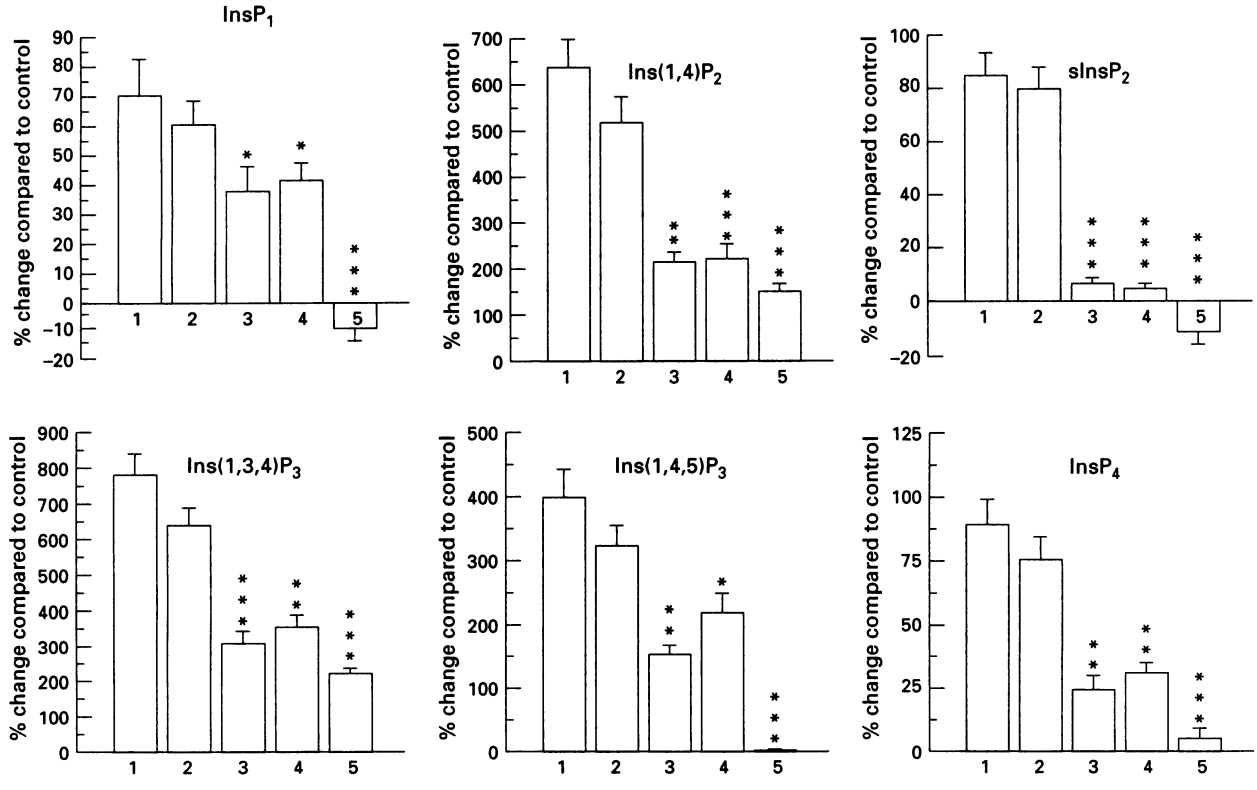

Figure 4 The effect of isobutylmethylxanthine (IBMX), isoprenaline, dibutyryl cyclic AMP and dibutyryl cyclic AMP with IBMX on levels of [^{3}H]-inositol phosphates in carbachol (CCh). [^{3}H]-inositol-labelled smooth muscle fragments were incubated for 10 min in the absence or presence of either isoprenaline, dibutyryl cyclic AMP or dibutyryl cyclic AMP with IBMX; 10 s before the end of the incubation period 100 μM CCh was added for 10 s and the reaction stopped. The histograms represent **(1)** CCh alone, **(2)** 1 mM IBMX plus CCh, **(3)** 1 μM isoprenaline plus CCh, **(4)** 10 μM dibutyryl cyclic AMP plus CCh, **(5)** 10 μM dibutyryl cyclic AMP with 1 mM IBMX plus CCh. Results represent the mean ± s.e. mean of three experiments performed on separate occasions and are expressed as the % change compared to control, where the control is taken as the value in the absence of CCh and in the presence of drug. Isoprenaline, IBMX alone, dibutyryl-cyclic AMP and dibutyryl-cyclic AMP plus IBMX had no effect on the basal production of [^{3}H]-inositol phosphates (data not shown).

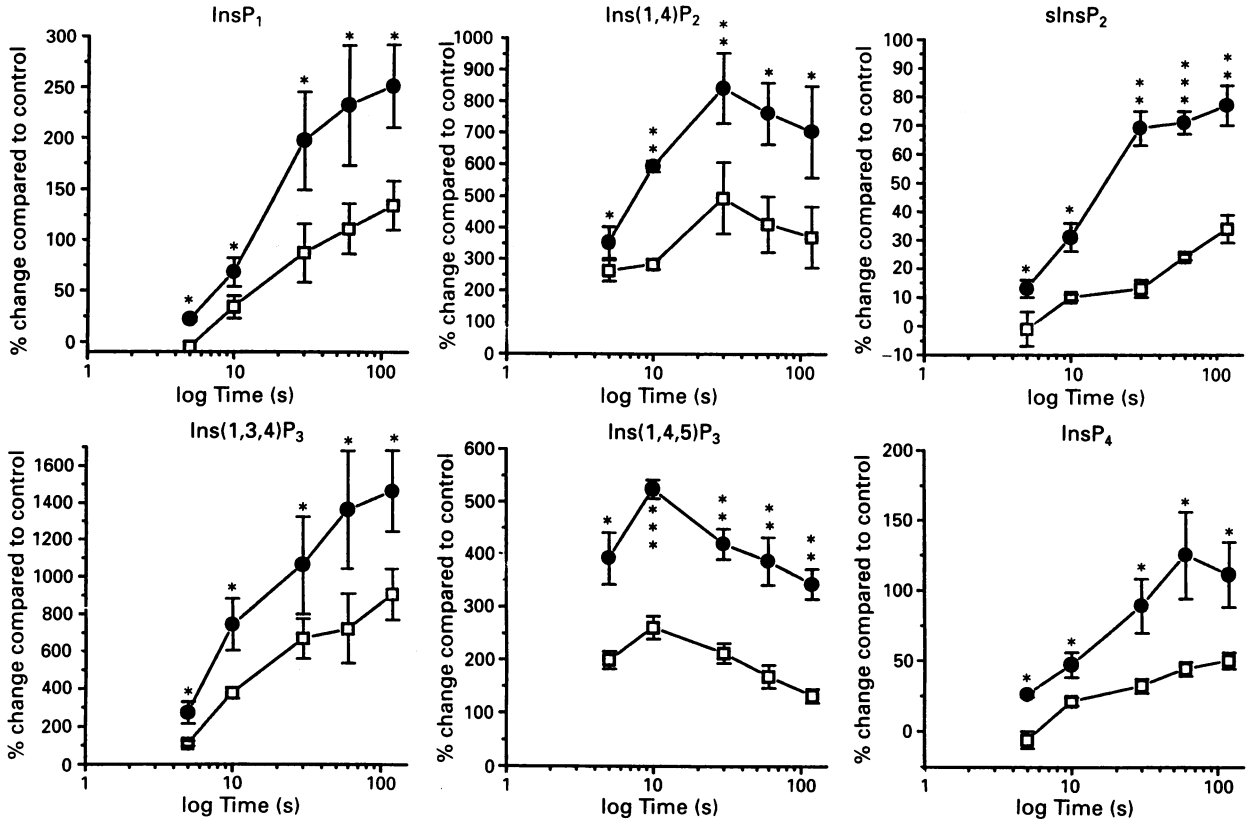

Figure 5 The effect of 12-O-tetradecanoylphorbol-13-acetate (TPA) on the time course of carbachol (CCh)-induced increases in the levels of [^{3}H]-inositol phosphates. [^{3}H]-inositol-labelled smooth muscle fragments were incubated for 10 min in the absence or presence of 1 μM TPA. CCh (100 μM) was added for either 5 s, 10 s, 30 s, 60 s or 120 s before the end of the incubation. Results are shown as the time-dependent increases in [^{3}H]-inositol phosphates in the presence of CCh alone (●) or in the presence of CCh plus TPA (□). TPA had no effect on the basal levels of [^{3}H]-inositol phosphates. Results represent the mean ± s.e. mean of three experiments performed on separate occasions and are expressed as the % change in [^{3}H]-inositol phosphates compared to control where the control is in the absence of CCh.

could not be detected in the presence of several different substances including isoprenaline, in the absence of IBMX. Therefore all experiments were performed with IBMX in the incubation buffer. Under these conditions isoprenaline (10 μM) increased the levels of cyclic AMP by 335 ± 43% ($n = 5$). CCh (100 μM, 10 min) had no significant effect on the basal levels of cyclic AMP (28.9 ± 6.7 pmol mg^{-1} protein) but significantly reduced the isoprenaline-induced increases by 44.8 ± 5.3% ($P<0.05$, $n = 5$). Treatment with PTX (6 μg ml^{-1} 20 h at 30°C) did not affect the basal levels of cyclic AMP but prevented the CCh-induced inhibition of isoprenaline-induced increases in cyclic AMP levels.

The effects of several other substances (under conditions where inhibition of CCh-induced increases in the levels of [^{3}H]-inositol phosphates had been observed) on the basal levels of cyclic AMP and in the presence of CCh (100 μM) were measured. However, caffeine (up to 30 mM), TPA (1 μM), D600 (10 μM) and aluminium fluoride (10 μM aluminium chloride and 10 mM sodium fluoride) had no effect on the basal levels of cyclic AMP in the presence or absence of IBMX and had no effect on the levels of cyclic AMP in the presence of CCh (100 μM).

Discussion

Except for thapsigargin and ryanodine, the substances used in this study inhibited the CCh-induced increases in the levels of all the [^{3}H]-inositol phosphates. However, only caffeine, or dibutyryl cyclic AMP in the presence of IBMX, could completely inhibit the effects of CCh and only caffeine affected the basal levels of the [^{3}H]-inositol phosphates.

Depletion of Ca^{2+} from the stores is unlikely to account for inhibition by caffeine of basal or agonist-induced changes in levels of [^{3}H]-inositol phosphates since neither thapsigargin nor ryanodine had any effects on [^{3}H]-inositol phosphate levels. The decrease in the basal levels of [^{3}H]-inositol phosphates by caffeine (Figures 1 and 2) may be due to its ability to inhibit PLC directly. However, the small increase in basal levels after 1 min incubation with caffeine may be due to the transient increase in $[Ca^{2+}]_i$ caused by the release of Ca^{2+} from sarcoplasmic reticulum stores. This small increase in $[Ca^{2+}]_i$ may be sufficient to increase the basal activity of PLC and may also be sufficient to activate Ca^{2+}-dependent K^+ channels in the plasma membrane which would result in hyperpolarization. This has recently been shown to inhibit agonist-induced inositol phospholipid hydrolysis (Yamagishi *et al.*, 1992; Yanagisawa *et al.*, 1993). Caffeine has been shown to induce a transient contraction in coronary artery smooth muscle followed by a sustained relaxation which occurs simultaneously with the relaxation caused by a hyperpolarization of the membrane (Van der Bent & Bény, 1991).

Isoprenaline causes hyperpolarization of smooth muscle through cyclic AMP-dependent protein kinase (Kume *et al.*, 1989) or directly via the α subunit of Gs (Scornik *et al.*, 1993). K^+-channel opening drugs which have been shown to inhibit agonist-induced inositol phosphate increases (Yamagishi *et al.* 1992), also cause hyperpolarization of the membrane and relaxation which is independent of changes in cellular cyclic nucleotide concentrations (Berry *et al.* 1991). So, hyperpolarization may be a major mechanism by which various substances may inhibit CCh-induced inositol phospholipid hydrolysis.

Although caffeine has been shown to inhibit phospho-

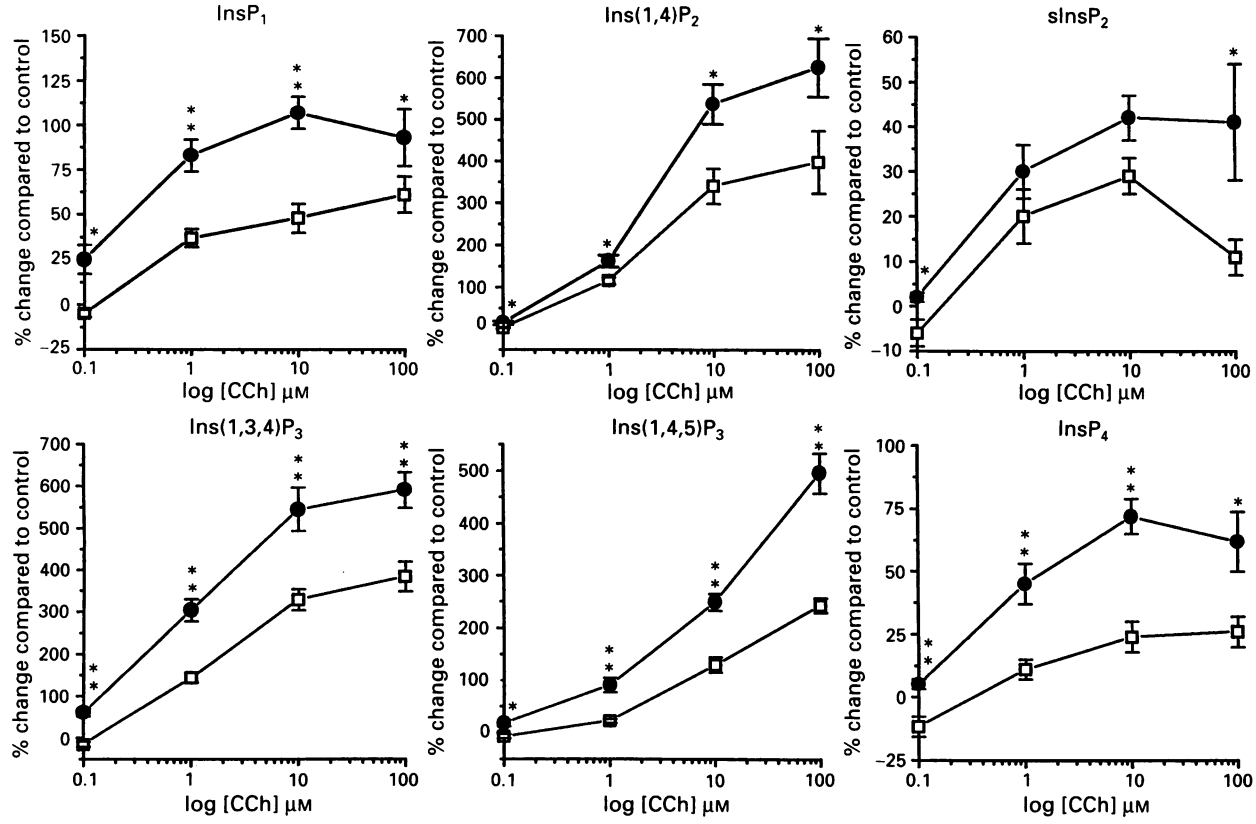

Figure 6 The effect of 12-O-tetradecanoylphorbol-13-acetate (TPA) on concentration-response curve to carbachol (CCh). [^{3}H]-inositol-labelled smooth muscle fragments were incubated in the absence or presence of 1 μM TPA for 10 min; 10 s before the end of the incubation period either 0.1 μM, 1 μM, 10 μM, or 100 μM CCh was added for 10 s and the incubation stopped. Results are shown in the presence of CCh alone (●), or CCh plus TPA (□). Results represent the mean ± s.e. mean of three experiments performed on separate occasions and are expressed as the % change in [^{3}H]-inositol phosphates compared to control where the control is in the absence of CCh.

diesterase activity (Butcher & Sutherland, 1962) thereby increasing the levels of cyclic AMP, this was not how caffeine inhibited the levels of [^{3}H]-inositol phosphates in this muscle. Under conditions where caffeine completely inhibited the CCh-induced increases in [^{3}H]-inositol phosphates it had no effect on the levels of cyclic AMP, when assayed either in the presence or absence of the phosphodiesterase inhibitor, IBMX. Thus, it may also be that caffeine can inhibit PLC activity directly.

However, when increases in the levels of cyclic AMP do occur, these may contribute to the observed inhibition of CCh-induced increases in the levels of [^{3}H]-inositol phosphates. Isoprenaline increased the levels of cyclic AMP in this study. Cyclic AMP has been shown to decrease $[Ca^{2+}]_i$ as a result of hyperpolarization due to stimulation of Ca^{2+}-activated K^+ channel opening (Sadoshima *et al.*, 1988), inhibition of Ca^{2+} influx into cells (Abe & Karaki, 1988), increased Ca^{2+} extrusion from cells through stimulation of the membrane Ca^{2+}-pump (Bülbring & den Hertog, 1980) and increased Ca^{2+} uptake into intracellular stores (Saida & Van Breemen, 1984). However, functional antagonism and crosstalk have been shown to occur following muscarinic AChR and β-adrenoceptor activation (Roffel *et al.*, 1993). The ability of isoprenaline to relax tone due to muscarinic AChR activation has been shown to be increased following treatment with PTX (Mitchell *et al.*, 1993), possibly due to loss of CCh inhibition of isoprenaline-induced increases in cyclic AMP following treatment with PTX. It is possible that the isoprenaline inhibition of CCh-induced inositol phospholipid hydrolysis may have been greater following PTX treatment, but this was not tested.

The membrane permeable analogue of cyclic AMP, dibutyryl cyclic AMP, also reduced CCh-stimulated [^{3}H]-inositol phosphate levels. The addition of IBMX (1 mM) which is a phosphodiesterase inhibitor (Smellie *et al.* 1979) with dibutyryl cyclic AMP resulted in a further inhibition. This suggests that when the hydrolysis of endogenous cyclic AMP is inhibited, a further increase of cyclic AMP inside the cell (from dibutyryl cyclic AMP) is enough to completely inhibit increases in [^{3}H]-inositol phospholipid levels following CCh-induced stimulation. However, direct inhibition of PLC acitivity by phosphodiesterase inhibitors has also been shown (Hall *et al.*, 1990) and non specific effects of the dibutyryl moiety have been suggested to occur in smooth muscle (Bülbring & Hardman, 1975). IBMX is a non selective phosphodiesterase inhibitor and inhibits cyclic GMP-dependent phosphodiesterase as well. However, the levels of cyclic GMP were not measured in this study.

β-Adrenoceptor activation, however, also increases the activity of β-adrenoceptor kinases (βARKs) and in the presence of βγ subunits they may phosphorylate the muscarinic AChR or the G-proteins involved in inositol phospholipid hydrolysis serving to uncouple the receptor from the G-protein (Richardson *et al.*, 1993). Other protein kinases exist distinct from β-ARK, PKC or other putative second messenger regulated kinases, which can phosphorylate the m3 AChR in CHO transfected cells (Tobin & Nahorski, 1993).

TPA can substitute for DAG in the activation of PKC even in the absence of increases in $[Ca^{2+}]_i$ (Castagna *et al.*, 1982) and inhibition of agonist-induced inositol phosphate formation in smooth muscle by phorbol esters has been shown (Olianas & Onali, 1993). Although in some studies activation of PKC has been shown to increase the levels of cyclic AMP (Katada *et al.*, 1985; Yoshimasa *et al.*, 1987) TPA had no effect on cyclic AMP levels in this study. Several

Table 1 Average percentage inhibition of the effects of a 10 s stimulation with 100 μM carbachol (CCh) on [^{3}H]-inositol phosphate formation following (**a**) a 10 min incubation with 1 μM TPA (**b**) a 2 h incubation with 1 μM TPA (**c**) a 10 min incubation with 100 μM OAG and (**d**) a 2 h incubation with 100 μM OAG

	(a) 10 min TPA + CCh ($n = 3$)	(b) 2 h TPA + CCh ($n = 2$)	(c) 10 min OAG + CCh ($n = 3$)	(d) 2 h OAG + CCh ($n = 2$)
[^{3}H]-$InsP_1$	55**	91	54*	84
[^{3}H]-$Ins(1,4)P_2$	42**	72	23*	62
[^{3}H]-$sInsP_2$	33*	52	25*	65
[^{3}H]-$Ins(1,3,4)P_3$	53*	79	42*	74
[^{3}H]-$Ins(1,4,5)P_3$	77**	92	55*	89
[^{3}H]-$InsP_4$	76**	88	52*	86

*$P<0.05$ and **$P<0.01$. For abbreviations, see text.

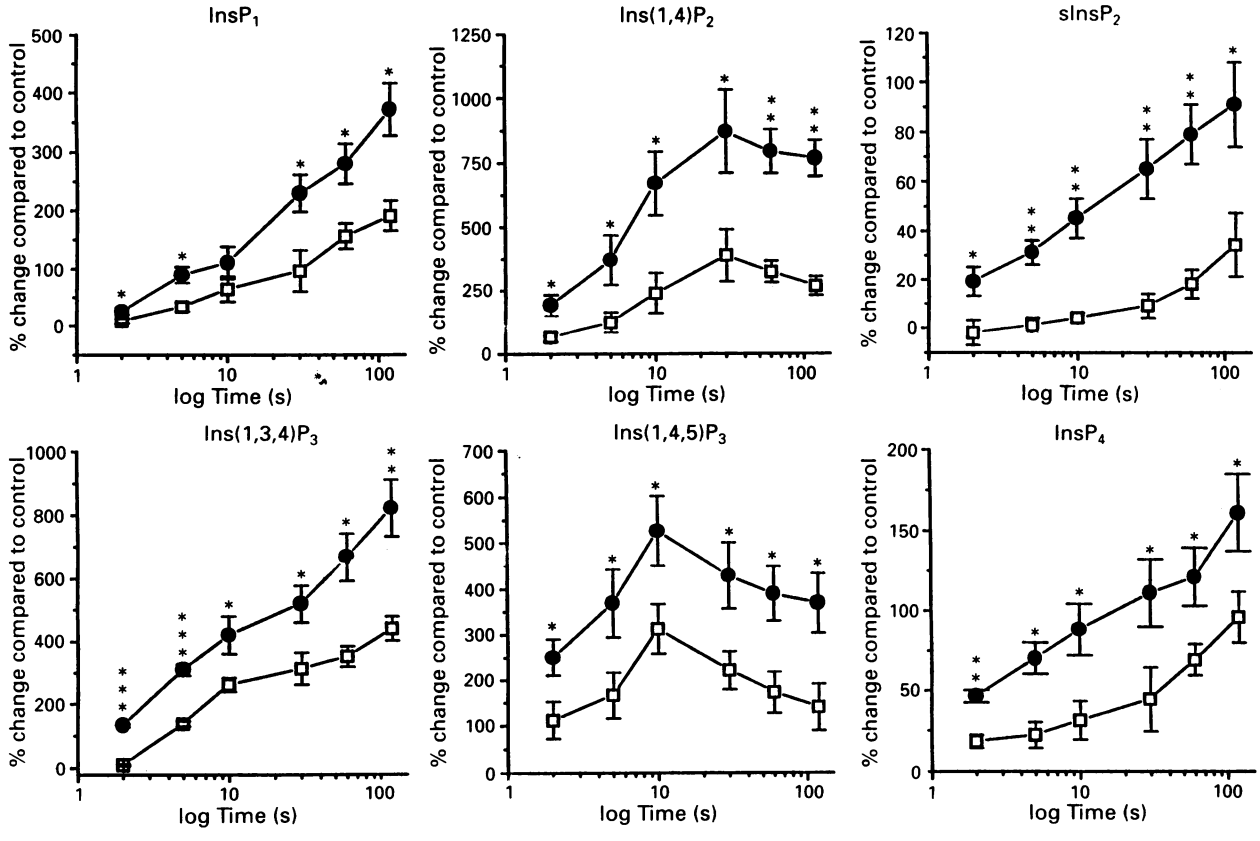

Figure 7 The effect of 2-methoxyverapamil (D600) on the carbachol (CCh)-induced increases in levels of [^{3}H]-inositol phosphates. [^{3}H]-inositol-labelled smooth muscle fragments were incubated in the absence or presence of 10 μM D600 for 10 min; 100 μM CCh was added at 2 s, 5 s, 10 s, 30 s, 60 s or 120 s before the end of incubation. Results are shown in the presence of CCh alone (●) or CCh plus D600 (□). Results represent the mean ± s.e. mean of three experiments performed on separate occasions and are expressed as the % change in [^{3}H]-inositol phosphates compared to control where the control is in the absence of CCh.

other effects of PKC activation could have contributed to the inhibition of the CCh effects: for example, phosphorylation of muscarinic AChRs resulting in desensitization of muscarinic AChR-mediated stimulation of inositol phospholipid hydrolysis and internalization of receptors (Orellana *et al.*, 1985; Creazzo & Wreen, 1988) or phosphorylation of PLCβ (Ryu *et al.*, 1990). Phorbol esters have also been shown to inhibit agonist-induced contraction (Holzer & Lippe, 1989) and decrease CCh-induced increases in $[Ca^{2+}]_i$ in several smooth muscles (Sasaguri & Watson, 1990; Mitsui & Karaki, 1993). It was suggested that this may occur via a direct inhibition of inositol phosphates or via activation of Na^+-K^+-ATPase resulting in membrane hyperpolarization and inhibition of voltage-dependent Ca^{2+} channels. However, the direct inhibition of Ca^{2+} channels by phorbol esters has also been reported (Sherman *et al.*, 1989).

Potentiation of the inositol phosphate responses due to Ca^{2+} influx (Sladeczek *et al.*, 1988) suggests that the effect of D600 on the levels of [^{3}H]-inositol phosphates measured during CCh-stimulation could be via its block of voltage-dependent Ca^{2+} channels and thereby inhibition of Ca^{2+} influx. Therefore some of the inhibition of CCh-induced increases in the levels of [^{3}H]-inositol phosphates by caffeine, PKC, D600 and isoprenaline, may also result from the inhibition of voltage-dependent Ca^{2+} channels and of Ca^{2+} influx either directly or as a result of hyperpolarization. However in permeabilized portal vein, D600 has also been suggested to uncouple the G-protein/PLC interaction (Kobayashi *et al.*, 1991).

Previous studies suggested that a major mechanism regulating muscarinic AChR-induced increases in inositol phospholipid turnover in this smooth muscle was via G-protein α and βγ subunits (Prestwich & Bolton, 1994). However changes in the levels of $[Ca^{2+}]_i$, membrane potential changes and alterations due to activation of protein kinases may also have important regulatory functions.

The authors thank the MRC for financial support.

References

ABE, A. & KARAKI, H. (1988). Mechanisms underlying the inhibitory effect of dibutyryl cAMP in vascular smooth muscle. *Eur. J. Pharmacol.*, **211**, 305–311.

BATTY, I.H., NAHORSKI, S.R. & IRVINE, R.F. (1985). Rapid formation of inositol 1,3,4,5-tetrakisphosphate following muscarinic receptor stimulation of rat cerebral cortical slices. *Biochem. J.*, **232**, 211–215.

BERRY, J.L., ELLIOTT, K.R., FOSTER, R.W., GREEN, K.A., MURRAY, M.A. & SMALL, R.C. (1991). Mechanical biochemical and electrophysiological studies of RP 49356 and cromakalin in guinea pig and bovine trachealis muscle. *Pulm. Pharmacol.*, **4**, 91–98.

BEST, L. & BOLTON, T.B. (1986). Depolarization of guinea-pig visceral smooth muscle causes hydrolysis of inositol phospholipids. *Naunyn-Schmied. Arch. Pharmacol.*, **333**, 78–82.

BOLTON, T.B. (1979). Mechanisms of action of transmitters and other substances on smooth muscle. *Physiol. Rev.*, **59**, 606–718.

BROADLEY, K.J. & GRASSBY, P.F. (1985). Alpha- and beta-adrenoceptor-mediated responses of the guinea-pig ileum and the effects of neuronal uptake inhibition. *Naunyn-Schmeid. Arch. Pharmacol.*, **331**, 316–323.

BÜLBRING, E. & DEN HERTOG, A. (1980). The action of isoprenaline on the smooth muscle of the guinea-pig taenia coli. *J. Physiol.*, **304**, 277–296.

BÜLBRING, E. & HARDMAN, J.H. (1975). Effects on smooth muscle of nucleotides and the dibutyryl analogues of cyclic nucleotides. In *Smooth Muscle Pharmacology & Physiology*. Vol. 50, pp. 114–120. ed. Worcel, M. & Vassort, G. Paris: INSERM.

BÜLBRING, E. & TOMITA, T. (1987). Catecholamine action in smooth muscle. *Pharmacol. Rev.*, **39**, 49–96.

BUTCHER, R.W. & SUTHERLAND, E.W. (1962). Adenosine 3'5'-phosphate in biological materials. *J. Biol. Chem.*, **237**, 1244–1250.

CASTAGNA, M., TAKAI, Y., KAIBUCHI, K., SANO, K., KIKKAWA, U. & NISHIZUKA, Y. (1982). Direct activation of calcium-activated, phospholipid-dependent protein kinase by tumour-promoting phorbol esters. *J. Biol. Chem.*, **251**, 7847–7851.

CREAZZO, T.L. & WREEN, R.W. (1988). Increased muscarinic receptor binding in heart membranes by an inhibitor of protein kinase C. *FEBS Lett.*, **242**, 175–177.

EHRLICH, B.E. & WATRAS, J. (1988). Inositol 1,4,5-trisphosphate activates a channel from smooth muscle sarcoplasmic reticulum. *Nature*, **336**, 583–586.

FLEISCHER, S., OGUNBUNMI, E.M., DIXON, M.D. & FLEER, E.A.M. (1985). Localisation of Ca^{2+} release channels with ryanodine in junctional terminal cisternae of sarcoplasmic reticulum of fast skeletal muscle. *Proc. Natl. Acad. Sci. U.S.A.*, **82**, 7256–7259.

GERTHOFFER, W.T. & MURPHY, R.A. (1983). Ca^{2+}, myosin phosphorylation, and relaxation of arterial smooth muscle. *Am. J. Physiol.*, **245**, C271–C277.

HALL, I.P., DONALDSON, J. & HILL, S.J. (1990b). Modulation of carbachol-induced inositol phosphate formation in bovine tracheal smooth muscle by cyclic AMP phosphodiesterase inhibitors. *Biochem. Pharmacol.*, **39**, 1357–1363.

HISAYAMA, T., TAKAYANAGI, I. & OKAMOTO, Y. (1990). Ryanodine reveals multiple contractile and relaxant mechanisms in vascular smooth muscle: simultaneous measurements of mechanical activity and of cytoplasmic free Ca^{2+} level with fura-2. *Br. J. Pharmacol.*, **100**, 677–684.

HOLZER, P. & LIPPE, TH. (1989). Protein kinase C may regulate the tonic component of intestinal smooth muscle contraction in response to substance P. *Naunyn-Schmied. Arch. Pharmacol.*, **339**, 214–220.

HUGHES, A.D., HERING, S. & BOLTON, T.B. (1990). The action of caffeine on inward barium current through voltage-dependent calcium channels in single rabbit ear artery cells. *Pflügers Arch.*, **416**, 462–466.

IRVINE, R.F., ÄNGGÄRD, E.E., LETCHER, A.J. & DOWNES, C.P. (1985). Metabolism of inositol 1,4,5-trisphosphate and inositol 1,3,4-trisphosphate in rat parotid glands. *Biochem. J.*, **229**, 505–511.

IYENGAR, R. & BIRNBAUMER, L. (1981). Hysteretic activation of adenylyl cyclases I. Effect of Mg ion on the rate of activation by guanine nucleotides and fluoride. *J. Biol. Chem.*, **256**, 11036–11041.

KARAKI, H., AHN, H.Y. & URAKAWA, N. (1987). Caffeine-induced contraction in vascular smooth muscle. *Arch. Int. Pharmacodyn.*, **285**, 60–71.

KATADA, T., GILMAN, A.G., WATANABE, Y., BAUER, S. & JAKOBS, K.H. (1985). Protein kinase C phosphorylates inhibitory guanine-nucleotide-binding regulatory component and apparently suppresses its function in hormonal inhibition of adenylate cyclase. *Eur. J. Biochem.*, **151**, 431–437.

KOBAYASHI, S., GONG, M.C., SOMLYO, A.V. & SOMLYO, A.P. (1991). Ca^{2+} channel blockers distinguish between G-protein-coupled pharmacomechanical Ca^{2+} release and Ca^{2+} sensitization. *Am. J. Physiol.*, **260**, C364–C370.

KOMORI, S. & BOLTON, T.B. (1991). Calcium release induced by inositol 1,4,5-trisphosphate in single rabbit intestinal smooth muscle cells. *J. Physiol.*, **433**, 495–517.

KONNO, F. & TAKAYANAGI, I. (1989). Relationship between the contractile responses and their coupling second messenger systems for muscarinic drugs in the guinea pig ileal longitudinal muscle. *Arch. Int. Pharmacodyn.*, **301**, 15–29.

KUME, H., TAKAI, A., TOKUMO, H. & TOMITA, T. (1989). Regulation of Ca^{2+}-dependent K^+ channel activity in tracheal myocytes by phosphorylation. *Nature*, **341**, 152–154.

LOW, A.M., GASPAR, V., KWAN, Y., DARBY, P.J., BOURREAU, J.P. & DANIEL, E.E. (1991). Thapsigargin inhibits repletion of phenylephrine-sensitive intracellular calcium pool in vascular smooth muscle. *J. Pharmacol. Exp. Ther.*, **258**, 1105–1113.

LOWRY, O.H., ROSEBROUGH, N.J., FARR, A.L. & RANDALL, R.J. (1951). Protein measurement with the folin phenol reagent. *J. Biol. Chem.*, **193**, 265–275.

MATSUMOTO, T., KANAIDE, H., SHOGAKINCHI, Y. & NAKAMURA, M. (1990). Characteristics of the histamine-sensitive calcium store in vascular smooth muscle. *J. Biol. Chem.*, **265**, 5610–5616.

MITCHELL, R.W., KOEING, S.M., POPOVICH, K.J., KELLY, E., TALLET, J. & LEFF, A.R. (1993). Pertussis toxin augments beta adrenergic relaxation of muscarinic contraction in canine trachealis. *Am. Rev. Respir. Dis.*, **147**, 327–331.

MITSUI, M. & KARAKI, H. (1993). Contractile and relaxant effects of phorbol ester in the intestinal smooth muscle of guinea pig taenia caeci. *Br. J. Pharmacol.*, **109**, 229–233.

NISHIZUKA, Y. (1992). Intracellular signalling by hydrolysis of phospholipids and activation of protein kinase C. *Science*, **258**, 607–614.

OLIANAS, M.C. & ONALI, P. (1993). Stimulation of phosphoinositide hydrolysis by muscarinic receptor activation in the rat olfactory bulb. *Biochem. Pharmacol.*, **45**, 281–287.

ORELLANA, S.A., SOLSKI, P.A. & BROWN, J.H. (1985). Phorbol ester inhibits phosphoinositide hydrolysis and calcium mobilization in cultured astrocytoma cells. *J. Biol. Chem.*, **260**, 5236–5239.

PACAUD, P. & BOLTON, T.B. (1992). Relation between muscarinic receptor cationic current and internal calcium in guinea-pig jejunal smooth muscle cells. *J. Physiol.*, **441**, 477–499.

PRESTWICH, S.A. & BOLTON, T.B. (1991). Measurement of picomole amounts of any inositol phosphate isomer separable by h.p.l.c. by means of a bioluminescence assay. *Biochem. J.*, **274**, 663–672.

PRESTWICH, S.A. & BOLTON, T.B. (1994). G-protein involvement in muscarinic receptor-stimulation of inositol phosphates in longitudinal smooth muscle from the small intestine of the guinea pig. *Br. J. Pharmacol.* (in press).

QUAST, U. (1993). Do the K^+ channel openers relax smooth muscle by opening K^+ channels? *Trends Pharmacol. Sci.*, **14**, 332–337.

RANA, R.S. & HOKIN, L.E. (1990). Role of phosphoinositides in transmembrane signalling. *Physiol. Rev.*, **70**, 115–164.

RASMUSSEN, H., TAKUWA, Y. & PARK, S. (1988). Protein kinase C in the regulation of smooth muscle contraction. *FASEB J.*, **1**, 177–185.

RICHARDSON, R.M., KIM, C., BENOVIC, J.L. & HOSEY, M. (1993). Phosphorylation and desensitization of human m2 muscarinic cholinergic receptors by two isoforms of the β-adrenergic receptor kinase. *J. Biol. Chem.*, **268**, 13650–13656.

ROFFEL, A.F., MEURS, H., ELZINGA, C.R.S. & ZAAGSMA, J. (1993). Muscarinic M2 receptors do not participate in the functional antagonism between methacholine and isoprenaline in guinea pig tracheal smooth muscle. *Eur. J. Pharmacol.*, **249**, 235–238.

RYUS, S.H., KIM, U-H., WAHL, M.I., BROWN, A.B., CARPENTER, G., HUANG, K-P. & RHEE, S.G. (1990). Feedback regulation of phospholipase Cβ by protein kinase C. *J. Biol. Chem.*, **265**, 17941–17945.

SADOSHIMA, J., AKAIKE, N., TOMOIKE, H., KANAIDE, H. & NAKAMURA, M. (1988). Ca^{2+}-activated K^+ channel in cultured smooth muscle cells of rat aortic media. *Am. J. Physiol.*, **255**, H410–H418.

SAIDA, K. & VAN BREEMEN, C. (1984). Characteristics of the norepinephrine-sensitive calcium store in rabbit aorta. *Blood Vessels*, **21**, 43–52.

SASAGURI, T. & WATSON, S.P. (1990). Phorbol esters inhibit smooth muscle contraction through activation of Na^+-K^+-ATPase. *Br. J. Pharmacol.*, **99**, 237–242.

SCORNIK, F.S., CODINA, J., BIRNBAUMER, L. & TORO, L. (1993). Modulation of coronary smooth muscle KCa channels by Gsα independent of phosphorylation by protein kinase A. *Am. J. Physiol.*, **265**, H1460–1465.

SHERMAN, W.R. (1989). Inositol homeostasis, lithium and diabetes. In *Inostiol Lipids in Cell Signalling*. ed. Michell, R.H., Drummond, A.H. & Downes, C.P. pp. 39–79. Academic Press: New York.

SHIMA, H. & BLAUSTEIN, M.P. (1992). Modulation of evoked contractions in rat arteries by ryanodine, thapsigargin and cyclopiazonic acid. *Circ. Res.*, **70**, 968–977.

SLADECZEK, F., SCHMIDT, B.H., ALONSO, R., VIAN, L., TEP, A., YASUMOTO, T., CORY, R.N. & BOCKAERT, J. (1988). New insights into maitotoxin action. *Eur. J. Biochem.*, **174**, 663–670.

SMELLIE, F.E., DAVIS, C.W., DALY, J.W. & WELLS, J.N. (1979). Alkylxanthines: inhibition of adenosine elicited accumulation of cyclic AMP in brain slices and of brain phosphodiesterase activity. *Life Sci.*, **24**, 2475–2482.

TOBIN, A.B. & NAHORSKI, S.R. (1993). Phosphorylation of a phosphoinositidase C-linked muscarinic receptor by a novel kinase distinct from β-adrenergic receptor kinase. *FEBS*, **335**, 353–357.

TOESCU, E.C., O'NEILL, PETERSEN, O.H. & EISNER, D.A. (1992). Caffeine inhibits the agonist-evoked cytosolic Ca^{2+} signal in mouse pancreatic acinar cells by blocking inositol trisphosphate production. *J. Biol. Chem.*, **267**, 23467–23470.

VAN DER BENT, V. & BÉNY, J.L. (1991). Mechanisms controlling caffeine-induced relaxation of coronary artery of the pig. *Br. J. Pharmacol.*, **103**, 1877–1882.

VAN DER VLIET, A., RADEMAKER, B. & BAST, A. (1990). A beta adrenoceptor with atypical characteristics is involved in the relaxation of the rat small intestine. *J. Pharmacol. Exp. Ther.*, **255**, 218–226.

YAMAGISHI, T., YANAGISAWA, T. & TAIRA, N. (1992). Activation of phospholipase C by the agonist U46619 is inhibited by cromakalim-induced hyperpolarization in porcine coronary artery. *Biochem. Biophys. Res. Commun.*, **187**, 1517–1522.

YANAGISAWA, T., YAMAGISHI, T. & OKADA, Y. (1993). Hyperpolarization induced by K^+ channel openers inhibits Ca^{2+} influx and Ca^{2+} release in coronary artery. *Cardiovas. Drugs Therapy*, **7**, 565–574.

YOSHIMASA, T., SIBLEY, D.R., BOUVIER, M., LEFKOWITZ, R.J. & CARON, M.G. (1987). Cross-talk between cellular signalling pathways suggested by phorbol ester-induced adenylate cyclase phosphorylation. *Nature*, **327**, 67–70.

(Received May 16, 1994
Revised September 27, 1994
Accepted October 10, 1994)

British Journal of Pharmacology (1995) 114, 612-617

Bradykinin B_1 receptors in the rabbit urinary bladder: induction of responses, smooth muscle contraction, and phosphatidylinositol hydrolysis

Semal K. Butt, Lee G. Dawson & [1]Judith M. Hall

Pharmacology Group, Biomedical Sciences Division, King's College London, Chelsea, London SW3 6LX

1 The aim of this study was to analyse the pharmacological characteristics, and second-messenger coupling-mechanisms, of bradykinin B_1 receptors in an intact tissue, the rabbit urinary bladder; and to investigate the influence of inhibition of endogenous peptidases on kinin activities.

2 In preparations of rabbit mucosa-free urinary bladder, at 90 min after mounting of the preparations, bradykinin (1 nM–10 μM) evoked contractile responses. In contrast, the B_1 receptor-selective agonist [des-Arg^9]-BK (10 nM–10 μM) was only weakly active at this time. Contractile responses to [des-Arg^9]-BK increased with time of tissue incubation in the organ bath, reaching a maximum after 3 h, when the pD_2 estimates were 6.4 ± 0.3 for bradykinin, and 6.9 ± 0.2 for [des-Arg^9]-BK.

3 Once stabilized, responses to [des-Arg^9]-BK in the bladder were competitively antagonized by the B_1 receptor-selective antagonists [Leu^8,des-Arg^9]-BK and D-Arg-[Hyp^3,Thi^5,D-Tic^7,Oic^8,des-Arg^9]-BK ([des-Arg^{10}]-Hoe140) (pK_B estimates were 6.1 ± 0.1 and 7.1 ± 0.1, respectively; $n = 17-21$), but responses were unaffected by the B_2 receptor-selective antagonist D-Arg-[Hyp^3,Thi^5,D-Tic^7,Oic^8]-BK (Hoe140) (100 nM; $n = 4$). Contractile responses to bradykinin itself were partially, but significantly, inhibited by the B_1 receptor-selective antagonist, [Leu^8,des-Arg^9]-BK (10 μM) ($P < 0.05$), or by the B_2 receptor-selective antagonist Hoe140 (100 nM) ($P < 0.005$) alone, and were largely blocked by a combination of the two antagonists ($P < 0.0001$).

4 The combined presence of the carboxypeptidase inhibitor DL-2-mercaptomethyl-3-guanidinoethylthiopropanoic acid (mergetpa; 10 μM), the neutral endopeptidase inhibitor, phosphoramidon (1 μM), and the angiotensin-converting enzyme inhibitor, enalaprilat (1 μM) increased the potency of bradykinin 17 fold ($P < 0.001$), but that of [des-Arg^9]-BK was unchanged ($P > 0.05$): pD_2 estimates were 7.6 ± 0.1 and 6.8 ± 0.1 for bradykinin and [des-Arg^9]-BK, respectively, in treated preparations. In the presence of peptidase inhibitors, the affinities of the antagonists [Leu^8,des-Arg^9]-BK and [des-Arg^{10}]-Hoe140 were unchanged as compared with those determined in the absence of peptidase inhibitors ($P > 0.05$). [Leu^8,des-Arg^9]-BK inhibited responses to bradykinin under these conditions ($n = 4$).

5 In endothelium-denuded preparations of the rabbit isolated aorta, an archetypal B_1 receptor preparation, contractile responses to the B_1 receptor-selective agonist [des-Arg^9]-BK (10 nM–10 μM) (and to bradykinin) increased progressively with time of tissue incubation; and [des-Arg^9]-BK responses were completely antagonized by the B_1 receptor antagonist [Leu^8,des-Arg^9]-BK (pK_B 6.3 ± 0.2; $n = 13$).

6 In experiments measuring stimulation of hydrolysis of phosphatidylinositol in rabbit urinary bladder, [des-Arg^9]-BK (10 μM–1 mM), and bradykinin (100 μM) significantly increased accumulation of inositol phosphates ($P < 0.0001$). The increase in accumulation of inositol phosphates evoked by [des-Arg^9]-BK (10 μM–1 mM) was significantly inhibited by [des-Arg^{10}]-Hoe140 (10 μM) ($P < 0.01$).

7 We conclude that in the mucosa-free rabbit urinary bladder, [des-Arg^9]-BK evokes contraction largely via activation of B_1 receptors which have similar properties, including time-dependent induction, to B_1 receptors in the rabbit isolated aorta. Bradykinin evokes contraction via stimulation of both B_1 and B_2 receptors, but does not require conversion by peptidases in order to activate B_1 receptors. We demonstrate, for the first time, B_1 receptor-coupling to phosphatidylinositol hydrolysis in an intact tissue preparation.

Keywords: Kinins; bradykinin; B_1 receptor; bradykinin receptor; urinary bladder (rabbit); phosphatidylinositol; receptor induction; peptidases; [des-Arg^9]-BK; [des-Arg^{10}]-Hoe140

Introduction

The recent introduction of receptor-selective agonist and antagonist kinin analogues has allowed confirmation of the long-standing proposal by Regoli and colleagues of the existence of two types of bradykinin receptor, termed B_1 and B_2 (see: Regoli & Barabé, 1980; Burch *et al.*, 1990; Hall, 1992). Further, the availability of active and stable B_2 receptor antagonist analogues of bradykinin has resulted in extensive study of the pharmacology and biological roles of the B_2 receptor type, and has led to proposals of the existence of further bradykinin receptor types (e.g. Farmer *et al.*, 1989; Farmer & DeSiato, 1994) and, additionally or alternatively, the existence of B_2 receptor species-homologues (Field *et al.*, 1992; Hall, 1992; Hall *et al.*, 1993). In contrast, there has been little study of the pharmacology of B_1 receptors, despite important recent proposals of a role for this receptor type in chronic hyperalgesia (Perkins & Kelly, 1993). This lack of research interest may be attributed, in part at least, to the paucity of reliable bioassay preparations for determining B_1 receptor characteristics and second-messenger coupling-mechanisms; and also the lack of selective, high specific activity, radiolabels for the B_1 receptor site.

This present study set out to identify a suitable non-vascular, functional (non-cell line) tissue preparation for the study of B_1 receptors characteristics; in particular second-messenger coupling-mechanisms. To this end, we chose the

[1] Author for correspondence.

rabbit isolated urinary bladder preparation which we found has the advantage of allowing measurement of B_1 receptor-coupling to phosphatidylinositol hydrolysis in an intact tissue. B_1 receptor-coupling to phosphatidylinositol hydrolysis has previously been demonstrated only in vascular cell lines in culture (Levesque *et al.*, 1993; Tropea *et al.*, 1993; Schneck *et al.*, 1994). In some experiments, peptidase inhibitors, including the carboxypeptidase inhibitor DL-2-mercaptomethyl-3-guanidino-ethylthiopropanoic acid (mergetpa), were used to investigate the influence of endogenous peptidases on agonist potency and antagonist affinity estimates (Hall *et al.*, 1990). In particular, we used the carboxypeptidase inhibitor, mergetpa, to investigate whether bradykinin itself required conversion (e.g. to the C-terminal-arginine deleted fragment, [des-Arg^9]-BK), by enzymes sensitive to this inhibitor, prior to its interaction with B_1 receptors.

Preliminary accounts of this work have been communicated to the Bayliss and Starling Meeting, Southampton, July 1994 (Butt *et al.*, 1994a) and the British Pharmacological Society Meeting, Sunderland, September, 1994 (Butt *et al.*, 1994b).

Methods

Tissue preparation and solutions

Male New Zealand albino rabbits (2.5–3.0 kg) were killed by an i.v. overdose of pentobarbitone sodium (Sagatal), and the urinary bladder and thoracic aorta were removed and placed in oxygenated Krebs solution (composition below). In all experiments, the urinary bladder and aorta were stored overnight in the refrigerator (4°C). Experiments were carried out in Krebs solution of composition (mM): NaCl 118, KH_2PO_4 1.17, KCl 4.7, $NaHCO_3$ 25, $MgSO_4$ 0.95, $CaCl_2$ 2.5 and glucose 11. The Krebs solution, at 37°C, was maintained at pH 7.4 by constant bubbling with 95% O_2:5% CO_2.

Isolated tissue studies

The preparations were attached to isometric Grass FT03B force-displacement transducers and suspended in 2.5 ml silanised organ baths. Mechanical activity was recorded with Grass model 7E polygraphs. The urinary bladder was cleared of mucosa and connective tissue and divided longitudinally into four preparations (length 10 mm) and set up under 2 g initial tension. The aorta was divided into strips (10 mm length) and set up under 2 g initial tension. Preparations were left to equilibrate for 60 min followed by determination of the maximum response to carbachol (bladder) or phenylephrine (aorta).

Urinary bladder Thirty minutes after determination of the maximal response to carbachol, cumulative concentration-response curves were obtained for bradykinin (1 nM–10 μM) or [des-Arg^9]-BK (10 nM–10 μM), and thereafter at 30 min intervals until consistent responses were obtained. Preliminary experiments had been carried out to determine antagonist incubation times resulting in optimum inhibition of submaximal kinin agonist responses (see Results). Once responses had stabilized, the antagonists (Hoe140, [Leu^8,des-Arg^9]-BK or [des-Arg^{10}]-Hoe140) were tested by applying the antagonist 5 min prior to determination of cumulative concentration-response curves in two preparations, whilst the other two preparations acted as concurrent time-controls (no antagonist). Each test preparation received one agonist and one antagonist only, with up to four antagonist concentrations tested in a single preparation. Some experiments were carried out in the additional continual presence (30 min pre-incubation) of the peptidase inhibitors mergetpa (10 μM), phosphoramidon (1 μM) and enalaprilat (1 μM). In a separate series of experiments, the effect of [Leu^8,des-Arg^9]-BK and Hoe140, alone and in combination, were tested against single submaximal responses to bradykinin (10 μM). After determination of control responses to bradykinin, one half of the preparations were re-tested following 5 min incubation with [Leu^8,des-Arg^9]-BK (10 μM), the other half following 5 min incubation with Hoe140 (100 nM). All preparations were then tested in the combined presence of [Leu^8,des-Arg^9]-BK (10 μM) and Hoe140 (100 nM). In some experiments, the effect of [Leu^8,des-Arg^9]-BK was tested against responses to bradykinin in the presence of peptidase inhibitors.

Aorta Cumulative concentration-response curves were obtained for bradykinin or [des-Arg^9]-BK (10 nM–10 μM) at 60 min intervals until consistent responses were obtained. The B_1 receptor antagonist, [Leu^8,des-Arg^9]-BK, was then applied 15 min prior to determination of the agonist responses in two preparations, whilst the other two preparations acted as concurrent time-control preparations. Each test preparation received one agonist and antagonist only, with up to three antagonist concentrations tested in a single preparation.

Phosphatidylinositol hydrolysis measurement

The methodology was adapted from Berridge *et al.* (1982) and Bristow *et al.* (1987). Briefly, cross-chopped tissues (350 × 350 μm, McIllwain tissue chopper) was washed three times at 37°C and then 25 μl aliquots added to tubes containing 2 μCi *myo*-[2-^{3}H]-inositol (844 GBq mol^{-1}) and 195 μl Krebs solution. Tubes were oxygenated with 95% O_2:5% CO_2 and placed in a shaking water bath for 60 min for prelabelling of inositol phospholipids. Following prelabelling, 20 μl lithium chloride (150 mM), and drug or drug-combination (to make up 250 μl total volume), was added to each tube; with each drug or drug-combination carried out in triplicate. Tubes were returned to the shaking water-bath following oxygenation, and incubated for a further 45 min at 37°C. Reaction was terminated by addition of 1.0 ml chloroform:methanol:hydrochloric acid (1 M) (100:200:1. v.v.v.), and total [^{3}H]-inositol phosphates extracted as described by Berridge *et al.* (1982). Distilled water (0.30 ml) and chloroform (0.31 ml) were added, the samples centrifuged (1000 *g* for 5 min). The aqueous phase (0.75 ml) was diluted with 2 ml deionised water and added, following 8 ml deionised water (pH 7.0), to a Dowex formate anion-exchange column (AG 1-X8 resin, 100–200 mesh). Total inositol phosphates were eluted with 6 ml ammonium formate:formic acid (800:100 mM) after removing [^{3}H]-inositol and [^{3}H]-glycerophosphoinositol by an 8 ml wash with sodium tetraborate:ammonium formate (5:60 mM). The lipid (0.40 ml) was removed and left overnight to evaporate off the chloroform. Samples were counted by liquid scintillation spectrometry to 2% error (Beckman LS1701) after addition of Liquiscint scintillation fluid and vortexing.

Preliminary experiments were carried out to determine concentrations of agonists (bradykinin, [des-Arg^9]-BK, and carbachol) producing submaximal increases in accumulation of total inositol phosphates (total-[^{3}H]-IPs). The effect of [des-Arg^{10}]-Hoe140 (10 μM) on submaximal increases in accumulation of total-[^{3}H]-IPs evoked by [des-Arg^9]-BK (10 μM and 1 mM) was investigated by co-incubation of agonist and antagonist in the same tubes.

Source of agents

Agents were obtained as follows: sodium pentobarbitone (Sagatal, Rhône Mérieux Limited, Essex), carbamylcholine chloride (carbachol), phosphoramidon (Sigma, Dorset), bradykinin, [des-Arg^9]-BK, [Leu^8,des-Arg^9]-BK (Bachem, Essex), D-Arg-[Hyp^3,Thi^5,D-Tic^7,Oic^8]-BK (Hoe140) (gift Sandoz Institute for Medical Research, London), D-Arg-[Hyp^3,Thi^5, D-Tic^7,Oic^8,des-Arg^9]-BK ([des-Arg^{10}]-Hoe140) (Peninsula Laboratories Europe, Cheshire).

DL-2-Mercaptomethyl-3-guanidino-ethylthiopropanoic acid

(mergetpa) (Calbiochem, CA, U.S.A.), enalaprilat (Merck, Sharp & Dohme, New Jersey, U.S.A.), *myo*-[2-^{3}H]-inositol (Amersham International plc, Buckinghamshire). All inorganic salts were of analytical grade and obtained from B.D.H., Essex. Dowex AG 1-X8 (100–200 mesh, formate form) was obtained from Biorad Laboratories, California, U.S.A., and Liquiscint from National Diagnostics, Buckinghamshire. All agents were dissolved in distilled water and peptides were stored at −20°C.

Expression of results and statistical analysis

The pD_2 (± s.e.mean) estimates were obtained from individual log concentration-response curves, and are defined as the $\log_{10}$ of the concentration producing 50% of the maximal response to the kinin receptor agonist. The pK_B estimates and their s.e.mean were obtained from individual dose-ratio estimates (x) by calculation from the Gaddum-Schild equation, $pK_B = \log_{10}(x\text{-}1) - \log_{10}[A]$, where [A] is the applied antagonist concentration (M), where Schild regressions do not differ from unity. In phosphatidylinositol hydrolysis experiments, increases in accumulation of total [^{3}H]-IPs were calculated and expressed as % over basal. Tests for significant differences were carried out using paired or unpaired Student's *t* tests, as appropriate. Analysis of Schild plots, and tests for unity and linearity of Schild regressions, were according to MacKay (1978); using conventional regression analysis (MINITAB 8.2, PA, U.S.A.) to estimate the coefficients of linear regression (b) and linear correlation (r). Numbers (*n*) shown are for individual estimates of pD_2 or pK_B of preparations (all other experiments); and experimental data are taken from at least 3 animals.

Results

Isolated tissue studies

Induction of agonist responses with time When tested after 90 min organ bath incubation, [des-Arg^9]-BK (10 nM–10 μM) evoked only small contractile responses in the isolated urinary bladder preparation (Figure 1), whereas responses to bradykinin were near the eventual maximum (not shown). Contractile responses to [des-Arg^9]-BK increased progressively with time of incubation of the preparation in the organ bath (Figure 1), but those to bradykinin showed little or no increase over this time period (not shown). Responses to both peptides were stable after 3 h of tissue incubation, and once stabilized, remained constant throughout the remainder of the experiment (a further 2–3 h). At this time, pD_2 estimates for bradykinin and [des-Arg^9]-BK were 6.4 ± 0.3, and 6.9 ± 0.2, respectively (Table 1). The presence of the peptidase inhibitors phosphoramidon (1 μM), enalaprilat (1 μM) and mergetpa (10 μM) resulted in a significant ($P<0.001$) 17 fold leftward-shift of the log concentration-responses curves for bradykinin, with no significant change ($P>0.05$) for [des-Arg^9]-BK (Figure 2; Table 1). In the presence of these inhibitors, pD_2 estimates for bradykinin and [des-Arg^9]-BK were 7.6 ± 0.1 and 6.8 ± 0.1, respectively (Table 1). There was little difference in the rate of induction of responses in peptidase inhibitor-treated preparations (data not shown). In the rabbit aorta, an archetypal B_1 receptor preparation, in the absence of peptidase inhibitors, B_1 response-induction was seen both with [des-Arg^9]-BK (data not shown) and with bradykinin (unpublished data).

Bradykinin receptor antagonist studies Preliminary studies in the bladder showed that maximal inhibition of agonist responses was obtained after 5 min antagonist incubation times for [Leu^8,des-Arg^9]-BK, [des-Arg^{10}]-Hoe140, or Hoe140. Increasing antagonist incubation time (to up to 15 min), in the absence of peptidase inhibitors, resulted in an apparent decrease in the affinities of [Leu^8,des-Arg^9]-BK and [des-

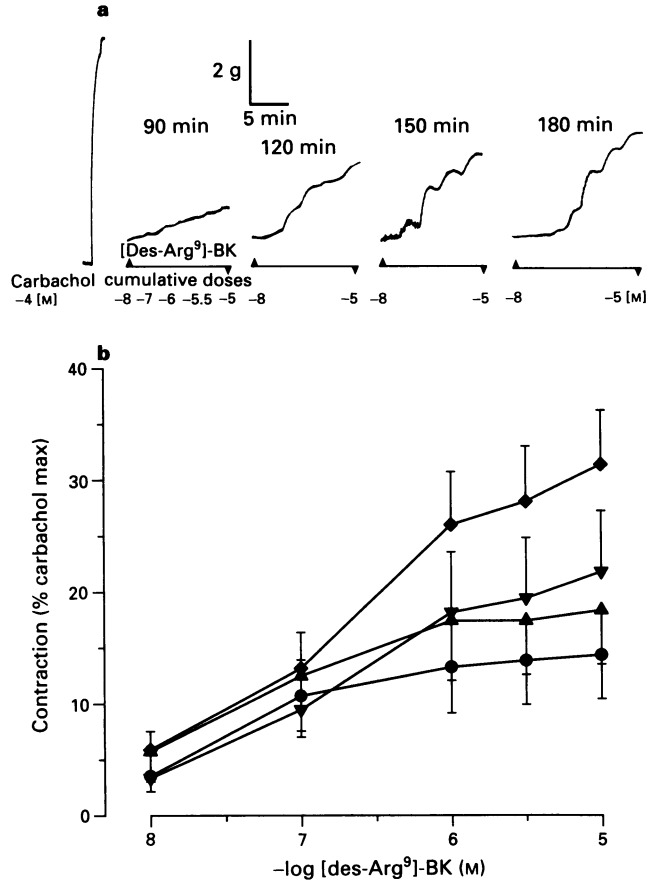

Figure 1 Time-dependent induction of contractile responses of rabbit isolated urinary bladder to [des-Arg^9]-BK. Contractile responses to [des-Arg^9]-BK were obtained by cumulative addition of the agonist. The first concentration-response curve was obtained 90 min following mounting the tissue, and subsequent concentration-response curves determined every 30 min thereafter until no further increase in contractile response was obtained (180 min). The upper panel (a) shows a representative original trace with addition of [des-Arg^9]-BK indicated by the arrows, and shown as the logarithm of the concentration. The lower panel (b) shows averaged data, expressed as % maximum response to carbachol obtained at the start of experiments, with each point representing the mean ± s.e.mean of experiments carried out in 8 preparations (times: ● 90 min; ▲ 120 min; ▼ 150 min; ◆ 180 min).

Table 1 Activity estimates for agonists and antagonists in the rabbit bladder

Contractile potency estimates for agonists (pD_2 ± s.e.mean)	*Control*	*+ Peptidase inhibitors*
Bradykinin	6.35 ± 0.30	7.63 ± 0.14**
[Des-Arg^9]-BK	6.94 ± 0.22	6.82 ± 0.09°
Affinity estimates for antagonists vs. [des-Arg^9]-BK (pK_B ± s.e.mean; *n*)	*Control*	*+ Peptidase inhibitors*
[Leu^8,des-Arg^9]-BK	6.06 ± 0.10	6.12 ± 0.09°
[Des-Arg^{10}]-Hoe 140	7.08 ± 0.13	7.09 ± 0.06°

Potencies of agonists are shown in terms of pD_2 ($-\log_{10}EC_{50}$) estimates ($n = 4$–29). Affinity estimates are given as pK_B values, since Schild slopes do not differ significantly ($P>0.05$; $n = 17$–57) from unity over the range used in analysis (see Figure 3 and Results). Significance differences between controls, and estimates in the presence of peptidase inhibitors phosphoramidon (1 μM), enalaprilat (1 μM) and DL-2-mercaptomethyl-3-guanidinoethylthiopropanoic acid (mergetpa; 10 μM), are shown as: **$P<0.001$; °$P>0.05$.

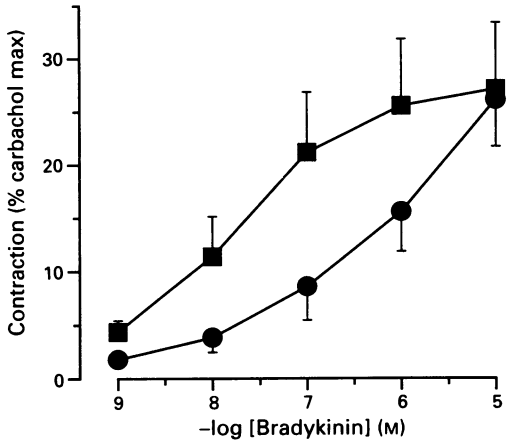

Figure 2 Peptidase inhibitors potentiate contractile responses to bradykinin in rabbit urinary bladder. Control log concentration-response curves (●) are compared to those obtained in the presence of the peptidase inhibitors enalaprilat (1 μM), phosphoramidon (1 μM) and DL-2-mercaptomethyl-3-guanidino-ethylthiopropanoic acid (mergetpa; 10 μM) (■). Contractile responses to bradykinin are expressed as % maximal response to carbachol, and are the mean ± s.e.mean of data obtained in 4–16 preparations.

Arg[10]-Hoe140 which was not prevented by the presence of peptidase inhibitors (data not shown). In concurrent time-control preparations, the lateral position and maximum response to [des-Arg[9]]-BK did not change with time (data not shown). Using a 5 min incubation time, the B_1 receptor antagonists [Leu[8],des-Arg[9]]-BK, and [des-Arg[10]]-Hoe140, showed competitive antagonism of contractile responses to the B_1 receptor-selective agonist [des-Arg[9]]-BK in the urinary bladder: pK_B estimates were 6.1 ± 0.1 and 7.1 ± 0.1, respectively (Figure 3 and Table 1). In these experiments under control conditions [Leu[8],des-Arg[9]]-BK gave a linear Schild regression of unity (slope 1.03 ± 0.22, correlation 0.8, $n = 17$). In contrast, [des-Arg[10]]-Hoe140 showed some flattening of the Schild regression at the highest concentration studied (10 μM), but when these data were excluded from analysis, the remaining range of concentrations (0.1–3 μM) gave satisfactory parameter estimates (slope 1.01 ± 0.24, correlation 0.7, $n = 21$). The reason for this behaviour of the antagonist at high concentration was not investigated further. In the rabbit isolated aorta preparation, [Leu[8],des-Arg[9]]-BK competitively antagonized responses to [des-Arg[9]]-BK (pK_B 6.3 ± 0.2, slope 1.04 ± 0.25, correlation 0.7, $n = 13$; Figure 3). The B_2 receptor-selective antagonist Hoe140 (100 nM) did not inhibit contractile responses to [des-Arg[9]]-BK in either preparation ($n = 4$, $P > 0.05$; data not shown). In the presence of the peptidase inhibitors phosphoramidon (1 μM), enalaprilat (1 μM) and mergetpa (10 μM), the affinities in the urinary bladder of [Leu[8],des-Arg[9]]-BK and [des-Arg[10]]-Hoe140 in antagonizing [des-Arg[9]]-BK were no different ($P > 0.05$) from those determined in the absence of peptidase inhibitors, with pK_B estimates of 6.1 ± 0.1 ($n = 20$) and 7.1 ± 0.1 ($n = 57$), respectively (Table 1). Contractile responses evoked by bradykinin in the urinary bladder were significantly inhibited by the B_1 receptor antagonists [Leu[8],des-Arg[9]]-BK (10 μM; $P < 0.05$), or by the B_2 receptor antagonist Hoe140 (100 nM; $P < 0.005$) (Figure 3) alone; and to a marked extent when used in combination at these concentrations, when bradykinin responses were reduced to 7.0% of control; $P < 0.0001$) (Figure 3). In the presence of the carboxypeptidase inhibitor mergetpa, responses to bradykinin were still inhibited by [Leu[8],des-Arg[9]]-BK (1–30 μM; $n = 6$; data not shown).

Phosphatidylinositol hydrolysis studies

Bradykinin (100 μM) and [des-Arg[9]]-BK (10 μM–1 mM) significantly increased accumulation of total-[^{3}H]-IPs ($P <$ 0.0001) (Figure 4). Submaximal increases in accumulation of total-[^{3}H]-IPs evoked by [des-Arg[9]]-BK were significantly inhibited by co-incubation with [des-Arg[10]]-Hoe140 (10 μM; $P < 0.01$, $n = 11–15$) (Figure 4). The antagonist [des-Arg[10]]-Hoe140 (10 μM) had no action in its own right (Figure 4).

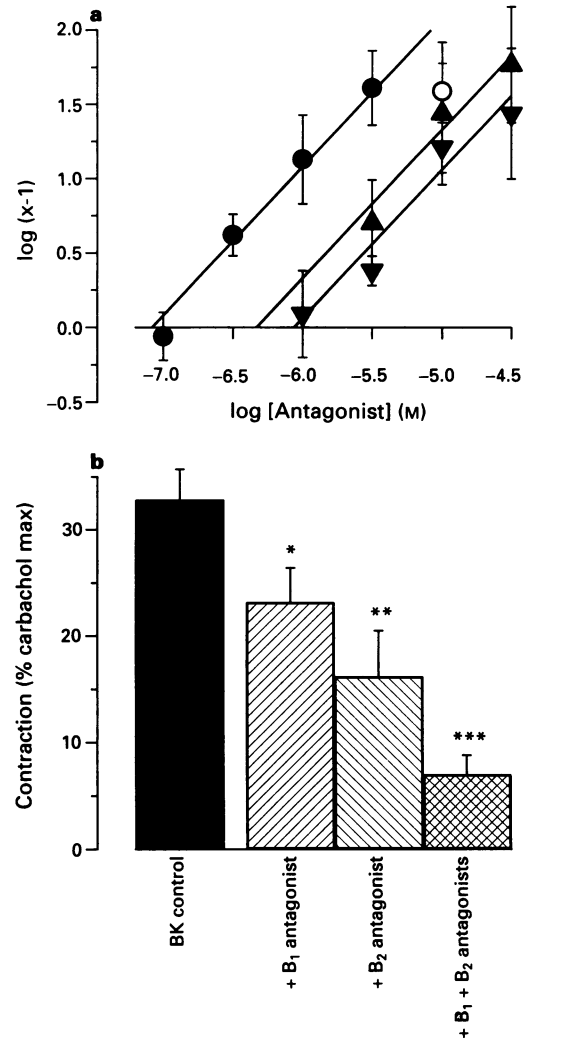

Figure 3 Antagonism of contractile responses to [des-Arg[9]]-BK and bradykinin in rabbit isolated urinary bladder by bradykinin receptor antagonists. In (a), Schild regressions are shown for antagonism of responses to [des-Arg[9]]-BK by [des-Arg[10]]-Hoe140 (●) and [Leu[8],des-Arg[9]]-BK (▼) in the urinary bladder; and for comparison, by [Leu[8],des-Arg[9]]-BK (▲) in the aorta. The lines fitted are of unity slope since the Schild regressions did not differ significantly ($P > 0.05$) from b = 1.0 over the range analysed and the correlation (r) was reasonably high. Estimates for [Leu[8],des-Arg[9]]-BK in the bladder were $pK_B = 6.06 \pm 0.10$, b = 1.03 ± 0.22, $r = 0.8$, $n = 17$; and in the aorta $pK_B = 6.33 \pm 0.24$, b = 1.04 ± 0.25, $r = 0.7$, $n = 13$. For [des-Arg[10]]-Hoe140 in the bladder, the estimates were $pK_B = 7.08 \pm 0.13$, b = 1.01 ± 0.24, $r = 0.7$, $n = 21$; analysed discounting the data at 10 μM (○) (see Results). The pK_B estimates are summarized in Table 1. In (b), submaximal control responses to bradykinin (10 μM; solid column) in the rabbit urinary bladder are significantly inhibited by the B_1 receptor antagonist [Leu[8],des-Arg[9]]-BK (10 μM; left-hatched column) and by the B_2 receptor antagonist Hoe140 (100 nM; right-hatched column), and further inhibited by a combination of the two antagonists (cross-hatched column). Data are shown as mean ± s.e.mean and represent data obtained from experiments carried out in 6–19 preparations. Significance is denoted: $*P < 0.05$, $**P < 0.005$, $***P < 0.0001$.

Discussion

This study demonstrates, in the mucosa-free rabbit urinary bladder preparation, that [des-Arg[9]]-BK causes contraction

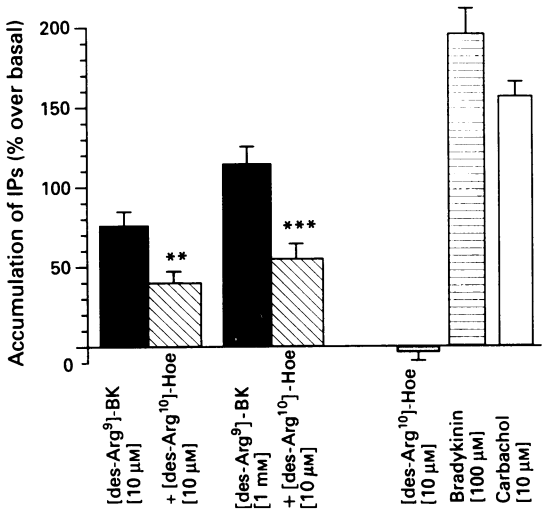

Figure 4 Effect of [des-Arg^{10}]-Hoe140 on [des-Arg^9]-BK-evoked accumulation of total-[^{3}H]-inositol phosphates (total-[^{3}H]-IPs). The filled columns show control increases in total-[^{3}H]-IPs evoked by [des-Arg^9]-BK (10 μM and 1 mM), the right-hatched columns show [des-Arg^9]-BK-evoked increases in total-[^{3}H]-IPs obtained in the presence of B_1 receptor antagonist [des-Arg^{10}]-Hoe140 (10 μM); the stippled column represents the effect of [des-Arg^{10}]-Hoe140 (10 μM) alone, on basal accumulation of total-[^{3}H]-IPs. Bradykinin-evoked (100 μM) and carbachol-evoked (10 mM) increases in total-[^{3}H]-IPs are shown as horizontal-fill and open columns, respectively. Data are shown as mean ± s.e.mean for at least 5 experiments carried out in triplicate. All agonists significantly increased accumulation of total-[^{3}H]-IPs ($P<0.0001$), and the increase evoked by [des-Arg^9]-BK was significantly inhibited by [des-Arg^{10}]-Hoe140 ($P<0.01$). [des-Arg^{10}]-Hoe140 did not significantly affect basal accumulation of total-[^{3}H]-IPs ($P>0.05$) in its own right.

largely via B_1 receptor-activation, whereas bradykinin contracts the urinary bladder via an interaction with both B_1 and B_2 receptors. The B_1 receptors in the urinary bladder have similar recognition properties and response characteristics, including time-dependent induction, to those in an archetypal B_1 receptor preparation, the rabbit isolated aorta. Metabolism of kinins by endogenous peptidases sensitive to the peptidase inhibitors used in this study does not influence B_1 receptor response-induction characteristics or antagonist affinities in this preparation, though does have the effect of decreasing the apparent potency of bradykinin (but not that of [des-Arg^9]-BK). Contractile responses to bradykinin are still obtained in the presence of mergetpa, and are in part inhibited by B_2 receptor antagonists (as well as by B_1 receptor antagonists). This suggests that conversion of bradykinin to [des-Arg^9]-BK by mergetpa-sensitive peptidases is not necessary for the interaction of bradykinin with B_1 receptors. We demonstrate, for the first time, B_1 receptor-coupling to phosphatidylinositol hydrolysis in a functional (non-cell line) preparation.

Contractile responses in the rabbit urinary bladder to the B_1 receptor-selective agonist [des-Arg^9]-BK increased progressively during tissue incubation time. Induction of B_1 receptor-responses has previously been described in other preparations including; the rabbit aorta (present study; see Regoli *et al.*, 1977), rabbit mesenteric artery (Regoli *et al.*, 1978; Boutillier *et al.*, 1987) and rat duodenum (Boschcov *et al.*, 1984). Once stabilized, responses to [des-Arg^9]-BK in both the rabbit bladder and aorta preparations were competitively antagonized by B_1 receptor-selective antagonists. The B_1 receptor-selective antagonist, [Leu^8,des-Arg^9]-BK had a similar affinity in both preparations (pK_B estimates of 6.1 and 6.3, respectively). The affinity of [Leu^8,des-Arg^9]-BK in these two preparations is lower than its affinity reported previously in the rabbit aorta (pA_2 6.8; Regoli *et al.*, 1978) and mesenteric artery (pA_2 6.5; Churchill & Ward, 1986). However, this discrepancy does not appear to result from a non-equilibrium state of the antagonist with the receptors, since increasing antagonist incubation time decreased, rather than increased, antagonist apparent affinities. Furthermore, the lower affinities do not seem to be a consequence of antagonist degradation by tissue peptidases, since affinity estimates determined in the presence of inhibitors of neutral endopeptidase (E.C. 3.4.24.11), angiotensin-converting enzyme (E.C. 3.4.15.1) and carboxypeptidases (see Orawski & Simmons, 1989), had no significant effect on antagonist affinity estimates. No appreciable interaction of the B_1 receptor-selective agonist [des-Arg^9]-BK with B_2 receptors seems likely, in as much as [des-Arg^9]-BK is without activity in the rabbit isolated jugular vein, a B_2 mono-receptor preparation (Regoli & Barabé, 1980; Butt *et al.*, 1994a,b), and no complication in interpretation due to differences between species needs to be taken into account (see Hall, 1992; Hall *et al.*, 1993). The novel B_1 receptor antagonist [des-Arg^{10}]-Hoe140 (Wirth *et al.*, 1991) has a ten fold higher affinity than [Leu^8,des-Arg^9]-BK. The relatively high affinity of this antagonist has previously been reported (Wirth *et al.*, 1991): we show here that at concentrations less than 10 μM it acts in a manner compatible with equilibrium competition, though shows a flattened Schild regression at 10 μM. Whether, amongst some plausible explanations, this was due to complications arising from non-equilibrium conditions, non-specific depression of the tissue, or cross-talk of [des-Arg^9]-BK to B_2 receptors at high dose-ratios, is not clear from the present experiments.

With respect to contractile responses to bradykinin itself in the rabbit urinary bladder; in contrast to those to [des-Arg^9]-BK, contractile responses to bradykinin were evident at the start of the experiment, and were little changed with time of tissue incubation. This suggests that bradykinin contracts the rabbit bladder predominantly via stimulation of B_2 receptors. This conclusion was supported by the finding that responses to bradykinin were partially inhibited by the B_2 receptor antagonist Hoe140 (100 nM), though some interaction with B_1 receptors also seems likely since responses to bradykinin were also partially inhibited by the B_1 receptor antagonist, [Leu^8,des-Arg^9]-BK (10 μM). Although bradykinin has been shown to have some pharmacological activity in both B_1 and B_2 receptor preparations (see Hall, 1992), it has not previously been established whether decarboxylation of bradykinin by mergetpa-sensitive peptidases (i.e. to [des-Arg^9]-BK), is required for its interaction with B_1 receptors. In the present study, we showed that, in the presence of peptidase inhibitors including the carboxypeptidase inhibitor mergetpa, the contractile responses evoked by bradykinin were still evident (indeed potentiated); and further, were in part inhibited by the B_1 receptor antagonist [Leu^8,des-Arg^9]-BK, thus suggesting that bradykinin can itself interact with B_1 receptors (although it is not possible to discount N-terminal cleavage by a mergepta-resistant carboxypeptidase).

In the present study, we demonstrated for the first time in an intact functional preparation, that B_1 receptor activation stimulates phosphatidylinositol hydrolysis. Thus, the B_1 receptor-selective agonist [des-Arg^9]-BK evoked a concentration-related increase in accumulation of total-[^{3}H]-IPs, and this increase was significantly inhibited by the B_1 receptor-selective antagonist [des-Arg^{10}]-Hoe140. Recently, B_1 receptor evoked stimulation of phosphatidylinositol hydrolysis was described in rabbit aorta (Schneck *et al.*, 1994), and superior mesenteric artery (Tropea *et al.*, 1993), smooth muscle cells in culture.

We conclude that in the mucosa-free rabbit urinary bladder, [des-Arg^9]-BK causes contraction via B_1 receptor activation, whereas bradykinin itself evokes contraction via B_1 and B_2 receptor activation. Although kinin agonists are degraded by endogenous peptidases, bradykinin does not require conversion by enalaprilat, mergetpa or phosphoramidon-sensitive peptidases in order to activate B_1 receptors in this preparation. The B_1 receptors of the urinary bladder have

similar recognition properties and response characteristics, including time-dependent induction, to those in the rabbit isolated aorta. We demonstrate for the first time, B_1 receptor-coupling to phosphatidylinositol hydrolysis in an intact functioning tissue preparation rather than in a cell line.

We thank Drs S.G. Farmer and R.M. Burch, Zeneca Pharmaceuticals, Delaware, U.S.A., and the Wellcome Trust for support. We thank the Sandoz Institute for Medical Research, London, U.K., for the gifts of Hoe140 and mergetpa. We are grateful to Dr Ian K.M. Morton for analysis and preparing the illustrations.

References

BERRIDGE, M.J., DOWNES, C.P. & HANLEY, M. (1982). Lithium amplifies agonist-dependent phosphatidylinositol responses in brain and salivary gland. *Biochem. J.*, **206**, 587–593.

BOSCHCOV, P., PAIVA, A.C.M., PAIVA, T.B. & SHIMUTA, S.I. (1984). Further evidence for the existence of two receptor sites for bradykinin responsible for the diphasic effect in the rat isolated duodenum. *Br. J. Pharmacol.*, **83**, 591–600.

BOUTILLIER, J., DEBLOIS, D. & MARCEAU, F. (1987). Studies on the induction of pharmacological responses to des-Arg^9-bradykinin *in vitro* and *in vivo*. *Br. J. Pharmacol.*, **92**, 257–264.

BRISTOW, D.R., CURTIS, N.R., SUMAN-CHAUHAN, N., WATLING, K.J. & WILLIAMS, B.J. (1987). Effects of tachykinins on inositol phospholipid hydrolysis in slices of hamster urinary bladder. *Br. J. Pharmacol.*, **90**, 211–217.

BURCH, R.M., FARMER, S.G. & STERANKA, L.R. (1990). Bradykinin receptor antagonists. *Med. Res. Rev.*, **10**, 237–269.

BUTT, S.K., DAWSON, L. & HALL, J.M. (1994a). Bradykinin receptors in rabbit urinary bladder: smooth muscle contraction and phosphatidylinositol hydrolysis. *Regul. Pept.*, **51**, 278.

BUTT, S.K., DAWSON, L., MORTON, I.K.M. & HALL, J.M. (1994b). Bradykinin B_1 receptors are induced in rabbit urinary bladder and are coupled to stimulation of phosphatidylinositol hydrolysis. *Br. J. Pharmacol.*, (in press).

CHURCHILL, L. & WARD, P.E. (1986). Relaxation of isolated mesenteric arteries by des-Arg^9-bradykinin stimulation of B_1 receptors. *Eur. J. Pharmacol.*, **130**, 11–18.

FARMER, S.G., BURCH, R.M., MEEKER, S.N. & WILKINS, D.E. (1989). Evidence for a pulmonary B_3 bradykinin receptor. *Mol. Pharmacol.*, **36**, 1–8.

FARMER, S.G. & DESIATO, M.A. (1994). Evidence of a novel nonpeptide bradykinin B_2 receptor antagonist on intestinal and airway smooth muscle: further evidence for the tracheal B_3 receptor. *Br. J. Pharmacol.*, **112**, 461–464.

FIELD, J.L., HALL, J.M. & MORTON, I.K.M. (1992). Bradykinin receptors in the guinea-pig taenia caeci are similar to proposed BK_3 receptors in the guinea-pig trachea and are blocked by Hoe140. *Br. J. Pharmacol.*, **105**, 293–296.

HALL, J.M. (1992). Bradykinin receptors: pharmacological properties and biological roles. *Pharmacol. Ther.*, **56**, 131–190.

HALL, J.M., CAULFIELD, M.P., WATSON, S.P. & GUARD, S. (1993). Receptor subtypes or species homologues: relevance to drug discovery. *Trends Pharmacol. Sci.*, **14**, 376–383.

HALL, J.M., FOX, A.J. & MORTON, I.K.M. (1990). Peptidase activity as a determinant of agonist potency in some smooth muscle preparations. *Eur. J. Pharmacol.*, **176**, 127–134.

LEVESQUE, L., DRAPEAU, G., GROSE, J.H., RIOUX, F. & MARCEAU, F. (1993). Vascular mode of action of kinin B_1 receptors and development of a cellular model for the investigation of these receptors. *Br. J. Pharmacol.*, **109**, 1254–1262.

MACKAY, D. (1978). How should values of pA_2 and affinity constants for pharmacological competitive antagonists be estimated? *J. Pharm. Pharmacol.*, **30**, 312–313.

ORAWSKI, A.T. & SIMMONS, W.H. (1989). Degradation of bradykinin and its metabolites by brain synaptic membranes. *Peptides*, **10**, 1063–1073.

PERKINS, M.R. & KELLY, D. (1993). Induction of B_1 receptors *in vivo* in a model of ultra-violet irradiation-induced thermal hyperalgesia in the rat. *Br. J. Pharmacol.*, **110**, 1441–1444.

REGOLI, D. & BARABÉ, J. (1980). Pharmacology of bradykinin and related kinins. *Pharmacol. Rev.*, **32**, 1–46.

REGOLI, D., BARABÉ, J. & PARK, W.K. (1977). Receptors for bradykinin in rabbit aortae. *Can. J. Physiol. Pharmacol.*, **55**, 855–867.

REGOLI, D., MARCEAU, F. & BARABÉ, J. (1978). *De novo* formation of vascular receptors for bradykinin. *Can. J. Physiol. Pharmacol.*, **56**, 674–677.

SCHNECK, K.A., HESS, J.F., STONESIFER, G.Y. & RANSOM, R.W. (1994). Bradykinin B_1 receptors in rabbit aorta smooth muscle cells in culture. *Eur. J. Pharmacol. (Mol. Pharmacol.)*, **266**, 277–282.

TROPEA, M.M., GUMMELT, D., HERZIG, M.S. & LEEB-LUNDBERG, L.M.F. (1993). B_1 and B_2 kinin receptors on cultured rabbit superior mesenteric artery smooth muscle cells: receptor-specific stimulation of inositol phosphate formation and arachidonic acid release by des-Arg^9-bradykinin and bradykinin. *J. Pharmacol. Exp. Ther.*, **264**, 931–937.

WIRTH, K., BREIPOHL, G., STECHL, J., KNOLLE, J., HENKE, S. & SCHÖLKENS, B. (1991). Des-Arg^9-D-Arg-[Hyp^3,Thi^5,D-Tic^7,Oic^8]-bradykinin (desArg^{10}-[Hoe140]) is a potent bradykinin B_1 receptor antagonist. *Eur. J. Pharmacol.*, **205**, 217–218.

(Received July 18, 1994
Revised October 4, 1994
Accepted October 10, 1994)

British Journal of Pharmacology (1995) 114, 618-623

Structural requirements at the melatonin receptor

[1]David Sugden, [2]Nelson W.S. Chong & *David F.V. Lewis

Physiology Group, Biomedical Sciences Division, King's College London, Campden Hill Road, Kensington, London W8 7AH and *School of Biological Sciences, University of Surrey, Guildford, Surrey GU2 5XH

1 High affinity, specific binding sites for the pineal hormone, melatonin (5-methoxy *N*-acetyltryptamine) can be detected in chick brain membranes by use of the radiolabelled agonist, 2-[^{125}I]-iodomelatonin (2-[^{125}I]-aMT).

2 The affinity of a number of analogues of melatonin at the 2-[^{125}I]-aMT binding site was determined and compared with an analysis of their electronic structure and significant quantitative relationships obtained.

3 The best correlations indicated that binding affinity was correlated with ΔE, the difference between the frontier orbital energies, and Q_NH, the electron density in the highest occupied molecular orbital of the side-chain nitrogen atom.

4 These findings suggest that ligand binding may involve hydrogen bonding between the 5-methoxy and amide moieties of melatonin and complementary amino acid residues, and charge transfer interactions between the indole ring of melatonin and an aromatic amino acid in the receptor binding site.

5 A molecular model of a putative binding site is proposed based on the predicted amino acid sequence of the cloned *Xenopus laevis* melanophore melatonin receptor and the quantitative structure-affinity relationships observed in the present study.

Keywords: Melatonin receptor; 2-[^{125}I]-iodomelatonin; chick brain binding; QSAR; molecular modelling

Introduction

Melatonin (5-methoxy *N*-acetyltryptamine, aMT) is synthesized in the pineal gland of vertebrates and secreted into the general circulation only at night (Sugden, 1989). A primary role for circulating melatonin in regulating various seasonal changes in physiology, such as reproduction, metabolism and hair growth, in many photoperiodic species is well-established (Tamarkin *et al.*, 1985; Bartness & Goldman, 1989). Pineal melatonin is also involved in regulating circadian rhythms in some species of birds and reptiles (Underwood, 1989) and, low doses of exogenous melatonin entrain free-running rhythms in mammals (Redman *et al.*, 1983; Folkard *et al.*, 1990; Thorpe & Coen, 1994), while larger doses of have a sleep-promoting and sedative effect in both experimental animals and man (Holmes & Sugden, 1982; Waldhauser *et al.*, 1990). Small amounts of melatonin are also synthesized by the photoreceptors of some species where it probably acts locally to regulate various aspects of retinal physiology such as photoreceptor retinomotor movements and photoreceptor outer segment disc shedding (Besharse *et al.*, 1988).

Recent studies using 2-[^{125}I]-iodomelatonin, a ligand originally developed for use in aMT radioimmunoassay (Vakkuri *et al.*, 1984), identified and characterized specific, high affinity receptors which probably mediate at least some of these actions of melatonin (Krause & Dubocovich, 1991; Morgan *et al.*, 1994). Our studies on the high affinity 2-[^{125}I]-iodomelatonin binding sites found in several tissues (brain, pars tuberalis and retina) and species (sheep, chicken and wallaby) using a series of novel melatonin analogues have indicated a considerable similarity of melatonin receptor characteristics (Sugden & Chong, 1991; Paterson *et al.*, 1992). In the present study we have combined radioreceptor data with an analysis of the electronic structure of a number of these melatonin analogues to provide a quantitative analysis of the structure-affinity relationships at the melatonin receptor. Our studies suggest a model of melatonin binding to its receptor in which hydrogen bonding occurs between 5-methoxy and amide groups of melatonin and complementary amino acid residues at the binding site.

[1] Author for correspondence.
[2] Present address: Department of Neuroscience, Institute of Psychiatry, De Crespigny Park, Denmark Hill, London SE5 8AF.

Methods

Membrane preparation and binding experiments

Chickens (*Gallus domesticus*, White Leghorn) were obtained from Orchard Farms (Buckinghamshire) at 1 day of age and were housed under a diurnal lighting cycle (12L:12D, lights on at 06 h 00 min) until killed between 14 h 00 min and 15 h 00 min at 15 days of age. Whole brain was removed and frozen in liquid nitrogen and stored at −70°C. Brains were homogenized in 20 vol of Tris-HCl (50 mM, pH 7.4) containing phenyl methylsulphonylfluoride (PMSF) (1 mM), leupeptin (50 μg ml^{-1}) and EGTA (1 mM). The homogenate was centrifuged (100,000 *g*, 4°C, 60 min) and the pellet rehomogenized in the same buffer and spun for a second time. The final membrane pellet was resuspended in Tris-HCl and aliquots frozen at −70°C until used. Binding assays were done in duplicate by incubating 2-[^{125}I]-iodomelatonin (30 to 50 pM) with membranes (60 μg of protein) for 60 min at 25°C. Nonspecific binding was defined with cold melatonin (1 μM). Protein was determined by a dye-binding method with bovine serum albumin as the standard (Bradford, 1976).

Data analysis

Saturation experiments were analysed by non-linear regression analysis using the ENZFITTER programme (Leatherbarrow, 1987) with the equation

$$B = B_{max} * F/(K_d + F)$$

where B = the concentration of ligand bound to the receptor, F = the concentration of free ligand, K_d = the equilibrium

dissociation constant and B_{max} = the maximal concentration of binding sites. IC_{50} values were determined in competition assays using the ALLFIT programme (DeLean *et al.*, 1978) with the four parameter logistic equation

$$Y = \frac{A - D}{1 + (X/C)^B} + D$$

where X and Y are the concentration of the competing compound and percentage inhibition of 2-[^{125}I]-iodomelatonin binding respectively, and A is the maximal binding (in the absence of competitor), B is the slope factor, C is the IC_{50} and D is the minimal binding (nonspecific binding). Inhibition constants (K_i) were then calculated with the Cheng-Prusoff equation (Cheng & Prusoff, 1973).

Reagents

2-[^{125}I]-iodomelatonin (2200 Ci mmol^{-1}) was purchased from DuPont U.K. Ltd. (Stevenage, U.K.). Melatonin analogues were obtained from the following sources: 2-chloromelatonin, Dr C.E. Smithen (Roche Products, U.K.); 6-fluoromelatonin and 6-chloromelatonin, Lilly Research Labs. (Indianapolis, U.S.A.); 6-methoxymelatonin, Dr D.C. Klein (National Institutes of Health, U.S.A.); 5-methoxy *O*-acetyltryptamine, Dr I. Smith (Middlesex Hospital Medical School, U.K.). 5-Methoxy *N*-isobutanoyltryptamine, 5-methoxy *N*-valeroyltryptamine, 5-methyl *N*-acetyltryptamine, 5-benzyloxy *N*-acetyltryptamine and N-acetyltryptamine were synthesized from the free amines as described previously (Ho *et al.*, 1968) and shown to be pure after recrystallization by thin-layer chromatography on silica gel plates (Anachem, Luton, U.K.) using two systems (I: ethyl acetate/n-butanol, 90/10; II: chlorform/methanol/acetic acid/water, 60/30/3/1). The structures were confirmed by ^{1}H n.m.r. (The Bruker WM 250 NMR University of London Intercollegiate Research Service for NMR at King's College). All other compounds were purchased from Sigma Chemical Co. (Poole, Dorset, U.K.) or Aldrich Chemical Co. (Gillingham, Dorset, U.K.).

Structural analysis

The molecular geometries of the melatonin analogues were optimised to give the minimum energy conformations using a combination of Newton-Raphson and Simplex methods found in the COSMIC molecular modelling package obtained from Smith Kline and French Ltd., Welwyn Garden City, U.K. (Vinter *et al.*, 1987).

Electronic structure calculations were executed on the minimized geometries using the CNDO/2 molecular orbital method (Pople *et al.*, 1965) using COSMIC. The resulting electronic distributions were used to generate molecular electrostatic potential energies for the melatonin analogues. QSARs were produced by stepwise multiple regression analysis of the electronic structural parameters, comprising a data set of 30 independent variables, with K_i values obtained in competition experiments using 2-[^{125}I]-iodomelatonin (Table 1). Molecular modelling and quantum chemical calculations were carried out on a MicroVAX II mini-computer and statistical processing was performed on a Cyber 176 mainframe at the University of Manchester Regional Computer Centre. The putative receptor binding site model was constructed using the SYBYL molecular modelling software package (Tripos Associates, St. Louis, U.S.A.).

Results

Binding of 2-[^{125}I]-iodomelatonin to chicken brain membranes

Binding of the melatonin agonist 2-[^{125}I]-iodomelatonin to chicken brain membranes was saturable and to a single population of binding sites with an equilibrium dissociation constant (K_d) of 29.4 ± 2.7 pM and a maximal density of binding sites (B_{max}) of 11.1 ± 0.4 fmól mg^{-1} protein ($n = 3$). The structures of the melatonin analogues used are shown in Figure 1. The results of the competition experiments are shown in Figure 2a and b and K_i values are presented in Table 1. All of the melatonin analogues examined displaced 2-[^{125}I]-iodomelatonin binding completely. In all cases the pseudo Hill coefficient was close to unity (0.80 to 1.10).

Substitution of chlorine in the 2-position of the indole ring of melatonin increased binding affinity, while fluorine or chlorine substitutions in the 6-position were reasonably well-tolerated. Other 6-position (methoxy, hydroxy) or 5-position substitutions (methyl, benzoyl) reduced affinity as did long side-chain acyl groups (valeroyl, isobutanoyl).

Table 1 Inhibition constants (K_i) for competition of 2-[^{125}I]-iodomelatonin (2-[^{125}I]-aMT) binding in chick brain membranes

	Compound	K_i (nM)	pK_i
1	2-Chloromelatonin	0.024 ± 0.004	−10.62
2	Melatonin	0.24 ± 0.01	−9.62
3	6-Fluoromelatonin	0.36 ± 0.04	−9.44
4	6-Chloromelatonin	0.58 ± 0.07	−9.24
5	6-Hydroxymelatonin	6.3 ± 0.4	−8.20
6	N-isobutanoyl 5-methoxytryptamine	6.1 ± 0.2	−8.21
7	N-valeroyl 5-methoxytryptamine	12.6 ± 0.4	−7.90
8	6-Methoxymelatonin	31.7 ± 2.6	−7.50
9	5-Methyl *N*-acetyltryptamine	146.8 ± 28.6	−6.83
10	5-Benzoyl *N*-acetyltryptamine	170.0 ± 6.1	−6.77
11	O-acetyl 5-methoxytryptamine	242.2 ± 24.2	−6.62
12	N-acetyltryptamine	730 ± 40	−6.14
13	N-acetyl 5-hydroxytryptamine	488 ± 14	−6.31
14	5-Methoxytryptamine	2528 ± 149	−5.60

IC_{50} values were determined in competition assays using a four parameter logistic equation on the ALLFIT programme (De Lean *et al.*, 1978) and K_i calculated using the Cheng-Prusoff equation (Cheng & Prusoff, 1973). The values given are the mean ± s.e.mean of 3 determinations. Hill coefficients were between 0.8 and 1.10.

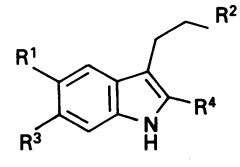

	Compound	R_1	R_2	R_3	R_4
1	2-Chloromelatonin	OMe	NHCOMe	H	Cl
2	Melatonin	OMe	NHCOMe	H	H
3	6-Fluoromelatonin	OMe	NHCOMe	F	H
4	6-Chloromelatonin	OMe	NHCOMe	Cl	H
5	6-Hydroxymelatonin	OMe	NHCOMe	OH	H
6	N-isobutanoyl 5-methoxytryptamine	OMe	$NHCOPr^i$	H	H
7	N-valeroyl 5-methoxytryptamine	OMe	NHCOBu	H	H
8	6-Methoxymelatonin	OMe	NHCOMe	OMe	H
9	5-Methyl *N*-acetyltryptamine	Me	NHCOMe	H	H
10	5-Benzoyl *N*-acetyltryptamine	OCH_2Ph	NHCOMe	H	H
11	O-acetyl 5-methoxytryptamine	OMe	OCOMe	H	H
12	N-acetyltryptamine	H	NHCOMe	H	H
13	N-acetyl 5-hydroxytryptamine	OH	NHCOMe	H	H
14	5-Methoxytryptamine	OMe	NH_2	H	H

Figure 1 Structures of melatonin analogues used in this study

Quantitative structure-affinity analysis

A quantitative relationship between the electronic structural parameters derived from CNDO/2 calculations and the affinity of the analogues at the chicken brain 2-[^{125}I]-iodomelatonin binding site was evident. The best correlations were:-

$$pK_i = -841.1\Delta E^{-1} - 62.6$$
$$(\pm 248.4) \qquad (n = 14,\ s = 1.125,\ R = 0.70,\ F = 11.5)$$

and,

$$pK_i = 770.7\Delta E^{-1} + 51.2\ Q_NH - 58.8$$
$$(\pm 229.3) \quad (\pm 27.5)$$
$$(n = 14,\ s = 1.024,\ R = 0.78,\ F = 8.7)$$

Where n = number of points, s = standard error, R = correlation coefficient, and F = variance ratio. It can be seen from Figure 3 that melatonin (2) is an outlier having a higher affinity than would be expected, and improved correlations were obtained if melatonin was excluded from the analysis:

$$pK_i = -4.9\Delta E + 45.3\ Q_NH + 64.8$$
$$(\pm 0.9) \quad (\pm 18.8)$$
$$(n = 13,\ s = 0.699,\ R = 0.90,\ F = 21.6)$$

This suggests that for the endogenous ligand additional factors, not represented in this analysis of electronic structure, may be important determinants of binding affinity. Given the similarities in their structures it seems unlikely that melatonin could bind to the receptor in an entirely different manner to the analogues. Thus the endogenous ligand is likely to possess specific molecular characteristics not entirely identifiable in the structural descriptors employed in the QSAR analysis. As the majority of the analogues of melatonin studied possess additional substituents or bulkier side-chains than melatonin itself, it might be that the greater conformational flexibility of melatonin relative to the other analogues allows it easier entry to the binding site, or confers an enhanced ability to adopt the appropriate shape needed for interaction with key amino acid residues in the binding site.

In each of these correlations the term ΔE is apparent. ΔE is the difference between the frontier orbital energies and relates to the ability of the molecule to participate in charge transfer interactions. Inclusion of a second parameter, Q_NH, the electron density in the highest occupied molecular orbital of the side-chain nitrogen atom (oxygen in the case of 11) improves the correlation, although the variance ratio diminishes. Log P, the hydrophobic parameter, has much the same effect as a secondary descriptor but the correlation is lower (data not shown).

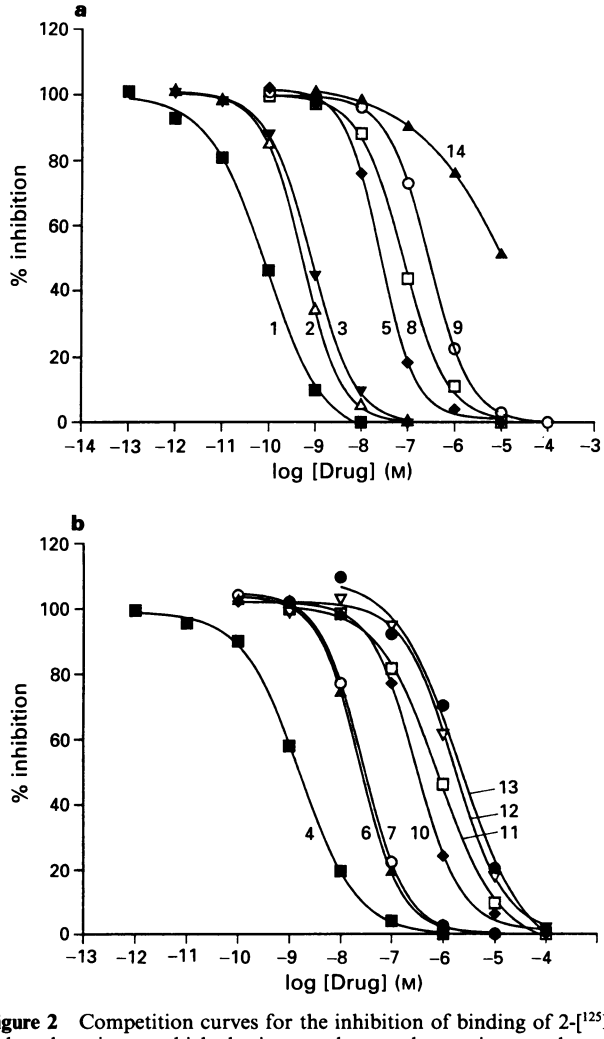

Figure 2 Competition curves for the inhibition of binding of 2-[^{125}I]-iodomelatonin to chick brain membranes by various melatonin analogues. (a) **1** 2-chloromelatonin; **2** melatonin; **3** 6-fluoromelatonin; **5** 6-hydroxymelatonin; **8** 6-methoxymelatonin; **9** 5-methyl *N*-acetyltryptamine; **14** 5-methoxytryptamine. (b) **4** 6-Chloromelatonin; **6** N-isobutyanoyl 5-methoxytryptamine; **7** N-valeroyl 5-methoxytryptamine; **10** 5-benzoyl *N*-acetyltryptamine; **11** O-acetyl 5-methoxytryptamine; **12** N-acetyltryptamine; **13** N-acetyl 5-hydroxytryptamine. The data shown are the mean of duplicate determinations from a representative experiment.

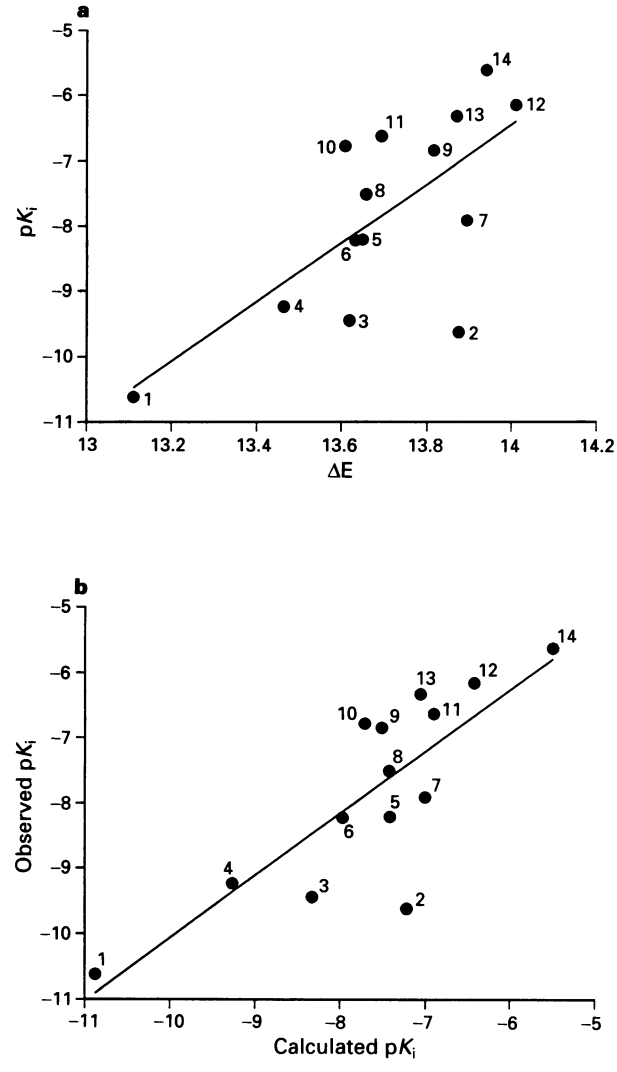

Figure 3 (a) Correlation of ΔE and inhibition constants (pK_i) for melatonin analogues for the displacement of 2-[^{125}I]-iodomelatonin binding from chick brain membranes. Compound numbers are given in the legend to Figure 2. (b) Graph of experimentally observed pK_i against calculated pK_i. Calculated pK_i values were obtained using the equation $pK_i = -4.9\ \Delta E + 45.3\ Q_NH + 64.8$, except for melatonin (**2**) which was determined from the equation $pK_i = 770.7\ \Delta E^{-1} + 51.2\ Q_NH - 58.8$.

Discussion

Our previous studies (Sugden & Chong, 1991) have shown that the binding site identified by 2-[^{125}I]-iodomelatonin in chick brain membranes is pharmacologically identical to the melatonin receptor in sheep pars tuberalis, at least as defined using a number of tryptamine analogues of melatonin including those used in the present analysis. Activation of melatonin receptors on pars tuberalis cells has been shown to inhibit forskolin stimulation of adenosine 3':5'-cyclic monophosphate (cyclic AMP) production (Morgan *et al.*, 1989), and it has been proposed that the pars tuberalis may be the site of action of melatonin in mediating photoperiodic changes in reproductive status (for discussion see Morgan *et al.*, 1994). The chick brain site also has very similar binding characteristics and pharmacology to the receptor in chick and rabbit neuronal retina which regulates dopamine release from amacrine cells (Dubocovich, 1985). In chick brain membranes, GTP inhibits 2-[^{125}I]-iodomelatonin binding suggesting that the binding site is coupled to a guanine nucleotide binding protein (G-protein) and thus is a functional receptor linked to an intracellular second messenger system. In some other tissues, for example, neonatal pituitary, pars tuberalis and *Xenopus laevis* melanophores, it has been shown that the melatonin receptor is negatively coupled to adenylate cyclase through a G_i-like protein as pertussis toxin blocks the biochemical effects or biological action of melatonin (White *et al.*, 1987; Vanecek & Vollrath, 1989; Carlson *et al.*, 1989; Sugden, 1991). Coupling to other transduction systems has also been reported (Vanecek & Vollrath, 1990; Vanecek & Klein, 1992). Using an expression cloning strategy, a melatonin receptor has recently been isolated from *Xenopus laevis* melanophores (Ebisawa *et al.*, 1994). The cDNA encodes a protein of 420 amino acids which has similarities to a wide range of G protein-coupled receptors rather than to any one particular group. Nevertheless, the melatonin receptor sequence contains seven hydrophobic segments which, like other G protein-coupled receptors, are thought to fold into transmembrane α-helical domains.

Existing receptor binding site models for adrenoceptors, dopamine, muscarinic and 5-HT_{2c} receptors have been devised from site-directed mutagenesis studies and the clear homology with the transmembrane domains of bacteriorhodopsin (Strader *et al.*, 1987; Hibert *et al.*, 1991; Lewis *et al.*, 1993). These models suggest that four or five of the transmembrane helical segments may be involved in ligand binding, and that a conserved aspartate on helix III and a serine or threonine residue on helix V are important for ligand binding. In the 5-HT_{2c} receptor site model (Lewis *et al.*, 1993) an alignment of helices II–VI in an approximately parallel symmetric arrangement gave rise to an interhelical channel of appropriate dimensions for binding of 5-HT. The putative binding site lies near the top of this channel and contains an aspartate and serine residue which pair with the protonated amino group and act as a hydrogen bond donor/acceptor with the indole 5-hydroxy group respectively. Two aromatic amino acid residues (phenylalanine and tryptophan) are found in transmembrane helix VI in the rat 5-HT_{2c} receptor which may enter into π–π stacking interactions with the indole ring of 5-HT (Lewis *et al.*, 1993). These residues are also found in the human β_1-adrenoceptor and muscarinic receptors and in bovine rhodopsin where a similar interaction may occur with the aromatic rings of the respective ligands.

An examination of the quantitative structure-affinity relationships for the melatonin analogues investigated and the similarity of the structures of 5-HT and melatonin, suggest that the amide moiety of melatonin may participate in hydrogen bonding. This is indicated by the appearance of the highest occupied molecular orbital frontier electron population on the amide nitrogen of the side-chain (Q_NH) in the QSAR equations which suggests that this group might act as a proton donor in a cooperative charge transfer interaction, assisted by the electronic donor-acceptor characteristics of the indole nucleus. Furthermore, the appearance of ΔE in the QSAR equations may reflect π–π stacking between the indole nucleus of the melatonin derivatives and an aromatic amino acid residue in the receptor binding site. This type of interaction between delocalized ring systems is assisted by frontier orbital (electron transfer) interactions between the two rings. Using the molecular electrostatic potential map of melatonin (Lewis *et al.*, 1990) and its similarity to 5-HT, and by modelling the putative transmembrane regions of the cloned melatonin receptor of *Xenopus* melanophores (Ebisawa *et al.*, 1994), it has been possible to construct a putative binding site model (Figure 4). In this model, it is envisaged that hydrogen bonding can occur between the 5-methoxy and amide groups of melatonin and complementary Ser_{115} and Asn_{167} residues in putative transmembrane helices III and IV respectively. The binding site model proposes that the single Trp_{256} residue in helix VI overlaps with the indole ring of melatonin allowing charge transfer between receptor and ligand as suggested by the appearance of ΔE in the QSAR correlations. Melatonin can be docked into this postulated binding domain in at least two ways such that hydrogen bonding can occur. The model shown (Figure 4) seems most probable in terms of the likely interactions between melatonin and complementary amino acid residues, namely the indole ring of melatonin and Trp_{256} via π–π stacking, hydrogen bonding between the -NH moiety of the melatonin side-chain and Asn_{167}, and Ser_{115} donating a hydrogen bond to the $-CH_3O$ moiety of melatonin. In addition, hydrophobic interactions between the three non-polar residues (Ile_{89}, Val_{170}, and Ile_{194}) and the methoxymethyl group at the 5-position, the amide methyl group and methylene side-chain of melatonin respectively are likely. From the model it appears that there is space for both an increase in the size of the amide side-chain and substitutions at the 2- and 6-position of the indole ring; such substitutions have been shown to be well-tolerated (Sugden & Chong, 1991).

The proposed model suggests that sufficient room exists for a water molecule between melatonin and the receptor, and does not preclude the possibility that hydrogen bonds may form either between the ligand and receptor or between the ligand and water molecule and the receptor. This is interesting in view of the recent observation that the van't Hoff plot of affinity against temperature for 2-[^{125}I]-iodomelatonin

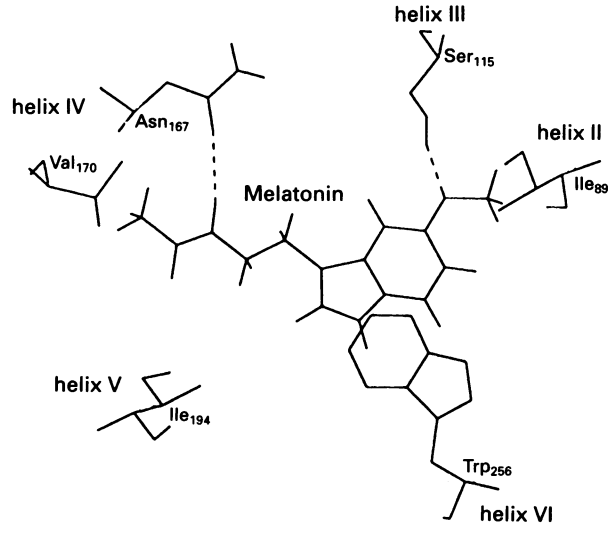

Figure 4 The postulated melatonin receptor binding site model. This model shows two possible hydrogen bonded interactions between melatonin and serine and asparagine residues in transmembrane helices III and IV of the receptor. Potential hydrogen bonds are denoted by dashed lines.

binding in chick brain membranes is not linear (Chong & Sugden, 1994). The fundamental properties of water molecules suggest that the ease of hydrogen bond formation between the ligand, water and the receptor would vary with temperature.

Assuming two hydrogen bonds are formed the thermodynamic binding energies for melatonin can be calculated using the equation of Williams *et al.* (1991):

$$\Delta G_{binding} = \Delta G_{T+R} + \Delta G_{Rotors} + \Delta G_{Hyd} + \Delta G_{Polar}$$

where $\Delta G_{binding}$ is the overall free energy of binding, ΔG_{T+R} is the loss in free energy due to restricted transition and rotation of the molecule, ΔG_{Rotors} is the loss in free energy due to loss in internal rotational freedom of associating components during binding, ΔG_{Hyd} is the favourable free energy change accompanying the association of hydrophobic species caused by desolvation, ΔG_{Polar} is the favourable free energy change due to interactions between polar functional groups, such as hydrogen bonding.

For melatonin the magnitude of each contribution to ΔG can be calculated from published data as follows: $\Delta G_{T+R} = 56$ kJ mol^{-1} for a molecule of mass 232 daltons binding to a macromolecule in an aqueous environment, $\Delta G_{Rotors} = 4-6$ kJ mol^{-1} for substrates with a relative molecular mass of a few hundred daltons, $\Delta G_{Hyd} = -0.19$ kJ mol^{-1} per A^2 of surface removed from exposure to water on binding. The surface area of melatonin is 488.2 A^2, ΔG_{Polar} = intrinsic binding energy of functional groups which would be between 12.552–16.736 kJ mol^{-1} per hydrogen-bond (as the energy varies according to the nature of the electronegative atoms involved in the hydrogen bond). Taking the averages for these contributions and assuming two hydrogen bonds are formed between the amide and 5-methoxy groups of melatonin and the receptor, $\Delta G_{binding} = 56 + 5 - 92.758 - 2(14.644) = -61.046$ kJ mol^{-1}.

Using the maximum and minimum values for ΔG_{Polar} and ΔG_{Rotors}, $\Delta G_{binding}$ varies between -57.86 and -64.23 kJ mol^{-1}. This calculation gives a value which agrees extremely well with experimentally determined value, predicting a K_i between 16 and 185 pM at 25°C. The experimentally determined K_i for melatonin at the chicken brain receptor at 25°C is 240 pM.

Further experiments will allow the molecular model proposed to be critically tested. First, a resurgence of interest in the pharmacology of melatonin has led to the synthesis and testing of novel analogues of melatonin by several groups. In particular, several novel series of potent melatonin analogues based on either a tetraline nucleus (Copinga *et al.*, 1993) or a naphthalene nucleus (Yous *et al.*, 1992) have recently been described. In addition, we have synthesized a series of high-affinity, conformationally restricted tetrahydrocarbazole analogues of melatonin (Garratt *et al.*, 1994) in which the amide side-chain has limited flexibility. It will be interesting to determine if these analogues can be docked into the proposed melatonin binding site. Second, the isolation of the cDNA for the melanophore melatonin receptor will facilitate the cloning of the mammalian melatonin receptor mediating the effects of the hormone on circadian and seasonal rhythms, and the identification of potential melatonin receptor subtypes (Krause & Dubocovich, 1991). Furthermore, site-directed mutagenesis studies will allow substitution or deletion of key amino acids enabling a direct test of the binding site model proposed.

We are grateful for the assistance of the WM 250 ULIRS NMR Service and to Drs Smithen, Klein and Smith for generously providing some of the melatonin analogues used in this study.

References

BARTNESS, T.J. & GOLDMAN, B.D. (1989). Mammalian pineal melatonin: a clock for all seasons. *Experientia*, **45**, 939–945.

BESHARSE, J.C., IUVONE, P.M. & PIERCE, M.E. (1988). Regulation of rhythmic photoreceptor metabolism: a role for post-receptoral neurons. In *Progress in Retinal Research*, ed. Osborne, N. & Chader, G.J. pp. 21–61. Oxford: Pergamon Press.

BRADFORD, M.M. (1976). A rapid and sensitive method for the quantitation of microgram quantities of protein utilizing the principle of protein-dye binding. *Anal. Biochem.*, **72**, 248–254.

CARLSON, L.L., WEAVER, D.R. & REPPERT, S.M. (1989). Melatonin signal transduction in hamster brain: inhibition of adenylyl cyclase through a pertussis toxin-sensitive G protein. *Endocrinology*, **125**, 2670–2676.

CHENG, Y.C. & PRUSOFF, W.H. (1973). Relationship between the inhibition constant (K_i) and the concentration of inhibitor which causes 50% inhibition (IC_{50}) of an enzymatic reaction. *Biochem. Pharmacol.*, **22**, 3099–3108.

CHONG, N.W.S. & SUGDEN, D. (1994). Thermodynamic analysis of agonist and antagonist binding to the chicken brain melatonin receptor. *Br. J. Pharmacol.*, **111**, 295–301.

COPINGA, S., TEPPER, P.G., GROL, C.J., HORN, A.S. & DUBOCOVICH, M.L. (1993). 2-Amido-8-methoxytetralins: a series of nonindolic melatonin-like agents. *J. Med. Chem.*, **36**, 2891–2898.

DELEAN, A., MUNSON, P.J. & RODBARD, D. (1978). Simultaneous analysis of families of sigmoidal dose-response curves: application to bioassay, radioligand assay and physiological dose-response curves. *Am. J. Physiol.*, **53**, E97–E102.

DUBOCOVICH, M.L. (1985). Characterization of a retinal melatonin receptor. *J. Pharmacol. Exp. Ther.*, **234**, 395–401.

EBISAWA, T., KARNE, S., LERNER, M.R. & REPPERT, S.M. (1994). Expression cloning of a high affinity melatonin receptor from *Xenopus* dermal melanophores. *Proc. Natl. Acad. Sci. U.S.A.*, **91**, 6133–6137.

FOLKARD, S., ARENDT, J., ALDHOUS, M. & KENNETT, H. (1990). Melatonin stabilizes sleep onset time in a blind man without entrainment of cortisol or temperature rhythms. *Neurosci. Lett.*, **113**, 193–198.

GARRATT, P.J., VONHOFF, S., ROWE, S.J. & SUGDEN, D. (1994). Mapping the melatonin receptor. 2. Synthesis and biological activity of indole-derived melatonin analogues with restricted conformations of the C-3 amidoethane side-chain. *Bioorg. Med. Chem. Lett.*, **4**, 1559–1564.

HIBERT, M.F., TRUMPP-KALLMEYER, S., BRUINVELS, A. & HOFLACK, J. (1989). Three-dimensional models of neurotransmitter G-binding protein-coupled receptors. *Mol. Pharmacol.*, **40**, 8–15.

HO, B.T., MCISAAC, W.M., TANSEY, L.W. & KRALIK, P.M. (1968). Hydroxyindole-O-methyltransferase II. Inhibitory activities of some N-acyltryptamines. *J. Pharmacol. Sci.*, **57**, 1988–2000.

HOLMES, S.W. & SUGDEN, D. (1982). Effects of melatonin on sleep and neurochemistry in the rat. *Br. J. Pharmacol.*, **76**, 95–101.

KRAUSE, D.N. & DUBOCOVICH, M.L. (1991). Melatonin receptors. *Annu. Rev. Pharmacol. Toxicol.*, **31**, 549–568.

LEATHERBARROW, R.J. (1987). *ENZFITTER – A Non-Linear Regression Data Analysis Program for the IBM PC.* Amsterdam: Elsevier-Biosoft.

LEWIS, D.F.V., ARENDT, J. & ENGLISH, J. (1990). Quantitative structure-activity relationships within a series of melatonin analogs and related indolealkylamines. *J. Pharmacol. Exp. Ther.*, **252**, 370–373.

LEWIS, D.F.V., KITCHEN, I., SUGDEN, D., ENGLISH, J. & ARENDT, J. (1993). Molecular modelling of G-protein coupled receptors: the interaction between specific ligands and their putative binding sites. In *Trends in QSAR & Molecular Modelling*, Vol 92, pp. 489–494. ed. Wermuth, C.G. Leiden: ESCOM.

MORGAN, P.J., BARRETT, P., HOWELL, H.E. & HELLIWELL, R. (1994). Melatonin receptors: localization, molecular pharmacology and physiological significance. *Neurochem. Int.*, **24**, 101–146.

MORGAN, P.J., LAWSON, W., DAVIDSON, G. & HOWELL, H.E. (1989). Melatonin inhibits cyclic AMP production in cultured ovine pars tuberalis cells. *J. Mol. Endocrinol.*, **3**, R5–R8.

PATERSON, A., CHONG, N.W.S., BRINKLOW, B.R., LOUDON, A.S.I. & SUGDEN, D. (1992). Characterization of 2-[^{125}I]-iodomelatonin binding sites in the brain of a marsupial, Bennett's wallaby (*Macropus Rufogriseus Rufogriseus*). *Comp. Biochem. Physiol.*, **102A**, 55–58.

POPLE, J.A., SANTRY, D.P. & SEGAL, G.A. (1965). Approximate self-consistent molecular orbital theory. I. Invariant procedures. *J. Chem. Physics*, **43 (suppl.)**, 129–135.

REDMAN, J.R., ARMSTRONG, S.M. & NG, K.T. (1983). Free-running activity rhythms in the rat: entrainment by melatonin. *Science*, **219**, 1089–1091.

STRADER, C.D., SIGAL, I.S., REGISTER, R.B., CANDELORE, M.R., RANDS, E. & DIXON, R.A.F. (1987). Identification of residues required for ligand binding to the β-adrenergic receptor. *Proc. Natl. Acad. Sci. U.S.A.*, **84**, 4384–4388.

SUGDEN, D. (1989). Melatonin biosynthesis in the mammalian pineal gland. *Experientia*, **45**, 922–932.

SUGDEN, D. (1991). Aggregation of pigment granules in single cultured *Xenopus laevis* melanophores by melatonin analogues. *Br. J. Pharmacol.*, **104**, 922–927.

SUGDEN, D. & CHONG, N.W.S. (1991). Pharmacological identity of 2-[^{125}I]iodomelatonin binding sites in chicken brain and sheep pars tuberalis. *Brain Res.*, **539**, 151–154.

TAMARKIN, L., BAIRD, C.J. & ALMEIDA, O.F.X. (1985). Melatonin: a co-ordinating signal for mammalian reproduction. *Science*, **227**, 714–720.

THORPE, D.J. & COEN, C.W. (1994). Entrainment of rat circadian rhythms by automated daily infusion of melatonin. *J. Physiol.*, **475**, 134P.

UNDERWOOD, H. (1989). The pineal and melatonin: regulators of circadian function in lower vertebrates. *Experientia*, **45**, 914–922.

VAKKURI, O., LAMSA, E., RAHKAMAA, E., RUOTSALAINEN, H. & LEPPALUOTO, J. (1984). Iodinated melatonin: preparation and characterisation of the molecular structure by mass and ^{3}H NMR spectroscopy. *Anal. Biochem.*, **142**, 284–289.

VANECEK, J. & KLEIN, D.C. (1992). Melatonin inhibits gonadotropin-releasing hormone-induced elevation of intracellular Ca^{2+} in neonatal rat pituitary cells. *Endocrinology*, **130**, 701–707.

VANECEK, J. & VOLLRATH, L. (1989). Melatonin inhibits cyclic AMP and cyclic GMP accumulation in the rat pituitary. *Brain Res.*, **505**, 157–159.

VANECEK, J. & VOLLRATH, L. (1990). Melatonin modulates diacylglycerol and arachidonic acid metabolism in the anterior pituitary of immature rats. *Neurosci. Lett.*, **110**, 199–203.

VINTER, J.G., DAVIS, A. & SAUNDERS, M.R. (1987). Strategic approaches to drug design 1. An integrated software framework for molecular modelling. *J. Comp.-Aided Mol. Design*, **1**, 31–51.

WALDHAUSER, F., SALETU, B. & TRINCHARD-LUGAN, I. (1990). Sleep laboratory investigations on hypnotic properties of melatonin. *Psychopharmacology*, **100**, 222–226.

WHITE, B.H., SEKURA, R.D. & ROLLAG, M.D. (1987). Pertussis toxin blocks melatonin-induced pigment aggregation in *Xenopus* dermal melanophores. *J. Comp. Physiol. B.*, **157**, 153–159.

WILLIAMS, D.H., COX, J.P.L., DOIG, A.J., GARDNER, M., GERHARD, U., KAYL, P.T., LAL, A.R., NICHOLLS, I.A., SALTER, C.J. & MITCHELL, R.C. (1991). Toward the semi-quantitative estimation of binding constants. Guides for peptide-peptide binding in aqueous solution. *J. Am. Chem. Soc.*, **113**, 7020–7030.

YOUS, S., ANDRIEUX, J., HOWELL, H.E., MORGAN, P.J., RENARD, P., PFEIFFER, B., LESIEUR, D. & GUARDIOLA-LEMAITRE, B. (1992). Novel naphthalenic ligands with high affinity for the melatonin receptor. *J. Med. Chem.*, **35**, 1484–1486.

(Received July 20, 1994
Revised September 15, 1994
Accepted October 10, 1994)

British Journal of Pharmacology (1995) 114, 624-631

Effect of crilvastatin, a new cholesterol lowering agent, on unesterified LDL-cholesterol metabolism into bile salts by rat isolated hepatocytes

Thierry Clerc, Véronique Sbarra, Nicolas Diaconescu, Huguette Lafont, *Guy Jadot, **Claude Laruelle & [1]Françoise Chanussot

INSERM, Unité 130, 18 Avenue Mozart, 13009 Marseille, France; *Laboratories Pan Medica, 94204 Ivry-sur-Seine, France and **CL Pharma, 06200 Nice, France

1 The aim of these experiments was to determine the effect of crilvastatin, a new cholesterol lowering agent, on the metabolism of unesterified low density lipoprotein (LDL)-cholesterol by rat freshly isolated hepatocytes. This preclinical model was developed as an alternative to *in vivo* experiments, to mimic the metabolic effects of a molecule on its target cells and to define optimal conditions for future experimentation on human hepatocytes.

2 Cells were obtained from normolipidaemic or hypercholesterolaemic rats, hypercholesterolaemia was nutritionally induced. Incubations were performed in a medium containing 600 μM taurocholate and 50 μM or 300 μM crilvastatin.

3 This molecule was shown *in vitro* to be carried by physiological transporters, i.e., albumin-bile salt micellar associations and LDL. Crilvastatin induced a significance increase in the synthesis and secretion by hepatocytes of bile salts resulting from the metabolism of unesterified LDL-cholesterol in both normolipidaemic and hypercholesterolaemic rats. Stimulation involved non-conjugated as well as tauro- and glyco-conjugated bile salts. These findings corroborate preliminary studies showing *in vivo* that crilvastatin enhances the secretion of bile acids by stimulating the uptake and incorporation of LDL-cholesterol by the liver.

Keywords: Isolated hepatocytes; cholesterol; bile salts; lipoproteins; hypercholesterolaemia; crilvastatin

Introduction

Crilvastatin (Esnault-Dupuy *et al.*, 1988) belongs to a new generation of cholesterol-lowering agents, the statins, inhibitors of the hydroxymethylglutaryl-coenzyme A reductase activity (Alberts, 1988a, b). In contrast to lovastatin, which in man lowers cholesterol and bile salt secretion in bile (Mitchell *et al.*, 1991), crilvastatin was shown in hypercholesterolaemic rats to stimulate bile cholesterol and bile salt secretion (Clerc *et al.*, 1993). Thus, in order to elucidate the mechanism of action of this drug in the hepatocyte, we have studied the fate of unesterified low density lipoprotein (LDL)-cholesterol in hepatocytes freshly isolated from normolipidaemic or hypercholesterolaemic rats.

In order to compensate for isolation effects, e.g. alteration of lipoprotein receptors (Gebhardt, 1986) due to disturbances in membrane polarity, addition of both taurocholate (TC) and LDL restored bile salt secretion by rat isolated hepatocytes to a level comparable to that observed *in vivo* (personal data). Bile cholesterol originates mostly from the LDL-cholesterol (Schwartz *et al.*, 1978; Robins & Brunengraber, 1982). Thus, in our experiment, freshly isolated LDL was added to the incubation medium. Since bile salts coming from the enterohepatic circulation (Henry *et al.*, 1987) are a major source of bile salt secretion, taurocholate was also added to the medium. In addition, it was important to incubate crilvastatin bound to physiological transporters: albumin, amphipathic molecules (bile salts), and lipoproteins such as LDL.

Methods

Animals

Sixteen 3-week-old male Wistar rats raised by Iffa Credo (L'Arbresle, France) were randomly placed in stainless steel cages. For 6 months, 8 rats (group A) received a low fat control diet (total fat content 5% : 3% lard and 2% corn oil), 8 rats (group B) received a high fat diet (29.2% fat: 26% lard, 2% corn oil, and 1.2% cholesterol). Both diets were isoprotidic (24% casein) and supplied daily requirements in essential fatty acids and protein.

After an overnight fast 3 days before the experiment, rats were anaesthetized with diethyl ether and blood (1 ml) was collected for plasma lipid analysis.

Physiological transport of crilvastatin

Tests were carried out to determine the binding of crilvastatin (cycloalkyl ester of pyroglutamic acid, Pan Medica, Ivry-sur-Seine, France) with physiological transporters : albumin, taurocholate and lipoproteins.

Emulsion of crilvastatin Taurocholate (TC) (Calbiochem, Meudon, France) 0.6 μmol in ethanol, crilvastatin 0.3 μmol in ethanol and [5-6 ^{3}H-cycloalkyl-]-crilvastatin (Isotopchim, Ganagobie-Peyruis, France, specific activity: 30 mCi mmol^{-1}) 0.1 μCi in ethanol, were mixed with gentle stirring. Solvent was carefully removed by evaporation under nitrogen. The resulting mixture was emulsified in 1 ml of RPMI 1640 (Flow Laboratories, Irvine, Scotland) without sodium bicarbonate or glutamine by 15 s pulses for 30 min in an ultrasonic device (Sonic-Bioblock, Illkirch, France). The radioactivity of a 20 μl aliquot of the emulsion in 10 ml scintillation liquid (Emulsifier Safe, Packard, Rungis, France) was counted in a Beckman LS 9000 liquid scintillation spectrophotometer equipped with an external standard.

Transport of crilvastatin To study transport of crilvastatin by albumin, taurocholate and lipoproteins, three dialysis assays were performed against a solution containing only NaCl 0.9% and TC 600 μM, using a membrane (Spectrapor

[1] Author for correspondence.

3500, Spectrum, Los Angeles CA, U.S.A.) retaining molecules greater than 3500 daltons. In the first dialysis, the medium contained the aforesaid emulsion; in the second dialysis, the medium contained the aforesaid emulsion and albumin, 22.3 mg ml^{-1}. In the third dialysis, the medium contained NaCl 0.9%, TC 600 μM, foetal calf serum (FCS), albumin and lipoproteins at the same concentrations as in hepatocyte incubation. After 1 h dialysis, radioactivity in the medium inside and outside the dialysis bag was counted as previously described.

To study transport of crilvastatin by lipoproteins, electrophoresis according to Moulin *et al.* (1979) was carried out using one volume of the third dialysis medium containing lipoproteins, in one volume of a solution containing Black Soudan (Pharmindustrie, IBF, Villeneuve la Garenne, France) at a concentration of 0.5% in ethylene glycol. After colour development in darkness for 24 h at 4°C, 25 μl of the mixture was deposited on a discontinuous gradient (2%–3%) polyacrylamide agarose gel electrophoresis. After migration, lipoproteins were removed, fractionated and oxidized in a bath of hydrogen peroxide, 30 V for 24 h at 70°C. Radioactivity in the different lipoproteic fractions was counted in 10 ml scintillation liquid (Hionic Fluor, Packard).

Experiment with isolated hepatocytes

Non-fasting rats were anaesthetized with sodium pentobarbitone (5 mg 100 g^{-1} body weight). Hepatocytes were isolated by perfusing the liver with type IV collagenase (Sigma, St Louis, Mo, U.S.A.) for 5 min according to the methods of Berry & Friend (1969) and Seglen (1962). A chelating agent (EDTA, 2.28 g l^{-1}) in Krebs buffer was pre-infused to eliminate calcium. This technique provides a yield greater than 85% with little contamination from non-parenchymal cells.

Freshly isolated hepatocytes were incubated under an atmosphere of 95% O_2, 5% CO_2, in a buffer containing RPMI 1640 without sodium bicarbonate or glutamine, with HEPES (20 mmol l^{-1}, Sigma), gentamycin (8 mg l^{-1}, Seromed, Frankfurt, Germany), insulin (0.05 u ml^{-1}, Actrapid HM, Novo, Boulogne, France) and foetal calf serum (4 μl ml^{-1}, Sigma).

Cells were suspended at a concentration range of $8-10 \times 10^6$ cells ml^{-1}. Bovine serum albumin (223 mg 10 ml^{-1} medium, fraction V powder, 98–99% albumin, Sigma) was added to prevent any toxic effects of incubated or newly synthesized bile salts. Cell viability was controlled throughout the experiment by counting stained cells under a light microscope in a Burker chamber after trypan blue exclusion. Viability was always over 85% of the total number of cells. We also checked that cell viability was not affected by the duration of experiment and addition of bile salts and crilvastatin. TC did not have a toxic effect, the level of alkaline phosphatases and β-glucuronidase in the medium being stable (± 10%) with or without 600 μM bile salts.

Aliquots were taken during the course and at the end of the experiment. Each sample was centrifuged at 3000 *g* for 5 min at 4°C, cells were removed, rinsed twice at 4°C with RPMI/HEPES buffer and centrifuged at 3000 *g* for 5 min at 4°C, to eliminate any traces of radioactivity. The wash buffer was added to the medium aliquot.

Preparation of ^{14}C-labelled unesterified cholesterol-LDL

Labelled LDL was obtained by incubation of rat plasma with [^{14}C]-unesterified cholesterol-liposomes.

Radiolabelled liposomes were prepared as follows: 1.66 mg dioleoyl-phosphatidylcholine (Sigma), 0.25 mg unlabelled cholesterol (Sigma) and 3.6 μCi [4-^{14}C]-cholesterol (NEN-Dupont de Nemours, Paris, France, specific activity: 50 mCi $mmol^{-1}$) were mixed in chloroform/ethanol/benzene. The solvent was carefully removed by evaporation under nitrogen. Trace amounts of solvent do not affect liposome structure. Dioleoyl-phosphatidylcholine was chosen in order to obtain liposomes of the smallest size (100 nm). After dispersion in 1 ml RPMI 1640 by 15 s pulses for 30 min in an ultrasonic device (Sonics-Bioblock), the resulting multilamellar liposomes were centrifuged at 100 000 *g* for 20 min at 10°C (Beckman L 5.75B ultracentrifuge, Palo Alto, CA, U.S.A., equipped with a fixed angle rotor type 60 Ti) to remove large particles. Integrity of the liposomes was checked by filtration on A4 gel (Ultrogel, IBF, Villeneuve la Garenne, France) with Tris buffer 0.5 M pH 7.5. Liposomes were eluted in a single peak.

Plasma (15 ml) from overnight fasted rats was collected into EDTA (0.1 mg ml^{-1}) and incubated for 24 h at 10°C with 3 ml of [^{14}C]-cholesterol-liposomes in order to label the plasma lipoproteins. Under these conditions, [^{14}C]-cholesterol-LDL labelling resulted from a direct exchange between plasma lipoproteins and liposomes.

Liposomes were removed by ultracentrifugation and flotation at 120 000 *g* at 10°C for 18 h in the density zone below 1.00. LDL were recovered after ultracentrifugation at 120 000 *g* at 10°C for 22 h in a sucrose solution of density 1.063, according to the method of Hatch & Less (1968). After labelling, LDL were dialyzed against NaCl 0.9% for 24 h at 10°C to remove sucrose and then concentrated on Amicon filter (B15, Amicon, Paris, France). Final concentration was adjusted with RPMI 1640 medium. Purity of the [^{14}C]-LDL fraction was confirmed by SDS gel electrophoresis showing only one fraction in the migration zone of LDL. Assays of apoproteins AI and B100 revealed that the [^{14}C]-LDL fraction contained only Apo B100. To verify that the esterfied cholesterol fraction was unlabelled, thin layer chromatography (t.l.c.) of lipids was carried out on silica gel F 1500 (Schleicher and Schüll, Dassel, Germany) using heptane/diethyl ether/ice cold acetic acid 90/30/1 v/v as developing solvent. Identification was achieved under iodine vapours and the spots were scrapped and counted in 10 ml scintillation liquid (Hionic Fluor, Packard). [^{14}C]-cholesterol in the LDL was exclusively on the unesterified cholesterol fraction. The negligible mass of radioactive cholesterol did not modify the metabolism of LDL. Radioactive LDL accounted for 50% of total labelling of incubated ^{14}C liposomes.

Incubation of hepatocytes with ^{14}C labelled unesterified cholesterol-LDL

Nine milliliters of hepatocyte preparation was incubated with 0.45 μCi [^{14}C]-unesterified cholesterol-LDL in the presence of 600 μM TC. Crilvastatin was added at the concentration 50 or 300 μM. Dispersion of the drug was performed with TC in 2 ml of RPMI 1640 and was then achieved by 15 s pulses for 30 min in an ultrasonic device. Each incubation (10 ml) contained 0.74 μg unesterified LDL-cholesterol.

The specific radioactivity of cholesterol in the incubation medium did not change during the experiment.

Distribution of radioactivity

Medium and cells were collected between 5 and 90 min in order to determine equilibrium steady-state conditions. Cell ^{14}C radioactivity was counted in 9 ml Ionic Fluor scintillation liquid (Packard) on pellets previously subjected to digestion in 1 ml of Soluene (Packard) for 2 h at 37°C.

Bile salts and cholesterol were extracted from the incubation medium and hepatocytes in a 10 fold volume of isopropanol in water (90/10, v/v) followed by boiling for 10 min to precipitate proteins. We verified that non-labelled material precipitated with the proteins and that extraction of bile salts and cholesterol was complete. After centrifugation at 2 500 *g* for 5 min, extracts were concentrated under nitrogen, bile salts (tauroconjugated, glycoconjugated, free cholate) and cholesterol were separated by t.l.c. using silica gel F1500 (Schleicher and Schüll), the ^{14}C radioactivity of the fractions

was counted. To ensure against possible contamination between components during chromatography, previous tests were carried out to compare migrations of [^{14}C]-cholesterol, [^{14}C]-taurocholate, [^{14}C]-glycocholate standards and blank. The elution medium consisted of a mixture of isoamyl acetate, propionic acid, isopropanol and water (40/30/20/10, v/v). Fractions were detected under a 350 nm u.v. light after spraying silica gel with a reagent containing 0.4 ml of a 10% solution $FeCl_3$ in ice-cold acetic acid diluted in 60 ml ice-cold acetic acid, 40 ml concentrated sulphuric acid and 100 ml absolute ethanol.

Assays

The protein content of the medium was measured by the method of Lowry *et al.* (1951) with bovine serum albumin used as a standard. Bile salts were assayed by the enzymatic method of Domingo *et al.* (1972), β-glucuronidase and alkaline phosphatase respectively by the methods of Morgenstern *et al.* (1965) and Fishman *et al.* (1967).

Statistical analysis

Differences were compared by Student's *t* test (Table 1 and Figure 1). Other results were assessed by using analysis of variance (ANOVA) for repeated values and the differences were determined by the Fischer's test at a probability value of 95%.

Results

Plasma cholesterol levels

Cholesterolaemia of overnight fasting animals was 2.5 mmol l^{-1} in the low-fat group and 8.0 mmol l^{-1} in the high-fat group (results only expressed in the text).

Emulsion of crilvastatin (Table 1, Figure 1)

When mixed in RPMI medium, TC and crilvastatin formed mixed micelles and mixed premicelles (Hauton *et al.*, 1986). [^{3}H]-crilvastatin was entirely in the aqueous phase (98% ± 0.4%, $n = 6$). Based on this finding, mixed micelles and mixed premicelles of the drug were prepared extemporaneously before being added to the incubation medium.

Crilvastatin having a molecular weight of 253, the drug dialyzes though a 3 500 Da membrane, in proportions depending on its association with components in the medium. When TC was added, 7.2% crilvastatin remained in the dialysis space. When albumin was added, 15% of crilvastatin remained in the dialysis space. When rat serum was added, measurement of ^{3}H radioactivity in the different migration zones of lipoproteins on polyacrylamide/agarose electrophoresis gel showed that 63% of the [^{3}H]-crilvastatin present on lipoproteins were associated with LDL. These observations strongly suggest that rat-LDL is implicated in the transport of crilvastatin. This phenomenon is probably of major importance in cases of high LDL levels, e.g. hypercholesterolaemia.

Incubation of rat isolated hepatocytes with TC, albumin, crilvastatin and [^{14}C]-cholesterol-LDL

Distribution of ^{14}C radioactivity in hepatocytes (Figure 2). The amounts of [^{14}C]-cholesterol incorporated into the hepatocytes were unchanged by addition of the drug (0 *vs* 50 or 300 μM crilvastatin). The quantity of radiolabelled material increased with the duration of the experiment and was lower in group B than in group A from 30 min to the end of the experiment.

Distribution of ^{14}C radioactivity in the incubation medium (Table 2, Figure 3). The quantity of [^{14}C]-cholesterol added to the medium was sufficient to induce a new synthesis of ^{14}C-labelled bile salts. The amount of [^{14}C]-cholesterol decreased and newly synthesized ^{14}C bile salts increased between 5 and 90 min of incubation. In group A, the increase was greater (x 1.5) when 50 μM or 300 μM crilvastatin was added. At both concentrations of crilvastatin, the amounts of ^{14}C bile salts secreted in the medium were comparable and showed a maximum at 30 and 90 min. In the high-fat group, the quantity of radiolabelled bile salts in the medium was always higher than in the control group. However the effect of crilvastatin on the new synthesis of radiolabelled bile salts seemed more efficient at 50 μM, no decrease was observed at 60 min.

Newly synthesized ^{14}C bile salts (Figures 4–6). New synthesis was the highest with unconjugated [^{14}C]-cholate partic-

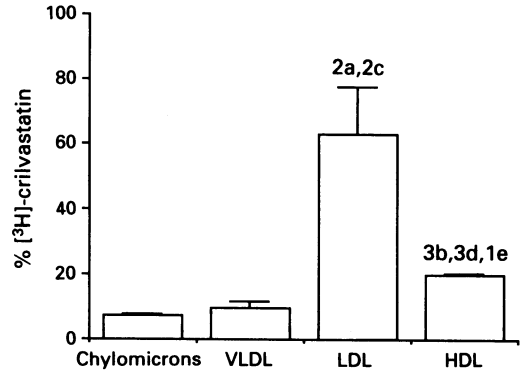

Figure 1 Lipoprotein carriers of crilvastatin: ^{3}H radioactivity was counted in the lipoprotein fraction after incubation of [^{3}H]-crilvastatin with rat serum added in the incubation medium. Results are expressed as means ± s.e.mean ($n = 6$). Differences were analysed by Student's *t* test and are significant at: $^1P<0.05$; $^2P<0.01$; $^3P<0.001$; ^{a}: chylomicrons vs LDL; ^{b}: chylomicrons vs HDL; ^{c}: VLDL vs LDL; ^{d}: VLDL vs HDL; ^{e}: LDL vs HDL. For abbreviations, see text.

Table 1 Mode of transport of crilvastatin (% [^{3}H]-crilvastatin recovered at the end of dialysis)

Dialysis conditions	*In the space of dialysis*	*In the dialysis buffer*
I Mixed micelles and mixed premicelles TC/[^{3}H]-crilvastatin	7.2 ± 0.1	92.8 ± 1.2
II Mixed micelles and mixed premicelles TC/albumin/[^{3}H]-crilvastatin	14.1 ± 0.1^{3a}	85.9 ± 0.2^{2a}
III Mixed micelles, mixed premicelles and lipoproteins TC/albumin/[^{3}H]-crilvastatin/lipoproteins/FCS	21.2 ± 0.4^{3b,3c}	78.8 ± 0.2^{3b,3c}

FCS: foetal calf serum. Results are expressed as means ± s.e.mean ($n = 4$). Differences were analysed by Student's *t* test and are significant at: ^{a}I vs II; ^{b}I vs III; ^{c}II vs III; $^2P<0.01$; $^3P<0.001$.

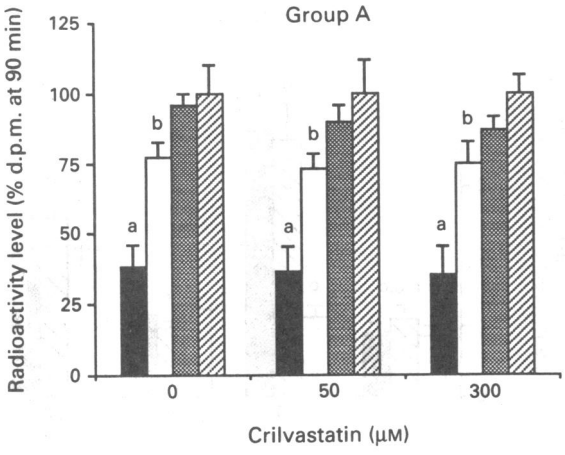

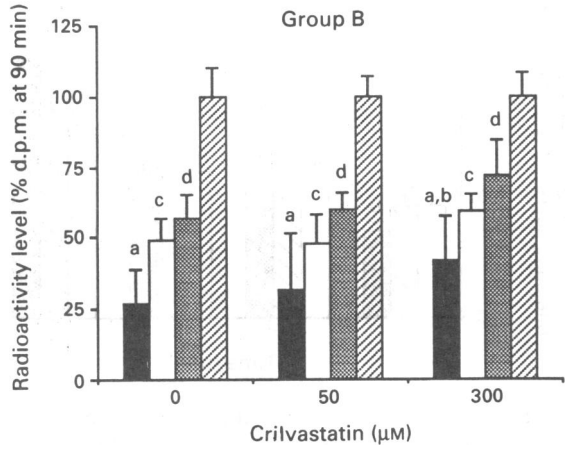

Figure 2 Distribution of ^{14}C radioactivity into hepatocytes: solid columns, time 0 min; open columns, time 30 min; stippled columns, time 60 min; hatched columns, time 90 min. Group A: low fat control group ($n = 7$). Group B: high fat group ($n = 8$). Samples A and B were assessed by using analysis of variance (ANOVA) for repeated values and the differences were determined by Fischers's test at a probability of 95%. Results are expressed as means ± s.e.mean.

Group A: [a]: time 5 min crilvastatin (C) 0 μM, 50 μM, 300 μM vs time 30 min, 60 min, 90 min, C 0 μM, 50 μM, 300 μM; [b]: time 30 min, C 0 μM, 50 μM, 300 μM vs time 90 min, C 0 μM, 50 μM, 300 μM.

Group B: [a]: time 5 min, C 0 μM vs time 30 min, 60 min, 90 min, C 0 μM; b: time 5 min, C 300 μM vs time 60 min, C 300 μM; [c]: time 30 min, C 0 μM, 50 μM, 300 μM vs time 90 min, C 0 μM, 50 μM, 300 μM; [d]: time 60 min, C 0 μM, 50 μM, 300 μM vs time 90 min, C 0 μM, 50 μM, 300 μM.

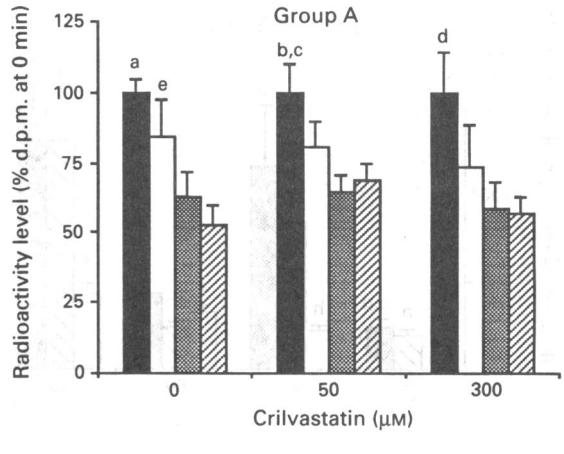

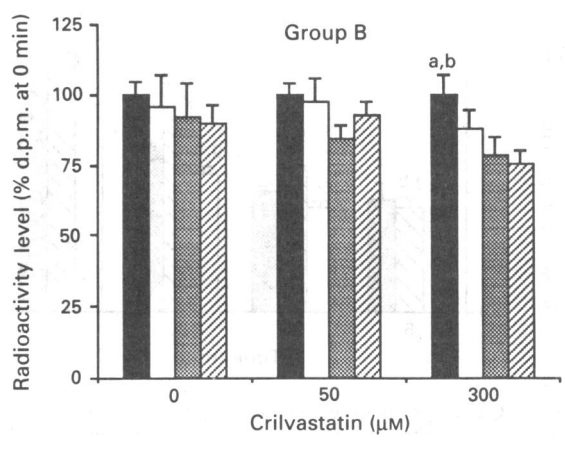

Figure 3 Distribution of ^{14}C radioactivity in the incubation medium: solid columns, time 0 min; open columns, time 30 min; stippled columns, time 60 min; hatched columns, time 90 min. Group A: low fat control group ($n = 7$). Group B: high fat control group ($n = 8$). Samples A and B were assessed by using analysis of variance (ANOVA) for repeated values and the differences were determined by Fischers's test at a probability of 95%. Results are expressed as means ± s.e.mean.

Group A: [a]: time 5 min crilvastatin (C) 0 μM vs time 60 min, 90 min, C 0 μM; [b]: time 5 min, C 50 μM vs time 30 min, C 50 μM; [c]: time 5 min, C 50 μM vs time 60 min, 90 min, C 50 μM; [d] time 5 min, C 300 μM vs time 60 min, 90 min, C 300 μM; [e]: time 30 min, C 0 μM vs time 90 min, C 0 μM.

Group B: [a]: time 5 min, C 300 μM vs time 60 min, C 300 μM; [b]: time 5 min, C 300 μM vs time 90 min, C 300 μM.

Table 2 Quantitites of ^{14}C-labelled bile salts synthesized by hepatocytes from LDL-[^{14}C]-unesterified cholesterol and secreted in the incubation medium (pmol secreted per 10^6 cells)

	Group A			*Group B*		
Crilvastatin (μM)	0	50	300	0	50	300
Time (min)						
5	92.8 ± 15.2	126.4 ± 22.4	127.2 ± 27.2	459.9 ± 47.4	462.7 ± 36.5	474.5 ± 13.0
30	140.8 ± 21.6	384.0 ± 80.0[a,i]	564.0 ± 191.2[e,j]	456.2 ± 69.3	468.5 ± 80.3	470.8 ± 51.1
60	184.8 ± 28.8	144.8 ± 20.0[e]	195.2 ± 39.2[g]	492.7 ± 36.5	737.3 ± 138.7[m,o,s]	704.4 ± 51.1[r]
90	247.2 ± 46.4	511.2 ± 160.8[b,d,k]	487.2 ± 128.0[f,h,l]	671.6 ± 135.0	1062.1 ± 208.0[n,p,q,t]	693.5 ± 69.3[u]

A: control group; B: hypercholesterolaemic group. Results are expressed as means ± s.e.mean (A: $n = 7$; B: $n = 8$). The ANOVA test for repeated values was used and differences were determined by Fisher's test at a probability of 95%. In group A: with 50 μM crilvastatin: [a]: 5 min vs 30 min; [b]: 5 min vs 90 min; [c]: 30 min vs 60 min; [d]: 60 min vs 90 min; with 300 μM crilvastatin: [e]: 5 min vs 30 min; [f]: 5 min vs 90 min; [g]: 30 min vs 60 min; [h]: 60 min vs 90 min; at 30 min; [i]: 0 μM vs 50 μM crilvastatin; [j]: 0 μM vs 300 μM crilvastatin; at 90 min: [k]: 0 μM vs 50 μM crilvastatin; [l]: 0 μM vs 300 μM crilvastatin. In group B: with 50 μM crilvastatin: [m]: 5 min vs 60 min; [n]: 5 min vs 90 min; [o]: 30 min vs 60 min; [p]: 30 min vs 90 min; [q]: 60 min vs 90 min; with 300 μM crilvastatin: [r]: 30 min vs 60 min; at 60 min: [s]: 0 μM vs 50 μM crilvastatin; at 90 min: [t]: 0 μM vs 50 μM crilvastatin; [u]: 50 μM vs 300 μM crilvastatin.

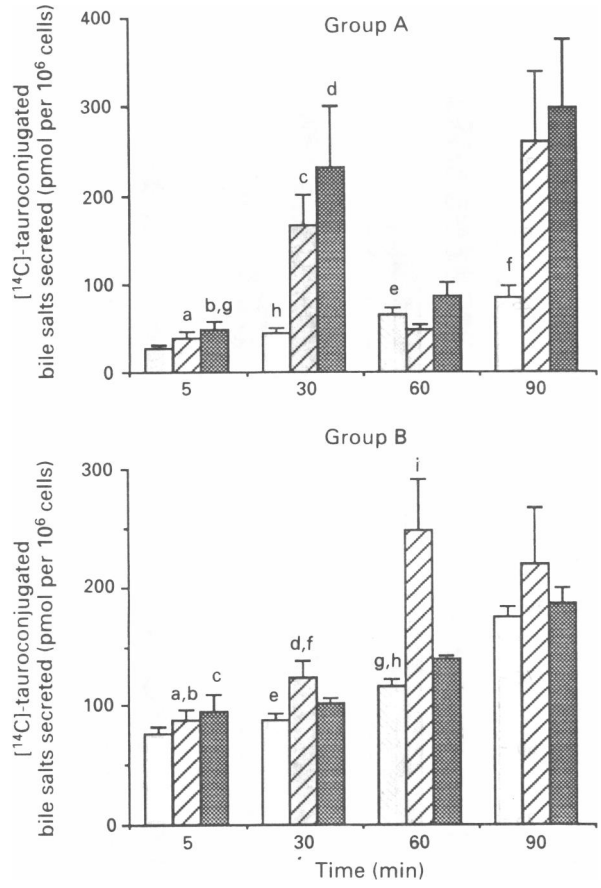

Figure 4 Quantities in the incubation medium of ^{14}C-tauro-conjugated bile salts synthesized from [^{14}C]-unesterified LDL-cholesterol: open columns, without crilvastatin; hatched columns, 50 μM crilvastatin; stippled columns, 300 μM crilvastatin. group A: low fat control group ($n = 7$). Group B: high fat group ($n = 8$). Samples A and B were assessed by using analysis of variance (ANOVA) for repeated values and the differences were determined by Fischers's test at a probability of 95%.

Group A: [a]: time 5 min, crilvastatin (C) 50 μM vs time 30 min, 90 min, C 50 μM; [b]: time 5 min, C 300 μM vs time 30 min, C 300 μM; [c]: time 30 min, C 50 μM vs time 60 min, C 50 μM; [d]: time 30 min, C 300 μM vs time 60 min, C 300 μM; [e]: time 60 min, C 0 μM, 50 μM, 300 μM vs time 90 min, C 0 μM, 50 μM, 300 μM; [f]: time 90 min, C 0 μM vs time 90 min, C 50 μM, 300 μM; [g]: time 5 min, C 300 μM vs time 90 min, C 300 μM; [h]: time 30 min, C 0 μM vs time 30 min, C 50 μM, 300 μM.

Group B: [a]: time 5 min, C 50 μM vs time 90 min, C 50 μM; [b]: time 5 min, C 50 μM vs time 60 min, C 50 μM; [c]: time 5 min, C 300 μM vs time 60 min, C 300 μM; [d]: time 30 min, C 50 μM vs time 60 min, C 50 μM; [e]: time 30 min, C 0 μM, 300 μM vs time 90 min, C 0 μM, 300 μM; [f]: time 30 min, C 50 μM vs time 90 min, C 50 μM; [g]: time 60 min, C 0 μM vs time 60 min, C 50 μM; [h]: time 60 min, C 0 μM vs time 90 min, C 0 μM; [i]: time 60 min, C 50 μM vs time 60 min, C 300 μM

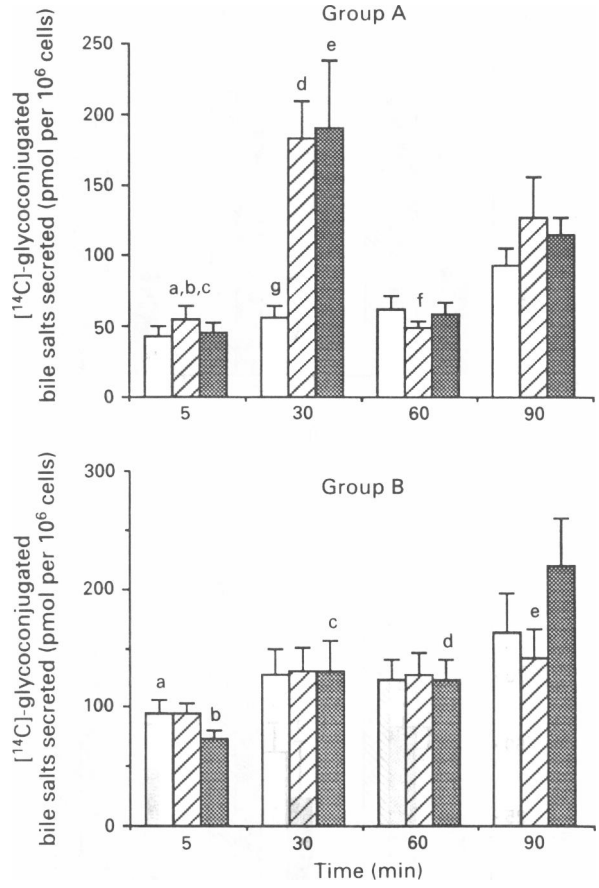

Figure 5 Quantities in the incubation medium of ^{14}C-glyco-conjugated bile salts synthesized from [^{14}C]-unesterified LDL-cholesterol: open columns, without crilvastatin; hatched columns, 50 μM crilvastatin; stippled columns, 300 μM crilvastatin. Group A: low fat control group ($n = 7$). Group B: high fat group ($n = 8$). Samples A and B were assessed by using analysis of variance (ANOVA) for repeated values and the differences were determined by Fischers' test at a probability of 95%.

Group A: [a]: time 5 min crilvastatin (C) 50 μM, 300 μM vs time 30 min, C 50 μM, 300 μM; [b]: time 5 min, C 50 μM vs time 90 min, C 50 μM; [c]: time 5 min, C 50 μM, 300 μM vs time 30 min, C 50 μM, 300 μM; [d]: time 30 min, C 50 μM vs time 60 min, C 50 μM; [e]: time 30 min, C 300 μM vs time 90 min, C 300 μM; [f]: time 60 min, C 50 μM vs time 90 min, C 50 μM; [g]: time 30 min, C 0 μM vs time 30 min, C 50 μM, 300 μM.

Group B: [a]: time 5 min, C 0 μM vs time 90 min, C 0 μM; [b]time 5 min, C 300 μM vs time 90 min, C 300 μM; [c]: time 30 min, C 300 μM vs time 90 min, C 300 μM; [d]: time 60 min, C 300 μM vs time 90 min, C 300 μM; [e]: time 90 min, C 50 μM vs time 90 min, C 300 μM.

ularly in the high fat group. In groups A and B, crilvastatin increased the amount of radiolabelled cholate in the medium. ^{14}C tauro-conjugated bile salts were stimulated by crilvastatin at 30 and 90 min (group A) and at 30 and 60 min (group B). ^{14}C glyco-conjugated bile salts were stimulated by crilvastatin at 30 min (group A).

Discussion

A priori, freshly isolated hepatocytes of the rat do not constitute the best model for studying metabolic processes involving the integrity of plasma membranes (Gebhardt, 1986). However, incubation of cells with bile salts and freshly isolated lipoproteins like LDL results in an enhanced bile salt secretion in the medium (personal observations). Although uptake of taurocholate decreases (Kukongviriyapan & Stacey, 1989), bile acid synthesis and cholesterol 7α-hydroxylase activity are maintained in rat cultured hepatocytes (Princen & Meijer, 1990) and probably in this model of freshly isolated rat hepatocytes (Alberts, 1988a; Blaanboer *et al.*, 1990). In addition, our results corroborate those obtained by Bouscarel *et al.* (1991) in the hamster showing that ursodeoxycholate has a direct effect on recruitment of LDL receptors from a latent pool in the hepatocellular membranes of isolated hepatocytes. Although rat hepatocyte membranes are poor in LDL receptors and thus non-specific uptake of LDL cannot be ruled out in our experiments, taurocholate appeared to stimulate LDL uptake.

A direct correlation has been observed between the rate of lipoprotein uptake by hepatocytes and bile salt secretion

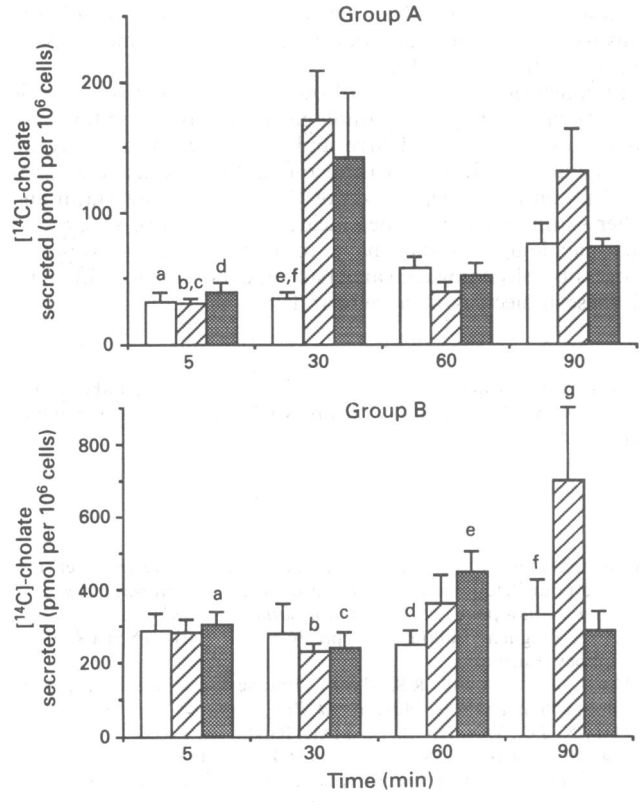

Figure 6 Quantities in the incubation medium of [^{14}C]-cholate synthesized from [^{14}C]-unesterified LDL-cholesterol: open columns, without crilvastatin, hatched columns, 50 μM crilvastatin; stippled columns, 300 μM crilvastatin. Group A: low fat control group ($n = 7$). Group B: high fat group ($n = 8$). Samples were assessed by using analysis of variance (ANOVA) for repeated values and the differences were determined by Fischer's test at a probability of 95%.

Group A: [a]: time 5 min, crilvastatin (C) 0 μM vs time 90 min, C 0 μM; [b]: time 5 min, C 50 μM vs time 30 min, C 50 μM; [c]: time 5 min, C 50 μM vs time 90 min, C 50 μM; [d]: time 5 min, C 300 μM vs time 30 min, C 300 μM; [e]: time 30 min, C 0 μM vs time 30 min C 50 μM, 300 μM; [f]: time 30 min, C 0 μM vs time 90 min, C 0 μM.

Group B: [a]: time 5 min, C 300 μM vs time 60 min, C 300 μM; [b]: time 30 min, C 50 μM vs time 90 min, C 50 μM; [c]: time 30 min, C 300 μM vs time 60 min, C 300 μM; [d]: time 60 min, C 0 μM vs time 60 min, C 300 μM; [e]: time 60 min, C 300 μM vs time 90 min, C 300 μM; [f]: time 90 min, C 0 μM vs time 90 min, C 50 μM; [g]: time 90 min, C 50 μM vs time 90 min, C 300 μM.

(Davis *et al.*, 1983). This correlation was particularly marked between uptake of cholesterol-rich lipoproteins (LDL, HDL) and synthesis of bile salts from lipoproteic cholesterol (Junker & Davis, 1989; Whiting *et al.*, 1989; Kwekkeboom *et al.*, 1990). Incorporation of lipoproteic cholesterol implies binding of bile salts to lipoproteins (Kramer *et al.*, 1979; Chitranukroh & Billing, 1983; Salvioli *et al.*, 1985; Ceryak *et al.*, 1993). Experimental evidence indicates that in the hepatic sinusoidal spaces, one third of bile salts are bound to lipoproteins and two thirds to albumin, this binding does not induce a denaturation even at high bile salt concentrations (Hauton *et al.*, 1982).

The ^{14}C total radioactivity remained unchanged in the cells and in the incubation medium during the experiment and there is no significant difference between incubations with or without crilvastatin. The intracellular ^{14}C radioactivity is the difference between ^{14}C taken up by the hepatocytes and ^{14}C secreted from the cells. This result does not significantly change by the addition of the drug, stimulating both uptake and secretion of ^{14}C materials. In addition, amounts of ^{14}C bile salts are small compared to the incubated [^{14}C]-cholesterol.

The incubation medium is a mixture of both plasma and bile. The bile salt concentration does not exceed 200 μM in the portal vein (Botham *et al.*, 1981). However, in the hepatic bile, the bile salt concentration reaches 30 mM. Thus we decided to choose 600 μM as an intermediate bile salt concentration in the incubation medium. The 600 μM bile salt value is 10 times lower than the critical micellar concentration of the added taurocholate. In addition, the amount of taurocholate required to achieve a stimulating effect on bile salt synthesis was more than 10 times higher than the concentration found to be efficient in rat cultured hepatocytes (Twisk *et al.*, 1993). Such differences can be explained by the need for greater quantities of bile salts with isolated cells than cultured cells in which bile canalicular spaces are already formed, contributing to a higher bile salt secretion. In addition, Alberts (1988a) noted that drugs like pravastatin induced greater inhibition of HMG CoA reductase in freshly isolated hepatocytes than cultured hepatocytes. Thus, our model could constitute a promising alternative to *in vivo* experiments or experiments using cultured cells.

Results of dialysis showed that crilvastatin was carried to a great extent by mixed micelles and to a lower extent by LDL. Thus in our cellular model, 50 or 300 μM crilvastatin was added in the physiological form of mixed micelles in presence of 600 μM taurocholate. Crilvastatin enhances significantly the new bile salts synthesis from unesterified LDL cholesterol, as compared to control without the drug. A similar increase was previously reported in the rat *in vivo* (Clerc *et al.*, 1993). Addition of 50 μM or 300 μM crilvastatin resulted in a 2 to 3 fold increase in the concentration of ^{14}C-labelled bile salts in the medium. The changes in the ^{14}C bile salt kinetics between 30, 60 and 90 min in the group A under crilvastatin may be related to different mechanisms. Interactions exist between the mixed micelles, LDL crilvastatin and bile salts. Bile salts such as taurocholate and crilvastatin were shown respectively to exhibit a stimulatory effect on the LDL-cholesterol uptake by the liver (Henry *et al.*, 1987; Clerc *et al.*, 1993). Thus, the two peaks of ^{14}C bile salts in the medium at 30 and 90 min could be linked to the presence of two forms of LDL: the first peak to crilvastatin associated LDL, the second peak to unassociated LDL. The changes in the ^{14}C bile salt kinetics may result from differences in the kinetics of [^{14}C]-cholesterol particle uptake and/or metabolism by hepatocytes. Results *in vivo* showed that HDL-cholesterol, as well as liposomes-/mixed micelles-cholesterol, was rapidly taken up by the hepatocytes. It was secreted in the bile in the form of unchanged cholesterol and bile salts with a maximum secretory rate at 30 min (Esnault-Dupuy *et al.*, 1987). In contrast, this secretory rate maximum was delayed when cholesterol was provided by LDL. In the group A of our experiment, the maxima in the ^{14}C bile salts at 30 and 90 min could be provided respectively by the metabolism of mixed micelles- and LDL, the [^{14}C]-cholesterol-mixed micelles resulting from the [^{14}C]-cholesterol exchange between LDL and mixed micelles. In addition, the changes in ^{14}C bile salt kinetics could be the result of secretion and re-uptake of bile salts by hepatocytes, particularly ^{14}C bile salts. The metabolic changes observed in group A do not exist in group B. In this last group, hepatocytes are provided by hypercholesterolaemic rats and the intracellular basal metabolic paths are more saturated than in the group A. This results in an increased ^{14}C dilution, compared to the low fat group.

Crilvastatin stimulated new synthesis of ^{14}C bile acids normally synthesized and secreted *in vivo* as well as by cultured rat hepatocytes (Davis *et al.*, 1983), i.e. glyco- and particularly tauro-conjugated bile salts. Bile acid may leave the peroxisome as free acid prior to reconjugation with CoA (Russell & Setchell, 1992). Johnson *et al.* (1991) showed that peroxisomal enzymatic proteins could have taurine and glycine as substrates and could ultimately be responsible for the conjugation of bile salts. These processes may also be active in our model.

In common with other statins, our results could be

explained by a crilvastatin stimulation of LDL receptors (Brown & Goldstein, 1983). Our findings further indicate that crilvastatin is transported mainly by lipoproteins and in a micellar form, the micellar transport was shown elsewhere, using another drug (Lasic, 1992). A possible explanation both *in vitro* and *in vivo* is that crilvastatin stimulates uptake of LDL-cholesterol by physico-chemical interactions involving the drug, LDL and LDL-hepatocyte receptors. These interactions could be enhanced during hypercholesterolaemia which is characterized by high LDL levels. In these conditions, it is likely that crilvastatin triggers an excess of LDL into the liver.

However, crilvastatin differs from other hypolipidaemic drugs in several respects. Fibrates such as clofibrate (The Coronary Drug Project, 1975) do not stimulate bile salt synthesis as demonstrated by the increase in the saturation index of gallbladder bile. Unlike crilvastatin which promotes cholesterol 7α-hydroxylase activity *in vivo*, gemfibrozil and simvastatin have an inhibitory effect on this enzyme (Leiss *et al.*, 1985; Björkhem, 1986).

In conclusion the interest of our cellular model is to mimic physiological or physiopathological *in vivo* conditions. It could constitute a predictive and valid preclinical study on the metabolic effect of a drug on its target cells. However, localization in the hepatocyte of the effect of crilvastatin and other statins remains to be elucidated. This work shows that pharmacological studies have to focus on drug transport process by physiological carriers to understand bioavailability of these molecules at a cellular level.

This work was supported by a grant from Pan Medica Laboratories (Grant No.89031). We wish to thank Mr Patrick Garzino for animal care.

References

ALBERTS, A.W. (1988a). Discovery, biochemistry and biology of lovastatin. *Am. J. Cardiol.*, **62**, 10–15.

ALBERTS, A.W. (1988b). Lovastatine et simvastatine. *Cah. Nutr. Diét.*, **23**, 231–233.

BERRY, M.N. & FRIEND, D.S. (1969). High yield preparation of isolated rat liver parenchymal cells. A biochemical and fine structural study. *J. Cell Biol.*, **43**, 506–520.

BJÖRKHEM, I. (1986). Effects of mevinolin in rat liver: evidence for a lack of coupling between synthesis of hydroxymethylglutaryl-coenzyme A (HMGCoA) reductase and cholesterol 7α-hydroxylase activity. *Biochim. Biophys. Acta*, **877**, 43–50.

BLAANBOER, B.J., WORTELBOER, H.M. & MENNES, W.C. (1990). The use of liver cell cultures derived from different mammalian species in *in vitro* toxicological studies: implementation in extrapolation models? *ATLA*, **18**, 251–258.

BOTHAM, K.M., LAWSON, M.E., BECKETT, G.J., PERCY-ROBB, I.W. & BOYD, G.S. (1981). Portal blood concentrations of conjugated cholic and chenodeoxycholic acids. Relationship to bile salt synthesis in liver cells. *Biochim. Biophys. Acta*, **665**, 81–87.

BOUSCAREL, B., FROMM, H., CERYAK, S. & CASSIDY, M.M. (1991). Ursodeoxycholic acid increases low-density lipoprotein binding, uptake and degradation in isolated hamster hepatocytes. *Biochem. J.*, **280**, 589–598.

BROWN, M.S. & GOLDSTEIN, J.L. (1983). Lipoprotein receptors in the liver, control signals for plasma cholesterol traffic. *J. Clin. Invest.*, **72**, 743–747.

CERYAK, S., BOUSCAREL, B. & FROMM, H. (1993). Comparative binding of bile acids to serum lipoproteins and albumin. *J. Lipid Res.*, **34**, 1661–1674.

CHITRANUKROH, A. & BILLING, B.H. (1983). Changes in the binding of radioactive conjugated bile salts to serum proteins in cholestatic jaundice. *Clin. Sci.*, **65**, 77–84.

CLERC, T., JOMIER, M., CHAUTAN, M., PORTUGAL, H., SENFT, M., PAULI, A.M., LARUELLE, C., MOREL, O., LAFONT, H. & CHANUSSOT, F. (1993). Mechanisms of action in the liver of crilvastatin, a new hydroxymethylglutaryl-coenzyme A reductase inhibitor. *Eur. J. Pharmacol.*, **235**, 59–68.

DAVIS, R.A., HYDE, P.M., KUAN, J.C., MALONE-MC NEAL, M. & ARCHAMBAULT-SCHEXNAYDER, J. (1983). Bile acid secretion by cultured rat hepatocytes. Regulation by cholesterol bioavailability. *J. Biol. Chem.*, **258**, 3661–3667.

DOMINGO, N., AMIC, J. & HAUTON, J. (1972). Dosage automatique des sels biliaires conjugués de la bile par la 3 alpha-hydroxystéroide déshydrogénase. *Clin. Chim. Acta*, **37**, 399–404.

ESNAULT-DUPUY, C., CHANUSSOT, F., LAFONT, H., CHABERT, C. & HAUTON, J. (1987). The relationship between HDL-, LDL-, liposomes-free cholesterol, biliary cholesterol and bile salts in the rat. *Biochimie*, **69**, 45–52.

ESNAULT-DUPUY, C., LAFONT, H., CHANUSSOT, F., CHAUTAN, M., HAUTON, J. & LARUELLE, C. (1988). Inhibition of hepatic HMG-CoA reductase activity by two new hypocholesterolemic drugs. In *Liver cells and Drugs*. ed. Guillouzo, A. pp. 99–102. Paris: INSERM/John Libbey Eurotext Ltd.

FISHMAN, W.H., KATO, K., ANSTISS, C.L. & GREEN, S. (1967). Human serum β-glucuronidase; its measurement and some of its properties. *Clin. Chim. Acta*, **15**, 435–447.

GEBHARDT, R. (1986). Utilisation des hépatocytes isolés et en culture pour l'étude de la formation de la bile. In *Hépatocytes isolés et en culture pour l'étude de la formation de la bile*. ed. Guillouzo, A. & Guguen-Guillouzo, C. pp. 367–391. Paris: INSERM/John Libbey Eurotext.

HATCH, F.T. & LESS, R.S. (1968). Practical methods for plasma lipoprotein analysis. *Adv. Lipid Res.*, **6**, 1–68.

HAUTON, J.C., DOMINGO, N., MARTIGNE, M., LAFONT, H., NALBONE, G., CHANUSSOT, F. & LAIRON, D. (1986). A quantitative dynamic concept on the interphase partition of lipids: application to bile salt-lecithin-cholesterol mixed micelles. *Biochimie*, **68**, 275–285.

HAUTON, J.C., VIGNE, J.L., NALBONE, G., LAFONT, H., LAIRON, D. & AUGEIRE-CHARBONNIER, M. (1982). Implications of a dynamic theory on the behaviour of the bile salt-lecithin association in water. In *Exposés Annuels de Biochimie Médicale*. ed. Polonovski, M., Boulanger, P. & Roche, J. pp. 39–73. Paris: Masson.

HENRY, J.C., DOMINGO, N., CHANUSSOT, F., LAFONT, H., HAUTON, J. & CANO, J.P. (1987). Bile lipid secretion in isolated perfused rat liver. A model for metabolic studies. *Lipids*, **22**, 1–5.

JOHNSON, M.R., BARNES, S., KNAKYE, J.B. & DIASIO, R.B. (1991). Purification and characterization of bile acid CoA amino acid N-acyltransferase from human liver. *J. Biol. Chem.*, **266**, 10227–10233.

JUNKER, L.H. & DAVIS, R.A. (1989). Receptor mediated uptake of low density lipoprotein stimulates bile acid synthesis by cultured rat hepatocytes. *J. Lipid Res.*, **30**, 1933–1941.

KRAMER, W., BUSCHER, H.P., GEROK, W. & KURZ, G. (1979). Bile salt binding to serum components. Taurocholate incorporation into high-density lipoprotein revealed by photoaffinity labelling. *Eur. J. Biochem.*, **102**, 1–9.

KUKONGVIRIYAPAN, V. & STACEY, N.H. (1989). Comparison of uptake kinetics in freshly isolated suspensions and short-term primary cultures of rat hepatocytes. *J. Cell. Physiol.*, **140**, 491–497.

KWEKKEBOOM, J., PRINCEN, H.M.G., VAN VOORTHUISEN, E.M. & KEMPEN, H.J.M. (1990). Cholesterol 7 α-hydroxylase activity and bile acid synthesis in hepatocytes of unweaned and weaned pigs in monolayer culture. *Biochim. Biophys. Acta*, **1042**, 386–394.

LASIC, D. (1992). Mixed micelles in drug delivery. *Nature*, **355**, 279–281.

LEISS, O., VON BERGMANN, K., GNASSO, A. & AUGUSTIN, J. (1985). Effect of gemfibrozil on biliary lipid metabolism in normolipemic subjects. *Metabolism*, **34**, 74–82.

LOWRY, O.H., ROSEBROUGH, N.F., FARR, A.L. & RANDALL, R.J. (1951). Protein measurement with the folin phenol reagent. *J. Biol. Chem.*, **193**, 265–275.

MITCHELL, J.C., LOGAN, G.M., STONE, B.G. & DUANE, C. (1991). Effect of lovastatin on biliary lipid secretion and bile acid metabolism in human. *J. Lipid Res.*, **32**, 71–78.

MORGENSTERN, S., KESSLER, G., AUERBACH, J., FLOR, R.V. & KLEIN, B. (1965). An automated p-nitrophenylphosphate serum alkaline phosphatase procedure for the autoanalyser. *Clin. Chem.*, **11**, 876.

MOULIN, S., FRUCHART, J.C., DEWAILLY, P. & SEZILLE, G. (1979). Electrophorèse des lipoprotéines sériques sur plaque de gel d'acrylamide-agarose, en gradient discontinu d'acrylamide. *Clin. Chim. Acta*, **91,** 159–163.

PRINCEN, H.M.G. & MEIJER, P. (1990). Maintenance of bile acid synthesis and cholesterol 7 α-hydroxylase activity in cultured rat hepatocytes. *Biochem. J.*, **272,** 273–275.

ROBINS, S.J. & BRUNENGRABER, H. (1982). Origin of biliary cholesterol and lecithin in the rat: contribution of new synthesis and preformed hepatic stores. *J. Lipid Res.*, **23,** 604–608.

RUSSELL, D.W. & SETCHELL, K.D.R. (1992). Bile acid biosynthesis. *Biochemistry*, **31,** 4737–4749.

SALVIOLI, G., LUGLI, R., PRADELLI, J.M. & GIGLIOTTI, G. (1985). Bile acid binding in the plasma: the importance of lipoproteins. *FEBS Lett.*, **187,** 272–276.

SCHWARTZ, C.C., HALLORAN, L.G., VLAHCEVIC, Z.R., GREGORY, D.H. & SWELL, L. (1978). Preferential utilization of free cholesterol from HDL for biliary cholesterol secretion in man. *Science*, **200,** 62–64.

SEGLEN, P.O. (1962). Preparation of isolated rat liver cells. *Methods Cell Biol.*, **13,** 29–83.

THE CORONARY DRUG PROJECT RESEARCH GROUP. (1975). Coronary Drug Project. Clofibrate and niacin in coronary heart disease. *J. Am. Med. Assoc.*, **231,** 360–381.

TWISK, J., LEHMANN, E.M. & PRINCEN, H.M.G. (1993). Differential feedback regulation of cholesterol 7 α-hydroxylase mRNA and transcriptional activity by rat bile acids in primary monolayer cultures of rat hepatocytes. *Biochem. J.*, **290,** 685–691.

WHITING, M.J., WISHART, R.A., LEWIS, G. & MACKINNON, A.M. (1989). Bile acid synthesis by cultured rabbit hepatocytes: stimulation by three lipoprotein fractions. *Biochim. Biophys. Acta*, **1005,** 137–142.

(Received July 8, 1994
Revised September 5, 1994
Accepted October 11, 1994)

British Journal of Pharmacology (1995) 114, 632-639

Effects of divalent cations and La^{3+} on contractility and ecto-ATPase activity in the guinea-pig urinary bladder

* †Airat U. Ziganshin, * †Lilia E. Ziganshina, *Charles H.V. Hoyle & [1]*Geoffrey Burnstock

*Department of Anatomy and Developmental Biology and Centre for Neuroscience, University College London, Gower Street, London WC1E 6BT and †Kazan Medical Institute, 49 Butlerov Street, Kazan, 420012, CIS

1 Several cations (Ba^{2+}, Cd^{2+}, Co^{2+}, Cu^{2+}, Mn^{2+}, Ni^{2+}, Zn^{2+} and La^{3+}, all as chloride salts, 1-1000 μM) were tested in the guinea-pig urinary bladder for their ability to: (i) modify contractile responses to electrical field stimulation (EFS), ATP, α,β-methylene ATP (α,β-meATP), carbachol (CCh), and KCl; (ii) affect ecto-ATPase activity.

2 Ba^{2+} (10-1000 μM) concentration-dependently potentiated contractile responses evoked by EFS (4-16 Hz), ATP (100 μM), α,β-meATP (1 μM), CCh (0.5 μM), and KCl (30 mM). Ni^{2+} at concentrations of 1-100 μM also potentiated contractility of the urinary bladder, but at concentrations tested its effect was not concentration-dependent. Cu^{2+} at a concentration of 10 μM and Cd^{2+} at a concentration of 1 μM potentiated responses to all stimuli, except KCl. Ni^{2+} at a concentration of 1000 μM and Cd^{2+} at a concentration of 100 μM inhibited contractions evoked by all stimuli, and at a concentration of 1000 μM Cd^{2+} abolished any contractions. Responses to ATP and α,β-meATP were selectively inhibited by Cu^{2+}, Zn^{2+} or La^{3+}, each at a concentration of 1 mM.

3 Cu^{2+}, Ni^{2+}, Zn^{2+} and La^{3+} (100-1000 μM) concentration-dependently inhibited ecto-ATPase activity in the urinary bladder smooth muscle preparations, while Ba^{2+} and Mn^{2+} were without effect, and Cd^{2+} and Co^{2+} caused significant inhibition only at a concentration of 1000 μM.

4 There was no correlation between the extent of ecto-ATPase inhibition and the effect on contractile activity of any of the cations.

5 In conclusion, the ability of some divalent cations to inhibit ecto-ATPase activity and to potentiate or inhibit contractile responses in the guinea-pig urinary bladder appear to be independent effects.

Keywords: Divalent cations; guinea-pig urinary bladder; ecto-ATPase; contractility

Introduction

The presence of ecto-ATPase (EC 3.6.1.3) has been shown in a wide range of human and animal tissues (see Ziganshin *et al.*, 1994a). Since extracellular ATP is very rapidly broken down by ecto-ATPase, an inhibitor of this enzyme would be very useful in clarifying the distribution of and relationship between P_1(adenosine)- and P_2(ATP)-purinoceptors, as well as for potentiation of P_2-purinoceptor-mediated responses. Although several compounds have been described as ecto-ATPase inhibitors (Grondal & Zimmermann, 1986; Dombrowski *et al.*, 1993; Ziganshin *et al.*, 1994b), none has been shown to be selective.

Ca^{2+} and Mg^{2+} cations have been found to play a significant role in ecto-ATPase activity. It has been shown in many studies that ecto-ATPase activity is highly dependent on Ca^{2+} and/or Mg^{2+}, and is usually described as Ca^{2+}/Mg^{2+} ATPase (see Dhalla & Zhao, 1988). Other divalent cations (Mn^{2+}, Cu^{2+}, Ba^{2+}, Co^{2+}, Ni^{2+}, Zn^{2+}) can substitute for Ca^{2+} or Mg^{2+}, albeit with lower potency (Majumder, 1981; Tuana & Dhalla, 1988; Culic *et al.*, 1990; Kurihara *et al.*, 1992). However, in the presence of Ca^{2+}, inorganic cations (Mg^{2+}, Mn^{2+}, Cu^{2+}, Ni^{2+}, Cd^{2+}, La^{3+}) markedly inhibit enzyme activity (Manery *et al.*, 1984; Tuana & Dhalla, 1988). On the other hand, in canine renal membrane vesicles, Zn^{2+} significantly stimulates ecto-ATPase activity (Hilden & Madias, 1990).

It has been shown that some divalent cations (Co^{2+}, Ni^{2+}, Mn^{2+}) can block voltage-operated Ca^{2+}- (Harrow *et al.*, 1978; Edwards, 1982; Rüegg *et al.*, 1989) and Na^{+}-channels (Ravindran *et al.*, 1991; Sheets & Hanck, 1992). Inhibition of calcium influx by La^{3+} has also been described (Weiss & Goodman, 1969; Van Breeman & McNaughton, 1970). Moreover, La^{3+} can block ATP- or KCl-evoked entry of $^{45}Ca^{2+}$ with an IC_{50} around micromolar concentration, while Cd^{2+}, Mn^{2+}, Co^{2+} and Ni^{2+} do the same at concentrations about 1000 times higher (Rüegg *et al.*, 1989; Wallnöfer *et al.*, 1989).

Co^{2+}, Ni^{2+} and Mn^{2+} inhibit agonist-mediated (noradrenaline, acetylcholine, histamine) contractions and relaxations in rat aorta preparations, and Cd^{2+} and Zn^{2+} virtually abolish contractions to high concentrations of KCl (Adeagbo & Triggle, 1991). In the rat urinary bladder, Mn^{2+} and La^{3+} both inhibit the amplitude of contractions evoked by electrical field stimulation (EFS), although Mn^{2+} was significantly more potent than La^{3+} (Huddart & Butler, 1986).

The aim of the present study was to compare the effects of several cations on ecto-ATPase activity with their ability to alter contractile responses of the guinea-pig urinary bladder. Contractions were evoked by EFS, the P_2-purinoceptor agonists, ATP and α,β-methylene ATP (α,β-meATP), the cholinoceptor agonist, carbachol (CCh), as well as KCl, which directly activates the contractile process by depolarization.

Methods

Organ bath experiments

Male Dunkin-Hartley guinea-pigs (250-400 g) were killed by a blow to the head and exsanguination. The urinary bladder was removed and strips of smooth muscle, approximately 2 by 10 mm, were prepared and suspended vertically in 10 ml organ baths for isometric recording of mechanical activity. An initial load of 1 g was applied to the strips which were

[1] Author for correspondence.

then allowed to equilibrate for at least 60 min. EFS was applied via two platinum-wire rings 2.5 mm in diameter, 10 mm apart, through which the strip was threaded. The modified Krebs solution used in these experiments had the following composition (mM): NaCl 133, KCl 4.7, $NaHCO_3$ 16.4, $MgSO_4$ 0.6, NaH_2PO_4 0.8, $CaCl_2$ 2.5 and glucose 7.7, gassed with 95% O_2 / 5% CO_2 (pH 7.3–7.4) and maintained at 37 ± 1°C. Contractions were recorded with a Grass FT0C3 force-displacement transducer, and displayed on a Grass 79D ink-writing oscillograph. EFS was provided by a Grass S9 stimulator and applied at a given frequency (4–16 Hz) with a pulse width of 0.5 ms and supramaximal voltage, until a maximum contraction had been reached and the tone had declined by about a third. ATP (100 μM), α,β-meATP (1 μM), CCh (0.5 μM) or KCl (30 mM) were added directly to the organ bath and washed out after a maximum contraction had been achieved. Intervals of at least 10 min were allowed for washout. Responses to EFS and to agonists were examined in preparations before and after incubation for at least 30 min with cations (1–1000 μM). In time-control preparations, which were carried out in parallel, but without incubation with tested cations, there was no significant change in response to EFS or to any agonist used throughout experiments. All contractile responses were calculated as a percentage of the response evoked by EFS at a frequency of 16 Hz (at which the largest contraction was obtained) before incubation with any drug. Frequency-response relationships for EFS and the effects of two or three different agonists were obtained on each preparation before and after incubation with different concentrations of a cation.

ATPase assay

The assay was carried out at 37 ± 1°C in buffer containing (mM): 4-(2-hydroxyethyl)-1-piperazine-ethanesulphonic acid (HEPES) 10, NaCl 135, KCl 5, $CaCl_2$ 2, $MgCl_2$ 2 and glucose 10, pH 7.4. Smooth muscle preparations of the guinea-pig urinary bladder were prepared as for organ bath experiments. Pieces of tissue (2–3 mg) were placed into 24-well cell culture dishes in 300 μl buffer and were pre-washed for 15–20 min. The pre-wash buffer was changed for 250 μl buffer containing 0.1 mM ATP, and the tissues were incubated for 30 min and shaken continuously. Incubation was terminated by removing the buffer and adding it to 0.9 ml of a 2.5% (w/v) solution of sodium dodecyl sulphate (SDS) for inorganic phosphate assay. Tissues were again washed with buffer for 10–15 min and then incubated with 250 μl buffer containing 0.1 mM ATP and a given concentration of one of the cations for 30 min. The buffer was again collected in SDS. For the inorganic phosphate assay 1 ml of 1.25% (w/v) ammonium molybdate solution in 2 M HCl and 0.1 ml of 16% (w/v) Fiske and SubbaRow reducing agent (Sigma) were added to the samples. The solutions were transferred to cuvettes and left for 30 min at room temperature to develop colour. The inorganic phosphate produced was measured spectrophotometrically at 700 nm in a Beckman Du-65 Spectrophotometer. KH_2PO_4 was used as a phosphate standard. The amount of phosphate produced in the presence of a cation (second incubation) was calculated as a percentage of that without any compound (first incubation). Only one concentration of a cation was tested on each piece of tissue. All results were expressed as the mean ± s.e.mean of at least two experiments performed in quadruplicate.

Analysis of results

Means were compared by Student's paired and unpaired *t* tests. A probability of less than or equal to 0.05 was considered as significant. Data are presented as mean ± s.e.mean (*n*).

Drugs

Barium chloride dihydrate and cobalt chloride hexahydrate were from BDH; cadmium chloride hydrate, cupric chloride hydrate, manganese chloride tetrahydrate, nickel chloride hexahydrate, zinc chloride, lanthanum chloride heptahydrate, adenosine-5'-triphosphate disodium salt (ATP), α,β-meATP lithium salt and carbamylcholine chloride (carbachol) were obtained from Sigma. All cations tested were dissolved in distilled water to produce a stock solution of 0.1 M.

Results

Organ bath experiments

EFS (4–16 Hz) caused frequency-dependent contractions of the urinary bladder detrusor muscle with the largest response at a frequency of 16 Hz (100%) and 38.9 ± 1.5% (42) and

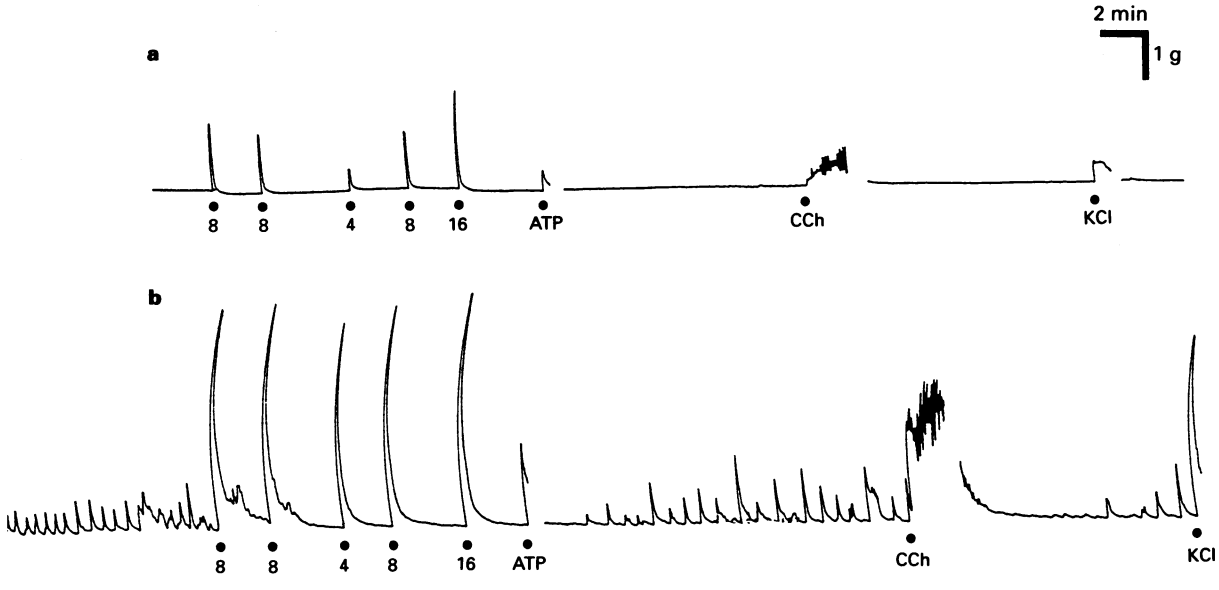

Figure 1 Original traces showing contractile responses of the guinea-pig urinary bladder evoked by electrical field stimulation (EFS; 4, 8 and 16 Hz), ATP (100 μM), carbachol (CCh; 0.5 μM) and KCl (30 mM) recorded before (a) and after (b) incubation of the tissue (for at least 30 min) with $BaCl_2$ at a concentration of 1 mM. EFS and addition of agonists are marked by dots. The first two responses to EFS at 8 Hz were used only for equilibration of tissue and not for calculations.

74.4 ± 1.9% (42) at frequencies of 4 and 8 Hz respectively, relative to the response at 16 Hz. Contractions evoked by ATP (100 μM), α,β-meATP (1 μM), CCh (0.5 μM) and KCl (30 mM) were 15.2 ± 0.3% (42), 24.1 ± 1.1% (34), 27.2 ± 2.5% (40) and 30.0 ± 2.0% (36), respectively, normalised to the response at 16 Hz.

Ba^{2+} at a concentration of 1 μM did not significantly change contractile responses of the bladder, but at 10–1000 μM concentration-dependently increased contractions evoked by all the tested stimuli (Figures 1 and 3a). This was accompanied by initiation of spontaneous activity of the tissue (Figure 1).

Cd^{2+} at a concentration of 1 μM potentiated contractions evoked by any stimuli, except KCl; at 100 μM it inhibited all contractions, and at 1 mM abolished them (Figures 2 and 3b). In some preparations Cd^{2+} at 1–10 μM either potentiated or provoked spontaneous contractions, which were completely blocked by 1 mM ion concentrations.

Ni^{2+} at concentrations of 1–100 μM potentiated responses to all the stimuli tested; at a concentration of 1 mM contractions evoked by CCh remained enhanced, while responses to other stimuli were significantly decreased (Figure 4a).

Cu^{2+} at a concentration of 10 μM potentiated responses to all the stimuli, except KCl (Figure 4b); at 10–1000 μM Cu^{2+} increased the basal tone of the preparations and evoked spontaneous contractions. At a concentration of 1 mM the cation inhibited contractions evoked by ATP and α,β-meATP, but not by any other stimuli (Figure 5).

Zn^{2+} and La^{3+} at a concentration of 1 mM caused significant inhibition of contractions evoked by ATP and α,β-meATP but not by any other stimuli (Figure 6).

Mn^{2+} and Co^{2+} (1–1000 μM) potentiated contractions evoked by CCh, while responses to other stimuli were not significantly affected (data not shown).

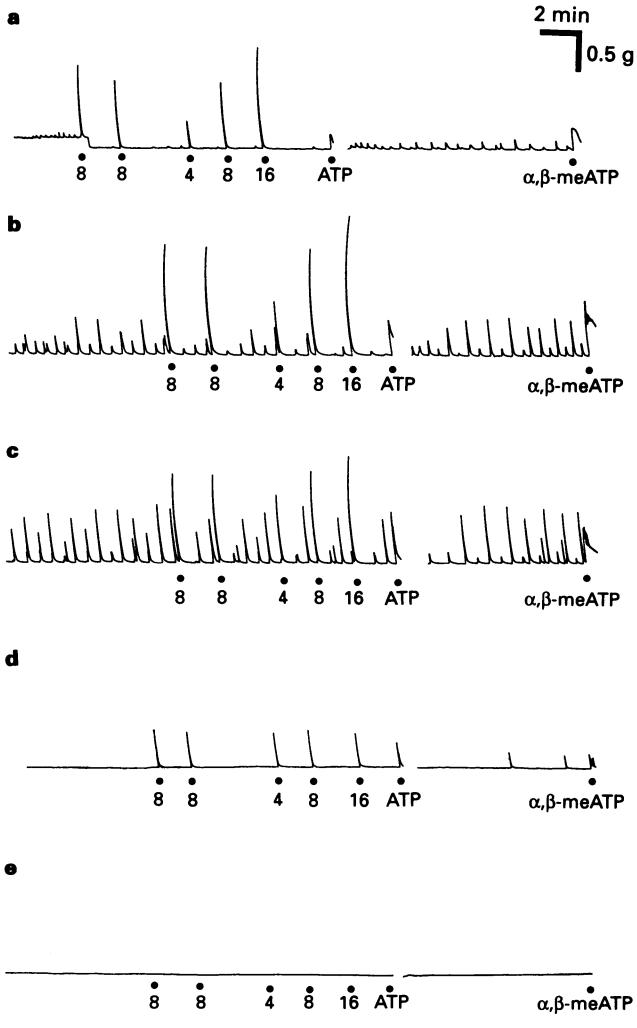

Figure 2 Original traces showing contractile responses of the guinea-pig urinary bladder evoked by electrical field stimulation (EFS; 4, 8 and 16 Hz), ATP (100 μM) and α,β-methylene ATP (α,β-meATP; 1 μM) recorded before (a) and after incubation of the tissue (for at least 30 min) with $CdCl_2$ at concentrations of 1 μM (b), 10 μM (c), 100 μM (d) and 1 mM (e). EFS and addition of agonists are marked by dots. The first two responses to EFS at 8 Hz were used only for equilibration of tissue and not for calculations.

ATPase assay

The actual rate of ATPase activity was 1.28 ± 0.038 (n = 70) nmol P_i $30\ min^{-1}\ mg^{-1}$ wet tissue in the urinary bladder, that was taken as a 100%. Spontaneous ATP breakdown when incubated in buffer without tissue for 30 min was negligible. There was no significant amount of inorganic phosphate when tissue was incubated without added ATP, which indicates that released or secreted ATP or inorganic phosphate does not interfere significantly with our assay.

Cu^{2+}, Ni^{2+}, Zn^{2+} and La^{3+} (100–1000 μM) concentration-dependently inhibited ecto-ATPase activity in the urinary bladder smooth muscle preparations, while Cd^{2+} and Co^{2+} caused significant inhibition only at a concentration of 1 mM, and Ba^{2+} and Mn^{2+} were without effect (Figure 7). The order of potency of cations at 1 mM for inhibition of ecto-ATPase was $La^{3+} > Zn^{2+} > Cu^{2+} > Cd^{2+} = Co^{2+} = Ni^{2+} > Ba^{2+} = Mn^{2+}$.

Discussion

In the present study we have established that divalent cations and La^{3+} have differential effects on ecto-ATPase activity and contractions of the guinea-pig urinary bladder. The most active cation for potentiation of the bladder contractions in organ bath experiments, Ba^{2+}, did not affect ecto-ATPase activity. On the other hand, the most active inhibitors of ecto-ATPase activity, Zn^{2+} and La^{3+}, did not potentiate responses to ATP, but inhibited contractions to the P_2-purinoceptor agonists, ATP and α,β-meATP.

Divalent cations have diverse biological activity. Despite unique comprehensive roles of calcium and magnesium, some other cations (copper, cobalt, zinc, manganese, iron) are essential for certain metalloproteins, coenzymes, metalloenzymes and vitamins. However, at concentrations above physiological levels cations produce other effects, such as stimulation or inhibition of calmodulin (Cox & Harrison, 1983; Chao *et al.*, 1984), or blockade of ion channels (Harrow *et al.*, 1978; Edwards, 1982; Ravindran *et al.*, 1991; Sheets & Hanck, 1992). The toxicity of heavy metals is also well known, and interestingly a correlation has been shown between divalent metal toxicity (LD_{50} for mice) and inhibition of calmodulin (IC_{50} for bovine brain calmodulin) (Cox & Harrison, 1983). Some effects of divalent cations have been found to be dependent on their radius. For example, Chao *et al.* (1984) have shown that Ca^{2+} is not a specific ion for bovine brain calmodulin, and other cations with ionic radii comparable to that of Ca^{2+} can replace it. However, this is not true in all cases since Ba^{2+} with an ionic radius 30% larger than Ca^{2+} can permeate into cells through Ca^{2+}-channels (Edwards, 1982) and replace calcium in its contractile effects (Kreye *et al.*, 1986). The order of crystal ionic radius for cations used in the present study is $Ba^{2+} > La^{3+} > Ca^{2+} > Cd^{2+} > Mn^{2+} > Zn^{2+} > Co^{2+} = Cu^{2+} > Ni^{2+}$. However, the order of potency of cations to inhibit ecto-ATPase activity was $La^{3+} > Zn^{2+} > Cu^{2+} > Cd^{2+} = Co^{2+} = Ni^{2+} > Ba^{2+} = Mn^{2+}$, which does not correlate with the order of ionic radii. Similarly, we did not find a correlation between ionic radius and effect of cations on either receptor- or depolarization-mediated contractions of the urinary bladder.

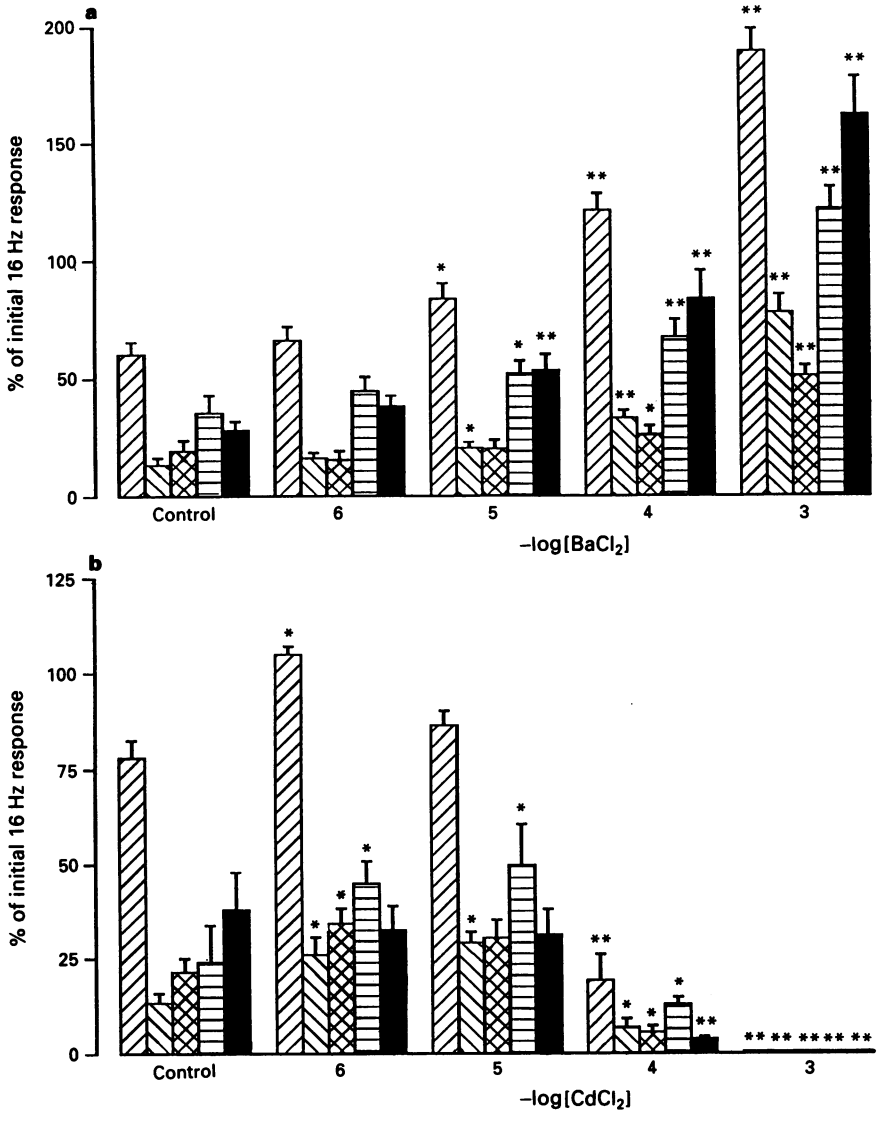

Figure 3 Effects of Ba^{2+} (a) and Cd^{2+} (b) on contractions of the guinea-pig urinary bladder evoked by electrical field stimulation (EFS; 8 Hz, ▨), ATP (100 μM, ▩), α,β-methylene ATP (1 μM, ▩), carbachol (0.5 μM, ▤) and KCl (30 mM, ■). Contractile responses to 4 and 16 Hz have also been tested; however, since effects of cations on EFS-evoked contractions were similar at all frequencies tested, only data for 8 Hz are shown. Columns represent mean ± s.e.mean of 4 to 6 experiments. $*P<0.05$; $**P<0.01$, paired t test.

Another feature which may be related to the biological activity of cations is their position in the Periodic table of elements. It has been shown that divalent cations of transition elements, such as Co^{2+}, Ni^{2+} and Mn^{2+}, but not of the nontransition elements, Cd^{2+}, Zn^{2+} and Sn^{2+}, markedly inhibit relaxation of rat aorta induced by acetylcholine and histamine, yet all cations antagonize KCl contraction (Adeagbo & Triggle, 1991). The metals we used in this study were from group IIA (Ba), group IIB (Zn, Cd, La) and some transition metals (Mn, Co, Ni and Cu). From the results of organ bath experiments the ions can be divided into three groups: (a) Cd^{2+}, Ni^{2+}, Cu^{2+}, which at low concentrations potentiated and at high concentrations inhibited (or did not affect) contractile responses of the bladder; (b) Co^{2+}, Mn^{2+}, Zn^{2+}, La^{3+}, which at most concentrations used did not significantly affect contractions to the stimuli tested, except that they potentiated the response to carbachol, Zn^{2+} and La^{3+} at 1000 μM inhibited responses to ATP and α,β-meATP; (c) Ba^{2+}, which concentration-dependently potentiated contractions to all stimuli. From the results of the ecto-ATPase assay the ions can be divided into: (a) Ba^{2+} and Mn^{2+}, which did not affect the enzyme activity; (b) Cd^{2+} and Co^{2+}, which inhibited ecto-ATPase only at high (1 mM) concentrations; (c) Cu^{2+}, Ni^{2+} and Zn^{2+}, which caused concentration-dependent inhibition of the enzyme activity; (d) La^{3+}, which at both concentrations (0.1 and 1 mM) inhibited ecto-ATPase activity by more than 80%. Thus, neither the results of organ bath experiments nor of the ATPase assay are related to the position of the metal cations in the Periodic table. Most likely, the effects of cations that we observed are dependent on several chemical and physical characteristics, and probably involve different mechanisms, and therefore each cation should be discussed separately.

Ba^{2+} is able to potentiate, as well as induce, contractions in smooth muscle preparations (this study and Kreye *et al.*, 1986), the effect of which is believed to be due to it permeating the voltage-operated Ca^{2+}-channels, releasing Ca^{2+} from intracellular stores, and directly activating contractile proteins via formation of a Ba^{2+}-calmodulin complex (Satoh *et al.*, 1987). It has been found, however, that Ba^{2+} is unable to activate calmodulin from bovine brain (Chao *et al.*, 1984). In our experiments, Ba^{2+} even at a high concentration (1 mM) did not significantly change ecto-ATPase activity. Similar results have been obtained in rat heart sarcolemma, where

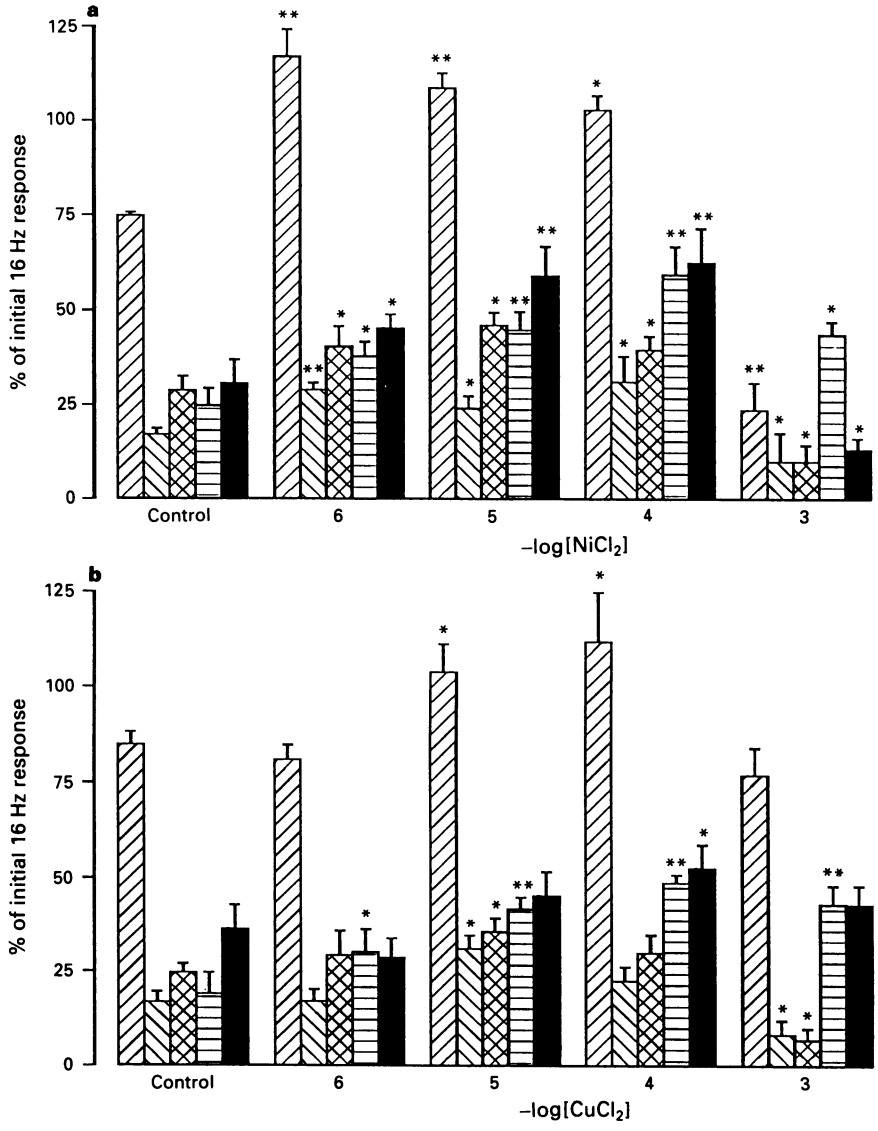

Figure 4 Effects of Ni^{2+} (a) and Cu^{2+} (b) on contractions of the guinea-pig urinary bladder evoked by electrical field stimulation (EFS; 8 Hz, ▨), ATP (100 μM, ▧), α,β-methylene ATP (1 μM, ▩), carbachol (0.5 μM, ▤) and KCl (30 mM, ■). Contractile responses to 4 and 16 Hz have also been tested; however, since effects of cations on EFS-evoked contractions were similar at all frequencies tested, only data for 8 Hz are shown. Columns represent mean ± s.e.mean of 4 to 6 experiments. $*P<0.05$; $**P<0.01$, paired t test.

Ba^{2+} (4 mM) was essentially without effect on Ca^{2+}/Mg^{2+} ecto-ATPase (Tuana & Dhalla, 1988). Thus, the effects of Ba^{2+} are mainly due to involvement of intracellular mechanisms, and are unlikely to be dependent on any receptor-mediated mechanisms.

The effect of Cd^{2+} on the contractile response of the urinary bladder was highly dependent on concentration; at low concentrations (1–10 μM) it potentiated, at 100 μM it inhibited and at a high concentration (1 mM) it abolished contractile responses. In isolated preparations of rat aorta Cd^{2+} at 3–30 μM inhibits Ca^{2+}-evoked contractions (Lawson & Cavero, 1989) and at 100 μM abolishes contractions to KCl (Adeagbo & Triggle, 1991). It has been shown that Cd^{2+} is able to activate (Chao *et al.*, 1984) or inhibit calmodulin (Cox & Harrison, 1983), as well as block Ca^{2+}- (Rüegg *et al.*, 1989) and Na^{+}-channels (Sheets & Hanck, 1992). It seems likely that micromolar concentrations of Cd^{2+} activate calmodulin in the urinary bladder and therefore potentiate evoked contractions, whereas at concentrations near millimolar this cation inhibits calmodulin, blocks ion channels and as a result inhibits contractility of the tissue. Interestingly, however, at 1 mM, when no contractions could be evoked, Cd^{2+} inhibited ecto-ATPase activity only by 20%.

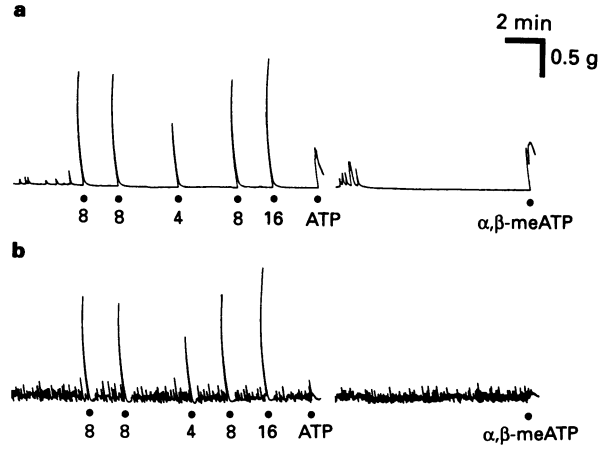

Figure 5 Original traces showing contractile responses of the guinea-pig urinary bladder evoked by electrical field stimulation (EFS; 4, 8 and 16 Hz), ATP (100 μM) and α,β-methylene ATP (α,β-meATP; 1 μM) recorded before (a) and after (b) incubation of the tissue (for at least 30 min) with $CuCl_2$ at concentration of 1 mM. EFS and addition of agonists are marked by dots. The first two responses to EFS at 8 Hz were used only for equilibration of tissue and not for calculations.

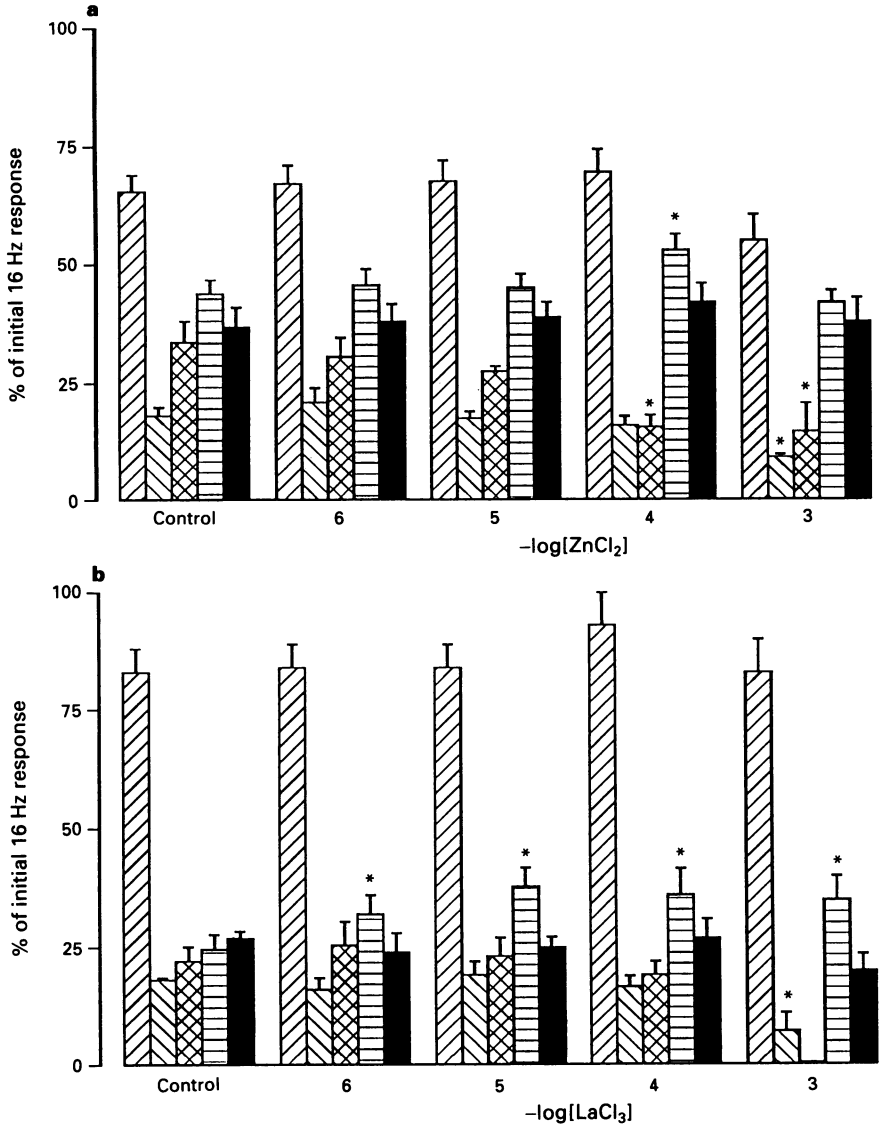

Figure 6 Effects of Zn^{2+} (a) and La^{3+} (b) on contractions of the guinea-pig urinary bladder evoked by electrical field stimulation (EFS; 8 Hz, ▨), ATP (100 μM, ▧), α,β-methylene ATP (1 μM, ▩), carbachol (0.5 μM, ▤) and KCl (30 mM, ■). Contractile responses to 4 and 16 Hz have also been tested; however, since effects of cations on EFS-evoked contractions were similar at all frequencies tested, only data for 8 Hz are shown. Columns represent mean ± s.e.mean of 4 to 6 experiments. $*P<0.05$; $**P<0.01$, paired t test.

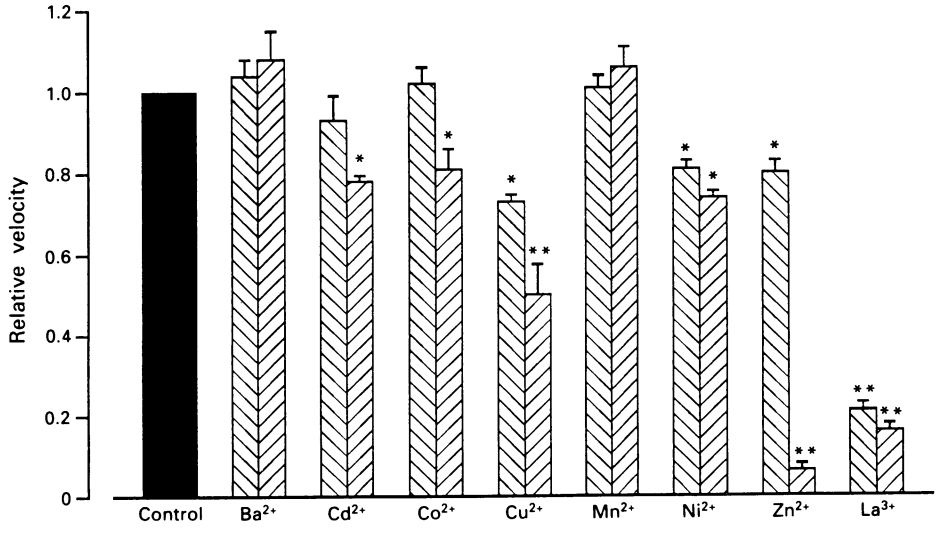

Figure 7 Effects of cations at concentrations of 100 μM (first columns, ▧) and 1 mM (second columns, ▨) on ecto-ATPase activity of isolated strips of the guinea-pig urinary bladder. Columns represent mean ± s.e.mean of 2 experiments performed in quadruplicate. Absolute ecto-ATPase activity in these experiments was 1.284 ± 0.038 (70) nmol P_i $30\ min^{-1}\ mg^{-1}$ wet tissue. $*P<0.05$; $**P<0.01$, paired t test.

Mn^{2+}, Co^{2+} and Ni^{2+} in a variety of tissues have been shown to be equipotent at blocking voltage-operated Ca^{2+}-channels (see Edwards, 1982). However, in our experiments only Ni^{2+} showed clear concentrations-dependent effects on contractions of urinary bladder, potentiating at 1–100 μM and inhibiting at 1 mM. Probably, in the guinea-pig urinary bladder, either the sensitivity of Ca^{2+}-channels to the cations is different, or these channels are not involved in the effects of Ni^{2+}.

Interestingly, La^{3+} has been found to be about 1000 times more potent at inhibiting stimulated Ca^{2+} influx via receptor-operated Ca^{2+} channels in cultured aortic smooth muscle cells (Rüegg *et al.*, 1989), whereas in rabbit aorta La^{3+} and Mn^{2+} were approximately equipotent in this effect (Deth & Lynch, 1981). In rat urinary bladder, Mn^{2+} (0.5 mM) was more potent than La^{3+} (1 mM) in inhibiting the amplitude of contractions evoked by EFS (Huddart & Butler, 1986); however, in our experiments both cations were without effect on contractions evoked by EFS.

Another interesting finding is that the most active ecto-ATPase inhibitors, La^{3+}, Zn^{2+} and Cu^{2+}, at a concentration of 1 mM, selectively inhibited contractions only to the P_2-purinoceptor agonists, ATP and α,β-meATP. One would expect potentiation, not inhibition, of purinoceptor mediated responses, especially of the response to ATP, since α,β-meATP is not readily degraded by ecto-ATPase (Welford *et al.*, 1986; 1987). However, it seems that the relationship between ecto-ATPase and purinoceptors is not so simple. Probably some agents can somehow interact with both molecules thus preventing ATP degradation and at the same time its action on receptors. Inhibition of ecto-ATPase activity by the P_2-purinoceptor antagonist, suramin, has been described in several tissues (Smolen & Weissmann, 1978; Hourani & Chown, 1989; Ziganshin *et al.*, 1994c), which is consistent with this idea. Further, it has been shown that suramin can potentiate effects of ATP in some tissues (Crack *et al.*, 1994; Bailey & Hourani, 1994). In the case of cations, however, only Cu^{2+} at a concentration of 10 mM potentiated ATP responses, but this did not occur when La^{3+} and Zn^{2+} were used.

In conclusion, we have demonstrated that several divalent cations and La^{3+} differentially affect ecto-ATPase activity and contractile responses in guinea-pig urinary bladder. The effects of some, but not all, of the cations can be explained by their known ability to affect permeability of ionic channels or their interaction with calmodulin. Inhibition of ecto-ATPase activity by some of the cations, did not contribute to potentiation of purinoceptor mediated responses in this tissue.

The Wellcome Trust is thanked for financial support of A.U.Z.

References

ADEAGBO, A.S.O. & TRIGGLE, C.R. (1991). Effects of some inorganic divalent cations and protein kinase C inhibitors on endothelium-dependent relaxation in rat isolated aorta and mesenteric arteries. *J. Cardiovasc. Pharmacol.*, **18**, 511–512.

BAILEY, S.J. & HOURANI, S.M.O. (1994). Differential effects of suramin on P_2-purinoceptors mediating contractions of the guinea-pig vas deferens and urinary bladder. *Br. J. Pharmacol.*, **112**, 219–225.

CHAO, S.-H., SUZUKI, Y., ZYSK, J.R. & CHEUNG, W.Y. (1984). Activation of calmodulin by various metal cations as a function of ionic radius. *Mol. Pharmacol.*, **26**, 75–82.

COX, L.J. & HARRISON, S.D. (1983). Correlation of metal toxicity with *in vitro* calmodulin inhibition. *Biochem. Biophys. Res. Commun.*, **115**, 106–111.

CRACK, B.E., BEUKERS, M.W., IJZERMAN, A.P., MCKENNIE, K.C.W. & LEFF, P. (1994). Inhibition of ATP degradation by L-2-methylthio-β,γ-dibromomethylene-ATP and suramin. *Drug Dev. Res.*, **31**, 259.

CULIC, O., SABOLIC, I. & ZANIC-GRUBISIC, T. (1990). The stepwise hydrolysis of adenine nucleotides by ectoenzymes of rat renal brush border membranes. *Biochim. Biophys. Acta*, **1030**, 143–151.

DETH, R. & LYNCH, C. (1981). Inhibition of alpha-receptor-induced Ca^{2+} release and Ca^{2+} influx by Mn^{2+} and La^{3+}. *Eur. J. Pharamacol.*, **71**, 1–11.

DHALIA, N.S. & ZHAO, D. (1988). Cell membrane Ca^{2+}/Mg^{2+} ATPase. *Prog. Biophys. Mol. Biol.*, **52**, 1–37.

DOMBROWSKI, K.E., TREVILLYAN, J.M., CONE, C., LU, Y. & PHILLIPS, C.A. (1993). Identification and partial characterization of an ecto-ATPase expressed by human natural killer cells. *Biochemistry*, **32**, 6515–6522.

EDWARDS, C. (1982). The selectivity of ion channels in nerve and muscle. *Neuroscience*, **7**, 1335–1366.

GRONDAL, E.J. & ZIMMERMANN, H. (1986). Ectonucleotidase activities associated with cholinergic synaptosomes isolated from *Torpedo* electric organ. *J. Neurochem.*, **47**, 871–881.

HARROW, J.A.C., DAS, P.K. & DHALLA, N.S. (1978). Influence of some divalent cations on heart sarcolemmal bound enzyme and calcium binding. *Biochem. Pharmacol.*, **27**, 2605–2609.

HILDEN, S.A. & MADIAS, N.E. (1990). Stimulation of canine kidney BBMV ATPase activity by acidic pH in the presence of Zn^{2+}: an ATPase activity distinct from transport ATPases and alkaline phosphatase that may be an ecto-ATPase. *Membr. Biochem.*, **9**, 69–81.

HOURANI, S.M.O. & CHOWN, J.A. (1989). The effects of some possible inhibitors of ectonucleotidases on the breakdown and pharmacological effects of ATP in the guinea-pig urinary bladder. *Gen. Pharmacol.*, **20**, 413–416.

HUDDART, H. & BUTLER, D.J. (1986). Field stimulation responses of rat urinary bladder detrusor smooth-muscle. Dependence upon slow calcium channel activity determined by K^+ depolarization and calcium antagonists. *Gen. Pharmacol.*, **17**, 695–703.

KREYE, V.A.W., HOFMANN, F. & MÜHLEISEN, M. (1986). Barium can replace calcium in calmodulin-dependent contractions of skinned renal arteries of the rabbit. *Pflügers Arch.*, **406**, 308–311.

KURIHARA, K., HOSOI, K. & UEHA, T. (1992). Characterization of ecto-nucleoside triphosphatase on A-431 human epidermoidal carcinoma cells. *Enzyme*, **46**, 213–220.

LAWSON, K. & CAVERO, I. (1989). Contractile responses to calcium chloride in rat aortic rings bathed in K^+-free solution are resistant to organic calcium antagonists. *Br. J. Pharmacol.*, **96**, 17–22.

MAJUMDER, G.C. (1981). Enzymic characteristics of ecto-adenosine triphosphatase in rat epididymal intact spermatozoa. *Biochem. J.*, **195**, 103–110.

MANERY, J.F., DRYDEN, E.E., STILL, J.S. & MADAPALLIMATTAM, G. (1984). Characteristics of skeletal muscle ecto-ATPase in situ. *Can. J. Biochem. Cell. Biol.*, **62**, 1015–1026.

RAVINDRAN, A., SCHILD, L. & MOCZYDLOWSKI, E. (1991). Divalent cation selectivity for external block of voltage-dependent Na^+ channels prolonged by batrachotoxin. *J. Gen. Physiol.*, **97**, 89–115.

RÜEGG, U.T., WALLNÖFER, A., WEIR, S. & CAUVIN, C. (1989). Receptor-operated calcium-permeable channels in vascular smooth muscle. *J. Cardiovasc. Pharmacol.*, **14** (Suppl. 6), S49–S58.

SATOH, S., KUBOTA, Y., ITOH, T. & KURIYAMA, H. (1987). Mechanisms of the Ba^{2+}-induced contraction in smooth muscle cells of the rabbit mesenteric artery. *J. Gen. Physiol.*, **89**, 215–237.

SHEETS, F.M. & HANCK, D.A. (1992). Mechanisms of extracellular divalent and trivalent cation block of the sodium current in canine cardiac Purkinje cells. *J. Physiol.*, **454**, 299–320.

SMOLEN, J.E. & WEISSMANN, G. (1978). Mg^{2+}-ATPase as a membrane ecto-enzyme of human granulocytes. Inhibitors, activators and response to phagocytosis. *Biochim. Biophys. Acta*, **512**, 525–538.

TUANA, B.S. & DHALLA, N.S. (1988). Purification and characterization of a Ca^{2+}/Mg^{2+}ecto-ATPase from rat heart sarcolemma. *Mol. Cell. Biochem.*, **81**, 75–88.

VAN BREEMAN, C. & MCNAUGHTON, E. (1970). The separation of cell membrane calcium transport from extracellular calcium exchange in vascular smooth muscle. *Biochem. Biophys. Res. Commun.*, **39**, 567–574.

WALLNÖFER, A., CAUVIN, C., LATEGAN, T.W. & RÜEGG, U.T. (1989). Differential blockade of agonist- and depolarization-induced $^{45}Ca^{2+}$ influx in smooth muscle cells. *Am. J. Physiol.*, **257**, C607–C611.

WEISS, G.B. & GOODMAN, F.R. (1969). Effects of lanthanum on contraction, calcium distribution and ^{45}Ca movements in intestinal smooth muscle. *J. Pharmacol. Exp. Ther.*, **169**, 46–55.

WELFORD, L.A., CUSACK, N.J. & HOURANI, S.M.O. (1986). ATP analogues and the guinea-pig taenia coli: a comparison of the structure-activity relationships of ectonucleotidases with those of the P_2-purinoceptor. *Eur. J. Pharmacol.*, **129**, 217–224.

WELFORD, L.A., CUSACK, N.J. & HOURANI, S.M.O. (1987). The structure-activity relationships of ectonucleotidases and of excitatory P_2-purinoceptors: evidence that dephosphorylation of ATP analogues reduces pharmacological potency. *Eur. J. Pharmacol.*, **141**, 123–130.

ZIGANSHIN, A.U., HOYLE, C.H.V. & BURNSTOCK, G. (1994a). Ectoenzymes and metabolism of extracellular ATP. *Drug Dev. Res.*, **32**, 134–146.

ZIGANSHIN, A.U., ZIGANSHINA, L.E. & BURNSTOCK, G. (1994b). Inhibitors of ecto-ATPase activity potentiate responses mediated via P_{2X}-purinoceptors. *Drug Dev. Res.*, **31**, 336.

ZIGANSHIN, A.U., ZIGANSHINA, L.E., KING, B.F. & BURNSTOCK, G. (1994c). Characteristics of ecto-ATPase of *Xenopus* oocytes and the inhibitory actions of suramin on ATP breakdown. *Pflügers Arch.*, (in press).

(Received August 16, 1994
Revised October 3, 1994
Accepted October 11, 1994)

British Journal of Pharmacology (1995) 114, 640-647

Influence of age on the signal transduction pathway of non-adrenergic non-cholinergic neurotransmitters in the rat gastric fundus

Geert J.M. Smits & [1]Romain A. Lefebvre

Heymans Institute of Pharmacology, University of Gent, De Pintelaan 185, B-9000 Gent, Belgium

1 The influence of aging on the relaxant response and the change in cyclic nucleotide content induced by vasoactive intestinal polypeptide (VIP), nitric oxide (NO), electrical field stimulation of the non-adrenergic non-cholinergic neurones and substances acting at different levels of the cyclic AMP and cyclic GMP transduction pathways was studied in longitudinal muscle strips of the rat gastric fundus.

2 The relaxant responses to VIP, sustained electrical stimulation, forskolin and 3-isobutyl-1-methylxanthine were reduced with age, while the responses to dibutyryl cyclic AMP were not. The increase in cyclic AMP content induced by sustained electrical stimulation and forskolin was lower in old rats.

3 The relaxant responses to NO and to short train electrical stimulation were similar in the three age groups. The inhibitory effect of N^G-nitro-L-arginine methyl ester on relaxations induced by short train electrical stimulation was more pronounced in old rats. The relaxant responses to sodium nitroprusside (SNP), 8-bromo-cyclic GMP and zaprinast were reduced with age. SNP induced a similar elevation of the cyclic GMP content in the three age groups.

4 These results suggest that aging differentially affects the cyclic AMP and cyclic GMP pathway for relaxation by VIP and NO in the rat gastric fundus, as the defect seems to occur at the level of the adenylate cyclase and cyclic GMP-dependent protein kinase respectively.

Keywords: Aging; rat gastric fundus; NANC; VIP; NO; cyclic AMP; cyclic GMP

Introduction

Aging is a highly complex biological process associated with a progressive decline in the performance of most organs, culminating in the inability to meet the environmental demands for continued existence (Linnane *et al.*, 1989). Although gastrointestinal symptoms are common in the elderly (Talley *et al.*, 1992), the gastrointestinal tract has received little attention in experimental studies on aging. However, some structural and functional changes have been observed e.g. a significant decrease in the number of neurones in the gut of old rodents (Santer & Baker, 1988; Gabella, 1989) and a change in contractile response to muscarinic agonists in the jejunum of old rats (Kobashi *et al.*, 1985).

The rat gastric fundus contains inhibitory non-adrenergic non-cholinergic (NANC) neurones (Lefebvre, 1986). Two co-transmitters have been proposed for these neurones: nitric oxide (NO) and vasoactive intestinal polypeptide (VIP), involved in initiating and sustaining NANC relaxation, respectively (Li & Rand, 1990; Boeckxstaens *et al.*, 1992; D'Amato *et al.*, 1992). Previously we demonstrated that the relaxant response to sustained electrical stimulation was decreased in old rats; this was mimicked by a decreased response to VIP, suggesting that there is a decreased muscular sensitivity to VIP in old rats. The relaxant response to short train electrical stimulation was not influenced by aging, while the response to low concentrations of NO was increased in old rats; this might suggest a postsynaptic increase in sensitivity to NO to compensate for a decreased NO release in old rats (Smits & Lefebvre, 1992).

NO and VIP exert their biological effect via two different signal transduction pathways resulting in the increase in concentration of two different cyclic nucleotide second messengers. NO is known to activate the soluble form of guanylate cyclase and thus cause accumulation of guanosine 3':5'-cyclic monophosphate (cyclic GMP) (Waldman & Murad, 1987), while VIP increases the adenosine 3':5'-cyclic monophosphate (cyclic AMP) content by activation of adenylate cyclase (Gozes & Brenneman, 1987). An increase in cyclic GMP and cyclic AMP content in the rat gastric fundus during sustained electrical stimulation has been observed, in which the cyclic GMP level raises quickly, while the cyclic AMP level raises gradually and attains a maximum later (Ito *et al.*, 1990).

In order to elucidate the mechanisms involved in the hyposensitivity to VIP and the hypersensitivity to NO in the gastric fundus of old rats, we have now studied the influence of aging on the signal transduction pathways of VIP and NO. The functional response to substances acting at different levels of these pathways and their influence on the cyclic nucleotide content was therefore investigated in the gastric fundus of young (3 months), adult (12 months) and old rats (24 months). In addition the influence of N^G-nitro-L-arginine methyl ester (L-NAME) and L-arginine on the relaxant responses to short train stimulation in the three age groups was also studied. Preliminary accounts of part of these results have been given (Smits & Lefebvre, 1993; 1994).

Methods

General methodology

Male Wistar rats (3, 12 and 24 months old) were obtained from the Centre For Experimental Animals of the University of Leuven, Belgium. They were killed by a blow on the head and bleeding after at least 22 h of fasting but with free access to water. The stomach fundus was removed rapidly and 2 to 4 longitudinal muscle strips (20 × 3 mm) were prepared from one fundus according to Vane (1957). The strips were

[1] Author for correspondence.

suspended in 5 ml organ baths containing Krebs solution (mM: NaCl 118.5, KCl 4.8, $CaCl_2$ 1.9, KH_2PO_4 1.2, $MgSO_4$ 1.2, $NaHCO_3$ 25.0 and glucose 10.1) held at 37°C and gassed with 95% O_2/5% CO_2. Atropine (10^{-6} M) and guanethidine (4×10^{-6} M) were continuously present from the beginning of the experiment to block cholinergic and noradrenergic responses respectively.

Functional experiments

Strips were mounted for recording of auxotonic tension via a Grass force-displacement transducer FT03 coupled in series with a 1 g cm^{-1} spring on a Graphtec linearcorder F WR3701. Transmural stimulation was performed via two platinum plate electrodes (22 × 7 mm, distance in between 6 mm) by means of a Grass S88 stimulator with a constant voltage unit (supramaximal voltage, 1 ms duration). After an equilibration period of 60 min at a load of 1 g the optimal load for each tissue was determined; the contraction to 50 mM KCl was determined for different loads ranging from 0.5 to 1.5 g. The optimal load, where the tissue showed the most pronounced contraction to KCl, was used for the rest of the experiment. To study the relaxant responses, tone was raised to a similar extent by the addition of different concentrations of prostaglandin $F_{2\alpha}$ ($PGF_{2\alpha}$) in the three age groups, based on our previous observations (6×10^{-8} M, 3×10^{-7} M and 10^{-6} M for young, adult and old rats respectively; Smits & Lefebvre, 1992). On each $PGF_{2\alpha}$-induced plateau only one type of relaxant stimulus was tested. A maximum of 4 $PGF_{2\alpha}$ additions was done in one tissue with a minimum washout period of 50 min in between; the contractile response to repetitive administration of $PGF_{2\alpha}$ was consistent. The following relaxant stimuli were investigated: electrical stimulation (10 s trains at increasing frequency with 3 min intervals in between, and sustained stimulation with cumulative increase of the frequency once a steady relaxant response was obtained; 0.25 to 16 Hz for both types of stimulation), VIP, forskolin, N^6, 2'-O-dibutyryl cyclic AMP (db cyclic AMP), 3-isobutyl-1-methylxanthine (IBMX), NO, sodium nitroprusside (SNP), 8-bromo-cyclic GMP and zaprinast. Except for NO, all exogenous substances were added in a cumulative way with stepwise increase of the concentration once a steady relaxant response to a preceding concentration was obtained. For db cyclic AMP, which caused very slow relaxations, a maximum incubation time of 15 min was allowed even when the plateau response was not reached. The relaxant responses to NO were short-lasting and bolus administrations of increasing concentrations of NO were given at 3 min intervals. The influence of L-arginine (10^{-3} M) or L-NAME (3×10^{-4} M) on the relaxant responses to train stimulation was studied by constructing a frequency-response curve upon a different exposure to $PGF_{2\alpha}$ before and in the presence of these agents; L-arginine or L-NAME were added 10 min before the administration of $PGF_{2\alpha}$. At the end of the experiments, the tissues were blotted and weighed.

Assay of cyclic nucleotides

Strips were now mounted in an isotonic set-up, that allowed quick clamping of the tissues (see below). Changes in length were recorded via a HSE lever transducer B type 368 on a Graphtec linearcorder WR3500. The mean optimal load determined in the functional experiments was used: 0.7, 0.9 and 1.1 g for young, adult and old rats, respectively (see Table 1). After equilibration, tone was raised with $PGF_{2\alpha}$ and one relaxant stimulus per tissue was applied. The following relaxant stimuli were investigated: electrical stimulation with a frequency of 4 Hz for 20 s and until maximal relaxation; addition of 10^{-7} M VIP, 3×10^{-7} M and 3×10^{-6} M forskolin, 3×10^{-5} M IBMX, 2×10^{-6} M and 10^{-5} M NO and 3×10^{-6} M SNP, until maximal relaxation. When the maximal relaxation was obtained, the tissue was quickly clamped between two liquid nitrogen cooled plates. Some tissues were clamped in basal condition or after induction of tone with $PGF_{2\alpha}$, without applying a relaxant stimulus (control tissues). The tissue was homogenized first with a membrane dismembrator (B. Braun A.G. Melsungen, 100%) for 45 s and second with an ultrasonic probe (B. Braun A.G. 300s, Melsungen) for 4 times 5 s in 6% TCA on ice. The homogenate was centrifuged for 20 min at 2600 *g* and the TCA was extracted from the supernatant 4 times with 5 volumes of water-saturated ether. The cyclic nucleotide content was measured in 100 µl aliquots of the supernatant. The cyclic AMP content was measured by a binding assay based on the method of Tovey *et al.* (1974) and the cyclic GMP content was determined by a radioimmunoassay with a commercially available kit. The protein content was determined on the pellet by the method of Lowry *et al.* (1951) with bovine serum albumin as standard.

Data analysis

Contractions are expressed as mN of tension per gram of tissue. Relaxations are expressed as percentage reduction of the $PGF_{2\alpha}$-induced tone, while the cyclic nucleotide content of the tissues is expressed as pmol cyclic nucleotide mg^{-1} protein. Data are given as means ± s.e.mean. The inhibitory effect of L-NAME on relaxant responses to short train stimulation was assessed as $(R_b\text{-}R_a)x100/R_b$ where R_b and R_a are the relaxant response to a given stimulation frequency before and after adding L-NAME.

Two-factor analysis of variance (ANOVA) was performed on the frequency- and concentration-response curves and on the curve for the inhibitory effect of L-NAME at different stimulation frequencies with age and frequency, concentration or % reduction as variables. If statistical significance was reached ($P < 0.05$) a multiple comparison test was performed (*t* test with Bonferroni correction) between young and adult, young and old and adult and old rats (Lundbrook, 1991). Other statistical comparisons between responses in the three age groups were also done by *t* test with Bonferroni correction for multiple comparison. Responses to train stimulation in the presence of L-arginine or L-NAME were compared to those before by a paired *t* test, while the cyclic nucleotide content between control strips and strips, relaxing under one of the stimuli studied, within one age group were compared by means of an unpaired *t* test. *P*-values less than or equal to 0.05 were considered to be statistically significant.

Substances used

Adenosine 3',5'-cyclic phosphate (Janssen Chimica, Beerse, Belgium), [5',8-^{3}H]-adenosine 3',5'-cyclic phosphate (Amersham, Buckinghamshire, U.K.), L-arginine hydrochloride (Sigma, St-Louis, U.S.A.), atropine sulphate (Merck, Brussels, Belgium), bovine serum albumin (Sigma), 8-bromoguanosine 3':5'-cyclic monophosphate (Sigma), N^6,2'-O-dibutyryladenosine 3':5'-cyclic monophosphate (Sigma), forskolin (Sigma), guanethidine sulphate (Ciba Geigy, Groot Bijgaarden, Belgium), 3-isobutyl-1-methylxanthine (Sigma), N^G-nitro-L-arginine methyl ester (Sigma), prostaglandin $F_{2\alpha}$ (Sigma), sodium nitroprusside (Sigma), VIP (CRB, Northwich, U.K.). The cyclic GMP[^{125}I] RIA-kit was bought from DuPont Canada Inc (Ontaria, Canada). Zaprinast was a gift from Rhone-Poulenc (Dagenham, England). All drugs were dissolved in Krebs solution except for IBMX which was dissolved in 50 vol% ethanol up to a concentration of 5×10^{-2} M, forskolin which was dissolved up to a concentration of 10^{-2} M in pure ethanol and zaprinast which was dissolved in 20 vol% triethanolamine up to a concentration of 10^{-1} M. Further dilutions of these substances were made in Krebs solution. VIP and $PGF_{2\alpha}$ stock solutions, prepared in distilled water, were stored at −70°C; all other solutions were prepared on the day of the experiment. A saturated NO solution was prepared from NO gas (Air Liquide, Belgium) as described by Kelm & Schrader (1990).

Results

Functional responses

Characterization of rats and tissues The body weight of the rats, the weights of the tissues, the optimal load and the contractile response to $PGF_{2\alpha}$ are given in Table 1. There were significant differences in body weight, in weight of the tissues and in optimal load. The contractile response to $PGF_{2\alpha}$ was similar in the three age groups as was intended by the use of different concentrations (6×10^{-8} M, 3×10^{-7} M and 10^{-6} M for young, adult and old rats respectively) based on our previous experiments (Smits & Lefebvre, 1992).

The VIP pathway The mean results of the relaxant responses to sustained NANC neurone stimulation and to VIP are given in Figure 1. A decrease in response to VIP in old rats as compared to young and adult rats was observed. A similar tendency was present for the electrically induced relaxations but no significance was reached.

A representative example of relaxant responses to forskolin, db cyclic AMP and IBMX on the gastric fundus of young rats is given in Figure 2. Forskolin-induced relaxations were slow in onset and sustained (Figure 2), and decreased with aging (Figure 3). db cyclic AMP caused very slow relaxations in the precontracted fundus of the rat (Figure 2). In some strips a plateau was not reached even after 15 min of incubation time, the maximum incubation time allowed for a given concentration. The mean results show no consistent difference within the three age groups (Figure 3). IBMX induced concentration-dependent relaxations that developed at a

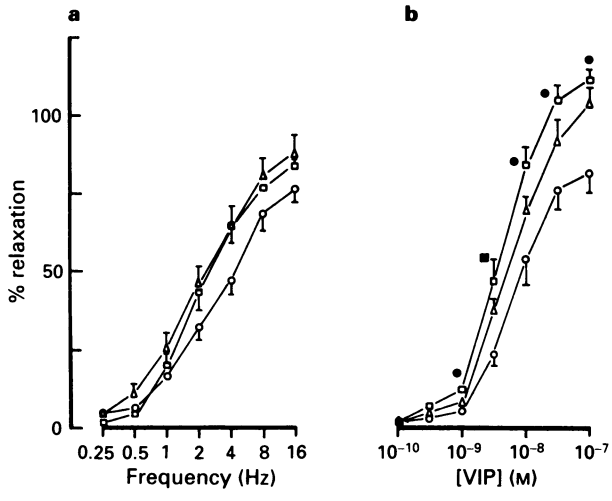

Figure 1 The cumulative frequency-response curve (a) under NANC conditions and the vasoactive intestinal polypeptide (VIP)-induced concentration response curve (b) in the gastric fundus of young (□), adult (Δ) and old (○) rats. Stimulation was with supramaximal voltage, 0.25 to 16 Hz and 1 ms duration. Mean ± s.e.mean, $n = 8-10$ for each age group. $^{\bullet}P < 0.05$, young versus old; $^{\blacksquare}P < 0.05$, adult versus old.

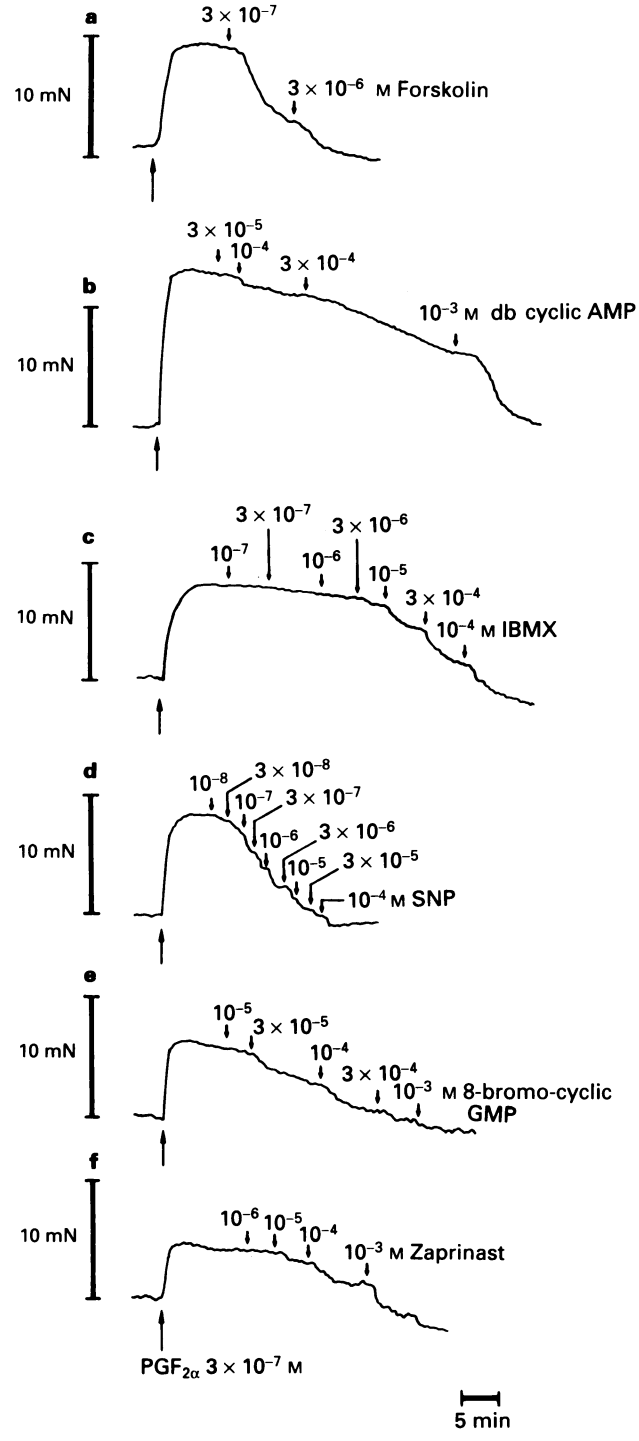

Figure 2 Representative examples of the relaxant responses to forskolin (a), db cyclic AMP (b), 3-isobutyl-1-methylxanthine (IBMX) (c), sodium nitroprusside (SNP) (d), 8-bromo-cyclic GMP (e) and zaprinast (f) in the gastric fundus of young rats. The arrow indicates the administration of 3×10^{-7} M prostaglandin $F_{2\alpha}$ ($PGF_{2\alpha}$).

Table 1 Body weight, tissue weight, optimal load and contractile response to prostaglandin $F_{2\alpha}$ ($PGF_{2\alpha}$) for young, adult and old rats

	Young	*Adult*	*Old*
Body weight (g)	313 ± 5	407 ± 7	532 ± 13^{aa,bb,cc}
	$n = 39$	$n = 33$	$n = 30$
Tissue weight (mg)	100 ± 4	121 ± 3	144 ± 4^{aa,bb,cc}
	$n = 65$	$n = 55$	$n = 52$
Optimal load (g)	0.69 ± 0.03	0.89 ± 0.04	1.06 ± 0.04^{aa,bb,c}
	$n = 65$	$n = 55$	$n = 52$
$PGF_{2\alpha}$ (mN g^{-1})	85.1 ± 3.7	90.4 ± 4.3	81.1 ± 3.3
	$n = 58$	$n = 52$	$n = 48$

Mean ± s.e.mean. $^{aa}P < 0.01$, young versus adult; $^{bb}P < 0.01$, young versus old; $^{c}P < 0.05$, $^{cc}P < 0.01$, adult versus old.

faster rate than those obtained with forskolin and db cyclic AMP (Figure 2). From a concentration of 3×10^{-6} M IBMX on, the relaxant responses were decreased in old rats as compared to young rats (Figure 3).

The NO pathway The mean relaxant responses to electrical stimulation with isolated trains and to NO showed no differences in the three age groups (Figure 4). SNP induced concentration-dependent relaxations. Especially at higher concentrations, the relaxations were fast in onset but tone tended to increase again quickly (Figure 2). The mean relaxant responses were significantly decreased with aging (Figure 5). 8-Bromo-cyclic GMP induced concentration-dependent relaxations which were slow in onset (Figure 2). The relaxant responses to this stimulus were generally decreased in old as compared to young rats (Figure 5). The relaxations induced by zaprinast in the fundus strips were well maintained (Figure 2). The mean results show an age-dependent decrease in relaxant response to zaprinast (Figure 5).

L-Arginine (10^{-3} M) did not affect the basal tone, but L-NAME (3×10^{-4} M) increased the basal tone by 12.2 ± 1.5, 5.5 ± 0.7 and 6.4 ± 1.0 mN g^{-1} in tissues of young, adult and old rats respectively ($n = 7-9$); these values were not statistically different. There was no influence of L-arginine on NANC relaxations induced by short train stimulation in any age group. L-NAME significantly decreased the responses to short train stimulation in the three age groups. The L-NAME-induced reduction was most pronounced in old rats (Figure 6).

Cyclic nucleotide measurements

Characterization of the rats and the tissues The body weight of the young rats (343 ± 7 g, $n = 34$) differed significantly ($P < 0.01$) from that of the adult (502 ± 11 g, $n = 34$) and old rats (476 ± 13, $n = 29$). The protein content of the tissues was similar in the three age groups (11.0 ± 0.3, $n = 101$; 11.9 ± 0.3, $n = 111$, and 11.3 ± 0.3, $n = 97$, mg for young, adult and old rats, respectively). The influence of age on the relaxant responses obtained under isotonic conditions was the same as measured under isometric conditions, except that the response to VIP was not clearly reduced with aging.

Cyclic AMP Preliminary experiments indicated that the cyclic AMP content of the tissues was not different between the 3 age groups ($n = 5-7$ for each age group). The ratio of the cyclic AMP content per mg protein in basal condition and after administration of $PGF_{2\alpha}$ did not change (1.3, 1.1 and 1.0 for young, adult and old rats respectively). The mean cyclic AMP content of the tissues in control conditions and after administration of the different relaxant stimuli are given in Table 2. VIP significantly increased the cyclic AMP content in each age group, without differences between the three age groups. Electrical stimulation until maximal relaxation increased the cyclic AMP content in young and adult but not old rats. Electrical stimulation for 20 s increased the cyclic AMP content in young rats. Only the higher concentrations of forskolin consistently increased the cyclic AMP content in the three age groups; a tendency for a lower response in the old rats was observed. The cyclic AMP content did not change after administration of IBMX in the three age groups.

Cyclic GMP Preliminary experiments indicated that the cyclic GMP content of the tissues did not differ between the three age groups ($n = 5-6$ for each age group). The ratio of the cyclic GMP content of strips in basal condition and after administration of $PGF_{2\alpha}$ did not change (1.2, 1.1 and 1.0 for young, adult and old rats respectively).

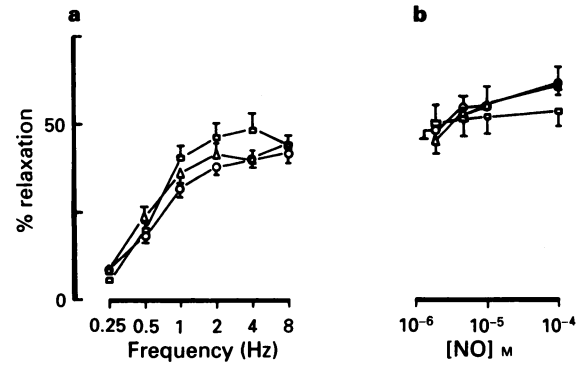

Figure 4 Concentration-response curves for the relaxant response of the gastric fundus strips to electrical stimulation with isolated trains (supramaximal voltage, 1 ms duration, 10 s trains and frequency between 0.25 and 16 Hz) (a) and to NO (b). Mean ± s.e.mean, $n = 8-9$ for each age group. (□) Young rats; (Δ) adult rats; (○) old rats.

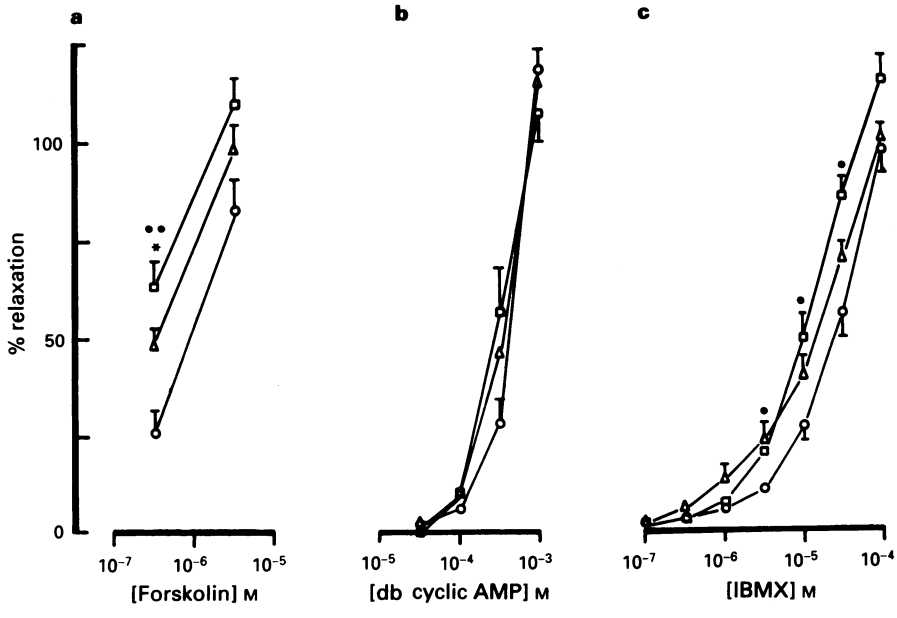

Figure 3 Concentration-response curves for the relaxant response of gastric fundus strips to forskolin (a), db cyclic AMP (b) and 3-isobutyl-1-methylxanthine (IBMX) (c). Mean ± s.e.mean, $n = 8-11$ for each age group. (□) Young rats; (Δ) adult rats; (○) old rats. $^{\bullet}P < 0.05$, $^{\bullet\bullet}P < 0.01$, young versus old; $^{*}P < 0.05$, young versus adult.

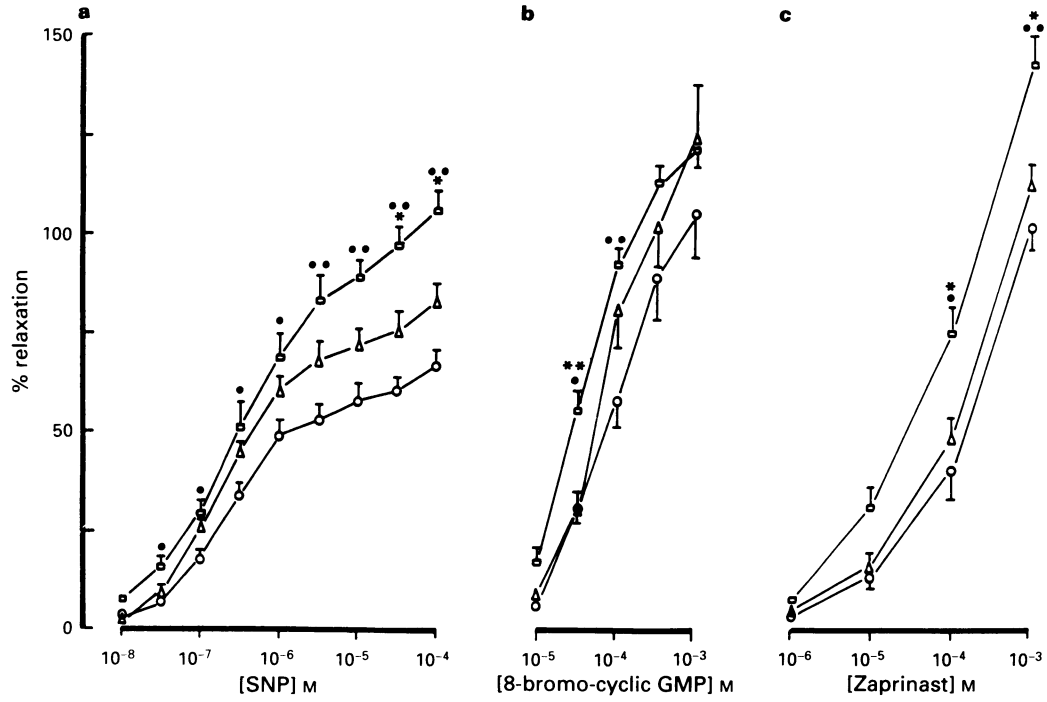

Figure 5 Concentration-response curves for the relaxant response of the gastric fundus strips to sodium nitroprusside (SNP) (a), 8-bromo-cyclic GMP (b) and zaprinast (c). Mean ± s.e.mean, $n = 7-10$ for each age group. (□) Young rats; (Δ) adult rats; (○) old rats. $^{\bullet}P<0.05$; $^{\bullet\bullet}P<0.01$, young versus old; $^{*}P<0.05$, $^{**}P<0.01$, young versus adult.

The mean cyclic GMP content of the tissues in control conditions and after administration of the different relaxant stimuli are given in Table 3. Electrical stimulation for 20 s and until maximal relaxation and administration of NO and SNP increased the cyclic GMP content significantly in all age groups. The cyclic GMP content after electrical stimulation for 20 s was significantly lower in old rats than in young and adult rats. A similar tendency was observed after the tissues were relaxed with the low NO concentration, but this did not reach statistical significance. IBMX did not influence the cyclic GMP content but VIP and the higher concentration of forskolin induced a modest increase in cyclic GMP content in the three age groups.

Discussion

As we previously obtained evidence suggesting the occurrence of hyposensitivity to VIP and hypersensitivity to NO in the fundus of aging rats (Smits & Lefebvre, 1992), this study was performed to evaluate further the mechanisms involved in these phenomena. The two inhibitory NANC co-transmitters, VIP and NO, act by activation of adenylate and guanylate cyclase respectively; the functional and cyclic nucleotide response to substances acting at different levels of the cyclic AMP and cyclic GMP transduction pathway was therefore studied. The tissues of the three age groups were investigated under optimal load and were contracted to an equivalent degree, which is an important prerequisite when comparing relaxant responses in tissues from different age groups (Cohen & Berkowitz, 1974).

Responses in young rats

The cyclic AMP pathway was studied by investigating the effect of forskolin, a direct activator of the catalytic subunit of adenylate cyclase (Seamon & Daly, 1981), IBMX, a non-specific phosphodiesterase inhibitor (Beavo & Reifsnyder, 1990) and db cyclic AMP. The relaxant responses to forskolin and IBMX in the gastric fundus of young rats were similar to those reported before by our group in rats of

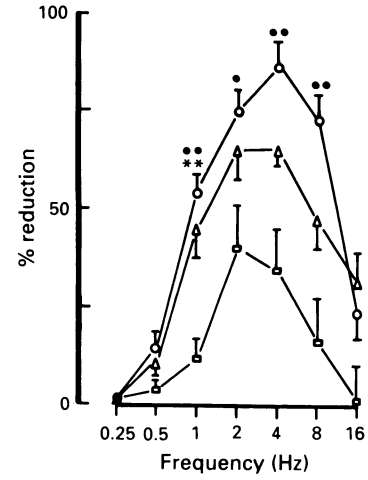

Figure 6 The N^{G}-nitro-L-arginine methyl ester (L-NAME)-induced reductions of the isolated frequency-response curve under NANC conditions in young (□), adult (Δ) and old (○) rats. Mean ± s.e.mean, $n = 8$ for each age group. $^{\bullet}P<0.05$, $^{\bullet\bullet}P<0.01$, young versus old; $^{**}P<0.01$, young versus adult.

similar age (Barbier & Lefebvre, 1992). As we had observed a very steep concentration-response curve, forskolin was now tested only at 2 concentrations. db cyclic AMP was now introduced to test the transduction pathway beyond cyclic AMP; it induced very slow relaxations. db cyclic AMP is a derivative of cyclic AMP which is more lipophilic (Nakatsu & Diamond, 1988) and thus penetrates the cell more easily than does cyclic AMP. After penetration into the cell, it needs intracellular degradation to N^{6}-monobutyryl cyclic AMP in order to activate further cyclic AMP-dependent protein kinase (Kaukel & Hilz, 1972; Kaukel *et al.*, 1972; Murray, 1990). The slow onset and the rate of action of db cyclic AMP might thus be related to the time needed to penetrate into the smooth muscle cells and to be degraded to its active part.

Table 2 The cyclic AMP content (pmol cyclic AMP mg^{-1} protein) in control condition (prostaglandin $F_{2\alpha}$, $PGF_{2\alpha}$ only) and after administration of different relaxant stimuli on top of $PGF_{2\alpha}$ in gastric fundus strips of young, adult and old rats

	Young	*Adult*	*Old*
Control	2.41 ± 0.15	3.07 ± 0.26	2.83 ± 0.18
	$n = 7$	$n = 7$	$n = 8$
ES max[b]	4.77 ± 0.40	4.08 ± 0.25	3.03 ± 0.30
	$n = 8$**	$n = 9$*	$n = 7$
VIP 10^{-7} M	6.29 ± 0.75	8.02 ± 0.69	8.31 ± 0.73
	$n = 7$**	$n = 7$**	$n = 6$**
Forskolin 3×10^{-7} M	3.46 ± 0.35	4.05 ± 0.44	3.49 ± 0.43
	$n = 5$*	$n = 6$	$n = 6$
Forskolin 3×10^{-6} M	6.79 ± 1.63	5.54 ± 0.88	4.31 ± 0.55
	$n = 6$*	$n = 6$*	$n = 6$*
IBMX[c] 3×10^{-5} M	2.99 ± 0.53	3.18 ± 0.25	2.19 ± 0.16
	$n = 5$	$n = 7$	$n = 3$
ES 20s	3.89 ± 0.36	3.09 ± 0.15	2.83 ± 0.17
	$n = 6$**	$n = 7$	$n = 7$
NO 2×10^{-6} M	3.04 ± 0.50	2.45 ± 0.33	3.03 ± 0.31
	$n = 3$	$n = 3$	$n = 3$
SNP 3×10^{-6} M	2.61 ± 0.18	2.61 ± 0.22	2.71 ± 0.06
	$n = 4$	$n = 5$	$n = 3$

ES 20s and ES max mean electrical stimulation at 4 Hz during 20 s and until maximal relaxation respectively. Mean ± s.e.mean. *$P<0.05$, **$P<0.01$, relaxant stimulus versus control; [b]$P<0.05$, young versus old; [c]$P<0.05$, adult versus old.

Table 3 The cyclic GMP content (pmol cyclic GMP mg^{-1} protein) in control condition (prostaglandin $F_{2\alpha}$, $PGF_{2\alpha}$, only) and after administration of different relaxant stimuli on top of $PGF_{2\alpha}$ in gastric fundus strips of young, adult and old rats

	Young	*Adult*	*Old*
Control[a,bb]	0.087 ± 0.056	0.135 ± 0.016	0.131 ± 0.010
	$n = 14$	$n = 16$	$n = 15$
ES max	0.470 ± 0.052	0.618 ± 0.099	0.359 ± 0.057
	$n = 8$**	$n = 9$**	$n = 7$**
VIP 10^{-7} M	0.140 ± 0.009	0.199 ± 0.033	0.175 ± 0.029
	$n = 7$**	$n = 7$	$n = 6$*
Forskolin 3×10^{-7} M	0.109 ± 0.007	0.095 ± 0.012	0.099 ± 0.010
	$n = 6$*	$n = 7$	$n = 7$*
Forskolin 3×10^{-6} M	0.136 ± 0.016	0.162 ± 0.027	0.133 ± 0.019
	$n = 6$**	$n = 6$	$n = 6$
IBMX 3×10^{-5} M	0.104 ± 0.012	0.130 ± 0.015	0.092 ± 0.008
	$n = 9$	$n = 8$	$n = 6$**
ES 20s[b,cc]	0.622 ± 0.056	0.761 ± 0.087	0.427 ± 0.028
	$n = 12$**	$n = 14$**	$n = 12$**
NO 2×10^{-6} M	0.490 ± 0.088	0.499 ± 0.144	0.271 ± 0.041
	$n = 5$**	$n = 6$	$n = 5$*
NO 10^{-5} M	0.710 ± 0.079	0.611 ± 0.173	0.693 ± 0.090
	$n = 5$**	$n = 6$**	$n = 5$**
SNP 3×10^{-6} M	0.243 ± 0.022	0.283 ± 0.021	0.258 ± 0.021
	$n = 6$**	$n = 8$**	$n = 7$**

ES 20s and ES max mean electrical stimulation at 4 Hz during 20 s and until maximal relaxation respectively. Mean ± s.e.mean. *$P<0.05$, **$P<0.01$, relaxant stimulus versus control; [a]$P<0.05$, young versus adult; [b]$P<0.05$, [bb]$P<0.01$, young versus old; [cc]$P<0.01$, adult versus old.

As expected, VIP and sustained electrical stimulation induced a clearcut increase in the cyclic AMP content; the same applied to the higher concentration of forskolin. The cyclic AMP response to 3×10^{-7} M forskolin, however, was modest, although this concentration already induced a pronounced relaxation. A similar discrepancy between cyclic AMP accumulation and relaxation to forskolin has been observed in other tissues e.g. the canine trachealis (Zhou *et al.*, 1992). A possible explanation is the compartmentation theory, stating that the tissues or even the cells contain different compartments or pools of cyclic nucleotide; the cyclic nucleotide content of the pool associated with smooth muscle relaxation must rise markedly before an increase in the total tissue cyclic nucleotide content can be detected (Nakatsu & Diamond, 1989; Murray, 1990). Compartmentation might also explain why the cyclic AMP (as well as the cyclic GMP) levels were not increased by IBMX. Alternatively, other mechanisms than adenylate cyclase activation or phosphodiesterase inhibition might contribute to the relaxant effect of forskolin and IBMX respectively (Bryson & Rodger, 1987; Laurenza *et al.*, 1989).

The cyclic GMP pathway was studied by investigating the effect of SNP, an exogenous NO-donor, zaprinast, a selective inhibitor of the cyclic GMP-specific phosphodiesterase (Beavo & Reifsnyder, 1990) and 8-bromo-cyclic GMP. The functional responses were as expected (Barbier & Lefebvre, 1992). With regard to the influence on the cyclic GMP content, the increase in the cyclic GMP content induced by SNP was less pronounced than that induced by NO and short train stimulation, although the relaxations were much more pronounced. Disproportionate changes in the tissue cyclic GMP content and relaxation to different stimuli are not uncommon (for review see Nakatsu & Diamond, 1989). Relaxations to SNP might have more to do with the rise or turnover of intracellular cyclic GMP than with the quantitative amount (see Rapoport *et al.*, 1985; 1987). A cyclic

GMP-independent mechanism of relaxation for SNP has been suggested in the dog femoral artery vein (Vidal *et al.*, 1991).

VIP induced a modest and sustained electrical stimulation a more pronounced increase in cyclic GMP content, similar to that reported by Ito *et al.* (1990) in adult rats. During the initial part of sustained electrical stimulation, mainly NO is released inducing an increase in cyclic GMP content. Ito *et al.* (1990) showed that the cyclic GMP content does not rise further after 40 s stimulation. The initial increase in cyclic GMP might thus just be maintained although some continuous release of NO during sustained electrical stimulation cannot be excluded. The VIP-induced increase in cyclic GMP content is more difficult to explain. VIP-induced release of NO from gastric smooth muscle cells has been proposed in the guinea-pig (Grider *et al.*, 1992) but in the rat gastric fundus, the VIP-induced relaxations are not influenced by NO synthase inhibitors (Boeckxstaens *et al.*, 1991). As forskolin also induced a modest increase in cyclic GMP content, some link between the cyclic AMP and cyclic GMP pathway cannot be excluded.

Influence of aging

The previously observed age-dependent decrease in the relaxant response to exogenously administered VIP and to prolonged electrical stimulation of the NANC neurones (which mainly releases VIP; Li & Rand, 1990; Boeckxstaens *et al.*, 1992; D'Amato *et al.*, 1992), was confirmed in all our experiments except for the response to 10^{-7} M VIP in the strips used for cyclic nucleotide measurement. We have no explanation for this exceptional result but as in general, the age-dependent decline in relaxation induced by prolonged electrical stimulation was mimicked by the age-dependent reduction in the response to VIP, the results point to an age-dependent decrease in muscular sensitivity to VIP in the rat gastric fundus. In this respect, it can be mentioned that a similar quantity of VIP-like immunoreactivity was observed in the stomach of young, adult and old rats (Ferrante *et al.*, 1991), although this does not exclude the release of a different amount. To explain the decreased relaxant response to the β-adrenoceptor agonist, isoprenaline, which also acts via the cyclic AMP pathway in vascular preparations of aging rats, a decrease in the function of the stimulatory GTP-binding protein (Kazanietz & Enero, 1991), an increase in phosphodiesterase activity (Schoeffter & Stoclet, 1990) and attenuated activation of cyclic AMP-dependent protein kinase (Deisher *et al.*, 1989) were suggested. The observation that the relaxant responses to forskolin but not to db cyclic AMP decreased with aging in a similar way to the response to VIP, suggest that the deficiency in old rats lies beyond the level of the VIP receptor but also that the intracellular mechanism for relaxation following cyclic AMP production is not influenced by aging. An age-dependent defect in adenylate cyclase might thus also be involved in the decreased muscular sensitivity to VIP in old animals. This is supported by the observation that the increase in cyclic AMP content induced by forskolin and by sustained electrical stimulation is lower in old rats. The decreased response to VIP and forskolin in the gastric fundus of aging rats cannot be explained by increased cyclic AMP phosphodiesterase activity, as one would expect in that case that the relaxant response to IBMX would increase with age while the opposite was observed.

As we previously observed an increased relaxant response to low concentrations of NO in the gastric fundus of old rats, while the relaxations induced by short train stimulation were not changed, we suggested the possibility of an age-dependent increase in sensitivity to NO in compensation for a decrease in stimulation-induced NO release (Smits & Lefebvre, 1992). This hypothesis cannot be maintained as the responses to both short train stimulation and to exogenous NO in the present study were similar in the three age groups. Furthermore, the inhibitory effect of L-NAME, used in a concentration that maximally inhibits the relaxations induced by short train stimulation in the rat gastric fundus (D'Amato *et al.*, 1992) was clearly most pronounced in old rats. This even suggests that the nitrergic contribution to the relaxations induced by short train stimulation increases with age. The less pronounced NO release in young rats cannot be attributed to a shortage of L-arginine, the substrate for NO synthesis, as exogenous L-arginine had no influence on the electrically induced relaxations in the three age groups. L-NAME increased the basal tone to a similar extent in the three age groups. This effect might be due to antagonism of a tonic inhibition of the rat gastric fundus via continuous release of NO. As tetrodotoxin did not influence the tone of the tissue, Boeckxstaens *et al.* (1991) concluded that this NO release is independent of action potential conduction. However, a non-specific contractile effect of L-NAME cannot be excluded.

The relaxant responses to SNP and 8-bromo-cyclic GMP in the rat gastric fundus were significantly decreased with age. A similar age-associated decrease in the nitroprusside- and 8-bromo-cyclic GMP-induced relaxation of the rat thoracic aorta was explained as due to age-related changes at the level of the guanylate cyclase and the cyclic GMP-dependent protein kinase (Moritoki *et al.*, 1988). As the action of SNP derives from enzymatic or non-enzymatic liberation of NO and subsequent activation of the guanylate cyclase (Feelisch & Noack, 1987; Waldman & Murad, 1987; Fung *et al.*, 1992), a decrease in the liberation of NO from nitroprusside in the aging gastric fundus might also explain the decreased response to this substance. However, both in this case and in the case of an age-induced deficiency of the guanylate cyclase, an age-dependent decrease in the cyclic GMP response to SNP should be observed. The similar cyclic GMP elevation induced by SNP in the three age groups thus points to a deficiency at the level of the cyclic GMP-dependent protein kinase in the aging rat gastric fundus. The more pronounced NO release after short train electrical stimulation in old rats, as indicated by the results with L-NAME, might thus compensate for this defect and explain why the relaxant responses to short train electrical stimulation were similar in the three age groups. Two observations do not correlate with the rest and are difficult to explain: the decreased cyclic GMP elevation to short train electrical stimulation in old rats as one would expect an increase with aging in view of the more pronounced NO release, and the similar relaxant responses to NO in the three age groups, as one would expect a decrease with age in view of the deficient cyclic GMP-dependent protein kinase.

The decreased response to nitroprusside and 8-bromo-cyclic GMP in the rat gastric fundus with aging is not due to increased cyclic GMP-specific phosphodiesterase activity, as the inhibitory effect of zaprinast, should increase with aging if this were the case (Ueda *et al.*, 1990; Moritoki *et al.*, 1992). In contrast, the response to zaprinast was found to decrease with aging, suggesting an age-dependent decline in cyclic GMP phosphodiesterase activity.

In conclusion, our results suggest that aging differentially affects the cyclic AMP and cyclic GMP pathway for relaxation in the rat gastric fundus. A decreased activity of adenylate cyclase contributes to the decline in the relaxant response to VIP with aging, while the decreased relaxant responses to SNP seem related to age-dependent changes at the level of the cyclic GMP-dependent protein kinase.

This study was financially supported by Grant 3.0007.92 from the Fund for Medical Scientific Research (FGWO).

References

BARBIER, A.J. & LEFEBVRE, R.A. (1992). Effect of 3-isobutyl-1-methylxanthine and zaprinast on non-adrenergic non-cholinergic relaxation in the rat gastric fundus. *Eur. J. Pharmacol.*, **210**, 315–323.

BEAVO, J.A. & REIFSNYDER, D.H. (1990). Primary sequence of cyclic nucleotide phosphodiesterase isozymes and the design of selective inhibitors. *Trends Pharmacol. Sci.*, **11**, 150–155.

BOECKXSTAENS, G.E., PELCKMANS, P.A., BOGERS, J.G., BULT, H., DE MAN, J.G., OOSTERBOSCH, L., HERMAN, A.G. & VAN MAERCKE, Y.M. (1991). Release of nitric oxide upon stimulation of nonadrenergic noncholinergic nerves in the rat gastric fundus. *J. Pharmacol. Exp. Ther.*, **256**, 441–447.

BOECKXSTAENS, G.E., PELCKMANS, P.A., DE MAN, J.G., BULT, H., HERMAN, A.G. & VAN MAERCKE, Y.M. (1992). Evidence for a differential release of nitric oxide and vasoactive intestinal polypeptide by nonadrenergic noncholinergic nerves in the rat gastic fundus. *Arch. Int. Pharmacodyn.*, **318**, 107–115.

BRYSON, S.E. & RODGER, I.W. (1987). Effects of phosphodiesterase inhibitors on normal and chemically-skinned isolated airway smooth muscle. *Br. J. Pharmacol.*, **92**, 673–681.

COHEN, M.L. & BERKOWITZ, B.A. (1974). Age-related changes in vascular responsiveness to cyclic nucleotides and contractile agonists. *J. Pharmacol. Exp. Ther.*, **191**, 147–155.

D'AMATO, M., CURRO D. & MONTUSCHI, P. (1992). Evidence for dual components in the non-adrenergic non-cholinergic relaxation in the rat gastric fundus: role of endogenous nitric oxide and vasoactive intestinal polypeptide. *J. Auton. Nerv. Syst.*, **37**, 175–186.

DEISHER, T.A., MANKANI, S. & HOFFMAN, B.B. (1989). Role of cyclic AMP-dependent protein kinase in the diminished beta adrenergic responsiveness of vascular smooth muscle with increasing age. *J. Pharmacol. Exp. Ther.*, **249**, 812–819.

FEELISCH, M. & NOACK, E.A. (1987). Correlation between nitric oxide formation during degradation of organic nitrates and activation of guanylate cyclase. *Eur. J. Pharmacol.*, **139**, 19–30.

FERRANTE, F., GEPPETTI, P. & AMENTA, F. (1991). Age-related changes in substance P and vasoactive intestinal polypeptide immunoreactivity in the rat stomach and small intestine. *Arch. Gerontol. Geriatr.*, **13**, 81–87.

FUNG, H.-L., CHUNG, S.-J., BAUER, J.A., CHONG, S. & KOWALUK, E.A. (1992). Biochemical mechanism of organic nitrate action. *Am. J. Cardiol.*, **70**, 4B–10B.

GABELLA, G. (1989). Fall in the number of myenteric neurons in aging guinea pigs. *Gastroenterology*, **96**, 1487–1493.

GOZES, I. & BRENNEMAN, D.E. (1989). VIP: molecular biology and neurobiological function. *Mol. Neurobiol.*, **3**, 201–236.

GRIDER, J.R., MURTHY, K.S., JIN, J.-G. & MAKHLOUF, G.M. (1992). Stimulation of nitric oxide from muscle cells by VIP: prejunctional enhancement of VIP release. *Am. J. Physiol.*, **262**, G774–G778.

ITO, S., KUROKAWA, A., OHGA, A., OHTA T. & SAWABE, K. (1990). Mechanical, electrical and cyclic nucleotide responses to peptide VIP and inhibitory nerve stimulation in rat stomach. *J. Physiol.*, **430**, 337–353.

KAUKEL, E. & HILZ, H. (1972). Permeation of dibutyryl cAMP into HELA cells and its conversion to monobutyryl cAMP. *Biochem. Biophys. Res. Commun.*, **46**, 1011–1018.

KAUKEL, E., MUNDHENK, K. & HILZ, H. (1972). N^6-monobutyryl-adenosine 3':5'-monophosphate as the biologically active derivative of dibutyryl adenosine 3':5'-monophosphate in HeLa S3 cells. *Eur. J. Biochem.*, **27**, 197–200.

KAZANIETZ, M.G. & ENERO, M.A. (1991). Decreased β-adrenoceptor-mediated vasodilation in aorta from aged rats: possible involvement of a stimulatory GTP-binding protein. *Eur. J. Pharmacol.*, **198**, 177–181.

KELM, M. & SCHRADER, J. (1990). Control of coronary vascular tone by nitric oxide. *Circ. Res.*, **66**, 1561–1575.

KOBASHI, Y.L., BREUING, E.P. & MARKUS, R.P. (1985). Age-related changes in the reactivity of the rat jejunum to cholinoceptor agonists. *Eur. J. Pharmacol.*, **115**, 133–138.

LAURENZA, A., MCHUGH SUTKOWSKI, E. & SEAMON, K.B. (1989). Forskolin: a specific stimulator of adenylyl cyclase or a diterpene with multiple sites of action? *Trends Pharmacol. Sci.*, **10**, 442–447.

LEFEBVRE, R.A. (1986). Study on the possible neurotransmitter of the non-adrenergic non-cholinergic innervation of the rat gastric fundus. *Arch. Int. Pharmacodyn.*, **280**, (Suppl.), 110–136.

LI, C.G. & RAND, M.J. (1990). Nitric oxide and vasoactive intestinal polypeptide mediate non-adrenergic, non-cholinergic inhibitory transmission to smooth muscle of the rat gastric fundus. *Eur. J. Pharmacol.*, **191**, 303–309.

LINNANE, A.W., MARZUKI, S., OZAWA, T. & TANAKA, M. (1989). Mitochondrial DNA mutations as an important contributor to ageing and degenerative diseases. *The Lancet*, **i**, 642–645.

LOWRY, O.H., ROSEBROUGH, N.J. & FARR, A.L. (1951). Protein measurement with folin phenol reagent. *J. Biol. Chem.*, **193**, 265–275.

LUNDBROOK, J. (1991). On making multiple comparisons in clinical and experimental pharmacology and physiology. *Clin. Exp. Pharmacol. Physiol.*, **18**, 379–392.

MORITOKI, H., TANIOKA, A., MAESHIBA, Y., IWAMOTO, T., ISHIDA Y. & ARAKI, H. (1988). Age-associated decrease in histamine-induced vasodilation may be due to reduction of cyclic GMP formation. *Br. J. Pharmacol.*, **95**, 1015–1022.

MORITOKI, H., YOSHIKAWA, T., HISAYAMA T. & TAKEUCHI, S. (1992). Possible mechanisms of age-associated reduction of vascular relaxation caused by atrial natriuretic peptide. *Eur. J. Pharmacol.*, **210**, 61–68.

MURRAY, K.J. (1990). Cyclic AMP and mechanisms of vasodilation. *Pharmacol. Ther.*, **47**, 329–345.

NAKATSU, K. & DIAMOND, J. (1988). Role of cGMP in relaxation of vascular and other smooth muscle. *Can. J. Physiol. Pharmacol.*, **67**, 251–262.

RAPOPORT, R.M., WALDMAN, S.A., GINSBURG, R., MOLINA, C.R. & MURAD, F. (1987). Effects of glycerol trinitrate on endothelium-dependent and -independent relaxation and cyclic GMP levels in the rat aorta and human coronary artery. *J. Cardiovasc. Res.*, **10**, 82–89.

RAPOPORT, R.M., WALDMAN, S.A., SCHWARTZ, K., WINQUIST, R.J. & MURAD, F. (1985). Effects of atrial natriuretic factor, sodium nitroprusside, and acetylcholine on cyclic GMP levels and relaxation in rat aorta. *Eur. J. Pharmacol.*, **115**, 219–229.

SANTER, R.M. & BAKER, D.M. (1988). Enteric neuron numbers and sizes in Auerbach's plexus in the small and large intestine of adult and aged rats. *J. Auton. Nerv. Syst.*, **25**, 59–67.

SCHOEFFTER, P. & STOCLET, J.-C. (1990). Age-related differences in cyclic AMP metabolism and their consequences on relaxation induced by isoproterenol and phosphodiesterase inhibitors in rat isolated aorta. *Mech. Ageing Dev.*, **54**, 197–205.

SEAMON, K.B. & DALY, J.W. (1981). Forskolin: a unique diterpine activator of cyclic AMP-generating systems. *J. Cyclic Nucleotide Res.*, **7**, 201–224.

SMITS, G.J.M. & LEFEBVRE, R.A. (1992). Influence of age on responsiveness of the rat gastric fundus to agonists and to stimulation of intrinsic nerves. *Eur. J. Pharmacol.*, **223**, 97–102.

SMITS, G.J.M. & LEFEBVRE, R.A. (1993). Possible involvement of adenylate cyclase in the decrease of NANC gastric relaxation in aging rats. *Acta Gastro-Enterologica Belgica*, **56**, b14.

SMITS, G.J.M. & LEFEBVRE, R.A. (1994). Influence of aging on nitrergic transmission in the rat gastric fundus. *Acta Gastro-Enterologica Belgica*, **57**, b2.

TALLEY, N.J., O'KEEFE, E.A., ZINSMEISTER, A.R. & MELTON III, L.J. (1992). Prevalence of gastrointestinal symptoms in the elderly: a population-based study. *Gastroenterology*, **102**, 895–901.

TOVEY, K.C., OLDHAM, K.G. & WHELAN, J.A.M. (1974). A simple direct assay for cyclic AMP in plasma and other biological samples using an improved competitive protein binding technique. *Clin. Chim. Acta.*, **56**, 221–229.

UEDA, H., HISAYAMA, T., HORIO, S. & MORITOKI, H. (1990). Age-associated decrease in cyclic GMP-mediated vasodilation may be in part due to increase in cyclic GMP-phosphodiesterase activity. *Eur. J. Pharmacol.*, **183**, 824.

VANE, J. (1957). A sensitive method for the assay of 5-hydroxytryptamine. *Br. J. Pharmacol. Chemother.*, **12**, 344–349.

VIDAL, M., VANHOUTTE, P.M. & MILLER, V.M. (1991). Dissociation between endothelium-dependent relaxations and increases in cGMP in systemic veins. *Am. J. Physiol.*, **29**, H1531–H1537.

WALDMAN, S.A. & MURAD, F. (1987). Cyclic GMP synthesis and function. *Pharmacol. Rev.*, **39**, 163–196.

ZHOU, H.-L., NEWSHOLME, S.J. & TORPHY, T.J. (1992). Agonist-related differences in the relationship between cAMP content and protein kinase activity in canine trachealis. *J. Pharmacol. Exp. Ther.*, **261**, 1260–1267.

(Received May 12, 1994
Revised September 26, 1994
Accepted October 12, 1994)

British Journal of Pharmacology (1995) 114, 648–655

Inhibition by cyclothiazide of neuronal nicotinic responses in bovine chromaffin cells

[1]J.M. Nooney & A. Feltz

Laboratoire de Neurobiologie Cellulaire. CNRS UPR 9009, 5 rue Blaise Pascal: 67084 Strasbourg, France

1 The desensitizing acetylcholine (ACh) response of bovine chromaffin cells maintained in culture was examined using rapid agonist applications (of 2 s duration) which imposed nominal drug concentrations within 50 ms. This study was aimed, firstly, at identifying which of the α3, α4 and α7 subunits known to be present in these cells is predominant in the ACh-evoked response and secondly, on the effects on these neuronal nicotinic ACh receptors (AChR) of cyclothiazide (CT), an agent acting as a modulator of a gating desensitization site on other ligand-gated channels.

2 Locally applied 100 μM ACh evoked peak currents (I_{ACh}) of -1.5 ± 0.1 nA ($n = 83$) at a holding potential of -60 mV. The ACh dose-response curve yielded an estimated EC_{50} of 60 μM. This current was not sustained but desensitized during the application period; it displayed strong inward rectification, but desensitized equally whether the evoked current was inward or outward going. The latter observation excludes α4 as a major contributor to the recorded current. Because the response was almost insensitive to a 1 μM α-bungarotoxin pretreatment ($I_{ACh} = -1.2 \pm 0.1$ nA; $n = 6$), and because 1, 1-dimethyl-4-phenylpiperazinium (DMPP) works as a potent agonist (peak current = -1.9 nA, $n = 2$ for 100 μM DMPP), the α7 subunit is also a minor contributor to the response. Taken together, these observations suggest a dominant α3 type of response.

3 Triple exponential fits were used to describe the characteristics of the ACh-evoked currents; one component to fit the rising phase, with 2 components to describe the decay phase. The decay times were 100 ms and 4 s for the fast and slow components respectively. The rate of the slow decay component increased systematically with recording time, approximately doubling from its initial value within 20–40 min. Furthermore there was a gradual rundown of the response, seen first as a loss of the late component of the current, measured at 2 s, with the peak current amplitude decreasing later in the recording.

4 CT, when coapplied with ACh, produced a dose-dependent inhibition of the ACh-evoked peak current. The effect showed little voltage-dependency with 100 μM CT producing $46 \pm 5\%$ (s.d.; $n = 3$) and $47 \pm 8\%$ (s.d.; $n = 7$) inhibition at -100 and -60 mV respectively. At $+60$ mV, inhibition was estimated to be $26 \pm 7\%$ (s.d.; $n = 3$).

5 After pre-exposure of the cells to CT by bath application, 10 and 30 μM CT produced poorly reversible $20 \pm 9\%$ ($n = 7$) and $42 \pm 5\%$ ($n = 4$) inhibitions of the peak current respectively. There were no discernible effects on the fitted decay constants at any CT concentration tested, although an increased inhibitory effect of CT was observed at higher concentrations (100 μM) on the amplitude of the late component measured at 2 s.

6 Similar effects were observed in conditions chosen to isolate the α3 type of receptor: namely when using DMPP as an agonist, or after α-bungarotoxin pretreatment.

7 The 2,3-benzodiazepine, GYKI 53655, is known to antagonize the action of CT on AMPA receptors. Coapplication of 50 μM GYKI 53655 with ACh (100 μM) produced a $29 \pm 4\%$ inhibition of the peak ACh-evoked current and $44 \pm 6\%$ inhibition of its amplitude at 2 s ($n = 4$). This response was fully reversible. Brief applications of both CT (100 μM) and GYKI 53655 (50 μM) with ACh via the microperfusion system produced a fully reversible inhibition that was not significantly different from the values obtained with either CT or GYKI 53655 alone, with $37 \pm 6\%$ inhibition of peak and $61 \pm 9\%$ inhibition of the amplitude at 2 s ($n = 3$).

8 The results obtained suggest that the CT effect is to impede recovery from a slow desensitization, with a more pronounced effect with longer CT applications. Globally, CT favours the 'rundown state' of the neuronal nicotinic AChR.

Keywords: Cyclothiazide; GYKI 53655; nicotinic receptor; desensitization; chromaffin cells; α-bungarotoxin

Introduction

Most known ligand-gated ion channels exhibit the phenomenon of desensitization during agonist application, wherein agonist-induced currents are poorly sustained in the continued presence of (high concentrations of) agonist; desensitization becoming more marked as the agonist concentration is increased. In its desensitized state, the receptor then displays increased affinity for antagonists (reviewed in Ochoa *et al.*, 1989; Changeux, 1990). The rates of desensitization vary between the millisecond and second time ranges, depending on the receptors, and even the receptor subtype, under study.

Cyclothiazide (CT) is a diuretic which reversibly relieves fast desensitization of AMPA receptors (Yamada & Tang, 1993; Patneau *et al.*, 1993), with little or no action apparent on the closely related kainate receptors (Partin *et al.*, 1993). This compound has therefore greatly aided the study of AMPA receptors and their pharmacology. That the effects of CT may be selectively antagonized by compounds such as 2,3-benzodiazepines (e.g. GYKI 53655; Palmer & Lodge, 1993) suggests that AMPA-preferring receptors contain a modulatory site that controls desensitization and which is

[1] Author for correspondence at present address: Lilly Research Centre Ltd., Erl Wood Manor, Windlesham, Surrey GU20 6PH.

sensitive to pharmacological agents. This leads to the question: do other ligand-gated receptors also contain a CT-sensitive modulatory site that controls desensitization?

Amongst the neuronal nicotinic acetylcholine receptors (AChR) described to date, chick (Couturier *et al.*, 1990a) and rat (Séguéla *et al.*, 1993) α7 homomers expressed in *Xenopus* oocytes, which form functional channels with high Ca^{2+} permeability and are sensitive to inhibition by α-bungarotoxin, display fast desensitization kinetics (Couturier *et al.*, 1990a) compared to other α subunits heteromerically expressed with β subunits in the same system (Couturier *et al.*, 1990b). It is this fast desensitization which underlies the failure until recently to observe functional native α7 receptors (Zhang *et al.*, 1994), despite suggestive evidence of their existence from α-bungarotoxin binding to CNS tissue (see Luetje *et al.*, 1990 for a review). Other neuronal nicotinic receptor subunits, such as α3 and α4, which are insensitive to α-bungarotoxin but may be inhibited by κ-bungarotoxin, also display desensitization, albeit at slower rates (Couturier *et al.*, 1990b). Expression of heteromeric nicotinic AChRs in *Xenopus* oocytes suggests that β subunits also contribute to the desensitization rate, though less markedly than α subunits, thus α3β2>α3β4>α4β2>α4β4 (Couturier *et al.*, 1990b). Following the observations of CT's effects on the desensitization of AMPA receptors, we decided to examine the possible effects of CT on nicotinic responses of bovine adrenomedullary chromaffin cells.

Acetylcholine (ACh)-evoked currents in bovine chromaffin cells arise from activation of a neuronal-type of nicotinic receptor (Fenwick *et al.*, 1982; Nooney *et al.*, 1992b) that is sensitive to κ-bungarotoxin (Nooney *et al.*, 1992a), but insensitive to α-bungarotoxin (Fenwick *et al.*, 1982; Nooney *et al.*, 1992a). The presence of high affinity α-bungarotoxin binding to adrenal medullary tissue (K_D = 1.6 nM; Wilson & Kirshner, 1977) and to chromaffin cells (K_D = 5–6 nM; Higgins & Berg, 1988) suggests, however, that an α7 receptor may also exist in these cells. Initially, we considered that CT might be a way of revealing these α7 receptors in chromaffin cells. The results obtained show, however, that CT inhibits ACh-evoked currents in these cells without changing the τ_{decay} values and in a voltage-independent manner. Furthermore, the same CT-inhibition was observed following incubation of the cells in high concentrations of α-bungarotoxin. These observations suggest that CT predominantly inhibits an α3-containing nicotinic AChR in these cells.

Methods

Bovine chromaffin cells were isolated according to the method of Bader *et al.* (1981). Cells were plated at 10^5 cells per 35 mm culture dish and maintained in 15% heat inactivated horse serum, 85% DMEM in 5% CO_2/95% O_2 at 37°C for 3–5 days before use.

Whole cell recordings were obtained from spherical cells, 10–15 μm in diameter and lacking obvious processes, voltage-clamped at −60 mV, unless otherwise stated. Agonist-evoked currents were recorded with an EPC-7 patch clamp amplifier (List Electronic, Darmstadt, Germany) and stored on an IBM compatible PC using the pClamp 5.5 suite of programmes. Currents were analysed off-line with Axograph 2 (Axon Instruments). The quality of the voltage-clamp in controlling large and fast ACh currents was systematically assessed by examining the activation kinetics of voltage-activated sodium currents, of similar amplitude, from the same cell (series resistance 2–8MΩ after Rs compensation).

ACh dose-response curves were obtained by bracketing the responses to different ACh concentrations with responses to 100 μM ACh. Drug effects were obtained by normalizing the current from ACh + drug application to the preceding control response in the presence of ACh alone. Results are expressed as mean ±s.e.mean (or s.d., where noted) from *n* cells. Where appropriate, data were tested for statistical significance by unpaired *t* tests.

Responses to different ACh concentrations, or to ACh in the presence of drug, were assessed by comparing currents evoked by application of agonist from one barrel to that, in the presence of drug, from a second barrel of a twin or triple barrelled microperfusion system. Agonists (± drugs) were dissolved in bath solution and fed by gravity to RNA injection cannulae (200 μm tip diam.) glued together. Agonist (± drug) applications were controlled by manual opening of a 3-way tap on each reservoir.

The triple barrelled pipette consisted of three cannulae glued together in the form of a triangle the apex of which was positioned at the base of the triangle, with the other two barrels, in the same plane, overlying this tubing. This was positioned so that the two 'outer' barrels were equidistant from the cell under study and gave almost identical (± 5%) agonist-evoked currents. The 'central' barrel contained control solution which flowed continuously, except during agonist applications. The remaining barrels contained agonist or agonist plus drug solution as required. When the central barrel tap was open, i.e. control solution flowing, either of the other taps could be opened (i.e. agonist solution flowing) with no agonist-induced current activity apparent (even at the single channel level) until such time as the central barrel tap was closed, at which time rapidly rising (τ_{rise} = 50–100 ms) agonist-induced currents were observed. In this way, agonist-induced currents could be controlled by closing the central 'control' tap, either manually or by means of an electrovalve controlled by the pClamp parameter file. Furthermore, by connecting one of the 'agonist' barrels to two reservoirs, each with a 3-way tap to control solution flow, its agonist solution could be exchanged for another without the need to remove and reposition the perfusion pipettes. Earlier experiments with direct agonist applications from a twin barrelled pipette allowed faster application rates

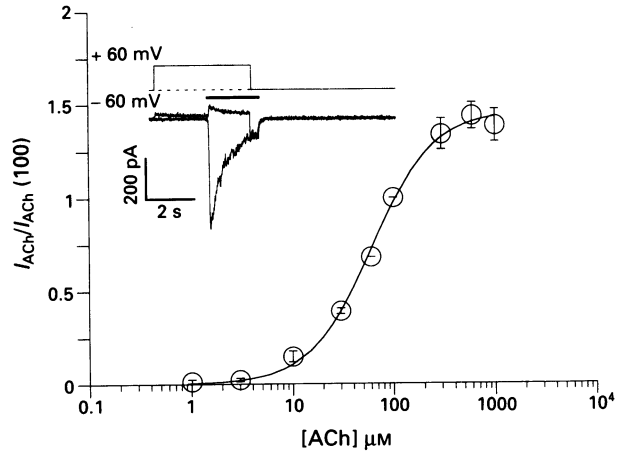

Figure 1 Characteristics of the acetylcholine (ACh) response in chromaffin cells. Insert: Traces illustrate the currents recorded in response to 100 μM ACh application at the holding potential −60 mV (inward current shown by downward deflection; broken line in voltage protocol), and at +60 mV (outward current shown by upward deflection; continuous line in voltage protocol) respectively. Note firstly the transient nature of the response which, after an initial peak, quickly desensitized and secondly, the strong inward rectification. Furthermore, when abruptly going from +60 mV to −60 mV during the ACh application (see voltage protocol), the desensitization was seen to have developed similarly at both potentials. Plot shows the dose-response curve of the ACh-evoked response at a holding potential of −60 mV. Values of peak current amplitude at different ACh concentrations were normalized to that obtained at 100 μM ACh. Data points represent mean values (± s.e.mean where appropriate and where larger than the symbol) obtained from 4–13 cells. Continuous line shows the best fit obtained with the equation: $y = M\ 10^{px}/(K^p + 10^{px})$, with x = log(ACh) and K = 61 μM, p = 1.41 and M = 1.464.

(τ_{rise} = 30–50 ms) but necessitated the removal and repositioning of the pipette in order to exchange the contents of one barrel to allow application of different drug solutions. The peak currents evoked by ACh application were similar with either system: -1.4 ± 0.06 nA ($n = 37$) compared to -1.6 ± 0.09 nA ($n = 46$) respectively. Henceforward further distinction between these two systems will not be made.

Solutions

Cells were continuously superfused with a bath saline containing (in mM): NaCl 140, KCl 2.8, $MgCl_2$ 2, $CaCl_2$ 1, HEPES 10, pH 7.2. Recording pipette solution contained (in mM): CsCl 140, HEPES 10, EGTA 1.1, $CaCl_2$ 0.1, $MgCl_2$ 2, pH 7.2. Stock solutions of all drugs were prepared and stored as aliquots at −20°C. ACh (Sigma) and 1,1-dimethyl-4-phenylpiperazinium iodide (DMPP; Sigma) were dissolved in distilled H_2O to give stock solutions of 10 mM; cyclothiazide (CT) was prepared as a 10 or 100 mM stock solution in dimethylsulphoxide (DMSO) and protected from light when in use. Most experiments were performed using 0.1–0.3% DMSO. ACh-induced currents recorded in the presence of 1% DMSO (the highest concentration used) were decreased by less than 15%. GYKI 53655 (1-(4'-aminomethyl)-3-methylcarbamoyl-4-methyl-3,4-dihydro-7,8-methylenedioxy-SH-2,3-benzodiazepine) was dissolved in HCl (10 mM) to give a 100 mM stock. α-Bungarotoxin (Sigma) was prepared as a stock solution of 10 mM in 140 mM NaCl plus 10 mM HEPES and stored as aliquots at −70°C.

Results

Acetylcholine-induced currents

Locally applied acetylcholine (ACh; 100 μM) evoked currents of -1.54 ± 0.06 nA ($n = 83$) at a holding potential of −60 mV. Typically, responses rose in 50–100 ms (τ_{rise} = 48 ± 0.3 ms at first application, $n = 25$) and decayed according to two time constants: the desensitization proceeding initially with a time constant of 100–200 ms, with a subsequent slower decline (time constant of 2–4 s, see below). Figure 1 illustrates the amplitude of peak ACh-induced currents (I_{ACh}), normalised to that evoked by 100 μM ACh, plotted as a function of ACh concentration. From this curve, an EC_{50} value of 60 μM was estimated and maximal I_{ACh} were observed at concentrations above 300 μM.

Figure 1 insert illustrates that (*i*) rapidly rising inward currents are evoked when ACh is applied to a holding potential −60 mV; (*ii*) this current is not sustained, but desensitizes during the 2 s application period; (*iii*) the outward current evoked 5 min later at +60 mV is much smaller than the preceding one at −60 mV; and (*iv*), nevertheless, returning to −60 mV during the 2 s ACh application fails to evoke a substantial inward current, but rather evokes a current the amplitude of which corresponds to the desensitized current which would have been recorded if the cell had been held at −60 mV throughout.

Because of the presence of this agonist-induced desensitization, agonist was applied to the cells at 5 min intervals, to allow full recovery of the response between applications and

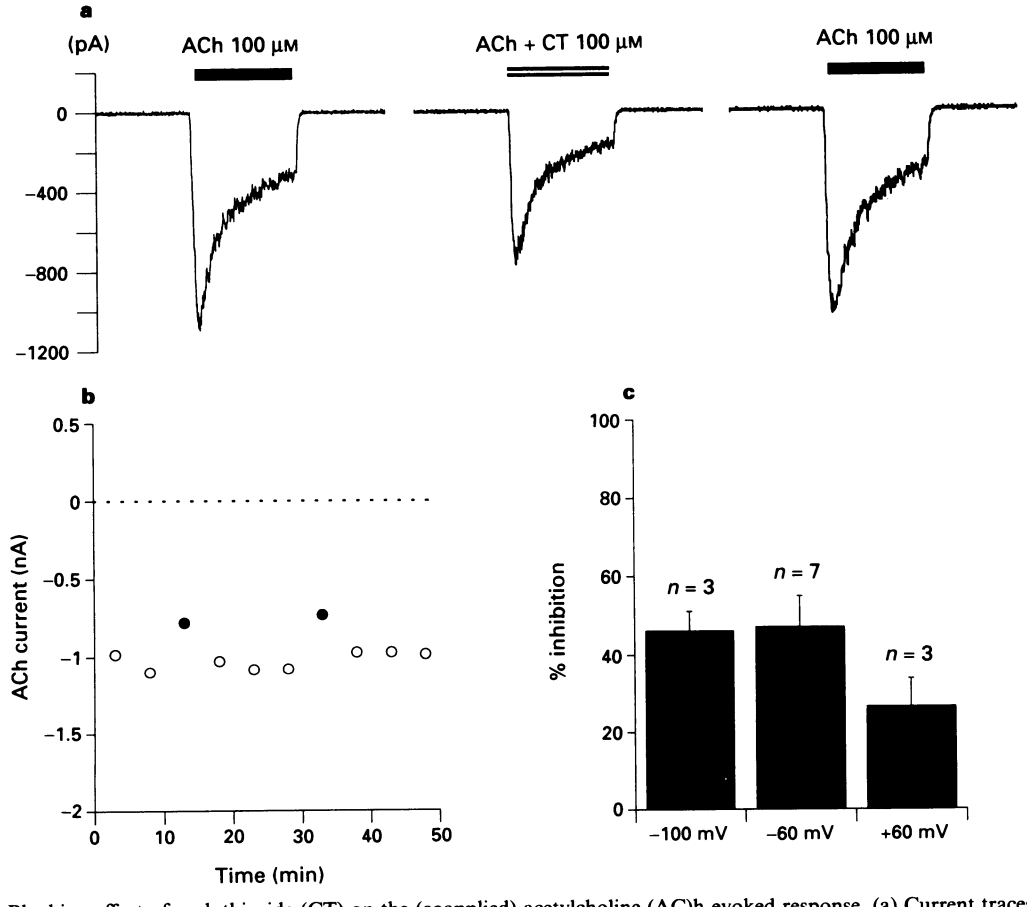

Figure 2 Blocking effect of cyclothiazide (CT) on the (coapplied) acetylcholine (AC)h-evoked response. (a) Current traces obtained by repeated 100 μM ACh application 5 min before (left) and after (right) coapplication of ACh plus 100 μM CT (for 2 s, as shown by bar). Note the reversibility of the effect. (b) Peak amplitude of the responses evoked by 100 μM ACh alone (○) and by coapplication of 100 μM ACh plus 100 μM CT (●) from the same cell as in (a), as a function of recording time. (c) Percentage inhibition induced by 100 μM CT (coapplied with 100 μM ACh for 2 s) at different holding potentials. Column height shows mean value and error bars, s.d.

to minimize rundown. Between individual applications this was true. Nevertheless, despite continuous washing, in the majority of the cells studied it was apparent that desensitization increased with recording time; becoming more pronounced as the recording continued. In fact, the amplitude at peak initially remained constant whilst that measured at 2 s gradually diminished with time. After 20–60 min, depending on the cell, the peak amplitude was also found to decrease (see Figure 3b). This phenomenon will be referred to hereafter as 'rundown'. Thus, although the decay of the first ACh-induced current recorded from any cell could occasionally be described by a single exponential, in most cells the first, and all subsequent responses, were best fitted by double exponentials ($\tau_{fast} = 171 \pm 16$ ms, $\tau_{slow} = 3.58 \pm 0.33$ s, $n = 25$), the rate of the slow component increasing further with time ($\tau_{slow} = 2.09 \pm 0.37$ s, $n = 22$ measured between 30 and 45 min; see Figure 3c) with no significant changes in τ_{fast} ($\tau_{fast} = 177 \pm 27$ ms, over the same time period). Also, the relative proportion of the fast to the slow component increased with time from 1.43 ± 0.18 to 2.62 ± 0.44 ($n = 22$) over 30 min, with, as a result, a typical loss of the slow component. The appearance of both the fast and slow components of the desensitization was not affected by pre-treating the cells for 90–120 min with 1 μM α-bungarotoxin ($n = 6$) (data not shown). Furthermore, 100 μM DMPP, which does not activate chick α7 homomers expressed in *Xenopus* oocytes (Bertrand *et al.*, 1992), evoked similar currents (−1.9 nA, $n = 2$) to ACh in these cells.

The effects of cyclothiazide

CT (30–500 μM) produced a dose-dependent inhibition of the peak ACh-evoked current when co-applied with agonist. The effects of CT were fully reversible when applied briefly

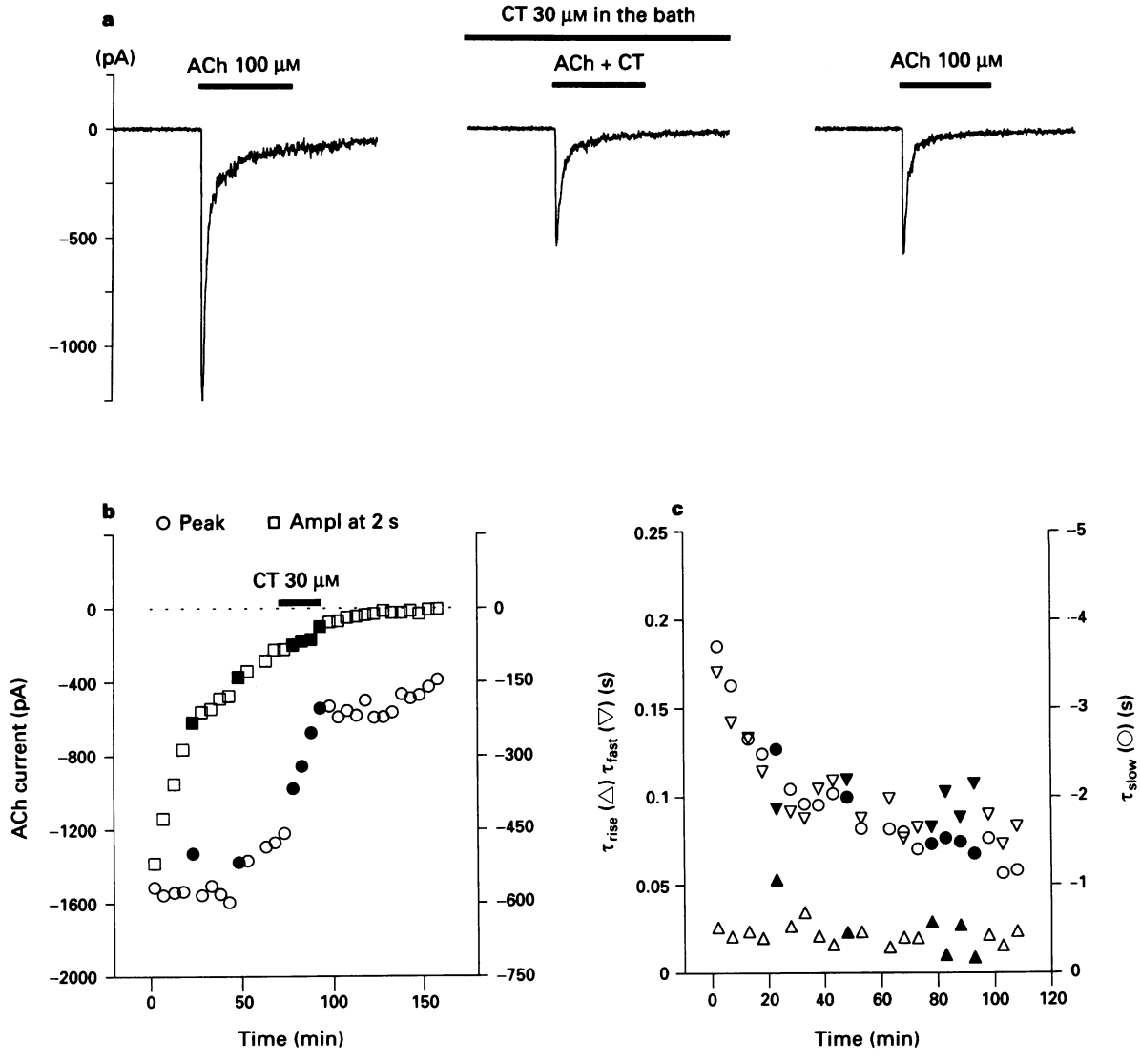

Figure 3 Cyclothiazide (CT) blocking effect in steady state conditions. (a) Same experimental conditions as in Figure 2 but CT (30 μM) was also preapplied, via the bath perfusate, to the test acetylcholine (ACh) (100 μM) plus CT (30 μM) application so as to obtain a steady-state concentration of CT. Note that the pronounced blocking effect induced by the steady-state CT application is not reversible. (b) Desensitization, with time, of the current evoked by 2 s applications of 100 μM ACh measured by the amplitude at peak (O) and at the end of the ACh application (□). Note that the decrease of the initial and late component of the ACh response is not synchronized: the late component decreases first, whereas peak amplitude starts to decrease only after some 50 min. The effect of 30 μM CT (coapplied with 100 μM ACh; filled symbols) before or during (at bar) bath application of CT is to accelerate rundown as seen by the effect on the evolution of the peak current. With 30 μM CT, the late component is almost unaffected. (c) Simultaneous evolution of the kinetic components of the ACh-evoked response. A 3 exponential fit was used to describe the characteristics of the individual responses yielding time constants and amplitudes of the rising phase, and the fast and slow components of the decay phase. Graph shows the evolution with recording time and CT application (filled symbol) of the three time constants from the same cell as in (a) and (b). Left ordinate corresponds to the time constants of the rising phase (△) and that of the fast component of decay (▽); right ordinate refers to the slow component of decay (○).

(Figure 2), by coapplication with ACh via the microperfusion system, with the subsequent ACh response being indistinguishable from the pre-CT control.

The effects showed little voltage-dependency (Figure 2), with brief applications of 100 μM CT producing 46 ± 5% (s.d.; $n = 3$) and 47 ± 8% (s.d.; $n = 7$) inhibition of the peak currents evoked at −100 and −60 mV respectively. At +60 mV, inhibition was estimated to be 26 ± 7% (s.d.; $n = 3$), although this may be an underestimation because of the increase in outward ACh-evoked currents with time (see Nooney *et al.*, 1992b; Ifune & Steinbach, 1993).

When the cells were exposed to CT by bath application, the effects of CT, although somewhat variable, became apparent at lower concentrations. Thus, 10 μM CT produced no discernible block when coapplied with ACh alone (103 ± 3% of control; $n = 15$) but produced 26 ± 9% inhibition when simultaneously bath and co-applied ($n = 7$). Similarly 30 μM CT produced 15 ± 2% inhibition when briefly coapplied with ACh alone ($n = 6$) but the inhibition was increased to 42 ± 5% ($n = 4$; Figure 3b) when CT was also present in the bath perfusate. Furthermore, in contrast to the brief applications, the effects of CT were poorly reversible when the cells were exposed for longer times (10 to 20 min) by inclusion of CT in the bath perfusate (Figure 3a,b). As a result, on repetitive CT and ACh applications, a cumulative decrease of the current amplitude is observed (Figure 3b).

At concentrations below 30 μM the effects of CT were observed only on the peak amplitude of the ACh-evoked current. The acceleration of the two components of decay with time described above was not modified during coapplications of CT with ACh (Figure 3c) at any of the concentrations tested.

At higher concentrations, an inhibitory effect of CT was also observed on the late component (see for example, Figure 4), although there was still no discernible effects on the fitted decay constants. Thus the current amplitude measured at 2 s was inhibited by 66 ± 4% ($n = 7$) compared to 44 ± 3% ($n = 7$) measured at peak with 100 μM CT in the same cells.

Cyclothiazide predominantly blocks α3 nicotinic receptors

Though DMPP-evoked currents are unlikely to arise from an α7 subset of receptors, similar effects of CT were seen when 100 μM DMPP was used as agonist (2 applications to 1 cell; Figure 4). This suggests that the predominant effect of CT is to inhibit α3 nicotinic receptors, in these cells. In the same line, pre-incubation of the cells at 37°C for 90–120 min in α-bungarotoxin (1 μM in DMEM containing 100 μg ml^{-1} bovine serum albumin, BSA) ($n = 2$) did not prevent the inhibitory effects of CT (Figure 4).

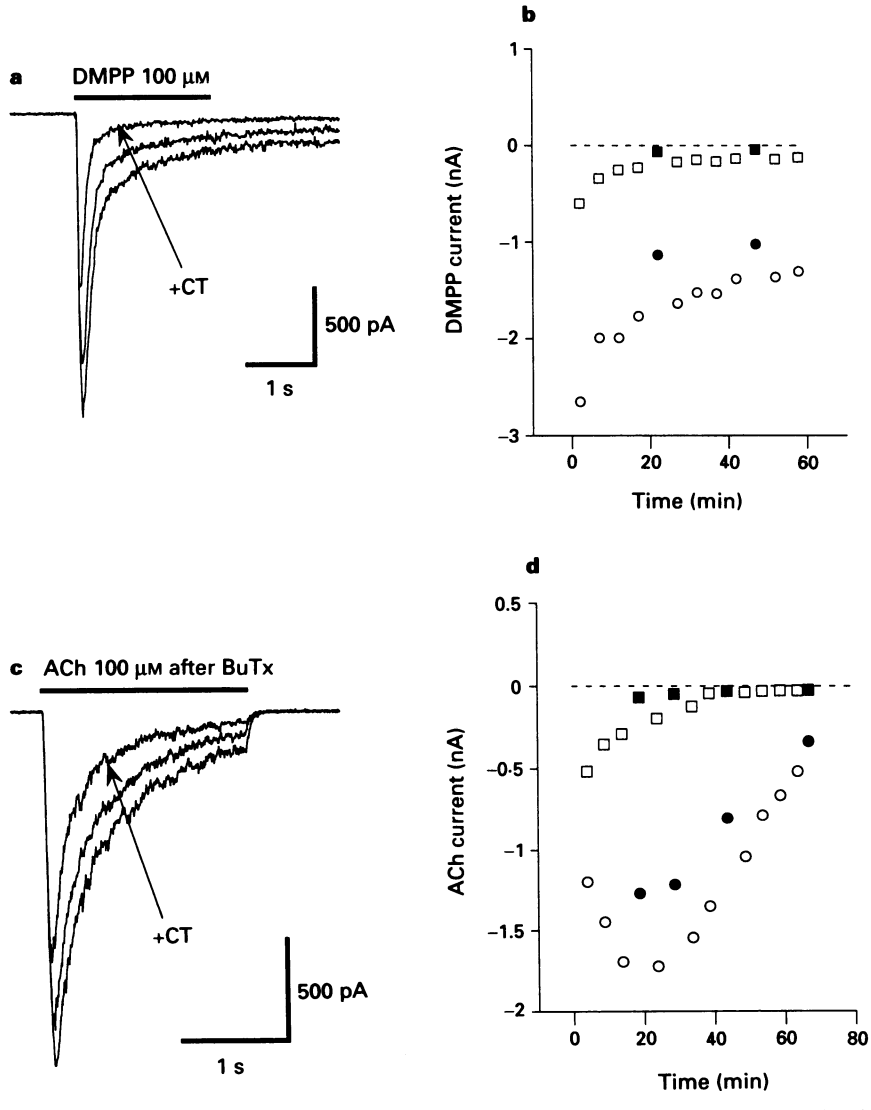

Figure 4 Preferential block of α3 nicotinic receptors by cyclothiazide (CT). (a,b) CT produces a similar block of DMPP-evoked currents. (c,d) Persistence of CT inhibition following α-bungarotoxin (BuTx) (see text for incubation details). For (a) and (b), same protocol as Figure 2a.

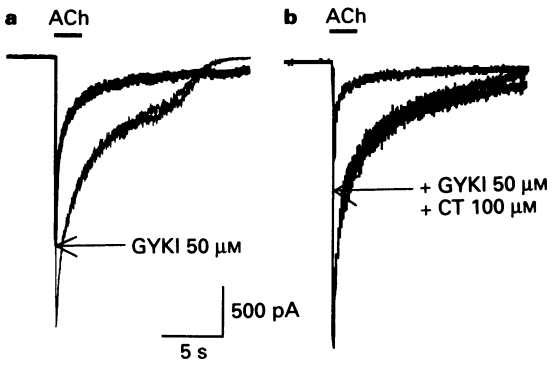

Figure 5 Blocking effects of GYKI 53655 and GYKI 53655 plus cyclothiazide (CT). (a) Inhibition of acetylcholine (ACh)-evoked current by coapplication of 50 μM GYKI 53655. Same experimental conditions as Figure 2(a). Note the full recovery of the response shown by identical ACh responses evoked before and after coapplication with GYKI 53655. (b) Inhibition of the ACh-evoked current by coapplication of GYKI 53655 (50 μM) plus CT (100 μM).

The effects of GYKI 53655

The effects of CT on AMPA receptors may be selectively antagonized by 2,3-benzodiazepines such as GYKI 53655. We therefore examined the actions of GYKI 53655 on ACh-evoked currents both alone and in the presence of CT. Coapplication of 50 μM GYKI 53655 with ACh (100 μM) produced a 29 ± 4% inhibition of the peak ACh-evoked current and 44 ± 6% of amplitude at 2 s ($n = 4$; Figure 5). This response was fully reversible, with the subsequent ACh response being identical to the preceding control. Application of lower doses (10 μM) via the bath perfusate produced poorly reversible inhibition ($n = 1$; data not shown). Brief application of both CT (100 μM) and GYKI 53655 (50 μM) with ACh via the microperfusion system produced an inhibition that was not significantly different from that obtained with either CT or GYKI 53655 alone, with 37 ± 6% inhibition of peak and 61 ± 9% inhibition of the amplitude at 2 s (Figure 5; $n = 3$) and was fully reversible as evidenced by the full sized ACh current when ACh was applied alone 5 min later.

Discussion

Cyclothiazide is a potent inhibitor of desensitization at the AMPA-preferring channels (Yamada, 1992; Patneau *et al.*, 1993), where its effect occurs without modification of the activation kinetics (Sahara *et al.*, 1993). On a neuronal nicotinic receptor, we show in contrast that cyclothiazide acts as an *enhancer* of desensitization, again without affecting the activation parameters. This set of observations makes cyclothiazide a potential tool for locating a major regulatory site for desensitization on channel forming molecules. The following discussion will first aim at an identification of the activated ACh receptor and subsequently at a characterization of the mechanism of action of cyclothiazide.

The ACh receptor inhibited by CT action

The activation of the nicotinic receptors present on chromaffin cells (Kilpatrick *et al.*, 1981; Fenwick *et al.*, 1982) elicits a transient response which is physiologically and pharmacologically similar to the neuronal receptors of the autonomic ganglia (see references in Nooney *et al.*, 1992b). The strong inward rectification observed in these cells (Nooney *et al.*, 1992b) as well as the EC_{50} of the ACh activation of this response (60 μM, comparable to the value of 150–450 μM estimated in rat chromaffin cells by Hirano *et al.*, 1987), its pharmacological profile previously described (Nooney *et al.*, 1992a,b), and the activation by DMPP, together suggest that this response could arise from activation of either α3- or α4-containing nicotinic receptors. The desensitization of the response which occurred at negative holding potentials was also observed at positive holding potentials, suggesting the prevailing involvement of an α3-containing receptor (Gross *et al.*, 1991) rather than α4-containing receptor which does not desensitize at positive holding potentials (when expressed with β2 in *Xenopus* oocytes; Gross *et al.*, 1991) and which may therefore represent the predominant native nicotinic AChR present in sympathetic ganglion cells (see Mathie *et al.*, 1990). Indeed α3 subunits have been shown to be present in the closely related PC12 cells (McLane *et al.*, 1990).

Nevertheless, chromaffin cells exhibit α-bungarotoxin binding sites (Higgins & Berg, 1987), which may indicate the additional presence of α7 subunits. However, α-bungarotoxin does not impair neurotransmission (Trifaro & Lee, 1980; Kilpatrick *et al.*, 1981; Higgins & Berg, 1987), nor does it affect the main characteristics of the ACh response (Nooney *et al.*, 1992a). An α7 component, if present, could make only a minor contribution to the measured ACh response. Most of the response we describe in chromaffin cells probably results, therefore, from the activation of α3 complexes, as often encountered in the peripheral nervous system (Deneris *et al.*, 1991).

However, an α7 component may have escaped our investigation because agonist application was too slow. If α7 is uniformally present in all chromaffin cells, it is obvious that CT did not transform the transient response expected for α7 nicotinic AChR into a sustained response as it does at AMPA-preferring channels. On the other hand, with fast simultaneous applications of ACh and CT (with no preapplication of CT), we observed if anything rather a slight increase of the peak ACh current, especially at low CT concentrations. In addition, in one case, large increases in amplitude (132 and 180% of control from two applications of 100 μM CT to the same cell; data not shown) and lengthening of the ACh response were observed. This may be linked to a differential expression of α7 receptors in these cells. Further investigations are required to clarify this point. However, when analyzing the effects of cyclothiazide, we kept in mind the possibility that the simultaneous activation of α3 and α7 receptors could come into play. This hypothesis was made more plausible following the recent demonstration that α-bungarotoxin binding sites correspond to functional channels (Zhang *et al.*, 1994).

CT versus 2,3-benzodiazepine binding site

An anti-relaxant effect has been reported for GYKI 53655, a 2,3-benzodiazepine (Smith *et al.*, 1991). This effect is unrelated to the benzodiazepine binding site of the $GABA_A$ channel which binds the classical 1,4-benzodiazepines. This new benzodiazepine increases desensitization of the non-NMDA channel resulting in protection against excitotoxicity (Zorumski *et al.*, 1993). Palmer & Lodge (1993) demonstrated recently that CT selectively antagonizes the actions of GYKI 53655 on a site located on AMPA-preferring channels. The present study shows that, on the ACh receptor, GYKI 53655 has the same effect as CT; suggesting, perhaps, that the two drugs also bind at the same site on this receptor.

Characterization of the cyclothiazide effect

Our main result is that this blocking effect does not alter the kinetics of the ACh response. Neither is the inhibition by CT strongly voltage-dependent. An inhibition through a channel block therefore seems unlikely. The conserved kinetics of the ACh response in the presence of CT rather implies a competitive antagonism on the nicotinic AChR or a favoured

desensitized state. Given the mode of action of cyclothiazide on AMPA receptors, we consider that the latter possibility is the more likely.

Though the α3 nicotinic AChR activation is determining the shape of the current recorded, an α7 nicotinic AChR activation, which results in a cationic flux that is difficult to record as a current because of its especially high rate of desensitization (Zhang *et al.*, 1994), elicits a measurable Ca entry (Zhou & Neher, 1993). In fact, cyclothiazide acting either directly through an increased α7 activation or indirectly in relation to a Ca entry is unlikely; we observed that cyclothiazide has similar action before and after α-bungarotoxin treatment. This set of observations led us to conclude that most of the cyclothiazide blocking effect is through its binding to α3 nicotinic AChR.

A possible scheme is one in which a single population of α3 nicotinic AChRs desensitizes along two time constants, CT only decreasing the proportion of the fast relative to the slow form. That is, the resting channel resides in two configurations; upon activation, one configuration exhibits fast desensitization, whilst the other is slow to desensitize. Both these states would be conducting, in contrast to the non-conducting desensitized forms. The fast desensitizing form recovers within 5 min, since the peak of the ACh-evoked current remains initially constant. By contrast, the recovery of the slowly desensitizing form proceeds at a slower rate, as shown by the gradual decrease of the late component on repeated ACh applications. On further activation the equilibrium must eventually shift from the fast to the slowly desensitizing form, producing a rundown of the response, seen here as a decreased peak current. In these terms, the rundown of the current represents a gradual failure of the nicotinic AChRs to recover from their desensitized state(s). Rundown is especially apparent during single channel recordings from isolated patches (e.g. Lester & Dani, 1994). Whether rundown is the result of a loss of functional receptors (e.g. channel dropout) or as a decreasing probability of channel opening is still unclear. The underlying causes of rundown, and the nature of the relationship, if any between rundown and desensitization are also unclear. However, the apparently constant amplitude of currents evoked by non-desensitizing ACh applications under otherwise similar conditions and recording times (J. Nooney unpublished observations; Nooney *et al.*, 1992a,b) would suggest that the rundown observed here is not simply due to intracellular dialysis. Further experiments are required to address this question.

Cyclothiazide appears to increase the phenomenon of rundown: with brief CT applications, more nicotinic AChRs are in their desensitized state, but the majority of these receptors are able to recover. At high concentrations, the slowly desensitizing form is preferentially blocked by CT. With longer applications (via the bath perfusate), CT prevents the receptors assuming or maintaining a form that is able to recover from desensitization. This CT effect is almost voltage insensitive.

In conclusion, this study shows that cyclothiazide acts as a gate modifier on ACh neuronal receptors. Cyclothiazide appears as the most potent of benzothiazide-related drugs at modifying the gate of AMPA-preferring non-NMDA channels (Yamada, 1992). From now on, one may wonder whether aniracetam and the other nootropic agents, which were the first gate modifiers to be identified (Isaacson & Nicoll, 1991; Tang *et al.*, 1991; Vycklicky *et al.*, 1991), also have an action on a number of other ligand-activated channels in addition to the AMPA receptor. A multiplicity of binding sites would require the aniracetam nootropic effect to be reinvestigated, with particular attention towards a specificity of action related to the glutamatergic pathways versus some cholinergic synaptic inputs.

The authors wish to thank Ms Danielle Thiersé, Unité Inserm 338, Strasbourg, for the generous provision of chromaffin cells; Dr David Lodge, Lilly Research Centre Ltd, U.K., for the gift of cyclothiazide and GYKI 53655; Dr John Clements, Vollum Institute, Portland, OR, U.S.A., for generously providing us with a prototype of Axograph 2; Dr Daniel Bertrand, University of Geneva, Switzerland, for helpful discussions. J.M.N. was a recipient of a Fondation de la Recherche Médicale fellowship.

References

BADER. M.F., CIESIELSKI-TRESKA, J., THIERSÉ, D., HESKETH, J.E. & AUNIS, D.J. (1981). Immunocytochemical study of microtubules in chromaffin cells in culture and evidence that tubulin is not an integral protein of the chromaffin granule membrane. *J. Neurochem.*, **37**, 917–933.

BERTRAND, D., BERTRAND, S. & BALLIVET, M. (1992). Pharmacological properties of the homomeric α7 receptor. *Neurosci. Lett.*, **146**, 87–90.

CHANGEUX, J.P. (1990). The functional architecture and dynamics of the nicotinic acetylcholine receptor: an allosteric ligand-gated ion channel. In *Fidia Research Foundation Neuroscience Award Lectures*, ed. Changeux, J.P., Llinas, R.R., Purves, D. & Bloom, F.E., pp. 21–168. New York: Raven Press.

COUTURIER, S., BERTRAND, D., MATTER, J.M., HERNANDEZ, A.C., BERTRAND, S., MILLAR, N., VALERA, S., BARKAS, T. & BALLIVET, M. (1990a). A neuronal nicotinic acetylcholine receptor subunit (α7) is developmentally regulated and forms a homo-oligomeric channel blocked by α-bungarotoxin. *Neuron*, **5**, 847–856.

COUTURIER, S., ERKMAN, L., VALERA, S., RUNGGER, D., BERTRAND, S., BOULTER, J., BALLIVET, M. & BERTRAND, D. (1990b). α5, α3, and non-α3, three clustered avian genes encoding neuronal nicotinic acetylcholine receptor-related subunits. *J. Biol. Chem.*, **265**, 17560–17567.

DENERIS, E.S., CONNOLLY, J., ROGERS, S.W. & DUVOISIN, R. (1991). Pharmacological and functional diversity of neuronal nicotinic acetylcholine receptors. *Trends Pharmacol. Sci.*, **12**, 34–40.

FENWICK, E.M., MARTY, A. & NEHER, E. (1982). A patch-clamp study of bovine chromaffin cells and of their sensitivity to acetylcholine. *J. Physiol.*, **331**, 577–597.

GROSS, A., BALLIVET, M., RUNGGER, D. & BERTRAND, D. (1991). Neuronal nicotinic acetylcholine receptors expressed in *Xenopus* oocytes: role of the α subunit in agonist sensitivity and desensitization. *Pflügers Arch.*, **419**, 545–551.

HIGGINS, L.S. & BERG, D.K. (1987). Immunological identification of a nicotinic acetylcholine receptor on bovine chromaffin cells. *J. Neurosci.*, **7**, 1792–1798.

HIGGINS, L.S. & BERG, D.K. (1988). A desensitized form of neuronal acetylcholine receptor detected by ^{3}H-nicotine binding on bovine adrenal chromaffin cells. *J. Neurosci.*, **8**, 1436–1446.

HIRANO, T., KIDOKORO, Y. & OHMORI, H. (1987). Acetylcholine dose-response relation and the effect of cesium ions in the rat adrenal chromaffin cell under voltage clamp. *Pflügers Arch.*, **408**, 401–407.

IFUNE, C.K. & STEINBACH, J.H. (1993). Modulation of acetylcholine-elicited currents in clonal rat phaeochromocytoma (PC12) cells by internal polyphosphates. *J. Physiol.*, **463**, 431–447.

ISAACSON, J.S. & NICOLL, R.A. (1991). Aniracetam reduces glutamate receptor desensitization and slows the decay of fast excitatory synaptic currents in the hippocampus. *Proc. Natl. Acad. Sci. U.S.A.*, **88**, 10936–10940.

KILPATRICK, D.L., SLEPETIS, R. & KIRSHNER, N. (1981). Ion channels and membrane potentials in stimuls-secretion coupling in adrenal medullary cells. *J. Neurochem.*, **36**, 1245–1255.

LESTER, R.A.J. & DANI, J.A. (1994). Time-dependent changes in central nicotinic acetylcholine channel kinetics in excised patches. *Neuropharmacology*, **33**, 27–34.

LUETJE, C.W., PATRICK, J. & SÉGUÉLA, P. (1990). Nicotine receptors in the mammalian brain. *FASEB*, **4**, 2753–2760.

MATHIE, A., COLQUHOUN, D. & CULL-CANDY, S.G. (1990). Rectification of currents activated by nicotinic acetylcholine receptors in rat sympathetic ganglion neurons. *J. Physiol.*, **427**, 625–655.

MCLANE, K.E., TANG, F. & CONTI-TRONCONI, B.M. (1990). Localization of sequence segments forming a κ-bungarotoxin-binding site on the α3 neuronal nicotinic receptor. *J. Biol. Chem.*, **265**, 1537–1544.

NOONEY, J.M., LAMBERT, J.J. & CHIAPPINELLI, V.A. (1992a). The interaction of κ-bungarotoxin with the nicotinic receptor of the bovine chromafin cells. *Brain Res.*, **573**, 77–82.

NOONEY, J.M., PETERS, J.A. & LAMBERT, J.J. (1992b). A patch clamp study of the nicotinic acetylcholine receptor of bovine adrenomedullary chromaffin cells in culture. *J. Physiol.*, **455**, 503–527.

OCHOA, E.L.M., CHATTOPADHYAY, A. & MCNAMEE, M.G. (1989). Desensitization of the nicotinic acetylcholine receptor: Molecular mechanisms and effect of modulators. *Cell. Mol. Biol.*, **9**, 141–178.

PALMER, A.J. & LODGE, D. (1993). Cyclothiazide reverses AMPA receptor antagonism of the 2,3-benzodiazepine GYKI 53655. *Eur. J. Pharmacol.*, **244**, 193–194.

PARTIN, K.M., PATNEAU, D.K., WINTERS, C.A., MAYER, M.L. & BUONANNO, A. (1993). Selective modulation of desensitization at AMPA versus kainate receptors by cyclothiazide and concanavalin A. *Neuron*, **11**, 1069–1082.

PATNEAU, D.K., VYKLICKY, Jr, L. & MAYER, M.L. (1993). Hippocampal neurons exhibit cyclothiazide-sensitive rapidly desensitizing responses to kainate. *J. Neurosci.*, **13**, 3496–3509.

SAHARA, Y., CLEMENTS, J.D., FELTZ, A. & WESTBROOK, G.L. (1993). How many agonist binding sites do AMPA/kainate receptor channels have? *Neurosci. Res.*, Supplement **18**, S42.

SÉGUÉLA, P., WADICHE, J., DINELEY-MILLER, K., DANI, J.A. & PATRICK, J.W. (1993). Molecular cloning, functional properties, and distribution of rat brain α7: A nicotinic cation channel highly permeable to calcium. *J. Neurosci.*, **13**, 596–604.

SMITH, S., DURMULLER, N. & MELDRUM, B.S. (1991). The non N-methyl-D-aspartate antagonists, GYKI 52466 and NBQX, are anticonvulsant in two animal models of reflex epilepsy. *Eur. J. Pharmacol.*, **201**, 179–183.

TANG, C.M., SHI, Q.Y., KATCHMAN, A. & LYNCH, G. (1991). Modulation of the time course of fast epscs and glutamate channel kinetics by aniracetam. *Science*, **254**, 288–290.

TRIFARO, J.M. & LEE, R.W.H. (1980). Morphological characteristics and stimulation-secretion coupling in bovine adrenal chromaffin cell cultures. *Neuroscience*, **5**, 1533–1546.

VYKLICKY, Jr, L., PATNEAU, D.K. & MAYER, M.L. (1991). Modulation of excitatory synaptic transmission by drugs that reduce desensitization at AMPA/kainate receptors. *Neuron*, **7**, 971–984.

WILSON, S.P. & KIRSHNER, N. (1977). The acetylcholine receptor of the adrenal medulla. *J. Neurochem.*, **28**, 687–695.

YAMADA, K.A. (1992). Thiazide diuretics reversibly block postsynaptic glutamate receptor desensitization in rat hippocampal neurons. *Soc. Neurosci. Abstr.*, **18**, 757.

YAMADA, K.A. & TANG, C.M. (1993). Benzothiadiazides inhibit rapid glutamate receptor desensitization and enhance glutamatergic synaptic currents. *J. Neurosci.*, **13**, 3904–3915.

ZHANG, Z.W., VIJAYARAGHAVAN, S. & BERG, D.K. (1994). Neuronal acetylcholine receptors that bind α-bungarotoxin with high affinity function as ligand-gated ion channels. *Neuron*, **12**, 167–177.

ZHOU, Z. & NEHER, E. (1993). Calcium permeability of nicotinic acetylcholine receptor channels in bovine adrenal chromaffin cells. *Pflügers Arch.*, **425**, 511–517.

ZORUMSKI, C.F., YAMADA, K.A., PRICE, M.T. & OLNEY, J.W. (1993). A benzodiazepine recognition site associated with the non-NMDA glutamate receptors. *Neuron*, **10**, 61–67.

(Received May 25, 1994
Revised October 13, 1994
Accepted October 18, 1994)

British Journal of Pharmacology (1995) 114, 656-661

Cardiovascular effects of the calcium sensitizer, levosimendan, in heart failure induced by rapid pacing in the presence of aortic constriction

[1]Éva Udvary, Julius Gy Papp & Ágnes Végh

Department of Pharmacology, Albert Szent-Györgyi Medical University, Dóm tér 12, Szeged, Hungary

1 The haemodynamic effects of a novel cardiotonic drug, levosimendan, which has both calcium-sensitizing and phosphodiesterase III (PDE III) inhibitory properties, were studied in conscious dogs in which heart failure had been induced by prolonged cardiac pacing in the presence of aortic constriction. These effects were compared with those in sham-operated dogs with essentially normal cardiac function.

2 Eighteen mongrel dogs were instrumented for the measurement of left ventricular pressure (LVSP, LVEDP) and contractile function (dP/dt; $dP/dt/P$). In twelve dogs a balloon catheter, positioned in the thoracic aorta, was inflated producing an approximate 60% reduction in effective aortic diameter. Twenty min later rapid ventricular pacing (240 beats mean^{-1}) was commenced and maintained for 48 h by means of a bipolar pacing electrode introduced into the right ventricle. This electrode served also for recording changes in the endocardial electrogram in the absence of pacing. Six of these dogs were used to evaluate the haemodynamic changes of pacing-induced heart failure; a further six of these dogs the haemodynamic changes elicited by levosimendan under these conditions. Six sham-operated dogs (group 2) served as controls.

3 In six dogs (group 1) the haemodynamic alterations were assessed after the development of heart failure. In the presence of aortic constriction, 48 h continuous rapid cardiac pacing resulted in a marked deterioration in left ventricular function which remained stable for at least 48 h after cessation of pacing. Thus, there was a marked reduction in LVSP (15%), $+dP/dt_{max}$ (35%), $-dP/dt_{max}$ (36%) and also in $dP/dt/P$ (29%), whereas LVEDP was increased considerably (from 6.4 ± 1.4 to 20.0 ± 2.2 mmHg). A marked elevation occurred in endocardial ST-segment (138%), lasting for 20 min.

4 Levosimendan was administered intravenously in doses of 0.005, 0.01 and 0.03 μmol kg^{-1} to 2 groups of conscious dogs. In the sham-operated dogs (group 2), only the higher dose (0.03 μmol kg^{-1}) produced significant increases in LVSP (19%), $+dP/dt_{max}$ (37%), and in $dP/dt/P$ (32%). In dogs with heart failure (group 3) doses of 0.005, 0.01 and 0.03 μmol kg^{-1} levosimendan resulted in an improvement in $+dP/dt_{max}$ (26%, 38% and 49%), $-dP/dt_{max}$ (20%, 25% and 38%) and in $dP/dt/P$ (19%, 34% and 50%) and reduction in the elevated LVEDP (from 20 ± 2.2 mmHg to 16 ± 1.0, 10 ± 1.3 and 9 ± 1.0 mmHg, respectively).

5 Levosimendan proved to be a potent cardiotonic drug at the doses used, and was approximately three times more effective under conditions of impaired left ventricular function than in normal hearts.

Keywords: Levosimendan; calcium sensitizer; heart failure; cardiac pacing

Introduction

Whether to treat heart failure with inotropic drugs remains an unanswered question. Recently, a new experimental approach has begun in this field with the development of 'calcium sensitizers', such as pimobendan (Rüegg *et al.*, 1984), EMD-53998 (Beier *et al.*, 1991), MCI-154 (Abe *et al.*, 1993) and levosimendan (Haikala *et al.*, 1992) which are reported to improve the contractile force of the failing heart by directly influencing the responsiveness of the contractile proteins to calcium. Since the contractile dysfunction in heart failure is associated with a reduced responsiveness of the myofilaments to calcium (Marban *et al.*, 1990), those drugs which are able to restore or increase the responses of the myofilaments by directly acting on the contractile protein system, appear to be potentially useful in the treatment of acute or chronic heart failure (Abe *et al.*, 1993; Lues *et al.*, 1993).

Some years ago simendan (OR 1259) was shown to be a powerful inodilator and antiarrhythmic compound in various *in vitro* and *in vivo* models (Haikala *et al.*, 1991; Végh *et al.*, 1992). The positive inotropic effect was attributed to a dual mechanism: increased sensitivity of troponin C to calcium and selective inhibition of phosphodiesterase III (PDE III) (Raasmaja *et al.*, 1991). In a model of acute heart failure induced by severe regional myocardial ischaemia (i.e. occlusion of the left anterior (LAD) and circumflex (LCX) branches of the left coronary artery; Végh *et al.*, 1987), simendan in a dose of 0.3 μmol kg^{-1} resulted in a marked improvement in cardiac output, positive dP/dt_{max} and in the local contractile performance of the impaired left ventricle (Végh *et al.*, 1992). However, simendan increased heart rate which was attributed to the PDE III inhibitory property of the compound. Recently, levosimendan, the negative enantiomer of simendan has been developed, and it was demonstrated that this negative enantiomer carries the calcium sensitizing action and the positive inotropic effect (Haikala *et al.*, 1992).

Apparently, levosimendan induces calcium sensitization by a mechanism different from that of other calcium sensitizers, such as EMD 53998. In skinned cardiac fibres Haikala *et al.* (1992) showed that, in contrast to EMD 53998, levosimendan did not enhance myosin ATP-ase activity and did not impair relaxation. Similarly in beating guinea-pig hearts simendan

[1] Author for correspondence.

preserved normal left ventricular relaxation (Édes *et al.*, 1992). In addition, and again in contrast to EMD 53998 and pimobendan, levosimendan did not increase calcium influx (Haikala *et al.*, 1993). Therefore levosimendan may avoid the possible deleterious effects of other calcium-sensitizing agents. For example there is some evidence that levosimendan does not aggravate the 'arrhythmogenic' cardiac electrophysiological alterations induced by simulated ischaemia in rabbit atrial and papillary muscles (Németh *et al.*, 1993) and indeed actually reduces arrhythmias resulting from coronary occlusion in anaesthetized dogs (unpublished data).

Unfortunately, evaluation of the effectiveness of cardiotonic compounds under conditions which mimic accurately the symptoms of either acute or congestive heart failure is hampered at least in part by the lack of suitable animal models. The objectives of the present study were therefore: (1) to establish a heart failure model in which ventricular dysfunction develops within a short time period and the effectiveness of cardiotonic agents can be tested easily before using a more difficult and expensive experimental model, and (2) to examine the haemodynamic effects of levosimendan under conditions of short-term heart failure induced by rapid pacing in the presence of aortic constriction in chronically instrumented conscious dogs.

Methods

Experiments were carried out in 18 healthy mongrel dogs of either sex, weighing between 16 and 24 kg (mean 22 ± 2.5 kg). The dogs were divided into three groups. In the first group (group 1) heart failure was induced without drug treatment, in order to evaluate haemodynamic changes during the development of heart failure due to rapid ventricular pacing combined with constriction of the aorta. The dogs in the second group (group 2) underwent a similar operational procedure but heart failure was not induced. These sham-operated dogs served as the levosimendan-control group. In a third group (group 3) heart failure was induced (as described below) and the haemodynamic effects of levosimendan were evaluated under these conditions.

Surgical procedure

Surgery was performed under general anaesthesia with sodium-pentobarbitone (Nembutal, Serva, 30 mg kg^{-1}, i.v.) under aseptic conditions. In all dogs a polyethylene catheter was introduced into the left ventricular cavity via the left carotid artery to measure pressure changes in the left ventricle. From the pressure trace left ventricular systolic pressure (LVSP) and end-diastolic pressure (LVEDP) were determined. The maximal rate of rise in the left ventricular pressure, i.e. positive dP/dt_{max} and also the negative dP/dt_{max} were measured by means of an electronic differentiator (Experimetria, Hungary) as was $dP/dt/P$, a measure of left ventricular contractility largely independent of changes in pre and afterload (Wolk *et al.*, 1971). Another catheter was introduced into the cavity of the right ventricle via the left external jugular vein for drug administration. In those dogs which underwent sham operation (group 2), the left carotid artery and the right jugular vein were ligated.

In twelve dogs (group 1 and group 3), in addition to the right and left ventricular catheterization, a pacing electrode was introduced into the right ventricle via the right jugular vein. This bipolar electrode served for pacing and also for measuring endocardial ST-segment changes when the stimulation was terminated. During surgery a balloon catheter was introduced into the thoracic aorta via the right carotid artery and positioned at the level of the diaphragm. All dogs were treated 1 hour before the surgery and throughout the entire investigation period with ticlopidine (125 mg) in order to avoid any complications resulting from introduction of the catheters (Nuttal *et al.*, 1985). If necessary, the animals were also treated with antibiotics for at least three days after the operation.

The animals were allowed to recover for one week before the initial study measurements. All subsequent studies were performed in the conscious state. Before starting the experiments, all dogs were conditioned and acclimatized to the laboratory environment for at least one week before the study. The animals were loosely suspended in a well fitting jacket (to protect the measuring devices) but allowed to move freely. The left ventricular catheter was attached to a pressure transducer (Viggo-Spectramed, Statham P23XL) and changes in left ventricular pressures (LVSP, LVEDP) and dP/dt were followed by means of an electromanometer (Experimetria, Hungary) and a differentiator (Experimetria, Hungary). In those groups in which heart failure was induced, the end of the pacing catheter was attached to a miniature stimulator, fixed under the collar of the dogs. Chest lead electrodes were positioned on the chest of the dogs and the ECG was measured telemetrically. The ECG trace was registered together with the haemodynamic parameters on an eight channel recorder (Medicor, Hungary). Parallel with recordings on paper, the ECG signals were transferred to an IBM-compatible computer and analysed by means of an ECG-Arrhythmia Analysing System (Innopoint, Hungary).

Experimental protocol

In the heart failure groups (group 1 and group 3) the balloon catheter was inflated by means of a syringe, containing approximately 1.5 ml saline. This volume was enough to produce about a 60% reduction in the diameter of the aorta and around a 45% reduction in aortic flow, as judged from preliminary studies performed in acute experiments. Heart failure was induced by rapid ventricular pacing. Twenty min after inflating the balloon catheter, rapid right ventricular pacing was started (240 beats min^{-1}, duration of 2 ms, at twice threshold) by means of a miniature pulse generator.

Experimental groups

Group 1 (heart failure control; $n = 6$) One week after surgery this group of conscious dogs underwent haemodynamic assessment as baseline. The balloon catheter was then inflated as described above with rapid ventricular pacing (240 beats min^{-1}) being started 20 min later and maintained for 48 h. Twenty four hours after commencing pacing the stimulator was switched off briefly (20 min) for measurement of haemodynamic parameters to assess whether or not heart failure was developing. Pacing was then resumed for a further 24 h. Forty eight hours after the initial start of pacing, the stimulation was stopped and haemodynamic measurements were performed for 200 min. The measurements were repeated 24 and 48 h after cessation of the rapid ventricular pacing.

Group 2 (sham operated animals, drug-control; $n = 6$) In this group of dogs, one week after operation and following the assessment of the baseline values, levosimendan was administered intravenously in doses of 0.005, 0.01 and 0.03 μmol kg^{-1} (over a period of 2 min). The effect of levosimendan on haemodynamic parameters was continuously assessed until the parameters returned to initial values; i.e. the observation period was 30 min after doses of 0.005 and 0.01 μmol kg^{-1}, whereas the changes were followed for 120 min when 0.03 μmol kg^{-1} was given.

Group 3 (heart failure treated group $n = 6$) In another group of dogs, heart failure was induced and haemodynamic measurements were performed as described above (group 1). When the stimulation was stopped and the baseline haemodynamic parameters were assessed, levosimendan was administered via intravenous bolus injection (over a period of

2 min) in doses of 0.005, 0.01 and 0.03 μmol kg^{-1} and the effects were continuously assessed until the haemodynamic parameters returned to initial values. Thus, as with the sham-operated animals after doses of 0.005 and 0.01 μmol kg^{-1}, haemodynamic changes were followed for 30 min, whereas after the dose of 0.03 μmol kg^{-1} the observation period was 120 min.

Levosimendan was dissolved in buffer containing 250 ml of 0.1 mol l^{-1} Na_2HPO_4 and 300 μl of 1 mol l^{-1} NaOH solution. The pH of the solvent was 10. This solvent administered intravenously was without significant effect on the haemodynamic parameters, such as LVSP (from 129 ± 7 to 130 ± 6 mmHg, NS) or positive dP/dt_{max} (from 5045 ± 296 to 5131 ± 277 mmHg s^{-1}, NS).

Statistical analysis

Data were expressed as mean ± s.e.mean. Statistical analysis was performed on data obtained at baseline and compared to following interventions and also differences between changes due to the interventions were analysed by two way analysis of variance (ANOVA) and modified t test. Differences are considered statistically significant at $P<0.05$. All studies were in accordance with the recommendations from the declaration of Helsinki and the internationally accepted principles in the care and use of laboratory animals.

Results

Development of heart failure induced by rapid ventricular pacing in the presence of aortic constriction

In 6 conscious dogs, the development of heart failure was assessed by means of evaluating haemodynamic indicators of contractility, filling pressure and ischaemia (Figure 1). Forty eight hours of rapid ventricular pacing combined with severe constriction of the aorta, resulted in a marked reduction in left ventricular pressure (LVSP from 152 ± 7 to 133 ± 4 mmHg, $P<0.05$), positive dP/dt_{max} (from 5332 ± 419 to 3316 ± 486 mmHg s^{-1}, $P<0.05$), negative dP/dt_{max} (from 2849 ± 206 to 1847 ± 300 mmHg s^{-1}, $P<0.05$) and $dP/dt/P$ (from 45.8 ± 4.4 to 31.5 ± 3.6 s^{-1}, $P<0.05$). After cessation of pacing all these parameters remained reduced for at least an additional 24 h and then started to return to the intial value.

After rapid ventricular pacing, there was a marked elevation in LVEDP (from 6 ± 1 to 20 ± 2 mmHg). This elevated LVEDP was present over a 24 h observation period. There was no statistically significant increase in heart rate from control baseline levels (from 113 ± 8 to 127 ± 6 beats min^{-1}, NS after cessation of pacing).

From the chest lead ECG, no significant changes occurred in the PQ and QT intervals, whereas the QRS interval was prolonged (from 35 ± 3 to 43 ± 2 ms, $P<0.05$). At the same time rapid ventricular pacing induced a significant elevation in ST segment measured from the bipolar pacing electrode site (from 2.2 ± 0.3 to 5.2 ± 0.5 mV, $P<0.05$) which was present for 20 min after cessation of pacing (Figure 1).

These results indicate that rapid ventricular pacing in the presence of aortic constriction resulted in a form of 'subacute' heart failure, characterized by a marked decrease in LVSP and in various indices of contractility, together with a parallel increase in LVEDP and considerable ST-segment alterations. The heart failure induced in such a way remained stable for at least 24 h after elimination of the frequency load. This period should be enough for testing and evaluating the effectiveness of drugs with positive inotropic properties under these experimental conditions of heart failure.

Effects of levosimendan in sham-operated dogs and in dogs with heart failure

The effects of levosimendan under normal conditions (sham-operated dogs, group 2) and in the presence of impaired

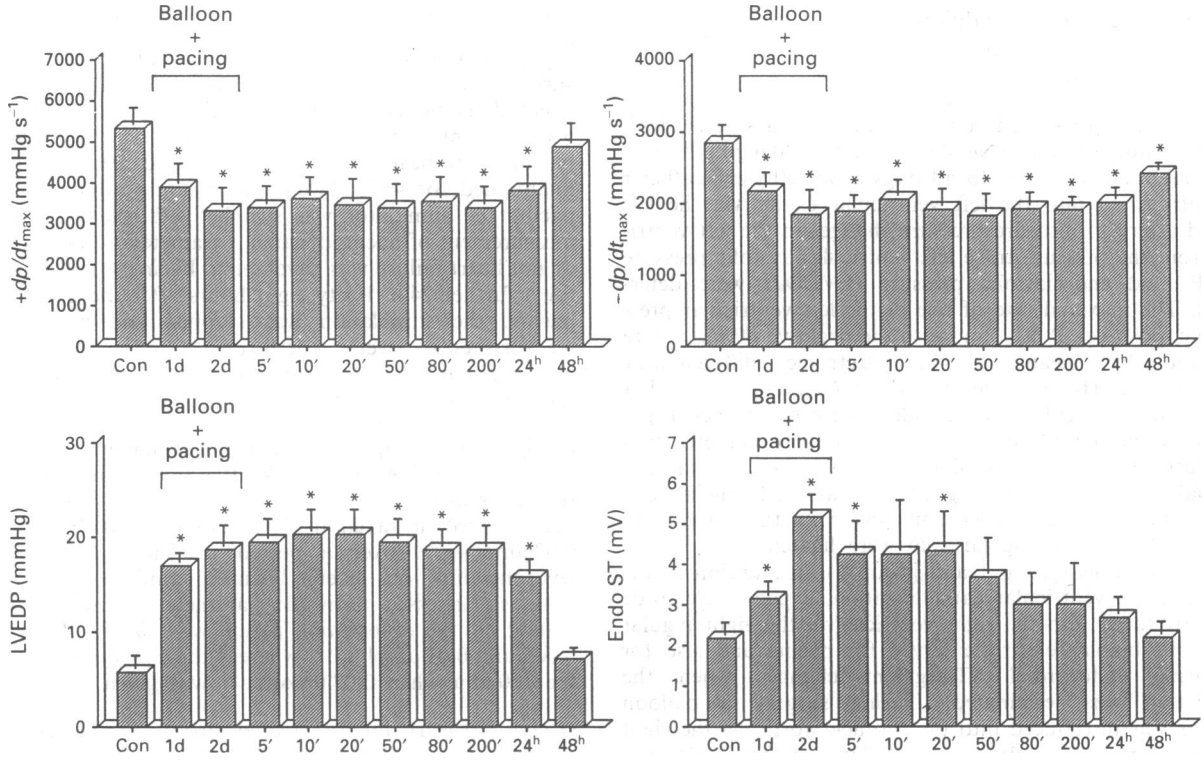

Figure 1 Development of heart failure induced by rapid ventricular pacing in the presence of aortic constriction characterized by haemodynamic parameters obtained from six conscious dogs; i.e. positive and negative dP/dt_{max} (mmHg s^{-1}), left ventricular end-diastolic pressure (LVEDP, mmHg) and ST-segment (mV) recorded from the right ventricular endocardial surface (Endo ST). Con = control baseline value, 1 d and 2 d = duration of pacing in days. *$P<0.05$ versus initial value.

Table 1 Haemodynamic effect of levosimendan in heart failure and in sham-operated dogs

Parameters	Groups	Before HF	Before drug	0.005 μmol kg^{-1} Max change	(%)	Before drug	Levosimendan 0.01 μmol kg^{-1} Max change	(%)	Before drug	0.03 μmol kg^{-1} Max change	(%)
LVSP (mmHg)	SO		153 ± 9	156 ± 10	2	151 ± 8	163 ± 8	8	150 ± 7	178 ± 8*	19
	HF	149 ± 7	138 ± 11	153 ± 14	11	135 ± 7	163 ± 8*	21	128 ± 8	152 ± 9*	19
LVEDP (mmHg)	SO		7.5 ± 1.1	7 ± 1.0	−7	9.2 ± 0.8	8.3 ± 1.0	−10	9.2 ± 0.8	4.4 ± 0.6	−52
	HF	6.4 ± 1.4	20 ± 2.2†°	16 ± 1.0†	−20	18 ± 1.7†	10 ± 1.3*	−44	15 ± 1.8†	9 ± 1.0†*	−40
+ dP/dt_{max} (mmHg s^{-1})	SO		4744 ± 240	5238 ± 302	10	4788 ± 311	5460 ± 706	14	4780 ± 362	6542 ± 271*	37
	HF	5240 ± 419	3419 ± 512†°	4313 ± 508*†	26	3519 ± 363†	4865 ± 612*	38	3602 ± 491	5325 ± 744*	49
$dP/dt/P$ (s^{-1})	SO		40 ± 0.9	44 ± 1.4	10	40 ± 1.7	49 ± 3.9	23	41 ± 1.9	54 ± 3.3*	32
	HF	49 ± 4.0	32 ± 3.0†°	38 ± 2.2†	19	35 ± 2.4	47 ± 3.6*	34	36 ± 2.9	54 ± 2.9*	50
− dP/dt_{max} (mmHg s^{-1})	SO		2768 ± 144	3000 ± 100	8	2652 ± 149	2960 ± 360	12	2762 ± 172	3136 ± 131	14
	HF	2759 ± 200	2082 ± 197†°	2490 ± 166†	20	2099 ± 147†	2625 ± 172*	25	2013 ± 140†	2769 ± 207*	38
HR (beats min^{-1})[a]	SO		117 ± 8	126 ± 8	8	117 ± 9	126 ± 9	8	114 ± 7	146 ± 8*	28
	HF	113 ± 8	123 ± 7	136 ± 6	11	123 ± 4	145 ± 6	18	121 ± 5	152 ± 7*	26

Values are mean ± s.e.mean.
Abbreviations: LVSP (left ventricular systolic pressure), LVEDP (left ventricular end-diastolic pressure), HR (heart rate), HF (heart failure), SO (sham-operated). °$P<0.05$ versus baseline value (before heart failure); *$P<0.05$ versus initial value (before drug); †$P<0.05$ versus sham-operated dogs.
[a]The solvent alone increased the heart rate by about 11% in both groups when given in a dose of 0.5 ml kg^{-1}.

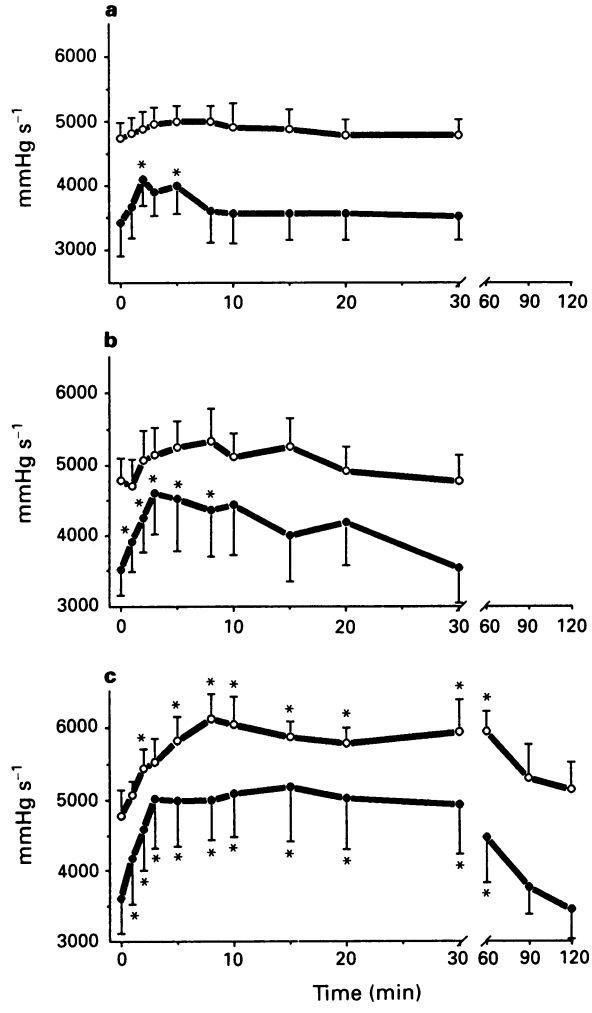

Figure 2 Effect of levosimendan on positive dP/dt_{max} (mmHg s^{-1}) in heart failure dogs ($n = 6$; ●), and in sham-operated dogs ($n = 6$; ○) after 0.005 μmol kg^{-1} (a), 0.01 μmol kg^{-1} (b) and 0.03 μmol kg^{-1} (c) doses. Values are means ± s.e. mean *$P<0.05$ versus initial value (before drug).

ventricular function (group 3) are presented in Table 1. When levosimendan was given intravenously in doses of 0.005 and 0.01 μmol kg^{-1} no significant haemodynamic changes occurred in sham-operated dogs. There were, however, significant increases in LVSP, positive dP/dt_{max}, negative dP/dt_{max} and also in $dP/dt/P$ when levosimendan was administered in a dose of 0.03 μmol kg^{-1}. The heart rate was also significantly increased (Table 1).

When levosimendan was given to conscious dogs with developed heart failure, a dose-dependent improvement occurred in the impaired left ventricular function. In contrast with the sham-operated dogs, the mean dose of levosimendan (0.01 μmol kg^{-1}) resulted in haemodynamic changes with significant increases in positive dP/dt_{max}, negative dP/dt_{max} and $dP/dt/P$ (Table 1). The highest dose (0.03 μmol kg^{-1}) of levosimendan resulted in further increase in left ventricular function (Table 1). Compared to the sham-operated group, this dose of levosimendan resulted in more pronounced improvement in positive dP/dt_{max}, negative dP/dt_{max} and in $dP/dt/P$ in the heart failure dogs, whereas the increase in heart rate was similar in both groups. Levosimendan also significantly reduced the elevated LVEDP (Table 1).

Figure 2 illustrates the dose-dependent increase in positive dP/dt_{mx} after levosimendan administration in sham-operated dogs and in dogs with developed heart failure. It is clear that levosimendan was more effective at increasing positive $dP/$

dt_{max} under conditions of heart failure than in dogs with intact heart function.

Discussion

A large number of compounds have been claimed to possess calcium sensitizing activity but most of them have additional inotropic activity, such as increase of calcium influx or selective inhibition of PDE III, which may also lead ultimately to an increase in intracellular calcium.

Levosimendan, a novel type of cardiotonic agent, is a powerful inodilator in various *in vitro* and *in vivo* models (Haikala *et al.*, 1992; Édes *et al.*, 1992; Udvary *et al.*, 1993). The proposed inotropic mechanism is that it increases the contractile state by stabilizing calcium-induced conformational changes in troponin C without enhancing myosin ATP-ase activity (Haikala *et al.*, 1992). Furthermore, levosimendan does not increase calcium influx (Haikala *et al.*, 1993); further evidence that the positive inotropic action might be due primarily to calcium sensitization.

The objective of the present study was to evaluate the haemodynamic effectiveness of levosimendan in a conscious canine model of heart failure. Evaluation of the effectiveness of a new cardiotonic agent under conditions which are able to mimic the clinical symptoms of heart failure remains a challenge. This is partially due to the lack of suitable animal models which provide an easy and quick evaluation of the effects of such compounds. In the present study one of our aims was to establish a conscious dog model in which the haemodynamic effects of cardiotonic drugs could be easily assessed under conditions mirroring the early phase of heart failure. It is well established that left ventricular dysfunction and heart failure can be induced by a 4 to 7 week period of continuous rapid ventricular pacing (Armstrong *et al.*, 1986; Wilson *et al.*, 1987; Moe *et al.*, 1992). This model exhibits haemodynamic and neural abnormalities closely resembling heart failure in man (Elsner & Riegger, 1991).

There is recent evidence that severely depressed left ventricular function can also be obtained by a shorter period of rapid ventricular pacing (i.e. 48 h), suggesting rapid adaptive changes in the receptor-effector systems (Pauw *et al.*, 1993). This model involves a technically easy surgical intervention and allows the evaluation of the effectiveness of a cardiotonic drug in a group of animals of sufficient size for valid statistical analysis. In our experiments the 48 h of rapid ventricular pacing was combined with constriction of the aorta in order to enhance the probability of the development of the left ventricular dysfunction over a relatively short period. In order to verify this model, heart failure was induced in one group of dogs without drug treatment and the haemodynamic changes were evaluated during and 48 h after rapid ventricular pacing. As the results indicate, a stable, overt heart failure develops 48 h following the onset of rapid ventricular pacing, if it is combined with constriction of the aorta. The depressed cardiac function was characterized by a decrease in ventricular pressure, a considerable reduction in left ventricular contractile function (i.e. positive and negative dP/dt_{max}, $dP/dt/P$), marked elevation in LVEDP and in the endocardial ST-segment. These changes remained stable for at least 24 to 48 h after cessation of pacing.

This experimental model was used to evaluate the effectiveness of levosimendan during the 2 day period after cessation of pacing. Levosimendan was administered intravenously in doses ranging from 0.005 to 0.003 $\mu mol\ kg^{-1}$ and the cardiotonic effects of the compound were estimated by recording changes in LVSP, LVEDP, positive and negative dP/dt_{max}, $dP/dt/P$ and heart rate. The effects of levosimendan under conditions of heart failure were compared to those present under normal conditions in sham-operated dogs. We found that levosimendan was a potent inotropic agent producing a dose-dependent cardiotonic action. Furthermore, levosimendan was somewhat more effective in improving left ventricular function under conditions of heart failure than in dogs with normal heart function. The ED_{25} values from dose-response curves of levosimendan on positive dP/dt_{max} in the sham-operated and heart failure dogs clearly demonstrate that levosimendan produced a more marked cardiotonic effect under conditions of impaired left ventricular function than when heart function was normal. Thus, in the sham-operated dogs, the ED_{25} was 0.0012 $\mu mol\ kg^{-1}$, whereas in dogs with heart failure, the ED_{25} was calculated to be 0.004 $\mu mol\ kg^{-1}$, indicating that levosimendan was approximately 3 times more effective in heart failure than in sham-operated animals.

Levosimendan, however, increased heart rate both in the sham-operated and in the heart failure dogs when given in a high dose, although in conscious dogs the solvent alone (0.5 $ml\ kg^{-1}$) increased the heart rate by about 11%. Similar increases in heart rate have been found in other canine models when levosimendan was administered in higher doses. For example, in anaesthetized dogs under conditions of acute heart failure, levosimendan in doses of 0.1 and 0.3 $\mu mol\ kg^{-1}$ resulted in a 20 to 26% increase in heart rate (unpublished data). This unfavourable effect of levosimendan was attributed to the phosphodiesterase inhibitory property of the compound. We aimed, therefore, to reduce the dose of levosimendan to determine the optimum dose-range which produces marked positive inotropic effects under conditions of heart failure but with less pronounced effects on heart rate. Thus, in the present study levosimendan was administered in doses 10 to 60 times lower than those used in our previous studies. Although these doses of levosimendan produced dose-dependent inotropic effects, the 0.03 $\mu mol\ kg^{-1}$ dose resulted in a similar increase in heart rate to that of doses of 0.1 or 0.3 $\mu mol\ kg^{-1}$. If we accept that the increase in heart rate after levosimendan administration can be attributed to inhibition of PDE III, we would suppose a dual mechanism of action; calcium sensitization and phosphodiesterase inhibition at higher doses.

This work was supported by the Hungarian National Scientific Foundation (OTKA; project numbers: T 5174). The authors are extremely grateful to Miss Ágnes Krajevszki and to Mr Gábor Girst for their valuable technical assistance.

Levosimendan was supplied by Orion Corporation (Orion-Farmos), Espoo, Finland.

References

ABE, Y., KITADA, Y. & NARIMATSU, A. (1993). Effect of MCI-154, a cardiotonic agent, on regional contractile function and myocardial oxygen consumption in the presence and absence of coronary artery stenosis in dogs. *J. Pharmacol. Exp. Ther.*, **256**, 819–825.

ARMSTRONG, P.W., STOPPS, T.P., FORD, S.E. & DEBOLD, A.J. (1986). Rapid ventricular pacing in the dog: pathophysiologic studies of heart failure. *Circulation*, **74**, 1075–1084.

BEIER, N., HARTING, J., JONAS, R., KLOCKOW, M., LUES, I. & HAEUSLER, G. (1991). The novel cardiotonic agent EMD 53998 is a potent calcium sensitizer. *J. Cardiovasc. Pharmacol.*, **18**, 17–27.

ÉDES, I., PAPP, J.G.Y. & CSANÁDI, M. (1992). The effects of a new calcium sensitizer, simendan, on intracellular protein phosphorylation. *J. Mol. Cell. Cardiol.*, **24**, (Suppl. V), S93. (abstract).

ELSNER, D. & RIEGGER, G.A.J. (1991). Animal models of heart failure. *Current Opinion Cardiol.*, **6**, 334–340.

HAIKALA, H., LEVIJOKI, J., LEINO, T., LINDÉN, I.-B. & POHTO, P. (1991). Antiarrhythmic effect and altered calcium sequestration by a cardiotonic agent OR-1259. *J. Mol. Cell. Cardiol.*, **23**, (Suppl. V), S130. (abstract).

HAIKALA, H., NISSINEN, E., ETEMADZADEH, E., LINDÉN, I.-B. & POHTO, P. (1992). Levosimendan increases calcium sensitivity without enhancing myosin ATP-ase activity and impairing relaxation. *J. Mol. Cell. Cardiol.*, **24**, (Suppl. V), S97. (abstract).

HAIKALA, H., LEVIJOKI, J., LEINO, T., LINDÉN, I.-B. & POHTO, P. (1993). Levosimendan, a novel calcium sensitizer, shifts favourably the velocity-time curve of twitch tension. *J. Mol. Cell. Cardiol.*, **25**, (Suppl. 1), S14. (abstract).

LUES, I., BEIER, N., JONAS, R., KLOCKOW, M. & HAEUSLER, G. (1993). The two mechanisms of action of racemic cardiotonic EMD 53998, calcium sensitization and phosphodiesterase inhibition, reside in different enantiomers. *J. Cardiovasc. Pharmacol.*, **21**, 883–892.

MARBAN, E., KITAKAZE, M., KORETSUNE, Y., YUE, D.T., CHACKO, V.P. & PIKE, M.M. (1990). Quantification of $[Ca^{2+}]_i$ in perfused hearts. Critical evaluation of the 5F-BAPTA and nuclear magnetic resonance method as to the study of ischemia and reperfusion. *Circ. Res.*, **66**, 1255–1267.

MOE, G.W., ANGUS, C., HOWARD, R.J., PARKER, T.G. & ARMSTRONG, P.W. (1992). Evaluation of indices of left ventricular contractility and relaxation in envolving canine experimental heart failure. *Cardiovasc. Res.*, **26**, 362–366.

NÉMETH, M. & PAPP, J.G.Y. (1993). Effects of levosimendan on the cardiac electrophysiological disorders induced by combined hyperkalaemia, hypoxia and acidosis. *J. Mol. Cell. Cardiol.*, **25**, (Suppl. I), S74. (abstract).

NUTTAL, A., SMITH, H.J. & LOVEDAY, B.E. (1985). A clinically relevant model of heart failure: effects of ticlopidine. *Cardiovasc. Res.*, **19**, 187–192.

PAUW, M., BAO, S.M. & HEIDRICKX, G.R. (1993). Decreased left ventricular contractile response to catecholamines in the early phase of heart failure induced by rapid pacing in chronically instrumented dogs. *J. Mol. Cell. Cardiol.*, **25**, (Suppl. I), S10 (abstract).

RAASMAJA, A., TALO, A., NISSINEN, E., LINDÉN, I.-B. & POHTO, P. (1991). Biochemical mechanisms of the novel cardiotonic agent OR-1259. *J. Mol. Cell. Cardiol.*, **23**, (Suppl. V), S130. (abstract).

RÜEGG, J.C., PFITZER, G., ELUBER, D. & ZEUGNER, C. (1984). Effect on contractility of skinned fibres from mammalian heart and smooth muscle by a new benzimidazole derivative, 4,5,-dihydro-6-[2-(4-methoxyphenyl)-1H-benzimidazole-5-yl]-5-methyl-3(2H)-piridazinonem. *Arzneim. Forsch./Drug Res.*, **34**, 1736–1738.

UDVARY, É., PAPP, J.G.Y., MESTER, L. & VÉGH, Á. (1993). Comparative study of levosimendan and EMD 53998 on cardiovascular function in conscious dogs. *J. Mol. Cell. Cardiol.*, **25**, (Suppl. I), S18. (abstract).

VÉGH, Á., SZEKERES, L. & UDVARY, É. (1987). Effects of the blood supply to the normal non-infarcted myocardium on the incidence and severity of early post-occlusion arrhythmias in dogs. *Basic Res. Cardiol.*, **82**, 159–171.

VÉGH, Á., UDVARY, É. & PAPP, J.G.Y. (1992). Effects of simendan in a model of acute heart failure produced by severe regional myocardial ischaemia in dogs. *J. Mol. Cell. Cardiol.*, **24**, (Suppl. V), S45. (abstract).

WILSON, J.R., DOUGLAS, P., HICKEY, W.F., LANOCE, V., FERRARO, N., MUHAMMAD, A. & REICHEK, N. (1987). Experimental congestive heart failure produced by rapid ventricular pacing in the dog: cardiac effects. *Circulation*, **75**, 857–867.

WOLK, M.J., KEEFE, J.F., BING, O.H.L., FINKELSTEIN, L.J. & LEVINE, H. (1971). Estimation of Vmax in auxotonic systoles from the rate of relative increase of isovolumic pressure: (dP/dt)kP. *J. Clin. Invest.*, **50**, 1276–1285.

(Received April 5, 1994
Revised September 26, 1994
Accepted October 20, 1994)

British Journal of Pharmacology (1995) 114, 662-672

Activation by intracellular GDP, metabolic inhibition and pinacidil of a glibenclamide-sensitive K-channel in smooth muscle cells of rat mesenteric artery

H. Zhang & [1]T.B. Bolton

Department of Pharmacology and Clinical Pharmacology, St George's Hospital Medical School, London SW17 0RE

1 Single-channel recordings were made from cell-attached and isolated patches, and whole-cell currents zwere recorded under voltage clamp from single smooth muscle cells obtained by enzymic digestion of a small branch of the rat mesenteric artery.

2 In single voltage-clamped cells 1 mM uridine diphosphate (UDP) or guanidine diphosphate (GDP) added to the pipette solution, or pinacidil (100 μM) a K-channel opener (KCO) applied in the bathing solution, evoked an outward current of up to 100pA which was blocked by glibenclamide (10 μM). In single cells from which recordings were made by the 'perforated patch' (nystatin pipette) technique, metabolic inhibition by 1 mM NaCN and 10 mM 2-deoxy-glucose also evoked a similar glibenclamide-sensitive current.

3 Single K-channel activity was observed in cell-attached patches only infrequently unless the metabolism of the cell was inhibited, whereupon channel activity blocked by glibenclamide was seen; pinacidil applied to the cell evoked similar glibenclamide-sensitive channel activity. If the patch was pulled off the cell to form an isolated inside-out patch, similar glibenclamide-sensitive single-channel currents were observed in the presence of UDP and/or pinacidil to those seen in cell-attached mode; channel conductance was 20 pS (60:130 K-gradient) and openings showed no voltage-dependence and noisy inward currents, typical of the nucleoside diphosphate (NDP) activated K-channel (K_{NDP}) seen previously in rabbit portal vein.

4 Formation of an isolated inside-out patch into an ATP-free solution did not increase the probability of channel opening which declined with time even when some single-channel activity had occurred in the cell-attached mode before detachment. However, application of 1 mM UDP or GDP, but not ATP, to inside-out patches evoked single-channel activity. Application of ATP-free solution to isolated patches, previously exposed to ATP and in which channel activity had been seen, did not evoke channel activity.

5 It is concluded that small conductance K-channels (K_{NDP}) open in smooth muscle cells from this small artery in response to UDP or GDP acting from the inside, or pinacidil acting from the outside; the same channels open during inhibition of metabolism presumably mainly due to the rise in nucleoside diphosphates, but a fall in the ATP concentration on the inside of the channel did not by itself evoke channel activity. Failure to respond to a fall in ATP concentration upon formation of an inside-out patch could not be due to dephosphorylation of the channel because sometimes it had been active previously during cell-attached recording. NDPs, instead of ATP, are more important regulators of K_{NDP} channels. It is suggested that the K_{NDP} is the main target K-channel for KCOs.

Keywords: Metabolic inhibition; cyanide; 2-deoxyglucose; pinacidil; GDP; uridine diphosphate; K_{NDP}

Introduction

K_{ATP} channels, by definition, are channels inhibited by intracellular ATP ($[ATP]_i$). If $[ATP]_i$ is the primary regulator of the channels, they should open when inside-out patches are made into ATP-free solution from a high-$[ATP]_i$ or normal-$[ATP]_i$ circumstances. This is true in the cases of both cardiac and pancreatic β-cells (Cook & Hales, 1984; Trube & Hescheler, 1984; Shen *et al.*, 1991). Standen *et al.* (1989) observed remarkable channel activity in inside-out patches in the absence of ATP in mesenteric artery smooth muscle cells which was clearly inhibited by ATP and reactivated by cromakalim. However, channel activity has not been observed by many groups when isolated inside-out patches were formed from smooth muscle cells into ATP-free solution (Kajioka *et al.*, 1991; Nakao & Bolton, 1991; Robertson *et al.*, 1992; Beech *et al.*, 1993a; Bonev & Nelson, 1993), unless GDP is present (Kajioka *et al.*, 1991; Beech *et al.*, 1993a,b). Furthermore, the channel conductance reported by Standen *et al.* (1989) is much higher than that in other tissues (Noma, 1983; Trube & Hescheler, 1984; Rorsman & Trube, 1985) and that in smooth muscle reported by Kajioka *et al.* (1991). While the channel conductance is quite similar in cardiac and pancreatic β-cells, the channel conductance of K_{ATP} channel in smooth muscle cells has been variously described as 258 pS (Lorenz *et al.*, 1992), 100-135 pS (Standen *et al.*, 1989; Kovacs & Nelson, 1991), 30 pS (Inoue *et al.*, 1989; Miyoshi & Nakaya, 1993), 24 pS (Beech *et al.*, 1993a), 15 pS (Kajioka *et al.*, 1991), 10 pS (Kajioka *et al.*, 1990) and 7 pS (Bonev & Nelson, 1993). Only a few of these differences can be explained by the different K-gradients used. As a consequence it is still unclear whether smooth muscle has a different type of K_{ATP} channel from other tissues and whether other factors rather than $[ATP]_i$ are more important in determining channel opening.

Many experiments have shown that relaxations of smooth muscle caused by potassium channel opener (KCO) drugs are blocked by glibenclamide (e.g. Winquist *et al.*, 1989; Standen *et al.*, 1989) which has been interpreted as indicating that the K_{ATP} channel is the target channel. In single cell and single channel experiments, glibenclamide, in micromolar concentrations blocked the whole cell currents induced by various KCOs including levcromakalim, pinacidil, nicorandil, diazoxide, minoxidil sulphate, RP 49356 (Noack *et al.*, 1992a;

[1] Author for correspondence.

Silberberg & van Breemen, 1992; Beech *et al.*, 1993b; Zhang & Bolton, unpublished) and the increase in probability of opening of K-channels produced by KCOs (Standen *et al.*, 1989; Kajioka *et al.*, 1991; Beech *et al.*, 1993b). However, the Ca-activated large conductance K-channel (BK_{Ca} channel) (Gelband & McCullough, 1993) and delayed rectifier K-channel (Edwards *et al.*, 1993) have been suggested as target channels for KCOs and the effect of KCOs on these are also inhibited by glibenclamide.

In our previous paper, we showed that GDP and other nucleoside diphosphates (NDPs) activated a K-channel with small (24 pS) conductance in rabbit portal vein cells (Beech *et al.*, 1993a). The action of NDPs on the channel was sensitive to the blocking action of glibenclamide and channel open probability was increased by the KCO, levcromakalim (Beech *et al.*, 1993b). We designated this channel K_{NDP} because nucleoside diphosphates needed to be present for the channel to open and $[ATP]_i$ could inhibit channel activity only when increased by NDPs; thus NDPs, and not ATP, seemed to be the primary regulator of channel activity because channel activity did not appear when isolated patches were formed into ATP-free solution if NDP was not present. In this paper, we use single smooth muscle cells isolated from rat mesenteric artery to test whether the channel activated by NDPs is also present in resistance arteries and whether there is a relation to the K_{ATP} channel which has been described in this tissue (Standen *et al.*, 1989). We also try to clarify whether KCO and metabolic inhibition can open the same channel as that opened by NDPs.

Methods

Single cell dispersion

Single smooth muscle cells were isolated from small branches of rat mesenteric artery. Adult, male Wistar rats (200~300 g) were killed by cervical dislocation. The second and third order branches of the artery were cut open along their longitudinal axis after careful dissection and incubated in a low-Ca (10 μM) and Mg-free physiological salt solution (PSS) at 37°C for 20 min. Tissue was then moved to the same solution which contained 0.4 mg ml^{-1} collagenase (type XI, Sigma), 0.4 mg ml^{-1} pronase (type E, Sigma) and 1 mg ml^{-1} bovine albumin (Sigma) at 37°C for 30 min. The tissue was washed with enzyme-free solution and triturated by sucking in and out of a wide bore, smooth-tipped pipette. The cells were used for experiments within 6 h of separation during which time they were stored at 4°C in low-Ca (10 μM) solution. All experiments were performed at room temperature (22°C). The solutions used for the whole procedure of the dispersion were oxygenated (100% O_2) vigorously and continuously and ice-cold solution was used for the tissue dissection to reduce as far as possible the reduction of ATP levels in the cells.

Electrophysiology

Conventional whole-cell, cell attached and isolated patch recording (Hamill *et al.*, 1981) and 'perforated patch' recording (Horn & Marty, 1988) were used in the experiments. The patch amplifier was a RK300 (Biologic). Patch pipettes were made from borosilicate glass (Plowden & Thompson); they had resistance of 2–5 MΩ after fire-polishing, and were coated with Sylgard (Dow Corning) for single channel recordings. Data were stored of FM-tape (Racal) (3.75 in s^{-1}, low-band pass 1250 Hz) and captured later to a 386 PC for data analysis after digitization using CED interface and software, or replayed using a Gould pen recorder (Gould Electronic Ltd.) for illustrations. All whole-cell current records were filtered at 500 Hz (4-pole Bessel filter, Barr and Stroud) and single channel records filtered as described in the legends of Figures 2 to 7. The input resistance was monitored in whole-cell experiments by square or ramp hyperpolarizing commands. The series resistance was estimated by the rate of decay of the capacity current after an instantaneous step in the command voltage and was estimated to be < 10 MΩ in conventional whole-cell and < 20 MΩ in 'perforated patch' experiments. Results are given as means ± standard error of the mean (s.e.mean).

Data analysis

Unitary current amplitude was determined by fitting amplitude histograms with Gaussian distributions. The channel open-state probability (P_o) was calculated using the following equation

$$P_o = \Sigma_{i=1}^{N} t_i \, i / (TN)$$

where the t_i is the time spent with $i = 1.2,3.....$, N channels open, N is the number of the channels, i is unitary current and T is the sample length. The calculation assumes the maximum number of unitary current levels observed in a patch to be equal to the number of active channels, N, in the patch. All data were expressed as means ± s.e.mean.

Solutions

Low-Ca and Mg-free solution (mM): NaCl 130, KCl 5, $CaCl_2$ 0.01, HEPES 10, glucose 10, pH 7.4 with NaOH. Solutions for whole-cell recording mode: physiological salt solution (PSS) in bath (mM): NaCl 130, KCl 5, $CaCl_2$ 1.7, $MgCl_2$ 1.2, HEPES 10, glucose 10, pH 7.4 with NaOH. Pipette (mM): KCl 130, $MgCl_2$ 2, EGTA 5, HEPES 20, pH 7.4 with KOH. Nystatin (Sigma) 100 μg ml^{-1} was added to the solution to make a 'perforated patch'. Solutions for single channel recording mode: Bath (mM): NaCl 9, KCl 117, $MgCl_2$ 3, HEPES 18, EGTA 5, pH 7.4 with KOH. Pipette (mM): NaCl 80, KCl 60, $CaCl_2$ 1.7, $MgCl_2$ 1.3, HEPES 10, glucose 10, pH 7.4 with NaOH. Glucose was replaced by 10 mM 2-deoxy-glucose (2DG) and sodium cyanide (CN) (1 mM) was added to the solution when metabolic inhibition was used. UDP, GDP and ATP were added as Na-salts and 100 mM stock solutions of these were prepared and frozen at −20°C. Dilution was made immediately prior to the application. Nystatin was prepared as a 5 mg ml^{-1} stock in methanol and diluted to the final concentration. Glibenclamide was prepared as a 10 mM stock solution in dimethylsulphoxide (DMSO). The final concentration of DMSO was 0.1% for 10 μM glibenclamide.

Drugs

GDP (guanosine diphosphate), UDP (uridine diphosphate), ATP (adenosine triphosphate), EGTA (ethylglycol-*bis*-(β-aminoethyl)-*N,N,N',N'*-tetraacetic acid), HEPES (N-2-hydroxyethylpiperazine-N'-2-ethanesulphonic acid) and glibenclamide were from Sigma. Pinacidil monohydrate was from Leo Pharmaceutical Company (Denmark). Levcromakalim was a gift from Dr T. Hamilton (SKB). Nicorandil was from Chugai Pharmaceutical Company (Japan).

Results

Pinacidil, metabolic inhibition and intracellular GDP all induce a glibenclamide-sensitive K-current in whole-cell recordings

Figure 1 shows three recordings in single cells isolated from rat mesenteric artery. Cells a and d are conventional whole-cell recordings, and cell c is a 'perforated-patch' whole cell recording (see Methods). All the cells were held at −37 mV. In cell a, a small transient outward current (about 8 pA in peak) developed about 4 min after breaking through the cell membrane. Similar currents were seen from another two cells

out of 8 cells observed. The mean amplitude of the currents from these three cells was 6 ± 2 pA (means ± s.e.mean). When pinacidil (100 μM) was applied via bath, a large outward current with a peak amplitude of about 97 pA developed which decayed slowly after reaching a peak (Figure 1a). Glibenclamide (10 μM) totally blocked the current induced by pinacidil. In another three cells, pinacidil (100 μM) induced outward currents of average amplitude of 46 ± 12 pA which were all blocked by glibenclamide (10 μM). Ramp voltage changes were applied to the cell to determine the reversal potential of the current induced by pinacidil. The currents, induced by ramp voltages from −117 mV to 20 mV before (i) and during (ii) application of pinacidil, intersected at −80 mV (Figure 1b), close to the calculated E_K (E_K was −88 mV), suggesting that most of the current induced by pinacidil was potassium current.

In Figure 1c, 100 μg ml^{-1} nystatin was included in the pipette to make a 'perforated patch'. After about 6 min when series resistance had fallen to less than 15 MΩ, metabolic poison solution (CN + 2DG) was applied. An outward current developed slowly with peak amplitude of 20 pA at a holding potential of −37 mV. The current did not decay before pinacidil (100 μM) was bath-applied. Pinacidil induced an additional outward current of 40 pA (peak). Both currents

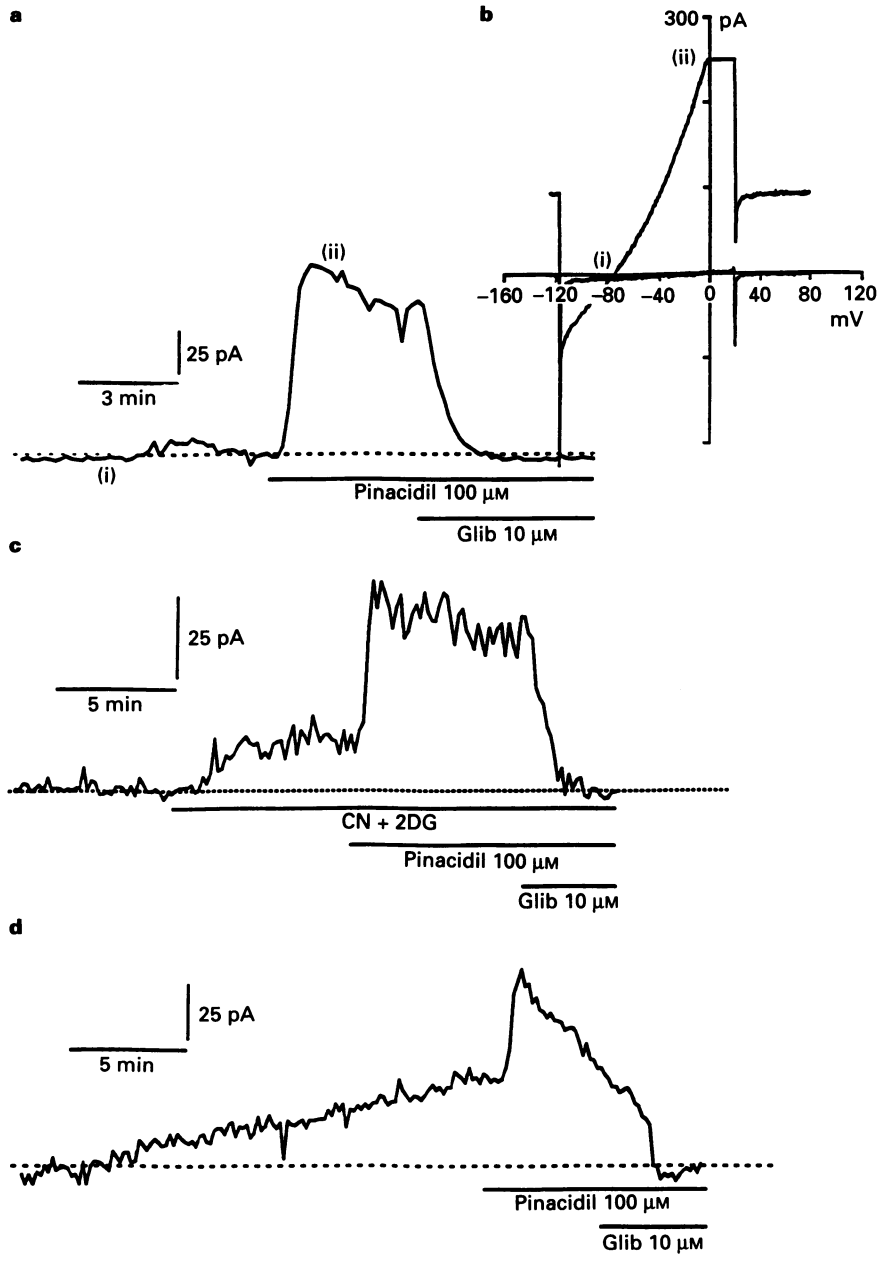

Figure 1 Pinacidil, metabolic inhibition and GDP_i activate a glibenclamide-sensitive K-current in single smooth muscle cells isolated from the rat mesenteric artery. The current traces were constructed from whole-cell currents sampled every 10 s at a holding potential of −37 mV. Pinacidil and glibenclamide were applied via bath solution as indicated. (a) Conventional whole-cell recording mode with KCl 130 mM, EGTA 5 mM, $MgCl_2$ 2 mM and HEPES 20 mM in the pipette solution; bath solution was 1.7 mM Ca PSS solution. The recording was started about 1 min after break-through to the whole cell recording mode. (b) Ramp change in voltage from −117 mV to +20 mV lasting 200 ms was applied during the recording shown at (a). (i) and (ii) indicate the responses to the ramp voltages before and at the peak of the response to pinacidil. (c) Perforated patch whole-cell recording mode. Nystatin (100 μg ml^{-1}) was included in the pipette solution which otherwise was same as in (a). The recording was started about 1 min after gaining electrical access to the interior of the cell which was indicated by a series resistance of less than 15 MΩ. The PSS in the bath was replaced by PSS containing cyanide (1 mM) and 2-deoxy-glucose (10 mM) as indicated. (d) Conventional whole-cell recording mode with 1 mM GDP included in the pipette solution. The recording was started about 30 s after break-though to the whole-cell recording mode.

were blocked by glibenclamide (10 μM). Similar results were seen in another three cells. However, we did not see currents developing in four cells during conventional whole-cell recordings either before or after metabolic inhibition, but pinacidil induced an average outward current in these cells of 36 ± 11 pA ($n = 4$).

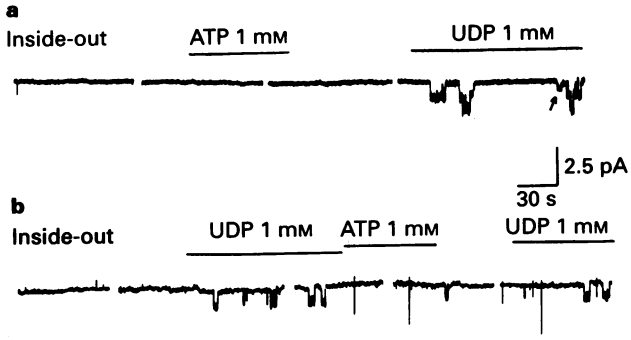

Figure 2 UDP activates a K-channel in isolated inside-out patches. Recordings of two cells isolated from rat mesenteric artery. The cells were held at −60 mV. KCl 117 mM, $MgCl_2$ 3 mM, EGTA 5 mM (Ca-free) were in the bath solution and the pipette solution contained KCl 60 mM, $CaCl_2$ 1.7 mM. In cell a, UDP (1 mM), applied via bath after ATP (1 mM) was washed out, activated the channel with an unitary current amplitude of about 0.85 pA at +60 mV. Notice that a smaller unitary current (↑) was also present. In cell b, UDP (1 mM) also activated the channel. After washing out UDP, channel activity ceased in the presence of ATP. Only one brief channel opening was seen after washing out ATP during a period of 5 min. UDP reactivated the channel again. The current traces were recorded continuously on FM-tape (3.75 in s^{-1}) with a 0.5 kHz low-pass filter (−3dB, 4-pole Bessel) and filtered for presentation at 100 Hz. The breaks in the records represented 3–4 min interruptions.

When 1 mM GDP was included in the pipette solution, an outward current slowly developed (Figure 1d) after breaking through the cell membrane into the whole-cell mode and this reached a maximum, on average, of 35 ± 7 pA ($n = 4$), after 10 to 15 min. Once the response to GDP had reached a maximum, pinacidil (100 μM), levcromakalim (10 μM) or nicorandil (100 μM) was bath-applied. These three KCOs induced an additional current of 40 (Figure 1c), 35 and 20 pA, respectively. Gilbenclamide (10 μM) blocked the currents induced by GDP and KCO. Ramp voltage was also applied to cell c and cell d; reversal potentials of −82 and −84 mV respectively, were obtained.

GDP and UDP activate a small conductance K-channel in inside-out patches

When inside-out patches were formed into zero-Ca EGTA solution in the absence of a nucleotide at the inner surface of the patch, no distinct channel activity was seen in most of the patches (35) held at −60 mV (Figure 2). However, some atypical channel activity did appear in two patches from two cells just once over a period of 2 to 5 min (an example is shown in Figure 3b; the unitary current is larger than that carried by K_{NDP} channels). When GDP (Figure 3) or UDP (Figure 2) (1 mM) were applied in the bathing solution to the inner surface of the patches, a channel was activated that showed long bursts of openings (mean open time 3.8 s in the case of Figure 3) separated by even longer closed periods (mean closed time 5.8 s in the case of Figure 3). There was a pronounced fluctuation in the channel open-state when the current direction was inward (Figure 3; see later; cf. Figure 7). When the patches were held at −60 mV, the unitary amplitude of the channel activated by UDP and GDP was

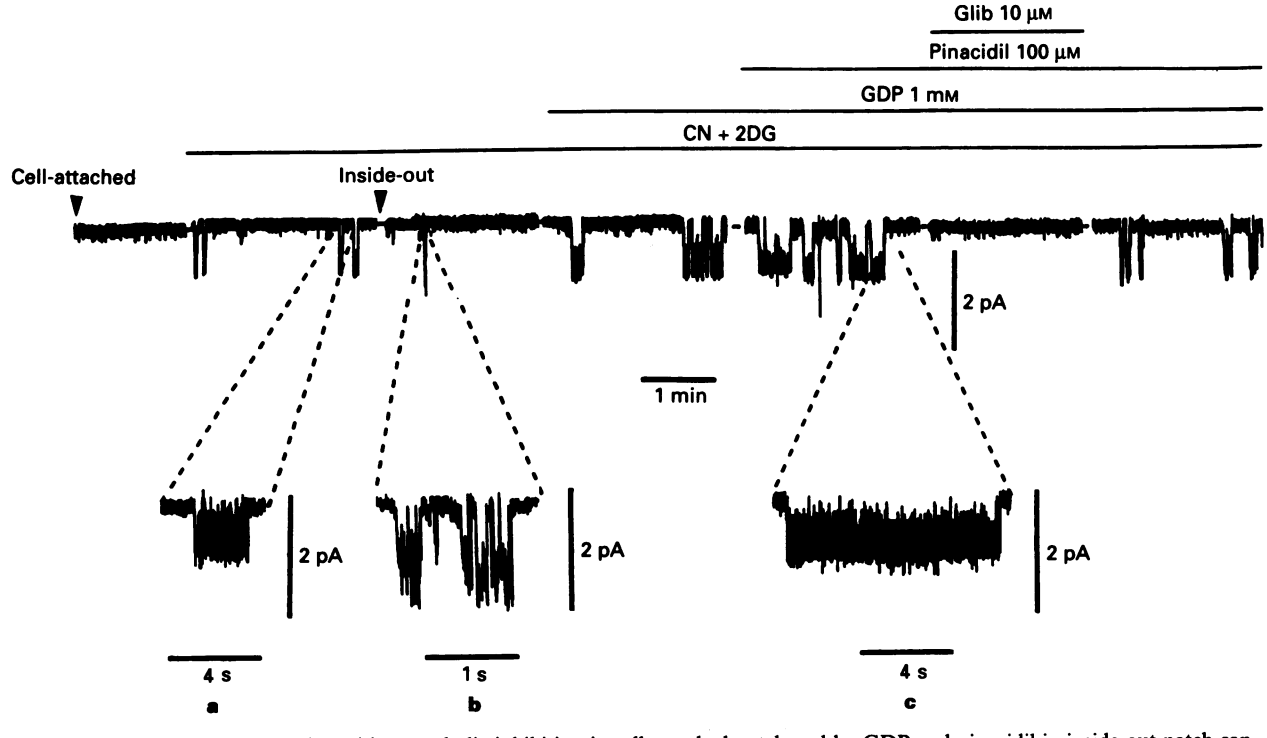

Figure 3 The K channel activated by metabolic inhibition in cell-attached patch and by GDP and pinacidil in inside-out patch can be blocked by glibenclamide. A patch from rat mesenteric artery was held at −60 mV. The same pipette solution (60 mM K) and bath solution (117mM K) were used as in Figure 2. Initially the patch was cell-attached and metabolic blocking agents, cyanide (CN, 1 mM) and 2-deoxy-glucose (2DG 10 mM), were applied via the bath; then an inside-out patch was formed in the ATP- and GDP-free, CN + 2DG solution. GDP (1 mM), pinacidil (100 μM) and glibenclamide (10 μM) were applied to the inside-out patch via bath as indicated. Glibenclamide totally abolished the channel activity induced by GDP and pinacidil and the effect of glibenclamide could be washed out. Notice that some atypical channel activity (unusually larger unitary current) can be seen just after forming an inside-out patch. The current traces were recorded continuously on FM-tape (3.75 in s^{-1}) with a 0.5 kHz low-pass filter (−3dB, 4-pole Bessel) and filtered for presentation at 100 Hz. The expanded sections of traces of cell-attached and inside-out patches showed that (a) and (c), but not (b), have the same unitary size and characteristics. The broken lines represented about 2–3 min interruption in each case.

0.85 ± 0.008 pA ($n = 9$). The conductance of the channel was 20 pS and the current reversed near E_K (−19.5 mV), suggesting K ions were the charge carrier (see later; cf. Figure 7). Pinacidil (100 μM) increased the channel activity and glibenclamide (10 μM) totally blocked it (Figure 3). All of these characteristics of channel activity are similar to those of the channel activated by GDP in rabbit portal vein smooth muscle cells described in our previous papers (Beech *et al.*, 1993a,b).

A low concentration of ATP, in the presence of Mg, is necessary to retain the ability of the K_{ATP} channel to open in both cardiac and pancreatic β-cells (Findlay & Dunne, 1986; Misler *et al.*, 1986; Findlay, 1987; Ohno-Shosaku *et al.*, 1987). So ATP (1 mM) in the presence of 3 mM $MgCl_2$ was applied to the inner surface of the patches in this experiment. In Figure 2a, no channel activity was observed before and after application of 1 mM ATP. However, when UDP (1 mM) was bath-applied after wash-out of ATP, the channel was activated. UDP (1 mM) activated the channel in another inside-out patch (Figure 2b); after washing out UDP and applying 1 mM ATP, channel activity ceased. When ATP was washed out, a brief channel opening was seen during a period of 5 min. UDP (1 mM) was applied again in this cell and the channel was re-activated by UDP (Figure 2b). Experiments using the same protocol as that used in Figure 2b were performed in two other cells and no channel activity was observed after washing out ATP but UDP always activated the channel.

Single-channel currents activated by pinacidil or metabolic inhibition in cell-attached and inside-out patches

The cell membrane was quiescent most of the time in cell-attached patches from rat mesenteric artery held at −60 mV. Occasionally, a channel with the same characteristics as the

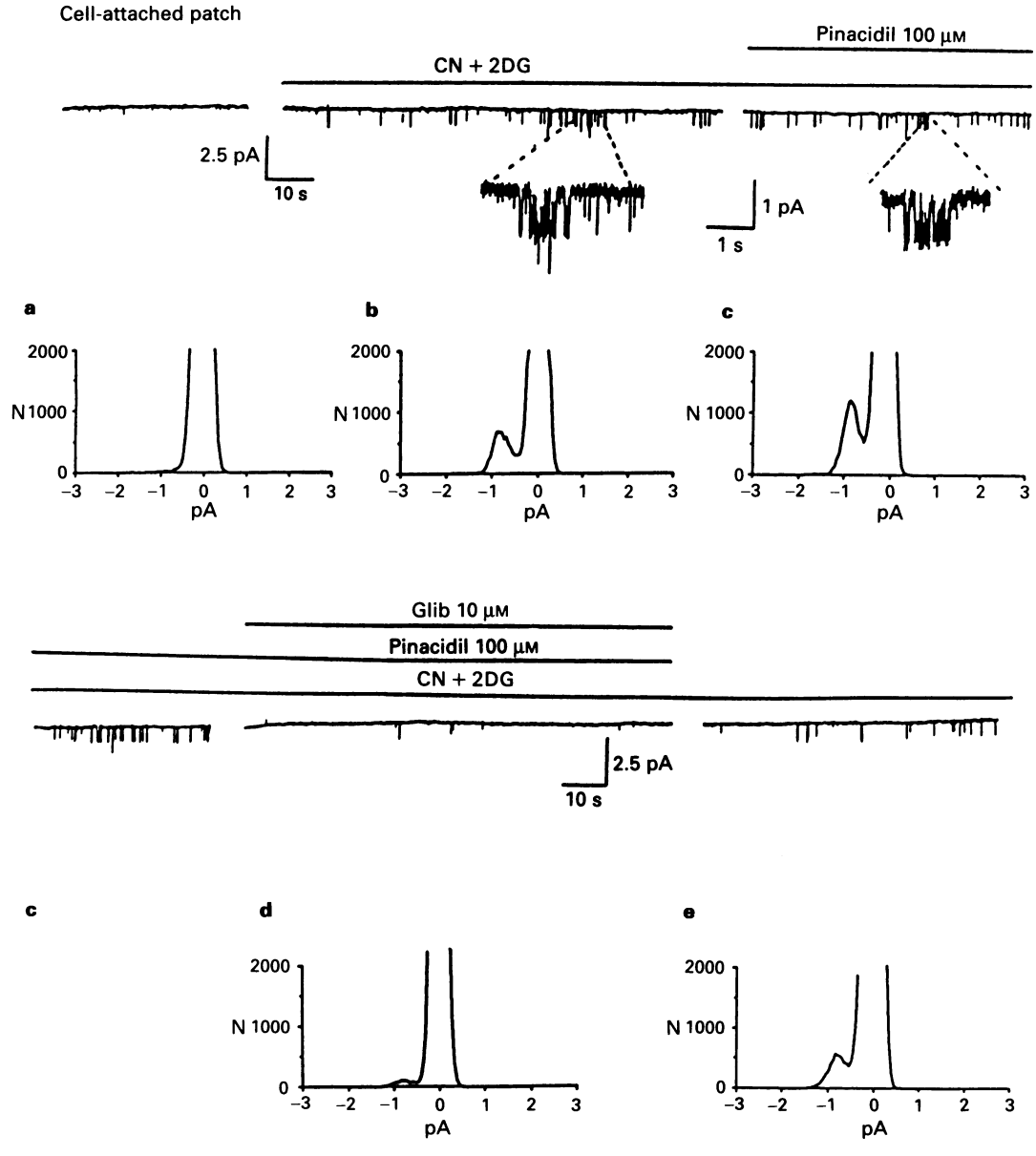

Figure 4 Metabolic block and pinacidil both activate a glibenclamide-sensitive K channel in cell-attached patch from a smooth muscle cell isolated from rat mesenteric artery. The cell was held at −60 mV. KCl 117 mM, $MgCl_2$ 3 mM and EGTA 5 mM (Ca-free) were in the bath solution and the pipette solution contained KCl 60 mM and $CaCl_2$ 1.7 mM. Cyanide (CN, 1 mM), 2-deoxy-glucose (2-DG, 10 mM), pinacidil (100 μM) and glibenclamide (Glib, 10 μM) were applied via the bath. (a–e) Recording of the current in a cell-attached patch. The control trace (a) was just before the application of CN + 2DG; later traces (b,c,d,e) were 2 to 3 min after the applications of CN + 2DG, pinacidil, or glibenclamide respectively; then pinacidil and glibenclamide were washed out. All-points histograms were constructed from a period of 4 min in each case with a sample frequency of 2 kHz and after filtering at 0.5 kHz. Notice the peak at about 0.8 pA representing activity of a single open channel.

channel activated by UDP and GDP in inside-out patches was seen in cell-attached patches but generally the patch was quiescent under control conditions (Figure 4a). However, when metabolic poisons (CN + 2DG) were applied to the cell, a channel was activated with an average unitary amplitude of 0.84 ± 0.02 pA ($n = 7$) at −60 mV. This channel also had open-state noise in an inward direction (Figure 4b; see later, cf. Figure 7), and was apparently similar to the type of channel activated by UDP and GDP in inside-out patches. Pinacidil (100 μM) added alone increased the channel activity and the open probability of the channel was increased from 0.014 to 0.025 (channel activity in control was 0.00093) (Figure 4c). However, application of glibenclamide (10 μM) completely abolished the channel activity induced by both CN + 2DG and pinacidil (histogram in Figure 4d was constructed just after the application of glibenclamide; channel activity was abolished 30 s after the application of glibenclamide). The effect of glibenclamide could be partly washed out (Figure 4e). The channel open probabilities were 0.0012 and 0.0063 in the presence and absence of glibenclamide, respectively. Figure 5 shows data from the same cell as Figure 4. The arrow in Figure 5 shows when an isolated inside-out patch was created after glibenclamide had been washed out. The channel activity declined after the inside-out patch was formed (5 min); one longer lasting opening (Figure 5b) was observed, presumably because the inhibition of the channel by ATP in the cell-attached mode was abolished in the inside-out patch (Kajioka *et al.*, 1991). After channel activity ceased, UDP (1 mM) and UDP (1 mM) plus pinacidil (100 μM) re-activated the channel with much greater channel activity and occasionally 3 channels were open simultaneously (Figure 5c). The sections of current record on a faster time base show that the characteristics of the channels open in the absence (Figure 5b) and presence (Figure 5c) of UDP and pinacidil, and in the cell-attached patch (Figure 4b,c and Figure 5a) were quite similar. The open probability of the channel in the presence of UDP + pinacidil was 0.16 and mean open time (one active channel in patch) was 1.8 s, compared with a mean open time of 164 ms in a cell-attached patch in the presence of pinacidil. In another 4 cells, the channel activity activated by CN + 2DG always ceased within 40 s after an inside-out patch was formed; UDP or GDP (1 mM) always re-activated the channel.

Although channel activity was not normally seen in cell-attached patches, in one particular cell pronounced channel activity was found even without CN + 2DG or KCO. In this cell, the channel which had an amplitude of 0.83 pA at −60 mV, opened frequently, and two channels could be seen to be open simultaneously. The channel activity decreased and ceased after about 1 min when inside-out patch was formed. This channel, with characteristic unitary current size, long open time and noisy open-state, was apparently the same type of channel as that activated by NDPs.

In another series of experiments, only pinacidil (10 μM) was applied to cell-attached patches and in three cells, pinacidil alone activated the channel with an average amplitude of 0.80 ± 0.02 pA at −60 mV. Figure 6a(i)(ii), b(i)(ii), shows a typical example of results from these cells. When an inside-out patch was formed in the presence of pinacidil (alone, no nucleoside diphosphate), channel open probability was increased from 0.093 to 0.28 and two channels were seen to be open simultaneously (Figure 6a(iii), b(iii)). These channels also showed similar characteristics to those of the channel activated by CN + 2DG or NDPs. In another cell, pinacidil did not activate channels in a cell-attached patch. However, a channel with similar characteristics to those described above was activated by pinacidil alone after an inside-out patch was formed. So, it seems that pinacidil can open the K_{ATP} channel in the absence of any nucleotide in rat mesenteric artery, which is different from cardiac cells (Shen *et al.*, 1991) and pancreatic β-cells (Dunne, 1990; Dunne *et al.*, 1990a,b) in which the effect of KCO needs the presence of ATP or NDP. However, in at least two cells, pinacidil (100 μM), applied after, rather than before an inside-out patch was formed, failed to activate the channel, although subsequently application of UDP proved the existence of the channel in the patches.

The BK_{Ca} channel was rarely seen because of the negative

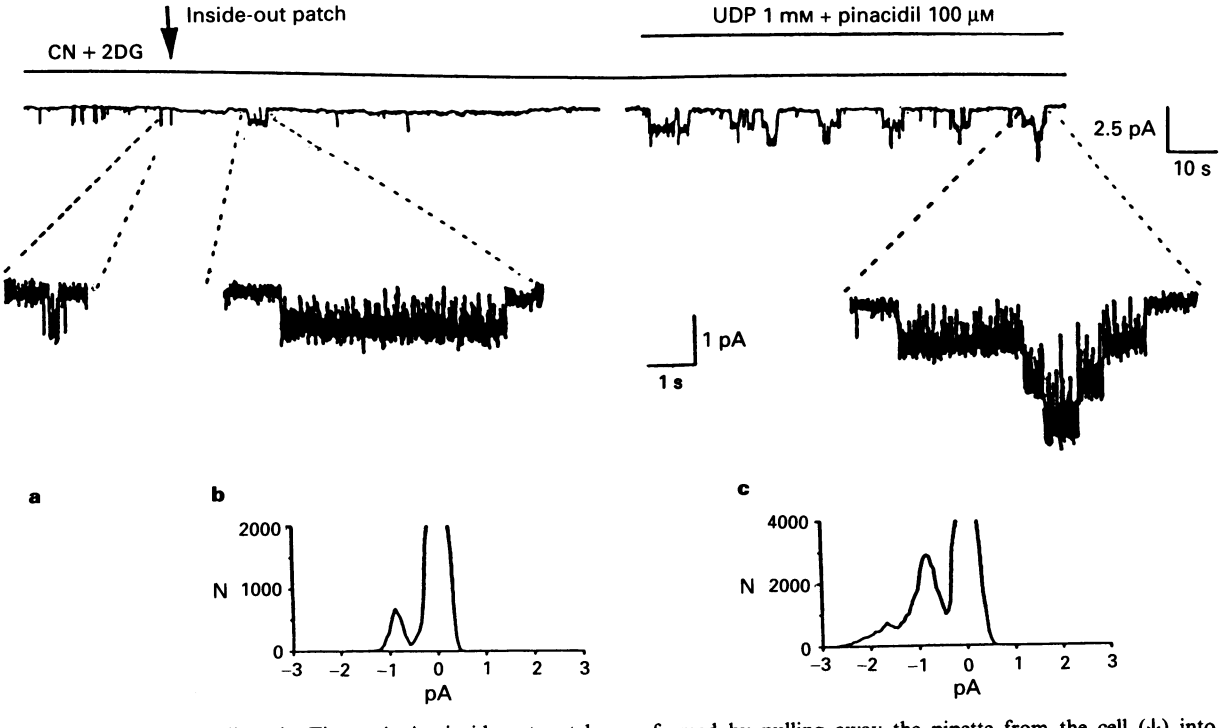

Figure 5 The same cell as in Figure 4. An inside-out patch was formed by pulling away the pipette from the cell (↓) into cyanide + 2-deoxy-glucose solution and held at −60 mV. The current with the same unitary size and the same characteristics (noisy open-state) as seen in the cell-attached mode (a) but with much longer open times was seen in the inside-out patch (b). The channel activity ceased in the trace (b) and was not seen for at least 5 min. The channel was reactivated by the application of UDP (1 mM) and pinacidil (100 μM) (c). The expanded section shows that as many as three channels were open simultaneously.

holding potential (−60 mV) and zero Ca in the bathing solution. However, when the holding potential was made positive (+60 mV), the BK_{Ca} channel was activated. Some cells were held at +60 mV but pinacidil and metabolic block had no effect on the BK_{Ca} channel. The conductance of the BK_{Ca} channel under the conditions of the present experiments (60:130 mM K-gradient) was about 150 pS in inside-out patches (see later, Figure 7).

The conductance of the channel activated by NDPs, metabolic inhibition and pinacidil

The current-voltage relationship was linear for the channel activated by pinacidil, CN + 2DG or NDPs (Figure 7c). Figure 7a is a record from a cell-attached patch in the presence of CN + 2DG and pinacidil and Figure 7b is an inside-out patch in the presence of UDP and pinacidil. A noisy open-state was observed only when the current direction was inward in both cases (Figure 7a,b). Two kinds of channels can be seen in Figure 7a, (i) BK_{Ca} channel with a conductance of 150 pS; (ii) the channel activated by CN + 2DG and pinacidil with a conductance of 20 pS. In Figure 7b, three different channels can be seen, (i) BK_{Ca} channel, (ii) 20 pS channel activated by UDP and pinacidil, (iii) 10 pS channel activated by UDP and pinacidil. The small conductance channel (10 pS) may be a sub-conductance state of the 20 pS channel, since it had similar characteristics apart from its conductance. However, current transfers from the subcon-

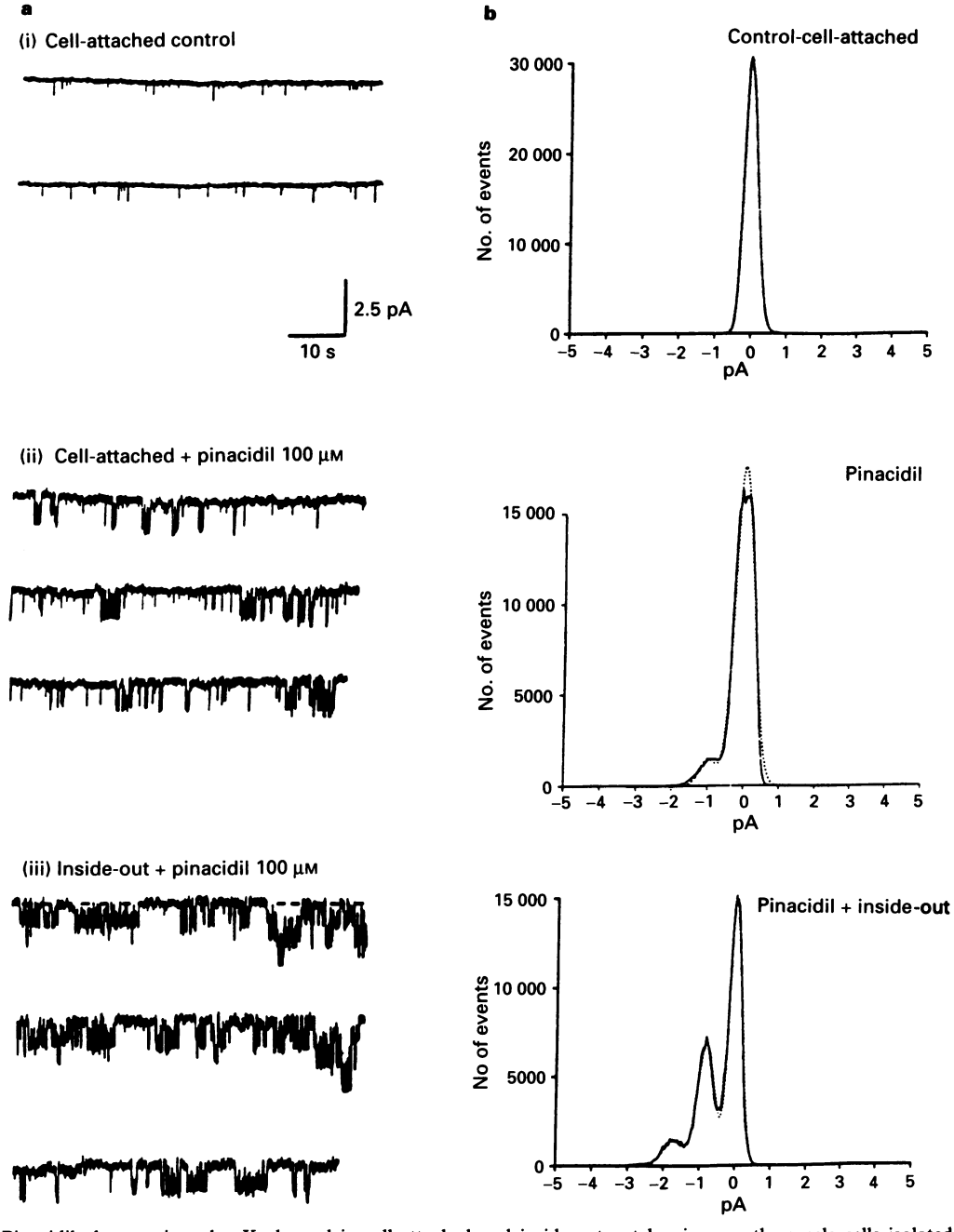

Figure 6 Pinacidil alone activated a K channel in cell-attached and inside-out patches in smooth muscle cells isolated from rat mesenteric artery. (a) Recordings, (b) all-point histograms. (i) The cell was held at −60 mV. KCl 117 mM, $MgCl_2$ 3 mM, and EGTA 5 mM (Ca-free) were in the bath solution and KCl 60 mM, and $CaCl_2$ 1.7 mM were in the pipette solution. (ii) Pinacidil (100 μM) was applied via bath in the cell-attached recording mode and (iii) an inside-out patch was formed in the presence of pinacidil. Pinacidil activated the channel with an unitary current amplitude of about 0.8 pA at −60 mV in the cell-attached mode and the channel activity was increased after an inside-out patch was formed. All points histograms were constructed from periods of 4 min in each case with a sample frequency of 2 kHz after filtering at 0.5 kHz.

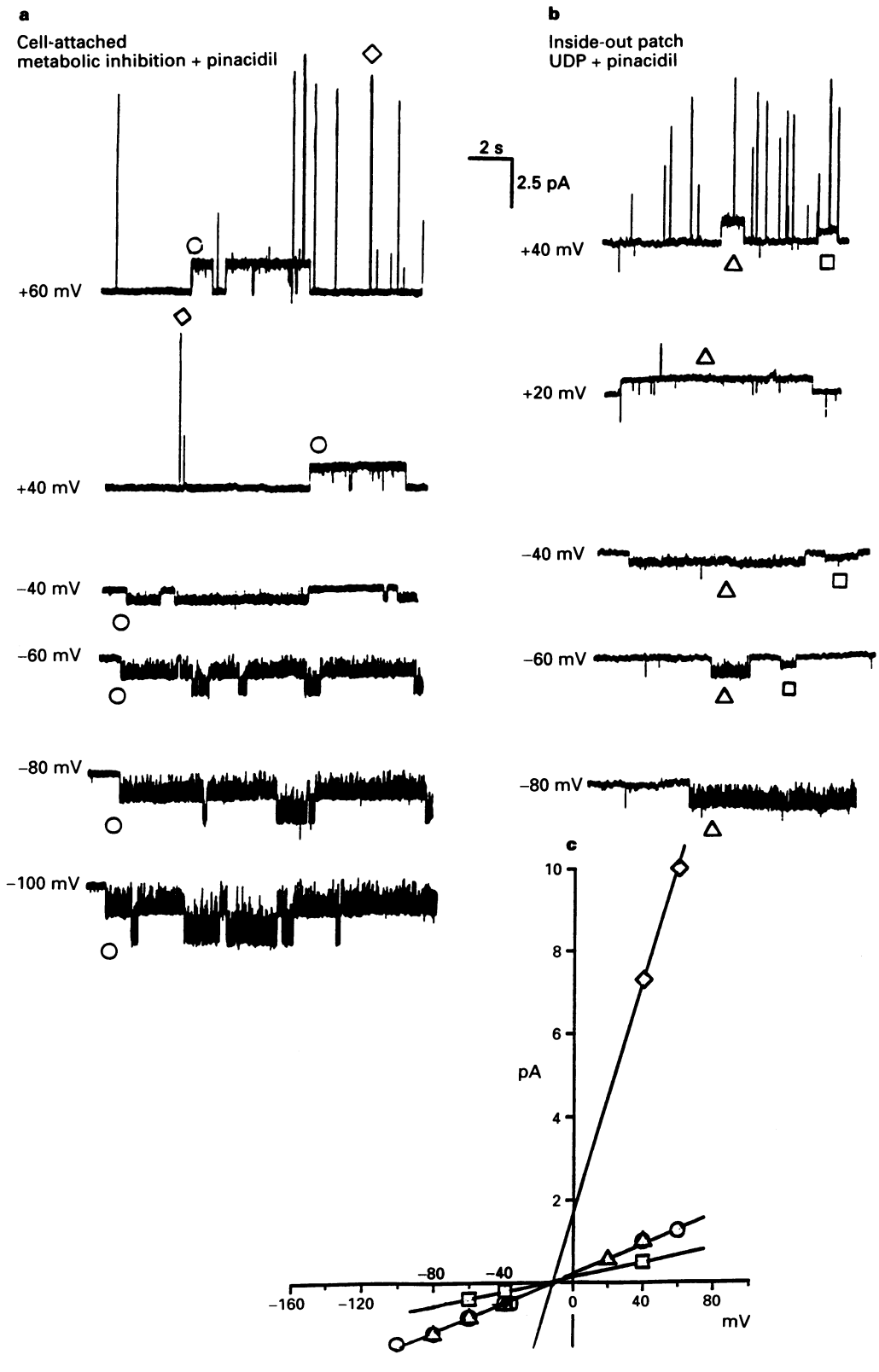

Figure 7 The conductance of the K channel activated by metabolic inhibition and pinacidil in cell-attached patches, and by UDP and pinacidil in inside-out patches was about 20 pS. Two cells from rat mesenteric artery were held at different voltages ranging from −100 mV to +60 mV. KCl 117 mM, $MgCl_2$ 3 mM and EGTA 5 mM (Ca-free) were in the bath solution and KCl 60 mM and $CaCl_2$ 1.7 mM were in the pipette. (a) Cell-attached patch from one cell in the presence of cyanide (CN) (1 mM) + 2-deoxy-glucose (2-DG) (10 mM) and pinacidil (100 μM). (b) Inside-out patch from another cell in the presence of UDP (1 mM) and pinacidil (100 μM). (c) The current-voltage relationship of the channel in both cases. Notice that the 20 pS channel was activated by CN + 2DG-pinacidil in the cell-attached patch (○) and by UDP + pinacidil in the inside-out patch (△). A smaller conductance channel (□) in inside-out patch, and the BK_{Ca} channel (◇) were also seen. The current traces were recorded continuously on FM-tape (3.75 in s^{-1}) with a 0.5 kHz low-pass filter (−3dB, 4-pole Bessel) and filtered for presentation at 300 Hz.

ductance to fully conducting state, or *vice versa* were not seen. All three current-voltage relationships reversed near E_K (−19.5 mV). The subconductance state of channels activated by pinacidil were also seen in a cell-attached patch. In Figure 2a, as well as the 20 pS channel activated by UDP in an inside-put patch, channel activity with a half-size unitary current was also present. The voltage-dependence of the 20 pS channel activated by pinacidil and UDP was checked over the voltage range from −80 mV to +40 mV. No modification was found in channel probability of opening upon changing the holding potential.

Discussion

In this paper, we have demonstrated that metabolic block, pinacidil and intracellular NDPs can induce K-currents in rat mesenteric artery cells, which are apparently from the same target channel. The channel activated by metabolic block, pinacidil and intracellular NDPs has similar characteristics to those of the channel we described in rabbit portal vein cells in our previous papers (Beech *et al.*, 1993a,b); it is a small conductance channel (probably about 15 pS in quasi-physiological K-gradient, Kajioka *et al.*, 1991). NDPs are a crucial regulator of these channels, which suggests that they should be designated K_{NDP} channels (Beech *et al.*, 1993a).

When recordings were made from the cells of rat mesenteric artery in the conventional whole-cell recording mode with ATP-free pipette solution, only a few cells developed a small transitory outward current at −37 mV (E_K was −88 mV). No further currents developed when metabolic inhibition was applied to these cells. However, when either GDP was added to the pipette solution, or metabolic block was applied during 'perforated patch' whole-cell recording, a sustained outward current developed consistently. Similar results were observed in rabbit portal vein cells where not only GDP but several other NDPs could induce the current. The simplest explanation for these observations is that the concentration of NDPs may rise, as well as that of ATP fall, during 'perforated patch' whole-cell recordings because of the metabolic block; ATP and NDPs may decline simultaneously in conventional whole-cell mode as a result of diffusion into the pipette, although at some stage of diffusion the ratio of NDPs to ATP might rise high enough for the channels to open and cause a small transient current. Hence, the effects of ATP in closing the channel are only possible once NDP has opened it. Pinacidil could induce an outward current during conventional whole-cell recording whether a transitory current had developed or not; pinacidil also induced an additional current after current had been induced by metabolic block or by intracellular GDP (Figure 1). Noack *et al.* (1992b) found a transient outward current (I_{met}) during whole-cell recording in rat portal vein cells held at −50 mV in the absence of ATP and metabolic substrates. After I_{met} had developed, no response to levcromakalin was observed. However, we always found that the responses to KCO and NDP were not exclusive (Beech *et al.*, 1993b; present results and unpublished results). The responses to NDP, metabolic inhibition and pinacidil were all blocked by glibenclamide, suggesting that the K_{NDP} channel was involved, since glibenclamide at this concentration had no significant effect on voltage-dependent K-current (Beech *et al.*, 1993b).

Although the K-channels in smooth muscle cells which can be inhibited by ATP have been observed to be active in the absence of ATP in inside-out patches in several vascular muscles, viz: in rabbit and rat mesenteric artery (Standen *et al.*, 1989), in the afferent artery of rabbit kidney (Lorenz *et al.*, 1992) and in porcine coronary artery (Wakatsuki *et al.*, 1992; Miyoshi *et al.*, 1992; 1993), we did not see such channels in inside-out patches in our previous experiments in rabbit portal vein smooth muscle cell (Beech *et al.*, 1993a,b). In the experiments on rat mesenteric artery cells in the absence of prior activation by metabolic inhibition or pinacidil in the cell-attached patch mode, when inside-out patches were created into nucleotide-free solution, no channel activity was observed unless NDPs were applied to the inner surface of the patches (Figure 2). However, when the channels were already activated by metabolic inhibition and/or pinacidil in cell-attached patches, channel activity could still be observed briefly after inside-out patches were created (Figure 5b, Figure 6c). However, these channel openings in inside-out patches were unlikely to be due to the absence of ATP since the channels had already been activated by metabolic inhibition and pinacidil in the cell-attached patch and the channel activity in Figure 5b did not increase when an inside-out patch was excised but declined with time. Other groups have also failed to identify K-channel activity, inhibitable by $[ATP]_i$, in inside-out patches in the absence of ATP and NDP in rabbit portal vein cells (Kajioka *et al.*, 1991; Kamouchi *et al.*, 1993) and in rat pulmonary artery cells (Robertson *et al.*, 1992). This is surprising because the K_{ATP} channel is supposed to be closed by ATP in normal cells, and should open in the absence of ATP; this characteristic can be used to define a K_{ATP} channel, in contradistinction to our K_{NDP} channels which do not open simply in the absence of ATP.

One explanation which has been offered for the lack of channel activity in ATP- and NDP-free solution is that the K_{ATP} channel rapidly 'runs-down' due to dephosphorylation of the channel, after patches are excised from the cell, a phenomenon which occurs in cardiac and pancreatic β-cells (Terzic *et al.*, 1994). However, K_{ATP} channels in cardiac and pancreatic β-cells always showed dramatic channel activity immediately after inside-out patches were formed into ATP-free solution, which could last several minutes before the channels ran down (Trube & Hescheler, 1984; Kakei *et al.*, 1985; Findlay & Dunne, 1986; Lederer & Nichols, 1989; Tung & Kurachi, 1991). It is difficult to imagine that the K_{ATP} channels in smooth muscle run down so fast (milliseconds) that we were unable to see their activity.

A second explanation which might be offered is that the K_{ATP} channels in smooth muscle has already been dephosphorylated in the intact cell because $[ATP]_i$ in these cells, for some reason, have become very low. This is unlikely to be true, at least in the present experiments, as we tried very carefully to prevent reduction of the $[ATP]_i$ level and the energy supply in the cells by oxygenating during the whole procedure of cell dispersion and by making the dissection solution ice-cold. The ratio of ATP to ADP in these cells (kindly measured using high performance liquid chromatography (h.p.l.c.) by S.A. Prestwich) was similar to that in fresh tissues which were taken immediately after death (the relative concentrations of ATP and ADP in fresh tissues were 13.3 and 4 nmol mg^{-1} protein respectively; the relative concentrations of ATP and ADP in the cells were 6.13 and 1.27 nmol mg^{-1} protein respectively). Even stronger evidence came from the effects of metabolic poisons applied to whole cells during cell-attached patch recording, which caused the development of a glibenclamide-sensitive K-channel activity in many patches which were otherwise quiescent. This result showed that ATP in these cells was high enough to maintain the K-channels closed and sufficiently phosphorylated (if that is necessary) to allow them to become active upon metabolic inhibition, so they should also open upon forming isolated patches into ATP- and NDP-free solution.

A third explanation, which is the one we prefer and which we have suggested in our previous paper (Beech *et al.*, 1993a), is that intracellular NDPs, instead of ATP, are the crucial regulators of these K-channels in smooth muscle. NDPs as well as ATP are lost when inside-out patches are formed. ATP, more likely binding to the open-state of the channel, inhibits the channel opening once the channel is activated by NDPs. This explanation agrees very well with our results above and there is more evidence supporting this. Firstly, ATP alone had no effects in patches in which UDP was able to activate the channel (Figure 2). However, it is

known that ATP reactivates the K_{ATP} channel in cardiac and pancreatic β-cells and prevents channel run down (Findlay & Dunne, 1986; Misler *et al.*, 1986; Ohno-Shosaku *et al.*, 1987; Takano *et al.*, 1990). Also, the mean open time of the channel activity induced by metabolic poisons in cell-attached patches was much shorter than that in inside-out patches activated by UDP, presumably because the inhibition of the channel by ATP in cell-attached patches was absent in inside-out patches (see also Kajioka *et al.*, 1991). Thus, the channels we describe according to our definitions should be designated K_{NDP} not K_{ATP}.

In cardiac muscle the view is forming that NDPs are important regulators of K_{ATP} channel activity and that the effects of NDPs depend on the operative state of the channel (Terzic *et al.*, 1994). However, cardiac K_{ATP} channels differ from those described in this paper and elsewhere (Kajioka *et al.*, 1991; Robertson *et al.*, 1992; Beech *et al.*, 1993a,b; Kamouchi *et al.*, 1993) in that lowering ATP_i results in a pronounced increase in activity. It seems likely that cardiac K_{ATP} and smooth K_{NDP} channels have some structural similarities but also important differences. It is significant that rat heart K_{ATP} channel mRNA was found to be expressed in a variety of peripheral and central tissues but not in smooth muscles (Ashford *et al.*, 1994).

Working on the same tissue (rat mesenteric artery) and under almost identical conditions (60:120 mM K-gradient; negative holding potentials) as those used in this paper, Standen *et al.* (1989) found an ATP-sensitive K-channel with a conductance of 135 pS. This large conductance channel was sensitive to ATP, activated by cromakalim, and the action of cromakalim was inhibited by glibenclamide. We did not see this channel in the present experiments nor did we see it in rabbit portal vein cells in our previous experiments (Beech *et al.*, 1993a,b). Apart from channel conductance, there are other differences in our channel characteristics, such as long channel opening and noisy channel open state. Conductances of the K-channels sensitive to $[ATP]_i$ in smooth muscle cells, ranging from 7 pA to 257 pA have been reported (Inoue *et al.*, 1989; Kajioka *et al.*, 1990; 1991; Kovacs & Nelson, 1991; Miyoshi & Nakaya, 1991; Lorenz *et al.*, 1992; Bonev & Nelson, 1993), with different channel characteristics such as Ca-sensitivity and voltage-dependence. Although many of these channels show sensitivity to one or more of the agents ATP, glibenclamide, or KCO, which has led to their designation at K_{ATP} channels, it seems reasonable to suggest that they are not, after all, the same type of channel. An important question which should now be asked is, what are the roles of all these different K channels sensitive to ATP, glibenclamide, or KCOs in smooth muscle?

The results from the experiments of Kajioka *et al.* (1991), Kamouchi *et al.* (1993) and those obtained by us (Beech *et al.*, 1993b) suggest that the K_{NDP} is the target channel KCO in rabbit portal vein smooth muscle cells. These results agree well with the observations that KCO hyperpolarizations and relaxations of intact smooth muscle are blocked by glibenclamide and are unaffected by blockers of BK channels (charybdotoxin or low concentrations of TEA) (Standen *et al.*, 1989; Winquist *et al.*, 1989; Daut *et al.*, 1990; Fujii *et al.*, 1990; Nelson *et al.*, 1990; Grant & Zuzack, 1991; Brayden & Nelson, 1992). The conclusion that a small conductance (about 15 pS under quasi-physiological K gradient) channel is the target for KCOs is consistent with estimates of single channel conductance made from whole-cell current noise (Beech & Bolton, 1989; Noack *et al.*, 1992a,b; Clapp *et al.*, 1994; Criddle *et al.*, 1994). However, although K_{NDP} is most likely the target channel of KCO in smooth muscle, KCOs can also modulate BK_{Ca} channel in isolated patches of smooth muscle cells (Gelband *et al.*, 1989; Klöckner *et al.*, 1989; Carl *et al.*, 1992; Gelband & McCullough, 1993), although this modulation may not be responsible for the effects of KCO on the whole tissue. In the present experiments, we found that pinacidil activated a glibenclamide-sensitive K current in both whole-cells and in patches. The channel activated by pinacidil had apparently similar characteristics to those of the channel activated by NDPs and metabolic poisons. Further, pinacidil potentiated the channel activity activated by NDPs but had no effect on the BK channel. These results suggest that K_{NDP} is the target channel of pinacidil in rat mesenteric artery.

We are grateful to Dr S.A. Prestwich for measuring the ATP and ADP levels by h.p.l.c. This work was supported by the MRC and by the British Heart Foundation.

References

ASHFORD, M.L.J., BOND, C.T., BLAIR, T.A. & ADELMAN, J.P. (1994). Cloning and functional expression of a rat heart K_{ATP} channel. *Nature*, **370**, 456–459.

BEECH, D.J. & BOLTON, T.B. (1989). Properties of the cromakalin-induced potassium conductance in smooth muscle cells isolated from the rabbit portal vein. *Br. J. Pharmacol.*, **98**, 851–864.

BEECH, D.J., ZHANG, H., NAKAO, K. & BOLTON, T.B. (1993a). K channel activation by nucleoside diphosphates and its inhibition by glibenclamide in vascular smooth muscle cells. *Br. J. Pharmacol.*, **110**, 573–582.

BEECH, D.J., ZHANG, H., NAKAO, K. & BOLTON, T.B. (1993b). Single channel and whole-cell K-currents evoked by levcromakalim in smooth muscle cells from the rabbit portal vein. *Br. J. Pharmacol.*, **110**, 583–590.

BONEV, A.D. & NELSON, M.T. (1993). ATP-sensitive potassium channels in smooth muscle cells from guinea-pig urinary bladder. *Am. J. Physiol.*, **264**, C1190–C1200.

BRAYDEN, J.E. & NELSON, M.T. (1992). Regulation of arterial tone by activation of calcium-dependent potassium channels. *Science*, **256**, 532–535.

CARL, A., BOWEN, S., GELBAND, C.H., SANDERS, K.M. & HUME, J.R. (1992). Cromakalim and Lemakalim activate Ca(2+)-dependent K^+ channels in canine colon. *Pflügers Arch.*, **421**, 67–76.

CLAPP, L.H., GURNEY, A.M., STANDEN, N.B. & LANGTON, P.D. (1994). Properties of the ATP-sensitive K^+ current activated by levcromakalim in isolated pulmonary myocytes. *J. Membr. Biol.*, **140**, 205–213.

COOK, D.L. & HALES, C.N. (1984). Intracellular ATP directly blocks K^+-channels in pancreatic β-cells. *Nature*, **311**, 271–273.

CRIDDLE, D.N., GREENWOOD, I.A. & WESTON, A.H. (1994). Levcromakalim-induced modulation of membrane potassium currents, intracellular calcium and mechanical activity in rat mesenteric artery. *Naunyn-Schmied. Arch. Pharmacol.*, **349**, 422–430.

DAUT, J., MAIER-RUDOLPH, W., VON BECKERATH, N., MEHRKE, G., GUNTHER, K. & GOEDEL-MEINEN, L. (1990). Hypoxic dilation of coronary arteries is mediated by ATP-sensitive potassium channels. *Science*, **247**, 1341–1344.

DUNNE, M.J. (1990). Effects of pinacidil, RP 49356 and nicorandil on ATP-sensitive potassium channels in insulin-secreting cells. *Br. J. Pharmacol.*, **99**, 487–492.

DUNNE, M.J., ASPINAL, R.J. & PETERSEN, O.H. (1990a). The effects of cromakalim on ATP-sensitive potassium channels in insulin-secreting cells. *Br. J. Pharmacol.*, **99**, 169–175.

DUNNE, M.J., YULE, D.I., GALLACHER, D.V. & PETERSEN, O.H. (1990b). Comparative study of the effects of cromakalim (BRL 34915) and diazoxide on membrane potential, $[Ca^+]_i$ and ATP-sensitive potassium currents in insulin-secreting cells. *J. Memb. Biol.*, **114**, 53–60.

EDWARDS, G., IBBOTSON, T. & WESTON, A.H. (1993). Levcromakalim may induce a voltage-independent K-current in rat portal veins by modifying the gating properties of the delayed rectifier, *Br. J. Pharmacol.*, **110**, 1037–1048.

FINDLAY, I. (1987). ATP-sensitive K channel in rat ventricular myocytes are blocked by internal divalent cations. *Pflügers Arch.*, **410**, 313–320.

FINDLAY, I.M. & DUNNE, J. (1986). ATP maintains ATP-inhibited K channel in an operational state. *Pflügers Arch.*, **407**, 238–240.

FUJII, K., FOSTER, C.D., BRADING, A.F. & PAREKH, A.B. (1990). Potassium channel blockers and the effects of cromakalim on the smooth muscle of the guinea-pig bladder. *Br. J. Pharmacol.*, **99**, 779–785.

GELBAND, C.H. & MCCULLOUGH, J.R. (1993). Modulation of rabbit aortic Ca^{2+}-activated K^+ channel by pinacidil, cromakalim, and glibenclamide. *Am. J. Physiol.*, **264**, C1119–C1127.

GELBAND, C.H., SILBERBERG, S.D., GROSCHNER, K. & VAN BREEMEN, C. (1990). ATP inhibits smooth muscle $Ca^{2(+)}$-activated K^+ channels. *Proc. R. Soc. B.*, **242**, 23–28.

GRANT, T.L. & ZUZACK, J.S. (1991). Effects of K^+ channel blockers and cromakalim (BRL 34915) on the mechanical activity of guinea-pig detrusor smooth muscle. *J. Pharmacol. Exp. Ther.*, **259**, 1158–1164.

HAMILL, O.P., MARTY, E., NEHER, B., SAKMANN, B. & SIGWORTH, F.J. (1981). Improved patch-clamp techniques for the high-resolution current recording from cells and cell-free membrane patches. *Pflügers Arch.*, **319**, 85–100.

HORN, R. & MARTY, A. (1988). Muscarinic activation of ionic currents measured by a new whole-cell recording method. *J. Gen. Physiol.*, **92**, 145–159.

INOUE, I., NAKAYA, Y. & MORI, H. (1989). Extracellular Ca^{2+}-activated K-channel in coronary artery smooth muscle cells and its role in vasodilation. *FEBS.*, **255**, 282–284.

KAJIOKA, S., KITAMURA, K. & KURIYAMA, H. (1991). Guanosine diphosphate activates an adenosine 5'-triphosphate-sensitive K+ channel in the rabbit portal vien. *J. Physiol.*, **444**, 397–418.

KAJIOKA, S., OIKE, M. & KITAMURA, K. (1990). Nicorandil opens a calcium-dependent potassium channel in smooth muscle cells of the rat portal vein. *J. Pharmacol. Exp. Ther.*, **254**, 905–913.

KAKEI, M., NOMA, A. & SHIBASAKI, T. (1985). Properties of adenosine-triphosphate-regulated potassium channels in guinea-pig ventricular cells. *J. Physiol.*, **363**, 441–462.

KAMOUCHI, M., KAJIOKA, S., SAKAI, T., KITAMURA, K. & KURIYAMA, H. (1993). A target K^+ channel for the LP-805-induced hyperpolarization in smooth muscle cells of the rabbit portal vein. *Naunyn-Schmied. Arch. Pharmacol.*, **347**, 329–335.

KLÖCKNER, U., TRIESCHMANN, U. & ISENBERG, G. (1989). Pharmacological modulation of calcium and potassium channels in isolated vascular smooth muscle cells. *Arzneimittel-Forschung.*, **39**, 120–126.

KOVACS, R.J. & NELSON, M.T. (1991). ATP-sensitive K+ channels from aortic smooth muscle incorporated into planar lipid bilayers. *Am. J. Physiol.*, **261**, H604–H609.

LEDERER, W.J. & NICHOLS, C.G. (1989). Nucleotide modulation of the activity of rat heart ATP-sensitive K^+ channels in isolated membrane patches. *J. Physiol.*, **419**, 193–211.

LORENZ, J.N., SCHNERMANN, J., BROSIUS, F.C., BRIGGS, J.P. & FURSPAN, P.B. (1992). Intracellular ATP can regulate afferent arteriolar tone via ATP-sensitive K^+ channels in the rabbit. *J. Clin. Invest.*, **90**, 733–740.

MISLER, S., FALKE, L.C., GILLIS, K. & MCDANIEL, M.L. (1986). A metabolite regulated potassium channel in rat pancreatic β-cells. *Proc. Natl. Acad. Sci. U.S.A.*, **83**, 7119–7123.

MIYOSHI, H. & NAKAYA, Y. (1993). Activation of ATP-sensitive K^+ channels by cyclic AMP-dependent protein kinase in cultured smooth muscle cells of porcine coronary artery. *Biochem. Biophys. Res. Commun.*, **193**, 240–247.

MIYOSHI, Y., NAKAYA, Y., WAKATSUKI, T., NAKAYA, S., FUJINO, K., SAITO, K. & INOUE, I. (1992). Endothelin blocks ATP-sensitive K^+ channels and depolarizes smooth muscle cells of porcine coronary artery. *Circ. Res.*, **70**, 612–616.

NAKAO, K. & BOLTON, T.B. (1991). Cromakalim-induced potassium currents in single dispersed smooth muscle cells of rabbit artery and vein. *Br. J. Pharmacol.*, **102**, 155P.

NELSON, M. T., PATLAK, J.B., WORLEY, J.F. & STANDEN, N.B. (1990). Calcium channels, potassium channels and the voltage-dependency of arterial smooth muscle tone. *Am. J. Physiol.*, **259**, C3–C18.

NOACK, T., DEITMER, P., EDWARDS, G. & WESTON, A.H. (1992a). Characterization of potassium currents modulated by BRL 38227 in rat portal vein. *Br. J. Pharmacol.*, **106**, 717–726.

NOACK, T., EDWARDS, G., DEITMER, P. & WESTON, A.H. (1992b). Potassium channel modulation in rat portal vein by ATP depletion: a comparison with the effects of levcromakalim (BRL 38227). *Br. J. Pharmacol.*, **107**, 945–955.

NOMA, A. (1983). ATP-regulated single channels in cardiac muscle. *Nature*, **305**, 147–148.

OHNO-SHOSAKU, T., ZÜNKLER, B. & TRUBE., G. (1987). Dual effects of ATP on K currents of mouse pancreatic β-cells. *Pflügers Arch.*, **408**, 133–138.

RORSMAN, P. & TRUBE, G. (1985). Glucose-dependent K-channels in pancreatic β-cells are regulated by intracellular ATP. *Pflügers Arch.*, **405**, 305–309.

ROBERTSON, B.E., CORRY, P.R., NYE, P.C. & KOZLOWSKI, R.Z. (1992). Ca^{2+} and Mg-ATP activated potassium channels from rat pulmonary artery [corrected and republished article originally printed in *Pflügers Arch* 1992, **421**, 97–99]. *Pflügers Arch.*, **421**, 94–96.

SHEN, W.K., TUNG, R.T., MACHULDA, M.M. & KURACHI, Y. (1991). Essential role of nucleoside diphosphates in nicorandil-mediated activation of cardiac ATP-sensitive K^+ channel. A comparison with pinacidil and lemakalim. *Circ. Res.*, **69**, 1152–1158.

SILBERBERG, S.D. & VAN BREEMEN, C. (1992). A potassium current activated by lemakalim and metabolic inhibition in rabbit mesenteric artery. *Pflügers Arch.*, **420**, 118–120.

STANDEN, N.B., QUAYLE, J.M., DAVIES, N.W., BRAYDEN, J.E., HUANG, Y. & NELSON, M.T. (1989). Hyperpolarizing vasodilators activate ATP-sensitive channels in arterial smooth muscle. *Science*, **245**, 177–180.

TAKANO, M., QIN, D & NOMA, A. (1990). ATP-dependent decay and recovery of K channels in guinea-pig cardiac myocytes. *Am. J. Physiol.*, **258**, H45–H50.

TERZIC, A., TUNG, R.T. & KURACHI, Y. (1994). Nucleotide regulation of ATP sensitive potassium channels. *Cardiovasc. Res.*, **28**, 746–753.

TRUBE, G. & HESCHELER, J. (1984). Inward-rectifying channel in isolated patches of the heart cell membrane: ATP-dependence and comparison with cell-attached patches. *Pflügers Arch.*, **407**, 178–184.

TUNG, R.T. & KURACHI, Y. (1991). On the mechanism of nucleotide diphosphate activation of the ATP-sensitive K^+ channel in ventricular cells of guinea-pig. *J. Physiol.*, **437**, 239–256.

WAKATSUKI, T., NAKAYA, Y. & INOUE, I. (1992). Vasopressin modulates K^+-channel activities of cultured smooth muscle cells from porcine coronary artery. *Am. J. Physiol.*, **263**, H491–H496.

WINQUIST, R.J., HEANEY, L.A., WALLACE, A.A., BASKIN, E.P., STEIN, R.B., GARCIA, M.L. & KACZOROWSKI, G.J. (1989). Glyburide blocks the relaxation response to BRL 34915 (cromakalin), minoxidil sulfate and diazoxide in vascular smooth muscle. *J. Pharmacol. Exp. Ther.*, **248**, 149–156.

(Received February 2, 1994
Revised October 6, 1994
Accepted October 12, 1994).

British Journal of Pharmacology (1995) 114, 673-677

Sustained negative inotropism mediated by α-adrenoceptors in adult mouse myocardia: developmental conversion from positive response in the neonate

[1]Hikaru Tanaka, Shigeru Manita, Tomoyuki Matsuda, Mika Adachi & Koki Shigenobu

Department of Pharmacology, Toho University School of Pharmaceutical Sciences, Miyama 2-2-1 Funabashi, Chiba 274, Japan

1 Inotropic responses to α-adrenoceptor stimulation and the effects of antagonists were examined in isolated ventricular preparations from neonatal and adult mice.

2 Phenylephrine, in the presence of propranolol, produced positive inotropic responses in neonates up to 1 week after birth, while it produced negative inotropic responses in mice older than 3 weeks.

3 Both positive and negative responses to phenylephrine in neonates and adults, respectively, were antagonized by prazosin, WB4101 (2-([2,6-dimethoxyphenoxyethyl]aminomethyl)-1,4-benzodioxane) and 5-methylurapidil, but not by atropine, yohimbine or chlorethylclonidine.

4 Noradrenaline (NA) produced positive inotropic responses both in the neonate and adult; the responses were observed in a lower concentration-range in the neonate than in the adult. WB4101 produced a significant leftward shift of the concentration-response curve for noradrenaline in adult preparations while only a slight rightward shift was observed in the neonate.

5 Our results demonstrate the presence of α-adrenoceptor-mediated inotropic responses in the mouse ventricular myocardia. The response to phenylephrine changes from a positive to a negative effect during postnatal development. The responses are mediated by α_1-adrenoceptors, and modulate the overall inotropic response to NA in the adult.

Keywords: Myocardium; inotropism; noradrenaline; α-adrenoceptor; development

Introduction

The sympathetic nervous system is a major regulator of myocardial function. Although myocardial effects of the neurotransmitter, noradrenaline (NA), are considered to be mediated through β-adrenoceptors, α-adrenoceptors are also present in myocardial tissue of various species, and their stimulation is known to affect cardiac rhythm and contractility (reviewed by Fedida, 1993; Terzic *et al.*, 1993). Although effects of α-adrenoceptor stimulation are considered to be mediated through mechanisms different from β-adrenoceptor stimulation, many questions on the mechanism and the species difference of α-adrenoceptor-mediated responses remained unsolved. Also, how α-adrenoceptors contribute to the overall inotropic action of NA or sympathetic stimulation is even less well understood.

Cardiac responsiveness to agents, including physiological neurotransmitters, is often different in developing animals when compared with adults (reviewed by Kojima *et al.*, 1990; Shigenobu, 1990). Many endogenous factors including autonomic innervation are known to affect cardiac responsiveness and in some cases abnormalities of the developing myocardium are considered to be involved in the pathogenesis of cardiovascular diseases (Tucker & Johnson, 1984; Tanaka *et al.*, 1988b). In our previous study (Tanaka *et al.*, 1994), we examined the positive inotropic responses to NA of isolated ventricular myocardia from neonatal and adult mice and demonstrated a developmental increase in sympathetic innervation and a tenfold decrease in the sensitivity to NA. In the present study, we examined whether α-adrenoceptor stimulation has any inotropic effect on mouse myocardia. We found that α-adrenoceptor-mediated inotropic responses in the mouse ventricular myocardia change from positive to negative during postnatal development and that this change contributes to the developmental decrease in the overall inotropic sensitivity to NA.

[1] Author for correspondence.

Methods

Right ventricular free wall strips were rapidly isolated from 1-day old neonatal and adult (5 to 6 weeks old) *ddy* strain mice. Preparations were placed horizontally in a 20 ml organ bath containing physiological salt solution of the following composition (mM concentration): NaCl 135, KCl 5, $CaCl_2$ 2, $MgCl_2$ 1, $NaHCO_3$ 15 and glucose 5.5 (pH 7.4). The nutrient solution was aerated with 95% O_2: 5% CO_2 and maintained at 36.5°C. The preparations were driven by a pair of platinum plate electrodes (field stimulation) with rectangular current pulses (1 Hz, 5 ms, 1.2 × threshold voltage) generated from an electronic stimulator (Dia Medical System, DPS-165B). Addition of propranolol (10^{-6}M) had no effect on the basal contractile force indicating that endogenous catecholamines which might be released by electrical stimulation did not modify the basal contractile activities. The resting tension applied to each preparation was adjusted so that the muscle was stretched to the peak of its length-tension curve. Developed tension was recorded isometrically with a force-displacement transducer (Nihon Kohden TB-611T) connected to a minipolygraph (Nihon Kohden RM-6100).

Drugs were added after preparations had been allowed to equilibrate for more than 30 min, after which the developed tension of the preparations was well maintained. All drug solutions were prepared immediately before the start of the experiments by dissolving them in distilled water. Small aliquots of the solutions were added to the bath to give the desired final concentrations. The preparations were incubated with antagonists (except for chlorethylclonidine) for 15 min before exposure to phenylephrine or NA. In the case of chlorethylclonidine, the preparations were exposed to the drug for 40 min and the drug was not removed during exposure to phenylephrine. Concentration-response curves were obtained by cumulative addition of agonists. Each curve was obtained in a different preparation to avoid exhaustion of preparations. Significance of difference in pD_2 values were evaluated by Duncan's multiple range test, and a P value less than 0.05 was considered significant. The drugs used were

(-)-noradrenaline hydrogen tatrate monohydrate (Wako), (-)-phenylephrine hydrochloride (Wako), propranolol hydrochloride (Sigma), atropine sulphate monohydrate (Tokyo Kasei), yohimbine hydrochloride (Tokyo Kasei), prazosin hydrochloride (Wako), chlorethylclonidine dihydrochloride (RBI), WB4101 hydrochloride (RBI) and 5-methylurapidil (RBI).

Results

Phenylephrine, in the presence of 10^{-6}M propranolol, produced a concentration-dependent positive inotropic effect in neonatal myocardia (Figure 1a,b). The maximum contractile force was about 200% of the basal contractile force and the pD_2 value was 5.23 ± 0.13. In contrast, in the adult (five to six weeks after birth), phenylephrine, in the presence of 10^{-6}M propranolol, produced a concentration-dependent negative inotropic effect. The contractile force decreased to about 50% of the basal value and the pD_2 value was 5.98 ± 0.20 (Figure 1a,b). Application of 10^{-4}M phenylephrine, in the presence of 10^{-6}M propranolol, resulted in increases in contractile force up to 1 week after birth, slight decreases or no effect were observed at 2 weeks after birth, and decreases were observed in myocardia from mice older than 3 weeks (Figure 1c).

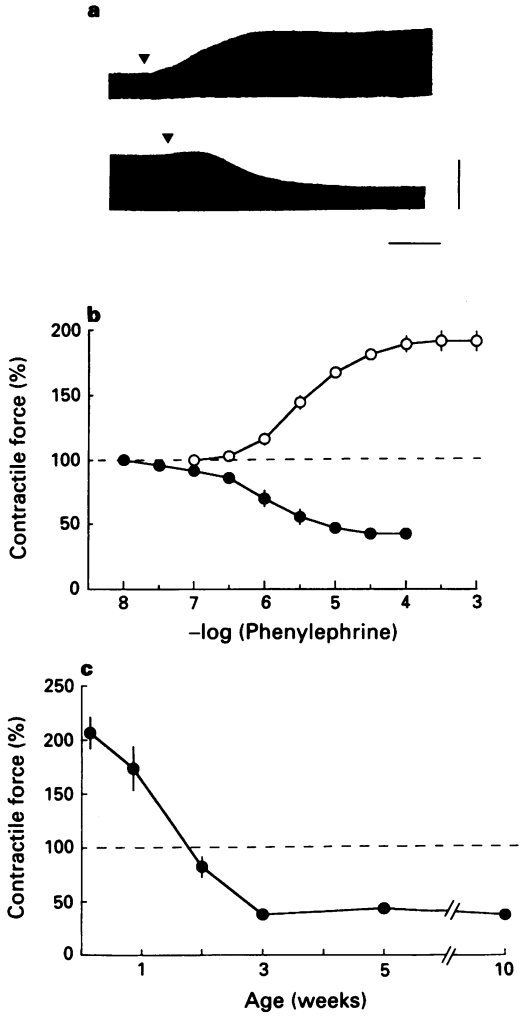

Figure 1 Inotropic responses of ventricular myocardia from neonatal and adult mice to phenylephrine. All experiments were performed in the presence of 10^{-6}M propranolol. (a) Traces of contractile force in neonatal (upper trace) and adult (lower trace) preparations; (▼) indicates the addition of 10^{-4}M phenylephrine. The horizontal bar indicates 1 min and the vertical bar indicates 100 mg. (b) Concentration-response curves for phenylephrine in neonatal (○) and adult (●) preparations. (c) Effect of 10^{-4}M phenylephrine on preparations from various ages. Each point in (b) and (c) represent the mean ± s.e. from five to ten experiments.

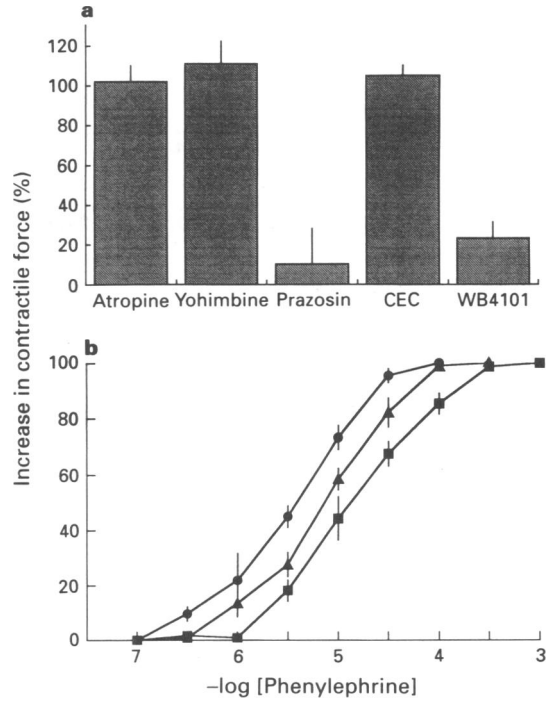

Figure 2 Effect of antagonists on the positive inotropic responses of neonatal myocardia to phenylephrine. All experiments were performed in the presence of 10^{-6}M propranolol. (a) Increases in contractile force by 10^{-4}M phenylephrine in the presence of antagonists were expressed as a percentage of the increase in the absence of antagonists in the same preparation. The concentration of the antagonists used were: atropine, 10^{-6}M; yohimbine, 10^{-6}M; prazosin, 10^{-6}M; chlorethylclonidine (CEC), 5×10^{-5}M and WB4101, 10^{-6}M. (b) Concentration-response curves for phenylephrine in the absence (●) and presence of 3×10^{-9}M (▲) and 10^{-8}M (■) 5-methylurapidil. Each column or point in (a) and (b) respectively, represent the mean ± s.e. from five experiments.

In neonatal preparations (1 day after birth), positive inotropic responses to 10^{-4}M phenylephrine, in the presence of 10^{-6}M propranolol, were inhibited by 10^{-6}M prazosin and 10^{-6}M WB4101, but not by 10^{-6}M atropine, 10^{-6}M yohimbine or 5×10^{-5}M chlorethylclonidine (Figure 2a). 5-Methylurapidil concentration-dependently shifted to the right the concentration-response curves for the positive inotropic effect of phenylephrine, in the presence of 10^{-6}M propranolol (Figure 2b); the slope of the Schild plot was close to unity (0.99 ± 0.11) and the pA_2 value was 8.59 ± 0.07.

In adult preparations, negative inotropic responses to 10^{-4}M phenylephrine, in the presence of 10^{-6}M propranolol, were inhibited by 10^{-6}M prazosin and 10^{-6}M WB4101, but not by 10^{-6}M atropine, 10^{-6}M yohimbine or 5×10^{-5}M chlorethylclonidine (Figure 3a). 5-Methylurapidil concentration-dependently shifted to the right the concentration-response curves for the negative inotropic effect of phenylephrine, in the presence of 10^{-6}M propranolol; the slope of the Schild plot was close to unity (0.91 ± 0.04) and the pA_2 value was 8.73 ± 0.11 (Figure 3b).

Noradrenaline produced positive inotropic responses both in the neonate and adult (Figure 4a). The response was observed with a lower concentration-range in the neonate than in the adult, pD_2 values for neonates and adults being 7.05 ± 0.01 and 6.09 ± 0.04, respectively. WB4101 (10^{-8}M) produced a significant leftward shift of the concentration-response curve for noradrenaline in adult preparations while only a slight rightward shift was observed in the neonate. pD_2 values for NA in the presence of 10^{-6}M WB4101 in

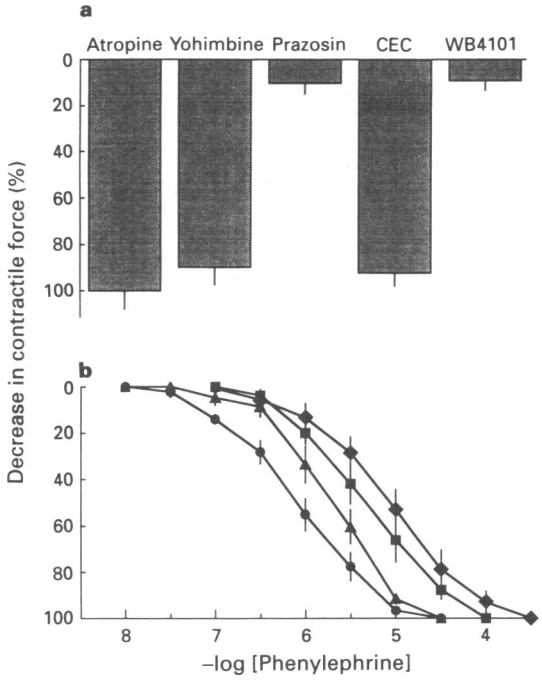

Figure 3 Effect of antagonists on the negative inotropic responses of adult myocardia to phenylephrine. All experiments were performed in the presence of 10^{-6}M propranolol. (a) Decreases in contractile force by 10^{-4}M phenylephrine in the presence of antagonists were expressed as a percentage of the decrease in the absence of antagonists. The concentration of the antagonists used were: atropine, 10^{-6}M; yohimbine, 10^{-6}M; prazosin, 10^{-6}M; chlorethylclonidine (CEC), 5×10^{-5}M and WB4101, 10^{-6}M. (b) Concentration-response curves for phenylephrine in the absence (●) and presence of 3×10^{-8}M (▲), 10^{-8}M (■) and 3×10^{-8}M (◆) 5-methylurapidil. Each column or point in (a) and (b) respectively, represent the mean ± s.e. from five experiments.

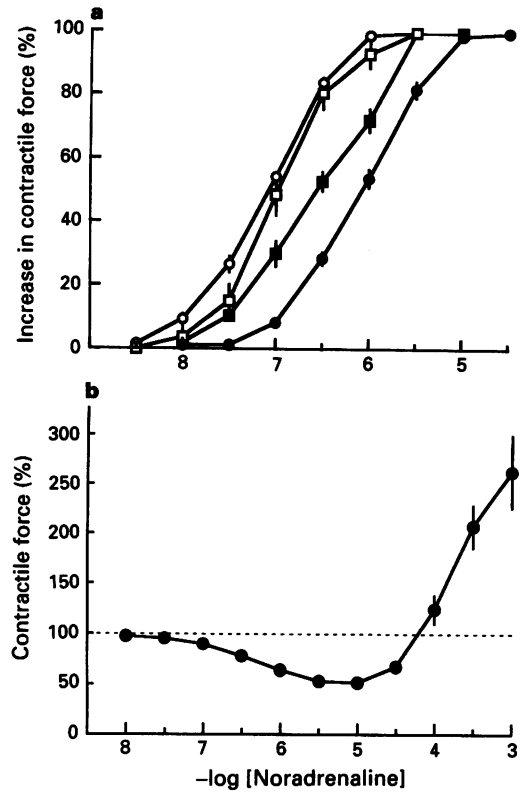

Figure 4 Effect of WB4101 and propranolol on the positive inotropic response to noradrenaline (NA) in ventricular muscles from neonatal (open symbols) and adult (closed symbols) mice. (a) Concentration-response curves for NA were obtained in the absence (circles) and presence (squares) of 10^{-8}M WB4101. (b) Concentration-response curves for NA of adult preparations in the presence of 10^{-6}M propranolol. Each point represents the mean ± s.e. from five experiments.

neonates and adults were 6.87 ± 0.09 and 6.79 ± 0.06, respectively. In the adult, 10^{-7} to 10^{-5}M NA, in the presence of 10^{-6}M propranolol, produced negative inotropic responses, while it produced positive responses at concentrations higher than 10^{-4}M (Figure 4b).

Discussion

We have previously reported a tenfold decrease in the sensitivity to NA during postnatal development of the mouse myocardium (Tanaka *et al.*, 1994). As sympathetic innervation of the mouse myocardium increases postnatally (Yamada *et al.*, 1980; Tanaka *et al.*, 1994), increased NA uptake into sympathetic nerve terminals may contribute to the decrease in sensitivity to NA; this was pharmacologically confirmed to be the case in our previous paper (Tanaka *et al.*, 1994). As the developmental decrease in sensitivity was also observed with isoprenaline, which is not taken up into sympathetic nerve endings, and with NA in the presence of desipramine, a neuronal uptake inhibitor, it was suggested that a decrease in the sensitivity of myocardial β-adrenoceptor-mediated mechanisms also takes place during development (Tanaka *et al.*, 1994). In addition to these two mechanisms, other mechanisms may be involved, i.e., the existence of an α-adrenoceptor-mediated inotropic response in the mouse ventricular myocardia and its change from positive to negative during postnatal development, as was revealed in the present study (Figure 1). In neonatal myocardium, the concentration-response curve for NA was only slightly affected by WB4101, indicating the small contribution of the α-adrenoceptor-mediated positive effect to the overall inotropic response to NA. This may be due to the greater sensitivity of the myocardium to the β-adrenoceptor-mediated positive effects of NA in the neonate (Tanaka *et al.*, 1994). In contrast, in adult myocardium, a significant leftward shift of the concentration-response curve for NA by WB4101 was observed (Figure 4a), indicating that the α-adrenoceptor-mediated negative effect significantly contributes to the overall inotropic response to NA. It was also confirmed that not only phenylephrine but also NA can produce negative inotropic responses during β-adrenoceptor blockade (Figure 4b). Thus, the developmental conversion of α-adrenoceptor-mediated inotropic response from positive to negative contributes to the postnatal decrease in the overall inotropic sensitivity to NA.

The factors triggering the developmental changes remain to be clarified. In the case of the ventricular myocardium of rats (reviewed by Shigenobu, 1990), a tenfold decrease in the sensitivity to NA and isoprenaline occurs in the early postnatal period concurrently with the increase in sympathetic innervation density (Shigenobu *et al.*, 1988; Tanaka & Shigenobu, 1990a). Sympathetic denervation studies (Ishii *et al.*, 1982; 1985; Goto *et al.*, 1985) and organ culture experiments (Tanaka *et al.*, 1988a; Tanaka & Shigenobu, 1990b) revealed that sympathetic innervation is not only responsible for the pre-junctional component of the decreased sensitivity, but also exerts a long-term influence on myocardial properties to maintain the sensitivity to agonists at normal level. Whether the developmental decrease in sensitivity of the β-adrenoceptor-mediated effects (Tanaka *et al.*, 1994) and conversion of α-adrenoceptor-mediated effects from positive to negative (Figure 1) in mouse myocardia have causal relationship with the concurrent increase in its

sympathetic innervation is a matter of interest. α-Adrenoceptor agonists are reported to increase automaticity in non-innervated ventricular myocytes or neonatal ventricles but decrease automaticity in innervated ventricular myocytes or adult ventricles (Malfatto *et al.*, 1990). Alternatively, it is also possible that developmental conversion of α-adrenoceptor-mediated responses is triggered by other *in vivo* factors. Myocardial α-adrenoceptor-mediated responses or sarcolemmal α-adrenoceptor density are reported to be altered by abnormal thyroid function (reviewed by Osnes *et al.*, 1985), in hypoxia (Heathers *et al.*, 1988), hypertension (Limas & Limas, 1987) and experimentally induced diabetes mellitus (Heijnis & van Zwieten, 1992).

The cellular mechanisms involved in the developmental conversion of α-adrenoceptor-mediated responses also remain to be investigated. Receptor-binding studies of mouse myocardia indicate that, the density of β-adrenoceptors is about 60% higher in the neonate than in the adult, while that of α-adrenoceptors is not different between early postnatal and adult periods (Yamada *et al.*, 1980). In the present study, both the positive and negative inotropic responses to phenylephrine were antagonized by prazosin but not by yohimbine indicating the involvement of α_1-receptors. This was further confirmed with the observation that the concentration-response curves for phenylephrine were shifted to the right by 5-methylurapidil (Figures 2b, 3b). The positive inotropic responses following α-adrenoceptor stimulation in several other species are reported to be mediated by α_1-adrenoceptors (reviewed by Endoh, 1991). α_1-Adrenoceptors can be further subdivided into at least two pharmacologically distinct subtypes, α_{1A} and α_{1B} (reviewed by Minneman, 1988). The α_{1A}-subtype has a higher affinity than the α_{1B}-subtype for the antagonist WB4101, 5-methylurapidil and (+)-nigludipine, while the α_{1B}-subtype is irreversively alkylated by chlorethylclonidine. The subtype responsible for the α_1-adrenoceptor mediated inotropic responses varies among species. For example, it is reported to be mainly the α_{1A}-subtype in rat myocardium (Rokosh & Sulakhe, 1991), while the α_{1B}-subtype mediates responses of the rabbit myocardium (Takanashi *et al.*, 1991). In the present study, both the positive and negative responses to phenylephrine in neonatal and adult mouse myocardia, respectively, were sensitive to WB4101 and 5-methylurapidil (Figures 2, 3), indicating that the receptors mediating both effects are of the α_{1A}-subtype. The pA_2 values for 5-methylurapidil against phenylephrine in neonatal and adult myocardium is close to those for α_1-adrenoceptors in the rabbit aorta (Suzuki *et al.*, 1990) and bronchus (Takayanagi & Moriya, 1991). As for the subclassification of receptor types, recent papers suggest the existence of additional types of α-adrenoceptors (Noguchi *et al.*, 1993) and the possibility remains that the inotropic responses of mouse myocardia are mediated by some of the novel types of receptors. In any case, no evidence for developmental changes in α-adrenoceptor subtypes mediating the inotropic effects was obtained in the present study. Thus it is likely that the developmental conversion of α-adrenoceptor-mediated response from positive to negative is due to developmental changes in the signal transduction pathways and/or excitation-contraction mechanisms of the mouse myocardium rather than to changes in α-adrenoceptor subtypes.

The contractile responses following α-adrenoceptor stimulation are reported to vary among species (reviewed by Fedida, 1993; Terzic *et al.*, 1993). In the myocardium of the rat (Tohse *et al.*, 1987), cat (Hartmann *et al.*, 1988) and rabbit (Skomedal *et al.*, 1990), α-adrenoceptor stimulation results in increases in contractile force, while in that of the dog (Endoh *et al.*, 1978), guinea-pig (Hescheler *et al.*, 1988) and ferret (Endoh *et al.*, 1989), inotropic effects are small or do not exist. Varying results have been reported with human myocardium (Jakob *et al.*, 1988; Osnes *et al.*, 1989). Many questions on the mechanisms of α-adrenoceptor-mediated inotropic responses remain unsolved. One reason for this may be the presence of both positive and negative effects. For example, in the rat ventricular myocardia, stimulation of α_1-adrenoceptors results in a triphasic inotropic response (Tohse *et al.*, 1987). An initial increase in contractile force is followed by a transient decline and finally reaches a maximum level which persists for more than 20 min. Also, in other species, it is possible that the positive response to α-adrenoceptor stimulation is obscured by a simultaneous unrecognized negative component. The adult mouse myocardium is unique in that α-adrenoceptor stimulation results in a sustained negative inotropic response (Figure 1a), and may be useful in studies of α-adrenoceptor-mediated inotropism.

In summary, our results demonstrated that the α-adrenoceptor-mediated inotropic response in the mouse ventricular myocardia changes from positive to negative during postnatal development. The effects are most likely mediated through α_{1A} receptors, and contribute to the overall inotropic response to NA. Thus, the mouse myocardium provides an interesting model for investigation of the factors regulating and the cellular mechanisms of α-adrenoceptor-mediated inotropism.

References

ENDOH, M. (1991). Signal transduction of myocardial α_1-adrenoceptors: regulation of ion channels, intracellular calcium, and force of contraction – a review. *J. Appl. Cardiol.*, **6**, 379–399.

ENDOH, M., HIRAMOTO, T. & KUSHIDA, H. (1989). Preponderance of β- over α-adrenoceptors in mediating the positive inotropic effect of phenylephrine in the ferret myocardium. *Naunyn Schmied. Arch. Pharmacol.*, **339**, 362–366.

ENDOH, M., SHIMIZU, T. & YANAGISAWA, T. (1978). Characterization of adrenoceptors mediating positive inotropic responses in the ventricular myocardium of the dog. *Br. J. Pharmacol.*, **64**, 53–61.

FEDIDA, D. (1993). Modulation of cardiac contractility by α1 adrenoceptors. *Cardiovasc. Res.*, **27**, 1735–1742.

GOTO, K., LONGHURST, P.A., CASIS, L.A., HEAD, R.J., TAYLOR, D.A., RICE, P.J. & FLEMING, W.W. (1985). Surgical sympathectomy of the heart in rodents and its effect on sensitivity to agonists. *J. Pharmacol. Exp. Ther.*, **234**, 280–287.

HARTMANN, H.A., MAZZOCA, N.J., KLEIMAN, R.B. & HOUSER, S.B. (1988). Effects of phenylephrine on calcium current and contractility of feline ventricular myocytes. *Am. J. Physiol.*, **255**, H1173–H1180.

HEATHERS, G.P., CORR, P.B. & RUBIN, L.J. (1988). Transient accumulation of inositol (1,3,4,5)-tetrakisphosphate in response to α1-adrenergic stimulation in adult cardiac myocytes. *Biochem. Biophys. Res. Commun.*, **156**, 485–492.

HEIJNIS, J.B. & VAN ZWIETEN, P.A. (1992). Enhanced inotropic responsiveness to α-adrenoceptor stimulation in isolated working hearts from diabetic rats. *J. Cardiovasc. Pharmacol.*, **20**, 559–559.

HESCHELER, J., NAWRATH, H., TANG, M. & TRAUTWEIN, W. (1988). Adrenoceptor-mediated changes of excitation and contraction in ventricular heart muscle from guinea-pigs and rabbits. *J. Physiol.*, **397**, 657–670.

ISHII, K., ISHII, N., SHIGENOBU, K. & KASUYA, Y. (1985). Acetylcholine supersensitivity in the rat heart produced by neonatal sympathectomy. *Can. J. Physiol. Pharmacol.*, **63**, 898–899.

ISHII, K., SHIGENOBU, K. & KASUYA, Y. (1982). Postjunctional supersensitivity in young rat heart produced by immunological and chemical sympathectomy. *J. Pharmacol. Exp. Ther.*, **220**, 209–215.

JAKOB, H., NAWRATH, H. & RUPP, J. (1988). Adrenoceptor-mediated changes of action potential and force of contraction in isolated human ventricular heart muscle. *Br. J. Pharmacol.*, **94**, 584–590.

KOJIMA, M., SPERELAKIS, N. & SADA, H. (1990). Ontogenesis of transmembrane signaling systems for control of cardiac Ca^{2+}channels. *J. Dev. Physiol.*, **14**, 181–219.

LIMAS, C.J. & LIMAS, J. (1987). Altered intracellular adrenoceptor distribution in myocardium of spontaneously hypertensive rats. *Am. J. Physiol.*, **253**, H904–H908.

MALFATTO, G., ROSEN, T.S. & STEINBERG, S.F. (1990). Sympathetic neural modulation of cardiac impulse initiation and repolarization in the newborn rat. *Circ. Res.*, **66**, 427–437.

MINNEMAN, K.P. (1988). α1-Adrenergic receptor subtypes, inositol phosphates, and sources of cell Ca^{2+}. *Pharmacol. Rev.*, **40**, 87–119.

NOGUCHI, H., MURAOKA, R., KIGOSHI, S. & MURAMATSU, I. (1993). α1-Adrenoceptor subtype involved in the positive inotropic response to phenylephrine in rat atria. *Eur. J. Pharmacol.*, **240**, 291–293.

OSNES, J.B., AASS, H. & SKOMEDAL, T. (1985). On adrenergic regulation of heart function: role of myocardial α-adrenoceptors. In *α-Adrenoceptor Blockers in Cardiovascular Disease*, ed. Refsum, S.H. & Mjos, O.D. pp. 69–102, Edinburgh: Churchill Livingstone.

OSNES, J.B., AASS, H. & SKOMEDAL, T. (1989). Adrenoceptors in myocardial regulation: concomitant contribution from both alpha- and beta- adrenoceptor stimulation to the inotropic response. *Basic Res. Cardiol.*, **84** (suppl. 1), 9–17.

ROKOSH, D.G. & SULAKHE, P.V. (1991). Characteristics of alpha 1-adrenoceptors coupled to inotropic response and phosphoinositide metabolism in rat myocardium. *Circulation*, **84**, 11–389.

SHIGENOBU, K. (1990). Electrophysiological properties of chick embryonic heart and some pharmacological studies with rat myocardium during pre- and postnatal development. In *Developmental Cardiology: Morphogenesis and Function* ed. Clark E.B. & Takao A. pp. 273–303. New York: Futura.

SHIGENOBU, K., TANAKA, H. & KASUYA, Y. (1988). Changes in sensitivity of rat heart to noradrenaline and isoproterenol during pre- and postnatal development and its relation to symphathetic innervation. *Dev. Pharmacol. Ther.*, **11**, 226–236.

SKOMEDAL, T., AASS, H. & OSNES, J.B. (1990). Prazosin-sensitive component of the inotropic response to noradrenaline in rabbit heart. *J. Pharmacol. Exp. Ther.*, **252**, 853–858.

SUZUKI, E., TSUJIMOTO, G., TAMURA, K. & HASHIMOTO, K. (1990). Two pharmacological distinct α1-adrenoceptor subtypes in the contraction of rabbit aorta: each subtype couples with a different Ca^{2+} signalling mechanism and plays a different role. *Mol. Pharmacol.*, **38**, 725–736.

TAKANASHI, M., NOROTA, I. & ENDOH, M. (1991). Potent inhibitory action of chlorethylclonidine on the positive inotropic effect and phosphoinositide hydrolysis mediated via myocardial α_1-adrenoceptors in the rabbit ventricular myocardium. *Naunyn Schmied. Arch. Pharmacol.*, **343**, 669–673.

TAKAYANAGI, I. & MORIYA, M. (1991). α_{1A}-Adrenoceptors in rabbit bronchus. *Eur. J. Pharmacol.*, **202**, 281–283.

TANAKA, H., KASUYA, Y., SAITO, H. & SHIGENOBU, K. (1988a). Organ culture of rat heart: maintained high sensitivity of fetal atria before innervation to noradrenaline. *Can. J. Physiol. Pharmacol.*, **66**, 901–906.

TANAKA, H., KASUYA, Y. & SHIGENOBU, K. (1988b). Altered responsiveness to autonomic transmitters of hearts from spontaneously hypertensive rats. *J. Cardiovasc. Pharmacol.*, **12**, 678–682.

TANAKA, H., MANITA, S. & SHIGENOBU, K. (1994). Increased sensitivity of neonatal mouse myocardia to autonomic transmitters. *J. Auton. Pharmacol.*, **14**, 123–128.

TANAKA, H. & SHIGENOBU, K. (1990a). Rat heart organ culture for the study of trophic substances involved in the maintenance of normal sensitivity to noradrenaline: possible involvement of cAMP and search for other factors. *Can. J. Physiol. Pharmacol.*, **68**, 898–902.

TANAKA, H. & SHIGENOBU, K. (1990b). Role of β-adrenoceptor-adenylate cyclase system in the developmental decrease in sensitivity to isoprenaline in foetal and neonatal rat heart. *Br. J. Pharmacol.*, **100**, 138–142.

TERZIC, A., PUCEAT, M., VASSORT, G. & VOGEL, S. (1993). Cardiac α_1-adrenoceptors: an overview. *Pharmacol. Rev.*, **45**, 147–175.

TOHSE, N., HATTORI, Y., NAKAYA, H. & KANNO, M. (1987). Effects of α-adrenoceptor stimulation on electrophysiological properties and mechanics in rat papillary muscle. *Gen. Pharmacol.*, **18**, 539–546.

TUCKER, D.C. & JOHNSON, A.K. (1984). Development of autonomic control of heart rate in genetically hypertensive and normotensive rats. *Am. J. Physiol.*, **246**, R570–577.

YAMADA, S., ROESKE, W.R. & YAMAMURA, H.I. (1980). Ontogeny of mammalian cardiac α1-adrenergic receptors. *Eur. J. Pharmacol.*, **68**, 217–221.

(Received May 10, 1994
Revised August 16, 1994
Accepted September 28, 1994).

British Journal of Pharmacology (1995) 114, 678-688

The relationship between density of α-adrenoceptor binding sites and contractile responses in several porcine isolated blood vessels

[1]I.K. Wright, N.A. Blaylock, D.A. Kendall & V.G. Wilson

Department of Physiology and Pharmacology, Medical School, Queen's Medical Centre, Nottingham NG7 2UH

1 The aim of this study was to investigate constrictor α-adrenoceptors in three isolated blood vessles of the pig, the thoracic aorta (TA), the splenic artery (SA) and marginal ear vein (MEV) and then compare the functional response with the densities of α_1- and α_2-adrenoceptor binding sites in these and several other porcine vascular tissues, palmar common digital artery (PCDA), palmar lateral vein (PLV) and ear artery (EA).

2 Noradrenaline (NA), phenylephrine (PE) and UK14304 (all at 0.03–10 μM) elicited concentration-dependent contractions in the TA and MEV, with a rank order of potency of UK14304>NA>PE. UK14304 produced maximal responses which were 58% (TA) and 65% (MEV) of that of NA. In the SA, UK14304 and PE produced maximal responses which were less than 10% and 50% of the NA-induced maximal response respectively, with an order of potency of NA>PE. In the SA, NA-induced contractions were competitively antagonized by prazosin ($pA_2 = 8.60 \pm 0.15$). Further, rauwolscine (1–10 μM) antagonized NA-induced contractions with an apparent pK_B of 6.09 ± 0.11 ($n = 6$), indicating an action at α_1-adrenoceptors. The combination of the two antagonists at concentrations selective for α_1- (0.1 μM) and α_2-adrenoceptors (1 μM) had no greater effect than either antagonist alone. This suggests that the SA expresses only post-junctional α_1-adrenoceptors.

3 In the TA, prazosin produced non-parallel shifts in the NA-induced CRC and this was also observed with rauwolscine, where reductions in the maximal responses were also observed. In the MEV, prazosin was largely inactive in antagonizing NA-induced contractions. In both these vessels a combination of these two antagonists had a greater effect than either alone, indicating the presence of functional α_1- and α_2-adrenoceptors. The post-junctional α_2-adrenoceptors in all of these vessels were resistant to prazosin, suggesting the α_2-adrenoceptor to be of the $\alpha_{2A/2D}$ subtype. The expression of functional α_2-adrenoceptors was MEV>TA>PLV>PCDA>SA.

4 In radioligand binding studies using TA P_2 pellet membranes, [^{3}H]-prazosin and [^{3}H]-RX821002 ([1,4-[6,7(n)-^{3}H] benzodioxan-2-methoxy-2-yl)-2-imidazole) labelled different high affinity sites, and in competition studies using identical membranes corynanthine displaced [^{3}H]-prazosin with 10 fold higher affinity than rauwolscine, indicating that [^{3}H]-prazosin was selectively binding to α_1-adrenoceptor sites. Further, rauwolscine displaced [^{3}H]-RX821002 with approximately 100 fold greater affinity compared to corynanthine, which is indicative of selective α_2-adrenoceptor binding.

5 Separation of the P_2 pellet into plasma membrane and mitochondrial fractions was carried out using a differential sucrose density gradient. [^{3}H]-prazosin and [^{3}H]-RX821002 binding sites were found in both the plasma membrane and mitochondrial fractions.

6 In saturation studies all tissues produced single site saturation curves with no difference in the K_d (range 0.13–0.20 nM) of the α_1-adrenoceptor sites for [^{3}H]-prazosin. However, there was considerable variation in B_{max} of α_1-adrenoceptor sites; the highest density was found in the TA (397.9 ± 52.7 fmol mg^{-1}, $n = 4$), followed by the PCDA (256.7 ± 22.7 fmol mg^{-1}, $n = 4$), the PLV and SA having approximately equal density (143.6 ± 3.9 and 159.1 ± 7.0 fmol mg^{-1} respectively, $n = 4$ for both), followed by the EA (91.3 ± 10.5 fmol mg^{-1}, $n = 3$) and the MEV had the lowest density (48.9 ± 11.4 fmol mg^{-1}, $n = 3$).

7 In saturation studies using [^{3}H]-RX821002, all tissues produced single site saturation curves with no differences in the K_d values (range 1.31 ± 2.16 nM) but the highest densities were found in the TA and MEV (545.3 ± 36.2 and 531.0 ± 40.9 fmol mg^{-1} respectively), followed by the PLV (418.4 ± 39.4 fmol mg^{-1}), then the EA (266.3 ± 40.0 fmol mg^{-1}), and low densities of [^{3}H]-RX821002 binding being found in the PCDA and SA (155.9 ± 18.1 and 117.5 ± 19.3 fmol mg^{-1} respectively).

8 The pattern of binding site distribution for α_1- and α_2-adrenoceptors is in reasonable agreement with functional studies carried out in these porcine vascular tissues; the TA has the highest densities of α_1- and α_2-adrenoceptors; in the SA and PCDA there is a predominance (although small) of α_1-adrenoceptor binding sites, the reverse of which is observed both in the PLV and MEV (i.e. greater density of α_2-adrenoceptor sites). Thus, it would appear that α_1- and α_2-adrenoceptor densities play a role in the expression of functional responses via these receptor subtypes; although it is interesting to note that the SA did have a small density of α_2-adrenoceptor binding sites, no functional response was observed after α_2-adrenoceptor activation.

Keywords: α-Adrenoceptors; [^{3}H]-prazosin; [^{3}H]-RX821002; radioligand binding; contractile responses; porcine vascular tissue

Introduction

It is now well established that α-adrenoceptors can be divided into α_1- and α_2-adrenoceptor subtypes. The existence of these

[1] Author for correspondence.

two subclasses has been demonstrated frequently by functional studies on arterial resistance *in vivo*, but the presence of α_2-adrenoceptors has been more difficult to demonstrate *in vitro* (see Agrawal *et al.*, 1987) with functionality often only being observed in the presence of an ancillary spasmogen (Daly *et al.*, 1988; Dunn *et al.*, 1991). However, overt α_2-adrenoceptor mediated contractions have been observed in a range of non-conduit/distal arteries and veins not generally used for routine experimentation, such as human arterioles (Nielsen *et al.*, 1989), canine saphenous vein (Flavahan & Vanhoutte, 1986), rabbit saphenous vein (Daly *et al.*, 1988), and feline middle cerebral artery (Fredholm *et al.*, 1985). A comparative study by Nielsen *et al.* (1991) examined the pharmacological characteristics of α-adrenoceptor-mediated contractions to noradrenaline in similar sized mesenteric arteries (200 μm diameter) from the rat, rabbit, pig and man and found α_2-adrenoceptor-mediated contractions detectable only in porcine and human blood vessels. Further, there are reports that indicate that α_1- and α_2-adrenoceptors participate in sympathetically mediated vasoconstriction of human vessels (Stevens & Moulds, 1985; Parkinson *et al.*, 1992), yet α-adrenoceptor mediated constrictor responses in small arteries from the rat, guinea-pig and rabbit appear to be exclusively via α_1-adrenoceptors (Angus *et al.*, 1988; McGrath *et al.*, 1989). It seems likely that in small mammals, neuronally activated α_2-adrenoceptors reside on blood vessels too small for routine experimentation (see Ohyanagi *et al.*, 1991).

It has been demonstrated that two superficial blood vessels from the pig, the palmar common digital artery and palmar lateral vein, possess constrictor α_2-adrenoceptors, with the latter preparation containing the larger, functional population (Blaylock & Wilson, 1995). In the present study we have extended our investigation and examined the presence and significance of α_1- and α_2-adrenoceptors using both functional and radioligand binding studies in four other porcine isolated blood vessels; namely, thoracic aorta, splenic artery, ear artery and marginal ear vein. It was then possible to determine whether any differences observed in α_1- and α_2-adrenoceptor binding site densities resulted in the differences in functional responses observed in these vessels (present study; Blaylock & Wilson, 1995).

Some of these results were presented in a preliminary form to the British Pharmacological Society (Blaylock & Wilson, 1993; Wright *et al.*, 1993).

Methods

Functional studies

Preparation of the blood vessel Ears, spleens, thoracic aortae (a length of 15 cm starting 10 cm down from the aortic arch) and trotters from the thoracic limbs were obtained within 30 min of the death of male pigs. The trotters and ears were placed on ice, while the spleens and aortae placed in Krebs-Henseleit saline (previously gassed with 95%O_2/5%CO_2 and maintained at 4°C), and transported to the laboratory. A 3–4 cm length of the palmar common digital artery (PCDA) and palmar lateral vein (PLV), a 4 cm segement of the splenic artery (SA), just proximal to the point where it gives rise to the left gastroepiploic artery, and a 2–3 cm segment of the marginal ear vein (MEV) (the location of these vessels is shown in Figure 1) were dissected out and stored overnight at 4°C in modified Krebs-Henseleit saline containing 2% Ficoll which had been previously gassed with 95%O_2/5%CO_2. In the case of the thoracic aorta (TA), preliminary experiments have established that these storage conditions produce excessive impairment of contractile function, so 7 mm ring segments (without the adventitia) were stored overnight at 37°C in Krebs-Henseleit saline containing 2% Ficoll and continually gassed with 95%O_2/5%CO_2. Krebs-Henseleit saline used for storage purposes was prepared with twice distilled water, while single distilled water was used for saline required for experimental purposes. The composition of the modified Krebs-Henseleit saline was (mM): NaCl 118.4, KCl 4.7, $CaCl_2$ 1.25, $MgSO_4$ 1.2, $NaHCO_3$ 24.9, KH_2PO_4 1.2 and glucose 11.1.

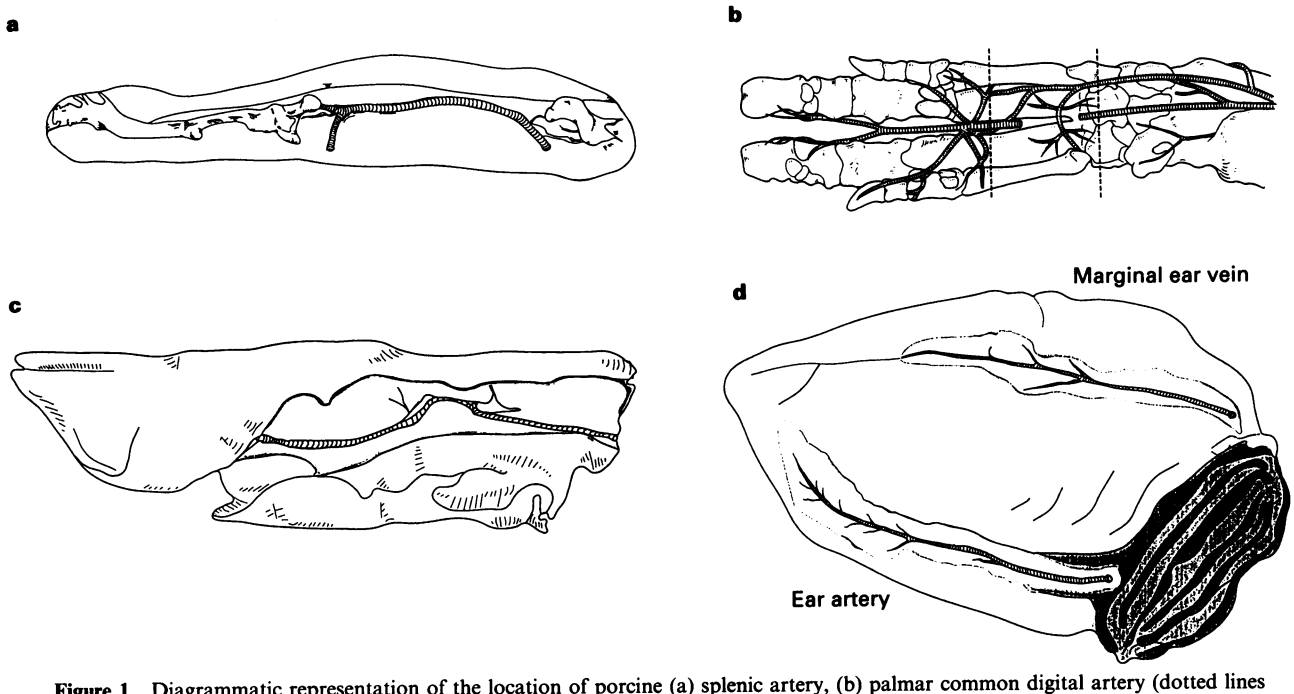

Figure 1 Diagrammatic representation of the location of porcine (a) splenic artery, (b) palmar common digital artery (dotted lines indicate region of the vessel used), (c) palmar lateral vein, and (d) ear artery and marginal ear vein. Each tissue is not to scale in comparison with the others.

Isometric tension recordings On the following day, the blood vessels were carefully cleaned of connective tissue and divided into 5 mm ring segments. Stainless steel wire supports (0.15 mm thick for ear veins, 0.2 mm thick for palmar lateral veins and palmar common digitial arteries and 0.5 mm thick for splenic arteries and thoracic aortae) were inserted into the lumen and each segment suspended in an isolated organ bath containing modified Krebs-Henseleit saline. Cocaine (10 μM), to inhibit uptake1, propranolol (1 μM), to inhibit β-adrenoceptors, and Na_2EDTA (23 μM), to prevent the oxidative degradation of NA, were included. The Krebs-Henseleit saline was maintained at 31°C for the ear vein, and at 37°C for the SA and TA, and gassed with $95\%O_2/5\%CO_2$. The superficial blood vessels were maintained at 31°C because previous studies have shown that α_2-adrenoceptor function is enhanced at lower temperature (Flavahan & Vanhoutte, 1986; Templeton *et al.*, 1989). No attempt was made to remove the endothelium. The lower support was fixed, and the upper support was connected to a Grass FT-03 transducer linked to Grass Polygraph. After 30 min equilibration in the Krebs-Henseleit saline, approximately 20 g wt. tension, 12 g wt. tension, and 2 g wt. tension was slowly applied to the TA, SA, and MEV, respectively, and allowed to relax to a final resting tension of 10–12 g wt., 3–4 g wt., and 0.3–0.4 g wt., respectively. After 60 min equilibration the preparations were exposed to either 60 mM KCl (TA) or 1 μM NA (the other vessels), and the contraction allowed to proceed to maximum. Following complete washout, the preparation was again challenged with the spasmogen, washed and an additional 1 h equilibration period allowed before starting the experiment. If these procedures resulted in excessive loss of resting tension (>30%), then preparations had tension reapplied prior to the beginning of the experiment. This procedure was found to minimize changes in the sensitivity of the preparation to further addition of NA.

In all experiments, cumulative concentration-response curves (CRC) were constructed by exposing the tissue to increasing concentrations (0.5 log unit increments) of the agonist until a maximum response was observed. Since contractile responses of the MEV to the α-adrenoceptor agonists were not well maintained over a period greater than 90 s, the addition of the next concentration of the agonist was made as close to the peak response as possible.

The effect of agonists For the TA, only one agonist concentration-response curve was generated per tissue and responses to NA, PE, and UK-14304 were compared to that produced by 60 mM KCl. For the other two vessels, two concentration-response curves were generated: NA followed by either UK-14304 or PE. The concentration-response curves were obtained 60 min apart, as measured from the time following washout and complete relaxation of the preparation.

The effect of the antagonists The α-adrenoceptor antagonists, prazosin (0.01–1 μM) and rauwolscine (0.1–10 μM) or a combination of the subtype-selective antagonists were added at least 40 min prior to the construction of a second or third CRC to NA. In the case of the TA, however, only one CRC was possible and the effects of the α-adrenoceptor antagonists were examined by a comparison of paired tissues.

Data analysis In the SA and MEV the sensitivity of the preparations to the agonists was assessed as the negative logarithm of the concentration required to cause 50% of the maximum response (pD_2). The agonist concentration-ratio in the presence and absence of the antagonist was determined at the level of 50% of the maximum response, or 40% level of response produced by 60 mM KCl (TA). Using the agonist concentration-ratio produced by the lowest effective concentration of the antagonist, an estimate of the negative logarithm of the dissociation constant (pK_B) was determined by the method of Furchgott (1972) or, where possible, a pA_2 value was determined by the method of Arunlakshana & Schild (1959).

In all experiments, one preparation was run in parallel with the experimental tissues, but received no antagonist, and was used to determine any time-dependent changes in agonist sensitivity (Furchgott, 1972). All responses are expressed as a percentage of the maximum response and given as the mean ± s.e.mean. Differences between means were considered statistically significant if $P<0.05$ for unpaired or paired observations (Student's *t* test). The logarithm of the concentration of NA producing either 50% of the control maximum response (pD_2) or agonist-concentration ratios were calculated with the logistic equation described by DeLean *et al.* (1978) with Kaleidagraph software (Synergy) on a MacIntosh LC II computer.

Radioligand binding

Tissue preparation Vessels were dissected out as described earlier. The amount of tissue (wet weight) required for each membrane preparation was approximately 1 TA (~15 g), 25 SA (~15 g), 30 PCDA, PLV, EA and MEV (~4 g).

Each tissue was crudely cut into pieces in a McIlwain tissue chopper and then homogenized with a Polytron disrupter (2 × 30 s, at maximum setting) in a minimum volume of ice-cold 50 mM Tris HCl buffer (pH 7.6 at 25°C) and then made up to approximately 10 volumes. This homogenate was subjected to step-wise differential centrifugation at 4°C, first at 1000 *g* for 10 min to remove unbroken tissue, nuclei, collagen and contractile protein. The post-nuclear supernatant (PNS) was then centrifuged at 40,000 *g* for 20 min to sediment the remaining fraction (P_2). The P_2 pellet was resuspended in 2 volumes original wet weight of 50 mM Tris HCl and saturation and competition binding studies were carried out as described below. All binding studies were carried out in freshly prepared PNS.

Differential sucrose density gradient (aorta only) The P_2 pellet was resuspended in 9 ml of 0.32 M sucrose and 6 × 1.5 ml layered on top of a differential sucrose density gradient composed of 3.5 ml each of 1.2 M, 0.8 M and 0.32 M sucrose solutions then centrifuged at 75,000 *g* for 60 min at 4°C. Three distinct bands were obtained: fraction 1 between the 0.32 M and 0.8 M sucrose solutions (myelin and connective tissue); fraction 2 between the 0.8 M and 1.2 M sucrose solutions (plasma membranes); fraction 3 the pellet (mitochondria and endoplasmic reticulum). The plasma membranes and mitochondrial fractions were removed by pasteur pipette and diluted in 50 mM Tris-HCl, disrupted by either shaking or low speed polytron and recentrifuged at 40,000 *g* for 20 min. The sedimented plasma membranes and mitochondrial fractions were resuspended in 2 volumes original wet weight of 50 mM Tris-HCl and used for radioligand binding. The presence and enrichment of the plasma membrane and mitochondrial fractions was determined by electron microscopy and enzyme markers (plasma membrane – 5'nucleotidase; mitochondria – succinate dehydrogenase).

For all enzyme marker and radioligand binding studies aliquots of the appropriate membrane (1 ml) were stored at −18°C for subsequent protein determination by the method of Bradford (1976).

Enzyme marker assays

5'Nucleotidase 5'Nucleotidase activity was measured as inorganic phosphate (P_i) released after incubation for 150 min in 5 ml of buffered 250 μmol 5'AMP, pH 7.0 at 37°C. Non-specific phosphatase activity was determined with glycerolphosphate as the substrate (250 μmol, pH 7.0 at 37°C) and taken into account when calculating 5'nucleotidase activity. After stopping the reaction with 1 ml 30% trichloroacetic acid and centrifuging down the precipitated protein, the liberated P_i was determined by the spect-

rophotometric method of Fiske & SubbaRow (1925). Results are expressed as μmol P_i h^{-1} mg^{-1} protein.

Succinate dehydrogenase

Succinate dehydrogenase was assayed based on the method of Pennington (1961), where succinate is oxidized to fumerate by succinate dehydrogenase and correspondingly (2-*p*-iodophenyl)-3-(*p*-nitrophenyl)-5-phenyl tetrazolium chloride (INT) is changed from an oxidized (yellow) to a reduced (red) state. This is then measured spectrophotometrically. Results are expressed as μmol formazan min^{-1} mg^{-1} protein.

Electron microscopy

Pellets were fixed in 2% glutaraldehyde:2% paraformaldehyde in 50 mM Tris-HCl (pH 7.4) for 2 h, post-fixed in 1% OsO_4 for 1 h, buffer washed, and treated with 2% aqueous uranyl acetate for 30 min. Samples were then dehydrated via graded acetone, embedded in Transmit resin (Tabb Laboratories Ltd.), and polymerised for 24 h at 70°C. Individual 90 nm thick sections were cut on a Reichart Ultracut E ultramicrotome and electron micrographs taken on a Philips EM410 electromicroscope.

Saturation binding

[^{3}H]-prazosin A final assay volume of 0.5 ml was employed; this comprised 200 μl membrane preparation (protein concentration 0.8–3.2 mg ml^{-1}), 200 μl 50 mM Tris HCl, 50 μl 50 mM Tris HCl or NA (10 μM), and 50 μl [^{3}H]-prazosin (specific activity 669.7 GBq $mmol^{-1}$) over a range of 8 concentrations from 0.04–5 nM. Each experiment was carried out in duplicate. The binding reaction was initiated by the addition of 200 μl membrane preparation and the mixture was incubated for 30 min at room temperature. NA (10 μM) was used to define non-specific binding (NSB). Membrane-bound radioactivity was recovered by filtration under vacuum through Whatman GF/B filters using a Brandel cell harvester. Filters were rinsed with cold buffer (6°C) immediately prior to filtration and filter-bound membranes were rapidly washed twice with cold buffer.

[^{3}H]-RX821002 [^{3}H]-RX821002 saturation studies were carried out which were identical to those with [^{3}H]-prazosin with the exception that the concentration-range of [^{3}H]-RX821002 (specific activity 1.78 TBq.$mmol^{-1}$) was 0.08–10 nM, with an incubation period of 60 min at room temperature.

Competition binding

Competition studies were performed with the P_2 pellet, plasma membrane and mitochondrial fractions of the thoracic aorta, employing a 0.5 ml assay volume (composition as for saturation binding) with a single concentration of either [^{3}H]-prazosin (0.1–0.3 nM), or [^{3}H]-RX821002 (1–1.5 nM) in the presence of increasing concentrations of either yohimbine or its stereoisomers rauwolscine and corynanthine (10 pM–100 μM). Incubation and assay conditions were as for those of saturation studies. Each experiment was carried out in triplicate.

Data analysis

In saturation studies, the equilibrium dissociation constant (K_d) and maximum density of binding sites (B_{max}) were determined by iterative fitting to a least squares non-linear equation (Kaleidagraph, MacIntosh). Competition data were also analysed using iterative fitting to generate IC_{50} values (concentration of drug displacing 50% specific binding). The IC_{50} was converted to the inhibitory constant (K_i) by the equation of Cheng & Prusoff (1973) where $K_i = IC_{50}/1 + ([ligand]/K_d)$.

Drugs

The following compounds were used: (−)-noradrenaline bitartrate (Sigma); prazosin HCl (Pfizer); rauwolscine HCl (Roth); UK-14304 (5-bromo-6-[2-imidazolin-2-ylamino]-quinoxaline bitartrate, Pfizer); propranolol HCl (Sigma); phenylephrine hydrochloride (Sigma); cocaine HCl (MacCarthys); yohimbine HCl (Sigma); corynanthine HCl (Sigma); Ficoll 70,000 (Sigma); [^{3}H]-prazosin (N.E.N. Research); [^{3}H]-RX821002 (Amersham); Tris HCl (Sigma); adenosine-5′-monophosphate (5′AMP, Sigma); glycerolphosphate (Sigma); trichloracetic acid (Sigma); Fiske and SubbaRow reagent (Sigma); succinic acid (Sigma); (2-*p*-iodophenyl)-3-(*p*-nitrophenyl)-5-phenyl tetrazolium chloride (INT, Sigma). For functional studies stock solutions of noradrenaline were prepared in distilled water with 23 μM Na_2EDTA, prazosin (1 mM) was dissolved in 0.1 M lactic acid and dilutions made in distilled water; all other drugs were dissolved in distilled water and added to the organ baths in a volume of 0.1 ml or less. For radioligand binding [^{3}H]-prazosin and [^{3}H]-RX821002 were made up fresh each day in 50 mM Tris HCl. Noradrenaline, yohimbine, rauwolscine and corynanthine were prepared fresh each day in 50 mM Tris HCl. Buffered 5′AMP and glycerolphosphate, trichloroacetic acid, Fiske and SubbaRow reagent, succinic acid and INT were prepared fresh on the day of the experiment.

Results

Functional studies

Overnight-storage of blood vessels In preliminary experiments with TA segments previously stored overnight at 4°C, 60 mM KCl failed to produce responses greater than 3 g wt. ($n = 5$). However, in 'fresh' (used same day) and 'overnight-stored' (37°C with 95%O_2/5% CO_2) segments 60 mM KCl produced larger contractions, 15.3 ± 2.5 g wt. ($n = 6$) and 11.3 ± 2.9 g wt. ($n = 12$), respectively, which took 20–30 min to reach maximum. All further experiments on the TA were conducted on segments stored overnight in Krebs-Henseleit saline with 2% Ficoll, gassed with 95%O_2/5%CO_2 and maintained at 37°C. Preparations that responded to 60 mM KCl with a contraction of less than 3 g wt. (approximately 1 in 6) were discarded. The other blood vessels were stored overnight at 4°C in Krebs-Henseleit saline with 2% Ficoll, a procedure which did not impair either contractile or dilator function (see Lot & Wilson, 1994).

Response to α-adrenoceptor agonists Noradrenaline (0.01–30 μM) produced concentration-dependent contractions of ring segments of the SA (Figure 2a), TA (Figure 2b) and MEV (Figure 2c) with a maximum response of 16.2 ± 1.1 g wt. ($n = 8$), 14.0 ± 3.8 g wt. ($n = 12$) and 2.21 ± 0.24 g wt. ($n = 8$), respectively. Contractions in the TA were considerably slower than those in SA and MEV, requiring up to 15 min to reach equilibrium. In the TA and MEV, NA was 3 to 10 fold more potent than PE but less potent UK-14304 (Table 1). In both tissues the maximum response to UK-14304 was 60% of that produced by NA (Figure 2a,c). In the SA, the maximum response to UK-14304 and PE was less than 10% and 50% respectively, of the maximum response to NA (Table 1, Figure 2b), and NA was 3 fold more potent than PE.

The effect of prazosin and rauwolscine against noradrenaline-induced contractions Prazosin produced qualitatively different inhibition against NA-induced contractions in the SA, TA and MEV (Figure 3). In the SA, NA-induced contractions were competitively antagonized by prazosin (pA_2 8.60 ± 0.15) with the slope of the Schild plot not being different from unity (0.95 ± 0.09) (Figure 3a). In the TA, 0.01 μM and 0.1 μM prazosin caused a non-parallel,

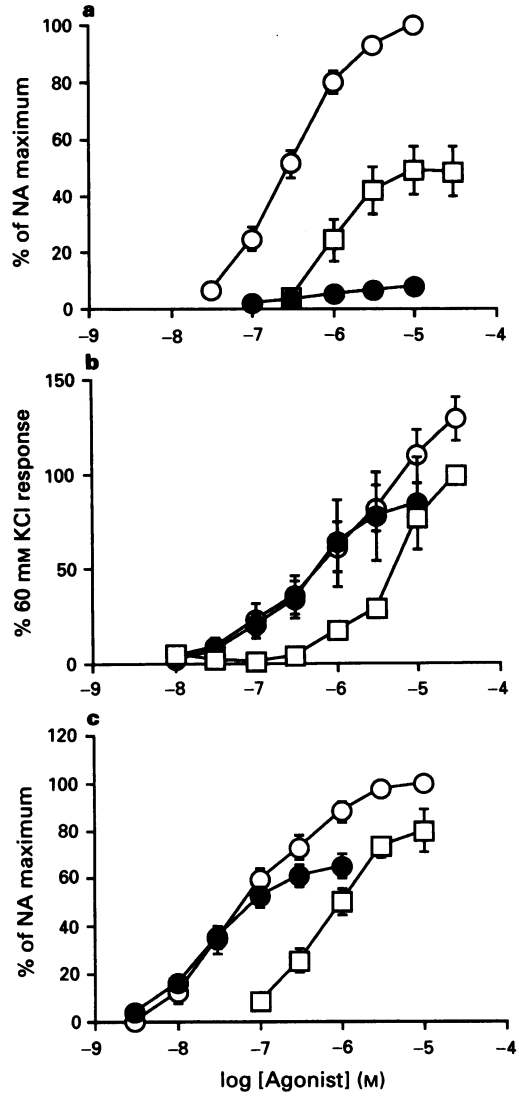

Figure 2 The effect of (○) noradrenaline, (□) phenylephrine and (●) UK-14304 in the porcine isolated (a) splenic artery, (b) thoracic aorta and (c) marginal ear vein. Responses have been expressed as a percentage of either the response to 60 mM KCl (a) or the maximum response to noradrenaline (b,c). All points represent the mean of 5–12 observations and the vertical lines indicate the s.e.mean.

concentration-dependent, rightward displacement of the NA concentration-response curve. At the level of 40% of the response to 60 mM KCl, 0.1 μM prazosin produced a 50 fold displacement of the NA CRC (Table 2), which was associated with a 35% reduction in the maximum response. Prazosin (1 μM) failed to cause a greater inhibition of the responses than that produced by 0.1 μM prazosin (Figure 3b). In the MEV, however, 0.01 μM and 0.1 μM prazosin were largely inactive, producing only a 2 fold rightward displacement of the noradrenaline CRC, while 1 μM prazosin caused a 30 fold rightward, displacement of the CRC (Figure 3c and Table 2).

In the SA, 1 μM and 10 μM rauwolscine produced a concentration-dependent, parallel displacement of the NA CRC; 0.1 μM rauwolscine was inactive (Figure 4a). Based upon the effect of 1 μM rauwolscine, the estimated $-\log K_B$ value was 6.09 ± 0.11 ($n = 6$). In contrast, 0.1 μM–10 μM rauwolscine produced a concentration-dependent, non-parallel, rightward displacement of responses in the TA, which was associated with a reduction in the maximum responses (Figure 4b).

In the SA, the combination of 0.1 μM prazosin and 1 μM

Table 1 Mean pD_2 (± s.e.mean) and E_{max} values for various agonists in several isolated blood vessels from the pig

		Thoracic aorta	*Splenic artery*	*Marginal ear vein*
Noradrenaline	pD_2	5.71 ± 0.09	6.82 ± 0.08	7.35 ± 0.09
	E_{max}	1	1	1
Phenylephrine	pD_2	5.2[a]	5.95 ± 0.09	6.24 ± 0.10
	E_{max}	>0.8	0.48	0.80
UK-14304	pD_2	6.24 ± 0.11	<6.5[a]	7.51 ± 0.09
	E_{max}	0.58	>0.08	0.65

The results shown are from observations in 7–12 animals. [a]A true maximum was not obtained, so the value shown has been estimated.

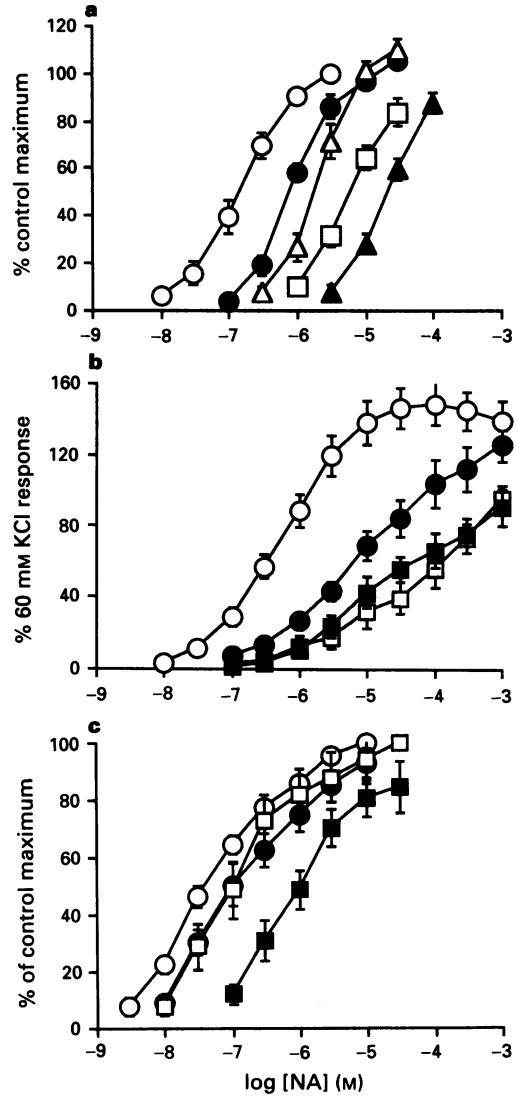

Figure 3 The effect of (●) 0.01 μM, (△) 0.03 μM, (□) 0.1 μM, (▲) 0.3 μM and (■) 1.0 μM prazosin against noradrenaline-induced contractions of the porcine isolated (a) splenic artery, (b) thoracic aorta and (c) marginal ear vein. The control concentration-response curve to noradrenaline is represented by (○). All points represent the mean of 5–10 observations and the vertical lines indicate the s.e.mean.

rauwolscine was no more effective than 0.1 μM prazosin alone (Table 2). This contrasts with observations in the TA and MEV, where the combination of the two antagonists produced more than a 1000 fold displacement of the noradrenaline CRC (Tabel 2), which was significantly greater than the effect of either antagonist alone.

Table 2 Logarithm of the concentration-ratio for noradrenaline produced by 'selective' concentrations of prazosin and rauwolscine, either alone or in combination, in the porcine isolated splenic artery (SA), thoracic aorta (TA) and marginal ear vein (MEV)

	SA	*TA*	*MEV*
Prazosin 0.1 μM	1.63 ± 0.12 ($n = 5$)	1.72 ± 0.32 ($n = 6$)	0.42 ± 0.16 ($n = 7$)
Rauwolscine 1 μM	0.09 ± 0.21 ($n = 6$)	0.58 ± 0.17 ($n = 6$)	1.20 ± 0.13 ($n = 4$)
Prazosin 0.1 μM + Rauwolscine 1 μM	1.85 ± 0.07 ($n = 5$)	2.62 ± 0.13 ($n = 6$)[a]	3.21 ± 0.20 ($n = 7$)[a]

Values shown are the mean ± s.e.mean of n experiments (shown in parentheses).
[a]$P < 0.05$ significantly different from the effect of the antagonist alone: Student's 2-tailed t test.
The values shown were calculated at the level of 40% of the response to 60 mM KCl (TA) or 50% of the maximum response to noradrenaline (SA, MEV).

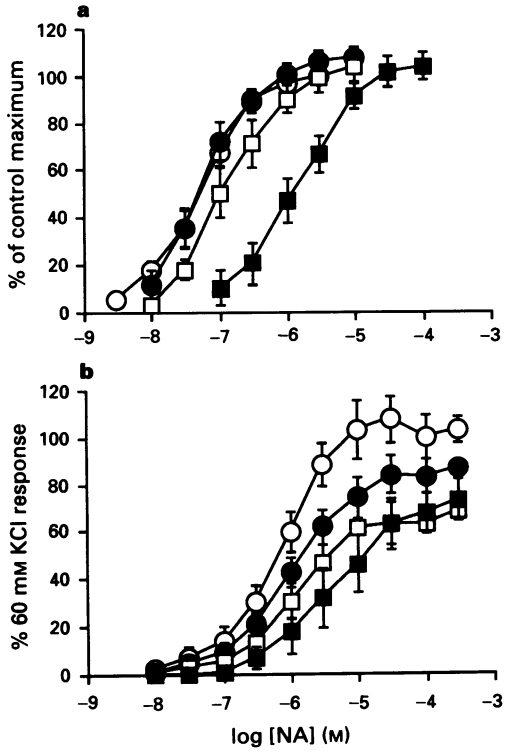

Figure 4 The effect of (●) 0.1 μM, (□) 1.0 μM, (■) 10 μM rauwolscine against noradrenaline-induced contractions of the porcine isolated (a) splenic artery and (b) thoracic aorta. The control concentration-response curve to noradrenaline is represented by (○). All points represent the mean of 6–10 observations and the vertical lines indicate the s.e.mean.

Radioligand binding

Porcine thoracic aorta saturation studies Saturation analysis of [^{3}H]-prazosin binding revealed a single, high affinity binding site in the P_2 pellet of the TA (Figure 5a illustrates an individual saturation isotherm), with an affinity (K_d) of 0.20 ± 0.03 nM and density (B_{max}) of 397.9 ± 52.7 fmol mg^{-1} ($n = 4$). Similarly, saturation analysis of [^{3}H]-RX821002 binding in the TA revealed a single, high affinity site (Figure 5b illustrates an individual saturation isotherm), with a K_d of 2.16 ± 0.18 nM and B_{max} 545.3 ± 36.2 fmol mg^{-1} ($n = 4$).

Competition studies Rauwolscine and corynanthine displaced [^{3}H]-prazosin and [^{3}H]-RX821002 binding to the TA membranes in a concentration-dependent manner (Figure 5c and 5d show displacement profiles from individual experiments). The competition curves generated were fitted to a one-site model and the mean pK_i values for yohimbine, rauwolscine and corynanthine against the two ^{3}H-ligands were calculated (Table 3). Corynanthine had a 5–10 fold greater affinity for [^{3}H]-prazosin binding compared to rauwolscine (Figure 5c and Table 3). Table 3 shows that the slopes of the displacement curves of [^{3}H]-prazosin by both rauwolscine and corynanthine were close to unity, indicating binding to a single site. Figure 5d (and Table 3) indicated that rauwolscine had approximately 100 fold higher affinity for [^{3}H]-RX821002 binding than corynanthine. However, the slopes of the displacement curves were different from unity with [^{3}H]-RX821002 (Table 3).

Competition binding carried out in the subcellular fractions obtained following differential sucrose gradient centrifugation revealed α_1- and α_2-adrenoceptor binding in both the plasma membrane and mitochondrial fractions. The affinity ratios of rauwolscine to corynanthine suggest that [^{3}H]-prazosin and [^{3}H]-RX821002 are labelling α_1- and α_2-adrenoceptor binding sites respectively in the two fractions, and the pK_i and Hill slope values obtained from analysis of the curve fitting indicate displacement of [^{3}H]-prazosin and [^{3}H]-RX821002 from separate high affinity sites (Table 3).

Enzyme markers and electron microscopy The highest 5'-nucleotidase activity was located in the plasma membrane fraction, an approximate 17 fold enrichment from the P_2 fraction, with very little enrichment in the mitochondrial fraction (Table 4). The highest succinate dehydrogenase activity was located in the mitochondrial fraction; about 2 fold greater than in the P_2 fraction, and activity was almost totally absent in the plasma membrane fraction (Table 4).

Electron micrographs of the plasma membrane and mitochondrial fractions revealed that the plasma membrane fraction is almost exclusively composed of vesicles of plasma membrane (Figure 6a), and the mitochondrial fraction (Figure 6b) shows a high density of mitochondria and some endoplasmic reticulum (often with ribosomes attached).

Saturation studies in other porcine blood vessels

There was no difference in the affinity (K_d) of [^{3}H]-prazosin for the binding site between the different tissues but marked variation was observed in the density of α_1-adrenoceptor binding sites (B_{max}). The highest density of [^{3}H]-prazosin binding was observed in the TA (approximately twice the density of the PCDA, 3 times higher than the PLV and SA, and 4–6 times greater than the EA and MEV), followed by the PCDA, and the PLV and SA having approximately equal density, followed by the EA and with MEV having the lowest density (Table 5).

As with [^{3}H]-prazosin, there was no difference in the affinity (K_d) of [^{3}H]-RX821002 for the α_2-adrenoceptor binding sites in each of the tissues but the density (B_{max}) of [^{3}H]-RX821002 binding varied considerably from tissue to tissue. The highest density was observed in the TA and MEV, followed by the PLV, then the EA, and low densities of [^{3}H]-RX821002 binding being found in the PCDA and SA (Table 5).

Correlations

[^{3}H]-RX821002 binding site density was plotted against [^{3}H]-prazosin binding site density for either all six vessels (Figure

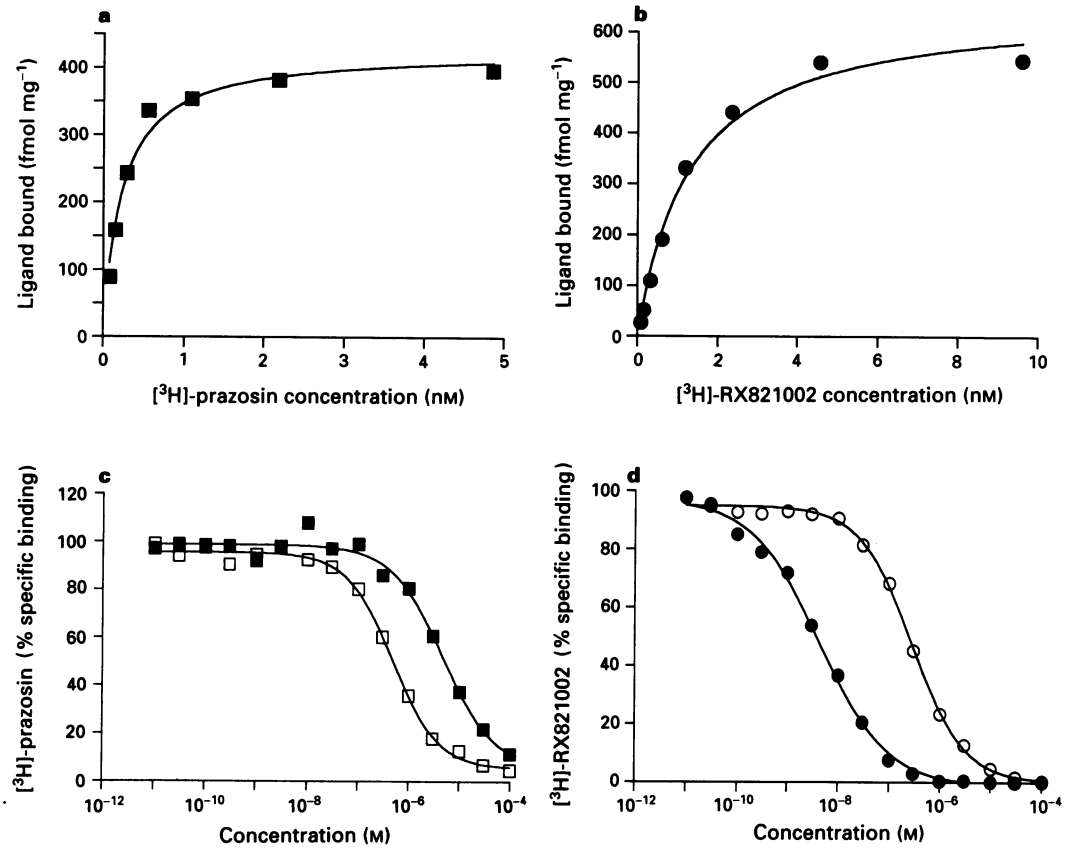

Figure 5 Specific saturation binding curves of (a) [^{3}H]-prazosin and (b) [^{3}H]-RX821002 to porcine thoracic aorta membranes, non-specific binding being defined as that remaining in the presence of 100 μM noradrenaline or 100 μM yohimbine respectively. Each saturation curve represents a typical experiment carried out in duplicate, and is a representative example of 3 to 4 experiments. The K_d and B_{max} values determined from these curves are given in Table 5. Competition for (c) [^{3}H]-prazosin and (d) [^{3}H]-RX821002 binding sites by rauwolscine (solid symbols) and corynanthine (open symbols) in porcine thoracic aorta membranes. The data represent a typical experiment carried out in triplicate, and are representative of 3 to 4 experiments. On the vertical axis, data are expressed as a percentage of control specific [^{3}H]-prazosin or [^{3}H]-RX821002 binding. The concentrations of [^{3}H]-prazosin and [^{3}H]-RX821002 used were 0.1–0.3 nM and 1–15 nM respectively. pK_i values of the antagonists and the Hill coefficients (slope) of the curves are given in Table 3.

Table 3 Inhibition constants of yohimbine, rauwolscine and corynanthine at [^{3}H]-prazosin and [^{3}H]-RX821002 labelled binding sites in porcine thoracic aorta P_2 pellet, plasma membrane fraction, and mitochondria fraction

	[^{3}H]-prazosin		*[^{3}H]-RX821002*	
P_2	pK_i	Slope	pK_i	Slope
Yohimbine	–	–	8.41 ± 0.02	−0.64 ± 0.02
Rauwolscine	5.22 ± 0.13	−0.96 ± 0.10	8.41 ± 0.02	−0.64 ± 0.02
Corynanthine	6.22 ± 0.16	−0.99 ± 0.14	6.50 ± 0.05	−0.81 ± 0.02
Membranes				
Rauwolscine	5.10 ± 0.15	−0.75 ± 0.08	8.43 ± 0.09	−0.80 ± 0.12
Corynanthine	6.16 ± 0.05	−0.82 ± 0.04	6.09 ± 0.12	−0.74 ± 0.03
Mitochondria				
Rauwolscine	5.12 ± 0.12	−0.76 ± 0.08	8.21 ± 0.09	−0.74 ± 0.12
Corynanthine	6.01 ± 0.05	−0.80 ± 0.04	6.09 ± 0.04	−0.76 ± 0.03

Each pK_i and Hill coefficient (slope) value is the mean ± standard error of the mean (s.e.mean) of 3 to 4 separate experiments, each carried out in triplicate. pK_i values were calculated from the Cheng & Prusoff equation (1973).

Table 4 5′-Nucleotidase and succinate dehydrogenase activities in the different fractions obtained in the preparation of the plasma membrane and mitochondrial fractions

	Enzyme			
	5′-Nucleotidase		*Succinate dehydrogenase*	
Fraction	μmol mg^{-1} h^{-1}	Relative to P_2	μmol min^{-1} mg^{-1}	Relative to P_2
Homogenate	0.25	0.22	0.0045	0.07
P_2	1.15	1	0.0612	1
Mitochondria	1.66	1.44	0.0952	1.59
Membranes	19.50	17.0	0.0004	0.006

7a) or all vessels except the TA (Figure 7b); using simple line regression analysis no correlation was found between the densities of the two binding sites in all 6 vessels (slope = 0.173, $r = 0.118$, $P = 0.825$; Figure 7a) but when the TA data were excluded a weak inverse relationship between the 2 binding site densities was observed (slope = 1.592, $r = 0.721$, $P = 0.175$; Figure 7b).

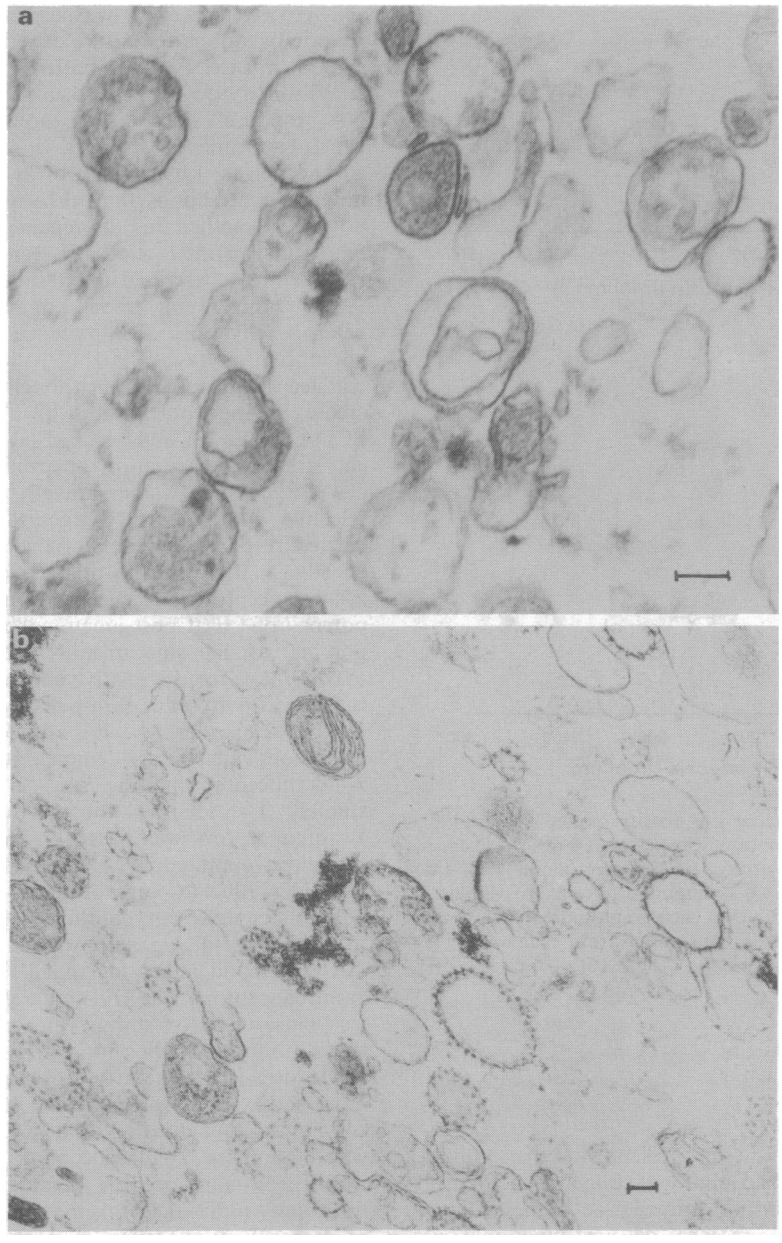

Figure 6 Electron micrographs of (a) plasma membrane vesicles and (b) intact and ruptured mitochondria (with the presence of some endoplasmic reticulum with attached ribosomes). Fractions of porcine thoracic aorta were prepared using differential sucrose density gradients. On both figures the size bar is equivalent to 0.1 μm.

Table 5 α_1-Adrenoceptor and α_2-adrenoceptor densities labelled with [^{3}H]-prazosin and [^{3}H]-RX821002 respectively in six porcine vascular tissues

Tissue	*[^{3}H]-prazosin*		*[^{3}H]-RX821002*	
	K_D (nM)	B_{max} (fmol mg^{-1})	K_D (nM)	B_{max} (fmol mg^{-1})
Thoracic aorta	0.20 ± 0.03	397.9 ± 52.7	2.16 ± 0.18	545.3 ± 36.2
Digital artery	0.14 ± 0.03	256.7 ± 22.7	1.80 ± 0.31	155.9 ± 18.1
Lateral vein	0.14 ± 0.03	143.6 ± 3.9	1.68 ± 0.39	418.4 ± 39.4
Splenic artery	0.15 ± 0.04	159.1 ± 7.0	2.11 ± 0.20	117.5 ± 19.3
Ear artery	0.15 ± 0.05	91.3 ± 10.5	1.43 ± 0.04	266.3 ± 40.0
Ear vein	0.13 ± 0.03	48.9 ± 14.4	1.31 ± 0.89	531.0 ± 40.9

Each value represents the mean ± standard error of the mean (s.e.mean) of 3 to 4 separate experiments for each radioligand. Each experiment was carried out in duplicate.

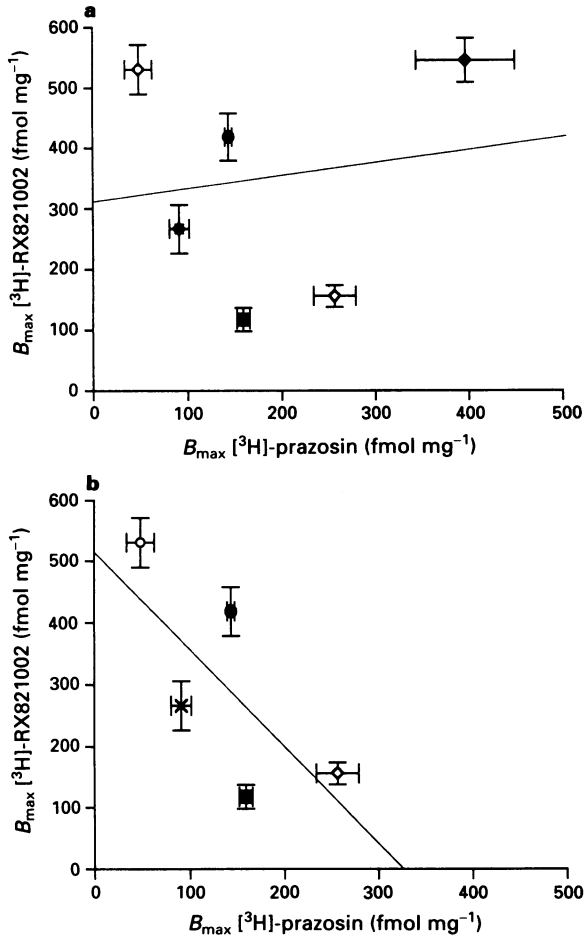

Figure 7 [^{3}H]-RX821002 binding site density plotted against [^{3}H]-prazosin binding site density in: (a) all six vessels: (◆) thoracic aorta, (◇) palmar common digital artery, (●) palmar lateral vein, (■) splenic artery, (×) ear artery, (○) marginal ear vein; (b) all vessels except the thoracic aorta. The line on each graph represents a simple regression analysis of the 6 or 5 data points from each vessel; (a) slope = 0.173, correlation coefficient = 0.118; (b) slope = −1.592, correlation coefficient = 0.721.

Discussion

As indicated by the results in the present study on porcine vascular smooth muscle, and those of Blaylock & Wilson (1995), the use of prazosin or rauwolscine alone may be sufficient to suggest the presence of post-junctional α_2-adrenoceptors that are activated by NA, i.e. either by the higher potency of rauwolscine or apparent resistance of responses to prazosin (McGrath *et al.*, 1989). However, unequivocal demonstration of the presence of α_2-adrenoceptors was provided by the use of 'selective' concentrations of the antagonists which, with the exception of the SA, produced a greater effect against responses to NA than either antagonist alone in the TA and MEV (present study) and the PCDA and PLV (Blaylock & Wilson, 1995). The insensitivity of responses to even a high concentration of prazosin (1 μM) indicates that the postjunctional α_2-adrenoceptors fall into the α_{2A}/α_{2D} category (Wilson *et al.*, 1991). The result in the SA, that the combination of antagonists was no more effective than prazosin alone, is of particular importance since several other observations also argue against the presence of a significant population of α_2-adrenoceptors. First, prazosin behaved as a competitive antagonist against NA-induced contractions with a pA_2 value (8.6); a value consistent with α_1-adrenoceptors (McGrath *et al.*, 1989). Second, the estimated dissociation constant for rauwolscine (approximately 6) is also consistent with an interaction with α_1-adrenoceptors. Third, UK-14304 failed to elicit a response larger than 5% of the NA maximum. Thus, expression of functional α_2-adrenoceptors in porcine blood vessels appears to increase in the order SA, PCDA, PLV, TA and MEV (data for PCDA and PLV is unpublished).

There are, however, two surprising observations that may have implications for future experiments on porcine vascular smooth muscle. First, in both the TA and PCDA (Blaylock & Wilson, 1995) 1 μM prazosin was no more effective against NA responses than 0.1 μM prazosin, while in the MEV, which appears to possess a larger population of α_2-adrenoceptors, 1 μM prazosin was more effective against NA-induced contractions than 0.1 μM prazosin. At present it is not clear whether this discrepancy between the preparations represents an interaction between α_1- and α_2-adrenoceptors, as previously described in rabbit blood vessels (Daly *et al.*, 1988; Dunn *et al.*, 1991), or is due to α_2-adrenoceptor heterogeneity, i.e. the presence of prazosin-sensitive α_2-adrenoceptors (α_{2B}/α_{2C}); this will form the basis of more detailed future studies. Although there is an apparent increase in the contribution of α_2-adrenoceptors from SA, PCDA, PLV, TA and MEV (Blaylock & Wilson, 1995; present study), the situation regarding α_1-adrenoceptors is less clear. PE, which was employed because it is regarded as a selective α_1-adrenoceptor agonist (McGrath *et al.*, 1989), elicited responses in each of the preparations but was least effective in the SA; the preparation with almost exclusively α_1-adrenoceptors. As we have not examined the relative potency of PE at post-junctional α_1- and α_2-adrenoceptors in porcine vascular smooth muscle, the only functional marker that we have for the relative contribution of α_1-adrenoceptors is the sensitivity of NA responses to prazosin (0.1 μM): these were in the order SA, TA and MEV.

Radioligand binding demonstrated the existence of α_1- and α_2-adrenoceptor binding sites in all the vascular tissues studied. The identification of these two sites as α_1- and α_2-adrenoceptors was based on the radiolabelled binding of the selective antagonists [^{3}H]-prazosin (α_1-adrenoceptors) and [^{3}H]-RX821002 (α_2-adrenoceptors) (Wilson *et al.*, 1991). At α_1-adrenoceptors, corynanthine has 5–10 fold greater affinity than rauwolscine, agreeing well with the competition binding in the TA and indicating that [^{3}H]-prazosin binding was to α_1-adrenoceptors. The Hill slope of [^{3}H]-prazosin binding was very close to unity, adding further support to evidence from the saturation binding that [^{3}H]-prazosin is binding to a single site. However, at α_2-adrenoceptors rauwolscine is the more active stereoisomer having 100 fold higher affinity than corynanthine, indicating that in this study [^{3}H]-RX821002 was binding to α_2-adrenoceptors. The Hill slopes obtained with the α_2-adrenoceptor binding were somewhat different from unity (0.65–0.8); this may possibly indicate the presence of more than one type of α_2-adrenoceptor, resulting in a shallow displacement curve.

Initial studies in the TA used membranes from the post-nuclear supernatant (PNS) or P_2 pellet as the yield obtained meant the initial amount of tissue required was not too great. However, when plasma membrane and mitochondrial fractions from the TA were purified using differential sucrose density gradient it greatly reduced the yield. Confirmation that the plasma membrane and mitochrondrial fractions were composed of predominantly these structures was obtained after observing that there was a 17 fold increase in 5'nucleotidase activity only in the plasma membrane fraction, and a 2 fold increase in the activity of succinate dehydrogenase in the mitochondrial fraction (and almost complete lack of activity in the plasma membrane fraction), agreeing with other reported studies (e.g. Matlib *et al.*, 1979). Further evidence of the separation of the two different structures can be seen when looking at the electron micrographs; the plasma membrane fraction was composed almost exclusively of vesicles of plasma membrane, whilst the other fraction contained a large proportion of mitochondria together with

some endoplasmic reticulum. However, no plasma membranes were observed in the mitochondrial fraction and *vice versa*.

It was noted that both α_1- and α_2-adrenoceptor binding were observed in plasma membrane and mitochondrial fractions. Reports in the literature are usually confined to binding being carried out either in the plasma membrane or mitochondrial fractions, and to our knowledge there have been no reports of α-adrenoceptor binding in the mitochondrial fraction. Although an enrichment in the enzyme markers has been observed, together with convincing electron microscopy the possibility of cross contamination cannot be ruled out. However, the fact that rauwolscine and corynanthine behaved almost identically in the two different fractions suggests that the [^{3}H]-prazosin and [^{3}H]-RX821002 binding sites exist within the mitochondrial fraction. The question is raised as to whether these mitochondrial α_1- and α_2-adrenoceptor binding sites have a function, or simply that other binding sites (i.e. non-adrenoceptor) found in the P_2 pellet would also be separated out into both fractions after a sucrose density gradient. The possibility exists that the binding sites observed in the mitochondrial fraction are a result of receptor turnover or 'traffic' in cells, as has been reported for α- and β-adrenoceptor binding sites in other tissues (for review see Mahan *et al.*, 1987). Because of the significant amount of binding in the mitochondrial fraction, and the large amount of tissue that would be required to look at the plasma membrane fraction solely, a comparative study of the densities of α_1- and α_2-adrenoceptor binding sites in the P_2 pellet was carried out in a variety of different porcine vascular tissues.

In saturation studies using [^{3}H]-prazosin, the K_d values did not significantly vary between the six different tissues, indicating that the α_1-adrenoceptor site which [^{3}H]-prazosin is binding to was identical in all six vascular tissues. However, the density of α_1-adrenoceptor binding sites (B_{max}) was highest in the TA, followed by the PCDA, the PLV and SA having approximately equal density, followed by the EA and with the MEV having the lowest density. Using the selective α_2-adrenoceptor antagonist [^{3}H]-RX821002, there were no differences in the K_d values but the density of [^{3}H]-RX821002 binding was highest in the TA and MEV followed by the PLV, then the EA, and low densities of [^{3}H]-RX821002 binding being found in the PCDA and SA. In agreement with Nishimura *et al.* (1987), the TA has a high density of both α_1- and α_2-adrenoceptor binding sites, with the density of α_2-adrenoceptor sites being slightly greater than that of α_1-adrenoceptor sites. The densities of these sites found in this study are 30% less than those reported by Nishimura *et al.* (1987), possibly as a result of their further purification of the PNS fraction, but the ratio of α_1-:α_2-adrenoceptor sites (this study: 1:1.4; Nishimura *et al.*: 1:1.9) is very similar. In the other vascular tissues studied it would appear that both in the SA and PCDA there is a predominance (although small) of α_1-adrenoceptor binding sites, the reverse of which is observed both in the PLV and MEV (i.e. greater density of α_2-adrenoceptor sites).

This pattern of binding site distribution is in reasonable agreement with the functional studies; functional α_1- and α_2-adrenoceptors were found in the TA and this tissue had the highest densities of α_1- and α_2-adrenoceptor binding sites. In the SA and PCDA, where there is a small predominance of α_1-adrenoceptor sites, greater α_1-adrenoceptor-mediated functional responses (compared to α_2-adrenoceptor) were observed (Blaylock & Wilson, 1995; present study); it is interesting to note that the SA did have a small density of α_2-adrenoceptor binding sites but no functional response was observed after α_2-adrenoceptor activation. The PLV and the MEV have overt α_2-adrenoceptor-mediated functional responses (Blaylock & Wilson, 1995; present study) and both were found to have high densities of α_2-adrenoceptor sites. The exception to this is the EA which, like the veins, has a dominance of α_2-adrenoceptor binding sites, and it would be of interest to determine how this vessel responds functionally to α_1- and α_2-adrenoceptor activation. It can observed from Figure 7a that there was no obvious relationship between the density of α_1- and α_2-adrenoceptor binding sites for the six vessels. However, if the results from the TA were excluded (Figure 7b) then there was evidence of a weak inverse relationship between α_1- and α_2-adrenoceptors in the five, largely, superficial, vessels examined. Whether this is true for the rest of the cardiovascular system (e.g. renal, pulmonary, coronary and cerebral vascular beds) remains to be determined. A possible explanation of the anomalous findings in the TA could be due to a large population of endothelial α_2-adrenoceptors, as recently reported (Bockman *et al.*, 1993). At the outset of this study it was decided that routine removal of the endothelium, particularly for the small veins, was not feasible. Thus, all blood vessels were essentially 'endothelium-intact'. In agreement with work carried out by Shi *et al.* (1989) using canine vascular tissue, it would appear that α_2-adrenoceptor density in porcine vascular tissue plays a role in the expression of functional responses via this receptor subtype. However, this does not exclude the possibility that a cellular factor (e.g. G-protein or second messenger) may also make an important contribution to the regional differences detected.

In connection with this, preliminary high resolution autoradiographic studies with [^{3}H]-RX821002 have been carried out to determine the exact location of the α_2-adrenoceptor binding sites in the SA. Specific binding of the ligand was evenly distributed throughout the tunica media with very little binding to either the endothelium or adventitia (unpublished observations, Dashwood and present authors). Thus, even though no functional response was observed in this vessel, α_2-adrenoceptor binding sites were detected and they appear to be located almost exclusively on the smooth muscle. We are currently examining the possibility that α_2-adrenoceptor-mediated contraction in the splenic artery can be uncovered by the presence of an ancillary spasmogen, as previously described in the rat isolated tail artery (Templeton *et al.*, 1989) and rabbit isolated distal saphenous artery (Dunn *et al.*, 1991).

In conclusion we have examined the pharmacological characteristics of α-adrenoceptors mediating contraction to noradrenaline in the TA, SA and MEV, and demonstrated the involvement of α_1-adrenoceptors in all three preparations and α_2-adrenoceptors in the TA and MEV. Complementary radioligand binding experiments have shown the presence of both α_1- and α_2-adrenoceptors which, with the exception of the TA, appear to exhibit an inverse relationship for the density of receptor expression. These observations support functional studies presented here and elsewhere (Blaylock & Wilson, 1995). Further experiments will capitalise on the routine availability of porcine blood vessels to assess the detailed pharmacological characteristics of vascular α_1- and α_2-adrenoceptors, and to undertake systematic examination of the associated second messenger systems (i.e. phosphoinositide hydrolysis and cyclic AMP formation).

We would like to thank Mr T. Self for his assistance with the electron microscopy, the Wellcome Trust for financial support and Mason Bros. abattoir (Nottingham) for the supply of tissues.

References

AGRAWAL, D.K., CRANKSHAW, D.J. & DANIEL, E.E. (1987). Postsynaptic alpha-adrenoceptors in vascular smooth muscle. In *Sarcolemmal Biochemistry*, Vol II, ed. Kidwai, A.M. pp. 99–152. Boca Raton, Florida: CRC Press Inc.

ANGUS, J.A., BROUGHTON, A. & MULVANY, M.J. (1988). Role of alpha-adrenoceptors in constrictor responses of rat, guinea-pig, and rabbit small arteries to neural activation. *J. Physiol.*, **403**, 495–510.

ARUNLAKSHANA, O. & SCHILD, H.O. (1959). Some quantitative uses of drug antagonists. *Br. J. Pharmacol. Chemother.*, **14**, 48–58.

BLAYLOCK, N.A. & WILSON, V.G. (1993). Evidence for functional α_2-adrenoceptor-mediated contractions in the porcine isolated thoracic aorta, but not in the splenic artery. *Br. J. Pharmacol.*, **109**, 35P.

BLAYLOCK, N.A. & WILSON, V.G. (1995). Pharmacological characterization of noradrenaline-induced contractions of the porcine isolated palmar lateral vein and palmar common digital artery. *Br. J. Pharmacol.* (in press).

BOCKMAN, C.S., JEFFRIES, W.B. & ABEL, P.W. (1993). Binding and functional characterization of alpha-2 adrenergic receptor subtypes on pig vascular endothelium. *J. Pharmacol. Exp. Ther.*, **276**, 1126–1133.

BRADFORD, M.M. (1976). A rapid and sensitive method for the measurement of microgram quantities of protein utilising the principle of protein dye binding. *Anal. Biochem.*, **72**, 248–254.

CHENG, Y.C. & PRUSOFF, W.H. (1973). Relationship between the inhibition constant (Ki) and the concentration of inhibitor which caused 50 per cent inhibition (I_{50}) of an enzymic reaction. *Biochem. Pharmacol.*, **22**, 3099–3108.

DALY, C.J., MCGRATH, J.C. & WILSON, V.G. (1988). An examination of the post-junctional α-adrenoceptor subtypes for (−)-noradrenaline in several isolated blood vessels from the rabbit. *Br. J. Pharmacol.*, **95**, 473–484.

DELEAN, A., MUNSON, P.J. & RODBARD, D. (1978). Simultaneous analysis of families of sigmoidal curves: applications to bioassay, radioligand assay and physiological dose response curves. *Am. J. Physiol.*, **235**, E97–E102.

DUNN, W.R., MCGRATH, J.C. & WILSON, V.G. (1991). Post-junctional α-adrenoceptors in the rabbit isolated distal saphenous artery: indirect sensitivity to prazosin of responses to noradrenaline mediated by post-junctional α_2-adrenoceptors. *Br. J. Pharmacol.*, **103**, 1484–1492.

FISKE, C.H. & SUBBAROW, Y. (1925). The colorimetric determination of phosphorus. *J. Biol. Chem.*, **66**, 375–400.

FLAVAHAN, N.A. & VANHOUTTE, P.M. (1986). The effect of cooling on α_1 and α_2-adrenoceptor responses in canine femoral veins. *J. Pharmacol. Exp. Ther.*, **238**, 139–147.

FREDHOLM, B.B., JANSSEN, I. & EDVINSSON, L. (1985). Neuropeptide Y is a potent inhibitor of cyclic AMP accumulation in feline cerebral blood vessels. *Acta Physiol. Scand.*, **124**, 467–469.

FURCHGOTT, R.F. (1972). The classification of adrenoceptors (adrenergic receptors). An evaluation from the standpoint of receptor theory. In *Handbook of Experimental Pharmacology*, Vol 33, *Catecholamines*, ed. Blaschko, H. & Muscholl, E. pp. 283–335. Berlin: Springer-Verlag.

LOT, T.Y. & WILSON, V.G. (1994). Overnight storage of the porcine isolated splenic artery enhances endothelium-dependent contractions to N^G-nitro-L-arginine methyl ester without impairing endothelium-dependent dilator function. *Naunyn-Schmied. Arch. Pharmacol.*, **349**, 95–100.

MAHAN, L.C., MCKERNAN, R.M. & INSEL, P.A. (1987). Metabolism of alpha- and beta-adrenergic receptors in vitro and in vivo. *Annu. Rev. Pharmacol. Toxicol.*, **27**, 215–235.

MATLIB, M.A., CRANKSHAW, J., GARFIELD, R.E., CRANKSHAW, D.J., KWAN, C.-Y., BRANDA, L.A. & DANIEL, E.E. (1979). Characterization of membrane fractions and isolation of purified plasma membranes from rat myometrium. *J. Biol. Chem.*, **254**, 1834–1840.

MCGRATH, J.C., BROWN, C.M. & WILSON, V.G. (1989). Alpha-adrenoceptors: a critical review. *Med. Res. Rev.*, **9**, 407–535.

NIELSEN, H., THOM, S., HUGHES, A.D., MARTIN, G.N., MULVANY, M.J. & SEVER, P.S. (1989). Post-junctional α_2-adrenoceptors mediate vasoconstriction in human subcutaneous resistance arteries. *Br. J. Pharmacol.*, **97**, 829–835.

NIELSEN, H., PIEGAARD, H.K., HASENKAM, J.M., MORTENSEN, F.V. & MULVANY, M.J. (1991). Heterogeneity of postjunctional alpha-adrenoceptors in the isolated mesenteric resistance vessels from rats, rabbits, pigs and humans. *J. Cardiovasc. Pharmacol.*, **18**, 4–10.

NISHIMURA, J., KANAIDE, H. & NAKAMURA, M. (1987). Characteristics of adrenoceptors and [3H]nitrendipine receptors of porcine vascular smooth muscle: differences between coronary artery and aorta. *Circ. Res.*, **60**, 837–844.

OHYANAGI, M., FABER, J.E. & NISHIGAKI, K. (1991). Differential activation of $alpha_1$- and $alpha_2$-adrenoceptors on microvascular smooth muscle during sympathetic nerve stimulation. *Circ. Res.*, **68**, 232–244.

PARKINSON, N.A., THOM, S.M., HUGHES, A.D., SEVER, P.S., MULVANY, M.J. & NIELSEN, H. (1992). Neurally-evoked responses of human isolated resistance arteries are mediated by both $alpha_1$- and $alpha_2$-adrenoceptors. *Br. J. Pharmacol.*, **106**, 568–573.

PENNINGTON, R.J. (1961). Biochemistry of dystrophic muscle. Mitochondrial succinate-tetrazolium reductase and adenosine triphosphatase. *Biochem. J.*, **80**, 649–654.

SHI, A.G., KWAN, C.Y. & DANIEL, E.E. (1989). Relation between density (maximum binding) of alpha adrenoceptor binding sites and contractile response in four canine vascular tissues. *J. Pharmacol. Exp. Ther.*, **250**, 1119–1124.

STEVENS, M.J. & MOULDS, R.F.W. (1985). Neuronally released norepinephrine does not preferentially activate post-junctional $alpha_1$-adrenoceptors in human isolated blood vessels in vitro. *Circ. Res.*, **57**, 399–405.

TEMPLETON, A.G.B., MACMILLAN, J., MCGRATH, J.C., STOREY, N.D. & WILSON, V.G. (1989). Evidence for a population of prazosin-resistant, rauwolscine-sensitive alpha-adrenoceptor mediating contractions in the isolated vascular bed of the rat tail. *Br. J. Pharmacol.*, **97**, 563–571.

WILSON, V.G., BROWN, C.M. & MCGRATH, J.C. (1991). Are there more than two types of α-adrenoceptors involved in physiological responses? *Exp. Physiol.*, **76**, 317–346.

WRIGHT, I.K., BLAYLOCK, N.A., KENDALL, D.A. & WILSON, V.G. (1993). Evidence for α_2-adrenoceptor binding sites on the porcine thoracic aorta and splenic artery. *Br. J. Pharmacol.*, **109**, 34P.

(Received June 20, 1994
Revised October 3, 1994
Accepted October 13, 1994)

British Journal of Pharmacology (1995) 114, 689-693

Sequential induction of nitric oxide synthase by *Corynebacterium parvum* in different organs of the mouse

D.D. Rees, F.Q. Cunha, J. Assreuy, A.G. Herman & S. Moncada

Wellcome Research Laboratories, Langley Court, Beckenham, Kent BR3 3BS

1 The ability of *Corynebacterium parvum* (*C. parvum*) to induce nitric oxide (NO) synthase in the macrophage, spleen, liver, aorta, heart and brain, and to elevate plasma NO_2^-/NO_3^- in the mouse was investigated. In addition, the relationship between NO synthase activity and blood pressure was studied.

2 *C. parvum* (100 mg kg^{-1}, i.p.) induced a time-dependent expression of a Ca^{2+}-independent NO synthase in the macrophage, spleen, liver, aorta and heart. The time course of induction of the NO synthase varied such that the maximum enzyme activity was at day 8 in the macrophage and liver, day 12 in the spleen and heart and day 16 in the aorta.

3 There was no significant induction of a Ca^{2+}-independent NO synthase in the brain, nor was there any change in the Ca^{2+}-dependent enzyme in this organ, during the study period.

4 *C. parvum* produced a gradual decrease in blood pressure, with a maximum fall at day 16 (from 108 ± 1 mmHg to 79 ± 3 mmHg), which recovered gradually by day 28.

5 Plasma NO_2^-/NO_3^- was significantly elevated between days 8 and 24, with a maximum increase at day 12.

6 These results show that *C. parvum* induces a Ca^{2+}-independent NO synthase in a number of tissues and that this induction occurs initially in macrophages and the liver. This suggests that induction of the NO synthase in the other tissues is secondary and probably the result of activation of macrophages and some cells of the liver.

7 Furthermore, the decrease in blood pressure induced by *C. parvum* is associated with the induction of NO synthase in the vasculature, whereas the increased concentration of plasma NO_2^-/NO_3^- seems to result from the generation of NO by a number of tissues.

Keywords: *C. parvum*; plasma nitrite/nitrate; blood pressure; inducible nitric oxide synthase

Introduction

The L-arginine: nitric oxide (NO) pathway (Moncada *et al.*, 1991) is now known to be involved in a variety of physiological processes in the cardiovascular and nervous system where NO is generated via constitutive Ca^{2+}-dependent NO synthases (Moncada *et al.*, 1991; Snyder & Bredt, 1992). On the other hand, an inducible Ca^{2+}-independent NO synthase is expressed in phagocytic and other cells following activation by endotoxin (lipopolysaccharide; LPS) and/or cytokines. Much larger amounts of NO are generated by this enzyme, which is responsible for the cytotoxicity of macrophages towards certain microorganisms and tumour cells and may account for the phenomenon of non-specific immunity (Moncada *et al.*, 1991). Endotoxin and/or cytokines also induce the expression of a Ca^{2+}-independent NO synthase in vascular endothelial and smooth muscle cells and cardiac myocytes. This accounts for the hypotension and probably the cardiac dysfunction characteristic of septic shock (Rees *et al.*, 1990a; Busse & Mulsch, 1990; Fleming *et al.*, 1991; Moncada, 1992; Wright *et al.*, 1992; Schulz *et al.*, 1992).

Administration of endotoxin *in vivo* activates macrophages, leading to the production of a variety of cytokines, including tumour necrosis factor (TNF; Suffredini *et al.*, 1989; De Groote *et al.*, 1992; Oliver *et al.*, 1993), the maximal release of which occurs 2 h after endotoxin administration (Oliver *et al.*, 1993). These cytokines, in turn, induce the Ca^{2+}-independent NO synthase simultaneously in a variety of tissues, with maximal induction occurring after a further 4-12 h (Knowles *et al.*, 1990; Salter *et al.*, 1991; Cunha *et al.*, 1994).

Administration of the heat-inactivated gram-positive bacterium *Corynebacterium parvum* (*C. parvum*) has been shown to induce NO synthase in rat and mouse liver hepatocytes *in vivo*, with a time course of several days (Geller *et al.*, 1993). *C. parvum* also induces the release of a number of cytokines over a period of weeks (Kawada *et al.*, 1990). Since the synthesis of NO is regulated by different cytokines in different cells, we wondered whether induction of NO synthase following *C. parvum* may vary significantly from one tissue to another. In view of this, we have investigated the effect of *C. parvum* on the induction of the NO synthase in various tissues of the mouse, and on the plasma concentrations of nitrite and nitrate (NO_2^-/NO_3^-), the breakdown products of NO. Furthermore, we have investigated the relationship between induction of the NO synthase and the blood pressure of the mouse.

Methods

Female CBA mice (Charles River, U.K. 30-35 g) were housed in a temperature-controlled room with water and food *ad libitum*. NO synthase activity in the spleen, liver, aorta, heart and brain, as well as blood pressure and plasma concentrations of NO_2^-/NO_3^-, were determined 2-28 days following administration of *C. parvum* (100 mg kg^{-1}, i.p., dissolved in sterile water, ~0.3 ml per mouse). In a separate series of experiments, the induction of NO synthase in peritoneal macrophages following *C. parvum* administration was also studied.

Measurement of plasma NO_2^-/NO_3^-

The animals were anaesthetized with isofluorane (2%) and blood samples (~0.5 ml) were obtained following exsanguination via the carotid artery. The plasma NO_2^- concentration was determined by first reducing the NO_3^- enzymatically, using NO_3^- reductase from *Aspergillus* species.

[1] Author for correspondence.

Briefly, plasma samples were diluted 1:4 or 1:10 with Milli-Q distilled water and incubated with assay buffer (composition, mM: KH_2PO_4 50, NADPH 0.6, FAD 5 and NO_3^- reductase 20 mu, pH 7.5) for 1 h at 37°C. A standard curve for NO_3^- was constructed by incubation of $NaNO_3^-$ (1–100 μM) with the assay buffer. The resultant NO_2^- concentrations were determined by chemiluminescence as described previously (Palmer *et al.*, 1987) and expressed as the amount of total plasma nitrite and nitrate (NOx) in μM.

Measurement of NO synthase activity in tissues

Immediately after collection of the blood sample, the tissues were removed and washed briefly in Krebs' buffer (containing in mM: NaCl 118, KCl 4.8, $CaCl_2$ 2.5, $MgSO_4$ 1.2, KH_2PO_4 1.2, $NaHCO_3$ 24 and glucose 11), gassed with 95% O_2/5% CO_2. The tissues were then freeze-clamped in liquid nitrogen and stored at − 80°C.

On the day of assay, the frozen tissues were homogenized in a cooled stainless steel pestle and mortar and then placed in homogenizing buffer (pH 7.4; Tris 50 mM, sucrose 3.2 mM, dithiothreitol 1 mM, leupeptin 10 μg ml^{-1}, soybean trypsin inhibitor 10 μg ml^{-1}, aprotinin 2 μg ml^{-1}) and the tissue sonicated for 3 s (x3) at 4°C. The homogenate was centrifuged at 10,000 *g* for 20 min at 4°C. The resultant supernatant, containing both the soluble and particulate NO synthase was added to assay buffer (pH 7.2; containing $KH_2PO_4^-$ 50 mM, $MgCl_2$ 1 mM, $CaCl_2$ 0.2 mM, valine 50 mM, L-citrulline 20 μM, L-arginine 20 μM, dithiothreitol 1 mM, NADPH 100 μM, tetrahydrobiopterin 3 μM, flavin adenine dinucleotide (FAD) 3 μM, flavin mononucleotide (FMN) 3 μM and L-[U-^{14}C]-arginine 0.05 μCi ~ 1 μM]. Following a 20 min incubation at 37°C, the reaction was terminated by removal of substrate by adding 1:1 (v/v) Milli-Q water/Dowex-AG50W (200–400, 8% cross linked, Na^+-form). The resin was left to settle for 30 min at room temperature and the supernatant carefully removed. NO synthase activity in the supernatant was determined from the conversion of L-[U-^{14}C]-arginine to [U-^{14}C]-citrulline. The activity of the Ca^{2+}-dependent enzyme was determined as the difference between the [U-^{14}C]-citrulline generated from control samples and samples containing EGTA (3 mM); the activity of the Ca^{2+}-independent enzyme was determined from the difference between samples containing EGTA (3 mM) and samples containing the NO synthase inhibitor, N$^{\omega}$-iminoethyl-L-ornithine (L-NIO, 1 mM; Rees *et al.*, 1990b). The soluble protein content of the supernatant was determined by the Coomassie blue binding method using BIO-RAD protein reagent with bovine serum albumin as a standard. NO synthase activity was expressed as pmol NO min^{-1} mg^{-1} protein. Due to the high arginase content and rapid utilisation of L-arginine in the liver, NO synthase levels in this tissue were determined from the conversion of L-[2,3,4,5 ^{3}H]-arginine to L[2,3,4,5 ^{3}H]-citrulline at 37°C for 10 min. Under these conditions the conversion of L-[^{14}C or ^{3}H]-arginine to L-[^{14}C or ^{3}H]-citrulline is linear in both assays.

Measurement of NO synthase in macrophages

The mice (n = 16) were killed by cervical dislocation. Culture medium (RPMI; 10 ml, 10 u ml^{-1} heparin) was injected into the peritoneum, agitated and withdrawn. The peritoneal suspension was centrifuged (10,000 *g*) for 10 min. The pellet was resuspended in distilled water for 5 s to lyse red blood cells, followed by phosphate buffered saline (PBS) and RPMI. The suspension was again centrifuged (10,000 *g*) for 10 min and the resulting pellet resuspended in RPMI. The macrophages were left to adhere in 12-well plates for 2 h. Non-adherent cells were discarded and adherent cells washed twice with fresh PBS and removed with a plastic scraper into homogenisation buffer. NO synthase activity was determined by the method described above. Macrophages from 4 mice were pooled to obtain each value.

Blood pressure

Mice (n = 6 per group) were anaesthetized with isofluorane (2%) at 0, 4, 8, 12, 16, 20, 24 and 28 days after *C. parvum* administration. A cannula line was implanted in the femoral artery, tunnelled subcutaneously to exit at the top of the back and connected to a swivel tether system for continuous monitoring of blood pressure. Normal physiological saline (154 mM) containing heparin (10 u ml^{-1}) was administered as a continuous infusion via the femoral artery (50 μl h^{-1}) to maintain patency of the blood pressure cannula line. Following a 1 h recovery from surgery, blood pressure was measured over the following 2 h period.

Materials

Corynebacterium parvum (*C. parvum*; Coparvax), N$^{\omega}$-iminoethyl-L-ornithine (L-NIO; Wellcome Research Laboratories) and NO_3^- reductase (Boehringer, England) were obtained from the sources indicated. All other materials were obtained from Sigma (England).

Statistics

Statistical significance ($P < 0.05$) was analysed by a one-way ANOVA test for multiple comparisons followed by Dunnett-adjusted analysis. Results are expressed as means ± s.e.mean, n = 3–10.

Results

Induction of NO synthase in various tissues

Ca^{2+}-independent NO synthase Administration of *C. parvum* (100 mg kg^{-1}, i.p.) stimulated the expression of a Ca^{2+}-independent NO synthase with different time courses in the various tissues studied (Figure 1). Induction of this enzyme was maximal in harvested peritoneal macrophages and the liver at day 8 (600 ± 44 pmol min^{-1} mg^{-1} protein and 1467 ± 362 pmol min^{-1} mg^{-1} protein respectively, n = 4 for each, $P < 0.05$), in the spleen and heart at day 12 (16 ± 0.8 pmol min^{-1} mg^{-1} protein and 8 ± 0.8 pmol min^{-1} mg^{-1} protein respectively, n = 3–10 for each, $P < 0.05$) and in the aorta at day 16 (124 ± 12 pmol min^{-1} mg^{-1} protein, n = 3–8, $P < 0.05$). *C. parvum* did not induce a Ca^{2+}-independent NO synthase in the brain.

Ca^{2+}-dependent NO synthase There was a smaller increase in activity of a Ca^{2+}-dependent NO synthase in the various tissues. This followed a similar time course to that of the Ca^{2+}-independent enzyme. The activity of the Ca^{2+}-dependent enzyme was maximal in harvested peritoneal macrophages and the liver at day 8 (132 ± 9 pmol min^{-1} mg^{-1} protein; n = 4, $P < 0.05$, and 36 ± 27 pmol min^{-1} mg^{-1} protein respectively, n = 3), in the spleen and heart at day 12 (2.4 ± 0.4 pmol min^{-1} mg^{-1} protein and 2.8 ± 0.6 pmol min^{-1} mg^{-1} protein respectively, n = 3–10 for each, $P < 0.05$) and in the aorta at day 16 (54 ± 18 pmol min^{-1} mg^{-1} protein, n '= 3–8, $P < 0.05$). There was no significant change in the activity of the Ca^{2+}-dependent NO synthase in the brain (n = 4; Figure 2).

Plasma NO_2^-/NO_3^- measurements

The basal concentration of nitrite/nitrate (NOx) in the plasma was 7 ± 3 μM (n = 10). *C. parvum* (100 mg kg^{-1}, i.p.) elevated plasma NO_2^-/NO_3^- concentrations from day 4 (13 ± 2 μM, n = 5, Figure 1), reaching a plateau at day 12 (1006 ± 23 μM, n = 5, Figure 1, $P < 0.05$) and gradually returning to control values by day 28 (22 ± 11 μM, n = 5, Figure 1).

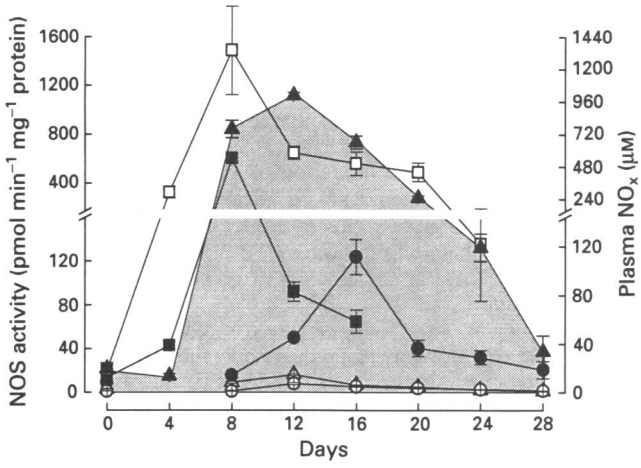

Figure 1 Time course of the sequential induction of the Ca^{2+}-independent NO synthase (NOS) in the liver (□), macrophages (■), spleen (△), heart (○) and aorta (●) and elevation of plasma concentrations of nitrite and nitrate (NO_x; $n = 4$, ▲, shaded area) following a single administration of *C. parvum* (100 mg kg^{-1}, i.p.; $n = 3-10$). Day 0 represents control, untreated group.

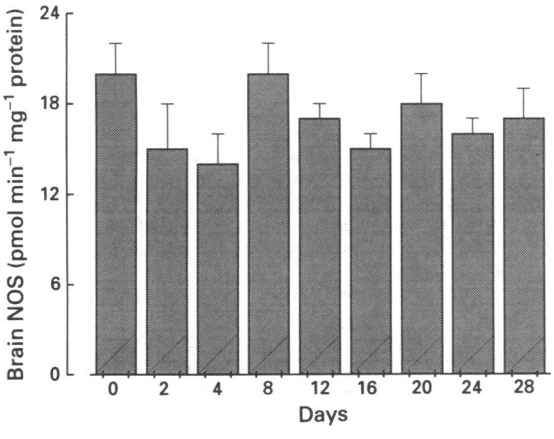

Figure 2 Ca^{2+}-dependent NO synthase (NOS) activity in the brain following a single administration of *C. parvum* (100 mg kg^{-1}, i.p.; $n = 4$). There was no induction of the Ca^{2+}-independent NO synthase over the time course studied. Day 0 represents control, untreated group.

Blood pressure measurements

Administration of *C. parvum* (100 mg kg^{-1}, i.p.) to the conscious mouse caused a progressive fall in mean arterial blood pressure (MABP) from a basal level of 108 ± 1 mmHg ($n = 6$, Figure 3) to a maximum fall at day 16 (79 ± 3 mmHg, $n = 9$, Figure 3, $P < 0.01$), which recovered gradually by day 28 (102 ± 1 mmHg, $n = 4$, Figure 3).

Discussion

Administration of endotoxin from gram-negative bacteria to animals induces the expression of a Ca^{2+}-independent NO synthase which plays a role in the immunological defence mechanism against invading microorganisms and cancer cells and also mediates the excessive vasodilatation characteristic of septic shock (Moncada *et al.*, 1991). The induction of the NO synthase by endotoxin occurs in many tissues and organs (Knowles *et al.*, 1990; Salter *et al.*, 1991; Mitchell *et al.*, 1993; Cunha *et al.*, 1994) and is relatively short-lasting, with a time course which starts typically 2 h following endotoxin administration, peaks between 6–12 h and is largely over by 24 h (Knowles *et al.*, 1990; Salter *et al.*, 1991; Mitchell *et al.*, 1993;

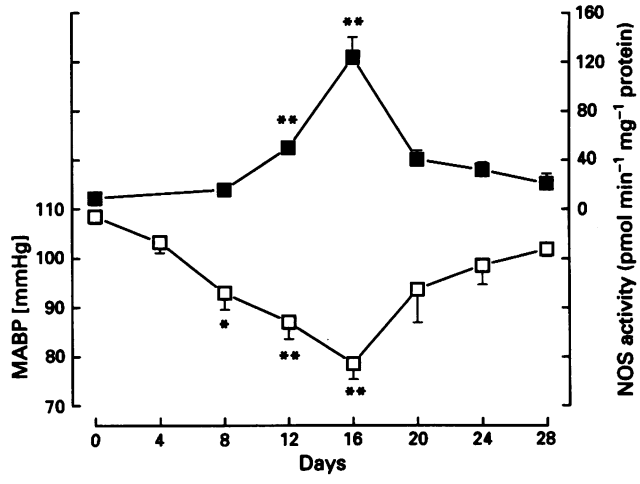

Figure 3 Time course of induction of the Ca^{2+}-independent NO synthase in the aorta (■, $n = 3-8$) and associated changes in mean arterial blood pressure (MABP; □, $n = 4-10$) following a single administration of *C. parvum* (100 mg kg^{-1}, i.p.). Day 0 represents control, untreated group. $^*P < 0.05$, $^{**}P < 0.01$.

Cunha *et al.*, 1994). This is accompanied by an increase in the concentration of NO_2^-/NO_3^- in the plasma which follows a similar time course (Cunha *et al.*, 1994). Although not yet studied in detail, the gram-positive exotoxins appear to induce the expression of NO synthase in various tissues with a similar, short-lasting, time course of induction (Zembowicz & Vane, 1992; Cunha *et al.*, 1993).

There is another group of bacteria which, unlike those described above, induce the NO synthase after a long period of latency (1–2 days) and, in the organs studied, this induction lasts for a period of days or weeks. This group includes *Mycobacterium bovis* (strain *bacillus Calmette Guérin*; BCG, Stuehr & Marletta, 1987) and *C. parvum* (Billiar *et al.*, 1990; 1992). Both bacteria induce profound and long-lasting reticuloendothelial system stimulation, as shown by increased carbon clearance from the blood, associated with a persistence of the intact bacteria within the macrophage (Cummins, 1984). Interestingly, these have been used as immunostimulants and it is likely that this effect is mediated, in part, by NO. Many reports have shown that macrophages activated by endotoxin, *C. parvum* and/or cytokines mediate non-specific anti-microbial and anti-tumour activities (Tuttle & Cantrell, 1981) by a mechanism which involves induction of NO synthase (Hibbs *et al.*, 1990; Adams *et al.*, 1990; Moncada *et al.*, 1991).

We have now shown that *C. parvum* induces a sequential and differential induction of NO synthase, which is first expressed in the macrophage and the liver, followed by the spleen, heart and aorta. The fact that NO synthase induction occurs first in the macrophage and liver suggests that following the sequestration of the bacteria by macrophages and probably Kupffer cells in the liver, their activation and subsequent generation of cytokines stimulates the induction of NO synthase in other tissues. Induction in these tissues will depend on their responses to different cytokines. This leads to a temporal and differential expression of the enzyme in various tissues. Thus, our results show that 12–20 days after the administration of *C. parvum* there is induction of NO synthase in the vasculature which coincides with the development of a small but significant hypotension. The time course of changes in plasma NO_2^-/NO_3^-, on the other hand, appears to reflect the production of NO in several different organs, predominantly the liver and macrophage in which NO synthase activity is greatest.

Interestingly, relatively small increases in the Ca^{2+}-dependent NO synthase were observed in all tissues over a similar time course. This may be artefactual in nature, since we

define Ca^{2+}-dependence as the residual activity after chelation of Ca^{2+}. Alternatively, induction of 'constitutive' NO synthases has been described previously in vascular tissue following shear stress (Nishida *et al.*, 1992) or oestrogen treatment (Weiner *et al.*, 1994). Whether induction of the Ca^{2+}-dependent enzyme occurs will therefore require further studies, including the measurement of mRNA for this enzyme.

The hypotension observed following administration of *C. parvum* was not as severe as that observed following treatment with endotoxin. The reasons for this are not clear at present, and detailed studies of the correlation between blood concentrations of NO_2^-/NO_3^-, induction of NO synthase in the vasculature and blood pressure are required. If, however, the maximum induction of NO synthase in the vessel wall is comparable after administration of endotoxin and *C. parvum* the question will remain as to why the fall in blood pressure following endotoxin is so severe and yet no hypotension has previously been described following *C. parvum* (Cummins, 1984). One possibility is that the cardiovascular system is able to adapt and compensate for the slow onset of the induction of NO in the vasculature that occurs following *C. parvum* administration.

Whether immunostimulants other than *C. parvum* also induce this form of long-lasting sequential and differential induction of NO synthase in different tissues remains to be determined. Furthermore, it is worth investigating whether selective and long-lasting induction of the NO synthase in the reticuloendothelial system can be achieved. If so, it will be very important to assess the anti-infective and anti-cancer potential of such manipulation.

The authors thank Tara Andrews, Jayne Monkhouse and Angela Deakin for their assistance with this work and Annie Higgs for critical appraisal of the manuscript. F.Q.C. is on leave from the Dept. of Pharmacology, Faculty of Medicine, Universidade de Sao Paulo, Brazil and is supported by a fellowship from Fundacao de Amparo a Pesquiso do Estado de Sao Paulo. J.A. is on leave from the Dept. of Pharmacology, Universidade Federal do Rio de Janeiro, Brazil and is supported by a fellowship from Conselho Nacional de Desenvolvimento Cientifico e Tecnologico, Brazil. A.G.H. is on leave from the Dept. of Pharmacology, University of Antwerp, Belgium.

References

ADAMS, L.B., HIBBS, J.B., TAINTOR, R.R. & KRAHENBUHL, J.L. (1990). Microbiostatic effect of murine macrophages for *Toxoplasma gondii*: role of synthesis of inorganic nitrogen oxides from L-arginine. *J. Immunol.*, **144**, 2725–2729.

BILLIAR, T.R., CURRAN, R.D., HARBRECHT, B.G., STADLER, J., WILLIAMS, D.L., OCHOA, J.B., DI SILVIO, M., SIMMONS, R.L. & MURRAY, S.A. (1992). Association between synthesis and release of cGMP and nitric oxide biosynthesis by hepatocytes. *Am. J. Physiol.*, **262**, C1077–C1082.

BILLIAR, T.R., CURRAN, R.D., STUEHR, D.J., STADLER, J., SIMMONS, R.L. & MURRAY, S.A. (1990). Inducible cytosolic enzyme activity for the production of nitrogen oxides from L-arginine in hepatocytes. *Biochem. Biophys. Res. Commun.*, **168**, 1034–1040.

BUSSE, R. & MULSCH, A. (1990). Induction of nitric oxide synthase by cytokines in vascular smooth muscle. *FEBS Lett.*, **275**, 87–90.

CUMMINS, C.S. (1984). *Corynebacterium parvum* and its fractions. *Immun. Ser.*, **25**, 163–190.

CUNHA, F.Q., ASSREUY, J., MOSS, D.W., REES, D.D., LEAL, L.M.C., MONCADA, S. & CARRIER, M. (1994). Differential induction of nitric oxide synthase in various organs of the mouse during endotoxaemia: role of TNFα and IL-1β. *Immunol.*, **81**, 211–215.

CUNHA, F.Q., MOSS, D.W., LEAL, L.M.C., MONCADA, S. & LIEW, F.Y. (1993). Induction of macrophage parasiticidal activity by *Staphylococcus aureus* and exotoxins through the nitric oxide synthesis pathway. *Immunol.*, **78**, 563–567.

DE GROOTE, D., ZANGERLE, P.F., GEVAERT, G., FASSOTTE, M.F., BEGUIN, Y., NOIZAT-PIRENNE, F., PIRENNE, J., GATHY, R., LOPEZ, M., DEHART, I., IGOT, D., BAUDRIHAYE, M., DELACROIX, D. & FRANCHIMONT, P. (1992). Direct stimulation of cytokines (IL-1β, TNFα, IL-6, IL-2, IFN-γ and GM-CSF) in whole blood. I. Comparison with isolated PBMC stimulation. *Cytokine*, **4**, 239–248.

FLEMING, I., GRAY, G.A., SCHOTT, C. & STOCLET, J.-C. (1991). Inducible but not constitutive production of nitric oxide by vascular smooth muscle cells. *Eur. J. Pharmacol.*, **200**, 375–376.

GELLER, D.A., NUSSLER, A.K., SILVIO, M., LOWENSTEIN, C.J., SHAPIRO, R.A., WANG, S.C., SIMMONS, R.L. & BILLIAR, T. (1993). Cytokines, endotoxin, and glucocorticoids regulate the expression of inducible nitric oxide synthase in hepatocytes. *Proc. Natl. Acad. Sci. U.S.A.*, **90**, 522–526.

HIBBS, J.B., TAINTOR, R.R., VAVRIN, Z., GRANGER, D.L., DRAPIER, J.-C., AMBER, I.J. & LANCASTER, J.R. (1990). Synthesis of nitric oxide from a terminal guanidino nitrogen atom of L-arginine: a molecular mechanism regulating cellular proliferation that targets intracellular iron. In *Nitric Oxide L-Arginine: a Bioregulatory System*. ed. Moncada, S. & Higgs, E.A. pp. 189–225. Amsterdam: Elsevier Science Publishers.

KAWADA, N., MIZOGUCHI, Y., SHIN, T., TSUTSUI, H., KOBAYASHI, K., MORISAWAR, S., MONNA, T. & YAMAMOTO, S. (1990). Synthesis of eicosanoids by Propionibacterium acnes – elicited liver adherent cells and their effect on production of interleukin 1 and tumor necrosis factor. *Prostaglandins Leukot. Essent. Fatty Acids*, **41**, 187–193.

KNOWLES, R., MERRETT, M., SALTER, M. & MONCADA, S. (1990). Differential induction of brain, lung and liver nitric oxide synthase by endotoxin in the rat. *Biochem. J.*, **270**, 833–836.

MITCHELL, J., KOHLHAAS, K.L., SORRENTINO, R., WARNER, T., MURAD, F. & VANE, J.R. (1993). Induction by endotoxin of nitric oxide synthase in the rat mesentery: lack of effect on action of vasoconstrictors. *Br. J. Pharmacol.*, **109**, 265–270.

MONCADA, S. (1992). The L-arginine: nitric oxide pathway. *Acta Physiol. Scand.*, **145**, 201–227.

MONCADA, S., PALMER, R.M.J. & HIGGS, E.A. (1991). Nitric oxide: physiology, pathophysiology and pharmacology. *Pharmacol. Rev.*, **43**, 109–142.

NISHIDA, K., HARRISON, D.G., NAVAS, J.P., FISHER, A.A., DOCKERY, S.P., UEMATSU M., NEREM, R.M., ALEXANDER, R.W. & MURPHY, T.J. (1992). Molecular cloning and characterization of the constitutive bovine aortic endothelial cell nitric oxide synthase. *J. Clin. Invest.*, **90**, 2092–2096.

OLIVER, J.C., BLAND, L.A., OETTINGER, C.W., ARDUINO, M.J. & MCALLISTER, S.K. (1993). Cytokine kinetics in an in vitro whole blood model following an endotoxin challenge. *Lymphokine Cytokine Res.*, **12**, 115–120.

PALMER, R.M.J., FERRIGE, A.G. & MONCADA, S. (1987). Nitric oxide release accounts for the biological activity of endothelium-derived relaxing factor. *Nature*, **327**, 524–526.

REES, D.D., CELLEK, S., PALMER, R.M.J. & MONCADA, S. (1990a). Dexamethasone prevents the induction by endotoxin of a nitric oxide synthase and the associated effects on vascular tone: an insight into endotoxin shock. *Biochem. Biophys. Res. Commun.*, **173**, 541–547.

REES, D.D., PALMER, R.M.J., SCHULZ, R., HODSON, H.F. & MONCADA, S. (1990b). Characterisation of three inhibitors of endothelial nitric oxide synthase *in vitro* and *in vivo*. *Br. J. Pharmacol.*, **101**, 746–752.

SALTER, M., KNOWLES, R.G. & MONCADA, S. (1991). Widespread tissue distribution, species distribution and changes in activity of Ca^{2+}-dependent and Ca^{2+}independent nitric oxide synthases. *FEBS Lett.*, **291**, 145–149.

SCHULZ, R., NAVA, E. & MONCADA, S. (1992). Induction and potential biological relevance of a Ca^{2+}-independent nitric oxide synthase in the myocardium. *Br. J. Pharmacol.*, **105**, 575–580.

SNYDER, S.H. & BREDT, D.S. (1992). Biological roles of nitric oxide. *Scientific American*, May, 28–35.

STUEHR, D.J. & MARLETTA, M.A. (1987). Induction of nitrite/nitrate synthesis in murine macrophages by BCG infection, lymphokines, or interferon-γ. *J. Immunol.*, **139**, 518–525.

SUFFREDINI, A.,F., FROMM, R.E., PARKER, M.M., BRENNER, M., KOVACS, J.A., WESLEY, R.A. & PARRILLO, J.E. (1989). The cardiovascular response of normal humans to the administration of endotoxin. *N. Engl. J. Med.*, **321**, 280–287.

TUTTLE, R.L. & CANTRELL, J. (1981). *C. Parvum* – determinants of biological activity. In *Augmenting Agents in Cancer Therapy*. ed. Hersh, E.M., Chirigoz, M.A. & Mastrangelo, M.J. pp. 53–69. New York: Raven Press.

WEINER, C.P., LIZASOAIN, I., BAYLIS, S.A., KNOWLES, R.G., CHARLES, I.G. & MONCADA, S. (1994). Induction of calcium-dependent nitric oxide synthases by sex hormones. *Proc. Natl. Acad. Sci. U.S.A.*, **91,** 5212–5216.

WRIGHT, C.E., REES, D. & MONCADA, S. (1992). Protective and pathological roles of nitric oxide in endotoxin shock. *Cardiovasc. Res.*, **26,** 48–57.

ZEMBOWICZ, A. & VANE, J.R. (1992). Induction of nitric oxide synthase activity by toxic shock syndrome toxin 1 in a macrophage-monocyte cell line. *Proc. Natl. Acad. Sci. U.S.A.*, **89,** 2051–2055.

(Received April 5, 1994
Revised September 1, 1994
Accepted October 4, 1994)

British Journal of Pharmacology (1995) 114, 694-702

Pharmacological characterization of noradrenaline-induced contractions of the porcine isolated palmar lateral vein and palmar common digital artery

N.A. Blaylock & [1]V.G. Wilson

Department of Physiology and Pharmacology, The Medical School, Queen's Medical Centre, Nottingham, NG7 2UH

1 The aim of this study was to examine the pharmacological characteristics of α-adrenoceptor-mediated contractions in two porcine isolated blood vessels, the palmar lateral vein (PLV) and the palmar common digital artery (PCDA). This was carried out with noradrenaline used as the agonist throughout, and either phentolamine (non-selective α-adrenoceptor antagonist), prazosin and YM-12617 (selective α_1-adrenoceptor antagonists) or rauwolscine and CH-38083 (selective α_2-adrenoceptor antagonists).

2 Noradrenaline (0.003–10 μM) produced concentration-dependent contractions in both vessels, with the PCDA ($pD_2 = 6.33 \pm 0.07$, $n = 10$) being approximately 10 fold less sensitive to noradrenaline compared to the PLV ($pD_2 = 7.39 \pm 0.09$, $n = 8$). Also, the maximal response to noradrenaline was greater in the PCDA compared to the PLV. Phentolamine (0.03–30 μM) produced parallel rightward shifts in the CRC to noradrenaline in both tissue preparations. The pA_2 values were similar and slopes of the Schild plots were not significantly different from unity, indicating an interaction between phentolamine and a single receptor in each preparation.

3 In the PCDA the α_1-adrenoceptor antagonists, prazosin (0.01–1 μM) and YM-12617 (0.01–1 μM) produced non-parallel rightwards shifts in the CRC to noradrenaline, with the lower 10–15% of the CRC exhibiting greater resistance to the effects of these antagonists compared to the upper part. In contrast, rauwolscine (1–10 μM) and CH-38083 (10 μM) produced parallel displacement of the CRC to noradrenaline. In the PLV, low concentrations of either α_1- (0.01 μM) or α_2-adrenoceptor antagonists (0.1–1 μM) produced a large shift in the CRC, but subsequent higher concentrations had only small additional effects. Based upon pK_B values estimated from the effects of the lower concentrations of antagonists, the results are consistent with a large population of α_1-adrenoceptors in the PCDA and a mixture of α_1- and α_2-adrenoceptors in the PLV.

4 In both tissues, when an α_1- and an α_2-adrenoceptor antagonist were used in combination the effect produced was greater than that with either agent alone. In contrast, the combination of the α_1-adrenoceptor antagonists (prazosin and YM-12617 together) or the α_2-adrenoceptor antagonists (CH-38083 and rauwolscine together) were no more effective than that produced by the individual antagonists. These findings suggest the presence of functional α_1- and α_2-adrenoceptors in the PLV and PCDA.

5 Phenoxybenzamine (0.3–3 μM, 60 min exposure) produced a concentration-dependent reduction in the maximal response to noradrenaline which was more pronounced in the PCDA than the PLV. After a 60 min exposure to a combination of phenoxybenzamine (1 μM) and rauwolscine (1 μM), the remaining NA-induced contraction after washout was resistant to prazosin (0.1 μM) and sensitive to rauwolscine (1 μM) in both tissue preparations, indicating the existence of functional α_2-adrenoceptors in both vessels.

6 Evidence suggests that post-junctional α_1- and α_2-adrenoceptors contribute to noradrenaline-induced contractions in the PCDA and PLV, with the latter possessing a larger population of functional α_2-adrenoceptors.

Keywords: Noradrenaline; porcine vascular smooth muscle; α_1-adrenoceptors; α_2-adrenoceptors; contraction

Introduction

Over the past 40 years, experimental studies on isolated blood vessels from standard laboratory animals, e.g. rat, rabbit, guinea-pig and, less commonly, cat, dog and primates, have yielded invaluable information on the properties of vascular smooth muscle. Although this information has been useful in the development of therapeutic agents for man, it is increasingly evident that the pharmacological characteristics vary between and also within individual vascular beds. The problem is further compounded by findings that even for the same vessel from different species, e.g. the thoracic aorta or mesenteric artery, substantial differences exist in the degree of sympathetic innervation (Patil *et al.*, 1972), utilization of cellular calcium and extracellular calcium for contraction (Beckeringh *et al.*, 1984; Jenkin *et al.*, 1991) and the pharmacological characteristics of α-adrenoceptors (Ruffolo & Waddell, 1982; Ruffolo *et al.*, 1982; Nielsen *et al.*, 1991). In view of the difficulty associated with access and viability of non-diseased human blood vessels, it is clearly important to widen the range of isolated blood vessels available for experimental studies and ensure that these adequately reflect the heterogeneous characteristics of vascular smooth muscle. There are several reasons to believe that the pig may be a useful model for this purpose.

First, porcine aortic and mitral valves have been successfully employed in man for over 15 years (Burdon *et al.*, 1992) and it has been suggested that pigs, genetically engineered to reduce hyperacute rejection, may eventually be used for xenotransplantation (First, 1992; Good *et al.*, 1992; Cooper 1992). Secondly, pulmonary (Kovitz *et al.*, 1993), renal

[1] Author for correspondence.

(Christie & Lewis, 1991), carotid (Ohgushi *et al.*, 1993), cerebral (Linnik & Lee, 1989; Kim *et al.*, 1992) and, in particular, coronary blood vessels (Shafiq *et al.*, 1992; Ohgushi *et al.*, 1993; Ito *et al.*, 1993) from the pig have been successfully used to examine the properties of vascular smooth muscle. Finally, the availability of large quantities of tissue has enabled radioligand binding and biochemical studies to be conducted on both aortic and coronary vascular smooth muscle (Nishimura *et al.*, 1987; Tsutsui *et al.*, 1990; Ito *et al.*, 1993), and it seems possible that this could be extended to other blood vessels.

In the present study we have focused on an examination of the pharmacological characteristics of α-adrenoceptor-mediated contraction of the porcine isolated palmar lateral vein (PLV) and palmar common digital artery (PCDA) to assess the suitability of the pig as a (cardiovascular) model for man. The corresponding human vessels were amongst the first shown to possess a population of constrictor α_2-adrenoceptors (Stevens & Moulds, 1981), while demonstration of this subtype in superficial vessels from standard laboratory animals often requires an ancillary spasmogen (rat tail; Templeton *et al.*, 1989), extensive pharmacological manipulation (rabbit isolated saphenous vein; Daly *et al.*, 1988c) or a combination of both (rabbit saphenous artery; Dunn *et al.*, 1991). We have used noradrenaline as the agonist throughout and examined the effect of prazosin and YM-12617, antagonists selective for α_1-adrenoceptors (Honda *et al.*, 1985; McGrath *et al.*, 1989), and rauwolscine and CH-38083, antagonists selective for α_2-adrenoceptors (Weitzell *et al.*, 1979; Vizi *et al.*, 1986). Our results indicate that the PLV and PCDA possess a population of α_1- and α_2-adrenoceptors which are stimulated by noradrenaline to produce a contraction.

Methods

Preparation of the blood vessel

Porcine trotters from the forelimbs were obtained within 30 min of death of the animal, placed on ice and transported to the laboratory. A 3–4 cm length of the palmar common digital artery and palmar lateral vein (Ghosal & Nanda, 1975) was dissected out and stored overnight at 4°C in modified Krebs-Henseleit saline containing 2% Ficoll which had been previously gassed with 95% O_2/5% CO_2. The composition of the modified Krebs-Henseleit saline was (mM): NaCl 118.4, KCl 4.7, $CaCl_2$ 1.25, $MgSO_4$ 1.2, $NaHCO_3$ 24.9, KH_2PO_4 1.2 and glucose 11.1. Previous experiments have established that this procedure neither impairs the contractility of the smooth muscle nor the ability of the endothelium to release nitric oxide (Wellman *et al.*, 1993; Lot & Wilson, 1994).

Isometric tension recordings

On the following day, the vein and artery were carefully cleaned of connective tissue and divided into 5 mm ring segments. Stainless steel wire (0.2 mm thick) supports were inserted into the lumen and each segment suspended in an isolated organ bath containing modified Krebs-Henseleit saline with 10 μM cocaine (to inhibit uptake$_1$), 1 μM propranolol (to inhibit β-adrenoceptors) and Na_2EDTA (23 μM) to prevent the oxidative degradation of noradrenaline. The Krebs-Henseleit saline was maintained at 31°C, as this has been shown to enhance the function of postjunctional α_2-adrenoceptors (Flavahan & Vanhoutte, 1986; Templeton *et al.*, 1989), and gassed with 95% O_2 and 5% CO_2. No attempt was made to remove the endothelium. The lower support was fixed, and the upper support was connected to a Grass FT-03 transducer linked to a Grass Polygraph. After 30 min equilibration in the Krebs-Henseleit saline, approximately 8 g wt. tension (artery) and 4 g wt. tension (vein) were slowly applied and the tissue allowed to relax to a final resting tension of 1.5–2 g wt. (artery) and 0.5–0.7 g wt. (vein). After 60 min equilibration, each preparation was exposed to 1 μM (−)-noradrenaline (NA) and allowed to contract for 5 min. Following complete washout, the preparation was again challenged with 1 μM noradrenaline, washed and an additional 1 h equilibration period allowed before starting the experiment. This procedure was found to minimize changes in the sensitivity of the preparation to further addition of noradrenaline. In experiments involving phenoxybenzamine the preparations were repeatedly exposed to 40 mM KCl, rather than noradrenaline, to establish reproducible responses.

In all experiments cumulative concentration-response curves (CRC) were constructed by exposing the tissue to increasing concentrations (0.5 log unit increments) of the agonist until a maximum response was observed. Since contractile responses of the palmar lateral vein to the α-adrenoceptor agonists were not well maintained over a period greater than 90 s, the addition of the next concentration of the agonist was made as close to the peak response as possible. For the palmar common digital artery, the CRC was terminated at 3 μM noradrenaline to avoid receptor desensitization. Successive CRCs were separated by 60 min, as measured from the time following washout and complete relaxation of the preparation, and a maximum of three CRCs was constructed in each preparation.

The effect of reversible α-adrenoceptor antagonists

The α-adrenoceptor antagonists, phentolamine (0.03–30 μM), prazosin (0.01–1 μM), rauwolscine (0.1–10 μM), CH-38083 (0.1–10 μM), YM-12617 (0.01–1 μM) or a combination of the subtype-selective antagonists were added at least 40 min prior to the construction of a second or third CRC. In one series of experiments, the effect of phentolamine against noradrenaline-induced contractions was also examined in the presence of 10 μM corticosterone (to inhibit extraneuronal uptake).

The effect of phenoxybenzamine

Preparations were exposed to a single concentration of phenoxybenzamine (0.3 μM, 1 μM or 3 μM) or saline for 60 min (after reproducible responses to KCl had been established) and then washed a minimum of five times over the next 60 min before exposure to increasing concentrations of noradrenaline. In another series of experiments, preparations were exposed to 1 μM rauwolscine 5 min before the addition of 1 μM phenoxybenzamine to increase the degree of protection for α_2-adrenoceptors (Daly *et al.*, 1988c). After 60 min, the phenoxybenzamine was removed by washing twice with Krebs-Henseleit saline containing 1 μM rauwolscine and this antagonist was removed 5 min later (total time; 60 min for phenoxybenzamine, 70 min for rauwolscine). The preparations were washed a further five times over 45 min and a concentration-response curve to noradrenaline constructed. The noradrenaline CRC was repeated 60 min later after 40 min exposure to either 0.1 μM prazosin, 1 μM rauwolscine or vehicle.

Data analysis

The sensitivity of the preparations to noradrenaline was assessed as the negative logarithm of the concentration required to cause 50% of the maximum response (pD_2). The agonist concentration-ratio in the presence and absence of the antagonist was determined at level of either 50% of the maximum response (palmar lateral vein) or 50% of the control response to 3 μM noradrenaline (palmar common digital artery). Using the agonist concentration-ratio produced by the lowest effective concentration of the antagonist, an estimate of the negative logarithm of the dissociation con-

stant (pK_B) was determined by the method of Furchgott (1972). In the case of phentolamine, a pA_2 value was determined by the method of Arunlakshana & Schild (1959).

In all experiments, one preparation was run in parallel with the experimental tissues, but received no antagonist, and was used to determine time-dependent changes in agonist sensitivity (Furchgott, 1972). All responses are expressed as a percentage of the maximum response and given as the mean ± s.e. mean. Differences between means were considered statistically significant if $P<0.05$ for unpaired or paired observations (Student's t test). The logarithm of the concentration of noradrenaline producing either 25% or 50% of the control maximum response or agonist-concentration ratios was calculated with the logistic equation described by DeLean *et al.* (1978) with Kalidegraph software (Synergy) on a MacIntosh LC II computer.

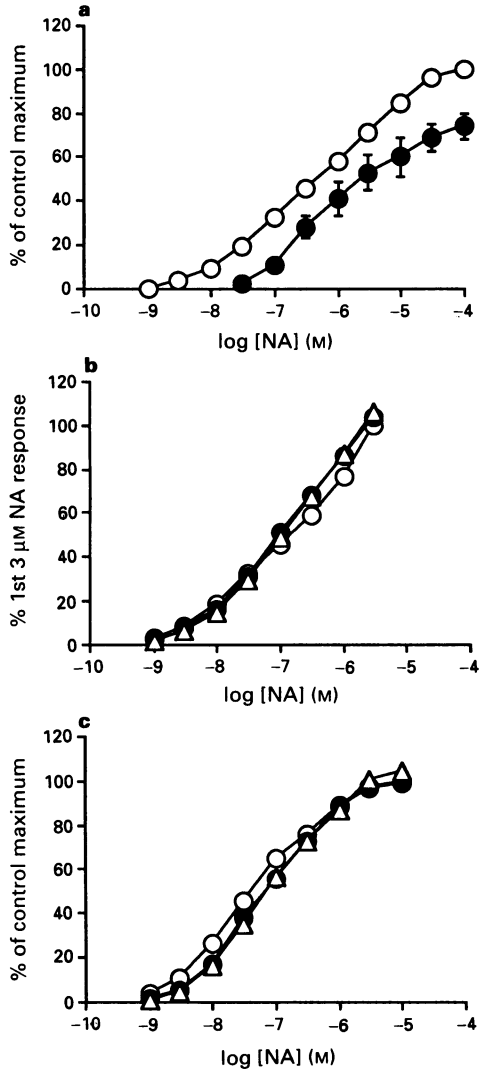

Figure 1 The reproducibility of noradrenaline (NA) concentration-response curves (CRCs) in the porcine isolated palmar common digital artery (a and b) and palmar lateral vein (c). The highest concentration of noradrenaline employed was 100 μM (a), 3 μM (b) and 10 μM (c), and (○) denotes the 1st CRC, (●) denotes the 2nd CRC and (△) denotes the 3rd CRC. All points represent the mean of 6 observations (a) or 9 observations (b and c) with the s.e. mean in (a). In (b) and (c) the s.e. mean, which were less than 6%, have been omitted to improve clarity.

Drugs

The following compounds were used: (−)-noradrenaline bitartrate (Sigma); prazosin HCl (Pfizer); rauwolscine HCl (Roth); YM-12617 (5-[2-[[2-(ethoxyphenoxy)ethyl]amino] propyl]-2-methoxy benzene-sulphonamide HCl) (Yamanouchi); CH-38083 (7,8-(methylenedioxi)-14-α-hydroalloberbane HCl) (Chinoin); phenoxybenzamine HCl (SKB); corticosterone (Sigma); phentolamine mesylate (Rogitine, Ciba Geigy); propranolol HCl (Sigma); cocaine HCl (MacCarthys), Ficoll 70,000 (Sigma). Stock solutions of noradrenaline were prepared in distilled water with 23 μM Na_2EDTA. Prazosin (1 mM) was dissolved in 0.1 M lactic acid and dilutions made in distilled water. Phenoxybenzamine (1 mM) was prepared in 20% absolute alcohol in distilled water and a drop of 1 N HCl to remove turbidity and further dilutions were made in distilled water. Corticosterone (10 mM) was dissolved in propylene glycol. All other drugs were dissolved in distilled water and added to the organ baths in a volume of 0.1 ml or less.

Results

The reproducibility of responses to noradrenaline and the effect of phentolamine

In the presence of 10 μM cocaine and 1 μM propranolol, noradrenaline (0.001–100 μM) produced concentration-dependent contractions of the PCDA and the PLV (Figure 1a,b). The maximum response of the PCDA was greater than that of the PLV, but the sensitivity of the arterial preparation to noradrenaline was 1/10th of that of the vein (Table 1). The addition of 10 μM corticosterone to the bathing medium caused a 2 fold increase in the sensitivity of the PCDA to noradrenaline, but did not alter the sensitivity of the PLV (Table 1).

Exposure of the PCDA to 100 μM noradrenaline (in order to achieve the maximum effect) required 2 h of repeated washing to effect complete relaxation of the smooth muscle. As shown in Figure 1a, the subsequent CRC was displaced approximately 3 fold to the right (pD_2 – 5.95 ± 0.13, $n=6$) and was associated with a 20–25% reduction in the max-

Table 1 Responses of the porcine isolated palmar common digital artery (PCDA) and palmar lateral vein (PLV) to noradrenaline

	Force (g wt)	pD_2
PCDA		
Cocaine 10 μM, propranolol 1 μM	10.4 ± 0.9 ($n=10$)	6.33 ± 0.07 ($n=10$)
Cocaine 10 μM, propranolol 1 μM, corticosterone 10 μM	9.2 ± 0.8 ($n=8$)	6.63 ± 0.08 ($n=8$)*
PLV		
Cocaine 10 μM, propranolol 1 μM	3.24 ± 0.22 ($n=8$)	7.39 ± 0.09 ($n=8$)
Cocaine 10 μM, propranolol 1 μM, cortisterone 10 μM	2.88 ± 0.19 ($n=8$)	7.48 ± 0.12 ($n=8$)

Values shown are the mean ± s.e.mean of n experiments (shown in parentheses). *Significantly different from value in the absence of corticosterone ($P<0.05$, unpaired t test).

imum response. Inclusion of 10 μM corticosterone to the bathing medium, reduced the time required to effect complete relaxation of the PCDA following exposure to 100 μM noradrenaline, but did not appreciably alter the apparent desensitization. By limiting the highest concentration of noradrenaline to 3 μM for the PCDA and 10 μM for the PLV, three reproducible CRCs could be constructed 75 min apart (Figure 1b,c).

Figure 2 shows the effect of phentolamine against noradrenaline-induced contractions of the PCDA and PLV in the presence of 10 μM cocaine and 1 μM propranolol. Phentolamine (0.03–30 μM) produced a parallel rightward displacement of the concentration-response curves for noradrenaline in both preparations. As shown in Table 2, the pA_2 value for phentolamine was similar in both preparations and the slopes of the Schild plots were not significantly different from unity. Neither the pA_2 value nor the slope of the Schild plot for phentolamine was significantly altered by the inclusion of 10 μM corticosterone in the bathing medium (Table 2). Since, corticosterone failed to alter the interaction between phentolamine and noradrenaline at α-adrenoceptors in either preparation, it was decided to conduct all subsequent experiments in the presence of only 10 μM cocaine and 1 μM propranolol.

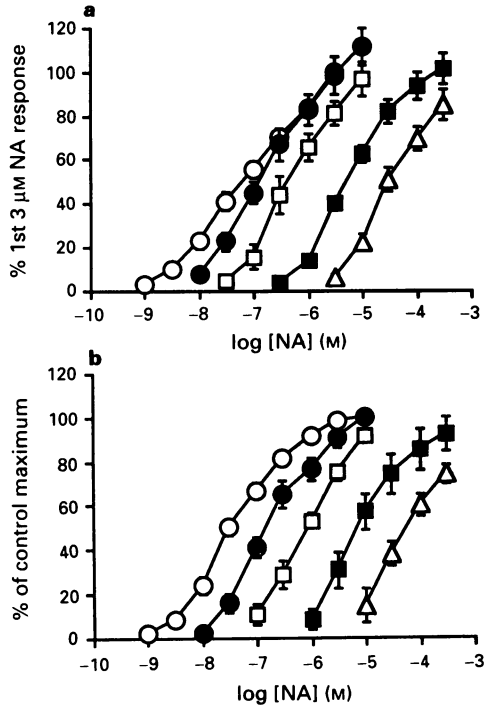

Figure 2 The effect of 0.03 μM (●), 0.3 μM (□), 3 μM (■) and 30 μM (△) phentolamine against noradrenaline (NA)-induced contraction of (a) the porcine isolated palmar common digital artery and (b) the porcine isolated palmar lateral vein. The control concentration-response curve to noradrenaline is represented by (○). All points represent the mean ± s.e. mean of 6 observations.

The effect of other α-adrenoceptor antagonists against noradrenaline-induced contractions

Figure 3 shows the effect of prazosin, YM-12617, rauwolscine and CH-38083 against noradrenaline-induced contractions in the PCDA. Prazosin (0.01–1 μM) and YM-12617 (0.01–1 μM) produced a non-parallel rightward displacement of noradrenaline CRCs, with the lower 10–15% of the CRC exhibiting greater resistance to the effect of these antagonists than the upper part of the CRC (Figure 3a, b). In contrast, rauwolscine (1–10 μM) and CH-38083 (10 μM) produced a parallel displacement of the noradrenaline CRC; lower concentrations of the antagonists failed to produce any effect. In the PLV, the lowest concentration of prazosin (0.01 μM) and YM-12617 (0.01 μM) examined produced a 10–20 fold rightward displacement of the noradrenaline CRC (Figure 4a,b). However, further increases in the concentration of the antagonists (to 1 μM) produced only a small additional displacement of the CRC. Qualitatively similar profiles were obtained for rauwolscine (0.1–10 μM) and CH-38083 (0.1–10 μM) against noradrenaline-induced contractions of the PLV (Figure 4c,d).

Based upon the displacement of the CRC produced by the lowest effective concentration of the antagonists (Table 3), the estimated -log K_B values for the antagonists are consistent with a large population of α_1-adrenoceptors in the PCDA and a mixture of α_1- and α_2-adrenoceptors in the PLV.

The effect of combinations of the α-adrenoceptor antagonists

Concentrations of the antagonists which produced a 15–50 fold rightward displacement of the noradrenaline CRC in PLV (see Table 4) were chosen in order to examine the effects of combinations of the antagonists against noradrenaline-evoked contractions in both preparations. Figure 5 shows that the combination of 1 μM prazosin and 1 μM rauwolscine produced a significantly greater rightward displacement of the noradrenaline CRC in the PCDA and PLV than either 1 μM rauwolscine and 10 μM CH-38083 in combination, or 1 μM prazosin and 0.1 μM YM-1267 in combination. In both cases, prazosin and rauwolscine caused more than a 1000 fold rightward displacement of the

Table 2 pA_2 values and slope for the Schild plot (with 95% confidence intervals) for phentolamine, in the presence of various ancillary agents, against noradrenaline-induced contractions of the porcine isolated palmar lateral vein (PLV) and palmar common digital artery (PCDA)

		(n)	pA_2	Slope
PLV	Cocaine 10 μM, propranolol 1 μM	19	7.78 (8.26–7.26)	0.91 (1.03–0.70)
	Cocaine 10 μM, propranolol 1 μM, corticosterone 10 μM	20	8.06 (8.41–7.70)	0.92 (1.05–0.78)
PCDA	Cocaine 10 μM, propranolol 1 μM	19	7.56 (8.08–7.04)	0.80 (1.14–0.68)
	Cocaine 10 μM, propranolol 1 μM, corticosterone 10 μM	17	7.52 (7.19–7.14)	0.88 (1.15–0.77)

The values shown are based on a minimum of 4 observations at each of 4 observations at each of 4 concentrations (0.03 μM, 0.3 μM, 3 μM and 30 μM) of phentolamine.

noradrenaline CRC; an effect greater than either agent alone (Table 4). In contrast, the combination of 1 μM prazosin with 0.1 μM YM-12617 was no more effective than either agent alone. Table 4 also shows that in both preparations the combination of 0.1 μM YM-12617 and 10 μM CH-38083 was more effective than either agent alone.

Attempts to isolate functional α_2-adrenoceptors

The above findings indicate that a combination of a selective α_1-adrenoceptor antagonist (prazosin or YM-12617) with a selective α_2-adrenoceptor antagonist (rauwolscine or CH-38083) is more effective than the combination of antagonists

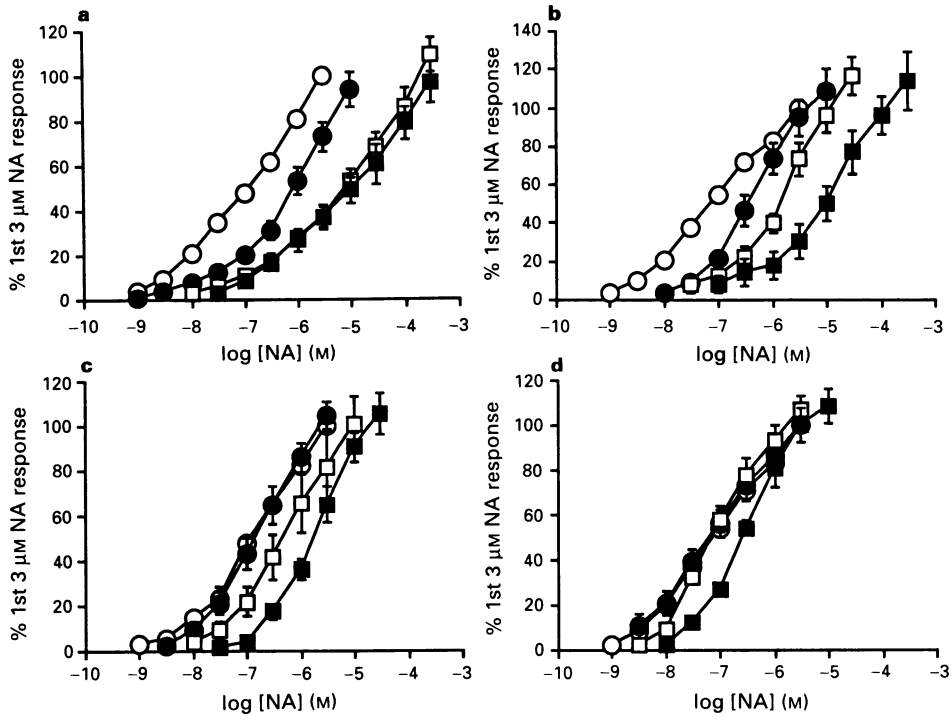

Figure 3 The effect of (a) 0.01 μM (●), 0.1 μM (□), 1 μM (■) prazosin; (b) 0.01 μM (●), 0.1 μM (□), 1 μM (■) YM-12617; (c) 0.1 μM (●), 1 μM (□), 10 μM (■) rauwolscine and (d) 0.1 μM (●), 1 μM (□) 10 μM (■) CH-38083 against noradrenaline (NA)-induced contractions of the porcine isolated palmar common digital artery. The control concentration-response curve to noradrenaline is represented by (○). All points represent the mean ± s.e. mean of 5–7 observations.

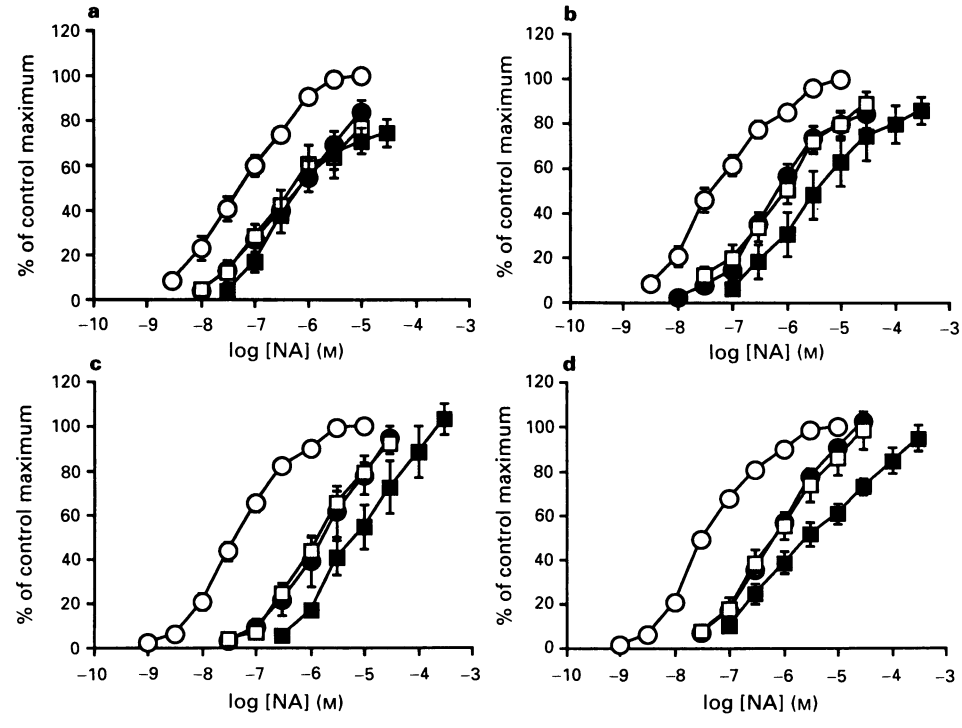

Figure 4 The effect of (a) 0.01 μM (●), 0.1 μM (□), 1 μM (■) prazosin; (b) 0.01 μM (●), 0.1 μM (□), 1 μM (■) YM-12617; (c) 0.1 μM (●), 1 μM (□), 10 μM (■) rauwolscine and (d) 0.1 μM (●), 1 μM (□) 10 μM (■) CH-38083 against noradrenaline (NA)-induced contractions of the porcine isolated palmar lateral vein. The control concentration-response curve to noradrenaline is represented by (○). All points represent the mean ± s.e. mean of 5–10 observations.

from the same group. This suggests that α_1- and α_2-adrenoceptors contribute to responses to noradrenaline in both preparations. Confirmation of this provided by the results in Figure 6. Figure 6a and b shows the effects of a 60 min exposure to phenoxybenzamine on contractions to noradrenaline in the PCDA and PLV, respectively. Phenoxybenzamine (0.3–1 μM) produced a concentration-dependent reduction in the maximum response to noradrenaline, which was more pronounced in the PCDA (Figure 6a) than in the PLV (Figure 6b). Phenoxybenzamine 3 μM practically abolished noradrenaline-induced contractions.

The α-adrenoceptor(s) contributing to the response to the noradrenaline remaining after exposure to a combination of 1 μM phenoxybenzamine and 1 μM rauwolscine was examined by investigating the effect of 0.1 μM prazosin and 1 μM rauwolscine. Figure 6c shows that 0.1 μM prazosin failed to affect responses to low concentrations of noradrenaline (0.03–1 μM) in the PCDA, but reduced responses to high concentrations of noradrenaline (> 1 μM). Rauwolscine 1 μM produced only a 10 fold rightward displacement of noradrenaline CRC in the PCDA. In contrast, 0.1 μM prazosin failed to affect responses to noradrenaline in the PLV, while 1 μM rauwolscine produced a 300 fold rightward displacement of the noradrenaline CRC (Figure 6d).

Table 3 Mean $-\log K_B$ values (± s.e.mean) for several antagonists at α-adrenoceptors in the porcine isolated palmar common digital artery (PCDA) and palmar lateral vein (PLV)

	PCDA	*PLV*
Prazosin	8.83 ± 0.09 (0.01 μM, $n = 9$)	8.73 ± 0.25 (0.01 μM, $n = 6$)
YM-12617	8.96 ± 0.22 (0.01 μM, $n = 6$)	8.63 ± 0.14 (0.01 μM, $n = 6$)
Rauwolscine	6.60 ± 0.22 (1.1 μM, $n = 5$)	8.31 ± 0.22 (0.1 μM, $n = 10$)
CH-38083	5.22 ± 0.08 (10 μM, $n = 5$)	8.20 ± 0.13 (0.1 μM, $n = 5$)
Comment: major α-adrenoceptor subtype	α_1	α_1 and α_2

Values shown are based on the shift in the concentration-response curve produced by the lowest effective concentration of the antagonist, measured at the 50% level of either the maximum control response (PLV) or the control response to 3 μM noradrenaline (PCDA). The concentration of the antagonist used for calculating the $-\log K_B$ value and the number of experimental observations are shown in parentheses.

Discussion

As indicated in the Introduction, the principal objective of this study was to examine the pharmacological characteristics of α-adrenoceptors mediating contractions of the PCDA and PLV and assess the suitability of these blood vessels as a model for man. The approach adopted during the course of this investigation was to use noradrenaline as the agonist, because it does not discriminate between α_1- and α_2-

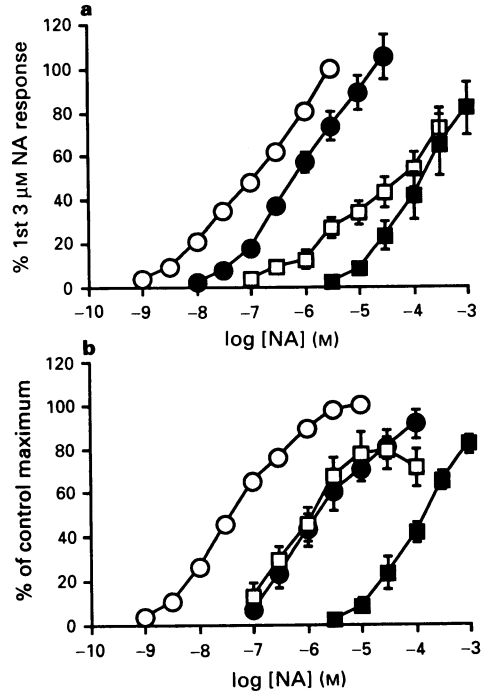

Figure 5 The effect of 1 μM rauwolscine and 10 μM CH-38083 (●); 0.1 μM YM-12617 and 1 μM prazosin (□); 1 μM prazosin and 1 μM rauwolscine (■) against noradrenaline (NA)-induced contractions in (a) porcine isolated palmar common digital artery and (b) porcine isolated palmar lateral vein. The control concentration-response curve to noradrenaline is represented by (○). All points represent the mean ± s.e. mean of 6–9 observations.

Table 4 Logarithm of the concentration-ratio for noradrenaline produced by 'selective' concentrations of the antagonists, either alone or in combination, in the porcine isolated palmar lateral vein (PLV) and palmar common digital artery (PCDA)

	PCDA	*PLV*
CH-38083* 10 μM	0.71 ± 0.10 ($n = 5$)	1.75 ± 0.13 ($n = 10$)
Rauwolscine* 1 μM	0.66 ± 0.22 ($n = 5$)	1.17 ± 0.08 ($n = 9$)
Combination	0.80 ± 0.15 ($n = 7$)	1.58 ± 0.11 ($n = 7$)
Prasozin* 1 μM	1.52 ± 0.18 ($n = 6$)	1.16 ± 0.19 ($n = 9$)
YM-12617* 0.1 μM	1.61 ± 0.14 ($n = 6$)	1.35 ± 0.18 ($n = 9$)
Combination	1.98 ± 0.17 ($n = 7$)	1.45 ± 0.14 ($n = 7$)
YM-12617* 0.1 μM	1.61 ± 0.14 ($n = 6$)	1.35 ± 0.18 ($n = 9$)
CH-38083* 10 μM	0.71 ± 0.22 ($n = 5$)	1.75 ± 0.13 ($n = 10$)
Combination	2.47 ± 0.21 ($n = 7$)†	2.50 ± 0.18 ($n = 7$)†
Prazosin* 1 μM	1.52 ± 0.18 ($n = 6$)	1.16 ± 0.19 ($n = 9$)
Rauwolscine* 1 μM	0.66 ± 0.22 ($n = 5$)	1.17 ± 0.08 ($n = 9$)
Combination	3.21 ± 0.23 ($n = 6$)†	3.38 ± 0.14 ($n = 9$)†

Values shown are the mean ± s.e.mean of n experiments (shown in parentheses). *Concentration-ratio calculated at the 50% level of the maximum control response to noradrenaline (PLV) or at the level of 25% of the control response to 3 μM noradrenaline (PCDA). *Values taken from a separate series of experiments (see Figures 3 and 4). †The effect of the combination of the antagonists is significantly more effective than either antagonist alone ($P < 0.05$. Student's unpaired t test).

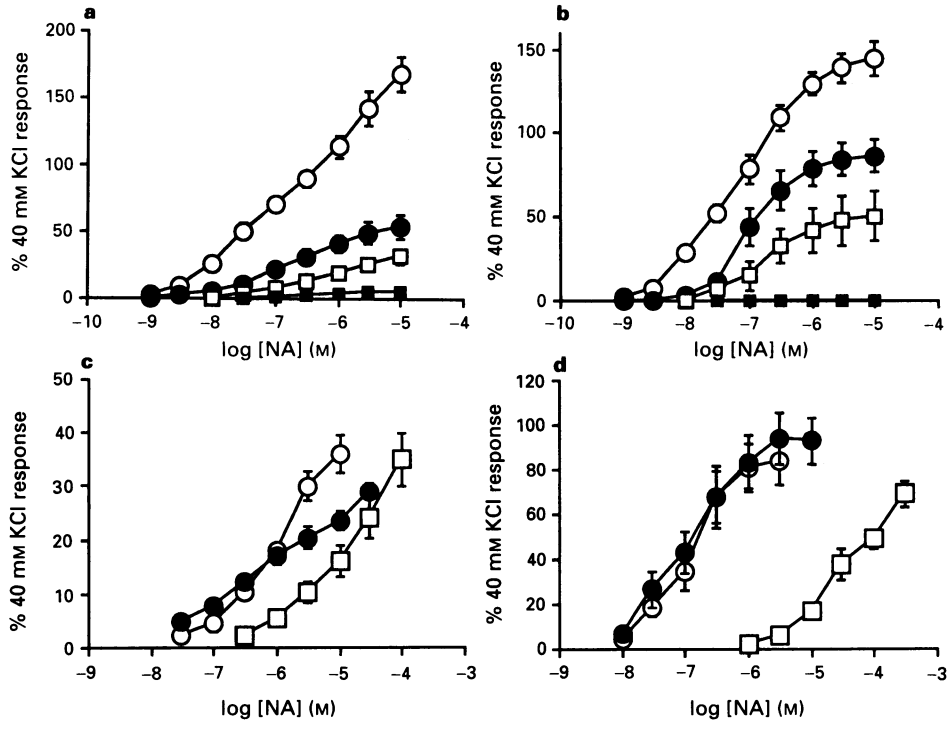

Figure 6 (a, b) The effect of prior exposure to 0.1 μM (●), 1 μM (□) and 3 μM (■) phenoxybenzamine (60 min exposure followed by 45 min washout) on noradrenaline (NA)-induced contractions of the (a) the porcine isolated palmar common digital artery and (b) porcine isolated palmar lateral vein. The control concentration-response curve to noradrenaline is represented by (○). All points represent the mean of 5–6 observations ± s.e. mean. (c,d) The effect of 0.1 μM prazosin (●) and 1 μM rauwolscine (□) against noradrenaline (NA)-induced contractions of the (c) the porcine isolated palmar common digital artery and (d) the porcine isolated palmar lateral vein, after exposure to a combination of 1 μM phenoxybenzamine (60 min) and 1 μM rauwolscine (70 min) followed by a several washes over 45 min. The control concentration-response curve to noradrenaline is represented by (□). All points represent the mean ± s.e. mean of 5–6 observations.

adrenoceptors (McGrath 1982; McGrath *et al.*, 1989), and rely upon selective antagonists to establish the presence of particular receptor subtypes. Support for this stance is provided by Sjöberg and coworkers (1987), who observed that B-HT 920 and clonidine, agonists which selectively activate α_2-adrenoceptors in other species, failed to elicit contractions of human blood vessels while the combination of noradrenaline and a selective α_1-adrenoceptor antagonist suggested the presence of postjunctional α_2-adrenoceptors.

There are three other aspects of the experimental conditions in our study that are worthy of comment. First, in preliminary experiments we observed that inhibition of neuronal uptake by cocaine, and blockade of β-adrenoceptors by propranolol, produced a 3 fold increase in the sensitivity of both preparations to noradrenaline (unpublished observations), and these agents were routinely incorporated in the Krebs-Henseleit saline. Secondly, although the inclusion of 10 μM corticosterone in the bathing medium further increased the sensitivity of the PCDA to noradrenaline, its failure to influence significantly either the slope of the Schild plot or pA_2 value for phentolamine (see below), coupled with a tendency to cause a slight reduction of the maximum response in both preparations, was taken as a basis for leaving extraneuronal uptake intact. Finally, no attempt was made to remove the endothelium, so the possibility exists that α-adrenoceptor-mediated contractions were reduced by either basal release or α_2-adrenoceptor-mediated release of endothelium-derived nitric oxide (Kovitz *et al.*, 1993; Ohgushi *et al.*, 1993). It should be noted, however, that endothelium-denudation in the PCDA failed to affect contractions to 5-hydroxytryptamine (Lot & Wilson, unpublished observations) and, α_2-adrenoceptor-mediated release of nitric oxide in the pig was not observed in mesenteric, renal or iliac arteries (Ohgushi *et al.*, 1993).

Noradrenaline produced concentration-dependent contractions in both preparations which were competitively antagonized by phentolamine. The pA_2 for phentolamine, approximately 7.3–7.7, is consistent with the presence of α-adrenoceptors (McGrath *et al.*, 1989). It was noticeable, however, that the potency of phentolamine was slightly higher in the PLV compared to the PCDA and that this difference was not influenced by the inclusion of 10 μM corticosterone in the bathing medium. The possibility exists that the decision to avoid full concentration-response curves in the PCDA, to reduce the potential for receptor desensitization, might have resulted in an underestimation of the potency of phentolamine in the arterial preparation.

To assess in greater detail the pharmacological characteristics of α-adrenoceptors in the two blood vessels, prazosin and YM-12617 were used as selective α_1-adrenoceptor antagonists and rauwolscine and CH-38083 used as selective α_2-adrenoceptor antagonists. Since, with the exception of prazosin (Akers *et al.*, 1987; Neilsen *et al.*, 1991), none of these agents has been used to characterize α-adrenoceptors on porcine vascular smooth muscle, no assumption was made about their selectivity for subtypes of α-adrenoceptor in the pig. Instead, we have relied upon agents of the same provisional class to produce qualitatively similar effects in each vessel. In this respect, the evidence suggests the presence of α_1- and α_2-adrenoceptors contributing to noradrenaline-induced contractions in the PCDA and PLV, with the latter possessing a larger population of functional α_2-adrenoceptors.

Prazosin and YM-12617 were potent antagonists in the PCDA but, unlike phentolamine, they produced non-competitive inhibition. Based upon the displacement produced by the lowest concentration employed (10 nM), the dissociation constant for both antagonists, approximately 9, is consistent with an effect at α_1-adrenoceptors (Wilson *et al.*, 1991). Significantly, higher concentrations of the antagonists tended to produce much smaller rightward displacement of

the lower component of the noradrenaline concentration-response curve, suggesting the presence of another receptor subtype. In the PCDA, only high concentrations of CH-38083 and rauwolscine (> 1 μM) produced significant inhibition of noradrenaline-induced responses which, when viewed in isolation, supports the presence of α_1-adrenoceptors. However, since the combination of a putative selective α_1- and α_2-adrenoceptor antagonist (prazosin and rauwolscine or YM-12617 and CH-38083) was more effective than the combination of either the putative α_1-adrenoceptor antagonists or α_2-adrenoceptor antagonists (prazosin with YM-12617 or CH-38083 and rauwolscine), this has been taken as evidence for the presence of α_2-adrenoceptors and also confirmation of the characteristics of the antagonists at α-adrenoceptors in the pig. Qualitatively similar observations were made in the PLV, except that the component of the noradrenaline response resistant to prazosin and YM-12617 was larger, and this was associated with a corresponding increase in the potency of rauwolscine and CH-38083; based upon the effect of the lowest concentration employed, rauwolscine and CH-38083 had an effect consistent with an action at α_2-adrenoceptors (see Wilson *et al.*, 1991). Finally, phenoxybenzamine, which has been reported to inactivate α_1-adrenoceptors preferentially (Constantine *et al.*, 1982), was more effective in the PCDA suggesting a larger population of α_1-adrenoceptors. Furthermore, following exposure to a combination of rauwolscine and phenoxybenzamine, to increase protection of α_2-adrenoceptors (Daly *et al.*, 1988c; Dunn *et al.*, 1991), the response to noradrenaline in PLV was completely resistant to prazosin but sensitive to rauwolscine; unequivocal evidence for a population of postjunctional α_2-adrenoceptors (McGrath *et al.*, 1989). In the case of the PCDA, however, only part of the remaining response was resistant to prazosin. The basis of this difference between the preparations is not known.

Although α_1- and α_2-adrenoceptors are currently divided into several further subtypes on the basis of both pharmacological characteristics of membrane sites in radioligand binding assays and receptor amino acid sequence (Wilson *et al.*, 1991; Lomasney *et al.*, 1991), the lack of genuinely subtype-specific antagonists, with selectivity comparable to that for either prazosin or rauwolscine, has precluded any attempt at detailed subclassification of α-adrenoceptors in these functional experiments. Moreover, since there is the potential for these receptor subtypes to interact (Daly *et al.*, 1988b,c; Dunn *et al.*, 1991), we have limited the scope of the pharmacological characterization simply to α_1- and α_2-adrenoceptors. It is noteworthy, however, that since we have used the resistance of responses to prazosin (0.1–1 μM) as a marker for the presence of postjunctional α_2-adrenoceptors, it seems likely that these belong to the $\alpha_{2A/D}$ subgroup. Also, the relative ease with which it is possible to obtain large quantities of porcine vascular smooth muscle has allowed us to perform preliminary radioligand binding experiments on the thoracic aorta and splenic artery (Wright *et al.*, 1993). Future experiments will be directed towards using membrane preparations of individual blood vessels for the purpose of detailed pharmacological characterization of the α-adrenoceptors.

Thus the PLV, like superficial veins from the rabbit, dog and man (Constantine *et al.*, 1982; Sjöberg *et al.*, 1987; Daly *et al.*, 1988a,b; Arner *et al.*, 1988) appear to possess α_1-adrenoceptors and a large population of α_2-adrenoceptors. Although α_1-adrenoceptors are the major subtype responsible for contractions to noradrenaline in the PCDA, observations with both competitive and irreversible antagonists indicate the presence of a small population of α_2-adrenoceptors which do not require the presence of an ancillary agent for functional expression (cf. Templeton *et al.*, 1989; Dunn *et al.*, 1991). In this respect, the PCDA is similar to both human skin and digital arteries (Stevens & Moulds, 1981; 1986; Borbujo *et al.*, 1989), and it provides support for the suggestion that the porcine blood vessels may be a good experimental model for man. Our results also suggest that demonstration of functional α_2-adrenoceptors on other human arteries, e.g. epigastric artery (Sjöberg *et al.*, 1987), may be more easily demonstrated by the use of noradrenaline and a combination of a selective α_1- and a selective α_2-adrenoceptor antagonist. It remains to be determined, however, whether the similarity between porcine and human α-adrenoceptor pharmacology in digital blood vessels extends to other vascular beds and, indeed, to other receptor systems, e.g. neuropeptidey and 5-HT_1-like, which have proved elusive in arterial vessels from standard laboratory animals.

We are grateful to the Wellcome Trust and Mason Brothers (Nottingham) for their support.

References

AKERS, I.A., COATES, J., DREW, G.M., GURDEN, J.M. & SULLIVAN, A.T. (1987). Does prazosin distinguish between subgroups of α_1-adrenoceptors? *Br. J. Pharmacol.*, **91**, 383P.

ARUNLAKSHANA, O. & SCHILD, H.O. (1959). Some quantitative uses of drug antagonists. *Br. J. Pharmacol. Chemother.*, **14**, 48–58.

ARNER, M., HÖGESTÄTT, E.D. & ANDERSSON, K-E. (1988). Effects of nimodipine, Bay K-8644 and pinacidil on α_1- and α_2-adrenoceptor-mediated vasoconstriction in human hand vein. *Acta Physiol. Scand.*, **133**, 417–422.

BECKERINGH, J.J., THOOLEN, M.J.M.C., DE JONGE, A., WILFFERT, B., TIMMERMANS, P.B.M.W.M. & VAN ZWEITEN, P.A. (1984). Differential effects of the calcium entry blocker D 600 on contractions of rat and guinea-pig aortae, elicited by various α_1-adrenoceptor agonists. *J. Pharmacol. Exp. Ther.*, **229**, 515–521.

BORBUJO, J., GARCIA-VILLALON, A.L., VALLE, J., GOMEZ, B. & DIEQUEZ, G. (1989). Postjunctional α_1- and α_2-adrenoceptors in human skin arteries. An *in vitro* study. *J. Pharmacol. Exp. Ther.*, **249**, 284–287.

BURDON, T.A., MILLER, D.G., OYER, P.E., MITCHELL, R.S., STINSON, E.B., STARNES, V.A. & SHUMWAY, N.E. (1992). Durability of porcine valves at fifteen years in a representative North American patient population. *J. Thorac. Cardiovac. Surg.*, **103**, 238–252.

CHRISTIE, M.I. & LEWIS, M.J. (1991). A comparison of endothelium-derived relaxing factor activity in the coronary and renal arteries of the pig. *Eur. J. Pharmacol.*, **202**, 143–149.

CONSTANTINE, J.W., LEBEL, W. & ARCHER, R. (1982). Functional postsynaptic α_2-, but not α_1-adrenoceptors in dog saphenous vein exposed to phenoxybenzamine. *Eur. J. Pharmacol.*, **85**, 325–329.

COOPER, D.K.C. (1992). Is xenotransplantation a realistic clinical option? *Transplantation Proc.*, **24**, 2393–2396.

DALY, C.J., MCGRATH, J.C. & WILSON, V.G. (1988a). An examination of α-adrenoceptors of postjunctional α-adrenoceptor subtypes for (−)-noradrenaline in several blood vessels from the rabbit. *Br. J. Pharmacol.*, **95**, 473–484.

DALY, C.J., MCGRATH, J.C. & WILSON, V.G. (1988b). Pharmacological analysis of the postjunctional α-adrenoceptors mediating contractions to (−)-noradrenaline in the rabbit isolated lateral saphenous vein can be explained by interacting responses to simultaneous activation of α_1- and α_2-adrenoceptors. *Br. J. Pharmacol.*, **95**, 485–500.

DALY, C.J., DUNN, W.R., MCGRATH, J.C. & WILSON, V.G. (1988c). An attempt at selective protection from phenoxybenzamine of post-junctional α-adrenoceptor subtypes mediating contractions to noradrenaline in the rabbit isolated saphenous vein. *Br. J. Pharmacol.*, **95**, 501–511.

DELEAN, A., MUNSON, P.J. & RODBARD, D. (1978). Simultaneous analysis of families of sigmoidal curves: applications to bioassay, radioligand assay and physiological dose response curves. *Am. J. Physiol.*, **235**, E97–E102.

DUNN, W.R., MCGRATH, J.C. & WILSON, V.G. (1991). Post-junctional α-adrenoceptors in the rabbit isolated distal saphenous artery: indirect sensitivity to prazosin of responses to noradrenaline mediated by post-junctional α_2-adrenoceptors. *Br. J. Pharmacol.*, **103**, 1484–1492.

FIRST, M.R. (1992). Transplantation in the nineties. *Transplantation*, **53**, 1–11.

FLAVAHAN, N.A. & VANHOUTTE, P.M. (1986). The effect of cooling on α_1- and α_2-adrenoceptor responses in canine and femoral veins. *J. Pharmacol. Exp. Ther.*, **238**, 139–147.

FURCHGOTT, R.F. (1972). The classification of adrenoceptors (adrenergic receptors). An evaluation from the standpoint of receptor theory. In *Handbook of Experimental Pharmacology*, Vol 33, *Catecholamines*. ed. Blaschko, H. & Muscholl, E. pp. 283–335. Berlin: Springer-Verlag.

GOOD, A.H., COOPER, D.K.C., MALCOLM, A.J., IPPOLITO, R.M., KOREN, E., NEETHLING, F.A. YE, Y., ZUDHI, N & LAMONTAGNE, L.R. (1992). Identification of carbohydrate structures that bind human antiporcine antibodies: implications for discordant xenografting in humans. *Transplantation Proc.*, **24**, 559–562.

GHOSHAL, N.G. & NANDA, B.S. (1975). Porcine heart and arteries. In *Sissons and Grossmans' Anatomy of Domestic Animals* ed. Getty, R. pp. 1306–1342. Philadelphia: Saunders and Co.

HONDA, K., TAKENAKA, T., MIYATA-OSAWA, A., TERAI, M. & SHIONO, K. (1985). Studies on YM-12617: a selective and potent antagonist of postsynaptic α_1-adrenoceptors. *Naunyn Schmied. Arch. Pharmacol.*, **328**, 264–272.

ITO, S., SUZUKI, S. & KURIYAMA, H. (1993). Effects of a water soluble forskolin derivative (NKH-477) and a membrane-permeable cyclic AMP analogue on noradrenaline-induced Ca^{2+} mobilization in smooth muscle of rabbit mesenteric artery. *Br. J. Pharmacol.*, **110**, 1117–1126.

JENKIN, R.A., BALDI, M.A., IWANOV, V. & MOULDS, R.F.W. (1991). Differences between rat and guinea-pig aorta in postreceptor mechanisms of α_1-adrenoceptors. *J. Cardiovasc. Pharmacol.*, **18**, 566–573.

KIM, P., SHIMOKAWA, H. & VANHOUTTE, P.M. (1992). Dietary omega-3 fatty acids and endothelium-dependent responses in porcine cerebral arteries. *Stroke*, **23**, 407–413.

KOVITZ, K.L., ALESKOWITCH, T.D., SYLVESTER, J.T. & FLAVAHAN, N.A. (1993). Endothelium-derived contracting and relaxing factors contribute to hypoxic responses of pulmonary arteries. *Am. J. Physiol.*, **265**, H1139–H1148.

LINNIK, M.D. & LEE, T-J. (1989). Effect of haemoglobin on neurogenic responses and cholinergic parameters in porcine cerebral arteries. *J. Cereb. Blood Flow Metab.*, **9**, 219–225.

LOMASNEY, J.W., COTECCHIA, S., LEFKOWITZ, R.J. & CARON, M.G. (1991). Molecular biology of α-adrenergic receptors: implications for receptor classification and for structure-function relationships. *Biochim. Biophysica. Acta.*, **1095**, 127–139.

LOT, T.Y. & WILSON, V.G. (1994). Overnight storage of porcine isolated splenic artery enhances endothelium-dependent constriction to N^G-nitro-L-arginine methyl ester without impairing endothelium-dependent dilator function. *Naunyn Schmied. Arch. Pharmacol.*, **349**, 95–100.

MCGRATH, J.C. (1982). Evidence for more than one type of postjunctional α-adrenoceptor. *Biochem. Pharmacol.*, **31**, 205–211.

MCGRATH, J.C., BROWN, C.M. & WILSON, V.G. (1989). α-Adrenoceptors: a critical review. *Med. Res. Rev.*, **9**, 408–531.

NILSEN, H., PILEGAARD, H.K., HASENKAM, J.M., MORTENSEN, F.V. & MULVANY, M.J. (1991). Heterogeneity of postjunctional α-adrenoceptors in isolated mesenteric resistance arteries from rats, rabbit, pigs and humans. *J. Cardiovasc. Pharmacol.*, **18**, 4–10.

NISHIMURA, J., KANAIDE, H. & NAKAMURA, M. (1987). Characterization of adrenoceptors and [^{3}H]-nitrendipine receptors of porcine vascular smooth muscle: differences between coronary artery and aorta. *Circ. Res.*, **60**, 837–844.

OHGUSHI, M., YASUE, H., KUGIYAMA, K., MUROHARA, T. & SAKAINO. (1993). Contraction and endothelium-dependent relaxation via α-adrenoceptors are variable in various pig arteries. *Cardiovasc. Res.*, **27**, 779–784.

PATIL, P.N., FUDGE, K. & JACOBWITZ, D.J. (1972). Steric aspects of adrenergic drugs XVIII: αα-adrenergic receptors of mammalian aorta. *Eur. J. Pharmacol.*, **19**, 79–87.

RUFFOLO, R.R. JR & WADDELL, J.E. (1982). Receptor interaction of imidazolines: α-adrenoceptors of rat and rabbit aortae differentiated by relative potencies, affinities and efficacies of imidazoline agonists. *Br. J. Pharmacol.*, **77**, 169–176.

RUFFOLO, R.R. Jr., WADDELL, J.E. & YADEN, E.L. (1982). Heterogeneity of postsynaptic α-adrenoceptors in mammalian aortae. *J. Pharmacol. Exp. Ther.*, **221**, 309–314.

SHAFIQ, J., SUZUKI, S., ITOH, T. & KURIYAMA, H. (1992). Mechanisms of vasodilatation induced by NKH744, a water soluble derivative of forskolin, in smooth muscle of the porcine coronary artery. *Circ. Res.*, **71**, 70–81.

SJÖBERG, T., STEEN, S., SKÄRBY, T., NORGREN, L. & ANDERSSON, K-E. (1987). Postjunctional α-adrenoceptors in human superficial epigastric arteries and veins. *Pharmacol Toxicol.*, **60**, 43–50.

STEVENS, M.J. & MOULDS, R.F.W. (1981). Heterogeneity of postjunctional α-adrenoceptors in isolated human vascular smooth muscle. *Arch. Int Pharmacodyn.*, **254**, 43–57.

STEVENS, M.J. & MOULDS, R.F.W. (1986). Antagonism by nifedipine of α_1- and α_2-adrenoceptor-mediated responses of human digital arteries. *J. Pharmacol. Exp. Ther.*, **236**, 764–769.

TEMPLETON, A.G.B., MACMILLAN, J., MCGRATH, J.C., STOREY, N.D. & WILSON, V.G. (1989). Evidence for a population of prazosin-resistant, rauwolscine-sensitive a-adrenoceptors mediating contractions in the isolated vascular bed of the rat tail. *Br. J. Pharmacol.*, **97**, 563–571.

TSUTSUI, H., TOMOIKE, H. & NAKAMURA, M. (1990). Quantitative autoradiographic analyses of α-adrenergic and serotonergic receptors on aorta and coronary. *Am. J. Physiol.*, **259**, H1343–H1350.

VIZI, E.S., HARSING, L.G., GALL, J., KAPOSCI, S., BERNATH, S. & SOMOGYI, G.T. (1986). CH-38083, a selective, potent antagonist of α_2-adrenoceptors. *J. Pharmacol. Exp. Ther.*, **238**, 701–706.

WEITZELL, R., TANAKA, T. & STARKE, K. (1979). Pre- and postsynaptic effects of yohimbine stereoisomers on noradrenergic transmission in the pulmonary artery of the rabbit. *Naunyn Schmied. Arch. Pharmacol.*, **308**, 127–136.

WILSON, V.G., MCGRATH, J.C. & BROWN, C.M. (1991). Evidence for more than two types of α-adrenoceptors involved in physiological responses. *Exp. Physiol.*, **76**, 316–346.

WELLMAN, G.C., WELLMAN, T.D., DUNN, W.R., BEVAN, R.D. & BEVAN, J.A. (1993). Preservation of function of isolated blood vessels after storage. *J. Vasc. Med. Biol.*, **4**, 47–53.

WRIGHT, I.K., BLAYLOCK, N.A., KENDALL, D.A. & WILSON, V.G. (1993). Evidence for α_2-adrenoceptor binding sites on the porcine isolated thoracic aorta, but not in the splenic artery. *Br. J. Pharmacol.*, **109**, 34P.

(Received February 3, 1994
Revised June 20, 1994
Accepted October 10, 1994)

British Journal of Pharmacology (1995) 114, 703-707

Relaxation and decrease in $[Ca^{2+}]_i$ by hydrochlorothiazide in guinea-pig isolated mesenteric arteries

Peter Pickkers & [1]Alun D. Hughes

Department of Clinical Pharmacology, Queen Elizabeth the Queen Mother Wing, St. Mary's Hospital Medical School, Imperial College of Science Technology and Medicine, South Wharf Rd, London W2 1NY

1 We examined the effect of the thiazide diuretic, hydrochlorothiazide, on intracellular calcium concentration ($[Ca^{2+}]_i$) and tone in guinea-pig mesentery arteries. Vessels were mounted on a microvascular myograph and loaded with the Ca^{2+}-sensitive fluorescent dye, Fura-2.

2 Hydrochlorothiazide caused relaxation of noradrenaline-precontracted arteries associated with a fall in $[Ca^{2+}]_i$. Preincubation of arteries with hydrochlorothiazide inhibited both contraction and rise in $[Ca^{2+}]_i$ in response to noradrenaline. Hydrochlorothiazide did not affect tone and $[Ca^{2+}]_i$ when this was elevated by a combination of depolarizing potassium solution and noradrenaline.

3 Hydrochlorothiazide-induced vasorelaxation and decrease of $[Ca^{2+}]_i$ was abolished by charybdotoxin, a blocker of large conductance Ca^{2+}-activated K channels.

4 The rise in $[Ca^{2+}]_i$ elicited by caffeine in Ca^{2+}-free physiological salt solution, and presumably reflecting Ca^{2+} release from intracellular stores, was not altered by preincubation with hydrochlorothiazide.

5 Under depolarizing conditions hydrochlorothiazide did not alter the relationship between the extracellular concentration of Ca^{2+} and $[Ca^{2+}]_i$; however, hydrochlorothiazide caused a small reduction in the contraction produced for a given rise in $[Ca^{2+}]_i$ suggesting hydrochlorothiazide may cause a slight desensitization of the contractile machinery.

6 These findings suggest that hydrochlorothiazide opens Ca^{2+}-activated K channels leading to hyperpolarization and consequent closing of voltage-operated calcium channels. The result of this is an impaired influx of extracellular Ca^{2+}, a decrease in $[Ca^{2+}]_i$ and vasorelaxation.

Keywords: Hydrochlorothiazide; diuretics; Ca^{2+}; Fura-2; K channels; calcium channels; vascular smooth muscle

Introduction

Almost four decades after their introduction in 1957, thiazide diuretics are still the mainstream of therapy of a large part of the hypertensive population (Ramsey *et al.*, 1994). Besides the well studied effect of thiazide diuretics on the nephron, little is known concerning direct vascular actions of this class of drug, despite the fact that in the long term, thiazide diuretics act by lowering vascular resistance, rather than by their diuretic effects (Van Brummelen *et al.*, 1980). Hydrochlorothiazide has been reported to relax isolated portal vein by Mironneau and colleagues (1981), and recently relaxant effects of hydrochlorothiazide and related drugs have been demonstrated in human isolated small arteries (Calder *et al.*, 1992; 1993).

It has long been recognized that Ca^{2+} ions are necessary to trigger and maintain the cascade of protein activation and deactivation that leads to a contractile response in vascular smooth muscle cells. The free concentration of Ca^{2+} ions that is present in the cytosol of vascular smooth muscle cells governs, to an important extent, the activity of the contractile machinery. The contraction of vascular smooth muscle in response to a vasoconstrictor is initiated by increases in free intracellular calcium ($[Ca^{2+}]_i$). This increase of $[Ca^{2+}]_i$ arises from two main sources: influx of extracellular Ca^{2+} ions, and mobilisation of intracellular calcium stores, probably associated with the sarcoplasmic reticulum (Somlyo & Himpens, 1989). There are also indications that vasoconstrictor agents increase the sensitivity of the contractile machinery to $[Ca^{2+}]_i$ (Nishimura *et al.*, 1988; Somlyo & Himpens, 1989; Jensen *et al.*, 1992).

In the opposite case of vasodilatation, $[Ca^{2+}]_i$ can decline as a result of blockade of calcium release from intracellular stores or through decrease of influx of extracellular Ca^{2+}, besides the possibility that some relaxants may desensitize the contractile apparatus to Ca^{2+} (Somlyo & Himpens, 1989).

In view of the key role played by $[Ca^{2+}]_i$ in regulating vascular tone, we have studied the interaction between the vasorelaxant, hydrochlorothiazide and $[Ca^{2+}]_i$ in isolated small arteries (internal diameter $\sim 300\,\mu m$) using the fluorescent indicator, Fura-2. Such arteries were used for this study since they are small enough to contribute significantly to peripheral vascular resistance *in vivo* (Mulvany & Aalkjaer, 1990) and may better reflect the behaviour of the resistance vasculature than larger upstream vessels.

Methods

Guinea-pig mesentery was removed from male animals ($\sim$300 g) killed by cervical dislocation. Resistance vessels (internal diameter $342 \pm 15\,\mu m$) were dissected free from surrounding tissue and mounted on two 40 μm wires in a single channel myograph dedicated to fluorescence measurements to allow simultaneous measurements of isometric tension (force) and $[Ca^{2+}]_i$ to be made.

The myograph contained 5 ml of a modified Krebs-Henseleit physiological saline solution (PSS composition, mM: NaCl 118, KCl 4.7, $CaCl_2.5H_2O$ 2.5, $MgSO_4.7H_2O$ 1.17, $NaHCO_3$ 25.0, $NaH_2PO_4.2H_4O$ 1.0, Na_2EDTA 0.03 and glucose 5) maintained at 37°C and aerated with 95% O_2, 5% CO_2. The vessels were allowed to equilibrate for 1 h and then set at a 'normalized' internal circumference 0.9 L_{100} estimated to be 90% of the circumference they would maintain if relaxed and exposed to 100 mmHg transmural pressure. L_{100} was calculated for each individual vessel on the basis of the passive length-tension characteristics of the artery and the Laplace relationship (Mulvany & Halpern, 1977). This procedure optimised active force generation by these vessels and

[1] Author for correspondence.

the internal diameters referred to were derived from this calculation.

Prior to the beginning of the studies, vessel viability was assessed by exposing arteries to 118 mM K^+ solution (KPSS; PSS with equimolar substitution of 118 mM KCl for NaCl), KPSS with noradrenaline (10 μM), and noradrenaline (10 μM) alone. Vessels which did not reproducibly produce tension equivalent to more than 100 mmHg effective pressure (by Laplace) in response to these stimulants were discarded.

Following assessment of vessel viability the vessels were incubated with the fluorescent calcium indicator Fura-2 AM (6 μM) for 2 h in PSS containing 0.02% Pluronic F-127, 0.1% cremaphor EL and 0.5% dimethyl sulphoxide to improve loading as previously described (Jensen *et al.*, 1992; 1993). Basal tone and contractile response to noradrenaline and potassium were not affected by exposure to this solution.

Fluorescence was measured with a Deltascan spectrofluorimeter (Photon Technology International Inc., South Brunswick, NJ, U.S.A.) connected to an inverted Axiovert 35 fluorescence microscope (Carl Zeiss Oberkochen, Germany). $[Ca^{2+}]_i$ was assessed on the basis of the ratio of fluorescence emission measured at 510 ± 5 nm which was evoked by excitation at 340 and 380 nm. Emission signals and force were measured simultaneously at 4 Hz and acquired on-line using an A/D interface (Photon Technology International Inc., South Brunswick, NJ, U.S.A.) connected to an IBM AT PC. Data were stored on an optical disc and later analysed off-line using commercially available software (Photon Technology International Inc., South Brunswick, NJ, U.S.A.). Both changes in force and $[Ca^{2+}]_i$ were normalized by expressing them as a percentage of control responses to KPSS for each individual vessel. Relaxation or fall in $[Ca^{2+}]_i$ was calculated as % reduction in stable active tone or $[Ca^{2+}]_i$ immediately prior to addition of drug.

Guinea-pig mesenteric arteries do not possess tone under resting conditions, therefore the relaxant effect of hydrochlorothiazide was examined on precontracted vessels. In some experiments a supramaximal concentration of noradrenaline (10 μM), or noradrenaline (10 μM) in the presence of KPSS were used to precontract the vessels and a near maximal concentration of hydrochlorothiazide (30 μM) was added once stable tone and $[Ca^{2+}]_i$ were attained. In other experiments we examined the effect of 20 min preincubation with hydrochlorothiazide (30 μM) or vehicle control on noradrenaline-induced rise in tone and $[Ca^{2+}]_i$. Hydrochlorothiazide had no effect on resting tone or $[Ca^{2+}]_i$. We also studied the effect of charybdotoxin on hydrochlorothiazide-induced relaxation in vessels precontracted with noradrenaline (10 μM) after pre-incubation with charybdotoxin (100 nM) for approximately 20 min. Charybdotoxin was present throughout these experiments.

The effect of hydrochlorothiazide on release of Ca^{2+} from intracellular stores was studied by examining the effect of caffeine (10 mM) in the absence of extracellular Ca^{2+}. Vessels were bathed in Ca^{2+}-free PSS (containing 1 mM BAPTA) for 3 min which is sufficient to remove extracellular Ca^{2+}, but not to deplete intracellular stores (Garcha & Hughes, 1994). The vessel was then exposed to Ca^{2+}-free PSS containing 10 mM caffeine for a further 3 min and then washed out into PSS. Hydrochlorothiazide (30 μM) or vehicle control (0.1% dimethylsulphoxide) was present in PSS and then in Ca^{2+}-free PSS for a total of 20 min before addition of caffeine.

The effect of hydrochlorothiazide on the sensitivity of the contractile machinery to $[Ca^{2+}]_i$ was examined by observing the effect of hydrochlorothiazide on contractile and $[Ca^{2+}]_i$ responses to addition of extracellular Ca^{2+} to a nominally Ca^{2+}-free high potassium solution. Concentrations of Ca^{2+} referred to are those added to the nominally Ca^{2+}-free high potassium solution and extracellular $[Ca^{2+}]$ is likely to differ from these. Vessels were bathed in Ca^{2+}-free KPSS for 3 min prior to cumulative addition of Ca^{2+} (1 nM–3 mM). Ca^{2+} concentration-response curves (Ca^{2+}:1 nM–3 mM) were constructed after either incubation with hydrochlorothiazide for 17 min in PSS prior to changing to Ca^{2+}-free KPSS containing hydrochlorothiazide (30 μM) or a similar incubation with vehicle control. In order to exclude time- or order-dependent effects in these studies the order of exposure to hydrochlorothiazide or vehicle was randomized.

Drugs

1,2-*bis*(2-Aminophenoxy) ethane *N',N',N',N'*, tetraacetic acid (BAPTA), caffeine, cremaphor-EL, dimethylsulphoxide, hydrochlorothiazide, noradrenaline bitartrate and verapamil were purchased from Sigma (Poole, Dorset, UK). Pluronic F-127 and pre-weighed aliquots (50 μg) of Fura-2 acetoxymethylester (Fura-2 AM) were purchased from Molecular Probes (Oregon, U.S.A.). One fresh aliquot of Fura-2AM was used for each experiment. Charybdotoxin was purchased from Peptide Institute (Osaka, Japan). With the exception of charybdotoxin which was stored as frozen aliquots, all drugs were prepared on the day of the experiments. Noradrenaline was dissolved in distilled water and hydrochlorothiazide in dimethylsulphoxide. The final concentration of dimethylsulphoxide 0.1% (v/v) had no effect on vessel reactivity.

Statistics

Data are presented as mean ± standard error of mean with the number of observations in parentheses. Data were analysed by Student's *t* test, in the case of paired comparisons, or two-way analysis of variance (ANOVA) in the case of multiple comparisons. $P<0.05$ was considered significant. Concentration-response data were fitted to a logistic function:

$$y = \frac{A + (B - A)}{1 + \left(\frac{10^c}{10^x}\right)^D}$$

Where y = effect at a given concentration of drug; A = minimum effect; B = maximum effect; c = EC_{50}; x = log [drug]; D = 'Hill slope', by non-linear regression using Excel 5.0 (Microsoft, U.S.A.) and a macro written by one of us (A.D.H.) on an IBM compatible PC.

Results

The effect of hydrochlorothiazide on responses to noradrenaline and the effect of charybdotoxin on hydrochlorothiazide-induced responses

As shown in Figures 1 and 2, the vasorelaxant effect of hydrochlorothiazide (30 μM) was associated with a fall in $[Ca^{2+}]_i$. In vessels preconstricted with noradrenaline (10 μM) in the presence of KPSS, hydrochlorothiazide had no significant effect on vascular tone or $[Ca^{2+}]_i$ (Figures 1 and 2). Incubation with charybdotoxin (20 min, 100 nM) had no effect on the subsequent contraction to noradrenaline, but under these conditions hydrochlorothiazide-induced relaxation was almost totally inhibited (Figures 1 and 2). This was associated with a marked inhibition of the fall in $[Ca^{2+}]_i$ induced by hydrochlorothiazide; $[Ca^{2+}]_i$ (Figures 1 and 2).

In vessels preincubated with hydrochlorothiazide (30 μM), noradrenaline (10 μM) induced a significantly smaller increase in $[Ca^{2+}]_i$ and force than in vessels preincubated with vehicle control. Force and $[Ca^{2+}]_i$ responses to noradrenaline alone were 69 ± 11% and 50 ± 4% respectively ($n = 10$); following preincubation with hydrochlorothiazide these were reduced to 29 ± 16% and 35 ± 17% respectively ($n = 5$; $P<0.05$ for force and $[Ca^{2+}]_i$).

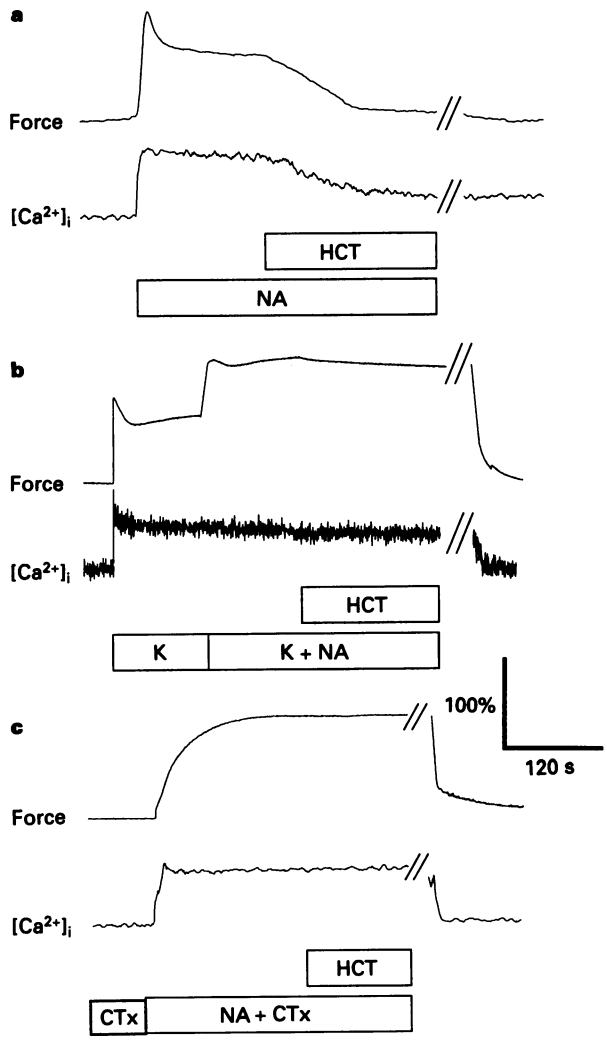

Figure 1 The effect of hydrochlorothiazide on force and $[Ca^{2+}]_i$ under various conditions. Representative traces are shown of simultaneously measured force (% KPSS) and $[Ca^{2+}]_i$ (% KPSS) in guinea-pig isolated small mesenteric arteries mounted in a myograph and loaded with Fura-2. (a) Vessel was precontracted with noradrenaline (NA; 10 μM) and hydrochlorothiazide (HCT; 30 μM) was added once stable tone and $[Ca^{2+}]_i$ were achieved. Periods of drug exposure are indicated by the horizontal bars, the parallel lines interrupting the traces indicate washout of drug. (b) Vessel was contracted with high potassium solution (KPSS) and then noradrenaline (NA; 10 μM) added. Hydrochlorothiazide (HCT; 30 μM) was added once stable tone and $[Ca^{2+}]_i$ were achieved. Periods of drug exposure are indicated by the horizontal bars, the parallel lines interrupting the traces indicate washout of drug. (c) Vessel was contracted with noradrenaline (NA; 10 μM) in the presence of charybdotoxin (CTx; 100 nM) following 20 min preincubation with CTx. Hydrochlorothiazide (HCT; 30 μM) was added once stable tone and $[Ca^{2+}]_i$ were achieved. Periods of drug exposure are indicated by the horizontal bars, the parallel lines interrupting the traces indicate washout of drug. Calibration bar is shown. Traces are representative of 4–9 similar experiments.

The effect of hydrochlorothiazide on calcium release from intracellular stores

Noradrenaline (10 μM) had no effect on force (−1 ± 2%) or $[Ca^{2+}]_i$ (0 ± 1%) in 3 vessels in Ca^{2+}-free PSS, although endothelin-1 (100 nM) induced a transient rise in force and $[Ca^{2+}]_i$ under the same conditions ($n = 2$). Preincubation with the calcium antagonist, verapamil (10 μM), also abolished force and $[Ca^{2+}]_i$ responses to noradrenaline (10 μM) in mesenteric arteries ($n = 3$), though both endothelin-1 (100 nM) and vasopressin (100 nM) induced an increase in tone

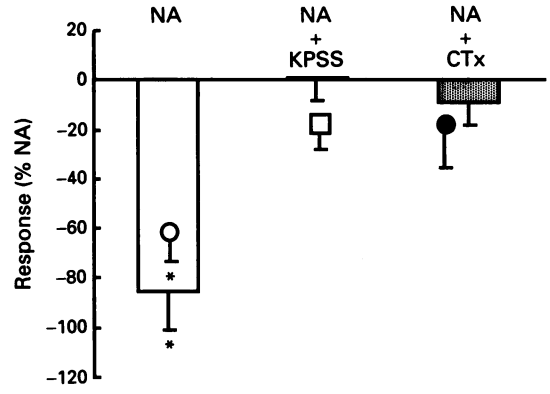

Figure 2 Combination chart showing the effect of hydrochlorothiazide (HCT; 30 μM) on contraction (columns) and elevated $[Ca^{2+}]_i$ (symbols) induced in guinea-pig mesenteric arteries by (a) noradrenaline (NA; 10 μM; $n = 9$); (b) noradrenaline (NA; 10 μM) in the presence of a depolarizing potassium solution (KPSS; $n = 5$) and (c) noradrenaline (NA; 10 μM) in the presence of charybdotoxin (CTx; 100 nM) and following 20 min preincubation with CTx ($n = 4$). Vessels were precontracted until stable tone and $[Ca^{2+}]_i$ were achieved. HCT was then added. Results were calculated as the % reduction in tone or $[Ca^{2+}]_i$ induced by HCT taking the response to NA as 100%. Values represent the mean ± s.e.means of n observations. $^*P < 0.001$ by Student's t test.

and a rise in $[Ca^{2+}]_i$ in the same arteries in the presence of verapamil (10 μM). It was therefore not possible to examine the effect of hydrochlorothiazide on noradrenaline-induced release of intracellular stores in this vessel.

Caffeine induced a small and transient increase in $[Ca^{2+}]_i$ and force of respectively 37.6 ± 12.5% and 20.3 ± 6.3% before and 37.5 ± 21.7% and 18.0 ± 5.6% after hydrochlorothiazide incubation ($n = 5$ in both cases). The action of caffeine was not significantly affected by the presence of hydrochlorothiazide.

The effect of hydrochlorothiazide on responses to extracellular Ca^{2+} under depolarized conditions: interaction between hydrochlorothiazide and the sensitivity of the contractile machinery

Ca^{2+} concentration-response curves were constructed in the presence and absence of hydrochlorothiazide. Data were analysed in terms of the effect of cumulative addition of extracellular Ca^{2+} on isometric force (Figure 3a), $[Ca^{2+}]_i$ (Figure 3b) and the relationship between isometric force and $[Ca^{2+}]_i$ derived from the previous two relationships. Hydrochlorothiazide caused a small rightward shift in the extracellular Ca^{2+}-force relationship (Figure 3a); the pD_2 for Ca^{2+} in the presence of hydrochlorothiazide was 5.2 ± 0.1 ($n = 5$), compared with 5.4 ± 0.1 ($n = 5$) under control conditions (NS), and there was little difference in the relationships between extracellular Ca^{2+} and $[Ca^{2+}]_i$ in the presence or absence of hydrochlorothiazide (Figure 3b; $pD_2 = 5.4 \pm 0.1$ ($n = 5$) in both cases). Examination of the $[Ca^{2+}]_i$-force relationship indicated a small rightward shift (desensitization) of this curve in the presence of hydrochlorothiazide, although this difference was not found to be statistically significant by 2-way analysis of variance.

Discussion

This study has confirmed that hydrochlorothiazide relaxes guinea-pig isolated mesenteric small arteries as Calder and colleagues (1994) have previously reported. We have shown that this effect of hydrochlorothiazide is associated with a fall in $[Ca^{2+}]_i$ and it seems likely that this fall in $[Ca^{2+}]_i$ largely

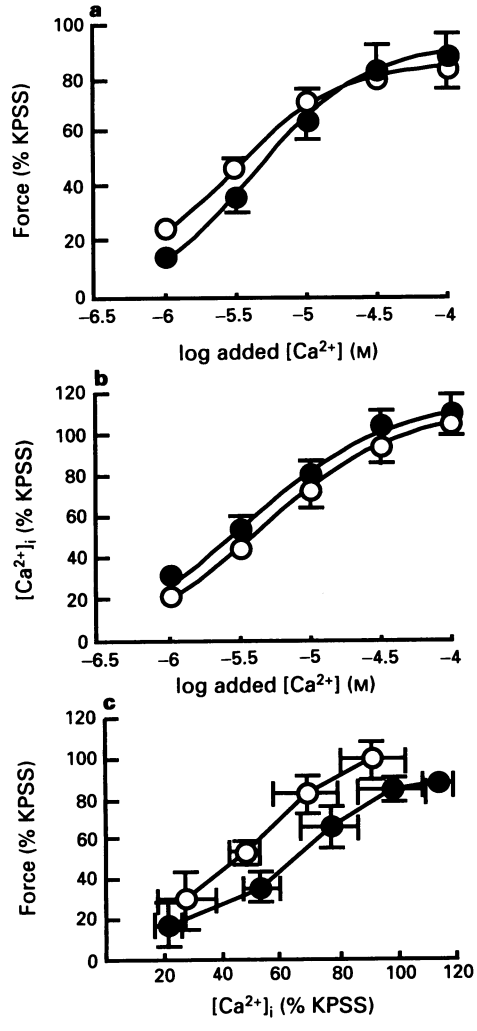

Figure 3 The effect of hydrochlorothiazide (HCT; 30 μM) on responses to cumulative addition of Ca^{2+} to nominally Ca^{2+}-free depolarized conditions. (a) Concentration-response relationships between added extracellular Ca^{2+} and force in the presence (●) or absence (○) of HCT. HCT was present for a total of 20 min prior to cumulative addition of Ca^{2+}. Increase in force is expressed as % contraction to KPSS in the same vessel. (b) Concentration-response relationship between added extracellular Ca^{2+} and $[Ca^{2+}]_i$ in the presence (●) or absence (○) of HCT. Change in $[Ca^{2+}]_i$ is expressed as % change in $[Ca^{2+}]_i$ in response to KPSS in the same vessel. (c) Relationship between $[Ca^{2+}]_i$ and force derived from data in (a) and (b). Each value represents the mean ± s.e.means of data from 5 separate experiments.

explains the direct vasorelaxant effects of hydrochlorothiazide. Both the reduction in $[Ca^{2+}]_i$ and force were blocked by charybdotoxin. Charybdotoxin is a 37-amino acid peptide present in the venom of the scorpion *Leiurus quinquestriatus hebraeus* which is a relatively selective inhibitor of large conductance Ca^{2+}-activated K^+ channels (K_{Ca}) (Anderson *et al.*, 1988; Gimenez-Gallego *et al.*, 1988). It inhibits K^+ channels by physically plugging the outer pore of the channel (Miller, 1990), but does not affect sodium or calcium channels (Miller *et al.*, 1985). The finding that charybdotoxin blocks the effect of hydrochlorothiazide on both force and $[Ca^{2+}]_i$ suggests that these actions of hydrochlorothiazide involve opening of K_{Ca} channels to increase K permeability and hyperpolarize the cell. Such a conclusion is supported by the failure of hydrochlorothiazide to alter tone and $[Ca^{2+}]_i$ in mesenteric arteries contracted by noradrenaline in the presence of potassium. Under these conditions the vessels will be depolarized and the membrane potential will be near to K equilibrium potential (probably near 0 mV under these ionic conditions). In this case opening K_{Ca} channels would have negligible effect on membrane potential and therefore should not reduce $[Ca^{2+}]_i$ or tone.

Hydrochlorothiazide had no detectable effect on caffeine-induced rises in $[Ca^{2+}]_i$ or tone. Caffeine is a widely used pharmacological tool which releases Ca^{2+} from intracellular stores (Leijten & Van Breemen, 1984), probably by activating channels in the sarcoplasmic reticulum involved in Ca^{2+}-induced Ca^{2+} release (Smith *et al.*, 1988). The failure of hydrochlorothiazide to affect responses to caffeine suggests that hydrochlorothiazide probably does not influence tone or $[Ca^{2+}]_i$ through an action on the caffeine-sensitive store in these arteries. In contrast, Mironneau (1988) reported that indapamide, a thiazide-like drug, depressed constrictions elicited by release of calcium from the endoplasmic reticulum. However, despite its structural similarities with thiazides there is evidence that indapamide-induced vasorelaxation shows considerable differences from thiazide-induced relaxation and probably acts through unrelated mechanisms (Mironneau *et al.*, 1981; Calder *et al.*, 1992). It was not possible to examine the effect of hydrochlorothiazide on noradrenaline-induced release of intracellular Ca^{2+} in these studies, since noradrenaline had very little or no detectable effect on tone or $[Ca^{2+}]_i$ in the absence of extracellular Ca^{2+} or the presence of verapamil, a calcium antagonist. Since other agonists, endothelin-1 and vasopressin were able to increase tone and $[Ca^{2+}]_i$ under these conditions, these preliminary data suggest that noradrenaline may be unable to mobilize Ca^{2+} from the intracellular store(s) in guinea-pig mesenteric small arteries, though further studies will be necessary to establish this unequivocally.

In our experiments using addition of increasing extracellular Ca^{2+} concentrations to a nominally Ca^{2+}-free depolarizing solution, we found that hydrochlorothiazide caused a small shift in the relationship between added extracellular Ca^{2+} and force. Although not statistically significant this magnitude of shift is similar to that previously reported by Calder and others (1993), which was interpreted by these authors as indicating a calcium antagonist action of hydrochlorothiazide. Our data where changes in $[Ca^{2+}]_i$ were measured, do not support such a conclusion and suggest that this modest effect of hydrochlorothiazide is due to a reduction in sensitivity of the contractile apparatus to $[Ca^{2+}]_i$ rather than interference with Ca^{2+} entry under depolarized conditions. Although such an effect may make some contribution to the vasorelaxant effect of hydrochlorothiazide, overall our data suggest that the effect of hydrochlorothiazide on K channels is a more important influence.

A recent study has shown that hydrochlorothiazide increased $^{86}Rb^+$ efflux, a marker of K^+ efflux, from guinea-pig mesenteric arteries (Calder *et al.*, 1994). A similar effect has also been seen using another thiazide drug, cyclothiazide, in tail artery smooth muscle (Moura & Worcel, 1983). Both these findings are consistent with the notion that thiazides increase the permeability of smooth muscle membranes to K^+, probably by opening K_{Ca}. It is not known how hydrochlorothiazide acts on K_{Ca} channels. It may be via an intracellular biochemical effect or by a direct interaction with the channel; electrophysiological studies represent the most direct approach to resolving this question.

The possibility that thiazides increase K^+ permeability may also have implications for thiazide-induced hyperglycaemia. In the pancreas, depolarization of the plasma membrane by inhibition of K^+ channels and opening of Cl^- channels leading to opening of voltage-dependent Ca^{2+} channels and increase of $[Ca^{2+}]_i$ is involved in the activation of insulin release (Sehlin, 1978; Wollheim & Sharp, 1981; Pedersen & Findlay, 1987). Recently it has been reported that hydrochlorothiazide reduced insulin release by isolated pancreatic β cells and that this was associated with a fall in glucose-stimulated $^{45}Ca^{2+}$ uptake (Sandstrom, 1993). It is known that diazoxide, a drug structurally related to the thiazides, hyper-

polarizes β-cells by opening ATP-dependent K channels (K_{ATP}) and that this impairs insulin release (Malaisse & Malaisse-Lagae, 1968; Henquin & Meissner, 1982; Trube *et al.*, 1986). This effect of diazoxide can be inhibited by agents such as glibenclamide which block K_{ATP} channels and are used as clinically hypoglycaemic agents. In contrast, blockers of K_{ATP} channels do not affect thiazide-induced relaxation (Calder *et al.*, 1992), or thiazide-induced $^{86}Rb^+$ efflux (Calder *et al.*, 1994). Hydrochlorothiazide does not affect the activity of K_{ATP} channels in the β-cell plasma membrane (Gillis *et al.*, 1989), but the effect of thiazide on K_{Ca} channels appears not to have been investigated. In view of our findings and those of others cited above a possible role for K_{Ca} channels in the inhibitory effect of hydrochlorothiazide on insulin release seems plausible.

In conclusion, we have shown that hydrochlorothiazide-induced vasorelaxation is associated with decreased influx of extracellular Ca^{2+}. This phenomenon is probably mediated through activation of large conductance Ca^{2+}-activated K^+ channels, as it was abolished by an antagonist of these channels, charybdotoxin. As a result of these studies we postulate that hydrochlorothiazide opens Ca^{2+}-activated K^+ channels, thereby leading to K^+ efflux and membrane hyperpolarization, and consequent closing of voltage-operated Ca^{2+} channels and smooth muscle cell relaxation. How hydrochlorothiazide acts on these channels remains to be established.

We would like to thank R. Garcha for technical assistance with some experiments and Dr M. Schachter for helpful discussions and his comments on this manuscript. P.P. was supported by a grant from the Dutch Heart Foundation, A.D.H. is a British Heart Foundation Intermediate Fellow.

References

ANDERSON, C.S., MACKINNON, R., SMITH, C. & MILLER, C. (1988). Charybdotoxin block of single Ca^{2+}-activated K^+ channel. Effect of channel gating, voltage and ionic strength. *J. Gen. Physiol.*, **91**, 317–333.

CALDER, J.A., SCHACHTER, M. & SEVER, P.S. (1992). Direct vascular actions of hydrochlorothiazide and indapamide in isolated small vessels. *Eur. J. Pharmacol.*, **220**, 19–26.

CALDER, J.A., SCHACHTER, M. & SEVER, P.S. (1993). Ion channel involvement in the acute vascular effects of thiazide diuretics and related compounds. *J. Pharmacol. Exp. Ther.*, **265**, 1175–1180.

CALDER, J.A., SCHACHTER, M. & SEVER, P.S. (1994). Potassium channel opening properties of thiazide diuretics in isolated guinea pig resistance arteries. *J. Cardiovasc. Pharmacol.*, **24**, 158–164.

GILLIS, K.D., GEE, W.M., HAMMOUD, A., MCDANIEL, M.L., FALKE, L.C. & MISLER, S. (1989). Effects of sulfonamides on a metabolic-regulated ATP_i-sensitive K^+ channel in rat pancreatic B-cells. *Am. J. Physiol.*, **257**, C1119–C1127.

GIMENEZ-GALLEGO, G., NAVIA, G., REUBEN, M.A., KATZ, J.P., KACZOROWSKI, G.J. & GARCIA, M.L. (1988). Purification, sequence and model structure of charybdotoxin a potent selective inhibitor of Ca^{2+}-activated potassium channels. *Proc. Natl. Acad. Sci. U.S.A.*, **85**, 3329–3333.

HENQUIN, J.-C. & MEISSNER, H.P. (1982). Opposite effects of tolbutamide and diazoxide on ^{86}Rb fluxes and membrane potential in pancreatic B cells. *Biochem. Pharmacol.*, **31**, 1407–1415.

JENSEN, P.E., HUGHES, A.D., BOONEN, H.C.M. & AALKJAER, C. (1993). Force, membrane potential, and $[Ca^{2+}]_i$ during activation of rat mesenteric small arteries with norepinephrine, potassium, aluminium fluoride and phorbol ester. Effects of changes in pH_i. *Circ. Res.*, **73**, 314–324.

JENSEN, P.E., MULVANY, M.J. & AALKJAER, C. (1992). Endogenous and exogenous agonist-induced changes in the coupling between $[Ca^{2+}]_i$ and force in rat resistance arteries. *Pflügers Arch.*, **420**, 526–543.

LEIJTEN, P.A. & VAN BREEMEN, C. (1984). The effects of caffeine on the noradrenaline-sensitive calcium store in rabbit aorta. *J. Physiol.*, **357**, 327–333.

MALAISSE, W.J. & MALAISSE-LAGAE, F. (1968). Effect of thiazides upon insulin secretion in vitro. *Arch. Int. Pharmacodyn.*, **171**, 235–239.

MILLER, C. (1990). Annus Mirabilis of K^+ channels. *Science*, **252**, 1092–1096.

MILLER, C., MOCZYDLOWSKI, E., LATORRE, R. & PHILLIPS, M. (1985). Charybdotoxin: a protein inhibitor of single Ca^{2+} activated K^+ channels from mammalian skeletal muscle. *Nature*, **313**, 316–318.

MIRONNEAU, J. (1988). Indapamide-induced inhibition of Ca^{2+} movement in smooth muscles. *Am. J. Med.*, **84**, 10–14.

MIRONNEAU, J., SAVINEAU, J.P. & MIRONNEAU, C. (1981). Compared effects of indapamide, hydrochlorothiazide and chlorthalidone on electrical and mechanical activities in vascular smooth muscle. *Eur. J. Pharmacol.*, **75**, 109–113.

MOURA, A.-M. & WORCEL, M. (1983). Mode of action of cyclothiazide and triamterene. Ex vivo effect on ^{22}Na and ^{86}Rb efflux from arterial smooth muscle. *Eur. J. Pharmacol.*, **86**, 129–133.

MULVANY, M.J. & AALKJAER, C. (1990). Structure and function of small arteries. *Physiol. Rev.*, **70**, 921–961.

MULVANY, M.J. & HALPERN, W. (1977). Contractile properties of small arterial resistance vessels in spontaneously hypertensive and normotensive rats. *Circ. Res.*, **41**, 19–26.

NISHIMURA, J., KOLBER, M. & VAN BREEMEN, C. (1988). Norepinephrine and GTP-γ-S increase myofilament Ca^{2+} sensitivity in α-toxin permeabilized arterial smooth muscle. *Biochem. Biophys. Res. Commun.*, **157**, 676–683.

PEDERSEN, O.H. & FINDLAY, I. (1987). Electrophysiology of the pancreas. *Physiol. Rev.*, **67**, 1054–1116.

RAMSEY, L.E., YEO, W.W., CHADWICK, I.G. & HOWES, L.G. (1994). Diuretics. In *Textbook of Hypertension*. ed. Swales, J.D. pp. 1046–1058. Oxford: Blackwell Scientific Publications.

SANDSTROM, P.-E. (1993). Inhibition by hydrochlorothiazide of insulin release and calcium influx in mouse pancreatic beta-cells. *Br. J. Pharmacol.*, **110**, 1359–1362.

SEHLIN, J. (1978). Interrelationship between chloride fluxes in pancreatic islets and insulin release. *Am. J. Physiol.*, **235**, C501–C508.

SMITH, J.S., IMAGAWA, T., MA, J., FILL, M., CAMPBELL, K.P. & CORONADO, R. (1988). Purified ryanodine receptor from rabbit skeletal muscle is the calcium-release channel of sarcoplasmic reticulum. *J. Gen. Physiol.*, **92**, 1–26.

SOMLYO, A.P. & HIMPENS, B. (1989). Cell calcium and its regulation in smooth muscle. *FASEB J.*, **3**, 2266–2276.

TRUBE, G., RORSMAN, P. & OHNO-SHOSAKU, T. (1986). Opposite effects of tolbutamide and diazoxide on ATP-regulated K^+ channel in mouse pancreatic β-cells. *Pflügers Arch.*, **407**, 493–499.

VAN BRUMMELEN, P., MAN IN'T VELD, A.J. & SCHALEKAMP, M.A. (1980). Hemodynamic changes during long-term thiazide treatment of essential hypertension in responders and nonresponders. *Clin. Pharmacol. Ther.*, **27**, 328–336.

WOLLHEIM, C. & SHARP, G.W.C. (1981). Regulation of insulin release by calcium. *Physiol. Rev.*, **61**, 914–973.

(Received August 4, 1994
Revised September 26, 1994
Accepted October 10, 1994)

British Journal of Pharmacology (1995) 114, 708–714

Pharmacological analysis of the local and reflex responses to bradykinin on rat urinary bladder motility *in vivo*

[1]A. Lecci, S. Giuliani, S. Meini & C.A. Maggi

Pharmacology Research Dept., 'A. Menarini' Pharmaceuticals, via Sette Santi 3, 50131 Florence, Italy

1 The topical application of bradykinin (BK) (0.05–5000 pmol/rat) onto the serosal surface of the urinary bladder in urethane-anaesthetized rats, evoked low amplitude tonic contractions (not exceeding 25 mmHg) or high amplitude (about 50 mmHg), phasic reflex contractions (chemoceptive micturition reflex) which were abolished by bilateral ablation of the pelvic ganglia. In ganglionectomized rats, BK induced only a local, tonic-type contraction.

2 Systemic capsaicin pretreatment (164 μmol kg^{-1}, 4 days before) reduced the incidence of chemoceptive reflex induced by BK (500 pmol/rat) but had no effect on the magnitude of the tonic-type contraction elicited by BK in ganglionectomized rats. Indomethacin (11 μmol kg^{-1}, 20 min before) reduced the incidence but not the amplitude of the reflex contractions induced by topical application of BK (500 pmol/rat). In ganglionectomized rats, indomethacin (11 μmol kg^{-1}, 20 min before) decreased the amplitude of the tonic contraction evoked by BK. Indomethacin did not affect the chemoceptive reflex induced by topical application of capsaicin (15 nmol/rat) onto the bladder.

3 Intrathecal administration of the tachykinin NK_1 receptor antagonists, RP 67,580 (10 nmol/rat) or SR 140,333 (10 nmol/rat), abolished the chemoceptive reflex induced by BK without modifying the magnitude of the tonic contraction. SR 140,333 (10 nmol/rat) also abolished the occurrence of the chemoceptive reflex induced by capsaicin.

4 Intravenous administration of the B_2 receptor antagonist, Hoe 140 (35 nmol kg^{-1}, 10 min before) abolished the reflex and local effects induced by BK on bladder motility but failed to modify the chemoceptive reflex induced by topical application of capsaicin (15 nmol/rat).

5 Intrathecal administration of Hoe 140 (10 nmol/rat) reduced the incidence of the chemoceptive reflex induced by BK but had no effect on the amplitude of the local motor response. Likewise, Hoe 140 (10 nmol/rat, i.t.) reduced the incidence of reflex bladder contractions induced by topical application of capsaicin (15 nmol/rat) without affecting the magnitude of the tonic-type contraction.

6 These findings indicate that BK stimulates motility through B_2 receptors in the rat urinary bladder. BK activates the reflex response by stimulating capsaicin-sensitive afferent nerves with a contribution from prostanoids. At the spinal cord level, tachykinin NK_1 and BK B_2 receptors could also be involved in the chemoceptive reflex induced by BK or capsaicin.

Keywords: Micturition reflex; bradykinin; capsaicin; tachykinin; rat urinary bladder

Introduction

Bradykinin (BK) is the most potent endogenous mediator producing pain (Dray & Perkins, 1993, for review). In laboratory animals the nociceptive effect induced by BK depends on the activation of a population of afferent nerves which are sensitive to capsaicin (Dray *et al.*, 1988a; 1989). The sensory stimulant action of peripherally applied BK is accompanied by a number of local effects such as vasodilatation, smooth muscle contraction, increased vascular permeability, etc (Marceau *et al.*, 1983, for review). These peripheral effects are partly a consequence of the direct action of BK on target cells and, to varying degrees in various systems, occur indirectly, through the local release of sensory neuropeptides from capsaicin-sensitive primary afferent nerves (Geppetti, 1993, for review) together with prostanoid generation from immune and muscle cells and sensory or sympathetic nerves (Dray & Bevan, 1993).

BK is generated during inflammation or by stimuli producing tissue injury (Bhoola *et al.*, 1992). However, the urine contains significant amounts of kinins (BK-related peptides) even in physiological conditions (Oza, 1988; Bhoola *et al.*, 1992). Therefore BK could be a stimulus producing pain in the lower urinary tract whenever the urothelial barrier is disrupted. BK induces urinary bladder contraction both *in vivo* (Maggi *et al.*, 1993) and *in vitro* (Maggi *et al.*, 1989). In the latter experimental conditions, indomethacin pretreatment but not capsaicin desensitization reduced the activity of BK. However, the role of prostanoids and of capsaicin-sensitive nerves in the sensory stimulant action of BK in the rat urinary bladder has not been investigated *in vivo*.

In the present study the motor effects produced by topical application of BK onto the urinary bladder of urethane-anaesthetized rats were compared with the effects induced by topical application of capsaicin. Since spinally administered NK_1 receptor antagonists block the capsaicin-evoked micturition reflex (Lecci *et al.*, 1992; 1993a) we also investigated the effect of intrathecal (i.t.) administration of NK_1 receptor antagonists, such as RP 67,580 or SR 140,333 (Garret *et al.*, 1991; Jung *et al.*, 1994) on the motor effects induced by the topical application of BK. In addition, the receptor subtype involved in the responses to BK was characterized by means of a potent and selective bradykinin B_2 receptor antagonist, Hoe 140 (Wirth *et al.*, 1991).

Methods

General

Male Wistar rats weighing 340–360 g were anaesthetized with urethane (1.2 g kg^{-1}, s.c.). After laparotomy, the bladder was exposed and both ureters were tied. Intrathecal (i.t.) administration of drugs was performed via a catheter (PE 10) inserted through the atlanto-occipital membrane for 8.5 cm, in such a way that the tip of the catheter was placed just

[1] Author for correspondence.

above the lumbosacral enlargement (L1–L2 segments), as previously described (Lecci *et al.*, 1993a). After catheter insertion, 25 μl of saline was rapidly flushed through the catheter and all animals responding with muscle myoclonus, hindleg, or tail movements were discarded. Rats were placed on a heating pad to keep body temperature between 36.5 and 37°C. Experiments were carried out 2 h after catheterization. Drugs or vehicle were administered in a volume of 10 μl and the cannula was rinsed with 15 μl of saline; the flow rate for injections was 10 μl min^{-1}. Some experiments were also performed in capsaicin pretreated animals (164 μmol kg^{-1}, s.c., 4 days before experiments). This protocol of capsaicin pretreatment has been shown to produce a selective impairment of a limited fraction of bladder afferents which accounts for the whole content of tachykinins in the rat urinary bladder (Maggi *et al.*, 1987a,b).

Bladder contractions induced by topical application of bradykinin or capsaicin (chemoceptive vesico-vesical reflex)

The intraluminal bladder pressure was measured by a catheter (PE 90) inserted through the proximal urethra. For topical application of BK or capsaicin, the bladder was exposed, kept separated from adjoining viscera by a piece of parafilm and covered with a saline moistened cotton gauze. The urinary bladder was filled with saline until high amplitude rhythmic contractions (micturition reflex) were observed in order to check the viability of the preparation. Afterwards, a small amount of saline was withdrawn until such contractions disappeared. Therefore the urinary bladder remained filled with just a subthreshold volume for eliciting the micturition reflex (about 0.35 ml of saline in controls and 1 ml in capsaicin-pretreated rats) and, after 30 min of equilibration, BK (500 pmol/50 μl) or capsaicin (15 nmol/50 μl) was applied onto the serosal surface of the urinary bladder by means of a microsyringe, as previously described (Lecci *et al.*, 1993a). Indomethacin was given 20 min before, Hoe 140, SR 140,333, RP 67,580 or the vehicle were administered intravenously or intrathecally 10 min before topical application of BK or capsaicin. In these experiments the following parameters were evaluated: presence of reflex bladder contractions (two or more phasic contractions of amplitude > 16 mmHg), the maximal amplitude of reflex contractions or of tonic-type contraction, as previously described (Maggi *et al.*, 1986).

In a series of experiments the pelvic ganglia were exposed and removed by means of microscissors. In these animals, bladder filling induced only low amplitude (1–4 mmHg) myogenic contractions; a volume of 0.35 ml was used to fill the bladder of control rats whereas 1 ml of saline was infused in capsaicin-pretreated rats. These volumes are the average threshold volumes of activation of micturition reflex in animals with intact urinary bladder innervation or sensory nerve lesion induced by pretreatment with capsaicin in adult rats. The experiments were carried out 1.5 h after bilateral surgical ablation. In ganglionectomized rats the maximal value of intravesical pressure (mmHg) produced within 20 min from agonist application was recorded.

Drugs

Capsaicin and indomethacin were from Sigma (St Louis, U.S.A.), BK was from Peninsula Laboratories Inc. (Merseyside, UK). Hoe 140 (D-Arg[Hyp^3, Thi^5, D-Tic^7, Oic^8] bradykinin), RP 67,580 ((3a**R**, 7a**R**)-7,7-diphenyl-2-[1-amino-2(2-methoxyphenyl) ethyl] perhydroisoindol-4-one) and SR 140,333 (S)1-{2-[3-(3,4-dichlorophenyl)-1-(3-isopropoxyphenyl-acetyl)-piperidin-3-yl] ethyl}-4-phenyl-1-azoniabicyclo[2.2.2.] octane chloride) were kindly provided by Drs K. Wirth (Hoechst, Frankfurt, Germany), C. Garret (Rhone-Poulenc Rorer, Vitry, France) and by X. Exmonds-Alt (Sanofi, Montpellier, France), respectively.

Data analysis

All values represent means ± standard error of the mean (s.e.mean). Dose-response experiments for the incidence of the chemoceptive reflex were evaluated by means of Chi^2 test. ED_{50} values for the activation of micturition reflex were calculated according to the Lichtfield-Wilcoxon method. The effect of antagonists on this parameter was analysed by Chi^2 test. The effect of antagonists on intravesical pressure was evaluated by one-way ANOVA followed by Tukey test or by Student's *t* test, when applicable.

Results

The topical application of BK onto the urinary bladder produced a dose-related increase in the incidence of the chemoceptive micturition reflex. The morphology of the intravesical pressure waves produced by BK is qualitatively similar to that observed in response to topical application of capsaicin (Lecci *et al.*, 1993a,b), i.e. a tonic-type contraction (4–25 mmHg in amplitude, lasting 2–6 min) on which a series of high amplitude (20–85 mmHg in amplitude, lasting 1–7 min) phasic contractions were superimposed. The tonic-type contraction could be seen when the reflex was not activated or was blocked by pharmacological or surgical means (Figure 1). The reflex response induced by topical application of BK is an all-or-none response, since the incidence but not the amplitude of this response is related to the dose of BK used (Table 1). In preliminary experiments ($n = 9$), we studied the response to 4 consecutive applications of BK (500 pmol/rat) at 20 min intervals: the reflex response faded on the second application of BK (9 out of 9 responders on the first challenge, 5 out of 9 on the second one, $P < 0.05$, Chi^2 test), with a partial recovery on the last two challenges (8 out of 9 and 7 out of 9 responders at the third and fourth challenge, respectively). To minimize these problems, the dose of BK was increased by a factor of 10 for consecutive additions of peptide (0.05–5000 pmol/rat) in either vehicle- or capsaicin-pretreated rats. The period between the administration of each BK dose was 20 min. The effect of other drug treatments (indomethacin, Hoe 140, SR 140,333 and RP 67,580) was evaluated toward a single dose of BK (500 pmol/rat).

In vehicle-pretreated rats the volume threshold for the activation of the micturition reflex (distension-induced) was 364 ± 76 μl ($n = 8$) and the ED_{50} for the activation of chemoceptive reflex by BK was 3.4 pmol/rat (0.3–40.8 pmol/rat, 95% confidence limits, $n = 8$). In capsaicin-pretreated rats (164 μmol kg^{-1}, s.c., 4 days before), the volume threshold for the activation of micturition reflex was 1324 ± 364 μl ($n = 8$, $P < 0.05$ vs vehicle). In these animals, BK was unable to activate the chemoceptive reflex, since, in a wide range of doses (0.05–5000 pmol/rat) the incidence of activation of the reflex response was never greater than 25% (Figure 1 and Table 1), although a tonic-type contraction was observed in all preparations at the highest doses used (500 and 5000 pmol/rat).

Indomethacin (5.5–11 μmol kg^{-1}, i.v.) reduced the incidence of reflex urinary bladder contractions induced by a submaximal dose of BK (500 pmol/rat) without affecting their amplitude (Table 2A). However, in those preparations where the chemoceptive reflex was inhibited (7 out of 12 at 5.5 μmol kg^{-1} indomethacin), the tonic-type contraction was still present (Table 2A). In order to evaluate the effect of indomethacin on the BK-induced tonic-type contractions, a series of experiments was performed in ganglionectomized animals. Indomethacin (11 μmol kg^{-1}, i.v.) reduced the amplitude of bladder contraction in rats subjected to the ablation of pelvic ganglia (Table 3). In these preparations, capsaicin pretreatment neither altered the effect of BK nor modified the inhibitory effect of indomethacin on the response induced by BK (Table 3). Indomethacin (11 μmol kg^{-1}, i.v.) was

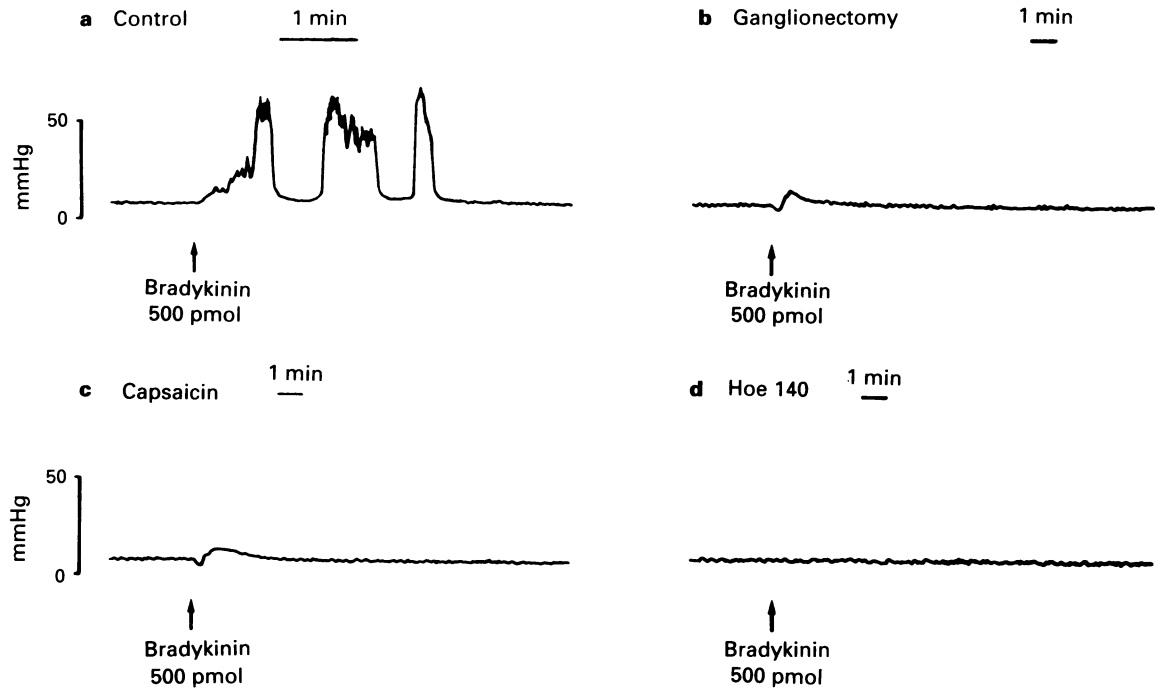

Figure 1 Representative traces showing the effects of application of bradykinin (500 pmol/rat) on urinary bladder in control rats (a), ganglionectomized rats (b), capsaicin (164 μmol kg^{-1}, s.c.) pretreated rats (c), Hoe 140 (35 nmol kg^{-1}, i.v.) pretreated rats (d).

Table 1 Cumulative dose-response of topical application of bradykinin in vehicle and capsaicin-pretreated rats (164 μmol kg^{-1}, 4 days before)

Dose/rat (pmol)	0.05	0.5	5	50	500	5000	Chi^2	ED_{50} (c.l.)
Vehicle								
Incidence of reflex contractions	2/8	3/8	3/8	5/8	7/8	8/8	$P<0.01$	3.4 (0.3–40.8)
Amplitude of reflex contractions (mmHg)	59 ± 17 ($n=2$)	46 ± 11 ($n=3$)	43 ± 9 ($n=3$)	48 ± 10 ($n=5$)	55 ± 8 ($n=7$)	56 ± 6 ($n=8$)		
Amplitude of tonic contraction (mmHg)	5 ± 2 ($n=6$)	4 ± 2 ($n=5$)	3 ± 2 ($n=5$)	6 ± 3 ($n=3$)	8 ($n=1$)	–		
Capsaicin								
Incidence of reflex contractions	0/8	2/8	2/8	2/8	2/8*	2/8**	NS	n.p.c.
Amplitude of reflex contractions (mmHg)	–	29 ± 1 ($n=2$)	29 ± 1 ($n=2$)	37 ± 9 ($n=2$)	29 ± 1 ($n=2$)	44 ± 16 ($n=2$)		
Amplitude of tonic contraction (mmHg)	2 ± 2 ($n=8$)	2 ± 1 ($n=6$)	3 ± 1 ($n=6$)	4 ± 1 ($n=6$)	12 ± 4 ($n=6$)	9 ± 1 ($n=6$)		

Chi^2: $*P<0.05$ and $**P<0.01$, respectively vs vehicle-pretreated rats. NS = not significant; n.p.c. = not possible to calculate.

Table 2 Effect of i.v. indomethacin on the chemoceptive vesico-vesical reflex induced by topical application of (**A**) bradykinin (BK, 500 pmol/rat) in vehicle or capsaicin-pretreated rats (164 μmol kg^{-1}, 4 days before), and (**B**) topical capsaicin (15 nmol/rat)

Dose (μmol kg^{-1})		*Incidence of the reflex*	*Amplitude of reflex contractions* (mmHg)	*Amplitude of tonic contraction* (mmHg)
A				
Vehicle	–	11/12	60 ± 5 ($n=11$)	8 ($n=1$)
Indomethacin	2.75	12/12	46 ± 5 ($n=12$)	–
Indomethacin	5.5	7/12	46 ± 5 ($n=7$)	9 ± 2 ($n=5$)
Indomethacin	11	5/12°°	49 ± 9 ($n=5$)	13 ± 4 ($n=7$)
Caps-Vehicle	–	2/10	30 ± 2 ($n=2$)	12 ± 3 ($n=8$)
Caps-Indometh	11	1/10	31 ($n=1$)	5 ± 1* ($n=9$)
B				
Vehicle	–	10/10	44 ± 5 ($n=10$)	–
Indomethacin	11	8/10	51 ± 5 ($n=8$)	10 ± 5 ($n=2$)

Student's t test: $*P<0.05$ vs Vehicle; Chi^2 test: $°°P<0.01$ vs Vehicle.

ineffective against the chemoceptive reflex induced by topical application of capsaicin (15 nmol/rat, Table 2B).

The non-peptide tachykinin NK_1 receptor antagonists, RP 67,580 (10 nmol/rat) or SR 140,333 (10 nmol/rat) blocked the activation of the chemoceptive reflex induced by topical application of BK (500 pmol/rat) while leaving the amplitude of the tonic-type detrusor contraction unaffected (Table 4A and Figure 2c). At the dose inhibiting the reflex response activated by BK, SR 140,333 (10 nmol/rat, i.t.) also completely prevented the activation of chemoceptive vesical reflex induced by topical application of capsaicin (15 nmol/rat); even in this case the tonic-type bladder contraction was preserved (Table 2B and Figure 2).

Table 3 Effect of i.v. indomethacin (11 μmol kg^{-1}, i.v.) and of capsaicin pretreatment (164 μmol kg^{-1}, 4 days before) on the tonic contraction induced by topical application of bradykinin (500 pmol/rat) in rats subjected to bilateral ablation of pelvic ganglia (1.5 h before)

Pretreatment-treatment	*Incidence of reflex*	*Amplitude of tonic contraction* (mmHg)
Vehicle-vehicle	0/8	7.7 ± 1.4 ($n = 8$)
Capsaicin-vehicle	0/8	6.2 ± 0.8 ($n = 8$)
Vehicle-indomethacin	0/8	3.4 ± 0.7** ($n = 8$)
Capsaicin-indomethacin	0/8	1.9 ± 0.5** ($n = 8$)

Tukey test: $^{**}P < 0.01$ vs respective vehicle.

I.v. administration of the selective B_2 receptor antagonist, Hoe 140 (10 and 35 pmol kg^{-1}) inhibited all the responses produced by topical application of BK (500 pmol/rat) (Table 5A) in a dose-dependent manner but at the dose of 35 nmol kg^{-1}, i.v. Hoe 140 did not alter the response to capsaicin (15 nmol/rat, Table 5B).

As a negative control, the effect of i.t. administration of Hoe 140 was also tested on BK-induced chemoceptive reflex. Surprisingly, Hoe 140 (10 nmol/rat, i.t.) reduced the incidence of the reflex activated by local application of BK onto the urinary bladder (Table 6A and Figure 2b). In order to exclude the possibility that the inhibitory effect of Hoe 140 was due to leakage out of the central nervous system and blockade of peripheral B_2 receptors, some experiments were performed after bilateral removal of pelvic ganglia. In these animals, only the tonic-type detrusor contraction to BK was evident; however, Hoe 140 (10 nmol/rat, i.t.) did not affect this response (Table 6B).

The specificity of the effect of Hoe 140 after i.t. administration was verified on the chemoceptive reflex induced by local application of capsaicin (15 nmol/rat). Hoe 140 blocked the reflex response without modifying the tonic-type contraction (Table 6C and Figure 2e).

Discussion

BK is a potent stimulant of urinary bladder motility both *in vitro* (Maggi *et al.*, 1989) and *in vivo* (Maggi *et al.*, 1993).

Table 4 Effect of i.t. SR 140,333 and RP 67,580 on the chemoceptive vesico-vesical reflex induced by topical application of (A) BK (500 pmol/rat) or (B) capsaicin (15 nmol/rat)

Dose (nmol/rat)		*Incidence of the reflex*	*Amplitude of reflex contractions* (mmHg)	*Amplitude of tonic contraction* (mmHg)
A				
Vehicle	–	7/8	53 ± 4 ($n = 7$)	12 ($n = 1$)
SR 140,333	1	6/7	43 ± 7 ($n = 6$)	14 ($n = 1$)
SR 140,333	10	0/8°°	–	18 ± 2 ($n = 8$)
RP 67,580	10	0/8°°	–	14 ± 3 ($n = 8$)
B				
Vehicle	–	8/9	57 ± 5 ($n = 8$)	10 ($n = 1$)
SR 140,333	10	0/9°°	–	20 ± 3 ($n = 9$)

Chi² test: $^{\circ\circ}P < 0.01$ vs Vehicle.

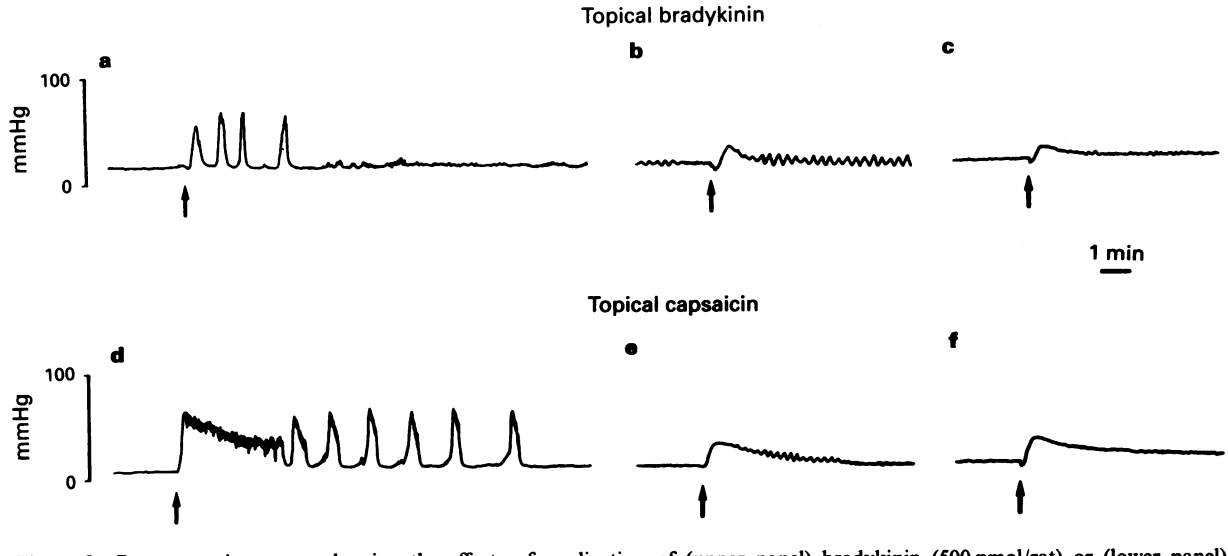

Figure 2 Representative traces showing the effects of application of (upper panel) bradykinin (500 pmol/rat) or (lower panel) capsaicin (15 nmol/rat) on urinary bladder in control rats (a and d), in rats pretreated with Hoe 140, 10 nmol/rat, i.t. (b and e), and in rats pretreated with SR 140,333, 10 nmol/rat, i.t. (c and f).

Table 5 Effect of i.v. Hoe 140 on the chemoceptive vesico-vesical reflex induced by (A) topical application of BK (500 pmol/rat) or (B) capsaicin (15 nmol/rat)

Dose (nmol kg^{-1})		*Incidence of the reflex*	*Amplitude of reflex contractions* (mmHg)	*Amplitude of tonic contraction* (mmHg)
A				
Vehicle	–	8/10	60 ± 5 (n = 8)	9 ± 5 (n = 2)
Hoe 140	10	3/10	44 ± 18 (n = 3)	3 ± 1 (n = 7)
Hoe 140	35	0/8°°	–	1 ± 1 (n = 8)
B				
Vehicle	–	7/8	46 ± 7 (n = 7)	15 (n = 1)
Hoe 140	35	7/8	40 ± 8 (n = 7)	20 (n = 1)

Chi^2 test: °°P<0.01 vs Vehicle.

Table 6 Effect of i.t. Hoe 140 on the chemoceptive vesico-vesical reflex induced by (A) topical application of BK (500 pmol/rat) in intact animals or (B) ganglionectomized animals or (C) topical application of capsaicin (15 nmol/rat) in intact rats

Dose (nmol/rat)		*Incidence of the reflex*	*Amplitude of reflex contractions* (mmHg)	*Amplitude of tonic contraction* (mmHg)
A				
Vehicle	–	8/8	51 ± 6 (n = 8)	–
Hoe 140	1	4/6	45 ± 7 (n = 4)	9 ± 3 (n = 2)
Hoe 140	10	1/8°°	52 (n = 1)	6 ± 1 (n = 7)
B				
Vehicle	–	0/8	–	7 ± 1 (n = 8)
Hoe 140	10	0/8	–	8 ± 1 (n = 8)
C				
Vehicle	–	8/8	54 ± 7 (n = 8)	–
Hoe 140	10	2/8°°	49 ± 1 (n = 2)	15 ± 3 (n = 6)

Chi^2 test: °°P<0.01 vs Vehicle.

Following topical application onto the urinary bladder, BK induced both high amplitude rhythmic contractions and a low amplitude tonic contraction. On the basis of previous studies in this model (Maggi *et al.*, 1984b; Lecci *et al.*, 1993c), it appears that the tonic contraction is a local response, while the high amplitude phasic contractions represent the activation of a chemoceptive micturition reflex. This assumption was verified in animals subjected to acute, bilateral removal of pelvic ganglia where, following topical application of BK, only the tonic contraction was evident.

In vitro, the urinary bladder contraction induced by BK is capsaicin-resistant, although a release of sensory neuropeptides is produced by BK (Maggi *et al.*, 1989; 1993). The present results show that, *in vivo*, a large component of urinary bladder response to BK is sensitive to capsaicin pretreatment. Since only the reflex response to BK was reduced in capsaicin-pretreated animals, we suggest that BK acts predominantly on the afferent rather than the efferent function of capsaicin-sensitive fibres in the rat urinary bladder. Alternatively, the motor component of the 'efferent' activation of capsaicin-sensitive fibres by BK is masked by other local motor effects induced by BK (Maggi *et al.*, 1989).

The activation of the reflex response by BK or by capsaicin is critically dependent on the integrity of the capsaicin-sensitive sensory innervation as indicated by the failure of BK (present results) or capsaicin (Maggi *et al.*, 1984b) to induce the chemoceptive reflex in capsaicin-pretreated rats. The suppression of the BK-induced chemoceptive reflex by capsaicin pretreatment does not follow a non-specific depression of the distension-induced micturition reflex, because, in similar experimental conditions, the reflexogenic effect of a selective tachykinin NK_2 receptor agonist was not modified by capsaicin pretreatment (Lecci *et al.*, 1993b). On the other hand, the reflex response induced by BK is not a direct consequence of the BK-evoked, local, tonic-type contraction since capsaicin pretreatment reduces the former but not the latter response. Therefore these results indicate that BK stimulates reflex bladder motility by stimulating those sensory fibres which are sensitive to the neurotoxic effect of topical capsaicin.

Present and previous (Dray *et al.*, 1992) studies indicate that prostanoids play an important role in the activation of reflex responses by BK. In fact indomethacin reduced the incidence of the BK-evoked chemoceptive reflex as well as the BK-induced neuropeptide release from the urinary bladder (Maggi *et al.*, 1989) or from the spinal cord (Andreeva & Rang, 1993). Since BK receptors are present on sensory nerves (Steranka *et al.*, 1988) and BK can directly excite sensory nerves without any contribution of arachidonic acid metabolites (Fox *et al.*, 1993), the relevance of prostaglandins in the stimulatory activity of BK on sensory nerves might vary between different tissues. The present results indicate that in the rat urinary bladder, prostanoids could play a permissive role (sensitization) on BK-induced activation of capsaicin-sensitive nerves, and that a large component of the local motor response produced by BK in the rat bladder is indomethacin-sensitive, thus confirming the results of previous investigations (Maggi *et al.*, 1989; Andersson *et al.*, 1992; Pinna *et al.*, 1992).

Although prostanoids modulate the micturition reflex (distension-induced) through an action on afferent innervation (Maggi *et al.*, 1984a; 1985; 1988), the effect of

indomethacin on the BK-evoked chemoceptive reflex does not depend upon a general depression of bladder-related reflexes. In fact when the chemoceptive reflex was triggered by capsaicin, indomethacin was ineffective, as previously observed for other kinds of capsaicin-induced reflexes (Staszewska-Woolley *et al.*, 1991). These results also indicate that the excitatory effect of BK and that of capsaicin are produced on the same population of bladder afferents through different mechanisms as established for the activation of intracellular effectors by these agents on sensory neurones in culture (Dray *et al.*, 1988a). The hypothesis that BK and capsaicin excite an overlapping population of sensory fibres in the rat urinary bladder, is also supported by the fact that the intrathecal administration of NK_1 receptor antagonists abolished the reflex response induced by either capsaicin (Lecci *et al.*, 1992; 1993a) or BK. These results would suggest that the application of capsaicin or BK onto the serosal surface of the urinary bladder causes the release of tachykinins from capsaicin-sensitive afferent neurones at the spinal cord level and that tachykinins act through NK_1 receptors to induce reflex motor response of the urinary bladder.

BK acts through two different receptors which have been termed B_1 and B_2. However, only B_2 receptors have been reported to mediate *in vivo* responses to BK in the absence of inflammation or other pathological conditions (Hall, 1993, for review). This proposal is in agreement with the finding that both reflex and local responses to topical BK were completely blocked by i.v. administration of the peptide B_2 receptor antagonist, Hoe 140.

Hoe 140 also reduced the incidence of the chemoceptive vesico-vesical reflex induced by BK or capsaicin when administered intrathecally. Despite the fact that this effect occurred at a dose of Hoe 140 which was similar to that producing full inhibition of the response to BK after systemic administration, the inhibition seen after i.t. administration of Hoe 140 does not depend on a leakage of the antagonist out of the central nervous system. On the other hand, systemic administration of Hoe 140 does not inhibit the reflex response induced by the local application of capsaicin. These results suggest that Hoe 140 may possess pharmacological properties which are not related to the BK antagonism. However, Hoe 140 does not block tachykinin NK_1 receptors in the rat bladder (Maggi *et al.*, 1993) or in the spinal cord (Lopes *et al.*, 1993b), thus excluding an effect of Hoe 140 on tachykininergic transmission. Another possibility is that either capsaicin or BK, when applied at the peripheral level, may stimulate the synthesis of BK-like material within the central nervous system. However, this hypothesis is not supported by previous studies showing that a nociceptive reflex induced by the peripheral application of capsaicin was not blocked by BK receptor antagonists applied to the spinal cord (Dray *et al.*, 1988b).

Although BK-like immunoreactivity (Correa *et al.*, 1979; Perry & Snyder, 1984) as well as BK receptors (Fujiwara *et al.*, 1988; Sharif & Whiting, 1991; Privitera *et al.*, 1992; Lopes *et al.*, 1993a) have been identified in the spinal cord there is no evidence to support BK as a neurotransmitter (Dray *et al.*, 1988b). Despite this, i.t. administration of B_2 receptor antagonists selectively blocked the effects of administration of BK in the spinal cord (Lopes *et al.*, 1993b) and induced an antinociceptive effect (Chapman & Dickenson, 1992) in a model sensitive to i.t. administration of NK_1 receptor antagonists (Yamamoto & Yaksh, 1991; Birch *et al.*, 1992; Chapman & Dickenson, 1993). The real significance of the inhibitory action of i.t. administered Hoe 140 on the reflex response elicited by peripherally applied BK or capsaicin, remains to be established.

In conclusion, the present findings indicate that BK and capsaicin excite with a different mechanism (indomethacin-sensitive and resistant, respectively) a common population of sensory fibres which use tachykinins (and possibly BK) as neurotransmitters for activation of a chemoceptive micturition reflex. This effect of BK is mediated by B_2 receptors in the bladder wall. These findings provide further evidence that BK and tachykinin receptor antagonists may prove useful for treatment of irritative symptoms of cystitis.

This work has been supported by IMI contract No. 56665. We are grateful to Drs X. Emonds Alt, C. Garret and K. Wirth for gifts of SR 140,333, RP 67,580 and Hoe 140, respectively.

References

ANDERSSON, K.E., HEDLUND, H. & STAHL, M. (1992). Contractions induced by angiotensin I, angiotensin II and bradykinin in isolated smooth muscle from the human detrusor. *Acta Physiol. Scand.*, **145**, 253–259.

ANDREEVA, L. & RANG, H.P. (1993). Effect of bradykinin and prostaglandins on the release of calcitonin gene-related peptide-like immunoreactivity from the rat spinal cord *in vitro*. *Br. J. Pharmacol.*, **108**, 185–190.

BHOOLA, K.D., FIGUEROA, C.D. & WORTHY, K. (1992). Bioregulation of kinins, kallikreins and kininases. *Pharmacol. Rev.*, **44**, 4–80.

BIRCH, P.J., HARRISON, S.M., HAYES, A.G., ROGERS, H. & TYERS, M.B. (1992). The non-peptide NK1 receptor antagonist, (±)-CP-96,345, produces antinociceptive and anti-oedema effects in the rat. *Br. J. Pharmacol.*, **105**, 508–510.

CHAPMAN, V. & DICKENSON, A.H. (1992). The spinal and peripheral roles of bradykinin and prostaglandins in nociceptive processing in the rat. *Eur. J. Pharmacol.*, **219**, 427–433.

CHAPMAN, V. & DICKENSON, A.H. (1993). The effect of intrathecal administration of RP 67,580, a potent neurokinin 1 antagonist on nociceptive transmission in the rat spinal cord. *Neurosci. Lett.*, **157**, 149–152.

CORREA, F., INNIS, R.B., UHL, G.R. & SNYDER, S. (1979). Bradykinin like immunoreactive systems localised histochemically in rat brain. *Proc. Natl. Acad. Sci. U.S.A.*, **76**, 1489–1493.

DRAY, A., BETTANEY, J., FORSTER, P. & PERKINS, M.N. (1988a). Bradykinin-induced stimulation of afferent fibres is mediated through protein kinase C. *Neurosci. Lett.*, **91**, 301–307.

DRAY, A., BETTANEY, J., FORSTER, P. & PERKINS, M.N. (1988b). Activation of a bradykinin receptor in peripheral nerve and spinal cord in the neonatal rat *in vitro*. *Br. J. Pharmacol.*, **95**, 1008–1010.

DRAY, A., BETTANEY, J. & FORSTER, P. (1989). Capsaicin desensitization of peripheral nociceptive fibres does not impair sensitivity to other noxious stimuli. *Neurosci. Lett.*, **99**, 50–54.

DRAY, A. & BEVAN, S. (1993). Inflammation and hyperalgesia: highlighting the team effort. *Trends Pharmacol. Sci.*, **14**, 287–290.

DRAY, A., PATEL, I.A., PERKINS, M.N. & RUEFF, A. (1992). Bradykinin-induced activation of nociceptors: receptor and mechanistic studies on the neonatal rat spinal cord-tail preparation *in vitro*. *Br. J. Pharmacol.*, **107**, 1129–1134.

DRAY, A. & PERKINS, M.N. (1993). Bradykinin and inflammatory pain. *Trends Neurosci.*, **16**, 99–104.

FOX, A.J., BARNES, P.J., URBAN, L. & DRAY, A. (1993). An *in vitro* study of the properties of single vagal afferents innervating guinea-pig airways. *J. Physiol.*, **469**, 21–35.

FUJIWARA, Y., MANTIONE, C.R. & YAMAMURA, H.I. (1988). Identification of B2 bradykinin binding sites in guinea-pig brain. *Eur. J. Pharmacol.*, **147**, 487–488.

GARRET, C., CARRUETTE, A., FARDIN, V., MOUSSAOUI, S., PEYRONEL, J.F., BLANCHARD, J.C. & LADURON, P.M. (1991). Pharmacological properties of a potent and selective nonpeptide substance P antagonist. *Proc. Natl. Acad. Sci. U.S.A.*, **88**, 10208–10212.

GEPPETTI, P. (1993). Sensory neuropeptide release by bradykinin: mechanisms and pathophysiological implications. *Regul. Pept.*, **47**, 1–23.

HALL, J.M. (1993). Bradykinin receptors: pharmacological properties and biological role. *Pharmacol. Ther.*, **56**, 131–190.

JUNG, M., CALASSI, R., MARUANI, J., BARNOUIN, M.C., SOUILHAC, J., PONCELET, M., GUEDET, C., EMONDS-ALT, X., SOUBRIE, P.H., BRELIERE, J.C. & LE FUR, G. (1994). Neuropharmacological characterization of SR 140,333, a non-peptide antagonist of NK_1 receptors. *Neuropharmacology*, **33**, 167–179.

LECCI, A., GIULIANI, S., GARRET, C. & MAGGI, C.A. (1993a). Evidence for a role of tachykinins as sensory transmitters in the activation of micturition reflex. *Neuroscience*, **54**, 827–837.

LECCI, A., GIULIANI, S. & MAGGI, C.A. (1992). Effect of the NK-1 receptor antagonist GR 82,334 on reflexly-induced bladder contractions. *Life Sci.* (Pharmacol Lett.), **51**, PL277–280.

LECCI, A., GIULIANI, S., MEINI, S. & MAGGI, C.A. (1993b). Tachykinin receptors on capsaicin-sensitive fibers in the rat urinary bladder: in vivo functional studies. *Soc. Neurosci. Abs.*, **19**, 511.

LECCI, A., GIULIANI, S., PATACCHINI, R. & MAGGI, C.A. (1993c). Evidence against a peripheral role of tachykinins in the initiation of micturition reflex in rats. *J. Pharmacol. Exp. Ther.*, **264**, 1327–1332.

LOPES, P., KAR, S., TOUSIGNANT, C., REGOLI, D., QUIRION, R. & COUTURE, R. (1993a). Autoradiographic localization of [^{125}I-Tyr^8]-Bradykinin receptor binding sites in the guinea pig spinal cord. *Synapse*, **15**, 48–57.

LOPES, P., REGOLI, D. & COUTURE, R. (1993b). Cardiovascular effects of intrathecally administered bradykinin in the rat: characterization of receptors with antagonists. *Br. J. Pharmacol.*, **110**, 1369–1370.

MAGGI, C.A., EVANGELISTA, S., GRIMALDI, G., SANTICIOLI, P., GIOLITTI, A. & MELI, A. (1984a). Evidence for the involvement of arachidonic acid metabolites in spontaneous and drug-induced contractions of rat urinary bladder. *J. Pharmacol. Exp. Ther.*, **230**, 500–513.

MAGGI, C.A., GEPPETTI, P., SANTICIOLI, P., SPILLANTINI, M.G., FRILLI, S. & MELI, A. (1987a). The correlation between sensory-efferent functions mediated by capsaicin-sensitive neurons and substance P content of the rat urinary bladder. *Neurosci. Lett.*, **76**, 351–356.

MAGGI, C.A., GIULIANI, S., CONTE, B., FURIO, M., SANTICIOLI, P., MELI, P., GRAGNANI, L. & MELI, A. (1988). Prostanoids modulate reflex micturition by acting through capsaicin-sensitive afferents. *Eur. J. Pharmacol.*, **145**, 105–112.

MAGGI, C.A., PATACCHINI, R., SANTICIOLI, P., GEPPETTI, P., CECCONI, R., GIULIANI, S. & MELI, A. (1989). Multiple mechanisms in the motor response of the guinea-pig urinary bladder to bradykinin. *Br. J. Pharmacol.*, **98**, 619–629.

MAGGI, C.A., SANTICIOLI, P., BORSINI, F., GIULIANI, S. & MELI, A. (1986). The role of capsaicin-sensitive innervation of the rat urinary bladder in the activation of micturition reflex. *Naunyn Schmied. Arch. Pharmacol.*, **332**, 276–283.

MAGGI, C.A., SANTICIOLI, P., DEL BIANCO, E., LECCI, A. & GIULIANI, S. (1993). Evidence of the involvement of bradykinin in chemically-evoked cystitis in anaesthetized rats. *Naunyn Schmied. Arch. Pharmacol.*, **347**, 432–437.

MAGGI, C.A., SANTICIOLI, P., FURIO, M. & MELI, A. (1985). The effect of cycloxygenase inhibitors on the low filling rate cystometrogram in urethane anesthetized rats. *J. Urol.*, **134**, 800–803.

MAGGI, C.A., SANTICIOLI, P., GEPPETTI, P., FURIO, M., FRILLI, S., CONTE, B., FANCIULLACCI, M., GIULIANI, S. & MELI, A. (1987B). The contribution of capsaicin-sensitive innervation to activation of the spinal vesico-vesical reflex in rats: relationship between substance P levels in the urinary bladder and the sensory efferent function of capsaicin-sensitive sensory neurons. *Brain Res.*, **415**, 1–13.

MAGGI, C.A., SANTICIOLI, P. & MELI, A. (1984b). The effects of topical capsaicin on rat urinary bladder motility in vivo. *Eur. J. Pharmacol.*, **103**, 41–50.

MARCEAU, F., LUSSIER, A., REGOLI, D. & GIROUD, J.P. (1983). Pharmacology of kinins: their relevance to tissue injury and inflammation. *Gen. Pharmacol.*, **14**, 209–229.

OZA, N.B. (1988). A new direct radioimmunoassay of rat urinary kininogen. *Biochem. Pharmacol.*, **37**, 1965–1970.

PERRY, D.C. & SNYDER, S.H. (1984). Identification of bradykinin in mammalian brain. *J. Neurochem.*, **43**, 1072–1080.

PINNA, C., CARATOZZOLO, O. & PUGLISI, L. (1992). A possible role for urinary bladder epithelium in bradykinin-induced contraction in diabetic rats. *Eur. J. Pharmacol.*, **214**, 143–148.

PRIVITERA, P.J., DAUM, P.R., HILL, D.R. & HILEY, C.R. (1992). Autoradiographic visualization and characteristics of [^{125}I]-bradykinin binding sites in guinea-pig brain. *Brain Res.*, **577**, 73–79.

SHARIF, N.A. & WHITING, R.L. (1991). Identification of B2 receptors in guinea-pig brain regions, spinal cord and peripheral tissues. *Neurochem. Int.*, **181**, 89–96.

STASZEWSKA-WOOLLEY, J., NOLAN, P.N. & LUK, D.E. (1991). Studies of reflexogenic effects of capsaicin and neuropeptides on neural afferents in the dog parietal pericardium. *Neuropeptides*, **20**, 191–200.

STERANKA, L.R., MANNING, D.C., DEHAAS, C.J., FERKANY, J.W., BOROSKY, S.A., CONNOR, J.R., VAVREK, R.J., STEWART, J.M. & SNYDER, S.H. (1988). Bradykinin as a pain mediator: receptors are localized to sensory neurons, and antagonists have analgesic actions. *Proc. Natl. Acad. Sci. U.S.A.*, **85**, 3245–3249.

WIRTH, K., HOCK, F.J., ALBUS, U., LIINZ, W., ALPERMANN, H.G., ANAGNOSTOPULOS, H., HENKE, S.T., BREIPHOL, G., KONIG, W., KNOLLE, J. & SCHOLKENS, B.A. (1991). Hoe 140 a new potent and long acting bradykinin antagonist: *in vivo* studies. *Br. J. Pharmacol.*, **102**, 774–777.

YAMAMOTO, T. & YAKSH, T.L. (1991). Stereospecific effects of a nonpeptidic NK1 selective antagonist, CP-96,345: antinociception in the absence of motor dysfunction. *Life Sci.*, **49**, 1955–1963.

(Received February 11, 1994
Revised September 15, 1994
Accepted October 4, 1994)

British Journal of Pharmacology (1995) 114, 715-719

Interaction between methotrexate and indomethacin on a human normal haemopoietic cell line

[1]S.J. Hollingsworth, *N.P. Shankley, [2]E.M. Anderson & A. Bennett

Department of Surgery, King's College School of Medicine and Dentistry, The Rayne Institute, 123 Coldharbour Lane, London, SE5 9NU and *James Black Foundation, King's College School of Medicine and Dentistry, 68 Half-Moon Lane, London, SE24 9JE

1 The interaction between methotrexate and indomethacin has been examined, at a physiological folate concentration (20 nM), on a human normal lymphoblast-like cell line (RPMI 1788) *in vitro*.

2 Indomethacin (1 $\mu g\,ml^{-1}$) increased the reduction of lymphoblast growth caused by methotrexate (10–80 $ng\,ml^{-1}$).

3 Indomethacin (0.1 and 1 $\mu g\,ml^{-1}$) potentiated the cytotoxicity of methotrexate (20 and 40 $ng\,ml^{-1}$) after 4 days in culture.

4 Indomethacin (0.4 $\mu g\,ml^{-1}$) reduced the accumulation of tritium in lymphoblasts incubated with [^{3}H]-methotrexate after 30 min; therefore initial drug accumulation was not responsible for the potentiation seen after 4 days.

5 If indomethacin increases the killing of human cancer cells by methotrexate *in vivo*, with a smaller potentiation on lymphoblasts, this combination may be beneficial in treating human malignancy.

Keywords: Haemopoietic cells; indomethacin; lymphoblasts; methotrexate

Introduction

Indomethacin (Indo) potentiates the cytotoxicity of the folate analogue, methotrexate (MTX) to the murine NC carcinoma *in vivo* and *in vitro* (Gaffen *et al.*, 1985; Bennett *et al.*, 1987) and, of particular clinical relevance, to two human breast cancer cell lines (T47D and DU4475, Bennett *et al.*, 1989). It has been suggested that this action is due to increased MTX uptake and/or retention (Bennett *et al.*, 1989; Bennett & Gaffen, 1989). Indo does not appear to potentiate MTX by blocking cyclo-oxygenase, since the effect is not mimicked by the selective inhibitors flurbiprofen or piroxicam, or counteracted by adding prostaglandin E_2 (PGE_2) (Bennett *et al.*, 1987; 1989). In contrast, Indo did not increase the MTX-induced killing of normal epithelial-like cells from human embryonic intestine, or their accumulation of tritium during incubation with [^{3}H]-MTX (Bennett *et al.*, 1987). We also have similar preliminary data showing no potentiation in two other epithelial-like cell lines from normal human gut (FHs 74 Int cells and HCMC cells, Bennett *et al.*, 1989). Thus Indo may be of use for increasing MTX cytotoxicity to human breast cancer, without simultaneously increasing gastrointestinal damage. However, bone marrow is also particularly sensitive to MTX toxicity, so we have now studied the Indo/MTX interaction on RPMI 1788 lymphoblasts, a continuous human haemopoietic cell line derived from a normal individual (Huang & Moore, 1969).

Methods

Cells and cell culture

RPMI 1788 cells were initially derived from peripheral blood leucocytes of a normal 33-year-old Caucasian male (Huang & Moore, 1969). Morphologically they are lymphoblast-like, secrete IgM-lambda chains, and are positive for HLA 2, 7 antigens.

Standard culture media typically contain supraphysiological levels of folates: the medium used for the lymphoblast cells (RPMI 1788; American Type Culture Collection, Rockville, Maryland, U.S.A.) was Iscove's modification of Dulbecco's medium (IMD) which contains 8 μM folic acid, i.e. 400 times that in normal blood (20 nM). For the studies with MTX, medium formulated without folic acid (Flow Laboratories) was used after adding folic acid to give a physiological level of 20 nM. The lymphoblast cells were maintained in roller suspension culture in IMD formulated with 20 nM folic acid and containing 10% heat-inactivated foetal bovine serum plus 50 units ml^{-1} each of penicillin and streptomycin (Gibco). Bulk cultures received additions of fresh medium (30–40% by volume) at 48–72 h intervals. The growth of bulk cultures was determined daily by counting cells in a 10 ml sample. Experiments were carried out on cultures grown for at least 15–20 cell cycles at the physiological folate concentration and with 10^6 cells ml^{-1} in the logarithmic phase of growth (>95% viability).

Determination of cell growth

Cell growth was determined by microturbidimetry (Gaffen *et al.*, 1985), by measuring the transmission of 600 nm light through cell suspensions (recorded as absorption units with a Dynatec MR600 microplate reader). This wavelength gave a linear correlation between light 'absorption' and cell numbers (1.25×10^4 to 2×10^5 cells in 200 μl; Figure 1a).

Cells from bulk suspension cultures were pelleted by centrifugation (200 *g*, 10 min), resuspended in 10–20 ml growth medium, gently disaggregated by repeated pipetting, and counted (Coulter counter). The cells were diluted in fresh medium to 1.25×10^4, 2.5×10^4, 5×10^4, 1×10^5 and 2×10^5 in 200 μl final volume and added to microplate wells. Light absorbance readings were taken immediately, and then on 4 consecutive days of incubation at 37°C, following gassing of the plates for 5 min with CO_2/O_2 (95:5) in a sealed Perspex box (separate plates for each day). As the cells grew and multiplied, the optical density of the cultures increased

[1] Author for correspondence at present address: Department of Haematological Medicine, King's College School of Medicine & Dentistry, Denmark Hill, London SE5 9RS.
[2]Present address, University Department of Surgery, Royal Free Hospital School of Medicine, Pond Street, London NW3 2QG.

linearly over 4 days. Figure 1b shows the growth curve for 10^5 cells per well as used in the drug assays.

In the studies of drug effects, aliquots of 100 µl medium containing vehicle alone or drugs at twice the desired final concentration were added to each of the 96 flat-bottomed wells of a microtest plate, followed by 100 µl of cell suspension (10^5 cells) or medium alone. After 4 days incubation (37°C, 5% CO_2 in humidified air) the plates were sealed in a Perspex box, gassed for 5 min with CO_2/O_2 (95:5), and light absorption was measured at 600 nm.

Concentration-growth curves were obtained to determine the sensitivity of the lymphoblasts to MTX at 10–80 ng ml^{-1} and Indo at 0.1–10 µg ml^{-1}. Later experiments examined the effect of Indo at 0.1 and 1 µg ml^{-1} alone or with MTX at 20 and 40 ng ml^{-1} on lymphoblast growth.

Methotrexate accumulation studies

Tritium accumulation was measured by a method modified from Henderson *et al.* (1978). Cells from bulk cultures were harvested, disaggregated and counted as described above, and were diluted to 8×10^6 cells ml^{-1} in IMD (without folic acid, as this would compete for uptake with MTX) supplemented only with penicillin and streptomycin (50 units ml^{-1} each). Assay tubes (30 ml universal containers placed on ice) contained 8×10^6 lymphoblasts, 3 ng ml^{-1} [^{3}H]-MTX (500,000 d.p.m.; [L-glutamyl-3,4-^{3}H]-MTX, 41.0 Ci mmol^{-1}. DuPont, UK), and nonradioactive MTX to various concentrations (5–140 ng ml^{-1} or 0.5–14 µg ml^{-1}), with or without Indo (0.4 µg ml^{-1}) in a total volume of 1.1 ml. Triplicate containers were then incubated at 37°C (to measure total accumulation) with identical controls at 0°C (blank). The difference between total and blank was taken as the 'specific accumulation'. After 30 min incubation, the reaction was stopped by placing the tubes on ice for 10 min prior to centrifugation (600 *g*, 5 min). Cell pellets were resuspended in 25 ml of ice-cold phosphate buffered saline pH 7.4 (PBS), centrifuged as above, transferred to scintillation vials by three aliquots of 200 µl twice distilled water, and 3 ml of scintillation cocktail (Packard Ultima Gold) was added. The accumulation of tritium was determined by standard spectrophotofluorimetric counting in a Packard 2200 CA scintillation counter (average ^{3}H efficiency ~ 50%).

Drugs and solvents

Sodium indomethacin trihydrate (Merck Sharp and Dohme) and MTX were made up in 154 mM NaCl, adjusted to pH 7.4 with 0.1 M NaOH, filter-sterilised and stored at −20°C.

Statistics

The results are expressed as means ± s.e.mean and analysed by Student's *t* test (2-tailed) for paired and unpaired data as appropriate.

Results

Cell studies

Indo alone had no significant effect on lymphoblast growth. With low concentrations of Indo (0.1 and 1 µg ml^{-1}) the mean growth at 4 days was slightly higher (13.9 ± 6.5 and 10.0 ± 6.0% respectively, $n = 12$, Figure 2) than controls, whereas with higher concentrations (5 and 10 µg ml^{-1}) it was slightly lower (1.2 ± 8.3 and 6.3 ± 6.7% respectively, Figure 2).

MTX at 40 and 80 ng ml^{-1} produced a concentration-dependent reduction of lymphoblast growth (both $P < 0.03$, Figure 3), but at 10 and 20 ng ml^{-1} had no significant effect (both $P < 0.5$). Indo (1 µg ml^{-1}) with MTX at 20, 40 and 80 ng ml^{-1} increased the growth reduction (105, 98, and 207% greater reduction than with MTX alone; $P < 0.02, < 0.001$ and < 0.001 respectively; Figure 3), and a similar trend occurred with Indo (1 µg ml^{-1}) + MTX at 10 ng ml^{-1} (38% greater reduction than with MTX alone; $P < 0.2$, Figure 3).

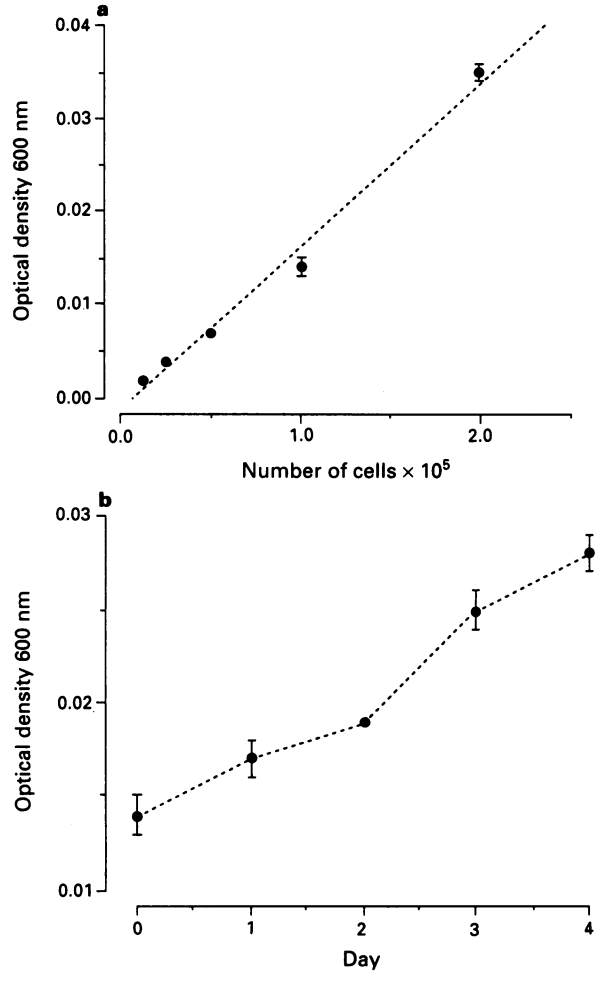

Figure 1 (a) The relationship between the numbers of lymphoblasts and light transmission was linear (linear regression analysis, $r = 0.988$). Each point is the mean ± s.e. of the separate means from 4 experiments each with 8–16 replicates. (b) The reduction of light transmission through each microplate well during a 4-day period of lymphoblast cell growth. Each point is the mean ± s.e. of the separate means from 4 experiments with cultures initially containing 10^5 cells, and there were 8–16 replicates in each experiment.

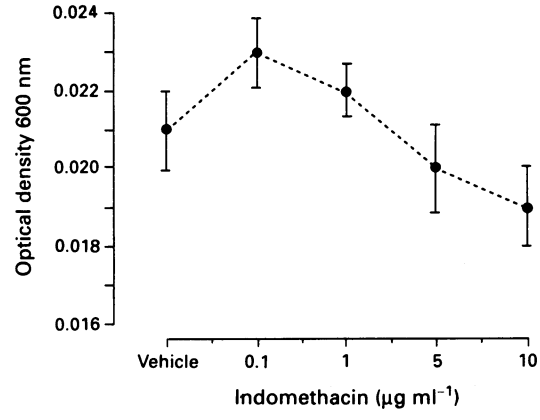

Figure 2 The effect of indomethacin on lymphoblast cell growth. Each point is the mean ± s.e. of the separate means from 12 experiments each with 16 replicates.

The MTX/Indo interaction was then evaluated in more detail. A possible drug interaction was examined by subtracting the sum of the separate mean percentage decreases in lymphoblast growth obtained with MTX and Indo alone, from the mean percentage decrease with the respective drug combinations. This can be summarised as follows:

$$\% \text{ interation} = \text{mean \% effect obtained with (MTX + Indo)} - \text{(MTX)} - \text{(Indo)}$$

A value above zero indicates potentiation, whilst a negative value indicates antagonism.

In further experiments, Indo potentiated the cytotoxicity of MTX at 20 and 40 ng ml^{-1}, calculated as described above, by 14.0 ± 5.8% and 16.8 ± 6.1% respectively with Indo at 0.1 μg ml^{-1}, and by 13.2 ± 5.2% and 18.3 ± 5.3% respectively with Indo 1 μg ml^{-1} (all P values <0.03, Figure 4).

Methotrexate accumulation

Initial experiments showed a linear active accumulation of label (3 ng ml^{-1} [^{3}H]-MTX) with time and increasing cell density, while the 0°C blanks showed only a very slow uptake of tritium (Figures 5a and b respectively).

The effect of Indo (0.4 μg ml^{-1}) was determined on the accumulation of tritium after 30 min incubation of cells with 3 ng ml^{-1} [^{3}H]-MTX + unlabelled MTX 5 ng ml^{-1} to 14 μg ml^{-1}, a range chosen to give concentrations expected to saturate the dihydrofolate reductase (DHFR). Four experiments, each on a separate population of cells, were performed in triplicate. Indo (0.4 μg ml^{-1}) reduced the accumulation of [^{3}H]-MTX, as shown by the difference in slope of the lines ($P<0.05$), and a decreased y-intercept ($P<0.005$) determined from linear regression analysis using the means of the three replicates from each of the four individual experiments (vehicle controls, $r = 0.996$; + Indo, $r = 0.994$; Figures 6a and b). The concentration-dependent increase in [^{3}H]-MTX accumulation did not appear to reach a maximum even at the highest concentration of MTX used (14 μg ml^{-1}).

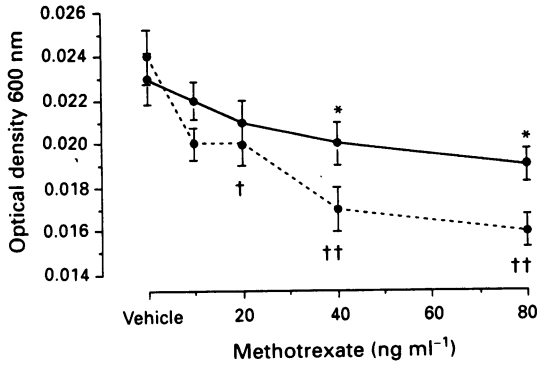

Figure 3 The effect of methotrexate (MTX) with and without indomethacin (Indo) on lymphoblast cell growth. (● —— ●) Vehicle controls; (● ..... ●) + 1 μg ml^{-1} indomethacin. P values: *<0.05 MTX vs vehicle; †<0.05 and ††<0.001 MTX + Indo vs MTX alone. Each point is the mean ± s.e. of the separate means from 18–42 experiments each with 4–16 replicates.

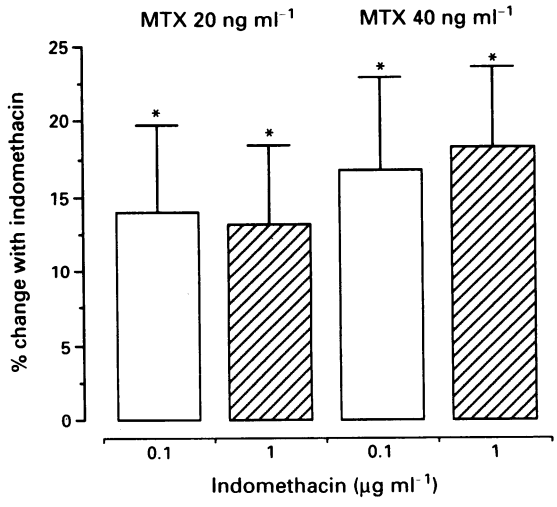

Figure 4 The potentiation of methotrexate (MTX) cytotoxicity to lymphoblasts (MTX at 20 and 40 ng ml^{-1}) by indomethacin (0.1 and 1 μg ml^{-1}, open and hatched columns, respectively). Each column is the mean ± s.e. of the separate means of 24–42 experiments each with 4–16 replicates.

Discussion

High doses of MTX (0.5–20 g m^{-2} for 6–24 h) are given to cancer patients, but these amounts are tolerated only when followed by folinic acid rescue, otherwise severe or even fatal myelosuppression may occur (Von Hoff *et al.*, 1977). Little is known about MTX pharmacokinetics in myeloid bone marrow cells. Four patients with non-Hodgkin's lymphoma infused with MTX for 24 h showed a much greater uptake and retention of MTX by cells in the proliferating (immature) myeloid compartment than by the mature myeloid cells and neutrophils (Schrøder, 1987). Long-term bone marrow cultures showed a concentration-related suppression of myelopoiesis with 1, 10 or 100 mM MTX followed

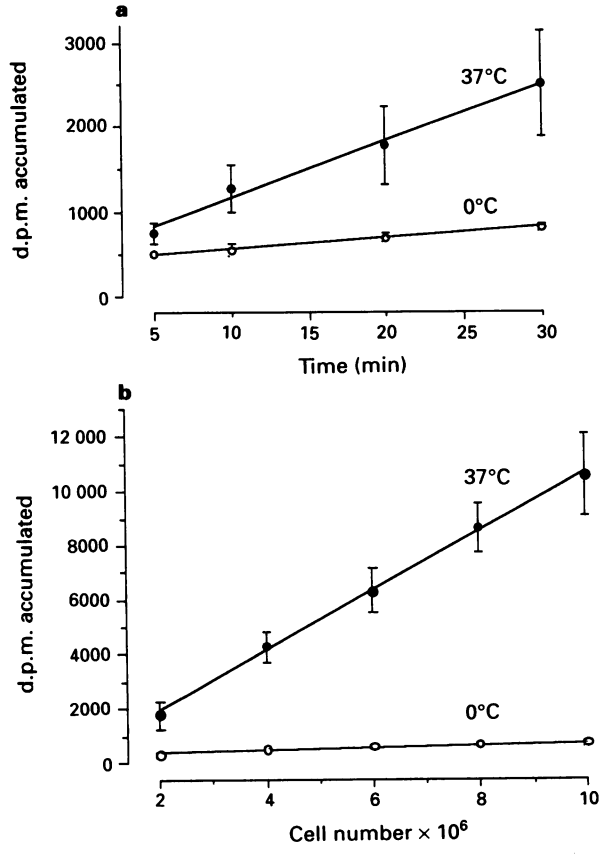

Figure 5 (a) Linear accumulation of tritium by lymphoblasts (8 × 10^6 cells) when incubated with 3 ng ml^{-1} [^{3}H]-methotrexate (MTX) (●, 37°C incubation, $r = 0.987$; ○, blanks incubated at 0°C, $r = 0.998$). Each point is the mean ± s.e. of the separate means from 4 experiments each with 3 replicates. (b) The influence of lymphoblast cell numbers in the accumulation of tritium when incubated for 30 min with 3 ng ml^{-1} [^{3}H]-MTX. Each point is the mean ± s.e. of the separate means from 4 experiments each with 3 replicates.

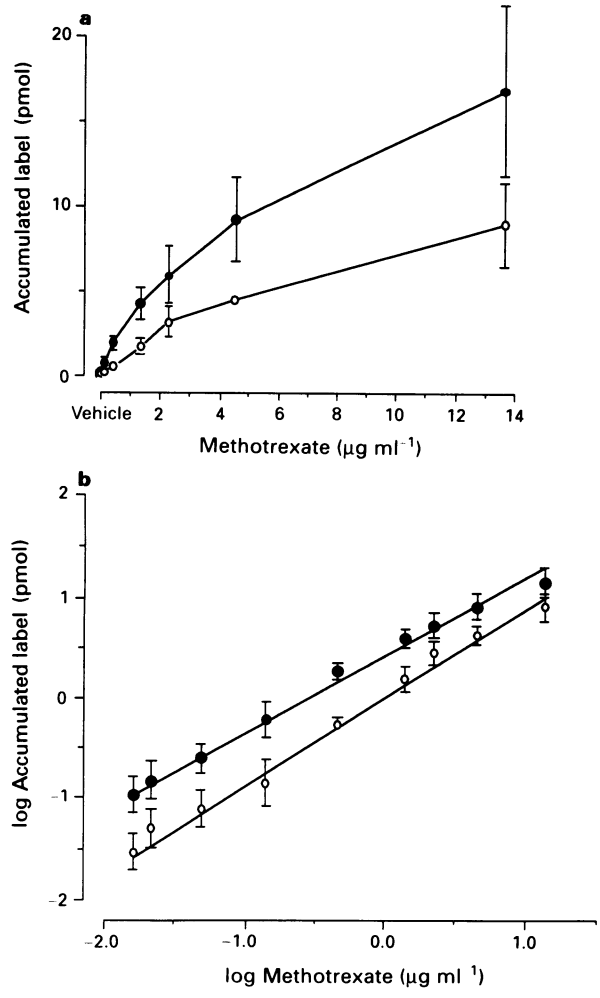

Figure 6 (a,b) The reduction by indomethacin (0.4 $\mu g\,ml^{-1}$) of tritium accumulation by 8×10^6 lymphoblasts incubated for 30 min with [^{3}H]-methotrexate. (●) Vehicle controls; (○) + indomethacin. Each point is the mean of the separate means from 4 experiments each with 3 replicates.

by folinic acid rescue (Williams *et al.*, 1988). Similarly, using an exogenous spleen-colony assay in irradiated mice, MTX inhibited the proliferative activity of transplanted haemopoietic stem cells in an exponential dose-response relationship (Jurásková, 1988).

Because our previous findings indicate that the cytotoxicity of MTX to human breast cancer cell lines is potentiated by Indo (Bennett & Gaffen, 1989; Bennett *et al.*, 1989), we have examined the safety of these drug combinations on the haemopoietic lymphoblast-like cell line RPMI 1788 derived from normal human peripheral blood.

Indo potentiated the cytotoxicity of MTX to RPMI 1788 normal human lymphoblast cells, the effect being slightly greater with higher concentrations of MTX. Compared to murine NC cells (derived from a spontaneously arising mammary tumour in WHT/Ht mice, Hewitt *et al.*, 1976), a much higher concentration of MTX was required to kill the lymphoblasts, and the potentiation by Indo was much less (Hollingsworth *et al.*, 1992). For example, in murine NC cells a concentration of MTX of only 4 $ng\,ml^{-1}$ caused a 55.1 ± 4.1% decrease in growth, and Indo at 1 $\mu g\,ml^{-1}$, a concentration that alone had little or no effect, caused a further 25.8 ± 4.1% increase in cell loss. Initial drug accumulation is an important factor in effective therapy with MTX (Jansen *et al.*, 1990), and it has been suggested that the potentiation by Indo is due to an increased uptake and/or retention of MTX (Bennett *et al.*, 1989; Bennett & Gaffen, 1989). Indo increased the accumulation of label by NC cells incubated with [^{3}H]-MTX (Bennett *et al.*, 1989; Kuonen *et al.*, 1992), whereas in this study with RPMI 1788 cells, Indo reduced the accumulation of label. Thus an increased initial drug accumulation does not explain the potentiation of MTX cytotoxicity to lymphoblasts by Indo. However, tritium accumulation in the present studies was measured after 30 min incubation, whereas cytotoxicity was measured at 4 days; what happens to MTX accumulation between 30 min and 4 days is not known. If Indo affects the K_m for MTX influx but not the V_{max}, in long incubation studies the initial changes in drug accumulation by Indo may not be important in the overall MTX/Indo interaction. Accumulation of tritium was apparently not saturated even on incubation with very high concentrations of MTX (well above those used in the cytotoxicity studies). It is therefore unlikely that Indo affects only the V_{max}, even though this could not be evaluated in these studies. Experiments with yet higher MTX concentrations, or longer incubation periods, would be limited by the need to maintain physiological conditions, except for the presence of drugs, and a reasonably high cellular viability. It is not known whether Indo potentiates MTX cytotoxicity to the lymphoblasts after 4 days in culture by inhibiting folate uptake and so increasing MTX accumulation, an effect that would not have been seen in the accumulation studies that were performed in the absence of folate. However, this would seem unlikely as the route by which folate enters the cell differs from that for reduced folates and MTX (Sirotnak, 1985). It is not clear from these studies how Indo reduces the accumulation of label at 30 min during incubation of lymphoblasts with [^{3}H]-MTX, or how cytotoxicity is potentiated at 4 days.

The kidney is also particularly at risk fom damage by MTX. Non-steroidal anti-inflammatory drugs (NSAIDs) competitively inhibit the *in vitro* accumulation of MTX by rabbit kidney slices (Nierenberg, 1983), and this may be related to the *in vivo* inhibition of renal MTX clearance by NSAIDs (Christophidis *et al.*, 1985). Using the ratio between the therapeutic plasma concentration and the K_i for this inhibition by each drug, Nierenberg (1983) predicted that drugs such as salicylates, fenoprofen, naproxen and phenylbutazone would be most likely to inhibit renal MTX excretion and cause toxicity, whereas Indo and meclofenamate would be least likely to do so. Seideman *et al.* (1987) found that in water-loaded rheumatic patients with normal kidney function, therapeutic doses of Indo decreased diuresis by 25–50%. Acute renal failure due to the concomitant action of MTX and Indo has been reported (Ellison & Servi, 1985; Maiche, 1986), and other life-threatening interactions between MTX and NSAIDs have been described (aspirin, Day *et al.*, 1984; ketoprofen, Thyss *et al.*, 1986; naproxen, Singh *et al.*, 1986; azapropazone, Daly *et al.*, 1986).

Our results suggest that Indo reduces the initial accumulation of label when human RPMI 1788 lymphoblasts are incubated with [^{3}H]-MTX, and although the long-term cytotoxicity of MTX is increased in the presence of Indo, the effect is much smaller than in murine NC adenocarcinoma cells. It remains to be seen how relevant these findings are to human disease, but if this difference is maintained in human malignant cells, the MTX/Indo interaction may have value in treating human cancer, with only a small increase of risk to the bone marrow.

We thank the Joint Research Committee of King's College London for financial support.

References

BENNETT, A. & GAFFEN, J.D. (1989). Interactions between anti-inflammatory drugs and cancer chemotherapy. In *Prostanoids and Drugs*, Vol. **177**, pp. 243–248. ed. Samuelsson, B, Berti, F. Folco, G.C. & Velo, G.P. New York, London: Plenum Press.

BENNETT, A., GAFFEN, J.D. & CHAMBERS, E. (1989). Cyclo-oxygenase inhibitors and cell killing by cytotoxic drugs. *Adv. Prostaglandin, Thromboxane, Leukot. Res.*, **19**, 427–430.

BENNETT, A., GAFFEN, J.D., MELHUISH, P.B. & STAMFORD, I.F. (1987). Studies on the mechanism by which indomethacin increases the anticancer effect of methotrexate. *Br. J. Pharmacol.*, **91**, 229–235.

CHRISTOPHIDIS, N., COSOLO, W., FRASKER, K., FRANCIS, G. & LOUIS, W. (1985). Pharmacokinetic studies of methotrexate. *Aust. N.Z. J. Med.*, **15**, (suppl), 180.

DALY, H.M., BOYLE, J., ROBERTS, C.J.C. & SCOTT, G.L. (1986). Interaction between methotrexate and nonsteroidal anti-inflammatory drugs. *Lancet.*, **i**, 557.

DAY, R.O., GRAHAM, G.G., CHAMPION, G.D. & LEE, E. (1984). Anti-rheumatic drug interactions. *Clin. Rheum. Dis.*, **10**, 251–257.

ELLISON, N.M. & SERVI, R.J. (1985). Acute renal failure and death following sequential intermediate-dose methotrexate and 5-FU: a possible adverse effect due to concomitant indomethacin administration. *Cancer Treat. Rep.*, **69**, 342–343.

GAFFEN, J.D., BENNETT, A. & BARER, M.R. (1985). A new method for studying cell growth in suspension, and its use to show that indomethacin enhances cell killing by methotrexate. *J. Pharm. Pharmacol.*, **37**, 261–263.

HENDERSON, G.B., ZEVERLY, E.M. & HUENNEKENS, F.M. (1978). Cyclic adenosine 3':5'-monophosphate and methotrexate transport in L1210 cells. *Cancer Res.*, **38**, 859–861.

HEWITT, H.B., BLAKE, E.R. & WALDER, A.S. (1976). A critique of the evidence for active host defence against cancer, based on personal studies of 27 murine tumours of spontaneous origin. *Br. J. Cancer*, **33**, 241–259.

HOLLINGSWORTH, S.J., ANDERSON, E.M. & BENNETT, A. (1992). Methotrexate/indomethacin interaction in normal and tumour cell lines: effects of folate concentration. *Br. J. Pharmacol.*, **107**, 262P.

HUANG, C.C. & MOORE, G.E. (1969). Chromosomes of 14 hematopoietic cell lines derived from peripheral blood of persons with and without chromosome anomalies. *J. Natl. Cancer Inst.*, **43**, 1119–1128.

JANSEN, G., WESTERHOF, G.R., JARMUSZEWSKI, M.J.A., KATHMANN, I., RIJKSEN, G. & SCHORNAGEL, J.H. (1990). Methotrexate transport in variant human CCRF-CEM leukaemia cells with elevated levels of the reduced folate carrier. *J. Biol. Chem.*, **265**, 18272–18277.

JURÁSKOVÁ, V. (1988). The cytotoxic effect of methotrexate as evaluated by colony-forming activity of hemopoietic and tumour cells. *Neoplasma*, **35**, 583–589.

KUONEN, D.R., ANDERSON, E.M., HOLLINGSWORTH, S.J. & BENNETT, A. (1992). Indomethacin increases the maximal velocity of [^{3}H]-MTX uptake by NC cancer cells. *Br. J. Pharmacol.*, **107**, 476P.

MAICHE, A.G. (1986). Acute renal failure due to concomitant action of methotrexate and indomethacin. *Lancet*, **i**, 1390.

NIERENBERG, D.W. (1983). Competitive inhibition of methotrexate accumulation in rabbit kidney slices by nonsteroidal anti-inflammatory drugs. *J. Pharmacol. Exp. Ther.*, **226**, 1–6.

SCHRØDER, H. (1987). Methotrexate kinetics in myeloid bone marrow cells and peripheral neutrophils. *Cancer Chemother. Pharmacol.*, **19**, 42–46.

SEIDEMAN, P., SOLLEVI, A. & FREDHOLM, B.B. (1987). Additive renal effects of indomethacin and dipyridamole in man. *Br. J. Clin. Pharmacol.*, **23**, 323–330.

SINGH, R.R., MALAVIYA, A.N., PANDEY, J.N. & GULERIA, J.S. (1986). Fatal interaction between methotrexate and niproxen. *Lancet*, **i**, 1390.

SIROTNAK, F.M. (1985). Obligate genetic expression in tumour cells of a fetal membrane property mediating 'folate' transport: biological significance and implications for improved therapy of human cancer. *Cancer Res.*, **45**, 3992–4000.

THYSS, A., MILANO, G., KUBAR, J., NAMER, M. & SCHNEIDER, M. (1986). Clinical and pharmacokinetic evidence of a life-threatening interaction between methotrexate and ketoprofen. *Lancet*, **i**, 256–258.

VON HOFF, D.D., PENTA, J.S., HELMAN, L.J. & SLAVIK, M. (1977). Incidence of drug related deaths secondary to high dose methotrexate-citrovorium factor administration. *Cancer Treat. Rep.*, **61**, 745–748.

WILLIAMS, L.H., KODETTHOOR, B., UDUPA, B. & LIPSCHITZ, D.A. (1988). Long-term marrow culture as a model for host toxicity: the effect of methotrexate on hematopoiesis and adherent layer function. *Exp. Hematol.*, **16**, 80–87.

(Received January 31, 1994
Revised September 9, 1994
Accepted October 20, 1994)

British Journal of Pharmacology (1995) 114, 720–726

Different pressor and bronchoconstrictor properties of human big-endothelin-1, 2 (1–38) and 3 in ketamine/xylazine-anaesthetized guinea-pigs

Jean-Philippe Gratton, *Giles A. Rae, Audrey Claing, †Sabine Télémaque & [1]Pedro D'Orléans-Juste

Department of Pharmacology, Medical School, Université de Sherbrooke, Sherbrooke (Québec) J1H 5N4, Canada; *Department of Pharmacology, Biological Sciences Center, Universidade Federal de Santa Catarina, Florianópolis, SC, Brazil and †Howard Hughes Medical Institute, UT Southwestern Medical Center, 5323 Harry Hines Blvd, Room Y5-224, Dallas, Texas 75235-9050, U.S.A.

1 In the present study, the precursors of endothelin-1, endothelin-2 and endothelin-3 were tested for their pressor and bronchoconstrictor properties in the anaesthetized guinea-pig. In addition, the effects of big-endothelin-1 and endothelin-1 were assessed under urethane or ketamine/xylazine anaesthesia.

2 When compared to ketamine/xylazine, urethane markedly depressed the pressor and bronchoconstrictor properties of endothelin-1 and big-endothelin-1.

3 Under ketamine/xylazine anaesthesia, the three endothelins induced a biphasic increase of mean arterial blood pressure. In contrast, big-endothelin-1, as well as big-endothelin-2 (1–38), induced only sustained increase in blood pressure whereas big-endothelin-3 was inactive at doses up to 25 nmol kg^{-1}.

4 Big-endothelin-1, but not big-endothelin-2, induced a significant increase in airway resistance. Yet, endothelin-1, endothelin-2 and endothelin-3 were equipotent as bronchoconstrictor agents.

5 Big-endothelin-1, endothelin-1 and endothelin-2, but not big-endothelin-2, triggered a marked release of prostacyclin and thromboxane A_2 from the guinea-pig perfused lung.

6 Our results suggest the presence of a phosphoramidon-sensitive endothelin-converting enzyme (ECE) which is responsible for the conversion of big-endothelin-1 and big-endothelin-2 to their active moieties, endothelin-1 and 2. However, the lack of bronchoconstrictor and eicosanoid-releasing properties of big-endothelin-2, as opposed to endothelin-2 or big-endothelin-1, suggests the presence of two distinct phosphoramidon-sensitive ECEs in the guinea-pig. The ECE responsible for the systemic conversion of big-endothelins possesses the same affinity for big-endothelin-1 and 2 but not big-endothelin-3. In contrast, in the pulmonary vasculature is localized in the vicinity of the sites responsible for eicosanoid release, an ECE which converts more readily big-endothelin-1 than big-endothelin-2.

Keywords: Endothelin-1; big-endothelin-2; eicosanoids; phosphoramidon; pressor response; bronchoconstriction (guinea-pig); endothelin-converting enzyme (ECE)

Introduction

The 21-amino acid peptide, endothelin-1, is a potent pressor and bronchoconstrictor agent in the anaesthetized guinea-pig. Unlike its hypertensive properties, the increase of airway resistance induced by endothelin-1 is markedly blunted by indomethacin, illustrating the indirect bronchoconstrictor properties of the peptide via the release of thromboxane A_2 in the guinea-pig (Payne & Whittle, 1988; Pons *et al.*, 1992).

Similarly to endothelin-1, big-endothelin-1 is also a potent pressor and bronchoconstrictor agent (Kashiwabara *et al.*, 1989; Fukuroda *et al.*, 1990; D'Orléans-Juste *et al.*, 1991b). Yet, unlike endothelin-1, both effects of big-endothelin-1 are suppressed by phosphoramidon, suggesting that the latter peptide must be converted to its active metabolite via an endothelin-converting enzyme (ECE) which is sensitive to this neutral endopeptidase inhibitor. In comparison, we have shown previously that the precursor of endothelin-3, big-endothelin-3 (Bloch *et al.*, 1990), is inactive both as a pressor agent *in vivo* and as a releaser of eicosanoids in the guinea-pig isolated perfused lung, illustrating the possible selectivity of the phosphoramidon-sensitive ECE for big-endothelin-1 (D'Orléans-Juste *et al.*, 1991b).

In different *in vivo* models, the conscious or anaesthetized rat, various groups have shown that big-endothelin-3 induces a phosphoramidon-sensitive pressor effect, demonstrating an interspecies variation in the ECE activity (Gardiner *et al.*, 1992; Matsumura *et al.*, 1993; Mattera *et al.*, 1993; Pollock *et al.* 1993). Furthermore, Matsumura *et al.* (1993) have suggested that different conditions of anaesthesia as well as the use of a ganglion blocker enhanced the pressor activity of big-endothelin-3 in the rat model.

Our initial observations on the lack of activity of big-endothelin-3 were obtained from urethane-anaesthetized guinea-pigs not treated with neuromuscular or ganglion blockers (D'Orléans-Juste *et al.*, 1991b). We were therefore interested to explore whether a different anaesthesia and the use of succinylcholine would unmask the pressor effects of big-endothelin-3 in this animal model.

Finally, although the pharmacological properties of endothelin-2 in the guinea-pig have been reported by Pons *et al.* (1991a,b), those of big-endothelin-2 remained to be investigated. It is of interest that the structure of human big-endothelin-2 (1–37), initially reported by Arinami *et al.* (1991), has recently been shown to be erroneous, for Yorimitsu *et al* (1992) have suggested that the structure of big-endothelin-2 includes an extra L-arginine amino acid in its C-terminal portion. Therefore, we have compared its pressor and bronchoconstrictor effects with big-endothelin-1 and 3 in the ketamine/xylazine-anaesthetized guinea-pig. Furthermore, its eicosanoid-releasing properties in comparison with

[1] Author for correspondence.

endothelin-2 were also investigated in the guinea-pig perfused lung.

Methods

In vivo *experiments*

Dunkin-Hartley guinea-pigs of either sex (250–350 g, Charles River, St-Constant, Canada), anaesthetized with either urethane (1.5 g kg^{-1}, i.p.) or ketamine/xylazine (90/15 mg kg^{-1}, i.m.), were used for the *in vivo* experiments. The type of anaesthetics and their dosage were chosen according to the regulations set by the Canadian Council of Animal Care in the 'Guide for the care and use of experimental animals' (Volume 1, page 188, 1993). Polyethylene catheters (PE-50) were inserted into the left external jugular vein for drug administration and in the right carotid artery to monitor mean arterial blood pressure (MAP) and heart rate. A cannula (PE-240) was then inserted in the trachea to facilitate respiration. A blood pressure analyser (Micro-Med, Louisville, KT, U.S.A.) was used to monitor MAP and heart rate. The data were recorded (at fixed 5 s time intervals) by an automated computer data acquisition system (Blood Pressure Analyzer Communications Program; MicroMed) linked to a Tandy 1000 RLX computer. Throughout the experiments, all above-mentioned parameters were constantly monitored.

After surgery, the anaesthetized animals were allowed to stabilize for 30 min. For the assessment of the bronchoconstrictor responses, spontaneous breathing was suppressed with succinylcholine (5 mg kg^{-1}, s.c.) and the animals were connected through the tracheal cannula to a respirator (Model 683, Harvard apparatus, South Natick, MA, U.S.A.) and ventilated (6 ml air kg^{-1}, 60 strokes min^{-1}). Pulmonary insufflation pressure (PIP) was monitored with a pressure transducer (Statham, model P23AC) connected to a side arm of the tracheal cannula, according to the method of Konzett & Rössler (1940), and recorded on a Grass physiograph (model 79). The pharmacological responses to the various agonists were assessed for at least 40 min following the administration of a single bolus dose ranging from 0.01 to 25 nmol kg^{-1} for the peptides. For some experiments, phosphoramidon (5 mg kg^{-1}) was administered i.v. 5 min prior to a single bolus injection of either endothelin-2 (1 nmol kg^{-1}) or big-endothelin-2 (1–38) (5 nmol kg^{-1}).

Measurements of eicosanoids from guinea-pig isolated perfused lungs

Dunkin-Hartley guinea-pigs (250–350 g, Charles River, St-Constant, Canada) of either sex were killed by cervical dislocation. Following thoracotomy, the pulmonary artery was cannulated and the pulmonary circulation immediately perfused with heparinized Krebs solution (100 units ml^{-1}). The lungs were then removed and suspended in a heated chamber (37°C) and perfused (5 ml min^{-1}) with oxygenated (95% O_2, 5% CO_2) Krebs solution. The lungs were left to stabilize for 60 min before the 3 min infusion of the various peptides, big-endothelin-1 (100 nM), big-endothelin-2 (1–38) (100 nM), endothelin-1 (5 nM) or endothelin-2 (5 nM). The effluent from the lungs was collected (1-min samples) before, during and after infusion of the various peptides. The samples were then stored (−20°C) and the stable, hydrolytic metabolites of prostacyclin (PGI_2), 6-keto-prostaglandin $F_{1\alpha}$ (6-keto-$PGF_{1\alpha}$), and thromboxane A_2 (TxA_2) (thromboxane B_2, TxB_2) were later determined by radioimmunoassay.

Drugs and statistical analysis

Synthetic big-endothelin-1, big-endothelin-3, endothelin-1, endothelin-2, endothelin-3 and phosphoramidon were purchased from Peninsula Laboratory (Belmont, CA, U.S.A.). Big-endothelin-2 (1–38) was obtained from Peptide Institute (Osaka, Japan), ketamine from Rogar/STB (Montréal, Canada), xylazine from Chemagro (Etobicoke, Canada) and succinylcholine from Burroughs Wellcome (Kirkland, Canada). Urethane (ethyl carbamate), heparin, TxB_2, TxB_2 antiserum, 6-keto-$PGF_{1\alpha}$ and 6-keto-$PGF_{1\alpha}$ antiserum were purchased from Sigma Chemical (St-Louis, MO, U.S.A.). The TxB_2 antiserum has a 100% cross-reactivity with TxB_2, less than 2% cross-reactivity with PGD_2 and $PGF_{2\alpha}$ and less than 0.1% cross-reactivity with 6-keto-$PGF_{1\alpha}$, PGE_1 and PGE_2 (Sigma). The 6-keto-$PGF_{1\alpha}$ antiserum has 100% cross-reactivity with 6-keto-$PGF_{1\alpha}$, 23% with PGE_1, 4% with PGE_2, 7% with $PGF_{2\alpha}$ and less than 1% with TxB_2 (Sigma). The eicosanoid antisera used in the present study did not cross-react with endothelin-1, endothelin-2, big-endothelin-1 or big-endothelin-2 (1–38). The tracers, [^{3}H]-6-keto-$PGF_{1\alpha}$ and [^{3}H]-TxB_2, were purchased from Amersham (Oakville, Canada). All agents were dissolved in phosphate-buffered saline (PBS, pH 7.4, Sigma).

Data used in the text and figures are expressed as mean ± s.e. mean of n observations. Change in MAP, increase in PIP or increased release of eicosanoids from the perfused lung, when compared to basal at time 0, were analysed by ANOVA followed by Bonferroni's test for multiple comparisons. P values of <0.05 were considered to be statistically significant.

Ethics

The care of animals and all research protocols conform to the guiding principles for animal experimentation as enunciated by the Canadian Council on Animal Care and approved by the Ethical Committee on Animal Research of the Université de Sherbrooke Medical School.

Results

Pressor effects of endothelins and their precursors in guinea-pigs anaesthetized with urethane or ketamine/xylazine

Basal MAP and heart rates were 45.8 ± 1.6 mmHg and 283.8 ± 9.6 beats min^{-1} in the urethane-anaesthetized, succinylcholine-treated and ventilated guinea-pig ($n = 21$) and 51.7 ± 1.2 mmHg and 189.6 ± 2.5 beats min^{-1} in the ketamine/xylazine-treated animals ($n = 52$). Endothelin-1 induced, both in the urethane and ketamine/xylazine anaesthetized guinea-pig, a biphasic pressor response characterized by an early transient increase in MAP and a late sustained phase. The transient increase was approximatively three fold higher under ketamine/xylazine anaesthesia than in urethane-treated animals, whereas the sustained phase remained unchanged (Table 1). The response to big-endothelin-1, which induces only a sustained increased in MAP, was two to three fold higher under ketamine/xylazine anaesthesia than with urethane anaesthesia (Table 1).

Comparison of the haemodynamic properties of the three endothelins and their intermediate precursors in the ketamine/xylazine anaesthetized guinea-pig

In ketamine/xylazine-treated animals, endothelin-1, -2 or -3 all induced biphasic pressor responses. Endothelin-1 and endothelin-2 were approximately equipotent in inducing both phases of the response (Δ MAP, endothelin-1 (1 nmol kg^{-1}), transient: 34.0 ± 5.5 mmHg; sustained: 13.9 ± 1.7 mmHg, $n = 3$; endothelin-2 (1 nmol kg^{-1}), transient: 34.0 ± 4.6 mmHg; sustained: 14.7 ± 2.0 mmHg, $n = 3$) (Figures 1 and 2). Endothelin-3 was less potent than either endothelin-1 or 2 at inducing a sustained increase of MAP (Figure 2), although the transient increase in MAP caused by endothelin-3 was similar to that produced by endothelin-1 and 2 (Figures 1

and 2) (Δ MAP, endothelin-3 (1 nmol kg^{-1}), acute: 36.0 ± 6.9 mmHg; sustained: 5.8 ± 2.0 mmHg, $n = 4$).

Big-endothelin-1 and big-endothelin-2 induced monophasic dose-dependent increases of the MAP in the ketamine/xylazine anaesthetized guinea-pigs. Big-endothelin-1 at 1 and 5 nmol kg^{-1} induced maximal increases of 24.7 ± 0.7 and 80.1 ± 5.9 mmHg, respectively ($n = 3-5$). Similarly, big-endothelin-2 at doses of 1 and 5 nmol kg^{-1} induced maximal increases of MAP of 11.5 ± 2.2 and 62.3 ± 2.6, respectively ($n = 3-4$) (Figure 2). In contrast, big-endothelin-3 did not produce significant increases in MAP even at a dose of 25 nmol kg^{-1} (Figure 2). Neither the endothelins nor their precursors caused any changes in heart rate in the guinea-pigs (results not shown).

Table 1 Effect of urethane (1.5 g kg^{-1}) or ketamine/xylazine (90/15 mg kg^{-1}) anaesthesia on the pressor and bronchoconstrictor response to endothelin-1 (ET-1) and big-endothelin-1 in the guinea-pig

		Urethane			*Ketamine/xylazine*		
	Dose (nmol kg^{-1})	Δ*MAP* (mmHg) *Acute*	*Sustained*	Δ*PIP* (mmHg)	Δ*MAP* (mmHg) *Acute*	*Sustained*	Δ*PIP* (mmHg)
ET-1	0.25	2.3 ± 1.2	5.0 ± 1.0	0.7 ± 0.3	12.5 ± 1.5*	4.7 ± 2.3	6.3 ± 2.4*
	0.5	8.0 ± 3.3	9.6 ± 2.1	1.4 ± 0.2	23.5 ± 5.8*	5.8 ± 1.9	15.5 ± 3.5**
Big-ET-1	0.5	–	6.3 ± 1.9	0	–	20.7 ± 3.0*	0.7 ± 0.3
	1.0	–	9.7 ± 0.3	0	–	24.7 ± 0.7*	1.5 ± 0.3
	5.0	–	41.3 ± 5.8	2.8 ± 1.2	–	80.1 ± 5.9*	7.8 ± 1.7*

Each value represents the mean ± s.e.mean of at least 3 experiments. *$P<0.05$ and **$P<0.01$ when compared to the urethane-anaesthetized guinea-pig.

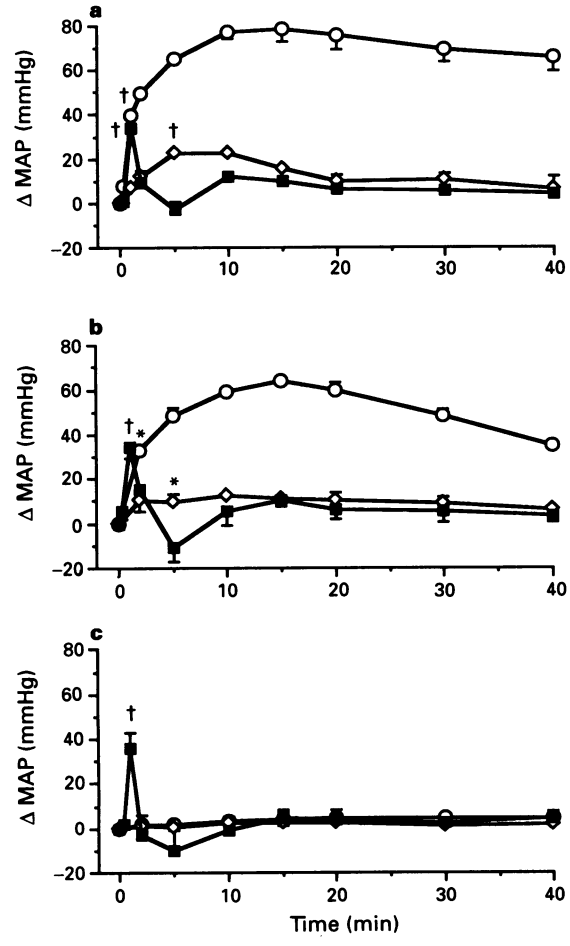

Figure 1 Change in mean arterial blood pressure (Δ MAP) in the ketamine/xylazine-anaesthetized guinea-pig induced by endothelin-1 (1 nmol kg^{-1}; ■) or big-endothelin-1 (1 nmol kg^{-1}; ◇ and 5 nmol kg^{-1}; ○) (a), endothelin-2 (1 nmol kg^{-1} ■) or big-endothelin-2 (1 nmol kg^{-1}; ◇ and 5 nmol kg^{-1}; ○) (b), endothelin-3 (1 nmol kg^{-1}; ■) or big-endothelin-3 (10 nmol kg^{-1}; ◇ and 25 nmol kg^{-1}; ○) (c). Each point represents the mean ± s.e.mean of at least 3 experiments. *$P<0.05$, †$P<0.01$. For the sake of clarity, significance is shown only for the first significant time point when compared to baseline at time 0.

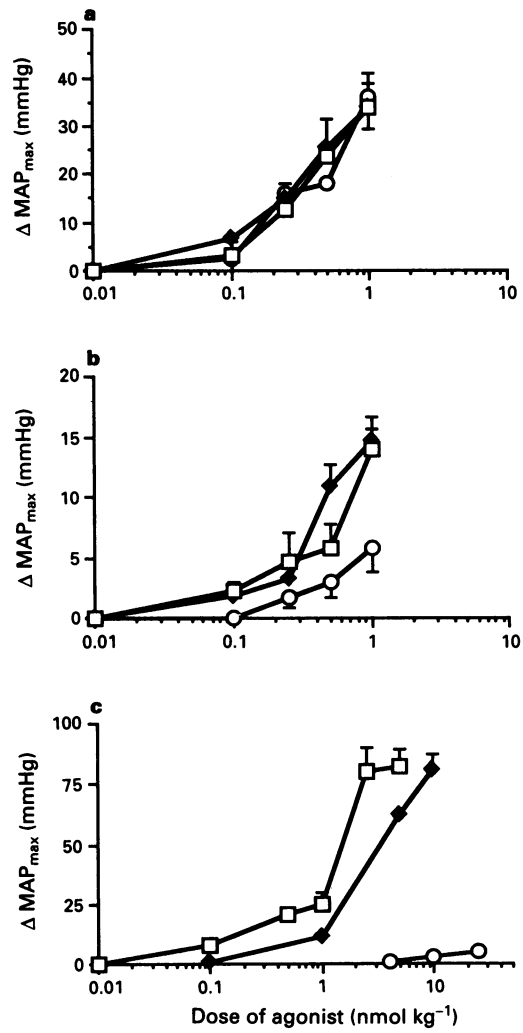

Figure 2 Dose-response curves showing transient (a) and sustained (b) phases of mean arterial pressure (MAP) response to endothelin-1 (□), endothelin-2 (◆), endothelin-3 (○) and (c) response to big-endothelin-1 (□), big-endothelin-2 (◆), and big-endothelin-3 (○) in the ketamine/xylazine-anaesthetized guinea-pig, Each point represents the mean ± s.e.mean of at least 3 experiments.

Effects of endothelins and their respective intermediate precursors on pulmonary insufflation pressure in the ketamine/xylazine-treated and ventilated guinea-pigs

Endothelins-1, 2 and 3 all induced similar dose-related increases in PIP in the anaesthetized guinea-pig (Figure 4). The three peptides induced a relatively short increase of PIP, lasting not more than 10 min (Figure 3). Big-endothelin-1 was approximately ten times less potent than endothelin-1 and a dose of 5 nmol kg^{-1} was necessary to elicit a significant and long-lasting (30 min) increase of PIP (Δ PIP, big-endothelin-1 (5 nmol kg^{-1}): 7.8 ± 1.7 mmHg, $n = 5$) (Figure 3a). In contrast, big-endothelin-2 (10 nmol kg^{-1}) and big-endothelin-3 (25 nmol kg^{-1}) did not alter the pulmonary insufflation pressure index significantly (Figures 3 and 4).

Effects of phosphoramidon on the increase of mean arterial blood pressure and pulmonary insufflation pressure induced by endothelin-2 or big-endothelin-2 in the guinea-pig

Phosphoramidon (5 mg kg^{-1}) markedly reduced the hypertensive effects of big-endothelin-2 (5 nmol kg^{-1}) (big-endothelin-2, control 62.3 ± 2.6 mmHg; in presence of phosphoramidon: 3.3 ± 0.9 mmHg, $n = 3$ each, $P<0.01$), but did not affect the pressor or bronchoconstrictor responses to endothelin-2 (Δ MAP, endothelin-2 (1 nmol kg^{-1}, control (transient phase): 34.0 ± 4.6 mmHg (sustained phase): 14.7 ± 2.0; in presence of phosphoramidon (transient phase): 36.3 ± 2.6 mmHg (sustained phase): 11.2 ± 2.5 mmHg, $n = 4$) (Δ PIP, endothelin-2 (1 nmol kg^{-1}, control: 28.7 ± 5.7 mmHg; in presence of phosphoramidon, 32.7 ± 4.8 mmHg, $n = 4$).

Different profiles of eicosanoid release stimulated by big-endothelin-1 and big-endothelin-2 in the isolated perfused lung of the guinea-pig

Endothelin-2 (5 nM) infused for 3 min into the pulmonary artery of the guinea-pig isolated perfused lung triggered a marked release of prostacyclin and thromboxane A_2 (Figures 5a and 6a). In contrast, big-endothelin-2 infused for 3 min at a 20 fold higher concentration than endothelin-2 did not stimulate the release of either eicosanoid (Figures 5a and 6a). Big-endothelin-1 (100 nM) or endothelin-1 (5 nM) induced the release of prostacyclin and thromboxane A_2 (Figure 5b and 6b).

Discussion

In the present study, we have investigated the pharmacological properties of the precursors of endothelin-1, endothelin-2 and endothelin-3 in the anaesthetized guinea-pig. Firstly, we found that urethane anaesthesia depressed the pressor and bronchoconstrictor properties of big-endothelins and endothelins. It was suggested by Couture & Kérouac (1987) that urethane, when compared to pentobarbitone anaesthesia, showed qualitatively different responses to other agonists, such as neurokinins in plasma extravasation studies. Ketamine/xylazine anaesthesia, unlike urethane or chloralose has the advantage of leaving unmodified basal mean arterial blood pressure in animals, such as the rat. Indeed, Wang &

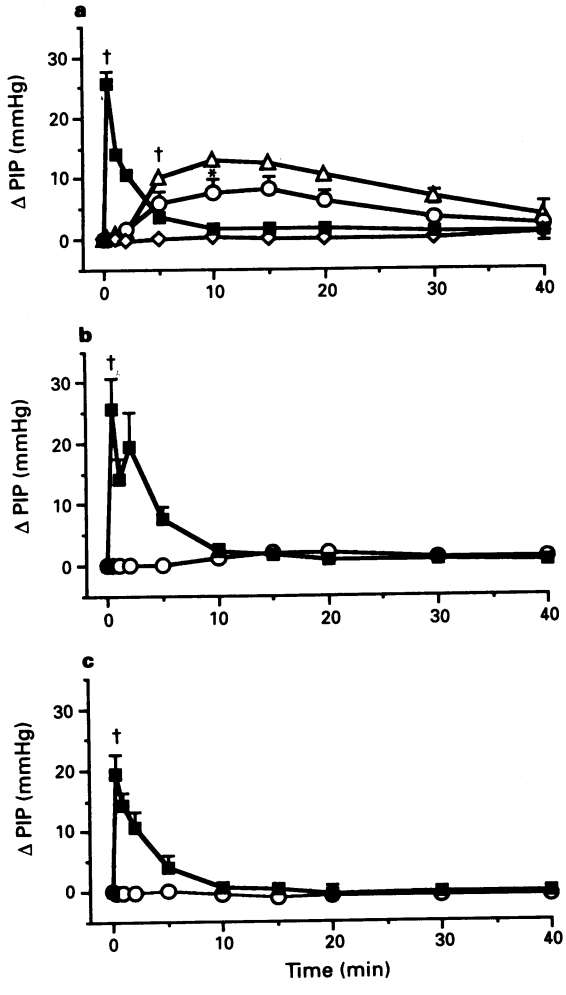

Figure 3 Change in pulmonary insufflation pressure (Δ PIP) in the ketamine/xylazine-anaesthetized guinea-pig induced by endothelin-1 (1 nmol kg^{-1}, ■) or big-endothelin-1 (1 nmol kg^{-1}, ◇; 5 nmol kg^{-1}, ○ and 10 nmol kg^{-1}, Δ). (a) endothelin-2 (1 nmol kg^{-1}; ■) or big-endothelin-2 (10 nmol kg^{-1}; ○) (b), endothelin-3 (1 nmol kg^{-1}; ■) or big-endothelin-3 (25 nmol kg^{-1}; ○) (c), Each point represents the mean with s.e.mean of at least 3 experiments: $*P<0.05$, $\dagger P<0.01$. For the sake of clarity, significance is shown only for the first significant time point when compared to baseline at time 0.

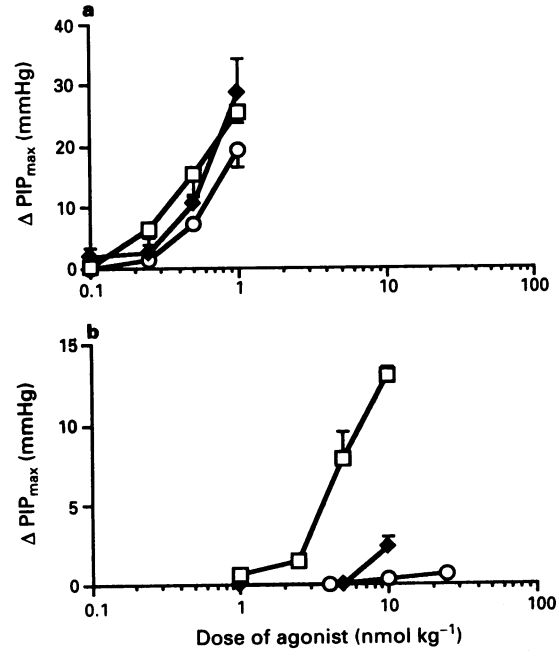

Figure 4 Dose-response curves of changes in pulmonary insufflation pressure (PIP) induced by endothelin-1 (□), endothelin-2 (◆), endothelin-3 (○) (a) and big-endothelin-1 (□), big-endothelin-2 (◆), big-endothelin-3 (○) (b) in the ketamine/xylazine-anaesthetized guinea-pig. Each point represents the mean with s.e.mean of at least 3 experiments.

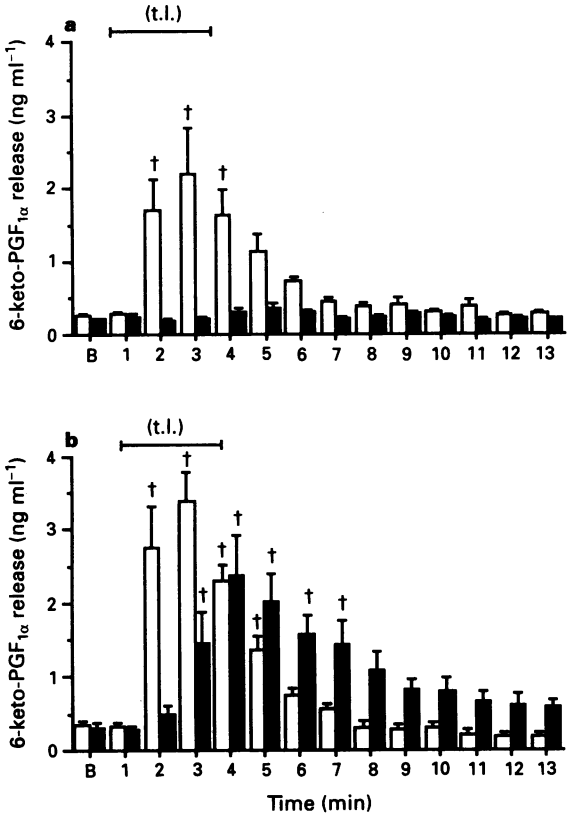

Figure 5 Profile of prostacyclin release (measured as 6-keto-$PGF_{1\alpha}$) from the guinea-pig isolated perfused lung induced by (a) endothelin-2 (5 nM, open columns) or big-endothelin-2 (100 nM, solid columns) and (b) endothelin-1 (5 nM, open columns) or big-endothelin-1 (100 nM, solid columns). Prostacylcin was monitored for 10 min after the cessation of a 3-min infusion of the peptide through the lung arterial vasculature (t.l.). B: Basal levels of prostacyclin measured before the infusion of the peptides. Each column represents the mean ± s.e. mean of at least 4 experiments. $*P<0.05$ and $\dagger P<0.01$ when compared with basal (B) levels of 6-keto-$PGF_{1\alpha}$.

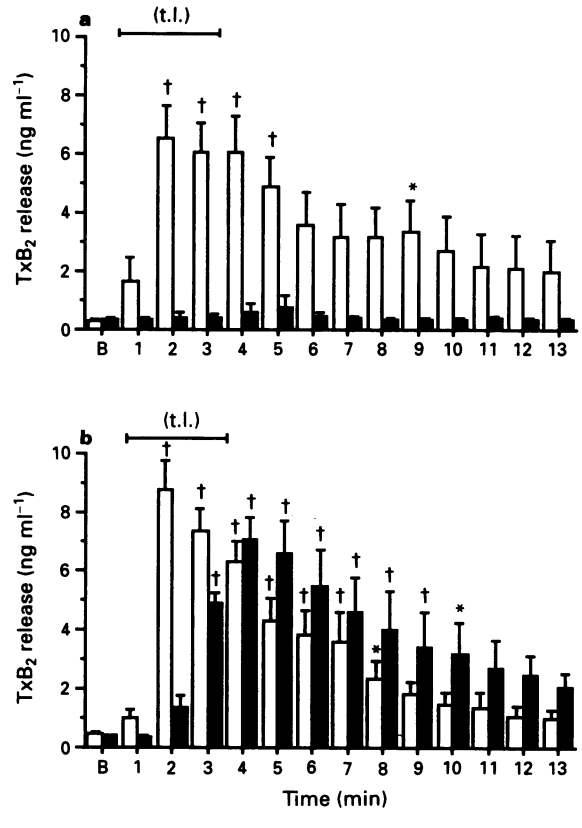

Figure 6 Profile of thromboxane A_2 release (measured as TxB_2) from the guinea-pig isolated perfused lung induced by (a) endothelin-2 (5 nM, open columns) or big-endothelin-2 (100 nM, solid columns) and (b) endothelin-1 (5 nM, open columns) or big-endothelin-1 (100 nM, solid columns). Thromboxane was monitored for 10 min after the cessation of a 3-min infusion of the peptide through the lung arterial vasculature (t.l.). B: Basal levels of thromboxane measured before the infusion of the peptides. Each column represents the mean ± s.e. mean of at least 4 experiments. $*P<0.05$ and $\dagger P<0.01$ when compared with basal (B) levels of TxB_2.

Pang (1993) have shown that ketamine-anaesthetized rats did not show a significantly different mean arterial blood pressure when compared to conscious rats. However, it is worthy of mention that ketamine activates the sympathetic nervous system (Traber & Wilson, 1969) by inhibiting neuronal noradrenaline uptake (Nedergaard, 1973). This mechanism was suggested by Wang & Pang (1993) to explain the E_{max} increase in the pressor effects of diphenyleneiodonium in ketamine-treated animals when compared to conscious rats. In the present study, we have not studied the effect of ketamine/xylazine on the sympathetic nervous system. Nonetheless, because of the enhanced sensitivity to various pressor agents of the ketamine/xylazine-treated animals, this type of anaesthesia was used in the present study in the guinea-pig, which has an intrinsically low mean arterial blood pressure.

As previously suggested (D'Orléans-Juste *et al.*, 1991b), big-endothelin-1 and endothelin-1 are approximately equipotent as pressor agents in this particular animal model. Like big-endothelin-1, big-endothelin-2 is also a potent pressor agent in the guinea-pig. Furthermore, we have shown that the pressor responses to big-endothelin-2 are phosphoramidon-sensitive, suggesting that the conversion pathway for big-endothelin-2 in the systemic circulation is similar to that reported for big-endothelin-1 (Fukuroda *et al.*, 1990; D'Orléans-Juste *et al.*, 1991b).

In contrast, although we found a marked enhancement of the response to endothelins and their precursors in ketamine/xylazine-anaesthetized guinea-pigs, big-endothelin-3 at very high doses (25 nmol kg^{-1}) remained inactive, unlike its active metabolite, endothelin-3. This observation confirms that big-endothelin-3 is indeed poorly recognized by the phosphoramidon-sensitive ECE localized in the systemic vasculature of the guinea-pig, as we suggested previously (D'Orléans-Juste *et al.*, 1991b).

It is also of interest to point out that urethane anaesthesia depresses the bronchoconstrictor response to endothelins in the guinea-pig. In ketamine/xylazine-anaesthetized animals, we confirmed the observation made by Pons *et al.* (1991a) that the three endothelins are equipotent bronchoconstrictor agents. Moreover, big-endothelin-1, but not big-endothelin-2, induced a marked increase in airway resistance yet being 10 fold less potent than that induced by endothelin-1 in the guinea-pig. The lack of responsiveness to big-endothelin-2, as opposed to endothelin-2, suggests that the former peptide may not be converted in the pulmonary vasculature, at least at the sites where the ECE is able to convert big-endothelin-1 to endothelin-1 to subsequently release thromboxane A_2. This however does not exclude the possibility that big-endothelin-2 may be more easily converted at other sites in the lungs. Indeed, Pons *et al.* (1992) have shown that, unlike the intravascularly administered peptide, aerosol administration of big-endothelin-1 induced a phosphoramidon-sensitive increase of airway resistance in the guinea-pig which was however unaffected by indomethacin. To that effect, it would be of interest to assess whether big-endothelin-2 enhances pul-

monary insufflation pressure when administered directly into the airways.

Nonetheless, we suggest that guinea-pig pulmonary vascular-ECE poorly recognizes big-endothelin-2 as opposed to big-endothelin-1. It is of interest that Shimada *et al.* (1994) have shown through the cloning and functional expression of an endothelin-converting enzyme from rat pulmonary endothelial cells that big-endothelin-1 but not big-endothelin-2 or 3 was efficiently converted by this particular enzyme. In addition, we have reported the phosphoramidon-sensitive release of prostacyclin by big-endothelin-1 in the rat perfused lung (D'Orléans-Juste *et al.*, 1991a). In contrast, big-endothelin-2 is unable, unlike endothelin-2, to enhance the release of prostacyclin from the rat pulmonary vasculature (Gratton *et al.*, unpublished observations).

We have previously suggested that the bronchoconstrictor properties of big-endothelin-1 in the guinea-pig may be the result of a phosphoramidon-sensitive release of TxA_2 in the pulmonary vasculature (D'Orléans-Juste *et al.*, 1991b). In agreement with the lack of bronchoconstrictor properties of big-endothelin-2 *in vivo*, we found that this particular peptide, in contrast to the active metabolite, endothelin-2, was unable to trigger the release of prostacyclin or TxA_2 in the guinea-pig perfused lung. As we have shown in the present study that the pressor responses induced by big-endothelin-2 were markedly reduced by phosphoramidon, we suggest that this particular peptide, prior to inducing marked pressor effects in the guinea-pig, may be converted by an ECE present in sites other than those near which endothelins trigger the release of eicosanoids in the pulmonary vasculature. It is of interest that endothelin-2 mRNA has been localized solely in the medullar part of the human kidney and not in the lung (Arinami *et al.*, 1991). Furthermore, endothelin-2 mRNA and big-endothelin-2 have been recently reported in the cytoplasm of endothelial cells derived from human blood vessels (Howard *et al.*, 1992). In the present study, we extend the observation of Arinami *et al.* (1991) in our experimental models, by suggesting that big-endothelin-2 is converted by a phosphoramidon-sensitive ECE (Yorimitsu *et al.*, 1992) present in the systemic but not the pulmonary vasculature of the guinea-pig.

In keeping with its lack of pressor activity, big-endothelin-3 also failed to cause bronchoconstriction in the ketamine/xylazine-anaesthetized guinea-pig. This latter finding reinforces the view that big-endothelin-3 is not susceptible to conversion by the ECE when given intravenously to this species. It is worthy of notice that the increase in airway resistance induced by endothelins in the guinea-pig appears to be mediated via the activation of ET_B receptors (Noguchi *et al.*, 1993; Ishikawa *et al.*, 1994). As endothelin-3 has been shown by this group to be as potent as endothelin-1 as a bronchoconstrictor *in vivo* in the guinea-pig, one may assume that even a slight conversion of big-endothelin-3 to its active metabolite should have been detected under the form of an increase of pulmonary insufflation pressure in this particular animal species.

In summary, we have shown in the present study that ketamine/xylazine is preferable to urethane as an anaesthetic for cardiovascular and bronchoconstrictor studies in guinea-pigs when testing the effects of endothelins and other vasopressor agents. Indeed, in rats, urethane has been showed to reduce baseline mean arterial blood pressure as well as it affected the pharmacological parameters (ED_{50} and E_{max}) of the dose pressor-response curve to diphenyleneiodonium when compared to conscious animals. The enhancement of the pressor response to endothelins in ketamine/xylazine-treated guinea-pigs may be due to activation of the sympathetic nervous system as suggested by Wang & Pang (1993) in the rat, although xylazine is also an α_2-adrenoceptor agonist.

Finally, as big-endothelin-2 does not share the ability of big-endothelin-1 to cause bronchoconstriction *in vivo* in the guinea-pig, nor the release of eicosanoids from perfused lungs, its pressor effects may depend on the conversion by a distinct ECE, which is phosphoramidon-sensitive and which may only be poorly encountered in the pulmonary vasculature of this species. It is worthy of notice that Sawamura *et al.* (1993) have shown that big-endothelin-1 was converted to endothelin-1 to a far greater extent than big-endothelin-2 and 3 in porcine lung homogenates. These observations would reinforce our suggestion that big-endothelin-2 is unable to induce bronchoconstriction or release eicosanoids because of its poor conversion by the ECE located in the pulmonary circulation of the guinea-pig.

The authors are grateful to H. Morin for her secretarial assistance and Dr D. Regoli for his constructive comments. The present study was supported financially by the Heart and Stroke Foundation of Québec and the Medical Research Council of Canada (Grants No. MA-11612 and PG-12350). G.A.R. is a researcher of the Brazilian National Research Council. A.C., S.T. and P.D.J. are in receipt of a studentship, fellowship and scholarship, respectively, of the Heart and Stroke Foundation of Canada.

References

ARINAMI, T., ISHIKAWA, M., INOUE, A., YANAGISAWA, M., MASAKI, T., YOSHIDA, M.C. & HAMAGUCHI, H. (1991). Chromosomal assignments of the human endothelin family genes: the endothelin-1 gene (EDN1) to 6p23–p24, the endothelin-2 gene (EDN2) to 1p34, and the endothelin-3 gene (EDN3) to 20q13.2–q13.3. *Am. J. Human Genet.*, **48**, 990–996.

BLOCH, K.D., EDDY, R.L., SHOWS, T.B. & QUERTERMOUS, T. (1989). cDNA cloning and chromosomal assignment of the gene encoding endothelin 3. *J. Biol. Chem.*, **264**, 18156–18161.

COUTURE, R. & KÉROUAC, R. (1987). Plasma protein extravasation induced by mammalian tachykinins in rat skin: influence of anaesthetic agents and an acetylcholine antagonist. *Br. J. Pharmacol.*, **91**, 265–273.

D'ORLÉANS-JUSTE, P., LIDBURY, P.S., WARNER, T.D., TÉLÉMAQUE, S. & VANE, J.R. (1991a). Human big-endothelin releases prostacyclin *in vivo* and *in vitro* through a phosphoramidon-sensitive conversion to endothelin-1. *J. Cardiovasc. Pharmacol.*, **17**, S251–S255.

D'ORLÉANS-JUSTE, P., TÉLÉMAQUE, S. & CLAING, A. (1991b). Different pharmacological profiles of big-endothelin-3 and big-endothelin-1 *in vivo* and *in vitro*. *Br. J. Pharmacol.*, **104**, 440–444.

FUKURODA, T., NOGUCHI, K., TSUCHIDA, S., NISHIKIBE, M., IKEMOTO, F., OKADA, K. & YANO, M. (1990). Inhibition of biological actions of big endothelin-1 by phosphoramidon. *Biochem. Biophys. Res. Commun.*, **172**, 390–395.

GARDINER, S.M., KEMP, P.A. & BENNETT, T. (1992). Inhibition by phosphoramidon of the regional haemodynamic effects of proendothelin-2 and -3 in conscious rats. *Br. J. Pharmacol.*, **107**, 584–590.

HOWARD, P.G., PLUMPTON, C. & DAVENPORT, A.P. (1992). Anatomical localization and pharmacological activity of mature endothelins and their precursors in human vascular tissue. *J. Hypertens.*, **10**, 1379–1386.

ISHIKAWA, K., IHARA, M., NOGUCHI, K., MASE, T., MINO, N., SAEKI, T., FUKURODA, T., FUKAMI, T., OZAKI, S., NAGASE, T., NISHIKIBE, M. & YANO, M. (1994). Biochemical and pharmacological profile of a potent and selective endothelin B-receptor antagonist. BQ-788. *Proc. Natl. Acad. Sci. U.S.A.*, **91**, 4892–4896.

KASHIWABARA, T., INAGAKI, Y., OHTA, H., IWAMATSU, A., NOMIZU, M., MORITA, A. & NISHIKORI, K. (1989). Putative precursors of endothelin have less vasoconstrictor activity *in vitro* but a potent pressor effect *in vivo*. *FEBS Lett.*, **247**, 73–76.

KONZETT, H. & RÖSSLER, R. (1940). Versuchsanordnung zu Untersuchungen an der Bronchialnuskulatur. *Naunyn-Schmied. Arch. Exp. Pathol. Pharmakol.*, **195**, 71.

MATSUMURA, Y., FUJITA, K., TAKAOKA, M. & MORIMOTO, S. (1993). Big endothelin-3-induced hypertension and its inhibition by phosphoramidon in anaesthetized rats. *Eur. J. Pharmacol.*, **230**, 89–93.

MATTERA, G.G., EGLEZOS, A., RENZETTI, A.R. & MIZRAHI, J. (1993). Comparison of the cardiovascular and neural activity of endothelin-1, -2, -3 and respective proendothelins: effects of phosphoramidon and thiorphan. *Br. J. Pharmacol.*, **110**, 331–337.

NEDERGAARD, O.A. (1973). Cocaine-like effect of ketamine on vascular adrenergic neurones. *Eur. J. Pharmacol.*, **23**, 153–161.

NOGUCHI, K., NOGUCHI, Y., HIROSE, H., NISHIKIBE, M., IHARA, M., ISHIKAWA, K. & YANO, M. (1993). Role of endothelin ET_B receptors in bronchoconstrictor and vasoconstrictor responses in guinea-pigs. *Eur. J. Pharmacol.*, **233**, 47–51.

PAYNE, A.N. & WHITTLE, B.J. (1988). Potent cyclo-oxygenase-mediated bronchoconstrictor effects of endothelin in the guinea pig *in vivo*. *Eur. J. Pharmacol.*, **158**, 303–304.

POLLOCK, D.M., DIVISH, B.J., MILICIC, I., NOVOSAD, E.I., BURRES, N.S. & OPGENORTH, T.J. (1993). *In vivo* characterization of a phosphoramidon-sensitive endothelin-converting enzyme in the rat. *Eur. J. Pharmacol.*, **231**, 459–464.

PONS, F., BOICHOT, E., LAGENTE, V., TOUVAY, C., MENCIA-HUERTA, J.M. & BRAQUET, P. (1992). Role of endothelin in pulmonary function. *Pulmonary Pharmacol.*, **5**, 213–219.

PONS, F., LOQUET, I., TOUVAY, C., ROUBERT, P., CHABRIER, P.-E., MENCIA-HUERTA, J.M. & BRAQUET, P. (1991a). Comparison of the bronchopulmonary and pressor activities of endothelin isoforms ET-1, ET-2, and ET-3 and characterization of their binding sites in guinea pig lung. *Am. Rev. Resp. Dis.*, **143**, 294–300.

PONS, F., TOUVAY, C., LAGENTE, V., MENCIA-HUERTA, J.M. & BRAQUET, P. (1991b). Bronchopulmonary and pressor activities of endothelin-1 (ET-1), ET-2, ET-3, and Big ET-1 in the guinea pig. *J. Cardiovasc. Pharmacol.*, **17**, S326–S328.

SAWAMURA, T., SHINMI, O., KISHI, N., SUGITA, Y., YANAGISAWA, M., GOTO, K., MASAKI, T. & KIMURA, S. (1993). Characterization of phosphoramidon-sensitive metalloproteinases with endothelin-converting enzyme activity in porcine lung membrane. *Biochem. Biophys. Acta*, **1161**, 295–302.

SHIMADA, K., TAKAHASHI, M. & TANZAWA, K. (1994). Cloning and functional expression of endothelin-converting enzyme from rat endothelial cells. *J. Biol. Chem.*, **269**, 18275–18278.

TRABER, D.L. & WILSON, R.D. (1969). Involvement of the sympathetic nervous system in the pressor response to ketamine. *Anaesth. Analg.*, **48**, 248–252.

WANG, Y.X. & PANG, C.C.Y. (1993). Halothane inhibits the pressor effect of diphenyleneiodonium. *Br. J. Pharmacol.*, **109**, 1186–1191.

YORIMITSU, K., SHINMI, O., NISHIYAMA, M., MOROI, K., SUGITA, Y., SAITO, T., INAGAKI, Y., MASAKI, T. & KIMURA, S. (1992). Effect of phosphoramidon on big endothelin-2 conversion into endothelin-2 in human renal adenocarcinoma (ACHN) cells. Analysis of endothelin-2 biosynthetic pathway. *FEBS Lett.*, **314**, 395–398.

(Received September 29, 1994
Accepted October 7, 1994)

British Journal of Pharmacology (1995) 114, 727-731

Differentiation by pyridoxal 5-phosphate, PPADS and IsoPPADS between responses mediated by UTP and those evoked by α,β-methylene-ATP on rat sympathetic ganglia

[1]Gerald P. Connolly

Department of Physiology, University College London, Gower Street, London, WC1E 6BT

1 The effect of pyridoxal 5-phosphate, and the 2',4' and 2',5'-disulphonic acid isomers of 6-azophenyl-pyridoxal 5-phosphate (PPADS and IsoPPADS respectively) on depolarization of the rat superior cervical ganglion evoked by α,β-methylene-adenosine 5'-triphosphate (α,β-Me-ATP) and uridine 5'-triphosphate (UTP) were determined by a grease-gap recording technique.

2 Pyridoxal 5-phosphate (10-100 μM) and PPADS (10-100 μM) enhanced UTP- and depressed α,β-Me-ATP-evoked depolarizations but did not significantly alter depolarizations evoked by potassium or hyperpolarizations evoked by adenosine. IsoPPADS (10 μM) depressed α,β-Me-ATP-evoked depolarizations but did not alter depolarizations evoked by UTP. Depolarizations evoked by muscarine were depressed by IsoPPADS but not by pyridoxal 5-phosphate.

3 It is concluded that pyridoxal 5-phosphate, PPADS and IsoPPADS are antagonists at P_{2X}-purinoceptors but not at the receptors that mediate UTP-evoked depolarization of the rat superior cervical ganglion. These observations substantiate the recent proposal that the rat superior cervical ganglia possess distinct receptors for purine and pyrimidine 5'-nucleotides, i.e. P_{2X}-purinoceptors and pyrimidinoceptors respectively.

Keywords: Rat superior cervical ganglion; UTP; pyridoxal-5-phosphate; PPADS; IsoPPADS; pyrimidinoceptor; P_{2X}-purinoceptor

Introduction

It has been suggested that some tissues contain extracellular receptors that recognise the purine nucleotide, adenosine 5'-triphosphate (ATP) and the pyrimidine nucleotide, uridine 5'-triphosphate (UTP), having equal affinity for ATP and UTP (Davidson *et al.*, 1990; reviewed by O'Connor *et al.*, 1991), i.e. a P_{2U}-purinoceptor. In addition it has also been proposed that ATP and UTP can activate distinct receptors, i.e. P_2-purinoceptors and pyrimidinoceptors respectively (reviewed by Seifert & Schultz, 1989). Pyrimidinoceptors have been suggested to exist on some vascular tissues, e.g. rabbit basilar and ear arteries (von Kugelgen *et al.*, 1987; von Kugelgen & Starke, 1990), the perfused isolated rat liver (Haussinger *et al.*, 1987), and on these tissues UTP rather than ATP activates pyrimidinoceptors. In contrast to these studies there have been few studies to examine the effects of pyrimidines on the nervous system or to determine if their effects are due to activation of pyrimidinoceptors.

Recently it has been proposed that neurones of the rat superior cervical ganglion (SCG) possess pyrimidinoceptors and that this preparation is a model tissue for the study of pyrimidinoceptors within the nervous system (Connolly & Harrison, 1993; Connolly *et al.*, 1993b; Connolly & Harrison, 1994; Connolly, 1994a). This hypothesis was based upon the observation that there are distinct receptors that are activated by UTP but not by ATP or α,β methylene adenosine 5'-triphosphate (α,β-Me-ATP) (a selective P_{2X}-purinoceptor agonist (Burnstock & Kennedy, 1985)). In addition SCG neurones possess P_1-purinoceptors of the A_1-subtype, which upon activation by adenosine or ATP (which presumably activates these receptors due to its rapid metabolism to adenosine) hyperpolarize ganglia. In contrast both α,β-Me-ATP and UTP depolarized rat SCG neurones and depolarizations elicited by UTP were not antagonized, rather they were enhanced in the presence of either suramin (a P_{2X}-purinoceptor antagonist) or reactive blue 2 (a P_{2Y}-purinoceptor antagonist) (see Connolly *et al.*, 1993b; Connolly & Harrison, 1994 respectively). Recently it has been proposed that pyridoxal 5-phosphate-6-azophenyl-2',4'-disulphonic acid (PPADS) is a novel and selective antagonist of P_{2X}-purinoceptors (Lambrecht *et al.*, 1992; Ziganshin *et al.*, 1993; McLaren *et al.*, 1994) however, the effect of PPADS on UTP-mediated responses has yet to be reported. Here the effects of pyridoxal 5-phosphate (a precursor of PPADS), PPADS and an isomer of PPADS, namely the 2',5'-disulphonic acid derivative of 6-azophenyl-pyridoxal 5-phosphate (IsoPPADS) on the responses of the rat SCG evoked by α,β-Me-ATP, adenosine and UTP are described. Preliminary reports of this study have been presented elsewhere (Connolly *et al.*, 1994; Connolly, 1994b).

Methods

Ganglia were prepared for recording of d.c. potentials via the internal carotid nerve and the body of the ganglion as described before (Connolly *et al.*, 1993a,b). SCG were removed from male Sprague-Dawley rats (200-330 g) killed with a lethal dose of urethane, desheathed and submerged between the greased barriers of a three compartment recording bath. The central chamber containing the ganglion body was superfused (about 2 ml min^{-1}) with a physiological salt solution (PSS) at pH 7.4 and 25 ± 1°C, containing (mM): NaCl 125, $NaHCO_3$ 25, KCl 1, KH_2PO_4 1, $MgSO_4$ 1, glucose 10, $CaCl_2$ 0.1 and pre-oxygenated (5% CO_2/95% O_2). Potential differences between the earthed central chamber and the internal carotid nerve were recorded with Ag/AgCl electrodes, the signals being filtered through a low pass filter, amplified via d.c. pre-amplifiers and recorded on a pen recorder.

Ganglia were equilibrated for at least 2 h before use. The effect of potassium and muscarine or the effects of purines and UTP on the d.c. potentials were determined by applying

[1] Present address: Biomedical Sciences Division, Physiology Group, King's College, Strand, London WC2R 2LS.

these substances for 1 or 2 min respectively. To avoid desensitization a minimum of 15 min was allowed between each application and responses to all agonists were reproducible with time (e.g. see results Figure 1).

With the exception of pyridoxal solutions all drugs were prepared in PSS as 10 mM stock solutions and frozen as aliquots (−20°C). Pyridoxal solutions were prepared immediately before use (as 10 mM stock solutions in PSS) and protected from light. Experiments with pyridoxal 5-phosphate were done in near darkness. In some experiments the effect of pyridoxal 5-phosphate (at 30 or 100 μM) on agonist-induced responses was determined and because after washing out (>25 min) pyridoxal 5-phosphate there was no significant difference in the control and subsequent responses (e.g. see results Figure 1), these ganglia were also used to determine the effect of PPADS. There was no significant difference between the effects of PPADS when determined on either ganglia previously exposed to pyridoxal 5-phosphate or when only PPADS was examined. In all other experiments the effect of only pyridoxal 5-phosphate or one of its derivatives at one concentration was examined on each ganglion. Responses in the presence of pyridoxal 5-phosphate, PPADS or IsoPPADS (30 to 150 min incubation) were compared (Student's paired t test) to control responses without each drug. P values were considered statistically significant if less than 0.05. Differences between responses are denoted by: $*P<0.05$, $**P<0.01$ and $**P<0.001$.

Adenosine hemisulphate, α,β-Me-ATP and UTP were obtained from Sigma Chemical Co. U.K. Pyridoxal 5-phosphate, PPADS and IsoPPADS were a gift from Tocris-Cookson, Langford, Bristol, U.K. (±)-Muscarine was bought from Research Biochemicals Inc. (Semat, U.K.) and salts for PSS were of Analar grade.

Results

Pyridoxal 5-phosphate, PPADS or IsoPPADS did not significantly alter the basal d.c. potential of ganglia (data not presented, but see Figure 1), depolarizations evoked by potassium, or hyperpolarizations evoked by adenosine (Figure 1 and Table 1). Depolarizations evoked by muscarine were significantly depressed by IsoPPADS but not PPADS (Table 1). In the presence of IsoPPADS (10 μM) of three out of fifteen ganglia that were depolarized by muscarine (control), two produced a hyperpolarization (−55 μV and −140 μV) preceding a depolarization and on a third ganglion muscarine evoked only a hyperpolarization (control = 140μV

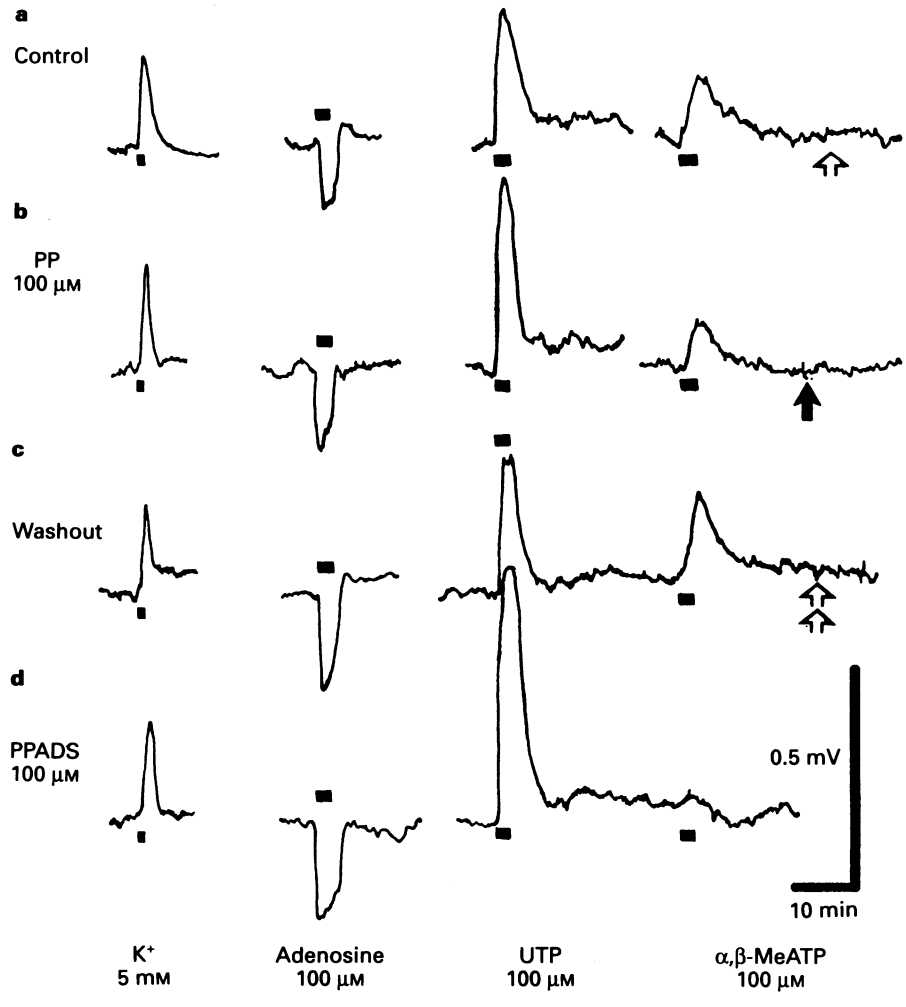

Figure 1 Effect of pyridoxal 5-phosphate (PP) and pyridoxal 5-phosphate-6-azophenyl-2',4'-disulphonic acid (PPADS) on the d.c. potential and responses of a single rat superior cervical ganglion evoked by potassium, adenosine, uridine 5'-triphosphate (UTP) and α,β-methylene adenosine 5'-triphosphate (α,β-Me-ATP). Responses evoked by 5 mM potassium (K^+), 100 μM adenosine, 100 μM UTP and 100 μM α,β-MeATP in (a) the absence (control), (b) presence of 100 μM PP, (c) after washing out PP (washout) and (d) in the presence of 100 μM PPADS. The scale in the bottom right hand corner of the trace applies to all the traces, which are a continuous record from a single ganglion. The bars refer to the time of application of drugs and depolarization is shown as an upward deflection of the trace. The open, solid and double open arrows show the times at which PSS was changed to PSS containing PP, from PP to PSS and then to PSS containing PPADS. N.B. The d.c. potential did not alter upon changing from one superfusate to another and the depolarizations evoked by α,β-Me-ATP were reduced in the presence of PP and reversed to a hyperpolarization in the presence of PPADS.

Table 1 Effect of pyridoxal 5-phosphate, PPADS and IsoPPADS on the response of the rat superior cervical ganglion evoked by adenosine, potassium and muscarine

Compound	Concentration (μM)	n	Control (0 μM)	Pyridoxal 5-phosphate (100 μM)	PPADS (10 μM)	PPADS (100 μM)	IsoPPADS (10 μM)
Adenosine	100	4	−116 ± 15	−138 ± 22			
	100	4	−134 ± 27		−131 ± 8		
	100	4	−156 ± 31			−181 ± 37	
	100	15	−124 ± 14				−126 ± 18
Potassium	5000	4	169 ± 15	199 ± 22			
	5000	4	146 ± 18		134 ± 24		
	5000	4	165 ± 41			175 ± 29	
	5000	15	181 ± 22				165 ± 25
Muscarine	0.1	4	243 ± 23		223 ± 43		
	0.1	15	207 ± 26				115 ± 28***

Responses are μV ± s.e.mean and n = number of ganglia. Statistical differences between responses (paired t test) in the absence (control) and presence of pyridoxal 5-phosphate. PPADs or IsoPPADS are indicated by: $*P<0.05$, $**P<0.01$ and $***P<0.001$.

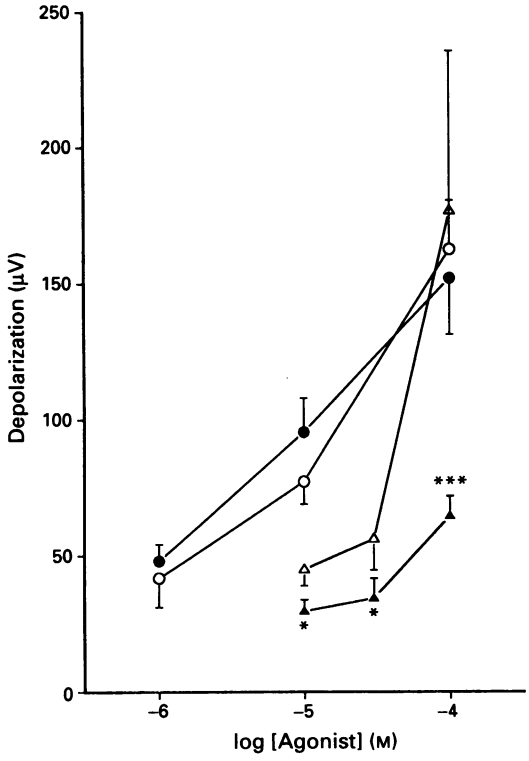

Figure 2 Effect of pyridoxal 5-phosphate-6-azophenyl-2',5'-disulphonic acid (IsoPPADS) on concentration-response curve of the depolarization of rat superior cervical ganglion evoked by uridine 5-triphosphate (UTP) or α,β-methylene-adenosine 5'-triphosphate (α,β-Me-ATP). Summary of the response of a minimum of eight ganglia evoked by UTP (circles) or α,β-Me-ATP (triangles) in the absence (○,△) and presence (●,▲) of 10 μM IsoPPADS respectively. Statistical differences between depolarizing responses in the absence and presence of IsoPPADS are indicated by: $*P<0.05$ and $***P<0.001$.

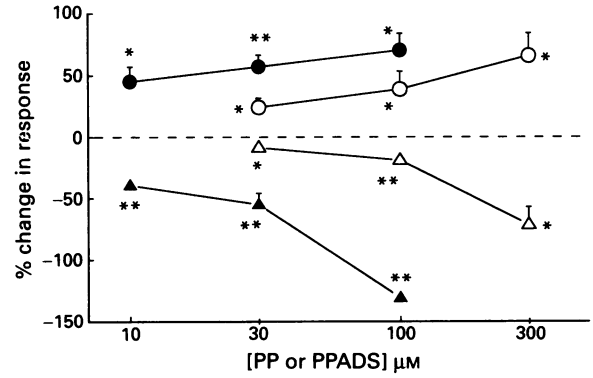

Figure 3 Effect of pyridoxal 5-phosphate and pyridoxal 5-phosphate-6-azophenyl-2',4'-disulphonic acid (PPADS) on the depolarizations of the rat superior cervical ganglion evoked by 100 μM α,β-Me-ATP (α,β-Me-ATP) and 100 μM uridine 5-triphosphate (UTP). Summary of the response of four to eight ganglia evoked by UTP (circles) or α,β-Me-ATP (triangles) in the presence of pyridoxal 5-phosphate (PP) (○,△) or PPADS (●,▲) respectively. Responses are expressed as a percentage of the response evoked by UTP or α,β-Me-ATP in the absence of pyridoxal 5-phosphate or PPADS. Statistical differences between responses in the absence and presence of pyridoxal 5-phosphate or PPADS are indicated by $*P<0.05$ and $**P<0.01$.

cf in IsoPPADS = −140 μV). Depolarizations evoked by 100 μM α,β-Me-ATP were significantly depressed by IsoPPADS (10 μM) by 43 ± 6% (n = 15) whereas depolarizations evoked by 100 μM UTP were not significantly altered (−2 ± 11%, n = 15). IsoPPADS (10 μM) significantly depressed concentration-dependent depolarizations evoked by α,β-Me-ATP but not depolarizations evoked by UTP (Figure 2).

Both pyridoxal 5-phosphate and PPADS produced a concentration-dependent enhancement of depolarizations evoked by UTP and a concentration-dependent depression of depolarizations evoked by α,β-Me-ATP (Figure 3). On some ganglia, pyridoxal 5-phosphate containing compounds as well as potentiating the peak response evoked by UTP, sharpened the time-course of the depolarization.

Discussion

The inability of pyridoxal 5-phosphate, PPADS or IsoPPADS to alter responses evoked by sub-maximal concentrations of either adenosine (which activates P_1-purinoceptors; Connolly *et al.*, 1993a) or potassium (a nonspecific depolarizing agonist) suggests that these drugs do not antagonize A_1-adenosine receptors or produce nonspecific effects on rat SCG neuronal membranes respectively. The inactivity of PPADS on adenosine-induced hyperpolarizations of the rat SCG is consistent with its reported lack of antagonism of A_1-adenosine receptors on the rabbit vas deferens (Lambrecht *et al.*, 1992).

The ability of PPADS, a putatively selective P_{2X}-purinoceptor antagonist (Lambrecht *et al.*, 1992; McLaren *et al.*, 1994) to depress depolarizations of the rat SCG evoked by α,β-Me-ATP (a selective P_{2X}-purinoceptor agonist, Burnstock & Kennedy, 1985) indicates these depolarizations were mediated by P_{2X}-purinoceptors. Similarly the ability of

pyridoxal 5-phosphate and IsoPPADS to depress depolarizations of the rat SCG evoked by α,β-Me-ATP indicates that these compounds are also antagonists of P_{2X}-purinoceptors. The receptor responsible for the hyperpolarization evoked by α,β-Me-ATP in the presence of PPADS is unknown. This hyperpolarization is unlikely to involve P_{2X}- or P_{2Y}-purinoceptors because of its resistance to a high concentration of PPADS and the virtual inactivity of 2-methylthio-ATP (a P_{2Y}-purinoceptor selective agonist) on the rat SCG (Connolly *et al.*, 1993b).

The similar degree of antagonism of depolarizations evoked by α,β-Me-ATP by both PPADS and IsoPPADS suggests that the position of the sulphonic acid group at the 4'- or 5'- position on 6-azophenylpyridoxal 5-phosphate is not particularly critical for the antagonistic activity of these compounds. Pyridoxal 5-phosphate had some, albeit weak antagonistic activity at P_2-purinoceptors, indicating that the pyridoxal 5-phosphate moiety of both PPADS and IsoPPADS is partly responsible for their antagonism at P_2-purinoceptors. However, the addition of the 6-azophenyl-disulphonic acid moiety clearly enhances the antagonistic potency of pyridoxal 5-phosphate at P_{2X}-purinoceptors.

IsoPPADS but not pyridoxal 5-phosphate altered depolarizations evoked by muscarine suggesting that IsoPPADS is an antagonist of muscarinic receptors of the rat SCG. The ability of IsoPPADS to depress depolarizations evoked by muscarine and reveal a muscarine-induced hyperpolarization on some ganglia is consistent with a selective depression of M_1-muscarinic receptor-mediated depolarization but not M_2-muscarinic receptor-mediated hyperpolarization. The observation that IsoPPADS depressed depolarizations of the rat SCG evoked by muscarine but not those produced by UTP also confirms the proposal that muscarine and UTP activate distinct receptors on the rat SCG (Connolly *et al.*, 1993b).

Over the range of concentrations examined, pyridoxal 5-phosphate, PPADS and IsoPPADS were never observed to depress responses evoked by UTP, only depressing depolarizations mediated by α,β-Me-ATP on the same ganglion. These results show the selectivity of these pyridoxal 5'-phosphate containing compounds for purine- rather than pyrimidine-nucleotide evoked depolarizations of the rat SCG, supporting the proposal that α,β-Me-ATP and UTP activate distinct receptors for nucleotides.

The mechanism by which pyridoxal 5-phosphate containing compounds potentiate UTP-evoked depolarizations of the rat SCG remains obscure, but it is unlikely to be due to an antagonism of an opposing P_{2Y}-purinoceptor mediated hyperpolarization, because of the virtual absence of P_{2Y}-purinoceptors on the rat SCG (Connolly *et al.*, 1993a). Interestingly, an enhancement of depolarizations of the rat SCG evoked by UTP was observed in the presence of the P_2-purinoceptors antagonists, suramin (Connolly *et al.*, 1993b) and reactive blue 2 (Connolly & Harrison, 1994). Thus one explanation of the potentiating effect of P_2-purinoceptor antagonists on UTP-evoked depolarizations is that this phenomenon is coupled to their ability to depress depolarizations evoked by α,β-Me-ATP. However the link between this potentiating effect and P_2-purinoceptor antagonism may be coincidental.

Evidence for these effects being independent of each other is suggested by the ability of IsoPPADS to depress depolarizations evoked by α,β-Me-ATP without any significant effect on UTP-evoked depolarizations. Here it should be noted that the effect of IsoPPADS was examined at only one concentration (10 μM) and thus it is possible that at higher concentrations IsoPPADS, like PPADS, would also have enhanced UTP-evoked depolarizations. Conversely the ability of reactive blue 2 (Connolly & Harrison, 1994, see Figure 1d) and uniblue A (unpublished observations) to enhance UTP-evoked depolarizations without altering depolarization evoked by α,β-Me-ATP suggests these two effects may be independent of each other. Alternative explanations for the potentiation of UTP-evoked depolarizations include antagonism of an underlying UTP-evoked hyperpolarization, a change in the metabolism of UTP or its metabolites or an allosteric interaction. These effects remain to be investigated, but some evidence in favour of the latter hypotheses is suggested by the observation that on some ganglia pyridoxal 5-phosphate containing compounds as well as potentiating the peak response evoked by UTP, sharpened the time-course of the response. Because unlike UTP, α,β-Me-ATP is relatively resistant to degradation by ectonucleotidases (Welford *et al.*, 1986; 1987), the ability of pyridoxal phosphate and PPADS to enhance depolarizations evoked by UTP (but depress α,β-Me-ATP-evoked depolarizations) could have arisen from the net effect of inhibition of ectonucleotidase activity and an antagonism of P_{2X}-purinoceptors, thus raising the possibility that UTP and α,β-Me-ATP activate the same receptor. An inhibition of ectonucleotidase activity by suramin (Hourani & Chown, 1989) could also account for the ability of suramin (but not reactive blue 2, which does not inhibit ectonucleotidases, Hourani & Chown, 1989) to enhance UTP-evoked depolarizations. Apart from studies using P_2-purinoceptor antagonists there is additional evidence that ATP and UTP activate distinct receptors, which is based upon desensitization studies (Connolly, 1994a). Further experiments to examine the effect of specific inhibitors of ectonucleotidases on purine and pyrimidine evoked responses of the rat SCG should help resolve these issues.

Because there are no suitable antagonists of the effects of UTP at pyrimidinoceptors (Seifert & Schultz, 1989) further studies to examine the modulatory effects of pyridoxal 5-phosphate and its derivatives on responses evoked by pyrimidines may lead to further discoveries on how pyrimidines (and purines) work on the nervous system.

It is concluded that pyridoxal 5-phosphate, PPADS and IsoPPADS are antagonists at P_{2X}-purinoceptors and like other P_2-purinoceptor antagonists they distinguish between purine and pyrimidine 5'-triphosphate-evoked depolarizations of the rat superior cervical ganglion. These results provide further justification for the proposal that SCG neurones possess both P_{2X}-purinoceptors and pyrimidinoceptors.

I thank Dr P.J. Harrison (U.C.L.) for his encouragement and facilities to perform this study and Laurence Ede (Tocris-Cookson) for the gifts of PP, PPADS and IsoPPADS.

References

BURNSTOCK, G. & KENNEDY, C. (1985). Is there a basis for distinguishing two types of P_2-purinoceptor? *Gen. Pharmacol.*, **16**, 433–440.

CONNOLLY, G.P. (1994a). Evidence from desensitisation studies for distinct receptors for ATP and UTP on the rat superior cervical ganglion. *Br. J. Pharmacol.*, **112**, 357–359.

CONNOLLY, G.P. (1994b). Pyridoxalphosphate (PP) and PP-6-azophenyl-2',4'-disulphonic acid (PPADS) enhance UTP- but depress α,β-MethyleneATP-evoked depolarisation of sympathetic ganglia. *Br. J. Pharmacol.* (in press).

CONNOLLY, G.P., BROWN, F. & STONE, T.W. (1993a). Characterization of the adenosine receptors on the rat isolated superior cervical ganglion. *Br. J. Pharmacol.*, **110**, 854–860.

CONNOLLY, G.P. & HARRISON, P.J. (1993). The isolated rat superior cervical ganglion (SCG) as a model tissue for the study of neuronal pyrimidine receptors. *Pharmacol. World Sci.*, **4**, F5.

CONNOLLY, G.P. & HARRISON, P.J. (1994). Reactive blue 2 discriminates between responses mediated by UTP and those evoked by ATP or α,β-methylene-ATP on rat sympathetic ganglia. *Eur. J. Pharmacol.*, **259**, 95–99.

CONNOLLY, G.P., HARRISON, P.J. & STONE, T.W. (1993b). Action of purine and pyrimidine nucleotides on the rat superior cervical ganglion. *Br. J. Pharmacol.*, **110,** 1297–1304.

CONNOLLY, G.P., HARRISON, P.J. & STONE, T.W. (1994). α,β-MethyleneATP but not UTP evoked depolarizations of the rat superior cervical ganglion are antagonised by a P_{2X}-purinoceptor antagonist. *Br. J. Pharmacol.*, **112,** 408P.

DAVIDSON, J.S., WAKEFIELD, I.K., SOHNIUS, U., VAN DER MERWE, P.A. & MILLAR, R.P. (1990). A novel extracellular nucleotide receptor coupled to phosphoinositase-C in pituitary cells. *Endocrinology*, **126,** 80–87.

HAUSSINGER, D., STEHLE, T. & GEROK, W. (1987). Actions of extracellular UTP and ATP in perfused rat liver. *Eur. J. Biochem.*, **167,** 65–71.

HOURANI, S.M.O. & CHOWN, J.A. (1989). The effects of some possible inhibitors of ectonucleotidases on the breakdown and pharmacological effects of ATP in the guinea-pig urinary bladder. *Gen. Pharmacol.*, **20,** 413–416.

LAMBRECHT, G., FRIEBE, T., GRIMM, U., WINDSCHEIF, U., BUNGARDT, E., HILDEBRANT, C., BAUMERT, H.G., SPATZ-KUMBEL, G. & MUTSCHLER, E. (1992). PPADS, a novel functionally selective antagonist of P_2-purinoceptor-mediated responses. *Eur. J. Pharmacol.*, **217,** 217–219.

MCLAREN, G.J., LAMBRECHT, G., MUTSCHLER, E., BAUMERT, H.G., SNEDDON, P. & KENNEDY, C. (1994). Investigation of the actions of PPADS, a novel P_{2X}-purinoceptor antagonist, in the guinea-pig isolated vas deferens. *Br. J. Pharmacol.*, **111,** 913–917.

O'CONNOR, S.E., DAINTY, I.A. & LEFF, P. (1991). Further subclassification of ATP receptors based on agonist studies. *Trends Pharmacol. Sci.*, **12,** 137–141.

SEIFERT, R. & SCHULTZ, G. (1989). Involvement of pyrimidinoceptors in the regulation of cell functions by uridine and by uracil nucleotides. *Trends Pharmacol. Sci.*, **10,** 365–369.

VON KUGELGEN, I., HAUSSINGER, D. & STARK, K. (1987). Evidence for a vasoconstriction-mediating receptor for UTP, distinct from the P_2-purinoceptor, in rabbit ear artery. *Naunyn-Schmied. Arch. Pharmacol.*, **336,** 556–560.

VON KUGELGEN, I. & STARK, K. (1990). Evidence for two separate vasoconstriction-mediating nucleotide receptors, both distinct from the P_{2X}-receptor, in rabbit basilar artery: a receptor for pyrimidine nucleotides and a receptor for purine nucleotides. *Naunyn-Schmied. Arch. Pharmacol.*, **341,** 538–546.

WELFORD, L.A., CUSACK, N.J. & HOURANI, S.M.O. (1986). ATP analogues and the guinea-pig taenia coli: a comparison of the structure-activity relationships of ectonucleotidases with those of the P2-purinoceptor. *Eur. J. Pharmacol.*, **129,** 217–224.

WELFORD, L.A., CUSACK, N.J. & HOURANI, S.M.O. (1987). The structure-activity relationships of ectonucleotidases and of excitatory P2-purinoceptors: evidence that dephosphorylation of ATP analogues reduces pharmacological potency. *Eur. J. Pharmacol.*, **141,** 123–130.

ZIGANSHIN, A.U., HOYLE, C.V., BO, X., LAMBRECHT, G., MUTSCHLER, E., BAUMERT, H.G. & BURNSTOCK, G. (1993). PPADS selectively antagonises P_{2X}-purinoceptor-mediated responses in the rabbit urinary bladder. *Br. J. Pharmacol.*, **110,** 1491–1495.

(Received August 9, 1994
Revised October 5, 1994
Accepted October 21, 1994)

British Journal of Pharmacology

VOLUME 114 (3) FEBRUARY 1995

PAPERS

STOCKTON

BRITISH JOURNAL OF PHARMACOLOGY

The *British Journal of Pharmacology* welcomes contributions in all fields of experimental pharmacology including neuroscience, biochemical, cellular and molecular pharmacology. The Board of Editors represents a wide range of expertise and ensures that well-presented work is published as promptly as possible, consistent with maintaining the overall quality of the journal.

Edited for the British Pharmacological Society by

A.T. Birmingham
(Chairman)

R.W. Horton **W.A. Large**
(Secretaries)

Submission of manuscripts: Manuscripts (two copies) should be sent to The Editorial Office, British Journal of Pharmacology, St. George's Hospital Medical School, Cranmer Terrace, London SW17 0RE.

Authors should consult the Instructions to Authors and the Nomenclature Guidelines for Authors in Vol. **114,** 245–255. These Instructions and Guidelines also appear with the journal Index for Volumes **111–113,** 1994. A checklist of the essential requirements is summarised in each issue of the journal, or as the last page of the issue.

The *British Journal of Pharmacology* is published by Stockton Press, a division of Macmillan Press Ltd. It is the official publication of the British Pharmacological Society.

Scope The *British Journal of Pharmacology* is published twice a month. It welcomes contribution in all field of experimental pharmacology including neuroscience, biochemical, cellular and molecular pharmacology. The Board of Editors represents a wide range of expertise and ensures that well-presented work is published as promptly as possible, consistent with maintaining the overall quality of the journal

This journal is covered by Current Contents, Excerpta Medica, BIOSIS and Index Medicus.

Editorial Manuscripts (plus two copies) and all editorial correspondence should be sent to: The Editorial Office, British Journal of Pharmacology, St George's Hospital Medical School, Cranmer Terrace, London SW17 0RE, UK. Tel: +44 (0)181 767 6765; Fax: +44 (0)181 767 5645.

Advertisements Enquiries concerning advertisements should be addressed to: Michael Rowley, Hasler House, High Street, Great Dunmow, Essex CM6 1AP, UK. Tel: +44 (0)1371 874613; Fax: +44 (0)1371 872273.

Publisher All business correspondence, supplement enquiries and reprint requests should be addressed to British Journal of Pharmacology, Stockton Press, Houndmills, Basingstoke, Hampshire RG21 2XS, UK. Tel: +44 (0)1256 29242; Fax: +44 (0)1256 810526. Publisher: Marija Vukovojac. Editorial Assistant: Alice Ellingham. Production Controller: Tony Holton.

Subscriptions – EU/Rest of World Subscription price per annum (3 volumes, 24 issues) £620, rest of world £820 (Airmail), £685 (Surface mail) or equivalent in any other currency. Orders must be accompanied by remittance. Cheques should be made payable to Macmillan Magazines and sent to: The Subscription Department, Macmillan Press Ltd, Houndmills, Basingstoke, Hampshire RG21 2XS, UK. Where appropriate, subscribers may make payments into UK Post Office Giro Account No. 519 2455. Full details must accompany the payment. Subscribers from EU territories should add sales tax at the local rate.

Subscriptions – USA USA subscribers call toll free 1-800-221-2123 or send check/money order/credit card details to: Stockton Press, 49, West 24th Street, New York, NY 10010; Tel: 212 627 5757, Fax: 212 627 9256. USA annual subscription rates: $1230 Airmail; $1030 Surface (Institutional/Corporate); $225 (Individual making personal payment).

British Journal of Pharmacology (ISSN 0007–1188) is published twice a month by Macmillan Press Ltd, c/o Mercury Airfreight International Ltd, 2323 Randolph Avenue, Avenel, NJ 07001, USA. Subscription price for institutions is $1030 per annum (surface). 2nd class postage is paid at Rahway NJ. Postmaster: send address corrections to Macmillan Press Ltd, c/o Mercury Airfreight International Ltd, 2323 Randolph Avenue, Avenel NJ 07001.

Reprints of any article in this journal are available from Stockton Press, Houndmills, Basingstoke, Hampshire RG21 2XS, UK. Tel: +44 (0)1256 29242; Fax: +44 (0)1256 810526.

ISSN 0007–1188

PREPARATION OF MANUSCRIPTS

Authors are strongly recommended to read the full *Instructions to Authors* and *Nomenclature Guidelines for Authors* (*Br. J. Pharmacol.* 1995, **114**, 245–255) before submitting a manuscript for publication in the *British Journal of Pharmacology*. The manuscript and cover letter should be checked against the following list before mailing.

The original and one copy of the manuscript must be supplied. Manuscripts must be typed in double-line spacing on one side of A4 paper, in type not smaller than 12 characters per inch or 10 point. Both copies to include Tables and a set of labelled Figures. One set of Figures without numbers or letters is also to be included. The text to be arranged in the following subsections:

1. **Title**—To have no more than 150 characters on a separate page, which should also include a Short Title (50 characters maximum) and the name and address of the author for correspondence.
2. **Summary**—To be arranged in numbered paragraphs (Full Papers) or a single paragraph (Special Reports).
   —to include aims, principal results and conclusions.
   —to include Key words (10 maximum) at end of summary.
3. **Introduction**—To contain concise statements of the problem and the aims of the investigation.
4. **Methods**—To have brief but adequate account of the procedures; *full names of drugs* (*including those referred to by manufacturer's code*), sources of drugs and statistical tests to be stated.
5. **Results**—To have no repetition of data in Figures, Tables and text.
6. **Discussion**—Findings and conclusions to be placed in context of other relevant work.
   NB Simple repetition of results and unwarranted speculation are not acceptable.
7. **Acknowledgements**—Sources of support. Sources of drugs not widely available commercially.
8. **References**—All references in the text to be included in the Reference List and *vice versa*. References in alphabetical order with complete citations; Journals publishing 'in press' papers identified.
   References to manuscripts submitted to other journals but not yet accepted are not allowed.
9. **Tables**—Each on a separate page and prepared in accordance with current requirements of the Journal.
10. **Figures**—Both labelled and non-labelled Figures to be prepared in accordance with current requirements of the Journal (see *Instructions to Authors*, 1995, **114**, 245–251) and provided with Figure Number and Authors' names on back (*in pencil*).
    —each legend to be typed on a separate page and carrying keys to symbols.
    —keys to symbols and histograms must not appear on the figures themselves, but in the respective legends.
    —'box style' figures are not in keeping with the Journal style; line drawings etc must have only left-hand and bottom axes.
11. **Manuscripts**—To be accompanied by a declaration signed by each author that
    (a) results are original
    (b) approval of all persons concerned has been given to submit manuscripts for consideration (see also 12b)
    (c) the same material is neither 'in press' (i.e. is in proof or has definitely been accepted for publication) nor under consideration elsewhere. Furthermore it will not be submitted or published elsewhere before a decision has been reached by the Editorial Board of the *British Journal of Pharmacology* and will not be submitted elsewhere if accepted by the *British Journal of Pharmacology*.
    (d) Copyright assignment is included.
12. **Cover letter**—To state clearly
    (a) Corresponding author's full postal address, telephone, telex or Fax number
    (b) where appropriate, that *either* ethical approval has been given for investigation *or* Company or Institutional permission to publish work has been received.
13. **Reminder**—Packaging to be sufficiently robust to protect Figures and to withstand mailing.

Failure to comply with *Instructions to Authors* may lead to substantial delays in processing, review and publication and may even jeopardize acceptance of the manuscript.

NOMENCLATURE

Authors are reminded that accepted receptor and associated terminology is laid out in *Nomenclature Guidelines for Authors*, as published in the *British Journal of Pharmacology*, *Br. J. Pharmacol.*, 1995, **114**, 253–255.

SPECIAL REPORTS

The purpose of *Special Reports* is to provide rapid publication for **new** and **important** results which the Editorial Board considers are likely to be of special pharmacological significance. *Special Reports* will have publication priority over all other material and so authors are asked to consider carefully the status of their work before submission.

In order to speed publication there is normally no revision allowed beyond very minor typographical or grammatical corrections. If significant revision is required, the Board may either invite rapid re-submission or, more probably, propose that it be re-written as a Full Paper and be re-submitted for consideration. In order to reduce delays, proofs of *Special Reports* will be sent to authors but **essential corrections must reach the Production Office within 48 hours of receipt.** Authors should ensure that their submitted material conforms exactly to the following requirements.

Special Reports should normally occupy no more than two printed pages of the Journal; two illustrations (Figures or Tables, with legends) are permitted. As a guideline, with type face of 12 pitch and double-line spacing, a page of A4 paper could contain about 400 words. The absolute maximum length of the *Special Report* is 1700 words. For each Figure or Table, please deduct 200 words. The manuscript should comprise a Title page with key words (maximum of 10), a Summary consisting of a single short paragraph, followed by Introduction, Methods, Results, Discussion and References (maximum of 10). In all other respects, the requirements are the same as for Full Papers (see current 'Instructions to Authors').

PAPERS

STOCKTON

Typeset by Elite Typesetting Techniques, Eastleigh, Hants
and printed in Great Britain by Unwin Brothers Ltd., The Gresham Press, Old Woking, Surrey